

MR-proADM as marker of endotheliitis predicts COVID-19 severity

Luis García de Guadiana-Romualdo¹  | María Dolores Calvo Nieves² | María Dolores Rodríguez Mulero³ | Ismael Calcerrada Alises⁴ | Marta Hernández Olivo⁵ | Wysali Trapiello Fernández² | Mercedes González Morales¹ | Cristina Bolado Jiménez⁶ | María Dolores Albaladejo-Otón¹ | Hilda Fernández Ovalle^{7,8} | Andrés Conesa Hernández⁹ | Eugenio Azpeleta Manrique⁶ | Luciano Consuegra-Sánchez¹⁰ | Leonor Nogales Martín¹¹ | Pablo Conesa Zamora¹ | David Andaluz-Ojeda¹¹

¹Laboratory Medicine Department, Hospital Universitario Santa Lucía, Cartagena, Spain

²Laboratory Medicine Department, Hospital Clínico Universitario, Valladolid, Spain

³Intensive Care Unit, Hospital Universitario Santa Lucía, Cartagena, Spain

⁴Primary Care Medina del Campo Urbano, Medina del Campo, Valladolid, Spain

⁵Pneumology Department, Hospital Universitario Santa Lucía, Cartagena, Spain

⁶Emergency Department, Hospital Clínico Universitario, Valladolid, Spain

⁷Primary Care Valladolid West Area, Centro de Salud Parque Alameda-Covaresa, Valladolid, Spain

⁸Endocrinology and Clinical Nutrition Research Center (ECNRC), Universidad de Valladolid, Valladolid, Spain

⁹Emergency Department, Hospital Universitario Santa Lucía, Cartagena, Spain

¹⁰Cardiology Department, Hospital Universitario Santa Lucía, Cartagena, Spain

¹¹Intensive Care Medicine Department, Hospital Clínico Universitario, Valladolid, Spain

Correspondence

Luis García de Guadiana-Romualdo, Luis. Laboratory Medicine Department, Hospital Universitario Santa Lucía, C/Mezquita, s/n, Paraje Los Arcos, 30202 Santa Lucía, Cartagena, Spain.

Email:

Funding information

Universidad Católica San Antonio de Murcia (UCAM), Grant/Award Number: PMAFI-COVID19/04; Gerencia Regional de Salud de Castilla y León, Grant/Award Number: GRS COVID 108/A/20

Abstract

Background: Early identification of patients at high risk of progression to severe COVID-19 constituted an unsolved challenge. Although growing evidence demonstrates a direct association between endotheliitis and severe COVID-19, the role of endothelial damage biomarkers has been scarcely studied. We investigated the relationship between circulating mid-regional proadrenomedullin (MR-proADM) levels, a biomarker of endothelial dysfunction, and prognosis of SARS-CoV-2-infected patients.

Methods: Prospective observational study enrolling adult patients with confirmed COVID-19. On admission to emergency department, a blood sample was drawn for laboratory test analysis. Primary and secondary endpoints were 28-day all-cause mortality and severe COVID-19 progression. Area under the curve (AUC) and multivariate regression analysis were employed to assess the association of the biomarker with the established endpoints.

Results: A total of 99 patients were enrolled. During hospitalization, 25 (25.3%) cases progressed to severe disease and the 28-day mortality rate was of 14.1%.

MR-proADM showed the highest AUC to predict 28-day mortality (0.905; [CI] 95%: 0.829-0.955; $P < .001$) and progression to severe disease (0.829; [CI] 95%: 0.740-0.897; $P < .001$), respectively. MR-proADM plasma levels above optimal cut-off (1.01 nmol/L) showed the strongest independent association with 28-day mortality risk (hazard ratio [HR]: 10.470, 95% CI: 2.066-53.049; $P < .005$) and with progression to severe disease (HR: 6.803, 95% CI: 1.458-31.750; $P = .015$).

Conclusion: Mid-regional proadrenomedullin was the biomarker with highest performance for prognosis of death and progression to severe disease in COVID-19 patients and represents a promising predictor for both outcomes, which might constitute a potential tool in the assessment of prognosis in early stages of this disease.

KEY WORDS

COVID-19, endotheliitis, mid-regional proadrenomedullin, prognosis, SARS-CoV-2, severity

1 | INTRODUCTION

In December 2019, severe acute respiratory syndrome coronavirus 2 (SARS-CoV-2) was identified as the etiological agent for the pneumonia cases of unknown origin in Wuhan (Hubei Province, China), a disease termed as coronavirus disease-2019 (COVID-19).¹ On March 11, COVID-19 was declared as a pandemic. According to the World Health Organization, nearly 2 million patients are currently dead after more than 82 million confirmed cases worldwide.²

Despite the exponential growth in research related to COVID-19 pandemic, the underlying pathophysiological mechanisms of this disease remain unclear. The incidence of complications associated to different organs and tissues and sepsis-like multiple organ dysfunction suggests the involvement of multiple pathways. Accordingly, recent studies have proposed that virus-induced endothelial dysfunction, resulting in impaired vascular blood flow, coagulation and leakage, may partially explain the development of organ dysfunction.³⁻⁵ Hence, the development of endotheliitis may be a prominent feature of COVID-19-induced severe illness.⁶

The role of clinical laboratories in this viral outbreak includes staging, prognostication and therapeutic monitoring.⁷ Different biomarkers have been identified as predictors of severe forms of COVID-19.⁸ Most of them are related to inflammation or the dysregulated immune response that characterizes this disease. Although endothelial damage has been shown to be a decisive pathophysiological factor, there are scarce studies that evaluate biomarkers of endothelial damage in severe forms of COVID-19. Here, mid-regional proadrenomedullin (MR-proADM), measured as a surrogate of adrenomedulin secretion,⁹ may be of interest within COVID-19-induced endotheliitis.¹⁰ This hormone is produced by endothelial and vascular smooth muscle cells throughout

the vascular tree to maintain endothelial barrier function. It freely diffuses through the blood and interstitium and binds to specific widespread receptors and has been showed to play a key role in reducing vascular permeability, promoting endothelial stability and integrity following severe infection.^{11,12} The extensive endothelial and pulmonary damage related to SARS-CoV-2 infection may cause a relevant disruption of the ADM system, mainly in severe cases and therefore an elevation of plasma levels of MR-proADM. This disruption of the adrenomedullin system results in vascular leakage that represents the first step of inflammation and coagulation cascade activation.⁶

Mid-regional proadrenomedullin has been widely reported as a prognostic marker in infectious and non-infectious diseases.¹³ In sepsis and community acquired pneumonia, this biomarker predicts organ damage, poor progression and mortality¹⁴⁻¹⁶ and this predictive ability is independent of the aetiology of pneumonia.¹⁷ MR-proADM has also been showed as a prognostic marker in viral infections^{18,19} and its measurement has been recently postulated in a consensus document as a potential tool in the future for prognosis of COVID-19 patients.²⁰

However, the role of MR-proADM in COVID-19 patients has been scarcely studied. Herein, the aim of this prospective study was to evaluate the relationship between MR-proADM levels and prognosis of hospitalized SARS-CoV-2-infected patients as well as its potential role as a marker of SARS-CoV-2-related widespread endothelial damage.

2 | MATERIAL AND METHODS

2.1 | Study design and population

This was a prospective observational study including consecutive adult patients admitted to Santa Lucía

University Hospital and Clínico Universitario Hospital, by confirmed SARS-CoV-2 infection between March and April 2020. COVID-19 was diagnosed by a positive result of real-time reverse transcriptase-polymerase chain reaction testing of a nasopharyngeal specimen. Exclusion criteria were as follows: (a) patients <18 years; (b) pregnant women; (c) patients transferred from or to other hospital and (d) lack of samples for the biomarkers measurement.

This study was approved by the Ethics Committee of both hospitals and performed under a waiver of informed consent. The work was carried out by following the guidelines of the Declaration of Helsinki of the World Medical Association.

2.2 | Data collection

Data collection was performed from electronic medical records and laboratory information systems. For eligible patients, we extracted the demographic information, comorbidities, laboratory test results and variables required for the previously defined endpoints.

2.3 | Blood sampling and laboratory analysis

In all patients, venous blood samples for biochemical analysis, including glucose, creatinine, sodium, potassium, albumin, bilirubin, alanine aminotransferase (ALT), ferritin, C-reactive protein (CRP), lactate dehydrogenase (LDH) and procalcitonin (PCT), haematological analysis, including haemoglobin, cell blood and platelet counts and coagulation markers, including D-dimer, were collected on admission to the Emergency Department and analysed in the laboratory within 1 hour, by using the habitual methods currently used in the participating laboratories. For measurement of MR-proADM and interleukin 6 (IL-6), blood samples collected in tubes containing EDTA K3 as anticoagulant were centrifuged at 2000 g for 10 min and plasma was subsequently frozen and stored to -80°C until testing, according to stability results previously reported.⁹

Mid-regional proadrenomedullin was measured by a homogeneous sandwich immunoassay with fluorescent detection using a time-resolved amplified cryptate emission (TRACE) technology assay (KRYPTOR[®], Brahms Thermo Fisher Scientific Inc). According to manufacturer's data, the detection limit, functional sensitivity and quantification limit were 0.05 nmol/L, 0.23 nmol/L and 0.25 nmol/L; intra-assay coefficient of variation (CV) and inter-assay CV were $\leq 10\%$ and $\leq 20\%$, for a level ranging from 0.2 to 0.5 nmol/L, respectively.

2.4 | Study endpoints

The primary endpoint was all-cause mortality at 28-days. Secondary endpoint was severe COVID-19 progression, defined as a composite of admission to Intensive Care Unit during the index hospital stay and/or need for mechanical ventilation and/or 28-day mortality, both verified by chart review.

2.5 | Statistical analysis

The normality of continuous variables was tested by Kolmogorov-Smirnov or Shapiro-Wilk test, and they are presented as median (interquartile range [IQR]) or mean (standard deviation [SD]), as appropriate. Comparisons for continuous variables were performed by Student's *t* test, for the normally distributed data; for skewed distribution, Mann-Whitney *U* non parametric tests were used for comparisons. Categorical variables are presented as frequency and percentage in each category. The significance of differences in percentages was tested by the chi-squared test. Discriminatory ability for both outcomes was evaluated by calculating the area under the receiver operating characteristic curve (ROC AUC). We additionally calculated the optimal ROC-derived cut-offs (Youden Index, corresponding to the maximum of the sum 'sensitivity + specificity') and sensitivity, specificity, likelihood ratios and predictive values. The association between the biomarkers and the risk for both outcomes was assessed by Cox regression analysis, adjusted by confounding variables. Variables yielding a $P < .10$ in the univariate regression analysis were further included in the multivariate using the backward stepwise selection method. In a further step, the impact of the biomarkers on outcomes along time was assessed by using Kaplan-Meier curves and the Mantel-Haenszel log-rank test. Time was censored at 28 days following admission to the Emergency Department. Software packages SPSS vs. 22 (SPSS Inc), and MedCalc 15.0 (MedCalc Software) were used for statistical analysis, with a $P < .05$ considered statistically significant.

Reporting of the study conforms to CONSORT-revised and the broader EQUATOR guidelines.²¹

3 | RESULTS

3.1 | Patient characteristics

Main baseline and clinical characteristics on admission according to the endpoints previously defined are listed in Table 1. A total of 99 patients, 60 from Santa Lucía University Hospital (Cartagena, Spain) and 39 from Clínico University Hospital

TABLE 1 Demographics, comorbidities and laboratory findings on admission, grouped according to survival status at 28 d and progression to severe disease

	All patients	Survivors	Non-survivors	P-value	Non-severe	Severe	P-value
n (%)	99	85 (13.3)	14 (14.1)		74 (75.7)	25 (25.3)	
Demographics							
Age (y), mean (SD)	66 (15)	64 (15)	76 (8)	.005	65 (16)	70 (12)	.054
Gender, male (n [%])	61 (61.6)	51 (60)	10 (71.4)	.415	45 (60.8)	16 (64.0)	.777
Medical history (n [%])							
Hypertension	54 (54.5)	41 (48.2)	13 (92.9)	.002	36 (48.6)	18 (72.0)	.043
Diabetes mellitus	28 (28.3)	21 (24.7)	7 (50.0)	.052	19 (25.7)	9 (36.0)	.322
COPD	6 (6.1)	5 (5.9)	1 (7.1)	.855	5 (6.8)	1 (4.0)	.617
Cardiovascular disease	18 (18.2)	12 (14.1)	6 (42.9)	.010	8 (10.8)	10 (40.0)	.001
Chronic kidney disease	9 (9.1)	3 (3.5)	6 (42.9)	<.001	2 (2.7)	7 (28.0)	<.001
Cancer	3 (3.0)	2 (2.4)	1 (7.1)	.333	5 (6.8)	1 (4.0)	.617
Cerebrovascular disease	7 (7.1)	6 (7.1)	1 (7.1)	.991	5 (6.8)	2 (8.0)	.834
Laboratory findings							
Glucose (mg/dL)	129 (110-154)	123 (108-146)	157 (114-270)	.007	126 (108-150)	138 (111-175)	.146
Sodium (mmol/L)	137 (134-139)	137 (134-139)	137 (129-143)	.805	136 (134-139)	137 (132-140)	.747
Potassium (mmol/L)	4.3 (0.6)	4.2 (0.6)	4.4 (0.7)	.243	4.2 (0.6)	4.4 (0.7)	.197
Creatinine (mg/dL)	0.93 (0.76-1.14)	0.91 (0.75-1.03)	1.49 (1.02-2.04)	.002	0.91 (0.75-1.00)	1.13 (0.80-1.73)	.015
Bilirubin (mg/dL)	0.41 (0.30-0.61)	0.40 (0.30-0.60)	0.55 (0.38-0.70)	.184	0.41 (0.30-0.60)	0.48 (0.37-0.65)	.241
Albumin (g/dL)	4.0 (3.6-4.2)	4.0 (3.7-4.2)	3.5 (3.2-4.0)	.016	4.0 (3.7-4.2)	3.7 (3.3-4.2)	.024
ALT (U/L)	26 (18-43)	26 (17-41)	22 (20-52)	.614	26 (17-41)	26 (21-50)	.342
LDH (U/L)	281 (220-374)	269 (213-360)	368 (288-511)	.005	260 (210-318)	376 (303-499)	<.001
Ferritin (μg/L)	432 (270-1250)	412 (244-1244)	845 (429-1401)	.043	360 (223-1109)	944 (468-1526)	.001
CRP (mg/L)	71 (27-128)	60 (23-118)	130 (95-276)	.001	57 (20-108)	109 (92-214)	<.001
PCT (μg/L)	0.09 (0.06-0.20)	0.08 (0.05-0.18)	0.19 (0.11-1.15)	.003	0.08 (0.05-0.16)	0.16 (0.11-0.61)	<.001
IL-6 (pg/mL)	34.8 (18.4-87.9)	30.5 (17.1-72.0)	126.9 (27.5-157.2)	.008	29.7 (16.0-60.4)	79.8 (29.9-135.7)	.003
Haemoglobin (g/dL)	13.7 (1.8)	13.8 (1.6)	13.3 (2.7)	.338	13.7 (1.7)	13.5 (2.1)	.548
WBC (*10 ⁹ /L)	7.03 (5.35-8.71)	7.03 (5.38-8.65)	6.78 (5.27-9.46)	.952	6.97 (5.38-8.76)	7.11 (5.33-8.65)	.994
Neutrophil count (*10 ⁹ /L)	4.92 (3.77-7.01)	4.92 (3.76-6.91)	5.39 (4.19-8.21)	.366	4.85 (3.76-6.89)	5.88 (4.19-7.58)	.280
Lymphocyte count (*10 ⁹ /L)	1.21 (0.81-1.48)	1.24 (0.88-1.63)	0.77 (0.45-1.23)	.015	1.27 (0.88-1.64)	1.01 (0.64-1.21)	.005
NLR	5.06 (2.87-7.48)	4.51 (2.73-6.98)	8.20 (4.17-10.98)	.025	4.32 (2.33-6.90)	6.55 (4.17-9.98)	.013

(Continues)

TABLE 1 (Continued)

	All patients	Survivors	Non-survivors	P-value	Non-severe	Severe	P-value
Platelet count (*10 ⁹ /L)	188 (165-243)	194 (167-251)	174 (126-209)	.037	193 (167-267)	181 (151-212)	.095
D-dimer (ng/mL FEU)	678 (470-1224)	624 (427-935)	1742 (946-4532)	.001	612 (447-935)	1044 (520-2679)	.007
MR-proADM (mmol/L)	0.74 (0.60-1.02)	0.68 (0.57-0.94)	1.54 (1.05-2.12)	<.001	0.68 (0.54-0.91)	1.36 (0.93-1.78)	<.001

Note: Laboratory tests levels are expressed as median (IQR) or mean (SD), as appropriate.

Abbreviations: ALT, Alanine aminotransferase; COPD, Chronic obstructive pulmonary disease; CRP, C-reactive protein; IL-6, Interleukin-6; LDH, Lactate dehydrogenase; MR-proADM, Mid-regional proadrenomedullin; NLR, Neutrophil-to-lymphocyte ratio; PCT, Procalcitonin; WBC, White blood cell.

FIGURE 1 Receiver operating characteristic curves of biomarker levels on admission to predict 28-d mortality (A) and progression to severe disease (B)

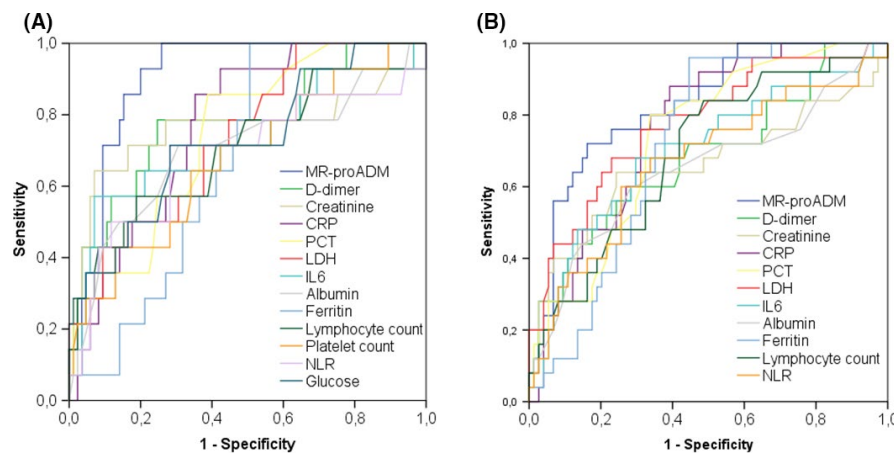


TABLE 2 Receiver operating characteristic (ROC) curves for prediction of primary and secondary endpoints

Biomarker	Prediction of 28-d mortality		Prediction of progression to severe disease	
	AUC	95% CI%; P	AUC	95% CI%; P
MR-proADM	0.905	0.829-0.955; <.001	0.829	0.740-0.897; <.001
Glucose	0.727	0.628-0.812; .004	–	–
Creatinine	0.764	0.668-0.843; .005	0.663	0.561-0.755; .031
Albumin	0.701	0.601-0.789; .024	0.651	0.548-0.744; .034
LDH	0.737	0.639-0.820; <.001	0.776	0.681-0.853; <.001
D-dimer	0.781	0.686-0.858; <.001	0.682	0.581-0.772; .006
CRP	0.769	0.673-0.848; <.001	0.766	0.670-0.845; <.001
Ferritin	0.670	0.568-0.761; .004	0.719	0.620-0.805; <.001
PCT	0.747	0.650-0.829; <.001	0.735	0.637-0.819; <.001
IL-6	0.724	0.625-0.809; .011	0.698	0.598-0.787; .002
NLR	0.687	0.586-0.777; .044	0.668	0.566-0.759; .014
Lymphocyte count	0.703	0.603-0.791; .020	0.688	0.587-0.777; .002
Platelet count	0.675	0.573-0.766; .035	–	–

Note: Only biomarkers with significant differences in comparisons among groups according to the outcome were included in the table.

Abbreviations: AUC, Area under the curve; CI, Confidence interval; CRP, C-reactive protein; IL-6, Interleukin-6; LDH, Lactate dehydrogenase; MR-proADM, Mid-regional proadrenomedullin; NLR, neutrophil-to-lymphocyte ratio; PCT, Procalcitonin.

(Valladolid, Spain), were admitted due to COVID-19, with a mean age of 66 years (61.6% were male). Hypertension was the most common comorbidity, with a greater prevalence among non-survivors (48.2% vs. 92.9%, $P = .002$), followed by diabetes mellitus (28.3%) and cardiovascular disease (18.2%). During hospitalization, 25 (25.3%) cases progressed to severe disease, of whom 16 (16.2%) required intensive care, 12 (12.1%) underwent mechanical ventilation and 14 (14.1%) died of any cause within the first 28 days of hospital stay. There were not significant differences between the two participating centres regarding to the rates of 28-day mortality (11.7% vs. 17.9%; $P = .381$) and progression to severe disease (23.3% vs. 28.2%; $P = .582$). In overall population, median hospital stay was 17 (IQR: 8-16) days and 12 (IQR: 7-19) days in patients requiring Intensive Care Unit care.

3.2 | Laboratory tests for prediction of 28-day mortality

According to survival status, the biomarker levels are summarized in Table 1. Glucose, creatinine, albumin, LDH, ferritin, CRP, IL-6, PCT, D-dimer and MR-proADM levels and

neutrophil-to-lymphocyte ratio (NLR) were significantly higher in patients who died, while platelet and lymphocyte counts were significantly lower.

The accuracy of biomarkers for predicting 28-days mortality, evaluated by ROC curve analysis, is showed in Figure 1.A and Table 2. MR-proADM was the biomarker with the highest AUC (0.905, 95% confidence interval [CI]: 0.829-0.955; $P < .001$).

According to the Youden index, we calculated the optimal cut-offs for differentiating between survivors and non-survivors (Table 3). Notably, Kaplan-Meier analysis showed that no patient with a MR-proADM value ≤ 0.88 nmol/L, recommended as cut-off by the manufacturer, died in the first 28 days following Emergency Department admission (Figure 2A). Survival analysis for the cut-off from Youden index is showed in Figure 2B.

In the multivariate Cox regression analysis (Table 4), after adjusting for confounders, MR-proADM > 1.01 nmol/L showed the strongest independent association with 28-day mortality risk (hazard ratio [HR]: 10.470, 95% CI: 2.066-53.049; $P = .005$). D-dimer > 935 ng/mL FEU (HR: 4.521, 95% CI: 1.185-17.238; $P = .027$) and IL-6 > 117.8 pg/mL (HR: 3.739, 95% CI: 1.207-11.585; $P = .022$) were also independent predictors associated with 28-day mortality.

TABLE 3 Accuracy of biomarkers for 28-d mortality

Biomarker	Cut-off	Sensitivity [95% CI] (%)	Specificity [95% CI] (%)	LR+ [95% CI]	LR- [95% CI]	PPV [95% CI] (%)	NPV [95% CI] (%)
MR-proADM (nmol/L)	$\leq 0.88^a$	100 (76.8-100)	68.2 (57.2-77.9)	3.2 (2.7-3.6)	0	34.1 (19.9-50.8)	100 (93.8-100)
	> 1.01	85.7 (57.2-98.2)	84.7 (75.3-91.6)	5.6 (4.4-7.1)	0.17 (0.04-0.7)	48.0 (27.8-68.7)	97.3 (90.6-99.7)
D-dimer (ng/mL FEU)	> 935	78.6 (49.2-95.3)	75.3 (64.7-84.0)	3.2 (2.4-4.3)	0.4 (0.1-0.8)	34.4 (18.6-53.2)	95.5 (87.4-99.1)
CRP (mg/L)	> 71	92.9 (66.1-99.8)	57.7 (46.4-68.3)	2.2 (1.7-2.8)	0.12 (0.02-0.8)	26.5 (14.9-41.1)	98.0 (89.2-100.0)
Creatinine (mg/dL)	> 1.37	64.3 (35.1-87.2)	92.9 (85.3-97.4)	9.1 (6.1-13.5)	0.38 (0.1-1.1)	60.0 (31.3-84.4)	94.0 (86.6-98.1)
PCT (μ g/L)	> 0.10	85.7 (57.2-98.2)	61.2 (50.0-71.6)	2.2 (1.7-2.9)	0.23 (0.06-0.9)	26.7 (14.5-42.1)	96.3 (87.3-99.5)
LDH (U/L)	> 331	57.1 (28.9-82.3)	69.4 (58.5-79.0)	1.9 (1.2-3.0)	0.62 (0.3-1.2)	23.5 (10.7-41.2)	90.8 (80.9-96.6)
Glucose (mg/dL)	> 139	71.4 (41.9-91.6)	71.8 (61.0-81.0)	2.5 (1.8-3.6)	0.4 (0.2-1.0)	29.4 (15.1-47.5)	93.8 (84.9-98.3)
IL-6 (pg/mL)	> 117.8	57.1 (28.9-82.3)	92.9 (85.3-97.4)	8.1 (5.1-12.8)	0.46 (0.2-1.2)	57.1 (27.8-83.1)	92.9 (85.3-97.4)
Lymphocyte count ($\times 10^9/L$)	≤ 0.79	57.1 (28.9-82.3)	81.2 (71.2-88.8)	3.0 (1.9-4.8)	0.53 (0.2-1.1)	33.3 (15.3-55.8)	92.0 (83.4-97.0)
Albumin (g/dL)	≤ 3.7	71.4 (41.9-91.6)	69.4 (58.5-79.0)	2.3 (1.6-3.3)	0.41 (0.2-1.0)	27.8 (14.2-45.2)	93.7 (84.4-98.3)
NLR	> 6.11	71.4 (41.9-91.6)	71.8 (61.0-81.0)	2.5 (1.8-3.6)	0.4 (0.2-1.0)	29.4 (15.1-47.5)	93.8 (84.9-98.3)
Platelet count ($\times 10^9/L$)	≤ 178	64.3 (35.1-87.2)	65.9 (54.8-75.8)	1.9 (1.2-2.9)	0.54 (0.3-1.2)	23.7 (11.4-40.2)	91.8 (81.8-97.3)
Ferritin (μ g/L)	> 381	92.9 (66.1-99.8)	49.4 (38.4-60.5)	1.8 (1.4-2.4)	0.14 (0.02-1.0)	23.2 (13.0-36.4)	97.7 (87.5-99.9)

Abbreviations: CI, confidence interval; CRP, C-reactive protein; IL-6, interleukin-6; LDH, Lactate dehydrogenase; LR, Likely hood ratio; MR-proADM, Mid-regional proadrenomedullin; NLR, neutrophil-to-lymphocyte ratio; NPV, Negative predictive value; PCT, Procalcitonin; PPV, Positive predictive value.

^aCutoff recommended by manufacturer to assess early the risk for progression to a more severe disease condition.

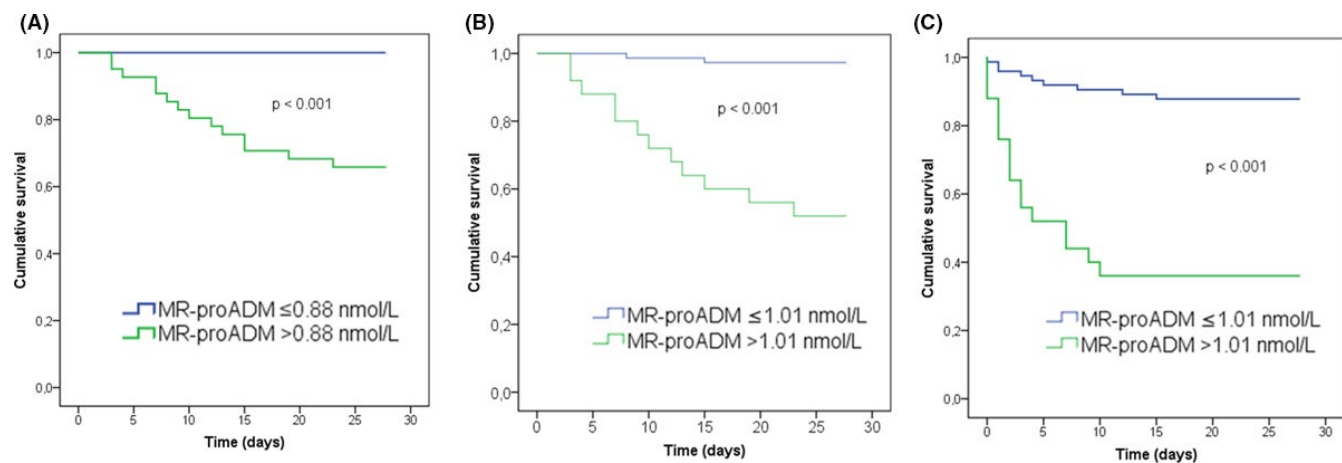


FIGURE 2 Cumulative incidence of (A) 28-d mortality during hospitalization stratified by MR-proADM on admission ≤ 0.88 nmol/L, (B) 28-d mortality during hospitalization stratified by MR-proADM on admission > 1.01 nmol/L, and (C) progression to severe disease stratified by MR-proADM on admission > 1.01 nmol/L

TABLE 4 Uni- and multivariate Cox regression analysis for 28-d mortality

Variable	Univariate analysis		Multivariate analysis	
	HR (CI 95%)	P-value	HR (CI 95%)	P-value
Age	1.061 (1.017-1.107)	.007	n.s	
Hypertension	12.346 (1.614-94.423)	.015	n.s	
Cardiovascular disease	4.053 (1.404-11.700)	.010	n.s	
Chronic kidney disease	10.208 (3.506-29.723)	<.001	n.s	
Diabetes melitus	2.739 (0.960-7.814)	.06	n.s	
Glucose	1.007 (1.003-1.011)	<.001	n.s	
Creatinine	2.433 (1.633-3.625)	<.001	n.s	
Albumin	0.235 (0.077-0.714)	.011	n.s	
NLR	1.122 (1.029-1.224)	.009	n.s	
Platelet count	0.989 (0.980-0.999)	.024	n.s	
Ferritin > 381 $\mu\text{g/L}$	11.051 (1.445-84.503)	.021	n.s	
CRP > 71 mg/L	15.079 (1.972-115.31)	.009	n.s	
PCT > 0.10 $\mu\text{g/L}$	8.386 (1.875-37.500)	.005	n.s	
IL-6 > 117.8 pg/mL	8.741 (3.051-25.042)	<.001	3.739 (1.207-11.585)	.022
MR-ProADM > 1.01 nmol/L	23.247 (5.189-104.152)	<.001	10.470 (2.066-53.049)	.005
D-Dimer > 935 ng/mL FEU	9.468 (2.637-33.995)	.001	4.521 (1.185-17.238)	.027
LDH > 331 U/L	2.816 (0.977-8.120)	.055	n.s	

Note: Only variables with a $P < .10$ for HR in univariate analysis were included in the table.

Abbreviations: CI, confidence interval; CRP, C-reactive protein; HR, hazard ratio; IL-6, interleukin-6; LDH, lactate dehydrogenase; MR-proADM, Mid-regional proadrenomedullin; n.s, non significant; NLR, neutrophil-to-lymphocyte ratio; PCT, procalcitonin.

3.3 | Laboratory tests for prediction of progression to severe disease

Creatinine, albumin, LDH, ferritin, CRP, PCT, IL-6 and MR-proADM levels and NLR were significant higher in patients who progressed to severe disease, while lymphocyte count was significant lower (Table 1).

Again, MR-proADM was the biomarker with the highest ROC AUC (0.829, 95% CI: 0.740-0.897; $P < .001$) (Figure 1B and Table 2). Optimal cut-offs for the biomarkers are showed in Table 5. Kaplan-Meier analysis showed a higher likelihood of progression to severe disease in patients with a MR-proADM level >1.01 nmol/L (Figure 2C).

Multivariate adjusted Cox regression model showed that MR-proADM >1.01 nmol/L [HR: 6.803, 95% CI: 1.458-31.750; $P = .015$] and ferritin >376 ng/ml (HR: 5.525, 95% CI: 1.042-29.308; $P = .045$) at admission were the only independent variables associated with progression to severe disease (Table 6).

4 | DISCUSSION

Our study suggests that MR-proADM may be used as an accurate marker of fatal outcome and progression to severe disease in COVID-19. Its accuracy was significantly better than that showed by other previously investigated biomarkers. Patients who presented MR-proADM levels above 1.01 nmol/L showed an association with 28-day mortality and progression to severe disease independent of other factors.

Endothelial dysfunction is known to be involved in organ dysfunction during bacterial sepsis^{22,23} and viral infections,²⁴ as it induces a pro-coagulant state, microvascular leak and organ failure.

Unlike other types of serious infections of different aetiology, epidemiological studies show that COVID-19 patients requiring hospital admission present frequently with accompanying conditions such as hypertension, diabetes, chronic renal failure and cardiovascular diseases.^{25,26} These comorbidities are associated with chronic endothelial dysfunction and could predispose these patients to a worse outcome.²⁷ The endothelium plays major roles in the response to infection: endothelial cells release chemokines, to guide leucocytes to the infected tissue, and cytokines that activate inflammatory responses. Patients with endothelial dysfunction present major alterations at the glycocalyx, intercellular junctions and endothelial cells, resulting in enhanced leucocyte adhesion and extravasation, and also in the induction of a procoagulant and antifibrinolytic state. Prior endothelial dysfunction could thus predispose to the development of severe forms of COVID-19.²⁸

In fact, emerging data suggest a crucial role of endothelial dysfunction during SARS-CoV-2 infection.²⁹ In this regard, recent histopathological studies have evidenced the presence of virus within endothelial cells of different organs beyond the lungs, suggesting a direct viral effect, as well as the accumulation of inflammatory cells, with evidence of endothelial and inflammatory cell death, thus contributing directly to severity. Shortly, SARS-CoV-2 infection would facilitate the induction of endotheliitis in different organs as a direct consequence of

TABLE 5 Accuracy of biomarkers for progression to severe disease

Biomarker	Cut-off	Sensitivity (%)	Specificity (%)	LR+	LR-	PPV (%)	NPV (%)
MR-proADM (nmol/L)	$\leq 0.88^a$	76.0 (54.9-90.6)	70.3 (58.5-80.3)	2.6 (2.0-3.3)	0.34 (0.2-0.7)	46.3 (30.5-62.8)	89.7 (78.8-96.1)
	>1.01	64.0 (42.5-82.0)	87.8 (78.2-94.3)	5.3 (3.9-7.1)	0.41 (0.2-0.9)	64.0 (42.0-82.4)	87.8 (78.2-94.3)
LDH (U/L)	>331	68.0 (46.5-85.1)	77.0 (65.8-86.0)	3.0 (2.2-4.0)	0.42 (0.2-0.8)	50.0 (32.4-67.6)	87.7 (77.2-94.5)
CRP (mg/L)	>67	88.0 (68.8-97.5)	60.8 (48.8-72.0)	2.3 (1.8-2.8)	0.20 (0.07-0.6)	43.1 (29.3-57.8)	93.7 (82.8-98.7)
PCT (μ g/L)	>0.10	80.0 (59.3-93.2)	66.2 (54.3-76.8)	2.4 (1.8-3.1)	0.30 (0.1-0.7)	44.4 (29.6-60.0)	90.7 (79.6-97.0)
Ferritin (μ g/L)	>376	96.0 (79.6-99.9)	55.4 (43.4-67.0)	2.2 (1.7-2.7)	0.07 (0.01-0.5)	42.1 (29.1-55.9)	97.6 (87.4-99.9)
IL-6 (pg/mL)	>50.6	58 (46.5-85.1)	70.3 (58.5-80.3)	2.3 (1.7-3.1)	0.46 (0.2-0.49)	43.6 (27.8-60.4)	86.7 (75.4-94.1)
Lymphocyte count ($\times 10^9/\text{L}$)	≤ 1.23	80.0 (59.3-93.2)	55.4 (43.4-67.0)	1.8 (1.4-2.4)	0.36 (0.2-0.8)	37.7 (24.8-52.1)	89.1 (76.2-96.4)
D-dimer (ng/mL FEU)	>935	56.0 (34.9-75.6)	75.7 (64.3-84.9)	2.3 (1.6-3.3)	0.58 (0.3-1.1)	43.8 (26.1-62.6)	83.6 (72.5-91.5)
NLR	>6.11	60.0 (38.7-78.9)	74.3 (62.8-83.8)	2.3 (1.7-3.3)	0.54 (0.3-1.0)	44.1 (27.2-62.1)	84.6 (73.4-92.4)
Creatinine (mg/dL)	>1.00	64.0 (42.5-82.0)	75.7 (64.3-84.9)	2.6 (1.9-3.6)	0.48 (0.2-0.9)	47.1 (29.5-65.1)	86.2 (75.3-93.5)
Albumin (g/dL)	≤ 3.7	60.0 (38.7-78.9)	71.6 (59.9-81.5)	2.1 (1.5-3.0)	0.56 (0.3-1.0)	41.7 (25.3-59.5)	84.1 (72.7-92.1)

Abbreviations: CI, confidence interval; CRP, C-reactive protein; IL-6, interleukin-6; LDH, lactate dehydrogenase; LR, likely hood ratio; MR-proADM, Mid-regional proadrenomedullin; NLR, neutrophil-to-lymphocyte ratio; NPV, negative predictive value; PCT, procalcitonin; PPV, positive predictive value.

^aCut-off recommended by manufacturer to assess early the risk for progression to a more severe disease condition.

TABLE 6 Uni- and multivariate Cox regression analysis for progression to severe disease

Variable	Univariate analysis		Multivariate analysis	
	HR (CI 95%)	P-value	HR (CI 95%)	P-value
Hypertension	2.320 (0.969-5.558)	.059	n.s	
Cardiovascular disease	3.646 (1.632-8.149)	.002	n.s	
Chronic kidney disease	6.145 (2.537-14.880)	<.001	n.s	
Glucose	1.006 (1.002-1.011)	.006	n.s	
Creatinine	3.062 (1.875-5.000)	<.001	n.s	
Albumin	0.334 (0.144-0.771)	.010	n.s	
Ferritin >376 ng/mL	10.861 (2.558-46.120)	.001	5.525 (1.042-29.308)	.045
CRP >67 mg/L	8.130 (2.429-27.205)	<.001	n.s	
PCT >0.10 µg/L	6.083 (2.278-16.243)	.002	n.s	
IL-6 >50.6 pg/mL	3.985 (1.717-9.247)	.001	n.s	
NLR	1.113 (1.033-1.199)	.005	n.s	
Platelet count	0.994 (0.988-1.000)	.059	n.s	
MR-ProADM >1.014 nmol/L	7.740 (3.392-17.661)	<.001	6.803 (1.458-31.750)	.015
D-Dimer >935 ng/mL FEU	3.129 (1.419-6.903)	.005	n.s	
LDH >331 U/L	5.330 (2.293-12.394)	<.001	n.s	

Note: Only variables with a $P < .10$ for HR in univariate analysis were included in the table

Abbreviations: CI, confidence interval; CRP, C-reactive protein; HR, hazard ratio; IL-6, interleukin-6; LDH, lactate dehydrogenase; MR-proADM, Mid-regional proadrenomedullin; n.s, non-significant; NLR, neutrophil-to-lymphocyte ratio; PCT, procalcitonin.

virus involvement and of the host inflammatory response.^{3,4} While endotheliopathy is thought to be a key factor of severe COVID-19 pathogenesis, markers indicative of this process have not been well-established. Only isolated little studies analyse the role of endothelium-related molecules such as thrombomodulin,⁵ angiopoietin 2,^{30,31} VCAM or ICAM³² in COVID-19.

Among the endothelial dysfunction markers associated with sepsis, MR-proADM appears to be the most promising, as reported by Martin-Fernandez et al. in a recent study.²² This biomarker can be automated with an adequate turn-around-time for its implementation as a stat laboratory test for clinical practice.⁹

In our study, MR-proADM was the biomarker with the highest accuracy for 28-day mortality, with a ROC AUC of 0.905. Furthermore, after adjusting for confounding variables, multivariate analysis showed the highest HR (10.47) when plasma MR-proADM levels on admission were above 1.01 mmol/L for the primary outcome, together with levels of D-dimer >935 ng/mL FEU and IL-6 > 117.8 pg/mL (HR: 4.521 and 3.739, respectively). These findings support the association of the triad composed of endothelial damage, inflammation and coagulopathy with COVID-19 severity.³³ In this line, there are numerous studies that describe the association between elevated plasma levels of D-dimer or IL-6 and poor prognosis.^{34,35}

Again, and similar to results for 28-day mortality, ROC AUC analysis evidenced that accuracy of MR-proADM was the highest to detect progression to severe disease (with AUC above 0.80), better than other inflammation markers, such as CRP, ferritin, LDH and PCT, all of them recommended for monitoring COVID-19 patients.⁸ In addition, MR-proADM, together with ferritin, was the only biomarkers independently associated with progression to severe disease in the multivariate analysis. The same cut-off (>1.01 nmol/L) for MR-proADM on admission showed the highest HR (6.803), while ferritin >376 ng/mL achieved a HR of 5.525. Serum ferritin, a feature of haemophagocytic lymphohistiocytosis, which is a known complication of viral infection, is closely related to poor recovery of COVID-19 patients, and those with impaired lung lesion are more likely to have increased ferritin levels.³⁶ Again, the binomial composed by an inflammatory marker, in this case ferritin, together with an endothelial damage marker, such as MR-proADM, seems crucial in the development of complications and fatal evolution in COVID-19.

In the setting of infectious disease, MR-proADM has been reported as a useful marker for differentiating between infection and sepsis^{22,37} and for an early stratification of severity in patients with sepsis.^{15,38,39} Few studies have evaluated the potential role of MR-ProADM in viral infections and most of them have been limited to

influenza virus. Thus, Valero-Cifuentes et al.¹⁹ reported a moderate ROC AUC (0.68) to predict a poor outcome in a cohort of patients admitted to hospital with influenza syndrome. On the contrary, Valenzuela et al.,¹⁸ in a small cohort of patients with influenza A virus pneumonia, obtained a ROC AUC of 0.871 to predict mortality, with an optimal cut-off of 1.12 nmol/L. In turn, Bello et al.,¹⁷ reported a ROC AUC of 0.859 and an optimal cut-off point of 1.09 nmol/L in patients with community-acquired pneumonia of different aetiology, including virus.¹⁶ These data are consistent with those obtained in our study.

To our knowledge, only a previous study has analysed the prognostic value of MR-proADM in COVID-19. Spoto et al.⁴⁰ have recently reported a ROC AUC for 28-day mortality of 0.89 in 69 patients, similar to that reported in our study (0.905) in a larger sample. Further, there were substantial differences regarding baseline characteristics between the populations of both studies. These disparities may partially explain the different optimal cut-offs (1.01 nmol/L vs. 2.0 nmol/L). This disagreement is likely due to differences in both study population characteristics. Hence, Spoto et al. cohort⁴⁰ included older patients than those in our study (79 years vs. 66 years), with a higher incidence of comorbidities such as cardiovascular disease (68.1% vs. 18.2%) and a greater severity, with a higher rate of death (23.2% vs. 14.1%) and of patients requiring admission to ICU (43.5% vs. 16.2%).

In addition, it is noteworthy that we observed that a MR-proADM level ≤ 0.88 nmol/L allows to rule out mortality in the 28 days following admission to hospital, as previously reported by Andaluz-Ojeda et al.^{15,41} in critically ill patients with sepsis diagnosis.

This study presents some limitations, namely the small sample size. Besides, the measurement of other blood biomarkers previously reported as predictors for a poor outcome, such as troponin,⁴² was not available in all the patients and it was not included in the study. Finally, we did not measure serial biomarkers and their values may therefore change during the patient's course, thereby making it possible to better identify deterioration or improvement.

In conclusion, the present study reports that plasma MR-proADM levels, measured on admission to Emergency Department, were increased in COVID-19 patients who died or progressed to severe disease. Besides, it was the biomarker with highest performance, expressed as ROC AUC, being MR-proADM value levels above 1.01 nmol/L the only independent factor predictor for both outcomes. Our results suggest that MR-proADM levels have a potential role in the assessment of prognosis in early stages of COVID-19 and might be a candidate to be incorporated in an early management protocol. Further studies, with a larger sample size, are required to confirm these findings.

ACKNOWLEDGEMENTS

This research has been partially funded by Universidad Católica San Antonio de Murcia (UCAM) (reference: PMAFI-COVID19/04) and Gerencia Regional de Salud de Castilla y León under grant number GRS COVID 108/A/20.

CONFLICT OF INTEREST

Authors state no conflict of interest.

AUTHOR CONTRIBUTIONS

LGGR and DAO designed this study, analysed the data and wrote the manuscript. All authors contributed to the enrollment of patients, data collection, sample collection and biomarkers measurement. LCS provided statistical advice. All authors reviewed and approved the final manuscript. All authors have accepted responsibility for the entire content of this manuscript and approved its submission.

ORCID

Luis García de Guadiana-Romualdo  <https://orcid.org/0000-0003-3028-3198>

REFERENCES

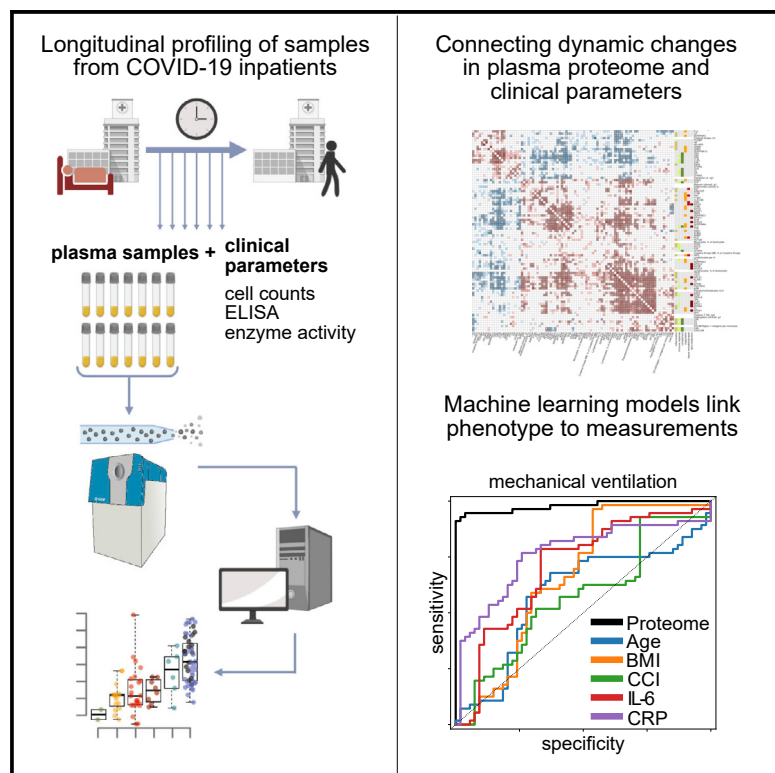
1. Zhu N, Zhang D, Wang W, et al. A novel coronavirus from patients with pneumonia in China, 2019. *N Engl J Med.* 2020;382:727-733.
2. WHO. Coronavirus disease 2019 (COVID-19) situation report. October 24, 2020. <https://www.who.int/emergencies/diseases/novel-coronavirus-2019>. Accessed January 2, 2021.
3. Varga Z, Flammer AJ, Steiger P, et al. Endothelial cell infection and endotheliitis in COVID-19. *Lancet.* 2020;395(10234):1417-1418.
4. Ackermann M, Verleden SE, Kuehnel M, et al. Pulmonary vascular endothelialitis, thrombosis, and angiogenesis in Covid-19. *N Engl J Med.* 2020;383:120-128.
5. Goshua G, Pine AB, Meizlish ML, et al. Endotheliopathy in COVID-19-associated coagulopathy: evidence from a single-centre, cross-sectional study. *Lancet Haematol.* 2020;7:e575-e582.
6. Wilson DC, Schefold JC, Baldirà J, Spinetti T, Saeed K, Elke G. Adrenomedullin in COVID-19 induced endotheliitis. *Crit Care.* 2020;24:411.
7. Lippi G, Plebani M. The critical role of laboratory medicine during coronavirus disease 2019 (COVID-19) and other viral outbreaks. *Clin Chem Lab Med.* 2020;58:1063-1069.
8. Del Sole F, Farcomeni A, Loffredo L, et al. Features of severe COVID-19: a systematic review and meta-analysis. *Eur J Clin Invest.* 2020;50:e13378.
9. Morgenthaler NG, Struck J, Alonso C, Bergmann A. Measurement of midregional proadrenomedullin in plasma with an immunoluminometric assay. *Clin Chem.* 2005;51:1823-1829.
10. Hupf J, Mustroph J, Hanses F, Evert K, Maier LS, Jungbauer CG. RNA-expression of adrenomedullin is increased in patients with severe COVID-19. *Crit Care.* 2020;24:527.
11. Temmesfeld-Wollbrück B, Brell B, Dávid I, et al. Adrenomedullin reduces vascular hyperpermeability and improves survival in rat septic shock. *Intensive Care Med.* 2007;33:703-710.
12. Vallet B. Endothelial cell dysfunction and abnormal tissue perfusion. *Crit Care Med.* 2002;30:S229-S234.

13. Morbach C, Marx A, Kaspar M, et al. Prognostic potential of mid-regional pro-adrenomedullin following decompensation for systolic heart failure: comparison with cardiac natriuretic peptides. *Eur J Heart Fail.* 2017;19:1166-1175.
14. Bernal-Morell E, García-Villalba E, Vera MDC, et al. Usefulness of midregional pro-adrenomedullin as a marker of organ damage and predictor of mortality in patients with sepsis. *J Infect.* 2018;76:249-257.
15. Andaluz-Ojeda D, Nguyen HB, Meunier-Beillard N, et al. Superior accuracy of mid-regional proadrenomedullin for mortality prediction in sepsis with varying levels of illness severity. *Ann Intensive Care.* 2017;7:15.
16. Liu D, Xie L, Zhao H, Liu X, Cao J. Prognostic value of mid-regional pro-adrenomedullin (MR-proADM) in patients with community-acquired pneumonia: a systematic review and meta-analysis. *BMC Infect Dis.* 2016;16:232.
17. Bello S, Lasierra AB, Mincholé E, et al. Prognostic power of proadrenomedullin in community-acquired pneumonia is independent of aetiology. *Eur Respir J.* 2012;39:1144-1155.
18. Valenzuela Sanchez F, Valenzuela Mendez B, Rodríguez Gutierrez JF, et al. Initial levels of mr-proadrenomedullin: a predictor of severity in patients with influenza a virus pneumonia. *Intensive Care Med Exp.* 2015;3:A832.
19. Valero Cifuentes S, García Villalba E, Alcaraz García A, et al. Prognostic value of pro-adrenomedullin and NT-proBNP in patients referred from the emergency department with influenza syndrome. *Emergencias.* 2019;3:180-184.
20. Julián-Jiménez A, García DE, González Del Castillo J, et al. Key issues in emergency department management of COVID-19: proposals for improving care for patients in Latin America. *Emergencias.* 2021;33:42-58.
21. Simera I, Moher D, Hoey J, Schulz KF, Altman DG. A catalogue of reporting guidelines for health research. *Eur J Clin Invest.* 2010;40:35-53.
22. Martin-Fernandez M, Vaquero-Roncero LM, Almansa R, et al. Endothelial dysfunction is an early indicator of sepsis and neutrophil degranulation of septic shock in surgical patients. *BJS Open.* 2020;4:524-534.
23. Johansen ME, Johansson PI, Ostrowski SR, et al. Profound endothelial damage predicts impending organ failure and death in sepsis. *Semin Thromb Hemost.* 2015;41:16-25.
24. Lin GL, McGinley JP, Drysdale SB, Pollard AJ. Epidemiology and immune pathogenesis of viral sepsis. *Front Immunol.* 2018;9:2147.
25. Zhou Y, Yang Q, Chi J, et al. Comorbidities and the risk of severe or fatal outcomes associated with coronavirus disease 2019: a systematic review and meta-analysis. *Int J Infect Dis.* 2020;99:47-56.
26. Ssentongo P, Ssentongo AE, Heilbrunn ES, Ba DM, Chinchilli VM. Association of cardiovascular disease and 10 other pre-existing comorbidities with COVID-19 mortality: a systematic review and meta-analysis. *PLoS ONE.* 2020;15:e0238215.
27. Bermejo-Martín JF, Martín-Fernandez M, López-Mestanza C, Duque P, Almansa R. Shared features of endothelial dysfunction between sepsis and its preceding risk factors (aging and chronic disease). *J Clin Med.* 2018;7:400.
28. Bermejo-Martín JF, Almansa R, Torres A, González-Rivera M, Kelvin DJ. COVID-19 as a cardiovascular disease: the potential role of chronic endothelial dysfunction. *Cardiovasc Res.* 2020;116:e132-e133.
29. Pons S, Fodil S, Azoulay E, Zafrani L. The vascular endothelium: the cornerstone of organ dysfunction in severe SARS-CoV-2 infection. *Crit Care.* 2020;24:353.
30. Smadjia DM, Guerin CL, Chocron R, et al. Angiopoietin-2 as a marker of endothelial activation is a good predictor factor for intensive care unit admission of COVID-19 patients. *Angiogenesis.* 2020;23:611-620.
31. Pine AB, Meizlish ML, Goshua G, et al. Circulating markers of angiogenesis and endotheliopathy in COVID-19. *Palm Circ.* 2020;10:2045894020966547.
32. Tong M, Jiang Y, Xia D, et al. Elevated expression of serum endothelial cell adhesion molecules in COVID-19 Patients. *J Infect Dis.* 2020;222:894-898.
33. Perico L, Benigni A, Casiraghi F, Ng LFP, Renia L, Remuzzi G. Immunity, endothelial injury and complement-induced coagulopathy in COVID-19. *Nat Rev Nephrol.* 2021;17:46-64.
34. Mojtabavi H, Saghazadeh A, Rezaei N. Interleukin-6 and severe COVID-19: a systematic review and meta-analysis. *Eur Cytokine Netw.* 2020;31:44-49.
35. Palogiannis P, Mangoni AA, Dettori P, Nasrallah GK, Pintus G, Zinelli A. D-dimer concentrations and COVID-19 severity: a systematic review and meta-analysis. *Front Public Health.* 2020;4(8):432.
36. Cheng L, Li H, Li L, et al. Ferritin in the coronavirus disease 2019 (COVID-19): a systematic review and meta-analysis. *J Clin Lab Anal.* 2020;34:e23618.
37. Baldirà J, Ruiz-Rodríguez JC, Wilson DC, et al. Biomarkers and clinical scores to aid the identification of disease severity and intensive care requirement following activation of an in-hospital sepsis code. *Ann Intensive Care.* 2020;10:7.
38. Elke G, Bloos F, Wilson DC, et al. The use of mid-regional proadrenomedullin to identify disease severity and treatment response to sepsis-a secondary analysis of a large randomised controlled trial. Critical care trials group. *Crit Care.* 2018;22:79.
39. Saeed K, Wilson DC, Bloos F, et al. The early identification of disease progression in patients with suspected infection presenting to the emergency department: a multi-centre derivation and validation study. *Crit Care.* 2019;23:40.
40. Spoto S, Agrò FE, Sambuco F, et al. High value of Mid-regional proAdrenomedullin in COVID-19: a marker of widespread endothelial damage, disease severity and mortality. *J Med Virol.* 2020. <https://doi.org/10.1002/jmv.26676>
41. Andaluz-Ojeda D, Cicuéndez R, Calvo D, et al. Sustained value of proadrenomedullin as mortality predictor in severe sepsis. *J Infect.* 2015;71:136-139.
42. Chapman AR, Bularca A, Mills NL. High-sensitivity cardiac troponin can be an ally in the fight against COVID-19. *Circulation.* 2020;141:1733-1735.

How to cite this article: García de Guadiana-Romualdo L, Calvo Nieves MD, Rodríguez Mulero MD, et al. MR-proADM as marker of endotheliitis predicts COVID-19 severity. *Eur J Clin Invest.* 2021;51:e13511. <https://doi.org/10.1111/eci.13511>

A time-resolved proteomic and prognostic map of COVID-19

Graphical abstract



Authors

Vadim Demichev, Pinkus Tober-Lau, Oliver Lemke, ..., PA-COVID-19 Study group, Markus Ralser, Florian Kurth

Correspondence

markus.ralser@charite.de

In brief

Demichev, Tober-Lau et al., present a time-resolved molecular map of the COVID-19, measuring plasma proteomes of patients with COVID-19 along with an extensive panel of clinical diagnostic parameters at 687-time points. They describe the specificity and dynamics, as well as the predictive and prognostic power of the molecular signatures in COVID-19.

Highlights

- Plasma proteomes combined with clinical parameters characterize COVID-19 progression
- Machine learning models allow highly precise prediction of the disease phenotype
- The early molecular host response is predictive of COVID-19 progression
- The molecular response to COVID-19 is age specific

Article

A time-resolved proteomic and prognostic map of COVID-19

Vadim Demichev,^{1,2,3,27} Pinkus Tober-Lau,^{4,27} Oliver Lemke,¹ Tatiana Nazarenko,^{8,11} Charlotte Thibeault,⁴ Harry Whitwell,^{9,10,26} Annika Röhl,¹ Anja Freiwald,¹ Lukasz Szyrwielski,² Daniela Ludwig,¹ Clara Correia-Melo,² Simran Kaur Aulakh,² Elisa T. Helbig,⁴ Paula Stubbemann,⁴ Lena J. Lippert,⁴ Nana-Maria Grüning,¹ Oleg Blyuss,^{10,12,13} Spyros Vernardis,² Matthew White,² Christoph B. Messner,^{1,2} Michael Joannidis,²⁵ Thomas Sonnweber,¹⁹ Sebastian J. Klein,²⁵ Alex Pizzini,¹⁹ Yvonne Wohlfarter,²¹ Sabina Sahanic,¹⁹ Richard Hilbe,¹⁹ Benedikt Schaefer,²⁰ Sonja Wagner,²⁰ Mirja Mittermaier,^{4,22} Felix Machleidt,⁴ Carmen Garcia,⁴ Christoph Ruwwe-Glösenkamp,⁴

(Author list continued on next page)

¹Charité Universitätsmedizin Berlin, Department of Biochemistry, 10117 Berlin, Germany

²The Francis Crick Institute, Molecular Biology of Metabolism Laboratory, London NW11AT, UK

³The University of Cambridge, Department of Biochemistry and Cambridge Centre for Proteomics, Cambridge CB21GA, UK

⁴Charité Universitätsmedizin Berlin, Department of Infectious Diseases and Respiratory Medicine, 10117 Berlin, Germany

⁵Charité Universitätsmedizin Berlin, Medical Department of Hematology, Oncology & Tumor Immunology, Virchow Campus & Molekulare Krebsforschungszentrum, 13353 Berlin, Germany

⁶Charité Universitätsmedizin Berlin, Department of Nephrology and Internal Intensive Care Medicine, 10117 Berlin, Germany

⁷Bernhard Nocht Institute for Tropical Medicine, Department of Tropical Medicine, and University Medical Center Hamburg-Eppendorf, Department of Medicine, 20359 Hamburg, Germany

⁸University College London, Department of Mathematics, London WC1E 6BT, UK

⁹National Phenome Centre and Imperial Clinical Phenotyping Centre, Department of Metabolism, Digestion and Reproduction, Imperial College London, London SW72AZ, UK

¹⁰Lobachevsky University, Department of Applied Mathematics, Nizhny Novgorod 603105, Russia

¹¹University College London, Department of Women's Cancer, EGA Institute for Women'S Health, London WC1E 6BT, UK

¹²University of Hertfordshire, School of Physics, Astronomy and Mathematics, Hatfield AL10 9AB, UK

¹³Sechenov First Moscow State Medical University, Department of Paediatrics and Paediatric Infectious Diseases, Moscow 119435, Russia

¹⁴Lobachevsky University, Laboratory of Systems Medicine of Healthy Ageing, Nizhny Novgorod 603105, Russia

¹⁵Chalmers Tekniska Högskola, Department of Biology and Biological Engineering, SE-412 96 Gothenburg, Sweden

¹⁶University of Edinburgh, Centre for Genomic and Experimental Medicine, Institute of Genetics and Cancer, Edinburgh EH4 2XU, UK

¹⁷University of Edinburgh, Usher Institute, Edinburgh EH16 4UX, UK

¹⁸University of Edinburgh, MRC Human Genetics Unit, Institute of Genetics and Cancer, Edinburgh EH4 2XU, UK

(Affiliations continued on next page)

SUMMARY

COVID-19 is highly variable in its clinical presentation, ranging from asymptomatic infection to severe organ damage and death. We characterized the time-dependent progression of the disease in 139 COVID-19 inpatients by measuring 86 accredited diagnostic parameters, such as blood cell counts and enzyme activities, as well as untargeted plasma proteomes at 687 sampling points. We report an initial spike in a systemic inflammatory response, which is gradually alleviated and followed by a protein signature indicative of tissue repair, metabolic reconstitution, and immunomodulation. We identify prognostic marker signatures for devising risk-adapted treatment strategies and use machine learning to classify therapeutic needs. We show that the machine learning models based on the proteome are transferable to an independent cohort. Our study presents a map linking routinely used clinical diagnostic parameters to plasma proteomes and their dynamics in an infectious disease.

INTRODUCTION

The coronavirus disease 2019 (COVID-19) has created unprecedented societal challenges, particularly for public health and the global economy (Alwan et al., 2020; Blumenthal et al., 2020; Rosenbaum, 2020). Efficient management of these challenges is hampered by the variability of clinical manifestations, ranging

from asymptomatic infection with severe acute respiratory syndrome coronavirus-2 (SARS-CoV-2) to death, despite maximum intensive care. Biomarkers and molecular signatures enabling accurate prognosis of future disease courses are needed to optimize resource allocation and personalize treatment strategies. Patients likely to progress to severe disease and organ failure and those likely to remain stable could be identified early, which

Tilman Lingscheid,⁴ Laure Bosquillon de Jarcy,⁴ Miriam S. Stegemann,⁴ Moritz Pfeiffer,⁴ Linda Jürgens,⁴ Sophy Denker,^{5,22} Daniel Zickler,⁶ Philipp Enghard,⁶ Aleksej Zelezniak,^{2,15} Archie Campbell,^{16,17} Caroline Hayward,¹⁸ David J. Porteous,^{16,17} Riccardo E. Marioni,¹⁶ Alexander Uhrig,⁴ Holger Müller-Redetzky,⁴ Heinz Zoller,²⁰ Judith Löffler-Ragg,¹⁹ Markus A. Keller,²¹ Ivan Tancevski,¹⁹ John F. Timms,¹¹ Alexey Zaikin,^{8,11,14} Stefan Hippenstiel,^{4,24} Michael Ramharter,⁷ Martin Witzenrath,^{4,24} Norbert Suttorp,^{4,24} Kathryn Lilley,³ Michael Mülleider,²³ Leif Erik Sander,^{4,24} PA-COVID-19 Study group, Markus Ralser,^{1,2,28,*} and Florian Kurth^{4,7}

¹⁹Medical University of Innsbruck, Department of Internal Medicine II, 6020 Innsbruck, Austria

²⁰Medical University of Innsbruck, Christian Doppler Laboratory for Iron and Phosphate Biology, Department of Internal Medicine I, 6020 Innsbruck, Austria

²¹Medical University of Innsbruck, Institute of Human Genetics, 6020 Innsbruck, Austria

²²Berlin Institute of Health, 10178 Berlin, Germany

²³Charité – Universitätsmedizin Berlin, Core Facility - High-Throughput Mass Spectrometry, 10117 Berlin, Germany

²⁴German Centre for Lung Research, 35392 Gießen, Germany

²⁵Medical University Innsbruck, Division of Intensive Care and Emergency Medicine, Department of Internal Medicine, 6020 Innsbruck, Austria

²⁶Imperial College London, Section of Bioanalytical Chemistry, Division of Systems Medicine, Department of Metabolism, Digestion and Reproduction, London SW7 2AZ, UK

²⁷These authors contributed equally

²⁸Lead contact

*Correspondence: markus.ralser@charite.de

<https://doi.org/10.1016/j.cels.2021.05.005>

is particularly valuable in scenarios where health care systems reach capacity limits. Prognostic panels would also optimize the monitoring of novel treatments, thereby accelerating clinical trials (Phua et al., 2020; Saxena, 2020; Wu et al., 2020). Knowledge of factors that differentiate recovery from deterioration throughout the disease will further enhance our understanding of the inflammatory host response as well as the underlying pathophysiology and provide new therapeutic targets.

A number of biomarkers that classify COVID-19 severity have recently been described. These are based on clinical chemistry, enzyme activities, immune profiling, single-cell sequencing, proteomics, and metabolomics (D'Alessandro et al., 2020; Laing et al., 2020; Liu et al., 2020b; Messner et al., 2020; Overmyer et al., 2020; Schulte-Schrepping et al., 2020; Shen et al., 2020; Shu et al., 2020; Wynants et al., 2020). As severity classifiers, the molecular signatures recorded in blood, serum, plasma, or immune cells characterize the COVID-19 pathology and host responses. Furthermore, markers of dysregulated coagulation, inflammation, and other organ dysfunction have been established as risk factors for severe illness, including low platelet count, elevated levels of D-dimer, C-reactive protein (CRP), interleukin 6 (IL-6), ferritin, troponin, and markers of kidney injury (Danwang et al., 2020; Henry et al., 2020). Proteomic investigations that characterize the comprehensive host response have revealed the activation of the complement cascade and acute phase response, both of which center around IL-6-driven pathways. In turn, these systematic studies have revealed that other common antiviral pathways, such as type I interferons (IFN), do not dominate the early response to COVID-19, probably reflecting evasion of the IFN system by SARS-CoV-2 and the subsequent activation of inflammatory cascades (Hadjadj et al., 2020; Yang et al., 2020). Furthermore, proteomic data and diagnostic parameters have pointed to underlying pathological mechanisms and possible therapeutic targets. For instance, using high-throughput proteomics, we reported a decline in plasma levels of gelsolin (GSN) in patients with severe COVID-19 in a previous study (Messner et al., 2020), and recombinant human

GSN is currently undergoing clinical testing for COVID-19 pneumonia in a phase II trial ([ClinicalTrials.gov](#) identifier: NCT04358406).

The severity of the disease, and the biomarker signatures that indicate severity, correlate with the outcome, but the highest diagnostic need is to stratify within therapeutically homogeneous patients. For instance, to identify those among the mildly affected individuals with the highest risk for deterioration, or among the most severely affected, those with the highest chance to respond positively to an augmentation of therapy. Predicting future trajectories on an individualized basis would also help accelerate therapeutic developments to judge the impact of the treatment on an individual disease course. To obtain a comprehensive picture of how the molecular COVID-19 phenotype develops over time, we deeply phenotyped a group of 139 COVID-19 inpatients at 687 sampling points. On the one hand, we measured a compendium of 86 clinical parameters, routine diagnostic markers, and clinically established risk scores using gold standard accredited clinical tests. On the other hand, we captured the patient's molecular phenotype by measuring plasma proteomes in an untargeted fashion. For this, we made use of liquid chromatography coupled with tandem mass spectrometry, using a recently developed platform technology that utilizes analytical flow rate chromatography, data-independent acquisition mass spectrometry (SWATH-MS), and deep-neural network-based data processing (Demichev et al., 2020; Messner et al., 2020) (Figure S1). By combining the compendium of diagnostic parameters with the proteomes in a time- and patient-resolved fashion, we obtained a comprehensive molecular picture that captures changes in the patient's molecular phenotype as they depend on the severity, age, and disease progression. We identify prognostic biomarkers and depict their distinct trajectories. We exemplify the power of our resource by showing that the biomarker profiles and diagnostic parameters classify treatment requirements, in particular, the need for mechanical ventilation. Furthermore, we report the future prediction of recovery time in mildly ill patients as well as the individual risk of

clinical deterioration. Our study demonstrates the predictability of COVID-19 disease trajectories based on the molecular phenotype of the early disease stage.

RESULTS

Covariation of clinical diagnostic parameters and the plasma proteome characterizes the host response to COVID-19

We longitudinally phenotyped 139 patients admitted to Charité University Hospital, Berlin, Germany, between March 01, 2020, and June 30, 2020, due to PCR-confirmed SARS-CoV-2 infection (Figure S2). The patients exhibited highly variable disease courses, graded according to the World Health Organization (WHO) ordinal scale for clinical improvement (Table S1), which reflects the treatment that the patient is receiving as a measure of disease severity. The patients included in our study range from WHO grade 3, which includes patients who require inpatient care without supplemental oxygen therapy, to WHO grade 7, which includes patients with severe COVID-19 who require invasive mechanical ventilation and additional organ support therapies such as renal replacement therapy (RRT) and extracorporeal membrane oxygenation (ECMO) (WHO, 2020). In total, 23 out of 139 (17%) patients in the WHO grade 3 category were stable, without requiring supplemental oxygen therapy and could be discharged after a median of 7 days of inpatient care (Table S2 and Figure S2); 47 (34%) patients required either low-flow or high-flow supplemental oxygen therapy; 69 (50%) patients either presented with severe COVID-19 (WHO grade 6 or 7, i.e., requiring invasive mechanical ventilation) or deteriorated and required invasive mechanical ventilation during their hospitalization; 46 patients (33%) required RRT; and 22 (16%) were treated with ECMO. A total of 20 (13%) patients died, including three patients with *do not intubate/do not resuscitate* (DNI/DNR) orders in place and one patient who died due to a non-COVID-19-related cause. Common risk factors for severe COVID-19 were reflected in the outcomes: patients with a severe course of disease were older than those with mild disease (49 years [IQR 35–70] for WHO grade 3 versus 62 years [IQR 53–72] for WHO grade 7, $p = 0.02$), and an age of 65 years or older was associated with a higher risk of death ($-OR\ 4.1$ [95% CI 1.5–11.5]). Our cohort further reflected that men and individuals with a high BMI have an increased likelihood to be hospitalized upon a COVID-19 infection; 68% of the patients were men, and the median BMI was 27.8 (IQR 24.7–31.9). However, we noted that within the group of patients hospitalized with COVID-19, sex and BMI were not further associated with disease severity or an increased risk of death. The median duration of hospitalization was 20 days (IQR 9–48) and correlated with severity (7 days for WHO grade 3 versus 46 days for WHO grade 7). The median time from admission to death despite receiving maximum treatment was 28 days (IQR 16–46).

To capture the diverse disease trajectories on a molecular and biochemical level, we systematically collected 86 clinical and accredited diagnostic parameters as measured with certified tests. Moreover, we monitored the development of risk scores such as the “sequential organ failure assessment” (SOFA) score, blood gas analyses, blood cell counts, enzyme activities, and inflammation biomarkers (Table S3). To complement these parameters

with an untargeted analysis, we employed a recently developed high-throughput proteomics platform (Messner et al., 2020). This platform makes use of the data-independent acquisition technique SWATH-MS (Gillet et al., 2012), a sample preparation pipeline designed to ISO13485 reporting standards, which is optimized for reducing batch effects, high-flow rate chromatography to provide highly consistent peptide separation in large sample series, and uses DIA-NN (Data-Independent Acquisition by Neural Networks) to analyze proteomics data recorded with 5-min chromatography (Messner et al., 2020; Demichev et al., 2020) (Figure S1 for a detailed overview of the proteomic workflow). In total, we measured 1,169 plasma proteome samples to determine 687 human proteomes, in which we quantified 321 plasma protein groups. Owing to the nature of the high-flow proteomics platform, data completeness was high; thus, we decided against the use of imputation strategies in the analysis of differential protein abundance. Total data completeness was 75%, with 200 proteins consistently quantified with 98% completeness, and 189 proteins with 99% completeness (Figure S1).

To identify interdependencies of the diagnostic parameters that are routinely used in clinical decision making and the plasma proteomes, we characterized their covariation and present a direct correlation map (Figures 1B and S3–S4; Tables S4, S5, and S6). We report a robust positive or negative correlation of IL-6 levels and other inflammatory markers (CRP, procalcitonin) with acute phase proteins (APPs) (APOA2, APOE, CD14, CRP, GSN, ITIH3, ITIH4, LYZ, SAA1, SAA2, SERPINA1, SERPINA3, and AHSG; the protein names corresponding to the gene identifiers are provided in Table S3), coagulation factors and related proteins (FGA, FGB, FGG, F2, F12, KLKB1, PLG, and SERPINC1), and the complement system (C1R, C1S, C8A, C9, CFB, CFD, and CFHR5). Our data, therefore, link the prominent role of the IL-6 response in COVID-19 (D'Alessandro et al., 2020) to coagulation and the complement cascade. Consistently, in our data, markers of cardiac (troponin T, NT-proBNP) and renal (creatinine, urea) function, as well as anemia and dyserythropoiesis (hemoglobin, hematocrit, erythrocytes, and red blood cell distribution width) correlate with various APPs (APOA2, APOE, CD14, GSN, LYZ, SAA1, SAA2, and SERPINA3; Figure 1B and Table S4) supporting the role of inflammation in COVID-19-related organ damage and its impact on erythropoiesis.

Increased levels of neutrophils and the occurrence of immature granulocyte precursors as markers of emergency myelopoiesis have been linked to severe COVID-19 (Schulte-Schrepping et al., 2020). Our data reveal covariation between neutrophil counts and the levels of two inhibitors of neutrophil serine proteases, SERPINA1 and SERPINA3 (Figure 1C). These two proteins show the highest correlation (0.72 and 0.79 Spearman R, respectively) with the neutrophil-to-lymphocyte ratio (NLR), a prognostic marker for COVID-19 (Lian et al., 2020; Liu et al., 2020a). We further report a strong correlation (Figure 1C) of alkaline phosphatase and gamma-glutamyl transferase activities, both characteristic of biliary disorders (Poynard and Imbert-Bismut, 2012), with plasma levels of the polymeric immunoglobulin receptor (PIGR). We notice that cholangiocytes (bile duct epithelium cells) express ACE-2 and can be directly infected with SARS-CoV-2 (Zhao et al., 2020), potentially leading to host viral

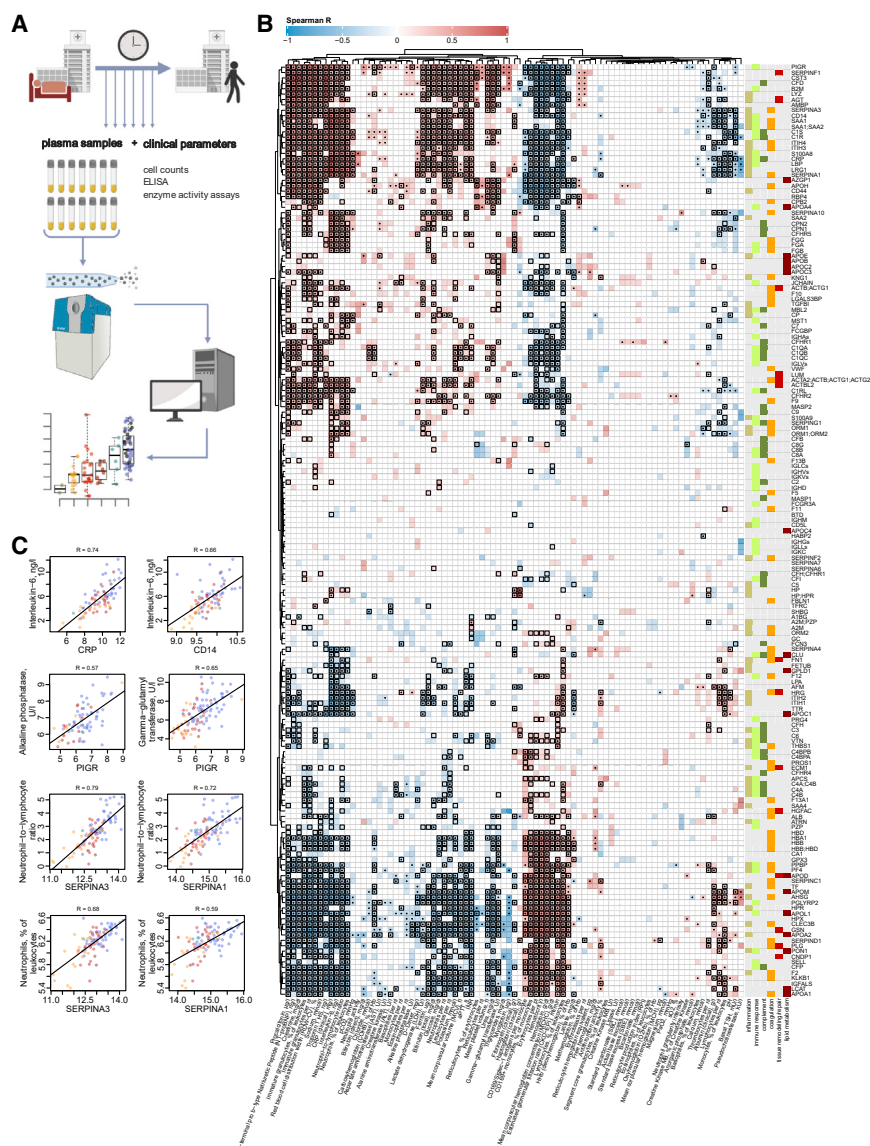


Figure 1. Interdependence of clinical, diagnostic, physiological and proteomic parameters during the clinical progression of COVID-19

(A) Study design. Schematic of the cohort of 139 patients with PCR-confirmed SARS-CoV-2 infection treated at Charité University Hospital Berlin. Plasma proteomics and accredited diagnostic tests were applied at 687 sampling points to generate high-resolution time series data for 86 routine diagnostic parameters and 321 protein quantities (see also Figures S1 and S2).

(B) Covariation map for plasma proteins and routine diagnostic and physiological parameters. Statistically significant correlations (Spearman; $p < 0.05$) are colored. Dots indicate statistical significance after row-wise multiple-testing correction (false discovery rate [FDR] < 0.05), black rectangles—column-wise. The panel on the right of the heatmap provides manual functional annotation for the proteins (see also Figures S3 and S4, and Tables S4, S5, and S6).

(C) Covariation of key diagnostic parameters and plasma protein markers (\log_2 -transformed) in COVID-19 (see also Tables S4, S5, and S6). Dots colors correspond to the WHO grade of the patient, see Figure 2B.

response-induced expression of PIGR and cell destruction (Schneeman et al., 2005; Turula and Wobus, 2018).

A map of plasma proteins and diagnostic parameters that depend on age and disease severity

113 proteins and 55 accredited diagnostic parameters responded in accordance to an increase in the WHO score as a measure of progressing COVID-19 severity (Figures 2, S5, and S6; STAR methods). To the best of our knowledge, more than 30 of these proteins have not been associated with COVID-19 severity previously (Table S3). The proteins that change dependent on disease severity include mediators of inflammation and immune response (CD44, B2M, PIGR, and A2M), components of the complement cascade (CFD, and CFHRs), and apolipoproteins (APOA2, APOC3, APOD, APOE, and APOL1). Furthermore, numerous markers of organ dysfunction (cardiac: NT-proBNP, troponin T; renal: creatinine,

urea; liver: aspartate aminotransferase, alanine aminotransferase, gamma-glutamyl transferase, and total bilirubin) and, inversely, markers of anemia (hemoglobin, erythrocytes, and hematocrit) were correlated with the WHO grade of the patient. In order to further dissect the proteomic signatures of the most severely ill patients requiring maximum treatment (WHO grade 7), we specifically characterized the impact of organ support treatments (RRT and ECMO) on the patients' molecular phenotype (Figures S7 and S8). We showed, for instance, that HP and HPX are reduced

in patients on RRT and ECMO as a sign of hemolysis in the extracorporeal circuit, whereas elevated SERPINC1 levels mirror substitution of antithrombin during ECMO. We discuss these findings in Note S1.

A total of 61 proteins and 18 diagnostic parameters varied with patients' age (Figure S9). Out of these, 37 proteins do not change with age in a pre-COVID-19 general population baseline (Generation Scotland cohort [Smith et al., 2006]), for which proteomes have been measured with the same proteomic technology (Messner et al., 2020) (Figure S10). We observed that a number of markers that increase with age in COVID-19 patients also correlated with a high WHO grade (Figures S6 and S9). To identify markers that are upregulated or downregulated in older patients in comparison with younger patients with a comparable therapy need, i.e. WHO grade, we tested the relationship between omics feature levels and age by accounting for WHO severity grade as a covariate using linear modeling

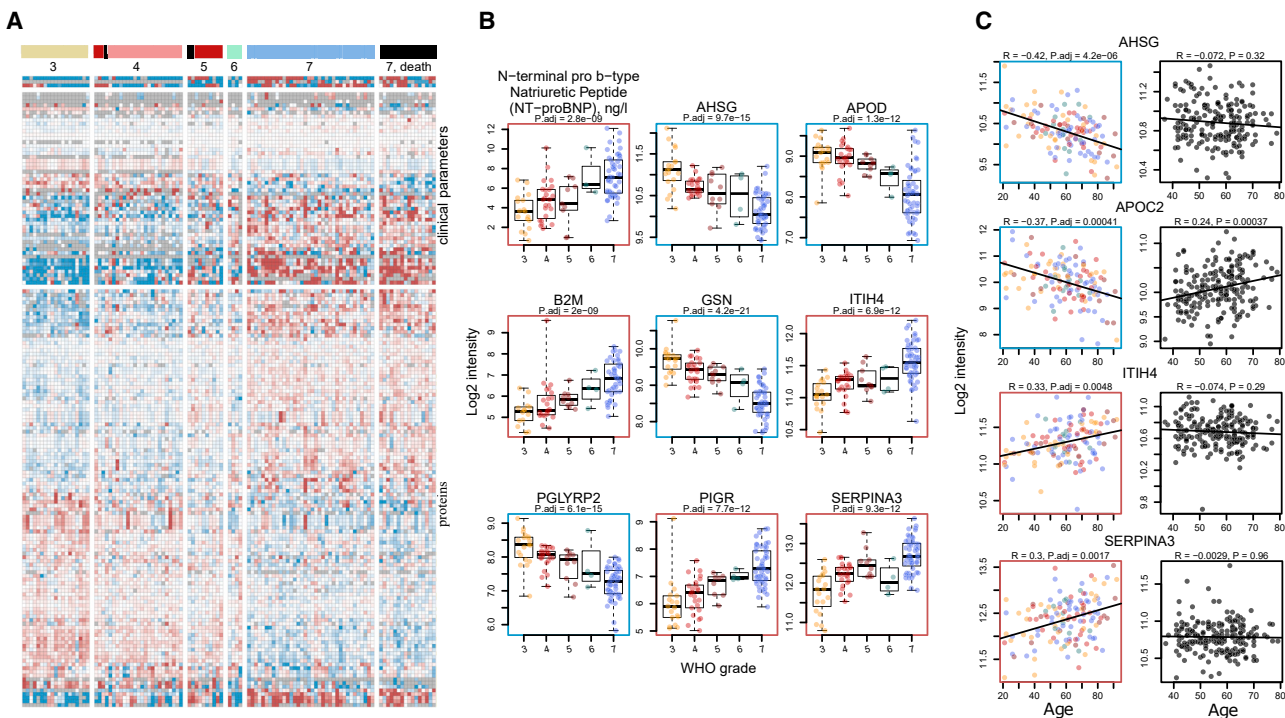


Figure 2. The molecular phenotype of patients with COVID-19 and its dependency on severity and age

(A) Plasma proteome and clinical diagnostic parameters in dependency of COVID-19 severity irrespective of age. The patients are grouped according to the maximum clinical treatment received (WHO ordinal scale), used as an indicator of disease severity (Table S1). 113 proteins and 55 routine diagnostic parameters vary significantly ($FDR < 0.05$) between patients of the different WHO groups upon accounting for age as a covariate using linear modeling (Ritchie et al., 2015). A fully annotated heatmap is provided in Figure S5 (see also Figure S6 and Table S3).

(B) Selected protein markers and routine diagnostic parameters (\log_2 -transformed) plotted against the WHO ordinal scale.

(C) Selected proteins differentially abundant depending on age ($FDR < 0.05$). Left, colored: this data set (\log_2 -transformed levels; statistical testing was performed by accounting for the WHO grade as a covariate Ritchie et al., 2015 and STAR methods; for visualization only, the data were corrected for the WHO grade); right, black: general population (\log_2 -transformed levels; Generation Scotland cohort).

(Ritchie et al., 2015) (STAR methods). This analysis identified 36 proteins and 12 clinical laboratory markers that are up- or are downregulated with age in COVID-19 patients within the same level of care, i.e., one WHO grade (Figures 2C and S11, summarized in Figure 5). Out of these, 20 proteins do not change with age in the pre-COVID-19 population baseline (Generation Scotland cohort proteome data, Messner et al., 2020; Figure S10), or show the opposite correlation with age in the general population (e.g., APOC2, Figure 2C). These proteins that only show an age-dependency in COVID-19 patients but not in the general population point toward age-dependent differences in host response patterns to SARS-CoV-2, and include markers involved in inflammation (SERPINA3, ITIH4, SAA1, SAA1, SAA2, ITIH3, CFB, C7, and AHSG), lipid metabolism (APOC1, APOC2, APOC3, APOB, and APOD), and coagulation (KLKB1, and FBLN1). We consider the implications of these findings in Note S2.

Time-dependent alleviation of severity indicators highlights the role of the early host response in COVID-19 progression

The time-resolved nature of our study facilitated a covariation analysis of protein levels and accredited diagnostic parameters along the patient trajectory over time (Figure S12; Table S7). Correlating the dynamics of omics features during the peak

period of the disease (STAR methods), we noted covariation of inflammatory markers, APPs, fibrinogen precursor proteins, and the NLR. The correlation between APPs and the markers of cardiac and renal impairment observed across different patients at the earliest time points (Figure 1B; Table S4) was not reflected as a trend over time (Figure S13).

To further dissect the dynamics of the patients' molecular phenotype during the course of COVID-19, we determined the longitudinal trend for all protein and diagnostic parameters during the peak period of the disease (i.e., while receiving maximum treatment; STAR methods). In total, 89 proteins and 37 clinical parameters significantly changed over time (Figure 3B, trends across all time points at the maximum WHO grade are provided in Figure S14; STAR methods). In general, we found that most proteins and diagnostic parameters that correlate with disease severity return toward baseline during the peak period of the disease. Many of these were most prominently changed in the early samples (Figure S6) but alleviated with time, irrespective of the outcome (Figure S14; summarized in Figure 5). For example, components of the coagulation cascade with known acute phase activity, such as fibrinogen, and many complement factors, significantly decreased over time. Proteins indicative of inflammatory response (e.g., ORM1, SERPINA1 and SERPINA3, SAA1, SAA2 [Luo et al., 2015; Sack, 2018; Wu et al., 2015]) and markers of inflammation,

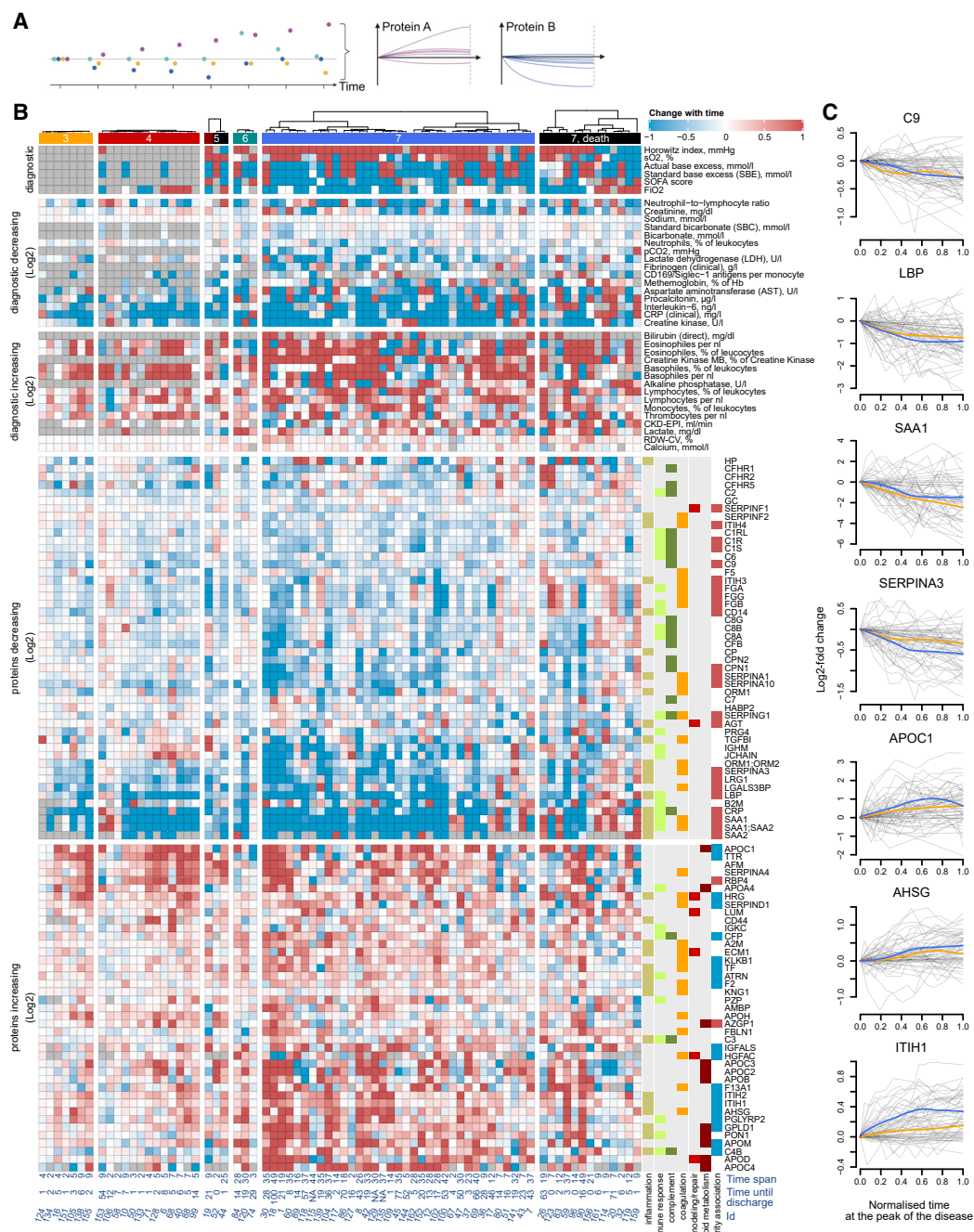


Figure 3. The progression of the COVID-19 molecular patient phenotype over time

(A) Schematic: each patient is followed during inpatient care by repetitive sampling, and the “trajectory” of each of the proteins and the routine diagnostic features is analyzed (points of different colors at each time point) (see also [Figure S2](#)).

(B) Protein levels and routine diagnostic parameters that change significantly ($FDR < 0.05$) over time during the peak of the disease, shown for individual patients stratified by their maximum treatment received (WHO grade): 89 proteins, 37 clinical diagnostic markers show time dependency during the disease course (illustrated as \log_2 -fold changes or absolute value changes, as indicated). The panel to the right of the heatmap provides manual functional annotation for the proteins. Known associations with COVID-19 severity are indicated (blue - downregulated in severe COVID-19, and red - upregulated) (D’Alessandro et al., 2020; Laing et al., 2020; Messner et al., 2020; Shen et al., 2020). Below the heatmap, the time span between the first and the last sampling time point at the peak of the disease is indicated as well as the remaining time until the discharge (see also [Figures S14](#) and [S15](#), and [Table S3](#)).

(C) Trajectories (change of \log_2 -transformed levels with time) for selected proteins. Sampling points during the peak period of the disease ([STAR methods](#)) are considered. x axis: 0 – first time point measured at the peak of the disease, 1 – last. The y axis reflects the change relative to the first valid measurement during the peak of the disease. Loess approximations are shown for patients, which did (blue), and did not (orange), require invasive mechanical ventilation. See also [Figure S16](#).

such as CRP or IL-6, also declined over time. Conversely, extracellular matrix (ECM) proteins, such as ECM1, LUM, and immunoregulatory factors (e.g. AHSG, A2M [Rehman et al., 2013](#), and HRG [Wakabayashi, 2013](#)) and proteins involved in lipid metabolism (e.g., APOC1, APOD, APOM, GPLD1, and PON1), and negative APPs (e.g., ITIH1, [Figure 3C](#)), which are downregulated in severe COVID-19 ([Figure S6](#), summarized in [Figure 5](#)), increased over time, approaching the baseline. This general alleviation of the initial molecular phenotype of COVID-19 was consistently detected in both mildly and severely ill patients (outlier trajectories discussed in Note S3). Indeed, only 13 proteins showed differences in trend depending on the WHO score ([Figure S15](#)). We provide visualization of individual trajectories for all omics features measured between the first and the last time points sampled at the peak of the disease ([Figures 3C and S16](#)).

Overall, the molecular patient phenotype reflected an initial spike in the systemic inflammatory response, which alleviated gradually, followed by a protein signature indicative of tissue repair, metabolic reconstitution, and immunomodulation. This was observed in both mildly and severely ill patients, highlighting the early disease phase as a major molecular determinant of the COVID-19 phenotype.

Proteomes and diagnostic clinical markers allow for prediction of disease severity by machine learning

Using a machine learning algorithm based on gradient boosted trees ([STAR methods](#)), we first evaluated the extent to which diagnostic parameters and proteomes characterize treatment requirements, as reflected by the WHO grade. Both proteomes and clinical diagnostic parameters were highly discriminative of the patient receiving invasive mechanical ventilation (WHO grade 6 or 7, clinical laboratory values AUROC = 0.97, proteomic data AUROC = 0.98, combined data AUROC = 0.99; [Figure 4C](#)). The machine learning models significantly outperformed the predictive scores derived from established COVID-19 risk factors such as age, BMI, Charlson comorbidity index (CCI), or molecular predictors such as CRP or IL-6 levels ([Figure 4C](#)). In order to assess the transferability of the proteomic predictors, we tested our model in an independent cohort of 99 hospitalized patients with COVID-19 from another hospital in a different healthcare system (Innsbruck cohort, [STAR methods](#)). The proteomic model trained on the main Charité cohort demonstrated a comparably high patient stratification performance when applied to this validation cohort ([Figure 4D](#); AUROC = 0.97). Scores reflecting the contribution of individual proteins and clinical parameters to the machine learning model are provided in [Table S3](#). Of note, we were able to establish machine learning models that not merely classified patients based on severity but were able to predict the current WHO severity grade from the proteome, from clinical measurements, and both ([Figure 4E](#)). Again, combined proteomic and clinical laboratory data performed best.

Having observed clear time trajectories for many proteins and diagnostic parameters, we hypothesized that the molecular signature of the initial host response can be exploited for the prediction of the future disease course. We started by investigating the potential of using the levels of proteins and diagnostic parameters for prediction of future clinical worsening, defined as progression to a higher severity grade on the WHO scale, i.e., a requirement for

supplemental low-flow oxygen therapy, high-flow oxygen therapy, or invasive mechanical ventilation. Upon using a linear model to account for current therapy (WHO grade) and age as covariates, 11 proteins and 9 clinical laboratory markers were identified as predictors of future worsening of the clinical condition, across all treatment groups ([STAR methods](#)) ([Figures 4A and S17; Box 1](#)). Increased or decreased plasma levels of these proteins functioning in inflammation (CRP, ITIH2, SERPINA3, AHSG, and B2M), coagulation (HRG, and PLG), and complement activation (C1R, and CFD), as well as levels of AGT and CST3, were predictive of future clinical deterioration.

Next, we investigated the predictability of the remaining time needed in the hospital for mildly ill patients with maximum WHO grade 3. We identified 26 protein biomarkers and 14 routine diagnostic markers ([Figures 4B and S18](#)) that correlate with the time between the first sampling point and discharge from inpatient care. The proteomic signature associated with a longer need for inpatient treatment is characterized by proteins of the complement system (C1QA, C1QB, and C1QC) and reflects altered coagulation (KLKB1, PLG, and SERPIND1) and inflammation (CD14, B2M, SERPINA3, CRP, GPLD1, PGLYRP2, and AHSG). As most of these proteins are also predictors of the required treatment ([Figure S6; Table S3](#)), we hypothesized that the time of inpatient care for mild (WHO grade 3) cases correlates with the severity of the disease in these patients. To test this hypothesis, we generated machine learning models for WHO grade prediction, similar to those shown in [Figure 4E](#), but trained the model only on the first time point data measured for each patient (to avoid using any future information with respect to that time point). We observed that the predictions derived from the first time point data correlated with the remaining time in the hospital ([Figure 4F](#)). We conclude that machine learning allows us to finely distinguish between more and less severe patients within a single treatment group, i.e. WHO grade.

DISCUSSION

Upfront clinical decision making is essential for optimum treatment allocation to patients as well as for efficient resource management within the hospital. For instance, early referral to intensive care treatment units has been shown to improve prognosis and outcome for patients with severe COVID-19 ([Sun et al., 2020](#)). One of the peculiarities of COVID-19 is that the examinable clinical conditions of patients often do not reflect the true severity of the disease, e.g., with respect to respiratory insufficiency. In contrast to patients with severe bacterial pneumonia, patients with COVID-19 often clinically appear to be only slightly affected, despite being in severe respiratory failure, a phenomenon termed “happy hypoxemia” ([Stawicki et al., 2020](#)). Clinical decisions therefore need to be supported by objective, molecular diagnostics. These diagnostic analyses help further in the monitoring of therapies and clinical trials as they allow for determining the extent to which a given patient has deviated from the disease trajectory that would be achieved without therapy.

Several recent investigations have identified protein biomarkers and clinical parameters that classify patients with COVID-19 according to disease severity and/or received treatment ([D'Alessandro et al., 2020](#); [Laing et al., 2020](#); [Liu et al., 2020b](#); [Messner et al., 2020](#); [Overmyer et al., 2020](#); [Schulte-Schrepping et al., 2020](#); [Shen et al., 2020](#); [Shu et al., 2020](#);

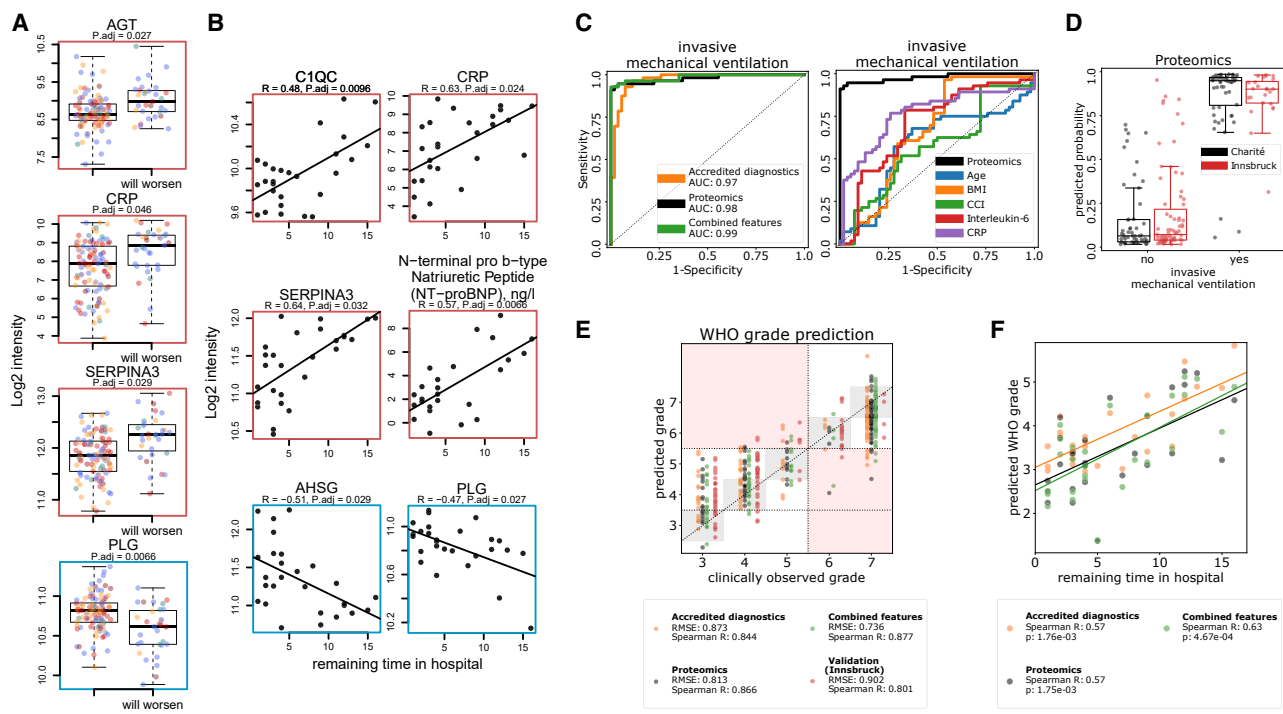


Figure 4. Predicting COVID-19 treatment requirement and future disease progression from the early molecular phenotype by using machine learning.

(A) Selected proteins that are predictive ($FDR < 0.05$) of the future clinical deterioration of the disease (that is progression to a higher WHO grade in the future; [STAR methods](#)). Illustrated are the \log_2 -transformed levels of the proteins at the first sampling point upon correction (for visualization only) for the impact of the WHO grade and age as covariates ([Ritchie et al., 2015](#)) (see also [Figure S17](#)).

(B) Selected proteins and routine diagnostic parameters predictive ($FDR < 0.05$) of the remaining time in hospital for patients receiving mild treatment (WHO grade 3). Statistical testing was performed by including patient's age as a covariate ([STAR methods](#)). Illustrated are the \log_2 -transformed levels of the proteins (upon correction for age as a covariate, for visualization only) at the first sampling point, plotted against the remaining time in hospital (days) (see also [Figure S18](#)).

(C) Left: performance of a machine learning model characterizing the need for invasive mechanical ventilation, based on either the proteomic data, accredited diagnostic parameters, or both. Right: comparison of the performance of a machine learning model characterising the need for invasive mechanical ventilation based on proteomic data to established prognostic parameters.

(D) Prediction performance, based on the proteome, visualized as boxplots. Cross-validation predictions on the Charité cohort are shown in black, predictions of a model trained on the Charité data and then applied to an independent cohort from another hospital (Innsbruck cohort) are shown in red.

(E) Prediction of the WHO grade itself using machine learning (cross-validated, first time point at the maximum treatment level for each patient is used, [STAR methods](#)), based on either the proteome, clinical diagnostic parameters, or both. The performance of the proteomic model trained on the Charité cohort and applied to the Innsbruck cohort is also shown.

(F) A machine learning model was trained to predict the level of necessary treatment (WHO grade) using the data (proteomics, clinical, or both) from the first time point measured for each patient. Derived predictions for patients who did not receive supplemental oxygen at this time point (WHO = 3) were plotted against the remaining time (days) in hospital for these patients.

[Wynants et al., 2020](#)). In other studies, the potential prognostic value of several established and newly discovered markers for predicting the future course of the disease was investigated, e.g., for IL-6, ferritin, or resistin ([Grifoni et al., 2020](#); [Meizlish et al., 2020](#)). Yet, it remained challenging so far, to put their prognostic value in relation to patient age and current level of care, the two most important apparent characteristics for prognosis in COVID-19. For instance, a patient at WHO grade 5 who requires high-flow oxygen therapy is significantly more likely to progress to mechanical ventilation and subsequently die than an inpatient at WHO grade 3 that does not require oxygen support. Likewise, a 90-year-old patient at WHO grade 3 is significantly more likely to progress to more severe disease and to stay in the hospital for a longer period of time than a 20-year-old patient at the same WHO grade.

To identify (1) which proteomic markers and laboratory parameters correlate with each other by being attributed to a common biological or physiological response, and (2) which markers reflect disease trajectories, we longitudinally phenotyped 139 individuals admitted at Charité University Hospital, Berlin, Germany, between March 01, 2020, and June 30, 2020, due to PCR-confirmed SARS-CoV-2 infection ([Figure S2](#)). We recorded a large panel of 86 parameters with accredited diagnostic tests. These tests capture the compendium of analytical parameters that are available for the clinical routine. In parallel, we record plasma proteomes using a recently developed mass spectrometry platform. This platform introduced the use of analytical (high-flow rate) chromatography to routine proteomics in order to increase throughput and measurement precision to the scale of clinical trials ([Messner et al., 2020](#)). The platform reaches a

Box 1. Proteins predictive of future worsening, i.e., disease progression to higher WHO grade

HIGH LEVELS INDICATIVE OF POOR PROGNOSIS

AGT: Angiotensinogen: Conversion via angiotensin-converting enzymes ACE and ACE2 produces AngI/AngII (pro-inflammatory, vasoconstrictive, pro-fibrotic) and Ang1-7/Ang1-9 (anti-inflammatory, vasodilative, anti-fibrotic), respectively (Turner, 2015; Zhang et al., 2020). Increased AGT likely reflects increased AngI/AngII due to SARS-CoV-2 mediated inactivation of ACE2 (Tay et al., 2020) and subsequently predominant conversion of AGT to AngII. AngII correlates with viral load (Liu et al., 2020c) and has tissue damaging effects (Zhang et al., 2020).

B2M: Beta-2-microglobulin: Component of major histocompatibility complex (MHC I) on all nucleated cells and platelets. Released abundantly by activated platelets leading to pro-inflammatory M1-like macrophage polarization (Hilt et al., 2019). Increase of B2M has been associated with death in patients with chronic kidney disease (Makridakis et al., 2020).

C1R: Complement C1r: Initiator of the classical complement pathway (Hajishengallis et al., 2017).

CFD: Complement Factor D: Initiator of the alternative complement pathway by cleaving Factor B (CFB) to form the C3bBb alternative pathway convertase (Volanakis and Narayana, 1996).

CRP: C-reactive protein: Acute phase protein, strongly upregulated in inflammation and infection, including COVID-19.

CST3: Cystatin C: Biomarker of kidney function (Peralta et al., 2011).

SERPINA3: Alpha-1-antichymotrypsin: Protease inhibitor of neutrophil cathepsin G (Benarafa, 2015). When cleaved at reactive site loop, it becomes stable to degradation and becomes a strong neutrophil chemoattractant (Banda et al., 1988; Potempa et al., 1991)

LOW LEVELS INDICATIVE OF POOR PROGNOSIS

AHSG: Alpha-2-HS glycoprotein (Fetuin-A): Negative acute phase protein attenuating macrophage activation and neutrophil degranulation (Ombrellino et al., 2001).

HRG: Histidine-rich glycoprotein: Negative acute phase protein, regulator of inflammation and immune response, clearance of pathogens and cell detritus as well as coagulation and fibrinolysis through a variety of interactions (Poon et al., 2011; Wakabayashi, 2013).

ITIH2: Inter-alpha-trypsin inhibitor heavy chain H2: Covalently linked to bikunin (AMBP), the complex binds to hyaluronan (HA) to form serum-derived hyaluronan-associated protein (SHAP) which has matrix-stabilizing and immunomodulatory effects (Fries and Blom, 2000; Zhuo et al., 2004).

PLG: Plasminogen, Plasmin: Mediator of fibrinolysis (Chapin and Hajjar, 2015). More recently, immunological functions including neutrophil attenuation as well as macrophage efferocytosis and polarization from pro-inflammatory M1 to tissue-repairing M2 phenotype have been identified (Heissig et al., 2020).

similar proteomic depth as other contemporary mass spectrometry technologies that address undepleted human plasma that is constrained by its huge dynamic range (Anderson and Anderson, 2002) (Box 2 for the resources generated).

The comprehensive and time-resolved molecular phenotyping of this patient cohort is complemented by a comparison with a healthy population baseline (Generation Scotland [Smith et al., 2006]) measured with the same proteomic platform (Messner et al., 2020), and the characterization of an independent cohort from an unrelated health care system (Innsbruck cohort, Austria) for validating the created predictors. The measurements were performed on samples collected during the early period of COVID-19, i.e., before immunomodulatory treatments such as dexamethasone became standard of care for severe COVID-19 (RECOVERY Collaborative Group, 2020). Our data thus reflect treatment-naïve trajectories, which are of major value as baseline data for future studies.

We report an initial spike in the early inflammatory host response as a determinant for the future course of the disease. As our results indicate, the patients in our cohort showed molecular marker signatures of higher basal inflammation with increasing age, which might be partially responsible for the higher risk of severe COVID-19 in older individuals. While several

approaches of targeted anti-inflammatory treatment have not been successful in preventing clinical deterioration in COVID-19 so far (Stone et al., 2020), our study indicates that this special population of older patients might benefit particularly from treatments that mitigate the inflammatory host response. We report numerous interdependencies between clinical laboratory markers and alterations in proteomes, linking, for example, clinical inflammatory markers to components of the complement cascade and the coagulation system. Using machine learning, we show that both plasma proteomes and the compendium of established diagnostic parameters can be used for accurate characterization of disease severity, significantly outperforming established individual risk markers, such as CRP or IL-6 levels. Of note, the combination of proteomic features and clinical laboratory markers repeatedly showed the best performance in the machine learning models. Furthermore, the models generated could be transferred for prediction in an independent cohort from another hospital and healthcare system, highlighting the robustness of this approach and its translational potential.

We observed a considerable overlap between prognostic markers and those that classify treatment according to COVID-19 severity (Figure 5). Out of 49 prognostic markers, 41 correlated with the WHO severity score. As an example, SERPINA3

Box 2. Overview of resources generated

We provide deep and time-resolved resources that characterize COVID-19 at the level of plasma proteomes and established diagnostic parameters. We demonstrate the extent to which proteomes and diagnostic parameters interdepend, in initial response to the disease and in dynamics during the disease course. We show how they change with age, differ depending on the disease severity, reflect the therapy received and evolve over time. Our data have been acquired for COVID-19 patients' samples and analyzed in the context of general population proteomics (Generation Scotland) for which samples have been measured with the same proteomic technology (Messner et al., 2020), but we also expect it to be of high value as a reference for studies of other types of viral pneumonia as well as any investigations involving both routine clinical phenotyping and plasma proteomics.

Summary of the resource data generated in the study.

1. Covariation maps. We provide a covariation map between plasma proteins measured with at least 3 peptides and clinical laboratory measurements (Figure 1B; Table S4). In addition, we provide a full covariation map between all features measured in the study (Figure S3; Table S5) as well as a COVID-19 specific protein-protein covariation map (Figure S4; Table S6). Finally, we also provide a correlation map for the changes of different omics features with time (Figure S12; Table S7).
2. A map of plasma protein levels and clinical laboratory measurements depending on disease severity (Figures S5 and S6; Table S3).
3. Characterization of age-dependency of plasma protein levels and clinical laboratory measurements in COVID-19, and in comparison with the general population (Figures 2C and S9–S11; Table S3).
4. Characterization of the dynamics of plasma protein levels and clinical laboratory measurements during the course of COVID-19 (Figures 3B, S14, and S15; Table S3).
5. Characterization of the predictive power of plasma protein levels and clinical laboratory measurements in COVID-19 (Figures 4, S17, and S18; Table S3).
6. Proteomic and clinical signatures observed in severe COVID-19 patients undergoing RRT and ECMO (Figures S7 and S8; Table S3).

(Alpha-1 antichymotrypsin) can be used for both the classification of severity and prediction of future disease course. Both SERPINA3 and SERPINA1, another classifier of severity, possess anti-inflammatory properties and are involved in the protection of tissues from neutrophil elastase- and cathepsin G-mediated tissue damage (Benarafa, 2015). Our data show a strong correlation of both serpins with levels of neutrophils and NLR in peripheral blood. SERPINA1 is mainly produced by the liver but it is also produced in epithelial cells, pulmonary alveolar cells, tissue macrophages, blood monocytes, and granulocytes. Hence, this finding presumably reflects a systemic response to the increased NLR. After binding to effector enzymes, SERPIN-proteinase complexes are normally rapidly cleared from the blood but become resistant to degradation when cleaved at the reactive site loop (Gettins and Olson, 2016). Cleaved SERPINA1 and SERPINA3 have been shown to act as strong neutrophil chemoattractants (Banda et al., 1988; Potempa et al., 1991). The observed increase in levels of SERPINA1 and SERPINA3 might therefore partly reflect the more stable, chemoattractant, pro-inflammatory cleaved forms, rather than the short-lived tissue-protective proteins in severe COVID-19. Given the prominent role of neutrophil activation in severe COVID-19 (Schulte-Schrepping et al., 2020), this finding merits further investigation.

Our data also highlight angiotensinogen (AGT) as a marker for future worsening. Activation of angiotensinogen occurs via the protease renin and the endogenous angiotensin-converting enzymes ACE or ACE2. ACE converts angiotensin I (AngI) to pro-inflammatory, vasoconstrictive, and pro-fibrotic angiotensin II (AngII) (Zhang et al., 2020). ACE2, in contrast, mediates conversion of angiotensins I and II to anti-inflammatory, vasodilative, anti-fibrotic, and anti-oxidant angiotensins 1–9 (Ang1–9) and 1–7 (Ang1–7) (Turner, 2015). SARS-CoV-2 invades host cells of the

lung, heart, kidneys, and other organs via ACE2, resulting in the internalization and downregulation of ACE2 (Hoffmann et al., 2020; Tay et al., 2020; Zhang et al., 2020). Subsequently, angiotensinogen is converted predominantly via ACE to AngII and is less degraded by ACE2, resulting in AngII accumulation (Batlle et al., 2012; Silhol et al., 2020). We can thus assume that the higher plasma levels of AGT gene products in severely ill patients, as measured in our study, mainly reflect the higher levels of AngII. Importantly, we observed a strong correlation of AGT with markers of acute kidney injury (AKI; creatinine, urea; Figures S3 and S13; Table S5), a frequent complication of COVID-19 and a risk factor for poor prognosis and fatal outcome (Fu et al., 2020). Aggravated by the absence of tissue-protective Ang1–7, elevated levels of AngII lead to activation of the renin-angiotensin-system (RAS) and contribute to hypoxic kidney injury (Kasal et al., 2020). Of note, apart from tissue damaging effects, AngII has been shown to linearly correlate with viral load and lung injury in SARS-CoV-2 infection (Liu et al., 2020c).

Overall, many of the markers that are both classifiers and predictors of the future disease course are initiators of the inflammatory response. This group includes some of the key initiators of the complement cascade: C1QA, C1QB, C1QC, C1R, and CFD. In contrast, severity markers without prognostic value largely include downstream effectors of inflammation-associated damage, such as GSN and the circulating actins ACTBL2 and ACTB, ACTG1, and ECM1. Thus, this high-precision, high-throughput approach can help us understand mechanisms of immune-mediated organ damage on a molecular basis.

Despite the high resolution and high throughput of the mass spectrometry platform deployed in our study, the direct translation of our results into clinical practice will require the development of a clinical assay according to FDA or EMA standards.

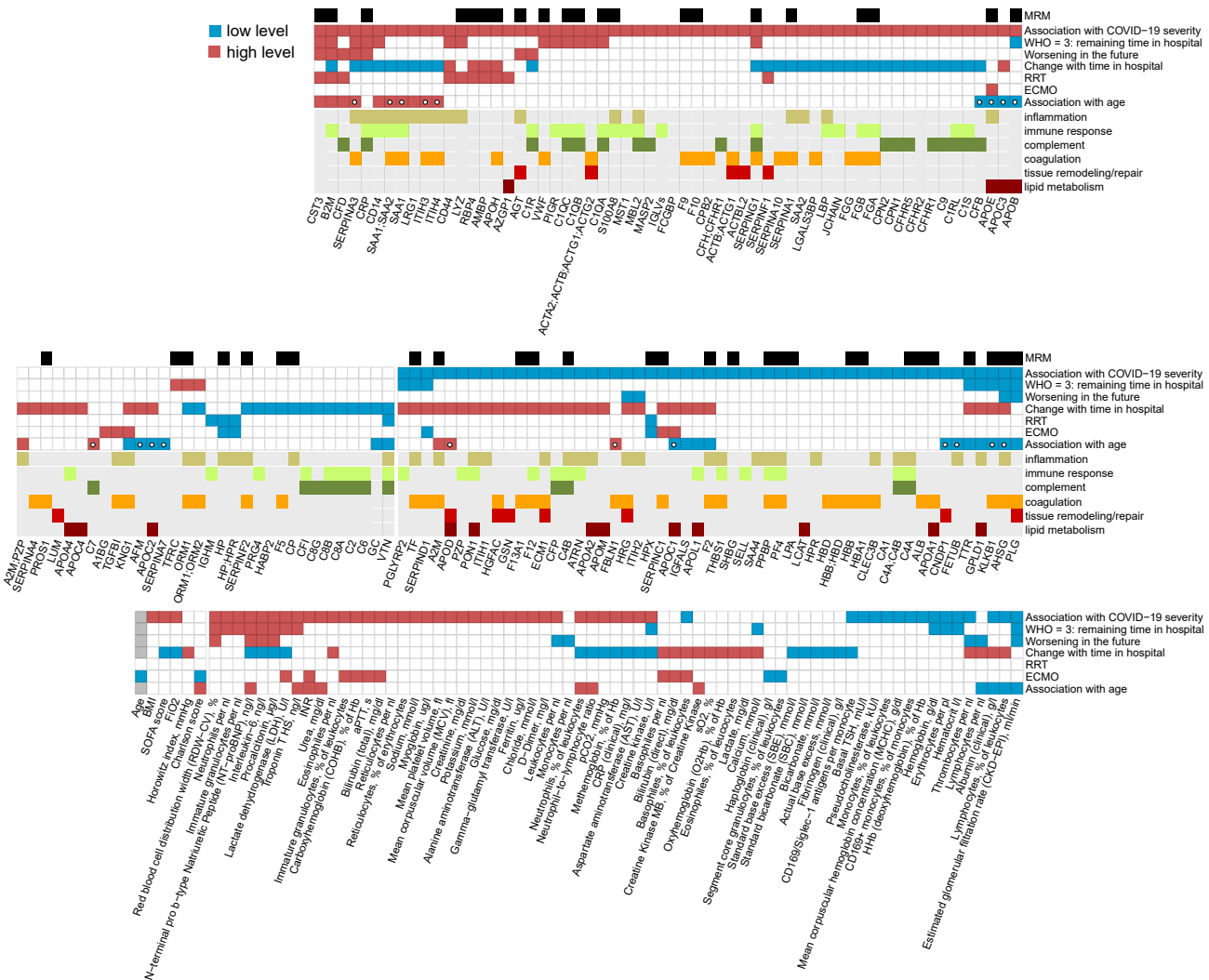


Figure 5. Summary: association of individual plasma proteins, routine diagnostic and physiological parameters with severity, necessary therapy, and progression of COVID-19.

For each statistical test considered (association with WHO grade, prediction of the remaining time in hospital for patients at WHO grade 3, prediction of worsening, i.e., progression to a higher WHO grade in the future, the trend during the peak period of the disease, association with RRT, association with ECMO and association with higher patient age), measurements, which show significant differences are highlighted, with the color indicating the trend, e.g., red for CST3 in the “Association with COVID-19 severity” test indicates higher levels of CST3 in severely ill patients. Proteins for which MRMAssayDB ([Bhowmick et al., 2018](#)) lists that a targeted proteomic assay has been developed are indicated with a black bar at the top. Proteins which change significantly with age in the Charité COVID-19 cohort (FDR < 0.05) but do not change significantly ($p < 0.05$) with age in the general population (Generation Scotland cohort), are highlighted with a white circle in the 7th row (“Association with age”). See also [Figures S6–S8, S10, S11, S14, S17, and S18](#), and [Table S3](#).

We further note that the use of machine learning is currently not a certified method to inform clinical decisions. However, in addition to multiple works that have successfully used machine learning for clinical prognosis previously (see recent reviews [Kelly et al., 2019; Lee and Lee, 2020; Nagendran et al., 2020; Shah et al., 2019; Vollmer et al., 2020]), our results bear a strong implication of the future potential of machine learning for clinical applications, including personalized medicine. This calls for a worldwide effort aimed at developing procedures, which would allow reliable clinical validation of machine learning predictors, their approval, and their routine deployment in the clinic.

In summary, by following a deeply phenotyped COVID-19 patient cohort over time at the level of the proteome and estab-

lished diagnostic biomarkers and physiological parameters, we have created a rich data resource for understanding the extent and progression of COVID-19. We have shown that an early spike in the inflammatory response is a key determinant of COVID-19, and that future disease progression is predictable by using panels of accredited diagnostic parameters as well as proteomic measurements from early time point samples. By using machine learning, we demonstrated that the proteome allows to precisely characterize the patients' phenotype and that the resulting machine learning models are robust and perform accurately when applied to samples from a different hospital and healthcare system. Our study provides comprehensive information about the key determinants of the varying COVID-19

trajectories as well as marker panels for early prognosis that can be exploited for clinical decision making, to devise personalized therapies, as well as for monitoring the development of much needed COVID-19 treatments.

CONSORTIA

Malte Kleinschmidt, Katrin M. Heim, Belén Millet, Lil Meyer-Arndt, Ralf H. Hübner, Tim Andermann, Jan M. Doebe, Bastian Opitz, Birgit Sawitzki, Daniel Grund, Peter Radünzel, Mariana Schürmann, Thomas Zoller, Florian Alius, Philipp Knape, Astrid Breitbart, Yaosi Li, Felix Bremer, Panagiotis Pergantis, Dirk Schürmann, Bettina Temmesfeld-Wollbrück, Daniel Wendisch, Sophia Brumhard, Sascha S. Haenel, Claudia Conrad, Philipp Georg, Kai-Uwe Eckardt, Lukas Lehner, Jan M. Kruse, Carolin Ferse, Roland Körner, Claudia Spies, Andreas Edel, Steffen Weber-Carstens, Alexander Krannich, Saskia Zvorc, Linna Li, Uwe Behrens, Sein Schmidt, Maria Rönnefarth, Chantip Dang-Heine, Robert Röhle, Emma Lieker, Lucie Kretzler, Isabelle Wirsching, Christian Wollboldt, Yinan Wu, Georg Schwanitz, David Hillus, Stefanie Kasper, Nadine Olk, Alexandra Horn, Dana Briesemeister, Denise Treue, Michael Hummel, Victor M. Corman, Christian Drosten, and Christof von Kalle

STAR★METHODS

Detailed methods are provided in the online version of this paper and include the following:

- **KEY RESOURCES TABLE**
- **RESOURCE AVAILABILITY**
 - Lead contact
 - Materials availability
 - Data and code availability
 - Experimental model and subject details
 - Innsbruck Patient cohort and clinical data
- **METHOD DETAILS**
 - Materials
 - Mass spectrometry
- **QUANTIFICATION AND STATISTICAL ANALYSIS**
 - Data analysis
 - Markers of the disease severity
 - Markers varying with age in COVID-19
 - Markers of RRT and ECMO
 - Markers predictive of time in hospital
 - Markers predictive of disease worsening
 - Peak period of the disease definition
 - Markers changing during the peak of disease
 - Correlation maps
 - Prediction of current mechanical ventilation
 - WHO grade prediction
 - Prediction of the remaining time in hospital
 - Supplementary Note 1. Diagnostic parameters and Proteome signatures that indicate therapeutic interventions
 - Supplementary Note 2. Age-specific response to COVID-19 in the context of severity markers
 - Supplementary Note 3. Diverging trends at the proteome level during the disease peak in individual patients

SUPPLEMENTAL INFORMATION

Supplemental information can be found online at <https://doi.org/10.1016/j.cels.2021.05.005>.

ACKNOWLEDGMENTS

We thank Robert Lane, Jean-Baptiste Vincendet and Nick Morrice (Sciex) for help with the TripleTOF 6600. This work was supported by the Berlin University Alliance (501_Massenspektrometrie, 501_Linklab, 112_PreEP_Corona_R-alser), by UKRI/NIHR through the UK Coronavirus Immunology Consortium (UK-CIC), the BMBF/DLR Projektträger (01KI20160A, 01ZX1604B, 01KI20337, 01KX2021), Charité-BIH Centrum für Therapieforschung (BIH_PA_covid-19_Ralser), the BBSRC (BB/N015215/1, BB/N015282/1), the Francis Crick Institute, which receives its core funding from Cancer Research UK (FC001134), the UK Medical Research Council (FC001134), and the Wellcome Trust (FC001134 and IA 200829/Z/16/Z), as well as the European Research Council (SyG 951475 to M.R.). This work was further supported by the Ministry of Education and Research (BMBF), as a part of the National Research Node ‘mass spectrometry in Systems Medicine (MScoresys), under grant agreement 031L0220A. This study was further supported by the German Federal Ministry of Education and Research (NaFoUniMedCovid19 – NUM-NAPKON, NUM-COVIM, FKZ: 01KX2021 and PROVID – FKZ: 01KI20160A) to F.K., L.E.S., M.W., N.S., and S.H.; L.E.S. is supported by the German Research Foundation (DFG, SFB-TR84 114933180) and by the Berlin Institute of Health (BIH), which receives funding from the Ministry of Education and Research (BMBF). M.W. is supported by grants from the German Research Foundation, SFB-TR84 C06 and C09, by the German Ministry of Education and Research (BMBF) in the framework of the CAPSyS (01ZX1304B), CAPSyS-COVID (01ZX1604B), SYMPATH (01ZX1906A) and PROVID project (01KI20160A) and by the Berlin Institute of Health (CM-COVID). S.H. is supported by the German Research Foundation (DFG, SFB-TR84 A04 and B06), and the BMBF (PROVID, and project 01KI2082). N.S. is supported by grants from the German Research Foundation, SFB-TR84 C09 und Z02, by the German Ministry of Education and Research (BMBF) in the framework of the PROGRESS 01KI07114. This study was further supported by Wellcome Trust (200829/Z/16/Z). The Generation Scotland study received core support from the Chief Scientist Office of the Scottish Government Health Directorates (CZD/16/6) and the Scottish Funding Council (HR03006), and is now supported by the Wellcome Trust (216767/Z/19/Z). A.C. is funded by HDR UK and the Wellcome Trust (216767/Z/19/Z). C.H. is supported by an MRC University Unit Programme grant (MC_UU_00007/10) (QTL in Health and Disease). R.M. is supported by an Alzheimer’s Research UK project grant (ARUK-PG2017B-10). H.W., J.F.T., A.Z., and T.N. are supported by a Medical Research Council grant (MR/R02524X/1) and H.W., A.Z., and O.B. by the Ministry of Science and Higher Education agreement no. 075-15-2020-808. H.W. is supported by the National Institute for Health Research (NIHR) Imperial Biomedical Research Centre (BRC). J.F.T is supported by the National Institute for Health Research (NIHR) UCLH/UCL Biomedical Research Centre. M.M. is a participant in the Bih-Charité Digital Clinician Scientist Program funded by the Charité – Universitätsmedizin Berlin, the Berlin Institute of Health, and the German Research Foundation (DFG). M.A.K. is supported by the Austrian Science Funds (FWF; P33333) and the Austrian Research Promotion Agency (FFG, #878654). Figures were created with biorender.com

AUTHOR CONTRIBUTIONS

L.E.S., M.R., and F.K. designed the study. A.F., D.L., and M.M. conducted experiments. P.T.-L., C.T., A.F., D.L., E.T.H., P.S., C.B.M., M.J., T.S., S.J.K., A.P., Y.W., S.S., R.H., B.S., S.W., M.M., F.M., C.G., C.R.-G., T.L., L.B.J., M.S.S., M.P., L.J., S.D., L.J.L., D.Z., P.E., A.U., H.Z., J.L.-R., M.A.K., I.T., H.M.-R., M.W., N.S., L.E.S., and F.K. acquired clinical samples and data. V.D., P.T.-L., O.L., T.N., C.T., H.W., S.K.A., A.R., N.-M.G., L.S., S.V., M.W., C.B.M., O.B., A.Z., A.C., C.H., D.J.P., R.E.M., J.F.T., A.Z., K.L., S.H., M.M., M.R., and F.K. analyzed the data. V.D., P.T.-L., C.T., C.C.-M., E.T.H., P.S., S.H., M.R., M.M., T.L., L.J.L., K.L., L.E.S., M.R., and F.K. interpreted the data. V.D., P.T.-L., M.R., F.K., and L.E.S. wrote the first draft of the manuscript. All authors contributed to finalizing the manuscript.

DECLARATION OF INTERESTS

The authors declare no competing interests.

Received: November 11, 2020

Revised: March 24, 2021

Accepted: May 7, 2021

Published: June 14, 2021

REFERENCES

- Agirbaşlı, M., Song, J., Lei, F., Wang, S., Kuselman, A.R., Clark, J.B., Myers, J.L., and Ündar, A. (2015). Apolipoprotein E levels in pediatric patients undergoing cardiopulmonary bypass. *Artif. Organs* 39, 28–33.
- Alwan, N.A., Burgess, R.A., Ashworth, S., Beale, R., Bhadelia, N., Bogaert, D., Dowd, J., Eckerle, I., Goldman, L.R., Greenhalgh, T., et al. (2020). Scientific consensus on the COVID-19 pandemic: we need to act now. *Lancet* 396, e71–e72.
- Anderson, N.L., and Anderson, N.G. (2002). The human plasma proteome: history, character, and diagnostic prospects. *Mol. Cell. Proteomics* 1, 845–867.
- ARDS Definition Task Force, Ranieri, V.M., Rubenfeld, G.D., Thompson, B.T., Ferguson, N.D., Caldwell, E., Fan, E., Camorota, L., and Slutsky, A.S. (2012). Acute respiratory distress syndrome: the Berlin definition. *JAMA* 307, 2526–2533.
- Banda, M.J., Rice, A.G., Griffin, G.L., and Senior, R.M. (1988). Alpha 1-proteinase inhibitor is a neutrophil chemoattractant after proteolytic inactivation by macrophage elastase. *J. Biol. Chem.* 263, 4481–4484.
- Battle, D., Wysocki, J., Soler, M.J., and Ranganath, K. (2012). Angiotensin-converting enzyme 2: enhancing the degradation of angiotensin II as a potential therapy for diabetic nephropathy. *Kidney Int* 81, 520–528.
- Benarafa, C. (2015). Regulation of neutrophil serine proteases by intracellular serpins. In *The Serpin Family: Proteins with Multiple Functions in Health and Disease*, M. Geiger, F. Wahrmüller, and M. Furtmüller, eds. (Springer International Publishing), pp. 59–76.
- Benjamini, Y., and Hochberg, Y. (1995). Controlling the false discovery rate: a practical and powerful approach to multiple testing. *Journal of the Royal Statistical Society: Series B (Methodological)* 57, 289–300.
- Bhowmick, P., Mohammed, Y., and Borchers, C.H. (2018). MRMAssayDB: an integrated resource for validated targeted proteomics assays. *Bioinformatics* 34, 3566–3571.
- Blumenthal, D., Fowler, E.J., Abrams, M., and Collins, S.R. (2020). Covid-19 – implications for the health care system. *N. Engl. J. Med.* 383, 1483–1488.
- Chapin, J.C., and Hajjar, K.A. (2015). Fibrinolysis and the control of blood coagulation. *Blood Rev* 29, 17–24.
- Chen, T., and Guestrin, C. (2016). XGBoost: A scalable tree boosting system. In *Proceedings of the 22nd ACM SIGKDD international conference on Knowledge Discovery and Data Mining*, pp. 785–794.
- Chung, H.Y., Kim, D.H., Lee, E.K., Chung, K.W., Chung, S., Lee, B., Seo, A.Y., Chung, J.H., Jung, Y.S., Im, E., et al. (2019). Redefining chronic inflammation in aging and age-related diseases: proposal of the Senoinflammation concept. *Aging Dis* 10, 367–382.
- Cox, J., Hein, M.Y., Luber, C.A., Paron, I., Nagaraj, N., and Mann, M. (2014). Accurate proteome-wide label-free quantification by delayed normalization and maximal peptide ratio extraction, termed MaxLFQ. *Mol. Cell. Proteomics* 13, 2513–2526.
- D'Alessandro, A., Thomas, T., Dzieciatkowska, M., Hill, R.C., Francis, R.O., Hudson, K.E., Zimring, J.C., Hod, E.A., Spitalnik, S.L., and Hansen, K.C. (2020). Serum proteomics in COVID-19 patients: altered coagulation and complement status as a function of IL-6 level. *J. Proteome Res.* 19, 4417–4427.
- Danwang, C., Endomba, F.T., Nkeck, J.R., Wouna, D.L.A., Robert, A., and Noubiap, J.J. (2020). A meta-analysis of potential biomarkers associated with severity of coronavirus disease 2019 (COVID-19). *Biomark. Res.* 8, 37.
- Dassati, S., Waldner, A., and Schweigreiter, R. (2014). Apolipoprotein D takes center stage in the stress response of the aging and degenerative brain. *Neurobiol. Aging* 35, 1632–1642.
- Demichev, V., Messner, C.B., Bernards, S.I., Lilley, K.S., and Ralser, M. (2020). DIA-NN: neural networks and interference correction enable deep proteome coverage in high throughput. *Nat. Methods* 17, 41–44.
- Do Carmo, S., Jacomy, H., Talbot, P.J., and Rassart, E. (2008). Neuroprotective effect of apolipoprotein D against human coronavirus OC43-induced encephalitis in mice. *J. Neurosci.* 28, 10330–10338.
- Ferrucci, L., Corsi, A., Lauretani, F., Bandinelli, S., Bartali, B., Taub, D.D., Guralnik, J.M., and Longo, D.L. (2005). The origins of age-related proinflammatory state. *Blood* 105, 2294–2299.
- Figueredo, D.M., Gordon, E.M., Yao, X., and Levine, S.J. (2019). Apolipoproteins as context-dependent regulators of lung inflammation. In *Mechanisms and Manifestations of Obesity in Lung Disease*, R.A. Johnston and B.T. Suratt, eds. (Academic Press), pp. 301–326.
- Franceschi, C., Garagnani, P., Parini, P., Giuliani, C., and Santoro, A. (2018). Inflammaging: a new immune-metabolic viewpoint for age-related diseases. *Nat. Rev. Endocrinol.* 14, 576–590.
- Fries, E., and Blom, A.M. (2000). Bikunin—not just a plasma proteinase inhibitor. *Int. J. Biochem. Cell Biol.* 32, 125–137.
- Fu, E.L., Janse, R.J., de Jong, Y., van der Endt, V.H.W., Milders, J., van der Willik, E.M., de Rooij, E.N.M., Dekkers, O.M., Rotmans, J.I., and van Diepen, M. (2020). Acute kidney injury and kidney replacement therapy in COVID-19: a systematic review and meta-analysis. *Clin. Kidney J.* 13, 550–563.
- Gettins, P.G.W., and Olson, S.T. (2016). Inhibitory serpins. New insights into their folding, polymerization, regulation and clearance. *Biochem. J.* 473, 2273–2293.
- Gillet, L.C., Navarro, P., Tate, S., Röst, H., Selevsek, N., Reiter, L., Bonner, R., and Aebersold, R. (2012). Targeted data extraction of the MS/MS spectra generated by data-independent acquisition: a new concept for consistent and accurate proteome analysis. *Mol. Cell. Proteomics* 11, O111.016717.
- Gordon, S.M. (2014). Proteomic diversity in HDL: a driving force for particle function and target for therapeutic intervention. In *The HDL Handbook*, Second Edition, T. Komoda, ed. (Academic Press), pp. 293–322.
- Goronzy, J.J., and Weyand, C.M. (2013). Understanding immunosenescence to improve responses to vaccines. *Nat. Immunol.* 14, 428–436.
- Grifoni, E., Valoriani, A., Cei, F., Lamanna, R., Gelli, A.M.G., Ciambotti, B., Vannucchi, V., Moroni, F., Pelagatti, L., Tarquini, R., et al. (2020). Interleukin-6 as prognosticator in patients with COVID-19. *J. Infect.* 81, 452–482.
- Gu, Z., Eils, R., and Schlesner, M. (2016). Complex heatmaps reveal patterns and correlations in multidimensional genomic data. *Bioinformatics* 32, 2847–2849.
- Hadjadj, J., Yatim, N., Barnabei, L., Corneau, A., Boussier, J., Smith, N., Pérez, H., Charbit, B., Bondet, V., Chenevier-Gobeaux, C., et al. (2020). Impaired type I interferon activity and inflammatory responses in severe COVID-19 patients. *Science* 369, 718–724.
- Hajishengallis, George, Reis, E.S., Mastellos, D.C., Ricklin, D., and Lambris, J.D. (2017). Novel mechanisms and functions of complement. *Nature Immunology* 18, 1288–1298. <https://doi.org/10.1038/ni.3858>.
- Han, S., Yang, K., Zhu, H., Liu, J., Zhang, L., and Zhao, J. (2018). Proteomics investigation of the changes in serum proteins after high- and low-flux hemodialysis. *Ren. Fail.* 40, 506–513.
- Harris, S.E., Riggio, V., Evenden, L., Gilchrist, T., McCafferty, S., Murphy, L., Wrobel, N., Taylor, A.M., Corley, J., Pattie, A., et al. (2017). Age-related gene expression changes, and transcriptome wide association study of physical and cognitive aging traits, in the Lothian Birth Cohort 1936. *Aging* 9, 2489–2503.
- Heissig, B., Salama, Y., Takahashi, S., Osada, T., and Hattori, K. (2020). The multifaceted role of plasminogen in inflammation. *Cell Signal* 75. <https://doi.org/10.1016/j.cellsig.2020.109761>.
- Henry, B.M., de Oliveira, M.H.S., Benoit, S., Plebani, M., and Lippi, G. (2020). Hematologic, biochemical and immune biomarker abnormalities associated with severe illness and mortality in coronavirus disease 2019 (COVID-19): a meta-analysis. *Clin. Chem. Lab. Med.* 58, 1021–1028.
- Hilt, Z.T., Pariser, D.N., Ture, S.K., Mohan, A., Quijada, P., Asante, A.A., Cameron, S.J., Sterling, J.A., Merkel, A.R., Johanson, A.L., et al. (2019).

- Platelet-derived β 2M regulates monocyte inflammatory responses. *JCI Insight* 4. <https://doi.org/10.1172/jci.insight.122943>.
- Hoffmann, M., Kleine-Weber, H., Schroeder, S., Krüger, N., Herrler, T., Erichsen, S., Schiergens, T.S., Herrler, G., Wu, N.-H., Nitsche, A., et al. (2020). SARS-CoV-2 cell entry depends on ACE2 and TMPRSS2 and is blocked by a clinically proven protease inhibitor. *Cell* 181, 271–280.e8.
- Kasal, D.A., De Lorenzo, A., and Tibiriçá, E. (2020). COVID-19 and microvascular disease: pathophysiology of SARS-CoV-2 infection with focus on the renin-angiotensin system. *Heart Lung Circ* 29, 1596–1602.
- Kelly, C.J., Karthikesalingam, A., Suleyman, M., Corrado, G., and King, D. (2019). Key challenges for delivering clinical impact with artificial intelligence. *BMC Med* 17, 195.
- Kurth, F., Roennefarth, M., Thibeault, C., Corman, V.M., Müller-Redetzky, H., Mittermaier, M., Ruwwe-Glösenkamp, C., Heim, K.M., Krannich, A., Zvorc, S., et al. (2020). Studying the pathophysiology of coronavirus disease 2019: a protocol for the Berlin prospective COVID-19 patient cohort (Pa-COVID-19). *Infection* 48, 619–626.
- Laing, A.G., Lorenc, A., Del Molino Del Barrio, I., Das, A., Fish, M., Monin, L., Muñoz-Ruiz, M., McKenzie, D.R., Hayday, T.S., Francos-Quijorna, I., et al. (2020). A dynamic COVID-19 immune signature includes associations with poor prognosis. *Nat. Med.* 26, 1623–1635.
- Lee, C.S., and Lee, A.Y. (2020). Clinical applications of continual learning machine learning. *Lancet Digit. Health* 2, e279–e281.
- Lian, J., Jin, C., Hao, S., Zhang, X., Yang, M., Jin, X., Lu, Y., Hu, J., Zhang, S., Zheng, L., et al. (2020). High neutrophil-to-lymphocyte ratio associated with progression to critical illness in older patients with COVID-19: a multicenter retrospective study. *Aging* 12, 13849–13859.
- Liu, J., Liu, Y., Xiang, P., Pu, L., Xiong, H., Li, C., Zhang, M., Tan, J., Xu, Y., Song, R., et al. (2020a). Neutrophil-to-lymphocyte ratio predicts critical illness patients with 2019 coronavirus disease in the early stage. *J. Transl. Med.* 18, 206.
- Liu, Y., Gao, W., Guo, W., Guo, Y., Shi, M., Dong, G., Ge, Q., Zhu, J., and Lu, J. (2020b). Prominent coagulation disorder is closely related to inflammatory response and could be as a prognostic indicator for ICU patients with COVID-19. *J. Thromb. Thrombolysis* 50, 825–832.
- Liu, Y., Yang, Y., Zhang, C., Huang, F., Wang, F., Yuan, J., Wang, Z., Li, J., Li, J., Feng, C., et al. (2020c). Clinical and biochemical indexes from 2019-nCoV infected patients linked to viral loads and lung injury. *Sci. China Life Sci.* 63, 364–374.
- Liu, Y.C., Zou, X.B., Chai, Y.F., and Yao, Y.M. (2014). Macrophage polarization in inflammatory diseases. *Int. J. Biol. Sci.* 10, 520–529.
- Luo, Z., Lei, H., Sun, Y., Liu, X., and Su, D.F. (2015). Orosomucoid, an acute response protein with multiple modulating activities. *J. Physiol. Biochem.* 71, 329–340.
- Makridakis, M., Kontostathi, G., Petra, E., Strogilos, R., Lygirou, V., Filip, S., Duranton, F., Mischak, H., Argiles, A., Zoidakis, J., and Vlahou, A. (2020). Multiplexed MRM-based protein quantification of putative prognostic biomarkers for chronic kidney disease progression in plasma. *Sci. Rep.* 10, 4815.
- McDonnell, T., Wincup, C., Buchholz, I., Pericleous, C., Giles, I., Ripoll, V., Cohen, H., Delcea, M., and Rahman, A. (2020). The role of beta-2-glycoprotein I in health and disease associating structure with function: more than just APS. *Blood Rev* 39, 100610.
- Meizlish, M.L., Pine, A.B., Bishai, J.D., Goshua, G., Nadelmann, E.R., Simonov, M., Chang, C.-H., Zhang, H., Shallow, M., Bahel, P., et al. (2020). A neutrophil activation signature predicts critical illness and mortality in COVID-19. *medRxiv*. <https://doi.org/10.1182/bloodadvances.2020003568>.
- Messner, C.B., Demichev, V., Wendisch, D., Michalick, L., White, M., Freiwald, A., Textoris-Taube, K., Vernardis, S.I., Egger, A.-S., Kreidl, M., et al. (2020). Ultra-high-throughput clinical proteomics reveals classifiers of COVID-19 infection. *Cell Syst* 11, 11–24.e4.
- Millard, S.P. (2014). EnvStats, an RPackage for environmental statistics. In Wiley StatsRef: Statistics Reference Online, N. Balakrishnan, T. Colton, B. Everitt, W. Piegorsch, F. Ruggeri, and J.L. Teugels, eds. (Wiley).
- Muffat, J., and Walker, D.W. (2010). Apolipoprotein D: an overview of its role in aging and age-related diseases. *Cell Cycle* 9, 269–273.
- Murphy, A.J., Akhtari, M., Tolani, S., Pagler, T., Bijl, N., Kuo, C.L., Wang, M., Sanson, M., Abramowicz, S., Welch, C., et al. (2011). ApoE regulates hematopoietic stem cell proliferation, monocytosis, and monocyte accumulation in atherosclerotic lesions in mice. *J. Clin. Invest.* 127, 4138–4149.
- Nagendran, M., Chen, Y., Lovejoy, C.A., Gordon, A.C., Komorowski, M., Harvey, H., Topol, E.J., Ioannidis, J.P.A., Collins, G.S., and Maruthappu, M. (2020). Artificial intelligence versus clinicians: systematic review of design, reporting standards, and claims of deep learning studies. *BMJ* 368, m689.
- WHO. (2020). R&D Blueprint—Novel Coronavirus COVID-19 Therapeutic Trial Synopsis (World Health Organization).
- Ombrellino, M., Wang, H., Yang, H., Zhang, M., Vishnubhakat, J., Frazier, A., Scher, L.A., Friedman, S.G., and Tracey, K.J. (2001). Fetuin, a negative acute phase protein, attenuates TNF synthesis and the innate inflammatory response to carrageenan. *Shock* 15, 181–185.
- Overmyer, K.A., Shishkova, E., Miller, I.J., Balnis, J., Bernstein, M.N., Peters-Clarke, T.M., Meyer, J.G., Quan, Q., Muehlbauer, L.K., Trujillo, E.A., et al. (2020). Large-scale multi-omic analysis of COVID-19 severity. *medRxiv*. <https://doi.org/10.1101/2020.07.17.20156513>.
- Page, C., Goicochea, L., Matthews, K., Zhang, Y., Klover, P., Holtzman, M.J., Hennighausen, L., and Frieman, M. (2012). Induction of alternatively activated macrophages enhances pathogenesis during severe acute respiratory syndrome coronavirus infection. *J. Virol.* 86, 13334–13349.
- Pascual, M., Steiger, G., Estreicher, J., Macon, K., Volanakis, J.E., and Schifferli, J.A. (1988). Metabolism of complement factor D in renal failure. *Kidney Int* 34, 529–536.
- Patrício, P., Paiva, J.A., and Borrego, L.M. (2019). Immune response in bacterial and candida sepsis. *Eur. J. Microbiol. Immunol. (Bp)* 9, 105–113.
- Pedregosa, F., Varoquaux, G., Gramfort, A., Michel, V., Thirion, B., Grisel, O., Blondel, M., Prettenhofer, P., Weiss, R., Dubourg, V., et al. (2011). Scikit-learn: machine learning in Python. *J. Mach. Learn. Res.* 12, 2825–2830.
- Peralta, C.A., Shlipak, M., Judd, S., Cushman, M., McClellan, W., Zakai, N.A., Safford, M.M., Zhang, X., Muntner, P., and Warnock, D. (2011). Detection of chronic kidney disease with creatinine, cystatin C, and urine albumin-to-creatinine ratio and association with progression to end-stage renal disease and mortality. *JAMA* 305, 1545–1552.
- Perez-Riverol, Y., Csordas, A., Bai, J., Bernal-Llinares, M., Hewapathirana, S., Kundu, D.J., Inuganti, A., Griss, J., Mayer, G., Eisenacher, M., et al. (2019). The PRIDE database and related tools and resources in 2019: improving support for quantification data. *Nucleic Acids Res* 47, D442–D450.
- Peters, M.J., Joehanes, R., Pilling, L.C., Schurmann, C., Conneely, K.N., Powell, J., Reinmaa, E., Sutphin, G.L., Zhernakova, A., Schramm, K., et al. (2015). The transcriptional landscape of age in human peripheral blood. *Nat. Commun.* 6, 8570.
- Pham, T.V., Henneman, A.A., and Jimenez, C.R. (2020). iq: an R package to estimate relative protein abundances from ion quantification in DIA-MS-based proteomics. *Bioinformatics* 36, 2611–2613.
- Phua, J., Weng, L., Ling, L., Egi, M., Lim, C.M., Divatia, J.V., Shrestha, B.R., Arabi, Y.M., Ng, J., Gomersall, C.D., et al. (2020). Intensive care management of coronavirus disease 2019 (COVID-19): challenges and recommendations. *Lancet Respir. Med.* 8, 506–517.
- Poon, I.K.H., Patel, K.K., Davis, D.S., Parish, C.R., and Hulett, M.D. (2011). Histidine-rich glycoprotein: the Swiss Army knife of mammalian plasma. *Blood* 117, 2093–2101.
- Potempa, J., Fedak, D., Dubin, A., Mast, A., and Travis, J. (1991). Proteolytic inactivation of alpha-1-anti-chymotrypsin. Sites of cleavage and generation of chemotactic activity. *J. Biol. Chem.* 266, 21482–21487.
- Poinnard, T., and Imbert-Bismut, F. (2012). Laboratory testing for liver disease. In Zakim and Boyer's Hepatology, Sixth Edition, T.D. Boyer, M.P. Manns, and A.J. Sanyal, eds. (W.B. Saunders), pp. 201–215.
- Ramasamy, I. (2014). Recent advances in physiological lipoprotein metabolism. *Clin. Chem. Lab. Med.* 52, 1695–1727.

Cell Systems

Article



- Rea, I.M., Gibson, D.S., McGilligan, V., Mc너너란, S.E., Alexander, H.D., and Ross, O.A. (2018). Age and age-related diseases: role of inflammation triggers and cytokines. *Front. Immunol.* 9, 586.
- RECOVERY Collaborative Group (2020). Dexamethasone in hospitalized patients with Covid-19 - preliminary report. *N. Engl. J. Med.* 384, 693–704.
- Rehman, A.A., Ahsan, H., and Khan, F.H. (2013). α -2-macroglobulin: a physiological guardian. *J. Cell. Physiol.* 228, 1665–1675.
- Ritchie, M.E., Phipson, B., Wu, D., Hu, Y., Law, C.W., Shi, W., and Smyth, G.K. (2015). limma powers differential expression analyses for RNA-sequencing and microarray studies. *Nucleic Acids Res* 43, e47.
- Rosenbaum, L. (2020). The untold toll - the pandemic's effects on patients without Covid-19. *N. Engl. J. Med.* 382, 2368–2371.
- Sack, G.H., Jr. (2018). Serum amyloid A - a review. *Mol. Med.* 24, 46.
- Saxena, S.K. (2020). *Coronavirus Disease 2019 (COVID-19): Epidemiology, Pathogenesis, Diagnosis, And Therapeutics* (Springer nature).
- Schneeman, T.A., Bruno, M.E.C., Schjerven, H., Johansen, F.E., Chady, L., and Kaetzel, C.S. (2005). Regulation of the polymeric Ig receptor by signaling through TLRs 3 and 4: linking innate and adaptive immune responses. *J. Immunol.* 175, 376–384.
- Schulte-Schrepping, J., Reusch, N., Paclik, D., Baßler, K., Schlickeiser, S., Zhang, B., Krämer, B., Krammer, T., Brumhard, S., Bonaguro, L., et al. (2020). Severe COVID-19 is marked by a dysregulated myeloid cell compartment. *Cell* 182, 1419–1440.e23.
- Shah, P., Kendall, F., Khuzin, S., Goosen, R., Hu, J., Laramie, J., Ringel, M., and Schork, N. (2019). Artificial intelligence and machine learning in clinical development: a translational perspective. *NPJ Digit. Med.* 2, 69.
- Shao, B., de Boer, I., Tang, C., Mayer, P.S., Zelnick, L., Afkarian, M., Heinecke, J.W., and Himmelfarb, J. (2015). A cluster of proteins implicated in kidney disease is increased in high-density lipoprotein isolated from hemodialysis subjects. *J. Proteome Res.* 14, 2792–2806.
- Sharma, N.K., Tashima, A.K., Brunialti, M.K.C., Ferreira, E.R., Torquato, R.J.S., Mortara, R.A., Machado, F.R., Assuncao, M., Rigato, O., and Salomao, R. (2017). Proteomic study revealed cellular assembly and lipid metabolism dysregulation in sepsis secondary to community-acquired pneumonia. *Sci. Rep.* 7, 15606.
- Shen, B., Yi, X., Sun, Y., Bi, X., Du, J., Zhang, C., Quan, S., Zhang, F., Sun, R., Qian, L., et al. (2020). Proteomic and metabolomic characterization of COVID-19 patient sera. *Cell* 182, 59–72.e15.
- Shu, T., Ning, W., Wu, D., Xu, J., Han, Q., Huang, M., Zou, X., Yang, Q., Yuan, Y., Bie, Y., et al. (2020). Plasma proteomics identify biomarkers and pathogenesis of COVID-19. *Immunity* 53, 1108–1122.e5.
- Silhol, F., Sarlon, G., Deharo, J.C., and Vaisse, B. (2020). Downregulation of ACE2 induces overstimulation of the renin-angiotensin system in COVID-19: should we block the renin-angiotensin system? *Hypertens. Res.* 43, 854–856.
- Singer, M., Deutschman, C.S., Seymour, C.W., Shankar-Hari, M., Annane, D., Bauer, M., Bellomo, R., Bernard, G.R., Chiche, J.D., Coopersmith, C.M., et al. (2016). The third international consensus definitions for sepsis and septic shock (Sepsis-3). *JAMA* 315, 801–810.
- Smith, B.H., Campbell, H., Blackwood, D., Connell, J., Connor, M., Deary, I.J., Dominiczak, A.F., Fitzpatrick, B., Ford, I., Jackson, C., et al. (2006). Generation Scotland: the Scottish Family Health Study; a new resource for researching genes and heritability. *BMC Med. Genet.* 7, 74.
- Smyth, G.K. (2004). Linear models and empirical bayes methods for assessing differential expression in microarray experiments. *Stat. Appl. Genet. Mol. Biol.* 3, article3.
- Soysal, P., Stubbs, B., Lucato, P., Luchini, C., Solmi, M., Peluso, R., Sergi, G., Isik, A.T., Manzato, E., Maggi, S., et al. (2016). Inflammation and frailty in the elderly: a systematic review and meta-analysis. *Ageing Res. Rev.* 31, 1–8.
- Stawicki, S.P., Jeanmonod, R., Miller, A.C., Paladino, L., Gajeski, D.F., Yaffee, A.Q., De Wulf, A., Grover, J., Papadimos, T.J., Bloem, C., et al. (2020). The 2019–2020 novel coronavirus (severe acute respiratory syndrome coronavirus 2) pandemic: a joint American College of Academic International Medicine-world academic council of emergency medicine multidisciplinary COVID-19 working group consensus paper. *J. Glob. Infect. Dis.* 12, 47–93.
- Stone, J.H., Frigault, M.J., Serling-Boyd, N.J., Fernandes, A.D., Harvey, L., Foulkes, A.S., Horick, N.K., Healy, B.C., Shah, R., Bensaci, A.M., et al. (2020). Efficacy of tocilizumab in patients hospitalized with Covid-19. *N. Engl. J. Med.* 383, 2333–2344.
- Sun, Q., Qiu, H., Huang, M., and Yang, Y. (2020). Lower mortality of COVID-19 by early recognition and intervention: experience from Jiangsu Province. *Ann. Intensive Care* 10, 33.
- Tavazoie, M.F., Pollack, I., Tanqueco, R., Ostendorf, B.N., Reis, B.S., Gonsalves, F.C., Kurth, I., Andreu-Agullo, C., Derbyshire, M.L., Posada, J., et al. (2018). LXR/ApoE activation restricts innate immune suppression in cancer. *Cell* 172, 825–840.e18.
- Tay, M.Z., Poh, C.M., Rénia, L., MacAry, P.A., and Ng, L.F.P. (2020). The trinity of COVID-19: immunity, inflammation and intervention. *Nat. Rev. Immunol.* 20, 363–374.
- Turner, A.J. (2015). ACE2 cell biology, regulation, and physiological functions. In *The Protective Arm of the Renin Angiotensin System (RAS)*, T. Unger, U.M. Steckelings, and R.A.S. dos Santos, eds. (Academic Press), pp. 185–189.
- Turula, H., and Wobus, C.E. (2018). The role of the polymeric immunoglobulin receptor and secretory immunoglobulins during mucosal infection and immunity. *Viruses* 10, 237.
- Virtanen, P., Gommers, R., Oliphant, T.E., Haberland, M., Reddy, T., Cournapeau, D., Burovski, E., Peterson, P., Weckesser, W., Bright, J., et al. (2020). SciPy 1.0: fundamental algorithms for scientific computing in Python. *Nat. Methods* 17, 261–272.
- Volanakis, J.E., and Narayana, S.V. (1996). Complement factor D, a novel serine protease. *Protein Sci* 5, 553–564.
- Vollmer, S., Mateen, B.A., Bohner, G., Király, F.J., Ghani, R., Jonsson, P., Cumbers, S., Jonas, A., McAllister, K.S.L., Myles, P., et al. (2020). Machine learning and artificial intelligence research for patient benefit: 20 critical questions on transparency, replicability, ethics, and effectiveness. *BMJ* 368, i6927.
- Wakabayashi, S. (2013). New insights into the functions of histidine-rich glycoprotein. In *International Review of Cell and Molecular Biology*, K.W. Jeon, ed. (Academic Press), pp. 467–493.
- Wermuth, P.J., and Jimenez, S.A. (2015). The significance of macrophage polarization subtypes for animal models of tissue fibrosis and human fibrotic diseases. *Clin. Transl. Med.* 4, 2.
- Wu, D., Koganti, R., Lambe, U.P., Yadavalli, T., Nandi, S.S., and Shukla, D. (2020). Vaccines and therapies in development for SARS-CoV-2 infections. *J. Clin. Med.* 9, 1885.
- Wu, Y., Potempa, L.A., El Kebir, D., and Filep, J.G. (2015). C-reactive protein and inflammation: conformational changes affect function. *Biol. Chem.* 396, 1181–1197.
- Wynants, L., Van Calster, B., Collins, G.S., Riley, R.D., Heinze, G., Schuit, E., Bonten, M.M.J., Dahly, D.L., Damen, J.A.A., Debray, T.P.A., et al. (2020). Prediction models for diagnosis and prognosis of covid-19 infection: systematic review and critical appraisal. *BMJ* 369, m1328.
- Yang, L., Liu, S., Liu, J., Zhang, Z., Wan, X., Huang, B., Chen, Y., and Zhang, Y. (2020). COVID-19: immunopathogenesis and immunotherapeutics. *Signal Transduct. Target. Ther.* 5, 128.
- Zhang, H., Penninger, J.M., Li, Y., Zhong, N., and Slutsky, A.S. (2020). Angiotensin-converting enzyme 2 (ACE2) as a SARS-CoV-2 receptor: molecular mechanisms and potential therapeutic target. *Intensive Care Med.* 46, 586–590.
- Zhao, B., Ni, C., Gao, R., Wang, Y., Yang, L., Wei, J., Lv, T., Liang, J., Zhang, Q., Xu, W., et al. (2020). Recapitulation of SARS-CoV-2 infection and cholangiocyte damage with human liver ductal organoids. *Protein Cell* 11, 771–775.
- Zhuo, L., Itano, N., Nonogaki, T., Shen, L., Wu, J., Watanabe, H., and Kimata, K. (2004). Chapter 9 - Biological Function of SHAP-Hyaluronan Covalent Complex. *Chemistry and Biology of Hyaluronan*, 205–222. <https://doi.org/10.1016/B978-008044382-9/50040-6>.

STAR★METHODS

KEY RESOURCES TABLE

REAGENT or RESOURCE	SOURCE	IDENTIFIER
Biological samples		
Human Serum	Sigma-Aldrich	Cat# S7023-50MB
Human Plasma (EDTA, Pooled Donor)	Genetex	Cat# GTX73265
Chemicals, peptides, and recombinant proteins		
Water for chromatography (LC-MS Grade)	Merck	Cat# 115333
LiChrosolv®		
Acetonitrile (Acetonitrile, Optima™ LC/MS Grade, Fisher Chemical™)	Fisher Scientific	Cat# A955-212
Methanol (Optima LC-MS Grade, Fisher Chemical)	Fisher Scientific	Cat# A456-212
DL-Dithiothreitol (BioUltra)	Sigma-Aldrich	Cat# 43815
Iodoacetamide (BioUltra)	Sigma-Aldrich	Cat# I1149
Ammonium Bicarbonate (Eluent additive for LC-MS)	Sigma-Aldrich	Cat# 40867
Urea (puriss. P.a., reag. Ph. Eur.)	Honeywell Research Chemicals	Cat# 33247H
Formic Acid, LC-MS Grade (Eluent additive for LC-MS)	Thermo Scientific™ Pierce™	Cat# 85178
Trypsin (Sequence grade)	Promega	Cat# V511X
Mass Spec-Compatible Human Extract	Promega	Cat# V6951
Retention time peptides Biognosys iRT kit	Biognosys	Cat# Ki-30002-b
MS synthetic peptide calibration kit	SCIEX	Cat# 5045759
Deposited Data		
Raw mass spectrometry proteomics data (commercial plasma and serum control samples)	This study	PXD025752
Software and algorithms		
Proteomics data analysis via Deep Neural Networks, DIA-NN	Demichev et al., 2020	https://github.com/vdemichev/DiaNN
DIA-NN R package	Demichev et al., 2020	https://github.com/vdemichev/diann-rpackage
ComplexHeatmap R package	(Gu et al., 2016)	https://github.com/jokergoo/ComplexHeatmap
EnvStats R package	(Millard, 2014)	https://CRAN.R-project.org/package=EnvStats
Limma R package	(Ritchie et al., 2015)	https://bioconductor.org/packages/limma/
eBayes R package	(Smyth, 2004)	https://github.com/cran/limma/blob/master/R/ebayes.R
XGBoost 1.2.0 Python package	(Chen and Guestrin, 2016)	https://pypi.org/project/xgboost/1.2.0/
scikit-learn 0.23.2 Python package	(Pedregosa et al., 2011)	https://scikit-learn.org/0.23/
scipy 1.5.2 Python package	(Virtanen et al., 2020)	https://pypi.org/project/scipy/1.5.2/
Other		
Zorbax RRHD Eclipse Plus 95A C18, 2.1 x 50mm, 1.8 um, 1200 bar	Agilent	Cat# 959757-902
Infinitylab Poroshell 120 EC-C18, 2.1x50mm 1.9um	Agilent	Cat# 699675-902
BioPureSPE Macro 96-Well, 100mg PROTO 300 C18	The Nest Group, Inc.	HNS S18V-L

RESOURCE AVAILABILITY

Lead contact

Further information and requests for resources and reagents should be directed to and will be fulfilled by the lead contact, Markus Ralser (markus.ralser@charite.de).

Materials availability

This study did not generate new unique reagents.

Data and code availability

- The processed proteomic and clinical source data is available in this paper's [supplemental information](#).
- The raw mass spectrometry proteomics source data for the quality control plasma and serum acquisitions has been deposited to the ProteomeXchange Consortium via the PRIDE partner repository ([Perez-Riverol et al., 2019](#)) with the dataset identifier PXD025752.
- This paper does not report original code.
- The machine learning scripts used to generate the figures reported in this paper are available in this paper's [supplemental information](#).
- Any additional information required to reproduce this work is available from the Lead Contact.

Experimental model and subject details

Charité patient cohort and clinical data

Patients were recruited within the Pa-COVID-19 study conducted at Charité - Universitätsmedizin Berlin, a prospective observational cohort study on the pathophysiology of COVID-19. The study protocol has been described in detail before ([Kurth et al., 2020](#)). All patients with PCR-confirmed SARS-CoV-2 infection were eligible for inclusion. Refusal to provide informed consent by the patient or a legal representative and any condition prohibiting supplemental blood collection for serial biosampling were exclusion criteria. Patients were treated according to current national and international guidelines. Three patients had *Do Not Intubate and Do Not Resuscitate* (DNI/DNR) orders in place, declining mechanical ventilation and other organ support or cardiopulmonary resuscitation. In 4 further cases, limitation of therapy was decided at a later time point according to the patient's presumed wish ("secondary DNR") and predictably unfavorable outcome. All other patients received maximum intensive care treatment including organ replacement therapies at the discretion of the responsible physicians.

Biosampling for proteome measurement was performed 3 times per week after inclusion. The WHO ordinal scale for clinical improvement ([Table S1](#)) was used to assess disease severity. ARDS was defined according to the Berlin ARDS criteria ([ARDS Definition Task Force et al., 2012](#)). Sepsis was defined according to sepsis-3 criteria ([Singer et al., 2016](#)). The study was approved by the ethics committee of Charité - Universitätsmedizin Berlin (EA2/066/20) and conducted in accordance with the Declaration of Helsinki and guidelines of Good Clinical Practice (ICH 1996). The study is registered in the German and the WHO international registry for clinical studies (DRKS00021688). Clinical data was captured in a purpose built electronic case report form data using the capture system SecuTrial®. All routine laboratory parameters were analyzed in accredited laboratories at Charité - Universitätsmedizin Berlin. Pseudonymized data exported from SecuTrial® were processed using JMP Pro 14 (SAS Institute Inc., Cary, NC, USA). If a laboratory value was missing for a given day, values from up to two preceding days were used for the analysis.

Innsbruck Patient cohort and clinical data

Serum samples from 99 patients admitted to the intensive care unit at the Department of Medicine, University Hospital of Innsbruck for the treatment of respiratory failure due to severe COVID-19 were collected within the first days (median 7.5, IQR 5-12) after admission. Written informed consent was either obtained before sampling or retrospectively after recovery, if patients were mechanically ventilated at the time of sampling. COVID-19 was diagnosed on the basis of a (i) positive SARS-CoV2 PCR within the last 7 days prior to study inclusion, (ii) respiratory failure defined as a partial pressure of oxygen < 60 mmHg on arterial blood gas analysis or a peripheral oxygen saturation of < 90% and (iii) typical infiltrates on computed tomography scanning of the chest. Patients were treated according to national guidelines. The study was approved by the local ethics research committee EK-Nr. 1107/2020, and EK-Nr. 1103/2020 for follow-up.

METHOD DETAILS

Materials

Water for chromatography (LC-MS Grade, LiChrosolv®, Merck; 115333), Acetonitrile (LC-MS Grade Optima; A955-212) and Methanol (LC-MS Grade, Optima; A456-212) were purchased from Fisher Chemicals. DL-Dithiothreitol (BioUltra, 43815), Iodoacetamide (BioUltra, I1149) and Ammonium Bicarbonate (Eluent additive for LC-MS, 40867) were purchased from Sigma Aldrich. Urea (puriss. P.a., reag. Ph. Eur., 33247H) and Formic Acid (Eluent additive for LC-MS, 85178) were purchased from Thermo Scientific. Trypsin

(Sequence grade, V511X) was purchased from Promega. Control samples were prepared from Human Serum (Sigma Aldrich, S7023-50MB) and Human Plasma (EDTA, Pooled Donor, Genetex GTX73265).

Mass spectrometry

Mass spectrometry-based proteomics analysis was performed as described previously (Messner et al., 2020) with minor adjustments to the workflow (Figure S1). Semi-automated sample preparation was performed in 96-well format, using in advance prepared stock solution plates stored at -80°C. Briefly, 5µl of thawed plasma samples were transferred to the pre-made denaturation/reduction stock solution plates (55µl 8M Urea, 100mM ammonium bicarbonate (ABC), 50mM dithiothreitol) resuspended and incubated at 30°C for 60 minutes. 5µl was then transferred from the iodoacetamide stock solution plate (100mM) to the sample plate and incubated in the dark at 23°C for 30 minutes before dilution with 100mM ABC buffer (340µl). 220µl of this solution was transferred to the pre-made trypsin stock solution plate (12.5µl, 0.1µg/µl) and incubated at 37°C for 17 h (Benchmark Scientific Incu-Mixer MP4). The digestion was quenched by addition of formic acid (10% v/v, 25µl). The digestion mixture was cleaned-up using C18 96-well plates (Bio-PureSPE Macro 96-Well, 100mg PROTO C18, The Nest Group) and redissolved in 60µl 0.1% formic acid with shaking. Insoluble particles were removed by centrifugation and the samples transferred to a new plate.

Each 96-well plate contained 8 plasma and 4 serum sample preparation controls, and the acquisition workflow included a pooled quality control sample every ~10 injections. Liquid chromatography was performed using the Agilent 1290 Infinity II system coupled to a TripleTOF 6600 mass spectrometer (SCIEX) equipped with IonDrive Turbo V Source (Sciex). A total of 5µl was injected, and the peptides were separated in reversed phase mode using a C18 ZORBAX Rapid Resolution High Definition (RRHD) column 2.1mm x 50mm, 1.8µm particles or Infinitylab Poroshell 120 EC-C18, 2.1 x 50mm 1.9 µm particles. A linear gradient was applied which ramps from 1% B to 40% B in 5 minutes (Buffer A: 0.1% FA; Buffer B: ACN/0.1% FA) with a flow rate of 800µl/min. For washing the column, the organic solvent was increased to 80% B in 0.5 minutes and was kept for 0.2 minutes at this composition before going back to 1% B in 0.1 min. The mass spectrometer was operated in the high sensitivity mode. The DIA/SWATH method consisted of an MS1 scan from m/z 100 to m/z 1500 (20 ms accumulation time) and 25 MS2 scans (25ms accumulation time) with variable precursor isolation width covering the mass range from m/z 450 to m/z 850 (Messner et al., 2020). An IonDrive Turbo V Source (Sciex) was used with ion source gas 1 (nebulizer gas), ion source gas 2 (heater gas) and curtain gas set to 50, 40 and 25, respectively. The source temperature was set to 450 and the ion spray voltage to 5500V. System suitability was evaluated using synthetic peptides (Sciex 5045759, Biognosys Ki-30002-b) and human protein extracts (Promega V6951).

QUANTIFICATION AND STATISTICAL ANALYSIS

Data analysis

The data were processed with DIA-NN (Demichev et al., 2020), an open-source software suite for DIA / SWATH data processing (<https://github.com/vdemichev/DiaNN>, commit 4498bd7) using a two-step spectral library refinement procedure as described previously (Messner et al., 2020), with filtering at precursor level q-value (1%), library q-value (0.5%) and gene group q-value (1%). Highly hydrophobic peptides (reference retention time > 110 on the iRT scale) were discarded. Batch correction was performed at the precursor level as described previously (Messner et al., 2020), using linear regression for intra-batch correction (for each MS batch) and control samples for inter-plate correction. Protein quantification was subsequently carried out using the MaxLFQ algorithm (Cox et al., 2014; Pham et al., 2020) as implemented in the DIA-NN R package (<https://github.com/vdemichev/diann-rpackage>). One of the 96-well plates (#12) featured technical replicates of a number of samples that were also analysed on other plates: in an extra batch correction step, the median log₂-protein levels across these replicates on plate 12 were matched to the respective median log₂-levels (across the same biological samples) throughout other plates, to correct protein levels on plate 12. Further batch correction was performed for Innsbruck data, to match the mean log₂-transformed protein levels in the respective control samples to log₂-transformed protein levels in control samples acquired for the Charité cohort. The Generation Scotland cohort proteomics raw data, which we described previously (Messner et al., 2020), have been reanalyzed using the updated software pipeline, to ensure comparability. Exclusion of precursors or proteins based on the data completeness was not performed.

Statistical testing was performed in the R environment for statistical computing, version 3.6.0 (R core team, www.R-project.org). All protein and clinical laboratory measurements (except for standard and actual base excess, oxyhemoglobin and sO2) were first log₂-transformed, to ensure optimal performance of linear models assuming Gaussian errors, as well as to reduce the impact of outliers. Imputation of the data was not performed, as all the statistical tests applied can accommodate missing values. Likewise, no data filtering based on missing value rates was applied. For differential abundance testing, only protein groups matched to at least three different unmodified peptide sequences were considered. Significance testing for a zero median (for analysing trajectories) or against binary variables (worsening, death) was performed using the Wilcoxon W test or Mann-Whitney U test, respectively, as implemented in the “wilcox.test” function of the “stats” R package. Testing against a continuous variable (e.g. when determining significance of pairwise correlations) was performed using the Kendall Tau test, with the slope estimated using the Theil-Sen method, as implemented in the “kendallTrendTest” function of the “EnvStats” (Millard, 2014) package. When covariates had to be taken into account, we used linear modelling with the “limma” (Ritchie et al., 2015) R package, with P-values obtained using “eBayes” (Smyth, 2004). Modelling with “limma” was likewise used to correct for these covariates for visualisation purposes. WHO grade was considered as a “factor-type” covariate (resulting in a “limma” design matrix with one-hot encoding for different WHO grades). Multiple-testing correction was performed using the Benjamini-Hochberg false discovery rate controlling procedure (Benjamini and Hochberg, 1995).

as implemented in the “*p.adjust*” function of the “*stats*” R package. The adjusted p-values below 0.05 were considered significant. Multiple-testing correction for differential abundance analysis was performed separately for proteins, for which MRMAssayDB lists a targeted assay (Bhowmick et al., 2018), the rest of proteins measured, the clinical laboratory measurements and the clinical factors (age, Charlson score, BMI, Horowitz index and FiO_2 , SOFA score), to ensure that the false discovery rate stayed below 0.05 for each of these categories of features. Likewise, when determining the significance of correlations in correlation matrices, correction was performed for each row or each column separately, to ensure less than 5% false discoveries in each row or column, respectively. For correlation map visualisations, black points were used to indicate row-wise significant correlations, and black rectangles at the border of the respective cell - column-wise significant correlations.

Quantities of gene products corresponding to open reading frames named IGxx (i.e. different types of immunoglobulin chains) were summed together to generate quantities representative of the overall levels of immunoglobulin classes (IGHVs , IGLVs , etc). This does not affect any conclusions of this work and was done purely to improve visualization and simplify the interpretation of the heatmaps and correlation maps. Full protein level tables, including levels of individual immunoglobulin gene products, are provided in supplementary materials. For visualisation, different WHO grades were color-coded throughout the manuscript (see [Figure S2](#)).

Markers of the disease severity

The first time point measured at the maximum WHO grade was chosen for each patient. For each omics feature, its values (\log_2 -transformed when necessary, as described above) were tested for a trend depending on the WHO grade. Age was included as a covariate in the linear model as described above.

Markers varying with age in COVID-19

The first sampling time point measured was chosen per patient. For each omics feature, its values (\log_2 -transformed when necessary, as described above) were tested for a trend depending on age. The test was performed either using the Kendall Tau test (as described above; [Figures S9](#) and [S10](#)), or by accounting for WHO grade as a covariate in the linear model (as described above; [Figures S11](#) and [5](#)).

Markers of RRT and ECMO

For each omics feature, the P-value was calculated using the Mann-Whitney test, comparing between the median levels (\log_2 -transformed when necessary, as described above) across all sampling time points at WHO grade 7 in patients who did not receive the therapy and the median levels (\log_2 -transformed when necessary, as described above) across all sampling time points at WHO grade 7 after initiation of the respective therapy in patients who did.

Markers predictive of time in hospital

Patients, for which the first sampling time point before the outcome corresponded to the WHO = 3 severity grade (that is the patient did not require supplemental oxygen on that day), were considered. Thus, no correction for disease severity was necessary. Testing of levels (\log_2 -transformed when necessary, as described above) of each omics feature (measured for the first sampling time point) vs the remaining time in hospital (days) was performed by including age as a covariate in the linear model as described above.

Markers predictive of disease worsening

The first sampling time point measured was chosen per patient. Future disease worsening was defined as a future increase in the WHO grade (for patients at WHO grade < 7) or death (for patients at WHO grade 7). For each omics feature, its levels (\log_2 -transformed when necessary, as described above) were compared between patients who did not worsen and patients who did, with age and current WHO grade (as factor) included as covariates in the linear model as described above.

Peak period of the disease definition

When studying the dynamic changes in omics values during the disease course, we focused on the time points sampled when the disease was the most severe for a particular patient. This allowed us to look at molecular changes over time without the need to take into account the potential impact of changes in disease severity and the level of treatment. For each patient, we thus defined the “peak period of the disease” as the time when the patient was receiving the most intensive treatment during their stay in hospital, that is the time when the patient was at WHO grade 6 or 7, for patients who received invasive mechanical ventilation at some point, or otherwise at their maximum WHO grade (3, 4 or 5).

Markers changing during the peak of disease

Only patients with at least two days between the first and last sampling time points at the peak of the disease (as defined above) were considered. For each omics feature, a linear regression model was fitted for its levels (\log_2 -transformed when necessary, as described above) vs the day number (with the slope estimated using the nonparametric Theil-Sen method, as implemented in the “*kendallTrendTest*” function of the “*EnvStats*” (Millard, 2014) R package), and the quantity $\text{slope}_{\text{adj}} = (\text{regression slope}) * (\text{number of days between first and last time points})$ was calculated. A non-parametric approach was chosen because of its superior robustness to outliers. A Wilcoxon W test was then applied to compare the median of $\text{slope}_{\text{adj}}$ to zero. The values of $\text{slope}_{\text{adj}}$ for each feature are visualised in [Figure S14](#). The non-parametric approach was chosen here due to its robustness with respect to outliers.

Correlation maps

General correlation maps were generated using the values (\log_2 -transformed when necessary, as described above) of features at the first time point measured at the maximum WHO grade for each patient. The correlation map between feature changes during the peak of the disease (as defined above) was generated by correlating the slope_{adj} values (as defined above). The map of significant protein correlations not detected in the general population was generated by excluding all correlations which were either significant ($P <= 0.05$, without multiple-testing correction) with the same trend in the Generation Scotland cohort, or could not be calculated reliably therein (less than 20 valid points).

Prediction of current mechanical ventilation

To reflect the power of omics measurements in characterising the phenotype, a classifier was constructed to predict mechanical ventilation (WHO grade > 5) at the present time point using the proteomic and/or accredited diagnostic data. For the proteomic data only proteins characterized by at least 3 peptides were taken into account. The first time point measured at the maximum WHO grade was selected per patient. We used a gradient boosted tree algorithm implemented in the XGBoost 1.2.0 (Chen and Guestrin, 2016) under Python 3.8.1. The classifier was constructed using leave-one-out cross-validation. To circumvent overfitting a subsampling of 0.5 of the training data per boosting step and an L2 regularization term “lambda” of 20 were applied.

For the assessment of classifier performance, the leave-one-out method was applied in the following way: the prediction was made for each sample separately, by excluding (withholding) this sample from the dataset, training the classifier on the remaining (independent) samples and then predicting the withheld sample using the trained model. The source code is provided in supplementary materials. For the determination of the feature importances, one classifier was trained on all data points using the same setup as described above. The feature importances were then extracted directly from the trained classifier.

For the validation of the trained models, samples from an independent cohort (Innsbruck) were used. A model was trained on the data collected at the Charité using the same setup and parameters as described above and the proteins that were characterized in both cohorts. The evaluation was performed on the Innsbruck cohort that was not used for training. ROC-curves and AUC were calculated using scikit-learn 0.23.2 (Pedregosa et al., 2011). The machine learning scripts are provided in [Data S1](#).

WHO grade prediction

For the prediction of the WHO grade an elastic net was applied as implemented in scikit-learn 0.23.2. The WHO grade was predicted for the first time point at maximum WHO grade per patient using a leave-one-out cross-validation procedure. A training/prediction based on proteomic (proteins with at least 3 peptides) and/or accredited diagnostic data from the Charité cohort was performed. Additionally, the proteomic model was validated using proteomic data set from the Innsbruck cohort that was not included in the training. Features with more than 10% missing values were removed. All data were \log_2 -transformed when necessary (as described above), standardized and kNN-imputed (5 neighbors). The latter two steps were fitted on the training data only. For the elastic net an “l1_ratio” of 0.05 was used coupled to a 5-fold cross-validated recursive feature-elimination algorithm (“step” = 10, “min_features” = 20). Calculations of metrics were performed using scikit-learn 0.23.2 and scipy 1.5.2 (Virtanen et al., 2020). The machine learning scripts are provided in [Data S1](#).

Prediction of the remaining time in hospital

For the prediction of the remaining time in hospital a WHO grade predictor as described above was trained on the first data points for every patient. The predicted WHO grades for every patient at WHO grade 3 who stayed in hospital for at least 1 day after sample time were correlated to the remaining time in hospital. The Spearman correlation was calculated using scipy 1.5.2. The machine learning scripts are provided in [Data S1](#).

Supplementary Note 1. Diagnostic parameters and Proteome signatures that indicate therapeutic interventions

We investigated to what extent specific organ replacement therapies in severely ill patients, (renal replacement therapy (RRT) and extracorporeal membrane oxygenation (ECMO)) were reflected in the proteome and at the level of accredited diagnostic parameters. HP and HPX were reduced in patients on RRT and ECMO, reflecting hemolysis in the extracorporeal circuits (Figures S7 and S8). Elevated SERPINC1 (Antithrombin III) levels mirror substitution of antithrombin during ECMO. The reason for elevated levels of APOE in patients with ECMO is unclear, but is in line with reports on increased levels of APOE in pediatric patients after cardiopulmonary bypass (Ağırbaşlı et al., 2015). The proteins increased in patients receiving RRT mainly reflect impaired kidney function and have been associated with RRT before (AMBP, B2M, CST3, LYZ, RBP4, Figure S7) (Shao et al., 2015). Of note, increased levels of AMBP, B2M and LYZ have been associated with death in chronic kidney disease (Makridakis et al., 2020). Levels of CFD and APOH, both involved in the complement system, were also increased (McDonnell et al., 2020; Volanakis and Narayana, 1996). CFD is eliminated renally and accumulates in end stage renal disease, possibly leading to enhanced complement activation via the alternative pathway (Pascual et al., 1988). In contrast, levels of APOH have even been reported to be slightly lower following high-flux hemodialysis (Han et al., 2018).

We note that the analysis of the effect of treatments on the proteome has two limitations. First, some of the markers identified might be prognostic for the treatment rather than reflect its effect. Age and the Charlson comorbidity index belong to this category: patients receiving ECMO were significantly younger and had a lower number of pre-existing chronic conditions than those who did not.

Second, the results might be partially confounded by the time elapsed from the onset of the disease, as we have shown (Figure 3) that omics signature changes with time in COVID-19 patients while on invasive mechanical ventilation.

Supplementary Note 2. Age-specific response to COVID-19 in the context of severity markers

Older age is one of the most significant risk factors for severe disease and adverse outcome in COVID-19. Enhanced understanding of underlying mechanisms for the age-specific response to SARS-CoV-2 infection is therefore important and needed for the development of effective age-specific strategies for prevention and treatment. Furthermore, dissecting the age-specific components of the host response will improve our knowledge of the pathogenicity of similar viruses, making the world better prepared for future pandemics. Current theories characterizing the link between the higher age and risk for severe disease include immunosenescence, elevated baseline inflammation, or altered protein glycosylation landscape leading to impaired antiviral response or reduced immune tolerance (Franceschi et al., 2018; Gorony and Weyand, 2013; Rea et al., 2018; Tay et al., 2020). However, a detailed and mechanistic understanding of the relation between COVID-19 and aging is lacking. In this work, we leverage the large size and high precision of the proteomic data acquired to map the age-related response to COVID-19, to provide a reference dataset (Figures 2C, 5, and S11) for future studies addressing this problem.

We report elevation of several inflammatory and acute phase proteins such as SERPINA3, ITIH4, SAA1, and ITIH3 in older patients with COVID-19. SAA1 has been shown to induce macrophage polarization to the M2-type which promotes tissue repair but also possesses pro-fibrotic properties involved in the pathogenesis of pulmonary fibrosis (Liu et al., 2014; Page et al., 2012; Wermuth and Jimenez, 2015). Moreover, SAA1 mediates displacement of APOA1 from HDL leading to loss of the cardio- and vasoprotective properties of high density lipoprotein (HDL) (Gordon, 2014). SERPINA3, as discussed above, has an ambivalent role as a neutrophil proteinase inhibitor but also a powerful neutrophil chemoattractant. Upregulation of SERPINA3 with age in COVID-19, along with the higher neutrophil-to-lymphocyte ratio, suggests that excessive neutrophil response is one of the aggravating factors in older COVID-19 patients. Taken together, our findings point toward a disproportionately dysregulated inflammatory response to SARS-CoV-2 with age, which may be explained by an increased baseline inflammation and immunosenescence in older patients (Chung et al., 2019; Ferrucci et al., 2005; Soysal et al., 2016). Age-dependent increase of FBLN1 and decrease of KLKB1 reflect alterations in blood coagulation which may aggravate this effect by predisposing older patients to thromboembolic events, one of the key clinical characteristics of severe COVID-19.

Interestingly, a number of apolipoproteins displayed a strong age-specific signature in COVID-19. For instance, APOC2, a component of chylomicrons, very low density lipoprotein (VLDL) and high density lipoprotein (HDL), and activator of lipoprotein lipase involved in triglyceride metabolism (Ramasamy, 2014), was downregulated with age in COVID-19, but upregulated with age in the general population (Harris et al., 2017; Peters et al., 2015) (Figure 2C). Dysregulation of apolipoproteins has been observed in community acquired pneumonia and associated with unfavourable outcome (Sharma et al., 2017). Remarkably, contrary to the general trend, APOD, APOC3 and APOE show opposite trends in older COVID-19 patients and in severe disease (Figure 5). APOD is expressed by many tissues, including the brain (Dassati et al., 2014). An increase in APOD has been previously observed in ischemic stroke and CNS inflammation and may reflect (subclinical) involvement of the central nervous system especially in older patients with more severe inflammation and more comorbidities (Muffat and Walker, 2010). Conversely, high levels of APOD have been shown to temper coronavirus-mediated encephalitis in mice, indicating its role as a marker of CNS damage as well as tissue protection and repair (Carmo et al., 2008). APOE, involved in inflammation, immune response and lipid metabolism, is upregulated in severe COVID-19 but downregulated with age in this cohort. APOE typically mediates anti-inflammatory effects by downregulation of NF κ B and inhibition of macrophage response to IFN γ and TLR3, both mediators of viral immune response. Moreover, it neutralizes bacterial LPS and enhances the adaptive immune response by facilitating antigen presentation (Figuerola et al., 2019). Downregulation with age may reflect a compromised immune response leading to over-activation of NF κ B and insufficient pathogen clearance in older patients. Finally, APOE has been described to reduce proliferation of myeloid progenitor cells (Murphy et al., 2011) and to reduce myeloid derived suppressor cell (MDSC) survival in mice (Tavazoie et al., 2018). Thus, lower levels of APOE in the elderly may favor expansion of immature and dysfunctional neutrophils that have been described as a hallmark in severe COVID-19 (Schulte-Schrepping et al., 2020). This broad involvement of APOE merits further investigation in future studies.

Supplementary Note 3. Diverging trends at the proteome level during the disease peak in individual patients

Some patients (59, 90, 96, 123) who died exhibited protein concentration trajectories distinctly similar to “typical” survivors (Figure 3B). Two of them (59, 90) had a prolonged ICU stay with repeated septic episodes and finally defined limitations of therapy according to presumed patients’ wishes (“secondary DNR”). Their protein signatures probably reflect the phenomenon of immune paralysis that can follow bacterial sepsis associated with a prolonged ICU treatment (Patricio et al., 2019). One patient (96) was receiving ongoing immunosuppressive therapy for an autoimmune disorder, and a fourth patient (123) had a history of kidney transplantation, both died of septic shock. Whether the particular group of solid organ recipients shows a distinct protein signature associated with the outcome requires further investigation.

We also note that some surviving patients do not show a trajectory characteristic of the typical ‘alleviation’ of the proteomic phenotype (WHO = 4: 58, 106, 153; WHO = 6 or 7: 43, 80). Specifically, the proteomic response in patients 106, 153 and 141 was indicative of overall ‘worsening’ of the proteome (Figure 3B). In contrast, patients 43 and 80 exhibited the overall ‘alleviation’ of the proteome, except for the spike in the levels of CRP and serum amyloid (Figure 3B). Shorter time spans between sampling days may explain these observations in four of these patients (43, 58, 80, 106), indicating that the host inflammatory response requires a certain time to resolve, especially in more severely ill patients, and some of the markers of systemic inflammation might linger, whereas a typical alleviation of the proteomic signature can be observed even within a few days in moderate disease courses. The unusual pattern of patient 153 was likely confounded by a skin infection that subsequently required antibiotic treatment.



Association of inflammatory markers with the severity of COVID-19: A meta-analysis



Furong Zeng^{a,b,1}, Yuzhao Huang^{c,1}, Ying Guo^{a,b}, Mingzhu Yin^{a,b}, Xiang Chen^{a,b}, Liang Xiao^{d,**}, Guangtong Deng^{a,b,*}

^a Department of Dermatology, Hunan Engineering Research Center of Skin Health and Disease, Hunan Key Laboratory of Skin Cancer and Psoriasis, Xiangya Hospital, Central South University, Changsha, Hunan 410008, China

^b National Clinical Research Center for Geriatric Disorders, Xiangya Hospital, Central South University, Changsha, Hunan 410008, China

^c Department of Orthopaedics, The Third Xiangya Hospital, Central South University, Changsha, Hunan 410008, China

^d Department of General Surgery, Xiangya Hospital, Central South University, Changsha, Hunan 410008, China

ARTICLE INFO

Article history:

Received 1 April 2020

Received in revised form 9 May 2020

Accepted 14 May 2020

Keywords:

COVID-19

SARS-CoV-2

Inflammatory markers

Severity

Meta-analysis

ABSTRACT

Objectives: Studies reported associations of inflammatory markers with the severity of COVID-19, but conclusions were inconsistent. We aimed to provide an overview of the association of inflammatory markers with the severity of COVID-19.

Methods: We searched PubMed, Embase, Cochrane Library, Wanfang and China National Knowledge Infrastructure (CNKI) database until March 20, 2020. Weighted mean difference (WMD) and 95% confidence intervals (CIs) were pooled using random or fixed-effects models.

Results: A total of 16 studies comprising 3962 patients with COVID-19 were included in our analysis. Random-effect results demonstrated that patients with COVID-19 in the nonsevere group had lower levels for CRP (WMD = -41.78 mg/l, 95% CI = [-52.43, -31.13], P < 0.001), PCT (WMD = -0.13 ng/ml, 95% CI = [-0.20, -0.05], P < 0.001), IL-6 (WMD = -21.32 ng/l, 95% CI = [-28.34, -14.31], P < 0.001), ESR (WMD = -8 mm/h, 95% CI = [-14, -2], P = 0.005), SAA (WMD = -43.35 µg/ml, 95% CI = [-80.85, -5.85], P = 0.020) and serum ferritin (WMD = -398.80 mg/l, 95% CI = [-625.89, -171.71], P < 0.001), compared with those in the severe group. Moreover, survivors had a lower level of IL-6 than non-survivors (WMD = -4.80 ng/ml, 95% CI = [-5.87, -3.73], P < 0.001). These results were consistent through sensitivity analysis and publication bias assessment.

Conclusions: The meta-analysis highlights the association of inflammatory markers with the severity of COVID-19. Measurement of inflammatory markers might assist clinicians to monitor and evaluate the severity and prognosis of COVID-19.

© 2020 The Author(s). Published by Elsevier Ltd on behalf of International Society for Infectious Diseases. This is an open access article under the CC BY-NC-ND license (<http://creativecommons.org/licenses/by-nc-nd/4.0/>).

Introduction

The ongoing worldwide Coronavirus Disease 2019 (COVID-19) pandemic has posed a huge threat to global public health (WHO, 2020a). The pathogen has been identified as a novel single-stranded ribonucleic acid (RNA) betacoronavirus named as severe acute respiratory syndrome coronavirus 2 (SARS-CoV-2), which shares an approximately 79% similarity at nucleotide level with

severe acute respiratory syndrome coronavirus (SARS-CoV) (Zhang and Holmes, 2020). As of March, 21, 2020, a total of 266, 073 confirmed cases from 150 countries and territories were reported, including 11,183 deaths (WHO, 2020b). COVID-19 represents a spectrum of clinical severity ranged from asymptomatic to critical pneumonia, acute respiratory distress syndrome (ARDS) and even death (Guan et al., 2020). Therefore, full monitoring the severity of COVID-19 and effective early intervention are the fundamental measures for reducing mortality.

Accumulating evidence has suggested that inflammatory responses play a critical role in the progression of COVID-19 (Mehta et al., 2020; Stebbing et al., 2020). Inflammatory responses triggered by rapid viral replication of SARS-CoV-2 and cellular destruction can recruit macrophages and monocytes and induce the release of cytokines and chemokines (Tay et al., 2020). These cytokines and chemokines then attract immune cells and activate immune

* Corresponding author at: Department of Dermatology, Xiangya Hospital, Central South University, 87# Xiangya Road, Changsha, 410008, Hunan, China.

** Corresponding author.

E-mail addresses: xiaoliangrick@csu.edu.cn (L. Xiao), dengguangtong@outlook.com (G. Deng).

¹ These authors contributed equally to this work.

responses, leading to cytokine storms and aggravations (Xu et al., 2020). Several inflammatory markers have some tracing and detecting accuracy for disease severity and fatality (Wu et al., 2020). Inflammatory markers such as procalcitonin (PCT), serum ferritin, erythrocyte sedimentation rate (ESR), C-reactive protein (CRP) and interleukin-6 (IL-6) have been reported to be significantly associated with the high risks of the development of severe COVID-19 (Cheng et al., 2020; Gao et al., 2020; Qin et al., 2020). Moreover, increased levels of serum amyloid A (SAA) are shown to be involved in COVID-19 pathogenesis and may serve as a potential biomarker for monitoring disease progression (Cheng et al., 2020; Xiang et al., 2020). However, these results remain controversial due to no observed difference in the levels of IL-6, SAA, ESR and CRP by other studies (Chen et al., 2020b; Wu et al., 2020; Zhang et al., 2020).

To the best of our knowledge, the overall inflammatory profile is missing to date due to the insufficient sample size. Here we performed a meta-analysis based on the current scientific literature to compare the levels of inflammatory markers between severe patients and nonsevere patients with COVID-19. Our study will highlight the association of inflammatory markers with the severity of COVID-19 and assist clinicians to monitor and evaluate the severity and prognosis of COVID-19.

Methods

Search strategy

This meta-analysis was performed according to the Preferred Reporting Items for Systematic Reviews and Meta-Analyses (PRISMA) guidelines (Moher et al., 2009). Original studies

reporting COVID-19 were searched until March 20, 2020 through PubMed, Embase, Cochrane Library, Wanfang and China National Knowledge Infrastructure (CNKI) database. The following combined search terms were used in PubMed, Embase and Cochrane: ("Novel coronavirus" OR "Coronavirus disease 2019" OR "Coronavirus 2019" OR "nCoV-2019" OR "2019-nCoV" OR "COVID-19" OR "SARS-CoV-2"). The Chinese translation of the search terms was used in Wanfang and CNKI database. We did not apply any restriction on language or date or study design. All eligible articles were retrieved, and their references to identified publications were searched for further potentially relevant articles (Gao et al., 2020; Zhou et al., 2020a).

Selection criteria

English-language or Chinese-language publications reporting levels of inflammation markers in patients with COVID-19 were included if they met the following criteria: (1) patients were diagnosed with COVID-19 and had positive results of SARS-CoV-2 RNA; (2) patients could be grouped into severe group and nonsevere group, or intensive care unit (ICU) group and non-ICU group, or survivors group and non-survivors group; (3) literature sources and levels of inflammatory markers were available. The diagnosis and severity classification of COVID-19 was based on the New Coronavirus Pneumonia Prevention and Control Program in China (National Health Commission of China, 2020), which classified COVID-19 into four types including mild, moderate, severe, and critical pneumonia. In our meta-analysis, severe or critical COVID-19 patients were grouped into the severe group, and mild or moderate COVID-19 patients were grouped into the

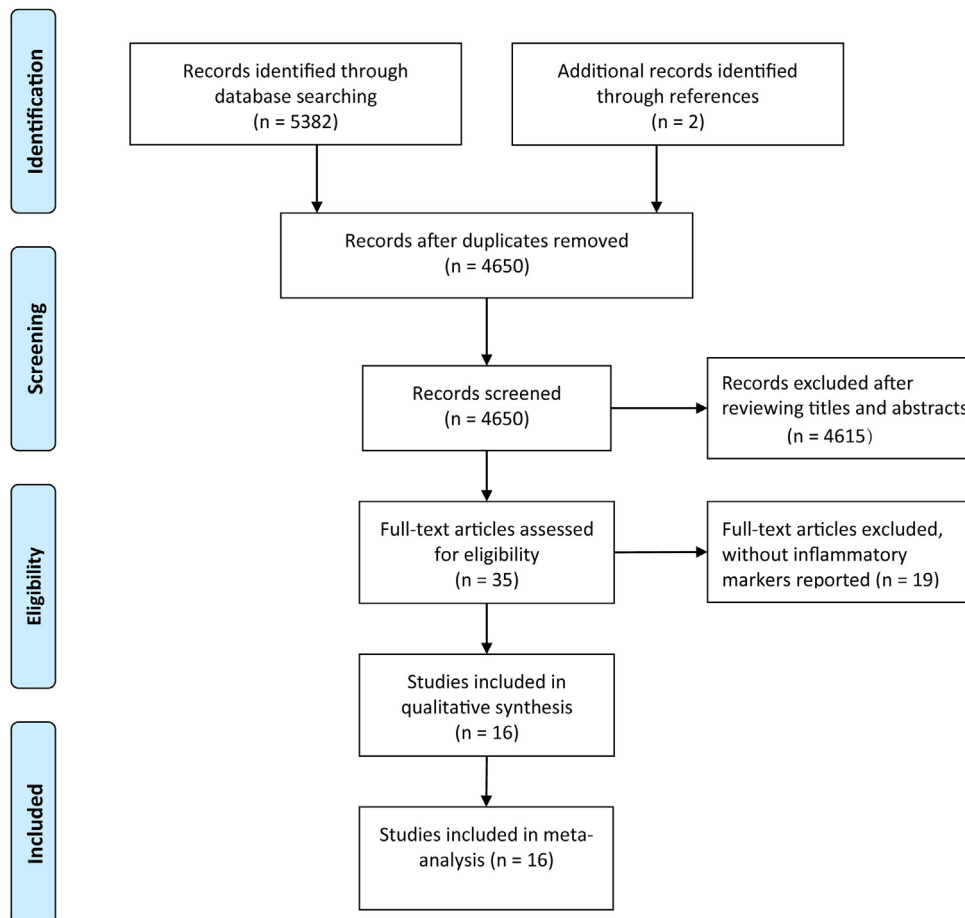


Figure 1. Literature search and filtering of studies.

nonsevere group. If there were two or more studies from the same authors or institutions, only the study with the largest sample size was chosen. Studies were excluded if patients were asymptomatic carriers and did not fulfil the inclusion criteria.

Data extraction and quality assessment

The records from the initial search were scanned by two authors to exclude any duplicate and irrelevant studies. The following data were extracted: first authors, publication date, country of origin, grouping situation, cases, age, sex and levels of inflammatory markers in different groups. Stratified data or interquartile range (IQR) were converted to mean (\pm SD) using mathematical formulas for meta-analysis (Luo et al., 2018; Wan et al., 2014). Any discrepancies were resolved by discussion. Quality assessments of all potentially eligible studies were conducted using the Newcastle-Ottawa Scale (NOS). There are eight items in three aspects: selection, comparability and exposure. The full score was 9 stars. Four to six stars was regarded as a moderate-quality study, and seven to nine stars as a high-quality study (Ga Wells et al., 2014). Studies with NOS scores lower than 7 were recognized to be of inferior quality and therefore excluded.

Statistical analysis

All the statistical analyses were carried out by STATA (Version 12.0; STATA Corporation, College Station, TX, USA) software. Statistical heterogeneity was assessed with I^2 and P-value. A fixed effects model was adopted without significant heterogeneity ($I^2 \leq 50\%$ and $P \geq 0.1$), while a random effects model was employed in all other instances ($I^2 > 50\%$ or $P < 0.1$) (Zeng et al., 2019; Zeng et al., 2020). Weighted mean difference (WMD) with 95% confidence interval (95% CI) was calculated for inflammatory

markers. Sensitivity analysis was performed by omitting one study each time through influence analysis to assess the stability of results. Additionally, standard mean difference (SMD) was used to explore the consistency of the conclusion. Publication bias was evaluated by Egger's test. If publication bias was conformed, the Duval's trim and fill method was implemented to adjust for this bias. $P < 0.05$ was considered statistically significant.

Results

Literature search and studies characteristics

The initial literature search generated altogether 5384 records with 734 studies subsequently excluded due to duplication (Figure 1). After a review of the titles and abstracts, we obtained 35 studies by excluding an additional 4615 studies. We further excluded 19 studies by scanning the full text which did not report inflammatory markers. Finally, 16 studies were included in our analysis (Chang et al., 2020; Chen et al., 2020a; Chen et al., 2020b; Cheng et al., 2020; Fang et al., 2020; Gao et al., 2020; Huang et al., 2020; Li et al., 2020; Peng et al., 2020; Qin et al., 2020; Ruan et al., 2020; Wu et al., 2020; Xiang et al., 2020; Xiao et al., 2020; Zhang et al., 2020; Zhou et al., 2020a). Characteristics of 16 eligible studies are presented in Table 1. All of these studies were published in 2020 and from China, involving 3962 patients. Eight studies were written in Chinese and the others in English. Twelve studies were grouped by nonsevere and severe groups, 2 studies grouped by non-ICU and ICU groups, and 2 studies grouped by survivors and non-survivors with COVID-19. Obviously, patients in the severe group, ICU group or non-survivors group were older than those in the corresponding control group. There was no obvious difference in the sex distribution of patients for each study. All studies were deemed of high quality with 7 or more NOS scores and details can be found in Table 2.

Table 1
Characteristics of enrolled studies in the meta-analysis.

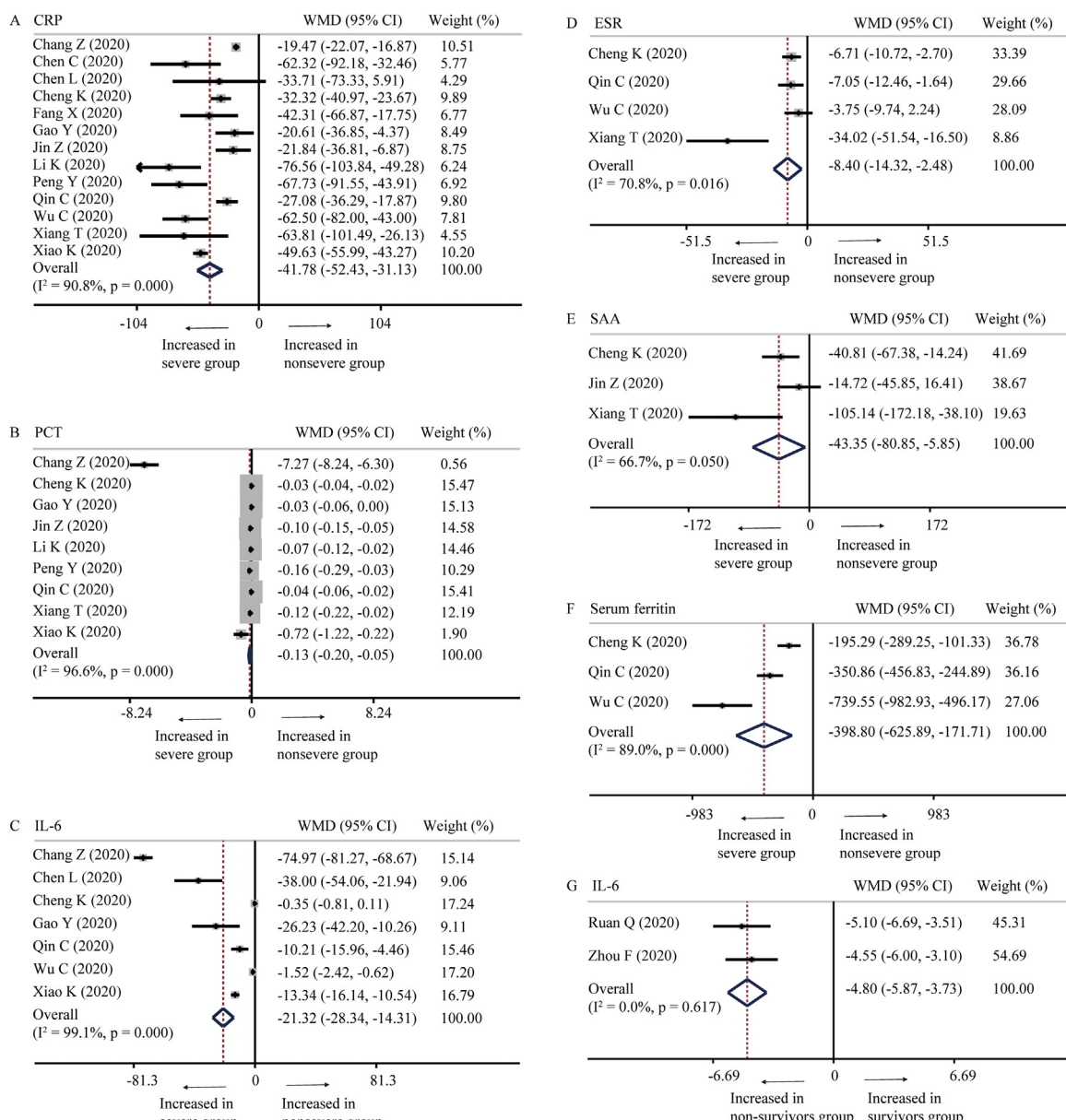
First author	Year	Country	Groups	Cases	Age	Sex (male, %)	Inflammatory markers	Quality
Chang Z	2020	China	Nonsevere	93	–	–	CRP, PCT, IL-6	8
			Severe	57				
Chen C	2020	China	Nonsevere	126	57.0 ± 15.6	66 (52.3)	CRP	7
			Severe	24	68.5 ± 13.6	18 (75.0)		
Chen L	2020	China	Nonsevere	15	–	–	IL-6, CRP	7
			Severe	14				
Cheng K	2020	China	Nonsevere	282	49.7 ± 11.9	145 (51.4)	IL-6, CRP, PCT, ESR, SAA, Serum ferritin	8
			Severe	181	54.7 ± 13.5	99 (54.7)		
Fang X	2020	China	Nonsevere	55	39.9 ± 14.9	27 (49.1)	CRP	7
			Severe	24	56.7 ± 14.4	18 (75.0)		
Gao Y	2020	China	Nonsevere	28	43.0 ± 14.0	17 (60.7)	IL-6, CRP, PCT, fibrinogen	9
			Severe	15	45.2 ± 7.7	9 (60.0)		
Jin Z	2020	China	Nonsevere	82	51.6 ± 10.7	38 (46.3)	CRP, PCT, SAA	7
			Severe	56	62.7 ± 13.6	33 (56.9)		
Li K	2020	China	Nonsevere	58	41.9 ± 10.6	29 (50.0)	CRP, PCT	7
			Severe	25	53.7 ± 12.3	15 (60.0)		
Peng Y	2020	China	Nonsevere	96	61.5 ± 9.4	44 (45.8)	CRP, PCT	8
			Severe	16	58.2 ± 7.3	9 (56.3)		
Qin C	2020	China	Nonsevere	166	52.0 ± 15.5	80 (48.2)	IL-6, CRP, PCT, ESR, Serum ferritin	7
			Severe	286	60.3 ± 13.4	155 (54.2)		
Wu C	2020	China	Nonsevere	117	47.3 ± 10.5	68 (58.1)	IL-6, CRP, ESR, Serum ferritin	7
			Severe	84	59.2 ± 14.3	60 (71.4)		
Xiang T	2020	China	Nonsevere	40	40.6 ± 14.3	25 (63.5)	CRP, PCT, ESR, SAA	8
			Severe	9	53.0 ± 14.0	8 (88.9)		
Xiao K	2020	China	Nonsevere	107	43.1 ± 1.1	52 (48.6)	IL-6, CRP, PCT	7
			Severe	36	51.3 ± 5.6	20 (55.6)		
Huang C	2020	China	Non-ICU	28	49.2 ± 12.9	19 (68.0)	PCT	9
			ICU	13	50.5 ± 16.6	11 (85.0)		
Ruan Q	2020	China	Survivors	82	51.6 ± 7.6	53 (65.0)	IL-6, CRP	7
			Non-survivors	68	64.3 ± 14.0	49 (72.0)		
Zhou F	2020	China	Survivors	137	51.6 ± 9.7	81 (59.0)	IL-6, PCT, Serum ferritin	7
			Non-survivors	54	69.4 ± 9.9	38 (70.0)		

CRP: C-reactive protein; PCT: procalcitonin; IL-6: interleukin-6; ESR: erythrocyte sedimentation rate; SAA: serum amyloid A.

Table 2

Methodological quality of enrolled studies based on Newcastle-Ottawa Scale (NOS).

Included studies	Year	Is the definition adequate?	Representativeness of the cases	Selection of controls	Definition of controls	Comparability of both groups	Ascertainment of diagnosis	Same ascertainment method for both groups	Nonresponse rate	Total scores
Chang Z	2020	☆	☆	☆	☆	☆	☆	☆	☆	8
Chen C	2020	☆	☆	☆	☆	—	☆	☆	☆	7
Chen L	2020	☆	☆	☆	☆	—	☆	☆	☆	7
Cheng K	2020	☆	☆	☆	☆	☆	☆	☆	☆	8
Fang X	2020	☆	☆	☆	☆	—	☆	☆	☆	7
Gao Y	2020	☆	☆	☆	☆	☆☆	☆	☆	☆	9
Jin Z	2020	☆	☆	☆	☆	—	☆	☆	☆	7
Li K	2020	☆	☆	☆	☆	—	☆	☆	☆	7
Peng Y	2020	☆	☆	☆	☆	☆	☆	☆	☆	8
Qin C	2020	☆	☆	☆	☆	—	☆	☆	☆	7
Wu C	2020	☆	☆	☆	☆	—	☆	☆	☆	7
Xiang T	2020	☆	☆	☆	☆	☆	☆	☆	☆	8
Xiao K	2020	☆	☆	☆	☆	—	☆	☆	☆	7
Huang C	2020	☆	☆	☆	☆	☆☆	☆	☆	☆	9
Ruan Q	2020	☆	☆	☆	☆	—	☆	☆	☆	7
Zhou F	2020	☆	☆	☆	☆	—	☆	☆	☆	7

**Figure 2.** Forest plot of inflammatory markers. (A–F) Forest plot between nonsevere and severe groups for levels of CRP (A), PCT (B), IL-6 (C), ESR (D), SAA (E), and serum ferritin (F); G. Forest plot between survivors group and non-survivors group for levels of IL-6.

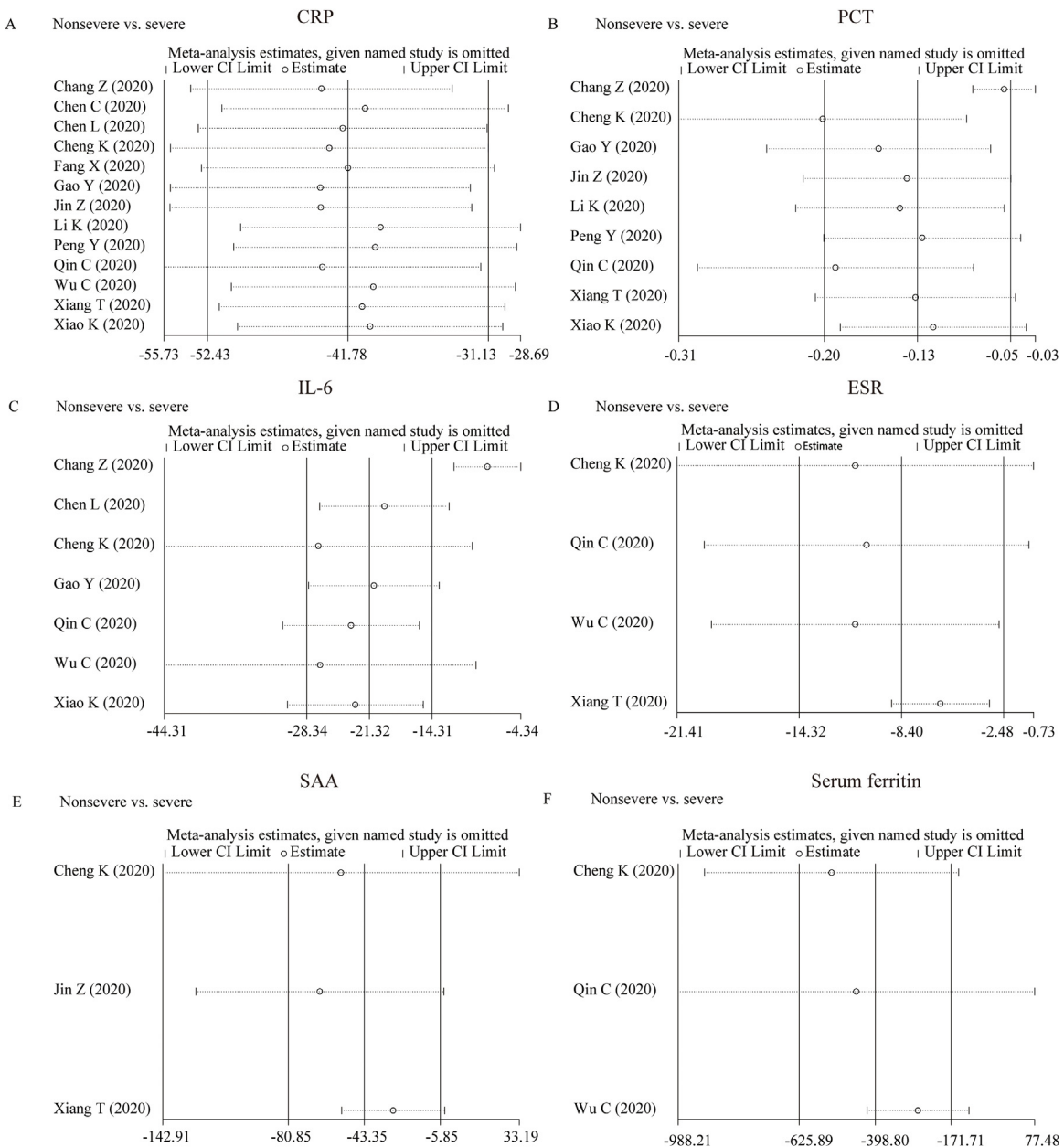


Figure 3. Sensitivity analyses. (A–F) Sensitivity analyses between nonsevere and severe groups for levels of CRP (A), PCT (B), IL-6 (C), ESR (D), SAA (E), and serum ferritin (F).

Association of inflammatory markers with the severity of COVID-19

For the patients stratified by severity of COVID-19, random-effect results demonstrated that compared with patients in the severe group, patients in the nonsevere group had lower levels for CRP (WMD = -41.78 mg/l, 95% CI = -52.43, -31.13], P < 0.001), PCT (WMD = -0.13 ng/ml, 95% CI = [-0.20, -0.05], P < 0.001), IL-6 (WMD = -21.32 ng/l, 95% CI = [-28.34, -14.31], P < 0.001), ESR (WMD = -8 mm/h, 95% CI = [-14, -2], P = 0.005), SAA (WMD = -43.35 µg/ml, 95% CI = [-80.85, -5.85], P = 0.020) and serum ferritin (WMD = -398.80 mg/l, 95% CI = [-625.89, -171.71], P < 0.001) (Figure 2A–F). Additionally, there are two studies grouped by survivors and non-survivors with COVID-19 reporting the level of IL-6, and fixed-effect results arrived at a similar conclusion that survivors had lower levels for IL-6 than non-survivors with COVID-19 (WMD = -4.80 ng/ml, 95% CI = [-5.87, -3.73], P < 0.001) (Figure 2G).

Additionally, one study on the level of fibrinogen between the nonsevere group and severe group, one study on the level of PCT between the non-ICU group and ICU group, and one study on the level of CRP and PCT between non-survivors and survivors, were not included in the meta-analysis due to their inadequate data; however, the results reported by these studies were consistent with the pooled results of our meta-analysis.

Investigation of heterogeneity

Strong evidence of heterogeneity was found in all the comparisons (Figure 2). Sensitivity analyses indicated that the results were not influenced by excluding any one specific study in CRP, PCT, IL-6 and ESR between the nonsevere and severe groups (Figure 3A–D). As for SAA and serum ferritin, the conclusions changed when deleting Cheng K's study and Qin C's study, separately, while the heterogeneity became larger,

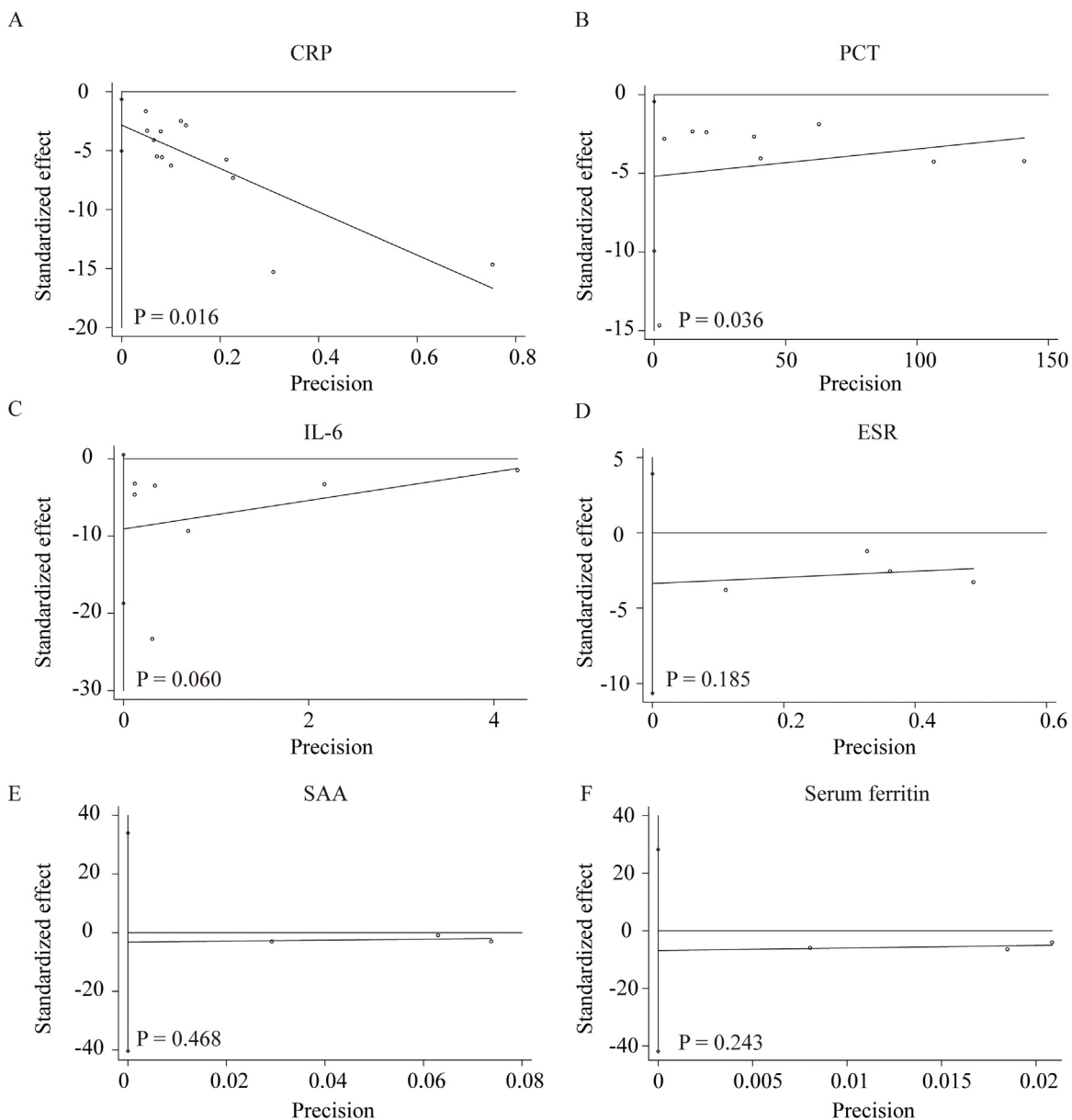


Figure 4. Publication bias by Egger's test. (A–F) Publication bias by Egger's test between nonsevere and severe groups in CRP (A), PCT (B), IL-6 (C), ESR (D), SAA (E), and serum ferritin (F).

suggesting that it is better to keep these studies in the meta-analysis (Figure 3E and F). Egger's test was conducted to evaluate the publication bias (Figure 4). No significant publication bias was detected in most of the studies except for CRP ($P = 0.012$) and PCT ($P = 0.036$). When applying the trim-and-fill method, there were no trials trimmed and filled in CRP. Regarding PCT, after filling one trial, the revised result was still consistent using a random model ($WMD = -0.17 \text{ ng/ml}$, $95\% \text{ CI} = [-0.26, -0.08]$, $P < 0.001$) or fixed model ($WMD = -0.06 \text{ ng/ml}$, $95\% \text{ CI} = [-0.07, -0.05]$, $P < 0.001$). Additionally, using standard mean difference (SMD) for the meta-analysis still did not change the conclusions (Table 3).

Discussion

COVID-19, caused by SARS-CoV-2, is rapidly expanding worldwide. Despite the fact that most cases have mild symptoms and a good prognosis, COVID-19 can develop into ARDS and even

death. To date, there is no effective therapy for COVID-19 (Li and De Clercq, 2020; Russell et al., 2020). Therefore, it is imperative to identify the markers monitoring the progression of disease and treat patients early.

Several studies have shown increased proinflammatory cytokines in serum of COVID-19 patients. Also, anti-inflammatory agents for COVID-19 therapy highlight the critical role of inflammation in the progression of COVID-19 (Mehta et al., 2020; Stebbing et al., 2020). However, the role of inflammatory markers in monitoring the severity of COVID-19 is still controversial. In this study, through analyzing the 16 retrospective studies, we concluded that inflammatory markers, especially CRP, PCT, IL-6 and ESR, were positively correlated with the severity of COVID-19.

IL-6 has been implicated in the 2003 SARS outbreak and the H5N1 avian influenza infections (Law et al., 2005; Saito et al., 2018). Recent studies showed that IL-6 and granulocyte-macrophage colony stimulating factor (GM-CSF) could be secreted by the

Table 3

The results of the meta-analysis based on standard mean difference (SMD).

Outcome	Studies	Participants	Heterogeneity		Model	SMD	95% CI	P
			I^2	P				
Nonsevere vs. Severe								
1. CRP	13	2092	95%	<0.001	Random	-1.48	[-1.95, -1.00]	<0.001
2. PCT	9	1633	94%	<0.001	Random	-1.11	[-1.58, -0.63]	<0.001
3. IL-6	7	1481	98%	<0.001	Random	-1.54	[-2.38, -0.71]	<0.001
4. ESR	4	1165	67%	0.03	Random	-0.34	[-0.57, -0.10]	0.005
5. SAA	3	650	73%	0.03	Random	-0.41	[-0.82, -0.00]	0.050
6. Serum ferritin	3	1116	80%	0.007	Random	-0.62	[-0.90, -0.34]	<0.001
Non-survivors vs. Survivors								
IL-6	2	341	9%	0.30	Fixed	-1.23	[-1.47, -0.98]	<0.001

CRP: C-reactive protein; PCT: procalcitonin; IL-6: interleukin-6; ESR: erythrocyte sedimentation rate; SAA: serum amyloid.

active pathogenic T cell upon SARS-CoV-2 infection. Also, CD14+CD16+ inflammatory monocytes activated by GM-CSF could secrete more IL-6 and other inflammatory factors (Zhou et al., 2020b). According to the New Coronavirus Pneumonia Prevention and Control Program (7th edition) published by the National Health Commission of China, decreasing level of IL-6 indicates the deterioration of COVID-19. Our study firstly provided evidence-based medicine evidence through meta-analysis. Moreover, the level of IL-6 could not be routinely detected in many hospitals in China, but some inflammatory markers such as CRP, PCT and ESR usually could be detected. Our study firstly put forward that in addition to IL-6, other inflammatory markers such as CRP, PCT and ESR were also positively correlated with the severity of COVID-19. These conclusions were consistent through sensitivity analysis and publication bias assessment.

CRP is an exquisitely sensitive systemic marker of acute-phase response in inflammation, infection, and tissue damage, which could be used as indicator of inflammation (Pepys and Hirschfield, 2003). In the study by Chen et al., although no statistically significant difference was found in the level of CRP between the nonsevere and the severe group, the mean level of CRP was higher in the severe group than in the nonsevere group (Chen et al., 2020b). Other studies all reported CRP level was positively related to the severity of COVID-19. PCT is also a main inflammatory marker routinely measured in clinical practice. Among 9 studies, the levels of PCT were all higher in the severe group than the nonsevere group. ESR is a non-specific inflammatory marker, which mainly reflects the changes of plasma protein types (Wu et al., 2018). In our meta-analysis, we found a higher ESR level in the severe group than in the nonsevere group. One reason is that patients in the severe group had higher inflammation. Another possible explanation is that patients with older age in the severe group contributed to the higher level of ESR considering that the level of ESR increased with age (Piva et al., 2001).

We also found patients with COVID-19 in the severe group had higher levels of SAA and serum ferritin than those in the nonsevere group. Considering that only three studies reported their levels and sensitivity analysis changed the conclusion, we temporarily could not conclude their association with the severity of COVID-19. SAA is a sensitive acute response protein and is used as a sensitive index to reflect the control of infection and inflammation. Serum ferritin is a surrogate marker of stored iron and increases in inflammation, liver disease, and malignancy (Cohen et al., 2010; Facciorusso et al., 2014; Kowdley et al., 2012). All of these highlight that an overexuberant inflammatory response is associated with the severity of COVID-19.

To our knowledge, this is the first meta-analysis on the associations of a series of inflammatory markers with the severity of COVID-19. Admittedly, our meta-analysis had some limitations. Firstly, noticeable heterogeneity exists in most of the analyses. Sensitivity analysis and SMD were used for the meta-analysis, yet

the heterogeneity could not be eliminated completely. Secondly, reporting and publication bias may result from the lack of information or unpublished negative studies although the conclusion did not change through the trim-and-fill method. Thirdly, the studies included in our meta-analysis were mainly from China and whether the conclusion is consistent in other countries needs to be further investigated. Finally, this study is underpowered to investigate the underlying mechanism of these inflammatory markers with the severity of COVID-19.

In conclusion, inflammatory markers, especially CRP, PCT, IL-6 and ESR, were positively correlated with the severity of COVID-19. The association of SAA and serum ferritin with the severity of COVID-19 needs to be further clarified. Measurement of inflammatory markers might assist clinicians to monitor and evaluate the severity and prognosis of COVID-19.

Authors contribution

GD, LX and FZ were responsible for study design; YH and YG were involved in data collection; GD and YH analyzed the data; FZ and YH wrote the manuscript. GD, LX, MY and XC revised the manuscript.

Funding

This research was funded by the grants from the National Natural Science Foundation of China, No. 62041208.

Ethics in publishing

Approval was not required.

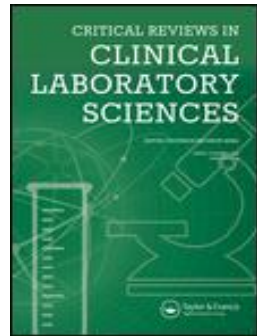
Declaration of interest

The authors declare no conflicts of interest.

References

- Chang Z, Yang W, Wang Q, Liao G. Clinical significance of serum hs-CRP, IL-16, and PCT in diagnosis and prognosis of patients with COVID-19 (In Chinese). Drugs Clin 2020;35(3).
- Chen C, Chen C, Yan JT, Zhou N, Zhao JP, Wang DW. Analysis of myocardial injury in patients with COVID-19 and association between concomitant cardiovascular diseases and severity of COVID-19 (In Chinese). Zhonghua Xin Xue Guan Bing Za Zhi 2020a;48:E008.
- Chen L, Liu HG, Liu W, Liu J, Liu K, Shang J, et al. Analysis of clinical features of 29 patients with 2019 novel coronavirus pneumonia (In Chinese). Zhonghua Jie He He Hu Xi Za Zhi 2020b;43(3):203–8.
- Cheng K, Wei M, Shen H, Wu C, Chen D, Xiong W, et al. Clinical characteristics of 463 patients with common and severe type coronavirus disease (In Chinese). Shanghai Med J 2020;1:15.
- National Health Commission of China. The notice of launching guideline on diagnosis and treatment of the novel coronavirus pneumonia. (In Chinese).

2020. http://www.gov.cn/zhengce/zhengceku/2020-02/19/content_5480948.htm.
- Cohen LA, Gutierrez L, Weiss A, Leichtmann-Bardoogo Y, Zhang DL, Crooks DR, et al. Serum ferritin is derived primarily from macrophages through a nonclassical secretory pathway. *Blood* 2010;116(9):1574–84.
- Facciorusso A, Del Prete V, Antonino M, Neve V, Crucinio N, Di Leo A, et al. Serum ferritin as a new prognostic factor in hepatocellular carcinoma patients treated with radiofrequency ablation. *J Gastroenterol Hepatol* 2014;29(11):1905–10.
- Fang X, Mei Q, Yang T, Zhang L, Yang Y, Wang Y, et al. Clinical characteristics and treatment strategies of 79 patients with COVID-19 (In Chinese). *Chin Pharmacol Bull* 2020;36(4).
- Wells GA, Shea Brooke, O'connell Dianne L, Peterson Joan, Welch V, Losos Michael, et al. The Newcastle-Ottawa Scale (NOS) for assessing the quality of nonrandomised studies in meta-analyses. *Open J Rheumatol Autoimmun Dis* 2014;4:.
- Gao Y, Li T, Han M, Li X, Wu D, Xu Y, et al. Diagnostic utility of clinical laboratory data determinations for patients with the severe COVID-19. *J Med Virol* 2020;.
- Guan WJ, Ni ZY, Hu Y, Liang WH, Ou CQ, He JX, et al. Clinical characteristics of coronavirus disease 2019 in China. *N Engl J Med* 2020;382(18):1708–20.
- Huang C, Wang Y, Li X, Ren L, Zhao J, Hu Y, et al. Clinical features of patients infected with 2019 novel coronavirus in Wuhan, China. *Lancet* 2020;395(10223):497–506.
- Kowdley KV, Belt P, Wilson LA, Yeh MM, Neuschwander-Tetri BA, Chalasani N, et al. Serum ferritin is an independent predictor of histologic severity and advanced fibrosis in patients with nonalcoholic fatty liver disease. *Hepatology* 2012;55(1):77–85.
- Law HK, Cheung CY, Ng HY, Sia SF, Chan YO, Luk W, et al. Chemokine up-regulation in SARS-coronavirus-infected, monocyte-derived human dendritic cells. *Blood* 2005;106(7):2366–74.
- Li G, De Clercq E. Therapeutic options for the 2019 novel coronavirus (2019-nCoV). *Nat Rev Drug Discov* 2020;19(3):149–50.
- Li K, Wu J, Wu F, Guo D, Chen L, Fang Z, et al. The clinical and chest CT features associated with severe and critical COVID-19 pneumonia. *Invest Radiol* 2020;55(6):327–31.
- Luo D, Wan X, Liu J, Tong T. Optimally estimating the sample mean from the sample size, median, mid-range, and/or mid-quartile range. *Stat Methods Med Res* 2018;27(6):1785–805.
- Mehta P, McAuley DF, Brown M, Sanchez E, Tattersall RS, Manson JJ, et al. COVID-19: consider cytokine storm syndromes and immunosuppression. *Lancet* 2020;395(10229):1033–4.
- Mohr D, Liberati A, Tetzlaff J, Altman DG, Group P. Preferred reporting items for systematic reviews and meta-analyses: the PRISMA statement. *BMJ* 2009;339:b2535.
- Peng YD, Meng K, Guan HQ, Leng L, Zhu RR, Wang BY, et al. [Clinical characteristics and outcomes of 112 cardiovascular disease patients infected by 2019-nCoV] (In Chinese). *Zhonghua Xin Xue Guan Bing Za Zhi* 2020;48:E004.
- Pepys MB, Hirschfield GM. C-reactive protein: a critical update. *J Clin Invest* 2003;111(12):1805–12.
- Piva E, Sanzari MC, Servidio G, Plebani M. Length of sedimentation reaction in undiluted blood (erythrocyte sedimentation rate): variations with sex and age and reference limits. *Clin Chem Lab Med* 2001;39(5):451–4.
- Qin C, Zhou L, Hu Z, Zhang S, Yang S, Tao Y, et al. Dysregulation of immune response in patients with COVID-19 in Wuhan, China. *Clin Infect Dis* 2020;.
- Ruan Q, Yang K, Wang W, Jiang L, Song J. Clinical predictors of mortality due to COVID-19 based on an analysis of data of 150 patients from Wuhan, China. *Intensive Care Med* 2020;46(5):846–8.
- Russell CD, Millar JE, Baillie JK. Clinical evidence does not support corticosteroid treatment for 2019-nCoV lung injury. *Lancet* 2020;395(10223):473–5.
- Saito LB, Diaz-Satizabal L, Evseev D, Fleming-Canepe X, Mao S, Webster RG, et al. IFN and cytokine responses in ducks to genetically similar H5N1 influenza A viruses of varying pathogenicity. *J Gen Virol* 2018;99(4):464–74.
- Stebbing J, Phelan A, Griffin I, Tucker C, Oechsle O, Smith D, et al. COVID-19: combining antiviral and anti-inflammatory treatments. *Lancet Infect Dis* 2020;20(4):400–2.
- Tay MZ, Poh CM, Renia L, MacAry PA, Ng LFP. The trinity of COVID-19: immunity, inflammation and intervention. *Nat Rev Immunol* 2020;1–12.
- Wan X, Wang W, Liu J, Tong T. Estimating the sample mean and standard deviation from the sample size, median, range and/or interquartile range. *BMC Med Res Methodol* 2014;14:135.
- WHO. WHO Virtual press conference on COVID-19 (March 11, 2020) [Accessed 16 March 2020]. 2020.
- WHO. WHO Virtual press conference on COVID-19 (March 21, 2020) [Accessed 21 March 2020]. 2020.
- Wu C, Chen X, Cai Y, Xia J, Zhou X, Xu S, et al. Risk factors associated with acute respiratory distress syndrome and death in patients with coronavirus disease 2019 pneumonia in Wuhan, China. *JAMA Intern Med* 2020;.
- Wu S, Zhou Y, Hua HY, Zhang Y, Zhu WY, Wang ZQ, et al. Inflammation marker ESR is effective in predicting outcome of diffuse large B-cell lymphoma. *BMC Cancer* 2018;18(1):997.
- Xiang T, Liu J, Xu F, Cheng N, Liu Y, Qian K, et al. Analysis of clinical characteristics of 49 patients with Novel Coronavirus Pneumonia in Jiangxi province (In Chinese). *Chin J Respir Crit Care Med* 2020;19(2).
- Xiao K, Shui L, Pang X, Mu H, Wang J, Lang C, et al. The clinical features of the 143 patients with COVID-19 in North-East of Chongqing (In Chinese). *J Third Mil Med Univ* 2020;1–5.
- Xu Z, Shi L, Wang Y, Zhang J, Huang L, Zhang C, et al. Pathological findings of COVID-19 associated with acute respiratory distress syndrome. *Lancet Respir Med* 2020;8(4):420–2.
- Zeng F, Chen B, Zeng J, Wang Z, Xiao L, Deng G. Preoperative neutrophil-lymphocyte ratio predicts the risk of microvascular invasion in hepatocellular carcinoma: a meta-analysis. *Int J Biol Markers* 2019;34(3):213–20.
- Zeng F, Chen L, Liao M, Chen B, Long J, Wu W, et al. Laparoscopic versus open gastrectomy for gastric cancer. *World J Surg Oncol* 2020;18(1):20.
- Zhang JJ, Dong X, Cao YY, Yuan YD, Yang YB, Yan YQ, et al. Clinical characteristics of 140 patients infected with SARS-CoV-2 in Wuhan, China. *Allergy Eur J Allergy Clin Immunol* 2020;.
- Zhang YZ, Holmes EC. A genomic perspective on the origin and emergence of SARS-CoV-2. *Cell* 2020;181(2):223–7.
- Zhou F, Yu T, Du R, Fan G, Liu Y, Liu Z, et al. Clinical course and risk factors for mortality of adult inpatients with COVID-19 in Wuhan, China: a retrospective cohort study. *Lancet* 2020a;395(10229):1054–62.
- Zhou Y, Fu B, Zheng X, Wang D, Zhao C, qi Y, Aberrant pathogenic GM-CSF+ T cells and inflammatory CD14+CD16+ monocytes in severe pulmonary syndrome patients of a new coronavirus 2020b;2020: 02.12.945576.



Biomarkers associated with COVID-19 disease progression

Giovanni Ponti, Monia Maccaferri, Cristel Ruini, Aldo Tomasi & Tomris Ozben

To cite this article: Giovanni Ponti, Monia Maccaferri, Cristel Ruini, Aldo Tomasi & Tomris Ozben (2020): Biomarkers associated with COVID-19 disease progression, Critical Reviews in Clinical Laboratory Sciences, DOI: [10.1080/10408363.2020.1770685](https://doi.org/10.1080/10408363.2020.1770685)

To link to this article: <https://doi.org/10.1080/10408363.2020.1770685>



Published online: 05 Jun 2020.



Submit your article to this journal



View related articles



View Crossmark data

REVIEW ARTICLE



Biomarkers associated with COVID-19 disease progression

Giovanni Ponti^a, Monia Maccaferri^b, Cristel Ruini^{a,c}, Aldo Tomasi^a and Tomris Ozben^d

^aDepartment of Surgical, Medical, Dental and Morphological Sciences with Interest in Transplant, Oncological and Regenerative Medicine, Division of Clinical Pathology, University of Modena and Reggio Emilia, Modena, Italy; ^bDermatology Unit, Azienda Ospedaliero-Universitaria of Modena, Modena, Italy; ^cDepartment of Dermatology and Allergology, University Hospital, LMU Munich, Munich, Germany; ^dDepartment of Clinical Biochemistry, Medical Faculty, Akdeniz University, Antalya, Turkey

ABSTRACT

The coronavirus disease 2019 (COVID-19) pandemic is a scientific, medical, and social challenge. The complexity of the severe acute respiratory syndrome coronavirus 2 (SARS-CoV-2) is centered on the unpredictable clinical course of the disease that can rapidly develop, causing severe and deadly complications. The identification of effective laboratory biomarkers able to classify patients based on their risk is imperative in being able to guarantee prompt treatment. The analysis of recently published studies highlights the role of systemic vasculitis and cytokine mediated coagulation disorders as the principal actors of multi organ failure in patients with severe COVID-19 complications. The following biomarkers have been identified: hematological (lymphocyte count, neutrophil count, neutrophil-lymphocyte ratio (NLR)), inflammatory (C-reactive protein (CRP), erythrocyte sedimentation rate (ESR), procalcitonin (PCT)), immunological (interleukin (IL)-6 and biochemical (D-dimer, troponin, creatine kinase (CK), aspartate aminotransferase (AST)), especially those related to coagulation cascades in disseminated intravascular coagulation (DIC) and acute respiratory distress syndrome (ARDS). New laboratory biomarkers could be identified through the accurate analysis of multicentric case series; in particular, homocysteine and angiotensin II could play a significant role.

Abbreviations: ACE: angiotensin-converting enzyme; ALT: alanine aminotransferase; Ang: angiotensin; aPTT: activated partial thromboplastin time; ARDS: acute respiratory distress syndrome; AST: aspartate aminotransferase; AT2R: AT2 receptor; BK: bradykinin; CI: confidence interval; CK: creatine kinase; CKD: chronic kidney disease; COVID-19: coronavirus disease 2019; CRP: C-reactive protein; CT: computer tomography; CTL: cytotoxic T lymphocyte; DIC: disseminated intravascular coagulation; ESR: erythrocyte sedimentation rate; FDP: fibrin degradation product; G-CSF: granulocyte-colony stimulating factor; Hcy: homocysteine; HPLC: high-performance liquid chromatography; HR: hazard risk; ICU: intensive care unit; IL: interleukin; INF: interferon; IP: interferon- γ inducible protein; LDH: lactate dehydrogenase; MasR: Mas receptor; MCP: monocyte chemoattractant protein; MIP: macrophage inflammatory protein; MOF: multiple organ failure; NCP: novel coronavirus pneumonia; NK: natural killer; NLR: neutrophil-lymphocyte ratio; NO: nitric oxide; OR: odds ratio; ORF: open reading frame; PCT: procalcitonin; PLR: platelet-to-lymphocyte ratio; PT: prothrombin time; RAS: renin-angiotensin system; ROCK: RhoA/Rho kinase; S: spike; SARS-CoV-2: severe acute respiratory syndrome coronavirus 2; TNF: tumor necrosis factor; WBC: white blood cell

ARTICLE HISTORY

Received 5 May 2020
Revised 12 May 2020
Accepted 14 May 2020

KEYWORDS

COVID-19; biomarkers of disease progression; hematological biomarkers; inflammatory biomarkers; immunological biomarkers; biochemical biomarkers; neutrophil-lymphocyte ratio (NLR)

1. Introduction

The scientific community is in urgent need for reliable biomarkers related to coronavirus disease 2019 (COVID-19) disease progression, in order to stratify high risk patients. The rapid disease spread necessitates the immediate categorization of patients into risk groups following diagnosis, to ensure optimal resource allocation. Novel biomarkers are needed to identify patients who will suffer rapid disease progression to severe complications and death. The identification of novel

biomarkers is strictly related to the understanding of viral pathogenetic mechanisms, as well as cellular and organ damage. Effective biomarkers would be helpful for screening, clinical management, and prevention of serious complications.

Preliminary studies describe vasculitic processes underlying organ damage in seriously ill patients, induced by the activation of inflammatory cascades, complement activation and pro-inflammatory cytokines (i.e. interleukin (IL)-6) [1,2]. Vasculitic damage causes

edema and acute respiratory distress syndrome (ARDS) in the lung, and plays a significant role in cardiovascular damage (ischemia, deep venous thrombosis, pulmonary thromboembolism) and cerebral injuries (embolism); its severity is unfortunately not easily predictable through currently used laboratory biomarkers such as D-dimer or prothrombin time/activated partial thromboplastin time (PT/aPTT) [3,4]. Epidemiological observations have associated a critical role of cardiovascular damage in severe acute respiratory syndrome coronavirus 2 (SARS-CoV-2) patients, with ischemic heart disease and hypertension among the most frequent preexisting comorbidities associated with SARS-CoV-2 mortality [5,6]. Current clinical practice suggests determining IL-6, D-dimer, lactate dehydrogenase (LDH), and transaminases in addition to routine laboratory tests, in order to identify patients at risk of fatal complications and those who will potentially benefit from anti-IL6 immunotherapies with tocilizumab [7]. However, as costly cytokine analysis is not routinely performed in most laboratories, surrogate markers of infection (ferritin, C-reactive protein (CRP)) correlated to IL-6 will be of increasing interest for prognostic value. Beyond D-dimer, prothrombin time (PT) and fibrin degradation product (FDP) [1], there are no specific predictive parameters of severe ischemic and thrombo-embolic disease. For this reason, it is not easy to cluster patients in risk categories for an appropriate early anticoagulant or fibrinolytic therapy.

According to the most recently published Diagnosis and Treatment Program of 2019 New Coronavirus Pneumonia (trial version seven) [8], COVID-19 patients are divided into mild, moderate, severe, and critical classifications. Some hematological parameters, including white blood cell (WBC), lymphopenia, CRP, and some biochemical parameters, such as LDH, creatine kinase (CK), and troponin were reported to be associated with COVID-19 severity [9,10].

Concerning new predictive parameters of specific cardiovascular risk, very recent data report that homocysteine (Hcy) (together with age, monocyte-lymphocyte ratio (MLR), and period from disease onset to hospital admission) may be a specific cardiovascular risk predictive parameter for severe pneumonia observed at chest computed tomography (CT) during the first week of COVID-19 infection; however, these observations did not report any additional organ involvement [11]. The aim of this review is to report the current state of knowledge regarding known biomarkers for COVID-19 infection, focusing on those potentially predictive of organ damage in patients with severe complications and death.

2. The mechanisms of action of COVID-19

The knowledge of molecular mechanisms related to virus damage on human cells is necessary to define efficacious pharmacologic strategies and to identify novel biomarkers predictive of severe cardiovascular damage or fatality.

The main mechanism for SARS-CoV-2 infection is the binding of the virus to membrane-bound form of angiotensin-converting enzyme 2 (ACE2) and the internalization of complex by the host cell.

ACE2, a glycoprotein and metalloprotease, exists in both membrane-bound and soluble forms [12]. The membrane-bound form contains a transmembrane domain which anchors its extracellular domain to the plasma membrane, whereas in its soluble form, it is cleaved and secreted, as the N-terminal ectodomain is barely measurable in circulation.

The significance of circulating ACE2 is unclear, although levels may be increased in chronic diseases such as diabetes, chronic kidney disease (CKD), and hypertension [13,14]. ACE2 has kinins, apelin, neurotensin, dynorphin, ghrelin, amyloid, and angiotensin as substrates. The main function of ACE2 is to physiologically counterbalance ACE and regulate angiotensin II (Ang II) by converting Ang I into Ang-(1-9), and by converting Ang II into Ang-(1-7), which is tissue-protective [15].

Recently, it has been demonstrated that the receptor-binding domain in the novel coronavirus spike (S) protein binds strongly to ACE2 receptors [16]. SARS-CoV-2 uses ACE2 and the serine protease TMPRSS2 for S protein priming. ACE2 and TMPRSS2 are not only expressed in lung, but also in the small intestinal epithelia, in the upper esophagus, liver, colon [17], in organs involved in blood pressure regulation (blood vessels, heart, kidneys) as well as in the ovaries and testes [15]. This wide distribution of the COVID-19 receptor could provoke systemic failure due to direct organ injury [18].

An additional SARS-CoV-2 mechanism of action was suggested by Wenzhong and Hualan who demonstrated that the open reading frame (ORF8) and surface glycoprotein may both bind to the porphyrin. At the same time, orf1ab, ORF10, and ORF3a proteins are presumed to coordinate an attack on the heme of the 1-beta chain of hemoglobin to dissociate the iron, forming the porphyrin and reducing the capacity of hemoglobin to carry oxygen and carbon dioxide [19] (not peer-reviewed). This mechanism of the virus inhibits the normal metabolic pathway of heme and provokes disease symptomatology.

Greater consensus exists on the pathogenetic mechanisms triggered by COVID-19 after entering the human body: inflammatory cascades, cytokine storms, and the activation of coagulation cascades. These are common in systemic vasculitis (pulmonary, renal, and cerebral), and lead to severe and even fatal complications, such as sepsis, disseminated intravascular coagulation (DIC), and acute cardiovascular events.

DIC has been identified in the majority of SARS-CoV-2 infected deceased patients. Patients with viral infection may develop sepsis associated with organ dysfunction. DIC, most commonly caused by sepsis, develops when monocytes and endothelial cells are activated, and following injury cytokines are released, with the expression of tissue factor and the secretion of von Willebrand factor. Free thrombin, uncontrolled by natural anticoagulants, can activate platelets and stimulate fibrinolysis. At late stages of novel coronavirus pneumonia (NCP), fibrin-related markers (D-dimer and FDP) were reported to be moderately or markedly elevated in all SARS-CoV-2 deaths, suggesting a common coagulation activation and secondary hyperfibrinolysis in these patients [1].

3. Markers of COVID-19 infection and severe progression

A pattern of hematologic, biochemical, inflammatory, and immune biomarker abnormalities has been identified in patients with severe disease compared to mild systemic disease, and warrant inclusion in risk stratification models (Table 1). Additionally, authors report the observation of significantly increased Hcy in patients with severe COVID-19 disease.

3.1. Hematologic biomarkers

Hematologic biomarkers used to stratify COVID-19 patients include WBC count, lymphocyte count,

neutrophil count, neutrophil-lymphocyte ratio (NLR), platelet count, eosinophil count, and hemoglobin.

Yang et al. [20] reported lymphopenia in 80% of critically ill adult COVID-19 patients, whereas Chen et al. [4] reported a rate of only 25% of patients with mild COVID-19 infection. These observations suggest that lymphopenia may correlate with infection severity. Qin et al. analyzed markers related to dysregulation of immune response in a cohort of 450 COVID-19 positive patients, reporting that severe cases tended to have lower lymphocyte-, higher leukocyte-counts and higher NLR, as well as lower percentages of monocytes, eosinophils, and basophils compared to mild cases [21]. Similarly, Henry et al. also concluded in a meta-analysis on 21 studies including 3377 COVID-19 positive patients that patients with severe and fatal disease had significantly increased WBC, and decreased lymphocyte and platelet counts compared to non-severe disease and survivors [22].

In COVID-19 patients, both helper T cells and suppressor T cells were below normal levels, with the lowest helper T cells levels associated with severe cases. Further, in severe cases, the percentage of naïve helper T cells were reportedly increased, and memory helper T cells were reportedly decreased. Patients with COVID-19 also have lower level of regulatory T cells, which are more obviously damaged in severe cases [21,23]. Cytotoxic lymphocytes, such as cytotoxic T lymphocytes (CTLs) and natural killer (NK) cells, are necessary for the control of viral infection, and the functional exhaustion of cytotoxic lymphocytes is correlated with disease progression [24]. On confirmed COVID-19 cases, laboratory testing showed that mean lymphocyte counts were below normal [3,25–27]. Changes in lymphocyte populations in patients severely affected by COVID-19 indicate a low T cells count, an increase in naïve helper T cells and a decrease in memory helper T cells [23]. The total number of NK, T cells, and B cells was decreased markedly in patients with SARS-CoV-2 infection

Table 1. Biomarker abnormalities in COVID-19 patients with severe systemic disease and potential new biomarkers.

Hematologic biomarkers		Biochemical biomarkers		Coagulation biomarkers		Inflammatory biomarkers		Potential new biomarkers	
↑	↓	↑	↓	↑		↑		↑	↓
WBC count	Lymphocyte count	ALT	Albumin	PT		ESR	Hcy	Ang-(1-7)	
Neutrophil count	Platelet count	AST		D-dimer		CRP	Ang II	Ang-(1-9)	
Eosinophil count		Total bilirubin			Serum ferritin	NLR		Alamandine	
T cell count		Blood urea nitrogen			PCT	MLR			
B cell count		CK			IL-2				
NK cell count		LDH			IL-6				
		Myoglobin			IL-8				
		CK-MB			IL-10				
		Cardiac troponin I							
		Creatinine							

WBC: white blood cell; NK: natural killer; ALT: alanine aminotransferase; AST: aspartate aminotransferase; CK: creatine kinase; LDH: lactate dehydrogenase; PT: prothrombin time; ESR: erythrocyte sedimentation rate; CRP: C-reactive protein; PCT: procalcitonin; IL: interleukin; Hcy: homocysteine; Ang: angiotensin; NLR: neutrophil-lymphocyte ratio; MLR: monocyte-lymphocyte ratio.

[21,28,29]. Lower CD8⁺ T cells count tended to be an independent predictor for COVID-19 severity and treatment efficacy [29]. Xu et al. reported that a decrease of specific T lymphocyte subsets is related to in-hospital death and severe illness. Lower counts of T lymphocyte subsets; lymphocyte (<500/ μ L), CD3+ T-cell (<200/ μ L), CD4+ T-cell (<100/ μ L), CD8+ T-cell (<100/ μ L), and B-cell (<50/ μ L) were associated with higher risks of in-hospital death of COVID-19. The warning values to predict in-hospital death of lymphocyte, CD3+ T-cell, CD4+ T-cell, CD8+ T-cell, and B-cell were 559/ μ L, 235/ μ L, 104/ μ L, 85/ μ L and 82/ μ L, respectively [30].

In a study of 32 COVID-19 patients, decreased eosinophil count was registered in 66% [31]. Eosinophil counts have been positively correlated to lymphocyte count ($r=0.305$, $p<.001$) [32]. In another study of 140 COVID-19 patients, eosinopenia was reported in 52.9% ($<0.02 \times 10^9/L$), and the eosinophil count was positively associated with lymphocyte count in mild ($r=0.449$, $p<.001$) and severe ($r=0.486$, $p<.001$) cases of COVID-19 [33]. Du et al. reported very low eosinophil counts in 81.2% patients at admission, which may indicate poor prognosis [9]. Liu et al. also reported low eosinophil values on initial hospitalization, which reportedly returned to normal before discharge, concluding that increasing eosinophils may be an indicator of clinical COVID-19 improvement [34]. However, results from a systematic literature review concluded that "eosinopenia may not be associated with unfavorable progression of COVID-19" [35]. Therefore, the diagnostic value of eosinopenia in COVID-19 requires further investigation with larger patient cohorts to establish the sensitivity and specificity of the eosinophil count.

The NLR, calculated simply by the ratio of neutrophils count/lymphocytes count, is an inflammatory marker that can predict the probability of death in patients with various cardiovascular diseases [36,37]. Moreover, NLR has been identified in a meta-analysis as a prognostic biomarker for patients with sepsis [38]. For COVID-19 patients, NLR has been shown to be an independent risk factor for severe disease [39–41]. Fifty (75.8%) patients with disease progression during hospitalization had a NLR ≥ 2.973 [42], which may indicate COVID-19 infection severity [43]. Binary logistic analysis identified elevated NLR (hazard risk (HR): 2.46, 95% confidence interval (CI): 1.98–4.57) as an independent factor for poor COVID-19 clinical outcome [44], which was confirmed by a meta-analysis which reported that NLR values were significantly increased in severe COVID-19 patients [45]. NLR elevation may be due to dysregulated expression of inflammatory cytokines, aberrant increase of pathological low-density neutrophil and the

upregulation of genes involved in lymphocyte cell death pathway, caused by the mechanism of SARS-CoV-2 infection [46].

Lymphopenia, excessive activation of the inflammatory cascade, and cardiac involvement are all crucial features of COVID-19 disease and have high prognostic value. However, the understanding of the underlying mechanisms is still limited [47]. Based on the observations derived from clinical practice, it has also been postulated that coronaviruses may directly infect bone marrow precursors, resulting in abnormal hematopoiesis, or trigger an auto-immune response against blood cells [48,49].

As platelet count is a simple, cheap, and easily available biomarker and has been independently associated with disease severity and mortality risk in intensive care unit (ICU) [50–52], it has been rapidly adopted as a potential biomarker for COVID-19 patients. The number of platelets was reported to be significantly reduced in COVID-19 patients [11,53] and was lower in non-survivor patients compared to survivors [54]. Low platelet count has been associated with increased risk of severe disease and mortality for COVID-19 patients, and can serve as an indicator of clinical disease worsening during hospitalization [55]. Another research group found that patients with severe pneumonia induced by SARS-CoV2 had higher platelet count than those induced by non-SARS-CoV2 [56]. The patients with significantly elevated platelets and higher platelet-to-lymphocyte ratio (PLR) during treatment had longer average hospitalization days [57]. Damaged lung tissue and pulmonary endothelial cells may activate platelets in the lungs, resulting in the aggregation and formation of microthrombi, thereby increasing platelet consumption [58].

In severe disease, WBCs show lymphocytopenia, affecting both CD4⁺ and CD8⁺ cells, as well as a decrease in monocytes and eosinophils, and a clear increase in neutrophils and NLR. These simple parameters can be used for early diagnosis and identification of critically ill patients [59,60].

3.2. Biochemical biomarkers

The main laboratory changes in severe or fatal COVID-19 patients were recently explored in a meta-analysis, including three large studies comparing survivors to non-survivors. A significant increase in total bilirubin and CK, together with serum ferritin, WBC count, and IL-6 was registered in non-survivors compared to survivors [20,26,61]. Further, given the strong association between thrombo-embolism and COVID-19 and to a

lesser extent, myocardial injury, D-dimer, and cardiac markers are crucial in COVID-19 patient monitoring.

Markers of muscular and in particular cardiac injury were elevated in patients with both severe and fatal COVID-19. At presentation, non-survivors had significantly higher cardiac troponin levels (weighted mean difference (WMD): 32.7 ng/L), which is probably due to both viral myocarditis and cardiac injury from disease progression to multiple organ failure (MOF). In MOF, significant elevation in liver enzymes (alanine aminotransferase (ALT) and aspartate aminotransferase (AST)) is associated with critical changes in renal function parameters (blood urea nitrogen, creatinine) and coagulation markers [60].

Chen et al. observed in a cohort of 799 patients (113 non-survivors and 161 recovered) markedly higher concentrations of ALT, AST, creatinine, CK, LDH, cardiac troponin I, N-terminal pro-brain natriuretic peptide, and D-dimer in non-survivors compared to recovered patients [62]. Du et al., in a prospective study of 179 patients with COVID-19 pneumonia (including 21 non-survivors), identified cardiac troponin $I \geq 0.05$ ng/mL as among the four risk factors predictive of mortality (age ≥ 65 years, preexisting concurrent cardiovascular or cerebrovascular diseases, CD3 + CD8+ T cells (≤ 75 cell/ μL) [9].

Liver function has also been identified as an important predictor for COVID-19 patient mortality. A recent study suggested that SARS-CoV-2 may directly bind to ACE2-positive cholangiocytes, and therefore, liver abnormalities in COVID-19 patients may be due to cholangiocyte dysfunction and other causes, such as drug-induced and systemic inflammatory response-induced liver injuries [63]. Regarding the specific and dynamic pattern of liver injury parameters, Lei et al., in a wide retrospective multicenter study involving a COVID-19 cohort-derived data set of 5771 patients, reported that AST is strongly associated with mortality risk compared to other parameters, reflecting liver injury [64]. This evidence is in contrast with the evidence of ALT elevation in other hepatitis-induced liver injury.

3.3. Inflammatory biomarkers

The increase in inflammation markers is the critical point underlying the systemic vasculitic processes and the defects in the coagulation processes that cause most parenchymal lesions in vital organs. The main inflammatory and immune biomarkers correlated with COVID-19 disease are summarized in Table 1.

The CRP marker was found to be significantly increased in the initial phases of the infection for severe

COVID-19 patients, also prior to indications of critical findings with CT. Importantly, CRP has been associated with disease development and is an early predictor for severe COVID-19 [65]. The authors also reported by correlation analysis that CRP ($R = 0.62, p < .01$), erythrocyte sedimentation rate (ESR) ($R = 0.55, p < .01$) and granulocyte/lymphocyte ratio ($R = 0.49, p < .01$) were positively associated with CT severity scores.

The immunological biomarkers of IL-6 and serum ferritin are reported to be significantly increased in non-survivors vs. survivors (WMD: 4.6 pg/mL and 760.2 ng/mL, respectively) and as compared to severe vs. non-severe disease (WMD: 1.7 pg/mL and 408.3 ng/mL, respectively) [60]. The significant increase of inflammatory cytokines, such as IL-6, is connected to a so-called "Cytokine Storm," behind acute lung injury and ARDS and can lead to further tissue damage and MOF [66]. This hyperbolic systemic inflammation relates to lymphopenia and is associated with severe disease [67]. Important inflammatory markers include IL-6, IL-2, IL-7, tumor necrosis factor (TNF)- α , interferon- γ inducible protein (IP)-10, monocyte chemoattractant protein (MCP)-1, macrophage inflammatory protein (MIP) 1- α , granulocyte-colony stimulating factor (G-CSF), CRP, procalcitonin (PCT), and ferritin [3,26,47,61,67,68].

Some of the above-mentioned parameters not only appear to be related to disease severity, but also to mortality. In a retrospective clinical series, non-survivors had higher levels of IL-6, ferritin, and CRP [26,61] compared to survivors. Current clinical practice suggests that the determination of IL-6, D-dimer, LDH, and transaminases in addition to routine laboratory tests, is useful for the stratification of high risk patients and the identification of those who might potentially benefit from anti-IL-6 immunotherapies with tocilizumab [7].

3.3.1. Procalcitonin

PCT, a glycoprotein, is the pro-peptide of calcitonin devoid of hormonal activity. Under normal circumstances, it is produced in the C-cells of the thyroid gland. In healthy humans, PCT levels are undetectable (< 0.1 ng/mL). During severe infection (bacterial, parasitic, and fungal) with systemic manifestations, PCT levels may rise to over 100 ng/mL, produced mostly by extra-thyroid tissue [69]. Although its biological action is largely unknown, the sequence homologies between PCT and other human cytokines, such as TNF- α family, IL-6, etc., support the hypothesis that PCT is a mediator of inflammation [70].

The synthesis of PCT can be increased as a result of endotoxins and/or cytokines (e.g. IL-6, TNF- α , and IL-1 β). The extra-thyroid synthesis of PCT has been found to occur in the liver, pancreas, kidney, lung, intestine, and within leukocytes. However, the synthesis of PCT has been shown to be suppressed within these tissues in the absence of bacterial infection. In contrast, cytokines, such as interferon (INF)- γ , which are released following viral infection, lead to down-regulation of PCT, thus highlighting another advantage of PCT assays [71]. PCT levels are either unmodified or only moderately increased in systemic inflammatory response to viral or to noninfectious stimuli (non-viral infections). Therefore, PCT values were more discriminative than WBC count and CRP in distinguishing a bacterial infection from another inflammatory process [72]. As for COVID-19 patients, more severe cases showed a more marked increase of PCT compared with non-severe cases [33,73–76]. A slight increase (much less than 0.5 ng/mL) in PCT levels is an important indicator to distinguish between SARS-CoV-2-positive and SARS-CoV-2-negative patients [77] and increased PCT values have been associated with a nearly fivefold higher risk of severe SARS-CoV-2 infection (odds ratio (OR): 4.76; 95% CI: 2.74–8.29). PCT value remains within reference ranges in patients with non-complicated SARS-CoV-2 infection; any substantial increase reflects bacterial co-infection and the development of a severe form of disease and a more complicated clinical picture [78]. PCT elevation has also been found in pediatric cases with lower respiratory tract infection, reflecting bacterial co-infection [79].

Although initial PCT value may be helpful in the determination of illness severity, it may not always be a reliable prognostic indicator. As PCT values may be influenced by preexisting comorbid conditions, such as CKD and congestive heart failure, baseline values may be high. However, PCT can provide invaluable information if considered within the clinical context [80].

3.4. Coagulation biomarkers

Abnormal coagulation parameters are associated with poor prognosis. Specifically, markedly elevated D-dimer and FDP are common in COVID-19 non-survivor patients [1].

D-dimer appears to be frequently increased in patients with COVID-19 (36–43%) [81] and may be related to severe complications and death. However, currently the interpretation of D-dimer during disease monitoring is unclear, as it may not be directly related

to disease severity. Similarities may exist with troponins (8), whose range does not always correspond to acute cardiac ischemia; not all increases in cardiac troponin require invasive assessments in the absence of clinical symptoms [82,83]. However, in some large-scale studies, PT has been shown to be correlated to disease severity. In a retrospective study involving 296 COVID-19 patients (with 17 non-survivors), the non-survivor group had higher D-dimer and thrombin time and lower aPTT than the survivor group [84]. In a retrospective, multicenter cohort study including 191 COVID-19 patients who had either been discharged or had died, factors associated with non-survival were PT, high-sensitive cardiac troponin I, CK, and D-dimer [61]. Wang et al. showed that 58% of patients with COVID-19 had prolonged PT [68]. Tang et al. investigated 207 non-survivor COVID-19 patients and revealed that non-survivors had remarkably higher D-dimer and FDP levels and longer PT at admission compared with survivors [1].

The activation of coagulation processes reaches its peak in the DIC, which appeared to occur before most of the COVID-19 positive patients' death. In fact, such patients may evolve to sepsis, which is one of the most common causes of DIC. DIC is the result of activation of monocytes and endothelial cells to release cytokines following injury, with expression of tissue factor and secretion of von Willebrand factor. Circulation of free thrombin, uncontrolled by natural anticoagulants, can activate platelets and stimulate fibrinolysis. At the late stages of NCP, levels of fibrin-related markers (D-dimer and FDP) are moderately or markedly elevated in all deaths, suggestive of a common coagulation activation and secondary hyperfibrinolysis condition.

This evidence could explain the rapid disease progression to death and the limited efficacy of mechanical ventilation in the treatment of COVID-19 patients. ARDS mechanical ventilation protocols are not always of significant benefit and may even cause additional lung damage. Conversely, the rapid and positive response of some patients to full anti coagulation therapy can be explained.

Terpos et al. showed that blood hypercoagulability is common among hospitalized COVID-19 patients. They reported that coagulation abnormalities in PT, aPTT, FDP, and D-dimer, along with severe thrombocytopenia, are associated with life-threatening DIC, which necessitates continuous vigilance and prompt intervention [85]. In large scale studies, D-dimer and PT have been found to be associated with severe disease and death [61,86].

3.5. Potential Novel Markers in COVID-19 positive patients

3.5.1. Homocysteine

Hcy has been under a lot of speculation since its discovery in 1932. The heating of the amino acid methionine with sulfuric acid led to this amino acid of interest [87].

High plasma levels of Hcy significantly increase the incidence of vascular damage in both small and large vessels [88,89]; concentrations above the 90th percentile are associated with increased risk of degenerative and atherosclerotic processes [90] in the coronary, cerebral and peripheral circulatory systems. Although Hcy is an effective cardiovascular risk biomarker, and the cardiovascular complications are critical in hospitalized COVID-19 patients, this parameter has not been adopted and studied in this clinical setting and in neither of the published prospective studies focused on laboratory markers useful for clinical evaluation of COVID-19.

The definition of hyperhomocysteinemia differs between studies [91]. Hyperhomocysteinemia is defined as a medical condition characterized by an abnormally high level ($>15 \mu\text{mol/L}$) of Hcy in the blood [92]. Total concentration of Hcy in plasma of healthy humans (fasting) is low, between 5.0 and $15.0 \mu\text{mol/L}$ when assessed with the use of high-performance liquid chromatography (HPLC), or 5.0– $12.0 \mu\text{mol/L}$ when immunoassay methods are used [93]. When the level is between 16 and $30 \mu\text{mol/L}$, it is classified as moderate, $31\text{--}100 \mu\text{mol/L}$ is considered as intermediate and a value $>100 \mu\text{mol/L}$ is classified as severe hyperhomocysteinemia [87,94]. Recent observations related hyperhomocysteinemia to cardiovascular disease, diabetes, CKD, and fatty liver disease [91,92,94].

Very recent data demonstrated a predictive value of Hcy (together with age, MLR, and period from disease onset to hospital admission) for severe pneumonia on chest CT at first week from COVID-19 patients, but did not report on additional organ involvement [11]. In the same study, the authors reported that MLR was significantly higher in imaging progression patients compared to that in imaging progression-free ones ($p < .001$).

3.5.2. Angiotensin II, Ang-(1-7), Ang-(1-9), and alamandine

ACE2 functions as a regulator of the renin–angiotensin system (RAS), modulating endogenous levels of Ang I and Ang II. Ang II levels were found to be significantly increased in the kidneys, hearts, and plasma of ACE2 null mice [95]. The level of Ang II was also significantly increased in the avian influenza A infected patients, indicating that Ang II is a biomarker for lethality in flu infections [96,97]. A strong correlation has been found

between increases in IL-6 and vascular macrophage accumulation and the degree of endothelial dysfunction produced by Ang II [98].

In an animal model, ACE2 and Ang-(1-7) infusion were shown to be protective via downregulation of RhoA/Rho kinase (ROCK) pathway. This pathway is deeply involved in changes of vascular tone and structure leading to hypertension and cardiovascular-renal remodeling, and it has a relevant role in the induction of lung fibrosis [99].

ACE2 converts Ang II to Ang-(1-7) and Ang I to Ang-(1-9). Ang-(1-7) and Ang-(1-9) produce biological effects through the Mas receptor (MasR) and AT2 receptor (AT2R), respectively. Ang-(1-7) induces regional and systemic vasodilation, diuresis, and natriuresis. Ang-(1-9) increases nitric oxide (NO) bioavailability by stimulating bradykinin (BK) release [100]. Activation of these pathways mediates anti-inflammatory and anti-fibrotic effects leading to cardiovascular, renal-protective actions, and acute lung injury protection [101,102].

Alamandine is generated by the catalytic action of ACE2 on Ang A or through a decarboxylation reaction on Ang-(1-7) in the N-terminal aspartate amino acid residue. Alamandine produces the same effects as Ang-(1-7), such as vasodilation and antifibrosis [103]. It modulates peripheral and central blood pressure regulation and cardiovascular remodeling [104].

Mechanistic evidence from related coronaviruses suggests that SARS-CoV-2 infection may downregulate ACE2, leading to toxic over-accumulation of Ang II that induces ARDS and fulminant myocarditis [105]. The Ang II level in the plasma samples from SARS-CoV-2 infected patients was markedly elevated and linearly associated to viral load and lung injury [106].

Up to date, there are no data regarding Ang-(1-7), Ang-(1-9), and alamandine plasma levels in COVID-19 patients. Following the loss of ACE2 function, due to the role of ACE2 as the viral binding site by SARS-CoV-2, we expect elevated level of Ang II and lower levels of Ang-(1-7), Ang-(1-9), and alamandine in severely infected patients than in mild ones.

4. Limitation of the study

A large proportion of the primary research is based on Asian patients; therefore, further verification is needed in populations in other areas. Some biomarkers, such as Hcy, have been evaluated in a few scientific reports and further analysis is needed in a large cohort of COVID-19 patients. There appears to be geographic variability in the percentage of patients with lymphopenia as shown in a retrospective study [107]. Further investigations

should be done to assess this geographic variability. This is a review of the current scientific literature with no statistical outcome measures. Therefore, these results may not be generalizable to all populations. Finally, with COVID-19 being a very novel disease, many clinical studies are still ongoing or undergoing publication.

5. Conclusions

Since the emergency pandemic situation began, it is of high scientific significance to analyze the discriminative ability of hematologic, biochemical, inflammatory, and immunologic biomarkers in patients with and without the severe or fatal forms of COVID-19. It is necessary to determine risk categories following COVID-19 diagnosis, to ensure an optimal resource allocation and to improve clinical management and prevention of serious complications.

To sum up, we can conclude from the analysis of published studies that hematological (lymphocyte count, neutrophil count, and NLR), inflammatory (CRP, ESR, IL-6), and especially biochemical (D-dimer, Troponins, CK) parameters correlate with severe prognosis or exitus in COVID-19 patients and can therefore be used as predictive biomarkers. Coagulation and liver parameters might play a crucial role in identifying severe cases of COVID-19.

Understanding the weight of the pathophysiological processes of systemic cardiovascular damage (vasculitis, DIC, myocardial infarction) and metabolic processes associated to the critical course of the infection, also thanks to autopsy cohorts [68,108–110], sets new light on biochemical biomarkers related to coagulation disorders. These are in fact not only predictive of disease severity, but are also helpful for the therapeutic management, based on drugs preventing the activation of coagulation processes. A laboratory score, taking into account hematological, inflammatory, biochemical and immunological parameters, would help to stratify COVID-19 positive patients into risk categories, which would be of outmost importance in the clinical setting and therapeutic management.

In addition to above discussed laboratory parameters, which are currently used in clinical practice, novel biomarkers potentially useful for screening, clinical management, and prevention of serious complications are under investigation. These include Hcy, Ang II, Ang-(1-7), Ang-(1-9), and alamandine, which need to be evaluated in larger case series in order to clearly determine their predictive clinical value as indicators of severe prognosis in COVID-19 patients.

Acknowledgements

We are grateful to Johanna Marie Chester for her language assistance.

Author contributions

GP, TO conceived of the idea for the review, searched the scientific literature and drafted the manuscript. MM searched the literature and drafted the manuscript. TO, CR and AT revised the manuscript. All authors read and approved the final manuscript.

Disclosure statement

The authors report no conflict of interest.

References

- [1] Tang N, Li D, Wang X, et al. Abnormal coagulation parameters are associated with poor prognosis in patients with novel coronavirus pneumonia. *J Thromb Haemost.* 2020;18(4):844–847.
- [2] Lin L, Lu L, Cao W, et al. Hypothesis for potential pathogenesis of SARS-CoV-2 infection—a review of immune changes in patients with viral pneumonia. *Emerg Microbes Infect.* 2020;9:1–14.
- [3] Huang C, Wang Y, Li X, et al. Clinical features of patients infected with 2019 novel coronavirus in Wuhan, China. *Lancet.* 2020;395(10223):497–506.
- [4] Chen N, Zhou M, Dong X, et al. Epidemiological and clinical characteristics of 99 cases of 2019 novel coronavirus pneumonia in Wuhan, China: a descriptive study. *Lancet.* 2020;395(10223):507–513.
- [5] Shi S, Qin M, Shen B, et al. Association of cardiac injury with mortality in hospitalized patients with COVID-19 in Wuhan, China. *JAMA Cardiol.* 2020.
- [6] Grasselli G, Zangrillo A, Zanella A, et al. Baseline characteristics and outcomes of 1591 patients infected with SARS-CoV-2 admitted to ICUs of the Lombardy Region, Italy. *JAMA.* 2020;323(16):1574.
- [7] Zhang C, Wu Z, Li J-W, et al. The cytokine release syndrome (CRS) of severe COVID-19 and interleukin-6 receptor (IL-6R) antagonist tocilizumab may be the key to reduce the mortality. *Int J Antimicrob Agents.* 2020. DOI:[10.1016/j.ijantimicag.2020.105954](https://doi.org/10.1016/j.ijantimicag.2020.105954)
- [8] Released by National Health Commission & National Administration of Traditional Chinese Medicine on March 3 2020. Diagnosis and treatment protocol for novel coronavirus pneumonia (trial version 7). *Chin Med J (Engl).* 2020;133:1087–1095.
- [9] Du R-H, Liang L-R, Yang C-Q, et al. Predictors of mortality for patients with COVID-19 pneumonia caused by SARS-CoV-2: a prospective cohort study. *Eur Respir J.* 2020;55:2000524.
- [10] Zhang G, Zhang J, Wang B, et al. Analysis of clinical characteristics and laboratory findings of 95 cases of 2019 novel coronavirus pneumonia in Wuhan, China: a retrospective analysis. *Respir Res.* 2020;21(1):74.

- [11] Yang Z, Shi J, He Z, et al. Predictors for imaging progression on chest CT from coronavirus disease 2019 (COVID-19) patients. *Aging.* 2020;12:6037–6048.
- [12] Donoghue M, Hsieh F, Baronas E, et al. A novel angiotensin-converting enzyme-related carboxypeptidase (ACE2) converts angiotensin I to angiotensin 1-9. *Circ Res.* 2000;87(5):E1–E9.
- [13] Anguiano L, Riera M, Pascual J, et al. Circulating angiotensin converting enzyme 2 activity as a biomarker of silent atherosclerosis in patients with chronic kidney disease. *Atherosclerosis.* 2016;253:135–143.
- [14] Li S, Wang Z, Yang X, et al. Association between circulating angiotensin-converting enzyme 2 and cardiac remodeling in hypertensive patients. *Peptides.* 2017;90:63–68.
- [15] Touyz RM, Li H, Delles C. ACE2 the Janus-faced protein – from cardiovascular protection to severe acute respiratory syndrome-coronavirus and COVID-19. *Clin Sci.* 2020;134(7):747–750.
- [16] Tai W, He L, Zhang X, et al. Characterization of the receptor-binding domain (RBD) of 2019 novel coronavirus: implication for development of RBD protein as a viral attachment inhibitor and vaccine. *Cell Mol Immunol.* 2020. DOI:10.1038/s41423-020-0400-4
- [17] D'Amico F, Baumgart DC, Danese S, et al. Diarrhea during COVID-19 infection: pathogenesis, epidemiology, prevention and management. *Clin Gastroenterol Hepatol.* 2020. DOI:10.1016/j.cgh.2020.04.001
- [18] Li S, Tang Z, Li Z, et al. Searching therapeutic strategy of new coronavirus pneumonia from angiotensin-converting enzyme 2: the target of COVID-19 and SARS-CoV. *Eur J Clin Microbiol Infect Dis.* 2020;39(6):1–6.
- [19] Wenzhong L, Huanlan L. COVID-19: attacks the 1-beta chain of hemoglobin and captures the porphyrin to inhibit human heme metabolism. 2020 [cited 2020 Apr 11]. Available from: https://chemrxiv.org/articles/COVID-19_Disease_ORF8_and_Surface_Glycoprotein_Inhibit_Heme_Metabolism_by_Binding_to_Porphyrin/11938173
- [20] Yang X, Yu Y, Xu J, et al. Clinical course and outcomes of critically ill patients with SARS-CoV-2 pneumonia in Wuhan, China: a single-centered, retrospective, observational study. *Lancet Respir Med.* 2020;8(5):475–481.
- [21] Qin C, Zhou L, Hu Z, et al. Dysregulation of immune response in patients with COVID-19 in Wuhan, China. *Clin Infect Dis.* 2020. DOI:10.1093/cid/ciaa248
- [22] Henry BM, de Oliveira MHS, Benoit S, et al. Hematologic, biochemical and immune biomarker abnormalities associated with severe illness and mortality in coronavirus disease 2019 (COVID-19): a meta-analysis. *Clin Chem Lab Med.* 2020.
- [23] Cossarizza A, De Biasi S, Guaraldi G, et al. SARS-CoV-2, the virus that causes COVID-19. *Cytometry.* 2020; 97(4):340–343.
- [24] Zhang C, Wang X, Li S, et al. NKG2A is a NK cell exhaustion checkpoint for HCV persistence. *Nat Commun.* 2019;10:1–11.
- [25] Luo S, Zhang X, Xu H. Don't overlook digestive symptoms in patients with 2019 novel coronavirus disease (COVID-19). *Clin Gastroenterol Hepatol.* 2020.
- [26] Ruan Q, Yang K, Wang W, et al. Clinical predictors of mortality due to COVID-19 based on an analysis of data of 150 patients from Wuhan, China. *Intensive Care Med.* 2020;46(5):846–848.
- [27] Ding Q, Lu P, Fan Y, et al. The clinical characteristics of pneumonia patients co-infected with 2019 novel coronavirus and influenza virus in Wuhan, China. *J Med Virol.* 2020.
- [28] Zheng M, Gao Y, Wang G, et al. Functional exhaustion of antiviral lymphocytes in COVID-19 patients. *Cell Mol Immunol.* 2020;17:1–3.
- [29] Wang F, Nie J, Wang H, et al. Characteristics of peripheral lymphocyte subset alteration in COVID-19 pneumonia. *J Infect Dis.* 2020;221(11):1762–1769.
- [30] Xu B, Fan C-Y, Wang A-L, et al. Suppressed T cell-mediated immunity in patients with COVID-19: a clinical retrospective study in Wuhan, China. *J Infect.* 2020. DOI:10.1016/j.jinf.2020.04.012
- [31] Yun H, Sun Z, Wu J, et al. Laboratory data analysis of novel coronavirus (COVID-19) screening in 2510 patients. *Clin Chim Acta.* 2020;507:94–97.
- [32] Qian G-Q, Yang N-B, Ding F, et al. Epidemiologic and clinical characteristics of 91 hospitalized patients with COVID-19 in Zhejiang, China: a retrospective, multi-centre case series. *QJM Mon J Assoc Phys.* 2020.
- [33] Zhang J-J, Dong X, Cao Y-Y, et al. Clinical characteristics of 140 patients infected with SARS-CoV-2 in Wuhan, China. *Allergy.* 2020.
- [34] Liu F, Xu A, Zhang Y, et al. Patients of COVID-19 may benefit from sustained lopinavir-combined regimen and the increase of eosinophil may predict the outcome of COVID-19 progression. *Int J Infect Dis.* 2020; 95:183–191.
- [35] Lippi G, Henry BM. Eosinophil count in severe coronavirus disease 2019 (COVID-19). *QJM Mon J Assoc Phys.* 2020.
- [36] Bhat T, Teli S, Rijal J, et al. Neutrophil to lymphocyte ratio and cardiovascular diseases: a review. *Expert Rev Cardiovasc Ther.* 2013;11(1):55–59.
- [37] Haybar H, Pezeshki SMS, Saki N. Evaluation of complete blood count parameters in cardiovascular diseases: an early indicator of prognosis? *Exp Mol Pathol.* 2019;110:104267.
- [38] Huang Z, Fu Z, Huang W, et al. Prognostic value of neutrophil-to-lymphocyte ratio in sepsis: a meta-analysis. *Am J Emerg Med.* 2019.
- [39] Liu Y, Du X, Chen J, et al. Neutrophil-to-lymphocyte ratio as an independent risk factor for mortality in hospitalized patients with COVID-19. *J Infect.* 2020.
- [40] Xia X, Wen M, Zhan S, et al. An increased neutrophil/lymphocyte ratio is an early warning signal of severe COVID-19. *Nan Fang Yi Ke Da Xue Xue Bao.* 2020;40: 333–336.
- [41] Liu J, Li S, Liu J, et al. Longitudinal characteristics of lymphocyte responses and cytokine profiles in the peripheral blood of SARS-CoV-2 infected patients. *EBioMedicine.* 2020;55:102763.
- [42] Long L, Zeng X, Zhang X, et al. Short-term outcomes of coronavirus disease 2019 and risk factors for progression. *Eur Respir J.* 2020.

- [43] Xia X-Y, Wu J, Liu H-L, et al. Epidemiological and initial clinical characteristics of patients with family aggregation of COVID-19. *J Clin Virol.* 2020;127: 104360.
- [44] Yang A-P, Liu J-P, Tao W-Q, et al. The diagnostic and predictive role of NLR, d-NLR and PLR in COVID-19 patients. *Int Immunopharmacol.* 2020;84:106504.
- [45] Lagunas-Rangel FA. Neutrophil-to-lymphocyte ratio and lymphocyte-to-C-reactive protein ratio in patients with severe coronavirus disease 2019 (COVID-19): a meta-analysis. *J Med Virol.* 2020.
- [46] Yan Q, Li P, Ye X, et al. Longitudinal peripheral blood transcriptional analysis of COVID-19 patients captures disease progression and reveals potential biomarkers. *medRxiv.* 2020.
- [47] Akhmerov A, Marban E. COVID-19 and the heart. *Circ Res.* 2020.
- [48] Jolicoeur P, Lamontagne L. Impairment of bone marrow pre-B and B cells in MHV3 chronically-infected mice. *Adv Exp Med Biol.* 1995;380:193–195.
- [49] Yang M, Ng MHL, Li CK. Thrombocytopenia in patients with severe acute respiratory syndrome (review). *Hematology.* 2005;10(2):101–105.
- [50] Khurana D, Deoke SA. Thrombocytopenia in critically ill patients: clinical and laboratorial behavior and its correlation with short-term outcome during hospitalization. *Indian J Crit Care Med.* 2017;21(12):861–864.
- [51] Vanderschueren S, De Weerdt A, Malbrain M, et al. Thrombocytopenia and prognosis in intensive care. *Crit Care Med.* 2000;28:1871–1876.
- [52] Hui P, Cook DJ, Lim W, et al. The frequency and clinical significance of thrombocytopenia complicating critical illness: a systematic review. *Chest.* 2011; 139(2):271–278.
- [53] Ganji A, Farahani I, Khansarinejad B, et al. Increased expression of CD8 marker on T-cells in COVID-19 patients. *Blood Cells Mol Dis.* 2020;83:102437.
- [54] Tang N, Bai H, Chen X, et al. Anticoagulant treatment is associated with decreased mortality in severe coronavirus disease 2019 patients with coagulopathy. *J Thromb Haemost.* 2020;18(5):1094–1099.
- [55] Lippi G, Plebani M, Henry BM. Thrombocytopenia is associated with severe coronavirus disease 2019 (COVID-19) infections: a meta-analysis. *Clin Chim Acta.* 2020;506:145–148.
- [56] Yin S, Huang M, Li D, et al. Difference of coagulation features between severe pneumonia induced by SARS-CoV2 and non-SARS-CoV2. *J Thromb Thrombolysis.* 2020.
- [57] Qu R, Ling Y, Zhang Y-H-Z, et al. Platelet-to-lymphocyte ratio is associated with prognosis in patients with coronavirus disease-19. *J Med Virol.* 2020.
- [58] Xu P, Zhou Q, Xu J. Mechanism of thrombocytopenia in COVID-19 patients. *Ann Hematol.* 2020;1–4.
- [59] Zheng Y, Xu H, Yang M, et al. Epidemiological characteristics and clinical features of 32 critical and 67 noncritical cases of COVID-19 in Chengdu. *J Clin Virol.* 2020;127:104366.
- [60] Henry BM, Oliveira MHS, de Benoit S, et al. Hematologic, biochemical and immune biomarker abnormalities associated with severe illness and mortality in coronavirus disease 2019 (COVID-19): a meta-analysis. *Clin Chem Lab Med.* 2020.
- [61] Zhou F, Yu T, Du R, et al. Clinical course and risk factors for mortality of adult inpatients with COVID-19 in Wuhan, China: a retrospective cohort study. *Lancet (Lond Engl).* 2020;395(10229):1054–1062.
- [62] Chen T, Wu D, Chen H, et al. Clinical characteristics of 113 deceased patients with coronavirus disease 2019: retrospective study. *BMJ.* 2020;368:m1091.
- [63] Chai X, Hu L, Zhang Y, et al. Specific ACE2 expression in cholangiocytes may cause liver damage after 2019-nCoV infection. *bioRxiv.* 2020.
- [64] Lei F, Liu Y-M, Zhou F, et al. Longitudinal association between markers of liver injury and mortality in COVID-19 in China. *Hepatology.* 2020.
- [65] Tan C, Huang Y, Shi F, et al. C-reactive protein correlates with CT findings and predicts severe COVID-19 early. *J Med Virol.* 2020.
- [66] Meduri GU, Headley S, Kohler G, et al. Persistent elevation of inflammatory cytokines predicts a poor outcome in ARDS. Plasma IL-1 beta and IL-6 levels are consistent and efficient predictors of outcome over time. *Chest.* 1995;107(4):1062–1073.
- [67] Mehta P, McAuley DF, Brown M, et al. COVID-19: consider cytokine storm syndromes and immunosuppression. *Lancet.* 2020;395(10229):1033–1034.
- [68] Wang D, Hu B, Hu C, et al. Clinical characteristics of 138 hospitalized patients with 2019 novel coronavirus-infected pneumonia in Wuhan, China. *JAMA.* 2020;323(11):1061–1069.
- [69] Karzai W, Oberhoffer M, Meier-Hellmann A, et al. Procalcitonin—a new indicator of the systemic response to severe infections. *Infection.* 1997;25(6): 329–334.
- [70] Russwurm S, Wiederhold M, Oberhoffer M, et al. Molecular aspects and natural source of procalcitonin. *Clin Chem Lab Med.* 1999;37(8):789–797.
- [71] Cleland DA, Ernster AP. Procalcitonin. *StatPearls; [Internet].* Treasure Island (FL): StatPearls Publishing; 2020 [cited 2020 Apr 22]. Available from: <http://www.ncbi.nlm.nih.gov/books/NBK539794/>
- [72] Delevaux I, Andre M, Colombier M, et al. Can procalcitonin measurement help in differentiating between bacterial infection and other kinds of inflammatory processes? *Ann Rheum Dis.* 2003;62(4):337–340.
- [73] Guan W, Liang W, Zhao Y, et al. Comorbidity and its impact on 1590 patients with Covid-19 in China: a nationwide analysis. *Eur Respir J.* 2020.
- [74] Zhang G, Hu C, Luo L, et al. Clinical features and short-term outcomes of 221 patients with COVID-19 in Wuhan, China. *J Clin Virol.* 2020;127:104364.
- [75] Chen T, Dai Z, Mo P, et al. Clinical characteristics and outcomes of older patients with coronavirus disease 2019 (COVID-19) in Wuhan, China (2019): a single-centered, retrospective study. *J Gerontol A Biol Sci Med Sci.* 2020.
- [76] Sun D, Li H, Lu X-X, et al. Clinical features of severe pediatric patients with coronavirus disease 2019 in Wuhan: a single center's observational study. *World J Pediatr.* 2020.
- [77] Chen X, Yang Y, Huang M, et al. Differences between COVID-19 and suspected then confirmed SARS-CoV-

- [78] 2-negative pneumonia: a retrospective study from a single center. *J Med Virol.* 2020;.
- [79] Lippi G, Plebani M. Procalcitonin in patients with severe coronavirus disease 2019 (COVID-19): a meta-analysis. *Clin Chim Acta.* 2020;505:190–191.
- [80] Xia W, Shao J, Guo Y, et al. Clinical and CT features in pediatric patients with COVID-19 infection: different points from adults. *Pediatr Pulmonol.* 2020;55(5):1169–1174.
- [81] Yunus I, Fasih A, Wang Y. The use of procalcitonin in the determination of severity of sepsis, patient outcomes and infection characteristics. *PLoS One.* 2018;13(11):e0206527.
- [82] Libby P. The heart in COVID19: primary target or secondary bystander? *JACC Basic Transl Sci.* 2020;.
- [83] Deng Q, Hu B, Zhang Y, et al. Suspected myocardial injury in patients with COVID-19: evidence from front-line clinical observation in Wuhan, China. *Int J Cardiol.* 2020;.
- [84] Wang K, Zuo P, Liu Y, et al. Clinical and laboratory predictors of in-hospital mortality in patients with COVID-19: a cohort study in Wuhan, China. *Clin Infect Dis.* 2020;.
- [85] Terpos E, Ntanasis-Stathopoulos I, Elalamy I, et al. Hematological findings and complications of COVID-19. *Am J Hematol.* 2020;.
- [86] Zou Y, Guo H, Zhang Y, et al. Analysis of coagulation parameters in patients with COVID-19 in Shanghai, China. *Biosci Trends.* 2020;.
- [87] Ganguly P, Alam SF. Role of homocysteine in the development of cardiovascular disease. *Nutr J.* 2015;14:6.
- [88] Balint B, Jepchumba VK, Guéant J-L, et al. Mechanisms of homocysteine-induced damage to the endothelial, medial and adventitial layers of the arterial wall. *Biochimie.* 2020;.
- [89] Pushpakumar S, Kundu S, Sen U. Endothelial dysfunction: the link between homocysteine and hydrogen sulfide. *Curr Med Chem.* 2014;21(32):3662–3672.
- [90] Graham IM, Daly LE, Refsum HM, et al. Plasma homocysteine as a risk factor for vascular disease. The European Concerted Action Project. *JAMA.* 1997;277(22):1775–1781.
- [91] Faeh D, Chiolero A, Paccaud F. Homocysteine as a risk factor for cardiovascular disease: should we (still) worry about? *Swiss Med Wkly.* 2006;136(47–48):745–756.
- [92] Guo H, Chi J, Xing Y, et al. Influence of folic acid on plasma homocysteine levels & arterial endothelial function in patients with unstable angina. *Indian J Med Res.* 2009;129:279–284.
- [93] Baszczuk A, Kopczyński Z. Hyperhomocysteinemia in patients with cardiovascular disease. *Postepy Hig Med Dosw.* 2014;68:579–589.
- [94] Hankey GJ, Eikelboom JW. Homocysteine and vascular disease. *Indian Heart J.* 2000;52(7 Suppl.):S18–S26.
- [95] Crackower MA, Sarao R, Oudit GY, et al. Angiotensin-converting enzyme 2 is an essential regulator of heart function. *Nature.* 2002;417(6891):822–828.
- [96] Zou Z, Yan Y, Shu Y, et al. Angiotensin-converting enzyme 2 protects from lethal avian influenza A H5N1 infections. *Nat Commun.* 2014;5:3594.
- [97] Huang F, Guo J, Zou Z, et al. Angiotensin II plasma levels are linked to disease severity and predict fatal outcomes in H7N9-infected patients. *Nat Commun.* 2014;5:1–7.
- [98] Gomolak JR, Didion SP. Angiotensin II-induced endothelial dysfunction is temporally linked with increases in interleukin-6 and vascular macrophage accumulation. *Front Physiol.* 2014;5:396.
- [99] Calò LA, Rigato M, Bertoldi G. ACE2/angiotensin 1-7 protective anti-inflammatory and antioxidant role in hyperoxic lung injury: support from studies in Bartter's and Gitelman's syndromes. *QJM Int J Med.* 2020;.
- [100] Mendoza-Torres E, Oyarzún A, Mondaca-Ruff D, et al. ACE2 and vasoactive peptides: novel players in cardiovascular/renal remodeling and hypertension. *Ther Adv Cardiovasc Dis.* 2015;9(4):217–237.
- [101] Arendse LB, Danser AHJ, Poglitsch M, et al. Novel therapeutic approaches targeting the renin–angiotensin system and associated peptides in hypertension and heart failure. *Pharmacol Rev.* 2019;71(4):539–570.
- [102] Rodrigues Prestes TR, Rocha NP, Miranda AS, et al. The anti-inflammatory potential of ACE2/angiotensin-(1-7)/Mas receptor axis: evidence from basic and clinical research. *Curr Drug Targets.* 2017;18(11):1301–1313.
- [103] Qaradakhi T, Apostolopoulos V, Zulli A. Angiotensin (1-7) and alamandine: similarities and differences. *Pharmacol Res.* 2016;111:820–826.
- [104] Hrenak J, Paulis L, Simko F. Angiotensin A/alamandine/MrgD axis: another clue to understanding cardiovascular pathophysiology. *Int J Mol Sci.* 2016;17.
- [105] Hanff TC, Harhay MO, Brown TS, et al. Is there an association between COVID-19 mortality and the renin–angiotensin system—a call for epidemiologic investigations. *Clin Infect Dis.* 2020;.
- [106] Liu Y, Yang Y, Zhang C, et al. Clinical and biochemical indexes from 2019-nCoV infected patients linked to viral loads and lung injury. *Sci China Life Sci.* 2020;63(3):364–374.
- [107] Xu X-W, Wu X-X, Jiang X-G, et al. Clinical findings in a group of patients infected with the 2019 novel coronavirus (SARS-CoV-2) outside of Wuhan, China: retrospective case series. *BMJ.* 2020;368:m606.
- [108] Hanley B, Lucas SB, Youd E, et al. Autopsy in suspected COVID-19 cases. *J Clin Pathol.* 2020;73(5):239–242.
- [109] Fu B, Xu X, Wei H. Why tocilizumab could be an effective treatment for severe COVID-19? *J Transl Med.* 2020;18(1):164.
- [110] Li H, Liu L, Zhang D, et al. SARS-CoV-2 and viral sepsis: observations and hypotheses. *Lancet (Lond Engl).* 2020;395(10235):1517–1520.

Diagnostic Value of D-Dimer in COVID-19: A Meta-Analysis and Meta-Regression

Clinical and Applied
Thrombosis/Hemostasis
Volume 27: 1-10
© The Author(s) 2021
Article reuse guidelines:
sagepub.com/journals-permissions
DOI: 10.1177/10760296211010976
journals.sagepub.com/home/cat



Haoting Zhan, PhD^{1,2} , Haizhen Chen, PhD^{1,2,3},
Chenxi Liu, PhD^{1,2}, Linlin Cheng, PhD^{1,2}, Songxin Yan, PhD^{1,2},
Haolong Li, PhD^{1,2}, and Yongzhe Li^{1,2}

Abstract

The prognostic role of hypercoagulability in COVID-19 patients is ambiguous. D-dimer, may be regarded as a global marker of hemostasis activation in COVID-19. Our study was to assess the predictive value of D-dimer for the severity, mortality and incidence of venous thromboembolism (VTE) events in COVID-19 patients. PubMed, EMBASE, Cochrane Library and Web of Science databases were searched. The pooled diagnostic value (95% confidence interval [CI]) of D-dimer was evaluated with a bivariate mixed-effects binary regression modeling framework. Sensitivity analysis and meta regression were used to determine heterogeneity and test robustness. A Spearman rank correlation tested threshold effect caused by different cut offs and units in D-dimer reports. The pooled sensitivity of the prognostic performance of D-dimer for the severity, mortality and VTE in COVID-19 were 77% (95% CI: 73%-80%), 75% (95% CI: 65%-82%) and 90% (95% CI: 90%-90%) respectively, and the specificity were 71% (95% CI: 64%-77%), 83% (95% CI: 77%-87%) and 60% (95% CI: 60%-60%). D-dimer can predict severe and fatal cases of COVID-19 with moderate accuracy. It also shows high sensitivity but relatively low specificity for detecting COVID-19-related VTE events, indicating that it can be used to screen for patients with VTE.

Keywords

COVID-19, coronavirus 2019, D-dimer, diagnosis, venous thromboembolism

Date received: 20 February 2021; revised: 21 March 2021; accepted: 29 March 2021.

Introduction

Since the outbreak of the pandemic in December 2019 in Wuhan, China, coronavirus disease 2019 (COVID-19) has affected over 120.77 million worldwide, and resulted in approximately 2,672,099 deaths. COVID-related mortality is largely associated with hypercoagulability and increased risk of venous thromboembolism (VTE) events, leading to thrombo-inflammation in severe conditions.¹ Therefore, coagulation biomarkers may indicate disease severity and mortality, and help determine patient triage, therapeutic strategies and prognosis supervision. D-dimer is the product of fibrin degradation, and plays a mechanistic role in thrombo-inflammation in COVID-19.¹ Several studies have correlated elevated D-dimer (prevalence up to 46.4%) with increased severity and adverse outcomes of COVID-19.²⁻⁴ Patients with D-dimer >1000 ng/ml present a 20-fold higher mortality risk compared to those with lower D-dimer values.³ Therefore, D-dimer is a potential screening tool for VTE in COVID-19 patients, and based on D-dimer elevation, adjusting therapeutic

anticoagulant doses is more beneficial to the patients compared to prophylactic doses.⁵ Thus, D-dimer levels should be monitored in COVID patients early after admission.

However, the diagnostic value of D-dimer in predicting disease severity, mortality and VTE events in COVID-19 has not

¹ Department of Clinical Laboratory, Peking Union Medical College Hospital, Chinese Academy of Medical Sciences and Peking Union Medical College, Beijing, People's Republic of China

² State Key Laboratory of Complex, Severe and Rare Diseases, Peking Union Medical College Hospital, Chinese Academy of Medical Sciences and Peking Union Medical College, Beijing, People's Republic of China

³ Department of Clinical Laboratory, The First Hospital of Jilin University, Changchun, People's Republic of China

Corresponding Author:

Yongzhe Li, Department of Clinical Laboratory, Peking Union Medical College Hospital, Chinese Academy of Medical Sciences and Peking Union Medical College, 1 Shuaifuyuan, Dongcheng District, Beijing 100730, People's Republic of China.

Email: yongzhelipumch@126.com



Creative Commons Non Commercial CC BY-NC: This article is distributed under the terms of the Creative Commons Attribution-NonCommercial 4.0 License (<https://creativecommons.org/licenses/by-nc/4.0/>) which permits non-commercial use,

reproduction and distribution of the work without further permission provided the original work is attributed as specified on the SAGE and Open Access pages (<https://us.sagepub.com/en-us/nam/open-access-at-sage>).

been elucidated yet, due to the small cohorts and the heterogeneity between studies. Up till now, most of studies didn't report harmonized D-dimer to single units. To recognize and verify its diagnostic performance in COVID-19, we systematically conducted a literature review and meta-analysis.

Materials and Methods

Literature Search

The systematic review and meta-analysis was performed based on the Preferred Reporting Items for Systematic Reviews and Meta-analyses (PRISMA) guidelines (Supplementary Table 1). The registration number is CRD42021230446. Two authors (HTZ and HZC) independently searched the PubMed, Embase, Cochrane Library and the core collection of Web of Science databases for studies published till September 1, 2020, using the following items: "d-dimer," "diagnostic marker," "biomarker" and "laboratory test" for D-dimer combined with "Coronavirus," "Beta coronavirus," "SARS CoV-2" and "COVID-19." The search strategies are detailed in Supplementary Table 2. Additional studies were retrieved manually from the references.

Eligibility Criteria

Without any restrictions on time, language, ethnicity or geographical region, studies satisfying the following criteria were included: (1) assessment of the diagnostic utility of D-dimer in distinguishing in-hospital severity, mortality and VTE events in COVID-19 patients, (2) sufficient data to construct a 2×2 table to determine diagnostic accuracy of D-dimer, and (3) confirmed diagnosis of COVID-19 by either real time-polymerase chain reaction (RT-PCR) or radiological imaging, with at least one adequate D-dimer result. Studies on animal and cellular models, case reports, case series, conference abstracts or letters without sufficient data were excluded.

Data Extraction and Quality Assessment

Two independent authors (HTZ and HZC) separately screened the literature, and extracted and evaluated the data. Any discrepancies were resolved by consensus or a third opinion. The study number, first author's name, study region, sample size, inclusion and exclusion criteria, demographic features (age, sex, comorbidity and ethnicity), reference standard, D-dimer assay method, time for D-dimer test (at admission or hospitalization) and VTE prevalence were extracted into pre-designed charts. Quality Assessment of Diagnostic Accuracy Studies (QUADAS-2) was used to evaluate the study quality. Further details of the pooled studies were obtained by directly contacting the authors as per requirement.

Statistical Analysis

STATA V.16.0 (Stata Corporation, College Station, TX, USA) and Meta-DiSc V.1.4 (Unit of Clinical Biostatistics, Ramony

Cajal Hospital, Madrid, Spain) was used to perform the meta-analysis. The primary outcomes were severity, mortality and VTE events in COVID-19 confirmed patients. A bivariate mixed-effects binary regression modeling framework was used to combine the pooled sensitivity, specificity, positive likelihood ratio ($LR+$), negative likelihood ratio ($LR-$), and diagnostic ratios (DOR) with 95% CI. Significant heterogeneity was ascertained based on Cochrane's Q-statistic P value ≤ 0.10 or $I^2 > 50\%$. The summary receiver operator characteristics (SROC) curve and the area under the curve (AUC) were analyzed to appraise the overall diagnostic performance of D-dimer in COVID-19 confirmed patients. Sensitivity analysis and multiple regression analysis were performed to identify the potential origin of heterogeneity and test robustness. P value <0.05 (2 sided) was considered statistically significant. The publication bias was also assessed.

Results

Search Results and Characteristics of Studies

The results of the literature search are outlined in Figure 1. A total of 5557 articles published till September 1, 2020 were extracted from 4 databases. After removing duplicate studies ($n = 2207$) and irrelevant publications ($n = 1048$), 2302 articles were further analyzed, and the full-text of 69 were read. Thirty-nine full-text articles were eliminated on account of incomplete data or unrelated outcomes (severe/dead/VTE events). Thirty-three eligible studies met our inclusion criteria,⁶⁻³⁴ of which one was excluded due to the combined model of dyslipidemia and D-dimer levels for VTE prediction in COVID-19, and 3 due to insufficient data. Finally, 8 studies on the predictive power of D-dimer for disease severity,⁶⁻¹³ 12 for mortality^{6,11,14-23} and 12 for COVID-19-related VTE events^{11,24-34} were included in the meta-analysis, which included 2014, 4468 and 2158 patients respectively. The main characteristics of the studies are summarized in Supplementary Table 3 and Supplementary Table 4. Most are retrospective studies ($n = 27$), one was prospective and one cross-sectional.

Study Quality

QUADAS-2 was used to assess the quality of the eligible studies, and indicated overall good quality, with positive results for at least 9/14 items (Figure S1).

Meta-Analysis of the Diagnostic Accuracy of D-Dimer for Disease Severity in COVID-19 Patients

The diagnostic sensitivity of D-dimer for severity in 2014 COVID-19 patients ranged from 43% to 100%, and the specificity was 57% to 89%. The pooled sensitivity and specificity were 77% (95% CI: 58%-89%) and 71% (95% CI: 64%-77%) respectively. The $LR+$ was 2.65 (95% CI: 2.22-3.17) and the $LR-$ was 0.33 (95% CI: 0.18-0.61). The pooled DOR was 8 (95% CI: 4-17) and the AUC of SROC was 77% (95% CI: 73%-

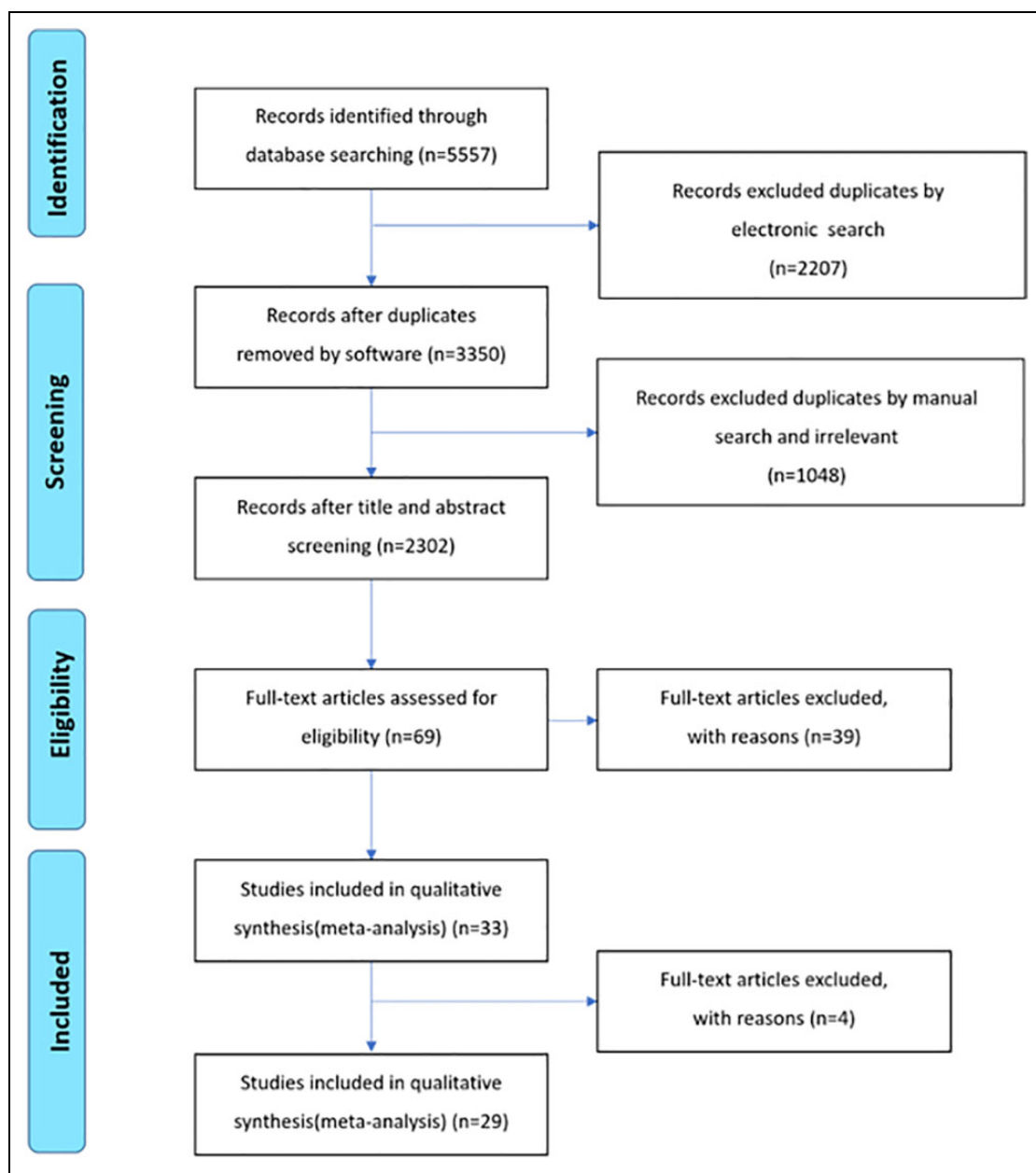


Figure 1. Flow diagram of studies included in the meta-analysis.

80%). The 95% confidence region of SROC was narrow and small, indicating the increased precision of studies in the pooled estimate. Forest plots of sensitivity and specificity, and the SROC curve are shown in Figure 2.

Meta-Analysis of the Diagnostic Accuracy of D-Dimer for Mortality in COVID-19 Patients

The diagnostic sensitivity and specificity of D-dimer for mortality in 4468 COVID-19 patients were 43% to 93% and 64% to 96% respectively, and the pooled estimates were 75% (95% CI: 65%-82%) and 83% (95% CI: 77%-87%). Comparing to severity, the LR+ was higher (4.35, 95% CI: 3.25-5.82) and the LR- was

comparable, (0.30, 95% CI: 0.22-0.42). The pooled DOR (14, 95% CI: 9-24) and the AUC of SROC (86%, 95% CI: 83%-89%) were higher than severity. Consistently, the narrow and small 95% confidence region of SROC indicated accuracy of the pooled estimate. The Forest plots and SROC curve are shown in Figure 3.

Meta-Analysis of the Diagnostic Accuracy of D-Dimer for VTE Events in COVID-19 Patients

The diagnostic sensitivity of D-dimer for VTE events in 2158 COVID-19 patients ranged from 67% to 100%, and the specificity from 29% to 89%. The pooled sensitivity and specificity were 90% (95% CI: 90%-90%) and 60% (95% CI: 60%-60%)

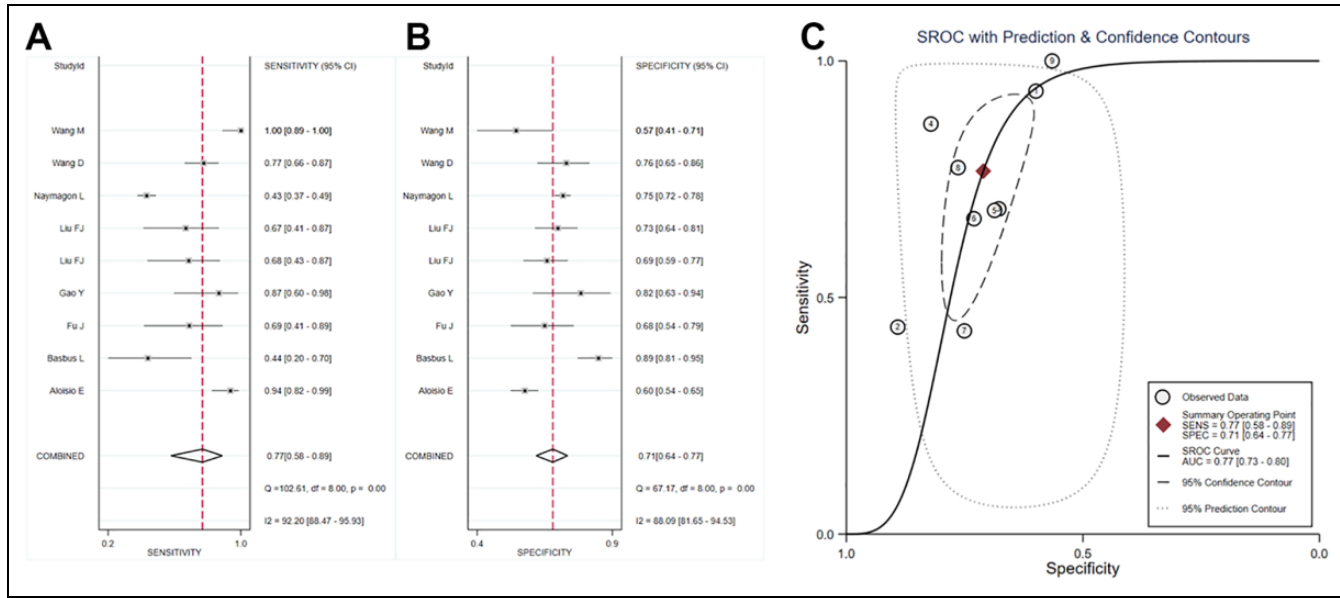


Figure 2. Forest plot and SROC of the accuracy of D-dimer for severity in COVID-19 patients.

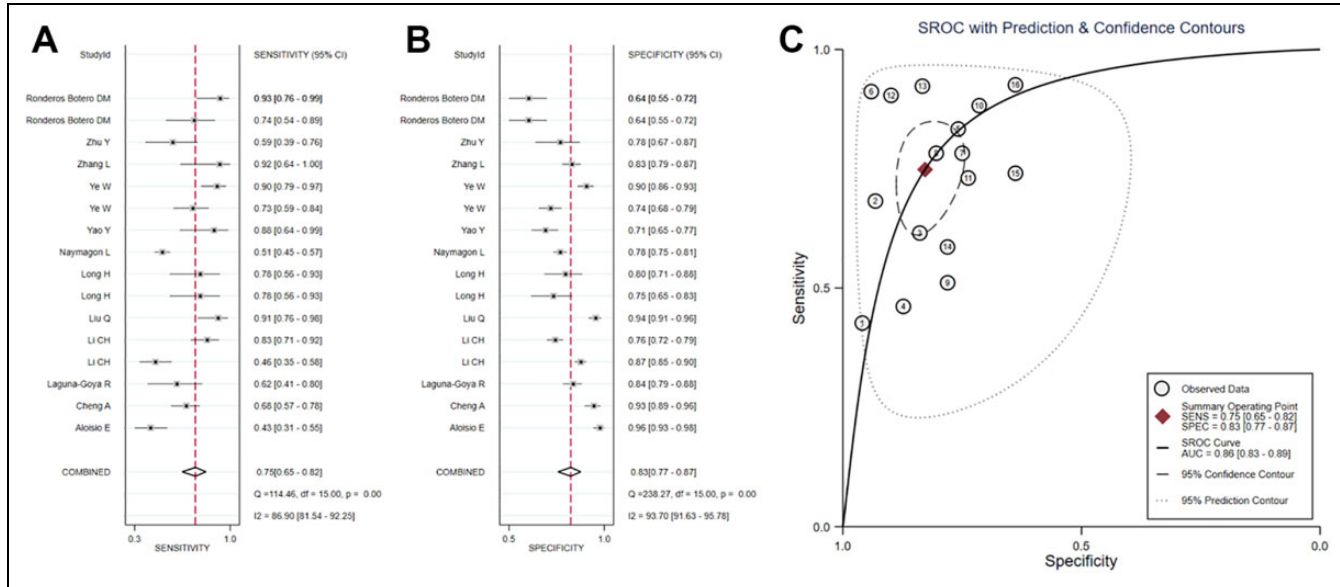


Figure 3. Forest plot and SROC of the accuracy of D-dimer for mortality in COVID-19 patients.

respectively. In this meta-analysis, LR+ and LR- showed slightly lower comparing to severity and mortality (2.24, 95% CI: 2.24-2.24; 0.16, 95% CI: 0.16-0.16, respectively). Similarly, the consistent pooled DOR was 14 (95% CI: 14-14) and the narrow and small AUC of SROC was 85% (95% CI: 81%-88%), which illustrated accurate pooled estimate. The Forest plots for pooled sensitivity and specificity, as well as the SROC curve are shown in Figure 4.

Multiple Regression and Exploration of Threshold Effect

Meta-regression analysis was performed to explore the potential origins of heterogeneity among the pooled studies.

The co-variates were country, study type, age, sex (percentage of males), patient inclusion and exclusion criteria, reference standards, time for D-dimer test, measurements of D-dimer, co-morbidity status, and clinical prevalence of VTE events.

For severity (Table 1 and Figure S2A), the reference standard (COVID-19 Diagnosis and Treatment Program Edition of China) and comorbidity status (percentage of diabetic patients) contributed to the heterogeneity in sensitivity ($P = 0.01$, $P = 0.00$, respectively), whereas country, sex and classification of severity outcome (admission to ICU/intubation/critical illness) led to heterogeneity in specificity ($P = 0.03$, $P = 0.03$, $P = 0.00$, respectively). Supplementary Table 5 showed the

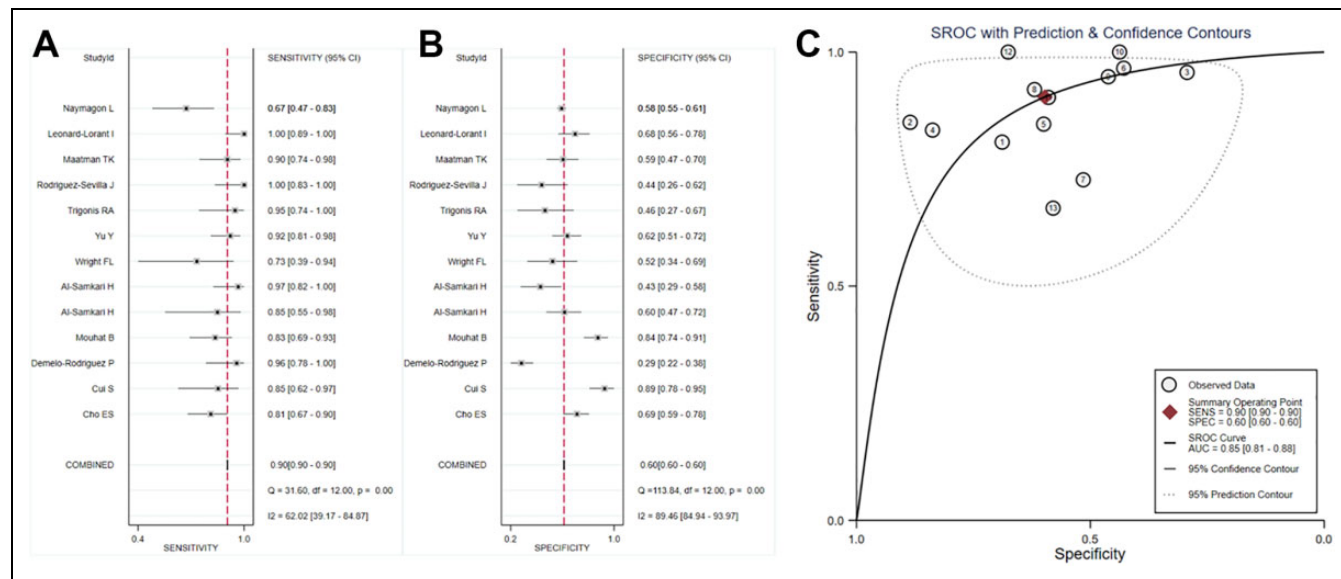


Figure 4. Forest plot and SROC of the accuracy of D-dimer for VTE events in COVID-19 patients.

results of sensitivity and specificity in meta-regression after adjusting the variable. For mortality (as shown in Table 1 and Figure S2B), country ($P = 0.03$) and exclusion of pregnancy ($P = 0.03$) led to heterogeneity in the diagnostic sensitivity, and the country ($P = 0.01$), mixed ($P = 0.00$) or single ($P = 0.02$) cohort patients (i.e. inclusion of mild/moderate/severe/critical COVID-19 patients), exclusion of no D-dimer test results ($P = 0.02$) and D-dimer test at peak level ($P = 0.00$) contributed to the heterogeneity in specificity. For VTE events (presented in Table 1 and Figure S2C), heterogeneity in sensitivity was attributed to the clinical prevalence of VTE ($P = 0.01$), whereas country ($P = 0.04$) was the source of heterogeneity in specificity.

Considering the heterogeneity of threshold (caused by different cut offs and D-dimer units) in individual study, we performed Spearman rank correlation to test the threshold effect and validated lack of threshold effect in this meta-analysis. The respective spearman correlation coefficients were 0.533 ($P = 0.139$), 0.283 ($P = 0.289$) and 0.368 ($P = 0.216$).

Exploration of Heterogeneity and Publication Bias

We conducted leave-one-out sensitivity analysis to explore the effect of every single study on the overall estimates, and the results indicated that our meta-analysis is stable (Supplementary Table 6 and Figure S3). We detected publication bias in the predictive role of D-dimer for mortality, as suggested by the asymmetric funnel plot and P values of 0.079 for Begg's test (Figure S4A), 0.000 for Egger's test (Figure S4B) and 0.04 for Deek's funnel plot (Figure S4C). However, the results of Begg's test should be interpreted with caution given small number of studies (<25). Additionally, a meta trim practice turns out the afterward heterogeneity ($Q = 230.447$, $P = 0.000$) is higher than it used to be ($Q = 116.636$, $P = 0.000$), suggesting adding imputed missing studies is more

likely to extend the distribution range of a meta-analysis and thus led to more heterogeneous of the whole set of studies (Figure S5). No publication bias was observed in the role of D-dimer for VTE events ($P = 0.95$ for Deek's funnel plot).

Discussion

Coagulation dysfunction in COVID-19 patients insidiously drives progression to severe illness and fatal outcome, and is characterized by elevated D-dimer and thrombi in the veins and arteries.¹ The high level of D-dimer in COVID-19 is triggered by excessive clots and hypoxemia. In addition, D-dimer elevation is frequently observed in COVID-19 patients with severe disease, and correlates significantly with mortality.^{2,3} Since D-dimer is the product of fibrin degradation, its presence can predict pulmonary embolism and deep venous thrombosis (DVT).^{3,5} In fact, COVID-19 patients with VTE events (both in deep venous thrombosis and pulmonary embolism) also exhibit high D-dimer levels in circulation.⁶⁻³⁴

The limited availability of duplex ultrasound or computer tomography pulmonary angiography (CTPA) and ICU equipment for COVID-19 patients due to the present quarantine warrants a novel predictor of VTE events. A recent study on 191 COVID-19 patients reported that D-dimer levels greater than 1 mg/ml on admission correlate to 18-fold increase in mortality risk.³ Furthermore, D-dimer >2600 ng/ml or more than 10 times higher than the upper limit of normal range calls for 4-extremity duplex ultrasound.³⁶ Although studies are increasingly focusing on the diagnostic performance of D-dimer for predicting the severity, mortality and VTE events in COVID-19, the results are ambiguous given the small study populations and heterogeneity between the studies. Therefore, we conducted a meta-analysis to assess the diagnostic value of D-dimer in COVID-19 patients.

Table I. Meta-Regression for Factors Associated With Variation in Sensitivity and Specificity.^a

Outcome	Variable	Sensitivity P value	Specificity P value
Severity	Country	0.18	0.03
	Age	0.95	0.93
	Study type	0.67	0.49
	Males	0.12	0.03
	Classification of outcome	0.58	0.00
	Reference standard used	0.01	0.29
	Diabetes	0.00	0.14
	Chronic respiratory disease	0.42	0.79
	Country	0.03	0.01
	Age	0.94	0.83
Mortality	Study type	0.47	0.66
	Males	0.08	0.48
	Recruitment criteria	0.52	0.00
	Severe patients only	0.46	0.02
	Exclusion criteria	0.15	0.02
	Study excluding no D-dimer results patients	0.03	0.08
	Study excluding pregnant patients	0.10	0.10
	Study excluding hematological system disease	0.67	0.10
	Time for index test	0.89	0.00
	At admission (within 3 days)	0.12	0.74
VTE events	Peak value of D-dimer	0.55	0.04
	Other time	0.93	0.97
	Country	0.11	0.08
	Age	0.31	0.06
	Study type	0.01	0.99
	Males	0.09	0.70
	Clinical prevalence of VTE	0.07	0.20
	Recruitment criteria	0.91	0.23
	DVT patients only	0.13	0.74
	PE patients only	0.40	0.06
Exclusion criteria	VTE patients only	0.23	0.84
	Mixed patient selection	0.10	0.20
	Severe patients only	0.91	0.23
	Study excluding prior VTE patients	0.41	0.74
	Study excluding therapeutic anticoagulation patients	0.23	0.84
	Reference standard used	0.10	0.20
	Use CPTA for radiographic examination	0.08	0.31
	Use ultrasound for radiographic examination	0.27	0.72
	Time for index test	0.54	0.68
	At admission	0.44	0.59
Treatment prior to index test	Peak value of D-dimer	0.28	0.79
	No treatment prior	0.71	0.13
	Hypertension	0.46	0.07
	Diabetes	0.80	0.59
	Respiratory disease	0.34	0.12
	Smoking history		

^aBold values represent $P < 0.05$ which means this variable is statistically correlated with sensitivity or specificity in meta-regression analysis.

D-dimer levels can distinguish severe COVID-19 patients with only moderate accuracy, as indicated by pooled sensitivity and specificity of 77% and 71% respectively, and AUC 77%. For predicting fatal outcome in COVID-19 patients, the pooled sensitivity, specificity and AUC were 75%, 83% and 86% respectively, suggesting a moderate chance of omission, relatively low risk of misdiagnosis and relatively high diagnostic accuracy. Finally, D-dimer can diagnose COVID-19 related VTE with high sensitivity (90%), low specificity (60%) and acceptable accuracy (AUC 85%). The respective pooled DORs for the above-mentioned analysis were 8 (95% CI: 4-17), 14

(95% CI: 9-24) and 14 (95% CI: 14-14), indicating that D-dimer can distinguish between mild and severe, fatal and non-fatal, and VTE and VTE-free cases of COVID-19.

Severity is not a solid endpoint as mortality in COVID-19 patients. In this analysis, we detailed described classification of severity in Supplementary Table 4. Definition of disease severity diversified according to different reference standard, which composed World Health Organization interim guidance for COVID-19, guidelines on the novel coronavirus-infected pneumonia diagnosis and treatment (issued by the National Health Commission of China), guidelines of national diagnosis and

treatment protocols for COVID-19 and the guidelines of American Thoracic Society. This source of heterogeneity of disease severity was confirmed by meta-regression analysis where the reference standard ($P = 0.01$) impact on the sensitivity and classification of severe outcome ($P = 0.00$) influenced specificity.

Threshold effect analysis only focused on true positive (TP), true negative (TN), false positive (FP) and false negative (FN) values to test diagnostic efficacy of D-dimer and distinguish if there exists heterogeneity caused by different cut offs and D-dimer units. On account of our analysis, we have identified that most of the pooled studies reported D-dimer using various units, such as D-dimer units (DDU), fibrinogen equivalent units (FEU) ($\sim 1.7\text{--}2.0$ differences), mg/L or $\mu\text{g}/\text{mL}$. This may give rise to concerns whether it is correct or not to pool all the sensitivity and specificity data without taking that into account. To reassure this consideration, we conducted a Spearman rank correlation to test the threshold effect. Inexistence of threshold effect was unveiled by spearman correlation coefficients as 0.533 ($P = 0.139$), 0.283 ($P = 0.289$) and 0.368 ($P = 0.216$). Thus, each metric can be combined for further analysis.

We found substantial heterogeneity among the studies, and performed multiple meta-regression analysis to identify the sources. For severity, the reference standard ($P = 0.01$) and percentage of diabetic patients ($P = 0.00$) affected the sensitivity, whereas country ($P = 0.03$), percentage of males ($P = 0.03$) and classification of severe outcome ($P = 0.00$) contributed to the heterogeneity in specificity. For mortality, country ($P = 0.03$) and exclusion of pregnancy ($P = 0.03$) predicted heterogeneity in sensitivity, while that in specificity was attributed to no D-dimer test results ($P = 0.02$), country ($P = 0.01$), recruitment of mixed or single cohort patients ($P = 0.00$ for mixed, $P = 0.02$ for severe only), and D-dimer test at peak value ($P = 0.00$). The heterogeneity in the sensitivity and specificity of diagnosing VTE were respectively due to clinical prevalence of VTE ($P = 0.01$) and country ($P = 0.04$).

Additional research could help us to understand this heterogeneity further, Yao et al¹⁹ retrospectively analyzed D-dimer upon admission and identified a cut off value $>2.14 \text{ mg/ml}$ predicting in-hospital mortality with a sensitivity of 88.2% and specificity of 71.3%. Creel-Bulos et al³⁷ rendered a comprehensive observation of D-dimer trajectories and represented a highly predictive value of a rise in D-dimer ($>2000 \text{ ng/ml}$) of any 24 hours within 10 days with 75% sensitivity and 74% specificity while baseline value was not associated with VTE. A Chinese study composed of 1114 patients³⁸ mentioned the meaningfulness of last D-dimer test before discharge or death in prognosing death using a cut off value of 2.025 mg/L rather than the first test at admission, the AUC of which was 0.909. Through meticulously reading of these articles, we have discovered the main source of inconsistency including age, comorbidity rates, mean duration of hospitalization, exclusion criteria for conditions that increases D-dimer levels (pregnancy, cancer or post trauma and surgery status), as well as

timing of D-dimer measurement (initial, peak or ultimate value), etc. In addition, lack of association between D-dimer and mortality in the study of Creel-Bulos et al³⁷ indicates anticoagulation treatment may potentially lead to decreased death and misunderstanding prognosis value of D-dimer. He and his colleges³⁸ also found participants with advanced age, male gender, dyspnea symptoms impact D-dimer value.

There can be several causes of heterogeneity. First, different reference standards can affect the sensitivity in discerning between severe and non-severe patients. Second, patients with diabetes have higher D-dimer levels and a significant higher risk of adverse prognosis, as well as shorter survival duration,³⁹ all of which influence diagnostic sensitivity. Third, males are more likely to develop severe illness and succumb, which can be attributed to the presence of androgens and angiotensin-converting enzyme 2 (ACE2) expression, along with a greater prevalence of unhealthy lifestyle choices like smoking, abuse alcohol and poor sleep.⁴⁰ Fourth, ethnicity can also affect diagnostic sensitivity and specificity due to the genetic predisposition to fatal comorbidities (diabetes, hypertension, asthma, etc.) and thrombotic events. For instance, polymorphism of mannose-binding lectin (MBL) genes and variations in ACE2 expression levels correlate to more severe and fatal outcomes in African American and Hispanic populations.⁴¹ Fifth, exclusion of pregnancy may reduce sensitivity by removing false positive results and exclusion of no D-dimer test results may increase specificity by removing false negative results. Sixth, recruiting only severe patients can increase the probability of death compared to a mixed cohort of severe and mild cases. Likewise, measuring D-dimer at its peak also increases the possibility of patients for progressing to severe or critical illness, thrombotic events and fatal outcomes.⁴² Finally, high clinical prevalence of VTE may avoid the potential diagnostic omission of VTE events in COVID-19 patients.

According to International Society on Thrombosis and Haemostasis (ISTH) guidance,⁴³ practice of utilizing thromboembolic prophylaxis is established for COVID-19 associated coagulopathy management, however, the optimal doses in severe COVID-19 patients based on increasing D-dimer values warrants adjustment and further investigation. Thus far, serial coagulation indices screening focused on D-dimer changes before and after anticoagulant as risk stratification is suggested. Dynamic alterations of D-dimer could demonstrate progression and prognosis of COVID-19. During 10 consecutive days of monitoring, D-dimer in admission escalated in improved and deteriorated groups after treatment and then gradually decreased in improved groups but remained high and fluctuated with disease progression in poor ones.⁴⁴ Coincidentally, initial elevated levels of D-dimer in baseline diminished after anticoagulant therapy with LMWH in DVT-COVID-19 patients and continuously higher than non-DVT-COVID-19 patients, indicating changes of D-dimer present an improvement in hypercoagulable state as well as a stable biomarker for anticoagulant effect in COVID-19 therapy.⁴⁵ Recently, researchers found D-dimer levels could affect anticoagulant doses. Prophylactic dose of heparin has been revealed its efficacy and better

prognosis among users with D-dimer >6 times the upper limit of normal value (ULN) by improving 28-day mortality than that of nonusers (32.8 vs 52.4%) while users with D-dimer ≤1 ULN of no benefit.⁴⁶ In comparison, another study unveiled improved survival rate in patients with D-dimer above 3000 ng/ml who administrated an intermediate dose of heparin than prophylactic doses.⁴⁷ Besides, prophylactic and therapeutic use of apixaban and enoxaparin prophylaxis is more beneficial in patients with D-dimer >10 µg/ml than UFH therapy while patients with D-dimer <1 µg/ml appears no benefit.⁴⁸ Benefit for extended thromboprophylaxis in the post-hospital discharge period (14-30 days) is also pronounced among patients with enhanced D-dimer >2 ULN and recognized 3-fold risk for VTE.⁴⁹ VTE risk stratification using very elevation of D-dimer may recommend intermediate or higher dose LMWH or UFH regimens.⁵⁰ Therefore, sequential measurement and careful assessment of D-dimer during disease worsening in addition to anticoagulation treatment may assist physicians to construct dynamic intervention, tailored prophylaxis or therapeutic doses and extended prophylaxis paradigms after hospitalization. We should apply D-dimer cautiously for anticoagulation considering the post-hoc feature of these studies and deficiency of clinical indications, its utility in adjusting antithrombotic strategies needs for prospective randomized controlled trials testing.

There are several limitations in our meta-analysis that ought to be considered. Although we conducted a meta-regression analysis to distinguish heterogeneity, much of it remains to be explained and reported. In addition, the funnel plots indicated publication bias in the predictive value of D-dimer for mortality, likely due to the fact that researchers would rather submit the favorable results, moreover, all the enrolled researches in our meta-analysis are published by September 1, 2020 which may also contribute to our publication bias. This publication bias may lead to overestimation of the pooled sensitivity and specificity. Data of race, comorbidities (respiratory failure, cardiovascular disease, smoking history, malignancy, previous VTE, etc.), pregnancy, recent surgery or trauma and anticoagulant treatment could not be retrieved, which may have led to missing values in meta-regression and omissions of covariates in the heterogeneity test. The test time, detection platform, cut offs and various units of D-dimer also potentially contributed to heterogeneity and bias. Availability of complete data on patient selection and exclusion, presence of comorbidities, treatment statistics of in-hospital COVID-19 patients, as well as the precise timing and method of D-dimer test would greatly reduce the bias in our estimates. In addition, although the existing heterogeneity can be partially explained by patient recruitment and methodological variance of individual studies, an exact conclusion cannot be drawn due to the lack of explanation for the remaining heterogeneity. Further studies with more comprehensive data can elucidate the diagnostic performance of D-dimer in COVID-19.

In conclusion, D-dimer can predict severe and fatal outcomes in COVID-19 patients with moderate sensitivity and specificity, and diagnose VTE with high sensitivity but low

specificity. It is a suitable to employ this indicator as a pre-radiographic screening tool, VTE risk stratification indicator as well as a routine investigation after anticoagulant therapy for hospitalized patients with COVID-19.

Authors' Note

YZL conceived and designed the research. HTZ and HZC extracted data and conducted quality assessment. HZC, CXL, LLC, SXY and HLL analyzed the data. HTZ wrote the paper. All authors are accountable for all aspects of the study, and attest to the accuracy and integrity of the results. All authors have read and approved the final manuscript as submitted. The data supporting this meta-analysis are from previously published studies and data sets, which have been cited. This article does not contain any studies with human participants performed by any of the authors. Trail Registry: PROSPERO (CRD42021230446).

Declaration of Conflicting Interests

The author(s) declared no potential conflicts of interest with respect to the research, authorship, and/or publication of this article.

Funding

The author(s) disclosed receipt of the following financial support for the research, authorship, and/or publication of this article: This research was supported by grants from the National Natural Science Foundation of China Grants (81871302) and Beijing Key Clinical Specialty for Laboratory Medicine - Excellent Project (No. ZK201000)

ORCID iD

Haoting Zhan  <https://orcid.org/0000-0001-5934-9141>

Supplemental Material

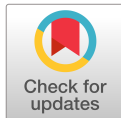
Supplemental material for this article is available online.

References

1. Bikdeli B, Madhavan MV, Jimenez D, et al. COVID-19 and thrombotic or thromboembolic disease: implications for prevention, antithrombotic therapy, and follow-up: *JACC* state-of-the-art review. *J Am Coll Cardiol.* 2020;75(23):2950-2973.
2. Guan WJ, Ni ZY, Hu Y, et al. Clinical characteristics of coronavirus disease 2019 in China. *N Engl J Med.* 2020;382(18):1708-1720.
3. Zhou F, Yu T, Du R, et al. Clinical course and risk factors for mortality of adult inpatients with COVID-19 in Wuhan, China: a retrospective cohort study. *Lancet.* 2020;395(10229):1054-1062.
4. Chen N, Zhou M, Dong X, et al. Epidemiological and clinical characteristics of 99 cases of 2019 novel coronavirus pneumonia in Wuhan, China: a descriptive study. *Lancet.* 2020;395(10223):507-513.
5. Llitjos JF, Leclerc M, Chochois C, et al. High incidence of venous thromboembolic events in anticoagulated severe COVID-19 patients. *J Thromb Haemost.* 2020;18(7):1743-1746.
6. Aloisio E, Chibireva M, Serafini L, et al. A comprehensive appraisal of laboratory biochemistry tests as major predictors of COVID-19 severity. *Arch Pathol Lab Med.* 2020;144(12):1457-1464.

7. Basbus L, Lapidus MI, Martingano I, Puga MC, Pollán J. Neutrophil to lymphocyte ratio as a prognostic marker in COVID-19 [in Spanish]. *Medicina (B Aires)*. 2020;80(suppl 3):31-36.
8. Fu J, Kong J, Wang W, et al. The clinical implication of dynamic neutrophil to lymphocyte ratio and D-dimer in COVID-19: a retrospective study in Suzhou China. *Thrombo Res*. 2020;192:3-8.
9. Gao Y, Li T, Han M, et al. Diagnostic utility of clinical laboratory data determinations for patients with the severe COVID-19. *J Med Virol*. 2020;92(7):791-796.
10. Liu FJ, Zhang Q, Huang C, et al. CT quantification of pneumonia lesions in early days predicts progression to severe illness in a cohort of COVID-19 patients. *Theranostics*. 2020;10(12):5613-5622.
11. Naymagon L, Zubizarreta N, Feld J, et al. Admission D-dimer levels, D-dimer trends, and outcomes in COVID-19. *Thromb Res*. 2020;196:99-105.
12. Tan CW, Chia WN, Qin X, et al. A SARS-CoV-2 surrogate virus neutralization test based on antibody-mediated blockage of ACE2-spike protein-protein interaction. *Nat Biotechnol*. 2020;38(9):1073-1078.
13. Wang M, Zhu Q, Fu J, Liu L, Xiao M, Du Y. Differences of inflammatory and non-inflammatory indicators in Coronavirus disease-19 (COVID-19) with different severity. *Infect Genet Evol*. 2020;85:104511.
14. Cheng A, Hu L, Wang Y, et al. Diagnostic performance of initial blood urea nitrogen combined with D-dimer levels for predicting in-hospital mortality in COVID-19 patients. *Int J Antimicrob Agents*. 2020;56(3):106110.
15. Laguna-Goya R, Utrero-Rico A, Talayero P, et al. IL-6-based mortality risk model for hospitalized patients with COVID-19. *J Allergy Clin Immunol*. 2020;146(4):799-807.e799.
16. Ronderos Botero DM, Omar AMS, Sun HK, et al. COVID-19 in the healthy patient population: demographic and clinical phenotypic characterization and predictors of in-hospital outcomes. *Arterioscler Thromb Vasc Biol*. 2020;40(11):2764-2775.
17. Li X, Xu S, Yu M, et al. Risk factors for severity and mortality in adult COVID-19 inpatients in Wuhan. *J Allergy Clin Immunol*. 2020;146(1):110-118.
18. Long H, Nie L, Xiang X, et al. D-Dimer and prothrombin time are the significant indicators of severe COVID-19 and poor prognosis. *BioMed Res Int*. 2020;2020:6159720.
19. Yao Y, Cao J, Wang Q, et al. D-dimer as a biomarker for disease severity and mortality in COVID-19 patients: a case control study. *J Intensive Care*. 2020;8:49.
20. Ye W, Chen G, Li X, et al. Dynamic changes of D-dimer and neutrophil-lymphocyte count ratio as prognostic biomarkers in COVID-19. *Respir Res*. 2020;21(1):169.
21. Zhang L, Yan X, Fan Q, et al. D-dimer levels on admission to predict in-hospital mortality in patients with Covid-19. *J Thromb Haemost*. 2020;18(6):1324-1329.
22. Zhu Y, Du Z, Zhu Y, Li W, Miao H, Li Z. Evaluation of organ function in patients with severe COVID-19 infections. *Med Clin (Barc)*. 2020;155(5):191-196.
23. Li C, Hu B, Zhang Z, et al. D-dimer triage for COVID-19. *Acad Emerg Med*. 2020;27(7):612-613.
24. Cho ES, McClelland PH, Cheng O, et al. Utility of D-dimer for diagnosis of deep vein thrombosis in coronavirus disease-19 infection. *J Vasc Surg Venous Lymphat Disord*. 2020;9(1):47-53.
25. Cui S, Chen S, Li X, Liu S, Wang F. Prevalence of venous thromboembolism in patients with severe novel coronavirus pneumonia. *J Thromb Haemost*. 2020;18(6):1421-1424.
26. Demelo-Rodriguez P, Cervilla-Munoz E, Ordieres-Ortega BL, et al. Incidence of asymptomatic deep vein thrombosis in patients with COVID-19 pneumonia and elevated D-dimer levels. *Thromb Res*. 2020;192:23-26.
27. Mouhat B, Besutti M, Bouiller K, et al. Elevated D-dimers and lack of anticoagulation predict PE in severe COVID-19 patients. *Eur Respir J*. 2020;56(4):2001811.
28. Al-Samkari H, Song F, Van Cott EM, Kuter DJ, Rosovsky R. Evaluation of the prothrombin fragment 1.2 in patients with coronavirus disease 2019 (COVID-19). *Am J Hematol*. 2020;95(12):1479-1485.
29. Wright FL, Vogler TO, Moore EE, et al. Fibrinolysis shutdown correlation with thromboembolic events in severe COVID-19 infection. *J Am Coll Surg*. 2020;231(2):193-203.e191.
30. Yu Y, Tu J, Lei B, et al. Incidence and risk factors of deep vein thrombosis in hospitalized COVID-19 patients. *Clin Appl Thromb Hemost*. 2020;26:1076029620953217.
31. Trigonis RA, Holt DB, Yuan R, et al. Incidence of venous thromboembolism in critically ill coronavirus disease 2019 patients receiving prophylactic anticoagulation. *Crit Care Med*. 2020;48(9):E805-E808.
32. Rodriguez-Sevilla J, Rodó-Pin A, Espallargas I, et al. Pulmonary embolism in patients with Covid-19 pneumonia: the utility of D-dimer. *Arch Bronconeumol*. 2020;56(11):758-759.
33. Maatman TK, Jalali F, Feizpour C, et al. Routine venous thromboembolism prophylaxis may be inadequate in the hypercoagulable state of severe coronavirus disease 2019. *Crit Care Med*. 2020;48(9):E783-E790.
34. Leonard-Lorant I, Delabranche X, Severac F, et al. Acute pulmonary embolism in patients with COVID-19 at CT angiography and relationship to D-dimer levels. *Radiology*. 2020;296(3):E189-E191.
35. van Belle A, Büller HR, Huisman MV, et al. Effectiveness of managing suspected pulmonary embolism using an algorithm combining clinical probability, D-dimer testing, and computed tomography. *JAMA*. 2006;295(2):172-179. doi:10.1001/jama.295.2.172
36. Klok FA, Kruip M, van der Meer NJM, et al. Incidence of thrombotic complications in critically ill ICU patients with COVID-19. *Thromb Res*. 2020;191:145-147.
37. Creel-Bulos C, Liu M, Auld SC, et al. Trends and diagnostic value of D-dimer levels in patients hospitalized with coronavirus disease 2019. *Medicine (Baltimore)*. 2020;99(46):e23186.
38. He X, Yao F, Chen J, et al. The poor prognosis and influencing factors of high D-dimer levels for COVID-19 patients. *Sci Rep*. 2021;11(1):1830.
39. Shang J, Wang Q, Zhang H, et al. The relationship between diabetes mellitus and COVID-19 prognosis: a retrospective cohort study in Wuhan, China. *Am J Med*. 2020;134(1):e6-e14.

40. Chanana N, Palmo T, Sharma K, Kumar R, Graham BB, Pasha Q. Sex-derived attributes contributing to SARS-CoV-2 mortality. *Am J Physiol Endocrinol Metab.* 2020;319(3):E562-E567.
41. Zhao Y, Zhao Z, Wang Y, Zhou Y, Ma Y, Zuo W. Single-cell RNA expression profiling of ACE2, the receptor of SARS-CoV-2. *Am J Respir Crit Care Med.* 2020;202(5):756-759.
42. Tang N, Li D, Wang X, Sun Z. Abnormal coagulation parameters are associated with poor prognosis in patients with novel coronavirus pneumonia. *J Thromb Haemost.* 2020;18(4):844-847.
43. Thachil J, Tang N, Gando S, et al. ISTH interim guidance on recognition and management of coagulopathy in COVID-19. *J Thromb Haemost.* 2020;18(5):1023-1026.
44. Li Y, Zhao K, Wei H, et al. Dynamic relationship between D-dimer and COVID-19 severity. *Br J Haematol.* 2020;190(1):e24-e27.
45. Cai C, Guo Y, You Y, et al. Deep venous thrombosis in COVID-19 patients: a cohort analysis. *Clin Appl Thromb Hemost.* 2020; 26:1076029620982669.
46. Tang N, Bai H, Chen X, Gong J, Li D, Sun Z. Anticoagulant treatment is associated with decreased mortality in severe coronavirus disease 2019 patients with coagulopathy. *J Thromb Haemost.* 2020;18(5):1094-1099.
47. Pavoni V, Gianesello L, Pazzi M, Stera C, Meconi T, Frigieri FC. Venous thromboembolism and bleeding in critically ill COVID-19 patients treated with higher than standard low molecular weight heparin doses and aspirin: a call to action. *Thromb Res.* 2020;196:313-317.
48. Billett HH, Reyes-Gil M, Szymanski J, et al. Anticoagulation in COVID-19: effect of enoxaparin, heparin, and apixaban on mortality. *Thromb Haemost.* 2020;120(12):1691-1699.
49. Spyropoulos AC, Lipardi C, Xu J, et al. Modified IMPROVE VTE risk score and elevated D-dimer identify a high venous thromboembolism risk in acutely ill medical population for extended thromboprophylaxis. *TH Open.* 2020;4(1):e59-e65.
50. Spyropoulos AC, Levy JH, Ageno W, et al. Scientific and Standardization Committee communication: clinical guidance on the diagnosis, prevention, and treatment of venous thromboembolism in hospitalized patients with COVID-19. *J Thromb Haemost.* 2020;18(8):1859-1865.



Nurshad Ali ORCID iD: 0000-0003-1649-0887

Elevated level of C-reactive protein may be an early marker to predict risk for severity of COVID-19

Nurshad Ali

Department of Biochemistry and Molecular Biology, Shahjalal University of Science and Technology, Sylhet 3114, Bangladesh

Corresponding author

Nurshad Ali, Ph.D.

Department of Biochemistry and Molecular Biology,

Shahjalal University of Science and Technology, Sylhet-3114, Bangladesh;

Phone: +880-1723205092

E-mail: nur_rubd@yahoo.com, nali-bmb@sust.edu

ORCID: <https://orcid.org/0000-0003-1649-0887>

To the Editor,

The outbreak of COVID-19 is an emerging global health threat. The healthcare workers are facing challenges in reducing the severity and mortality of COVID-19 across the world. Severe patients with COVID-19 are generally treated in the intensive care unit (ICU), while mild or non-severe patients treated in the usual isolation ward of the hospital. However, there is an emerging challenge that a small subset of mild or non-severe COVID-19 patients develops into a severe disease course. Therefore, it is

This article has been accepted for publication and undergone full peer review but has not been through the copyediting, typesetting, pagination and proofreading process, which may lead to differences between this version and the Version of Record. Please cite this article as doi: 10.1002/jmv.26097.

important to early identify and give the treatment of this subset of patients to reduce the disease severity and improve the outcomes of COVID-19. Clinical studies demonstrated that altered levels of some blood markers might be linked with the degree of severity and mortality of COVID-19 patients¹⁻⁵. Of these clinical parameter, serum C-reactive protein (CRP) has been found as an important marker that changes significantly in severe patients with COVID-19³. CRP is a type of protein produced by the liver that serves as an early marker of infection and inflammation⁶. In blood, the normal concentration of CRP is less than 10 mg/L; however, it rises rapidly within 6-8 hours and gives the highest peak in 48 hours from the disease onset⁷. Its half-life is about 19 hours⁸ and its concentration decreases when the inflammatory stages end and the patient is healing. CRP preferably binds to phosphocholine expressed highly on the surface of damaged cells⁹. This binding makes active the classical complement pathway of the immune system and modulates the phagocytic activity to clear microbes and damaged cells from the organism⁷. When the inflammation or tissue damage is resolved, CRP concentration fall, making it a useful marker for monitoring disease severity⁷.

The available studies that have determined serum concentration of CRP in COVID-19 patients are presented in Table 1. A significant increase of CRP was found with levels on average 20-50 mg/L in patients with COVID-19¹⁰⁻¹², Elevated levels of CRP were observed up to 86% in severe COVID-19 patients^{10,13,14}. Patients with severe disease courses had a far elevated level of CRP than mild or non-severe patients. For example, a study reported that patients with more severe symptoms had on average CRP concentration of 39.4 mg/L and patients with mild symptoms CRP concentration of 18.8 mg/L¹². CRP was found at increased levels in the severe group at the initial stage than

those in the mild group¹. In another study, the mean concentration of CRP was significantly higher in severe patients (46 mg/L) than non-severe patients (23 mg/L)¹¹. The patients who died from COVID-19 had about 10 fold higher levels of CRP than the recovered patients (median 100 mg/L vs 9.6 mg/L).¹⁵ A recent study showed that about 7.7% of non-severe COVID-19 patients were progressed to severe disease courses after hospitalization³, and compared to non-severe cases, the aggravated patients had significantly higher concentrations of CRP (median 43.8 mg/L vs 12.1 mg/L). A significant association was observed between CRP concentrations and the aggravation of non-severe patients with COVID-19 [1], and the authors proposed CRP as a suitable marker for anticipating the aggravation probability of non-severe COVID-19 patients, with an optimal threshold value of 26.9 mg/L³. The authors also noted that the risk of developing severe events is increased by 5% for every one-unit increase in CRP concentration in patients with COVID-19.

Furthermore, it was observed that patients with low oxygen saturation ($\text{SpO}_2 \leq 90\%$) had significantly higher levels of CRP (median 76.5 mg/L) compared to patients with high oxygen saturation ($\text{SpO}_2 > 90\%$) (median 12.7 mg/L)¹⁶, indicating that more severe patients with lung damage have elevated levels of CRP. So, higher levels of CRP indicate more severe disease course-linked to lung injury and worse prognosis. CRP levels are correlated well with the severity of symptoms of patients with COVID-19; therefore, it may be a suitable marker in assessing a patient's conditions together with other clinical findings.

The elevated levels of CRP might be linked to the overproduction of inflammatory cytokines in severe COVID-19 patients. Cytokines fight against the microbes but when

the immune system becomes hyperactive, it can damage lung tissue. Thus, CRP production is induced by inflammatory cytokines and by tissue destruction in COVID-19 patients. In conclusion, elevated level of CRP may be a valuable early marker in predicting the possibility of disease progression in non-severe COVID-19 patients, which can help health workers to identify those patients at an early stage for early treatment. Besides, COVID-19 patients with elevated levels of CRP need close monitoring and treatment even though they did not develop symptoms to meet the criteria for the severe disease course. However, CRP levels in COVID-19 patients who may progress from non-severe to severe cases need to be further studied in large scale multicenter studies.

Conflict of interest: The author has no conflict of interest to declare.

Funding source: None

Author contributions: NA wrote and revised the manuscript.

Author ORCID: <https://orcid.org/0000-0003-1649-0887>

References

1. Tan C, Huang Y, Shi F, et al. C-reactive protein correlates with computed tomographic findings and predicts severe COVID-19 early. *J Med Virol*. Published online April 25, 2020:jmv.25871. doi:10.1002/jmv.25871
2. Tian W, Jiang W, Yao J, et al. Predictors of mortality in hospitalized COVID-19 patients: A systematic review and meta-analysis. *J Med Virol*. Published online May 22, 2020. doi:10.1002/jmv.26050
3. Wang G, Wu C, Zhang Q, et al. C-Reactive Protein Level May Predict the Risk of COVID-19 Aggravation. *Open Forum Infectious Diseases*. 2020;7(5):ofaa153. doi:10.1093/ofid/ofaa153
4. Ali N. Is SARS-CoV-2 associated with liver dysfunction in COVID-19 patients? *Clinics and Research in Hepatology and Gastroenterology*. Published online May 2020:S2210740120301406. doi:10.1016/j.clinre.2020.05.002

5. Lagunas-Rangel FA. Neutrophil-to-lymphocyte ratio and lymphocyte-to-C-reactive protein ratio in patients with severe coronavirus disease 2019 (COVID-19): A meta-analysis. *J Med Virol.* Published online April 8, 2020. doi:10.1002/jmv.25819
6. Marnell L, Mold C, Du Clos TW. C-reactive protein: Ligands, receptors and role in inflammation. *Clinical Immunology.* 2005;117(2):104-111. doi:10.1016/j.clim.2005.08.004
7. Young B, Gleeson M, Cripps AW. C-reactive protein: A critical review. *Pathology.* 1991;23(2):118-124. doi:10.3109/00313029109060809
8. Pepys MB, Hirschfield GM. C-reactive protein: a critical update. *J Clin Invest.* 2003;111(12):1805-1812. doi:10.1172/JCI200318921
9. Ballou SP, Kushner I. C-reactive protein and the acute phase response. *Adv Intern Med.* 1992;37:313-336.
10. Chen N, Zhou M, Dong X, et al. Epidemiological and clinical characteristics of 99 cases of 2019 novel coronavirus pneumonia in Wuhan, China: a descriptive study. *The Lancet.* 2020;395(10223):507-513. doi:10.1016/S0140-6736(20)30211-7
11. Mo P, Xing Y, Xiao Y, et al. Clinical characteristics of refractory COVID-19 pneumonia in Wuhan, China. *Clinical Infectious Diseases.* Published online March 16, 2020:ciaa270. doi:10.1093/cid/ciaa270
12. Gao Y, Li T, Han M, et al. Diagnostic Utility of Clinical Laboratory Data Determinations for Patients with the Severe COVID-19. *J Med Virol.* Published online March 17, 2020:jmv.25770. doi:10.1002/jmv.25770
13. Chen T, Wu D, Chen H, et al. Clinical characteristics of 113 deceased patients with coronavirus disease 2019: retrospective study. *BMJ.* Published online March 26, 2020:m1091. doi:10.1136/bmj.m1091
14. Guan W, Ni Z, Hu Y, et al. Clinical Characteristics of Coronavirus Disease 2019 in China. *N Engl J Med.* 2020;382(18):1708-1720. doi:10.1056/NEJMoa2002032
15. Luo X, Zhou W, Yan X, et al. *Prognostic Value of C-Reactive Protein in Patients with COVID-19.* Infectious Diseases (except HIV/AIDS); 2020. doi:10.1101/2020.03.21.20040360
16. Xie J, Covassin N, Fan Z, et al. Association Between Hypoxemia and Mortality in Patients With COVID-19. *Mayo Clinic Proceedings.* Published online April 2020:S0025619620303670. doi:10.1016/j.mayocp.2020.04.006
17. Chen N, Zhou M, Dong X, et al. Epidemiological and clinical characteristics of 99 cases of 2019 novel coronavirus pneumonia in Wuhan, China: a descriptive study. *The Lancet.* 2020;395(10223):507-513. doi:10.1016/S0140-6736(20)30211-7

18. Guan W, Ni Z, Hu Y, et al. Clinical Characteristics of Coronavirus Disease 2019 in China. *N Engl J Med.* 2020;382(18):1708-1720. doi:10.1056/NEJMoa2002032
19. Jin X, Lian J-S, Hu J-H, et al. Epidemiological, clinical and virological characteristics of 74 cases of coronavirus-infected disease 2019 (COVID-19) with gastrointestinal symptoms. *Gut.* 2020;69(6):1002-1009. doi:10.1136/gutjnl-2020-320926
20. Liu J, Li S, Liu J, et al. Longitudinal characteristics of lymphocyte responses and cytokine profiles in the peripheral blood of SARS-CoV-2 infected patients. *EBioMedicine.* Published online April 18, 2020. doi:10.1016/j.ebiom.2020.102763
21. Mo P, Xing Y, Xiao Y, et al. Clinical characteristics of refractory COVID-19 pneumonia in Wuhan, China. *Clin Infect Dis.* Published online March 16, 2020. doi:10.1093/cid/ciaa270
22. Shang W, Dong J, Ren Y, et al. The value of clinical parameters in predicting the severity of COVID-19. *J Med Virol.* Published online May 21, 2020:jmv.26031. doi:10.1002/jmv.26031
23. Shi H, Han X, Jiang N, et al. Radiological findings from 81 patients with COVID-19 pneumonia in Wuhan, China: a descriptive study. *The Lancet Infectious Diseases.* 2020;20(4):425-434. doi:10.1016/S1473-3099(20)30086-4
24. Young BE, Ong SWX, Kalimuddin S, et al. Epidemiologic Features and Clinical Course of Patients Infected With SARS-CoV-2 in Singapore. *JAMA.* 2020;323(15):1488. doi:10.1001/jama.2020.3204

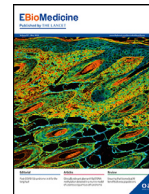
Table 1 Levels of C-reactive protein (CRP) in patients with COVID-19

Reference	Group	Patients (n)	CRP (mg/L)	P-value	N and % of patients with Elevated CRP
Chen et al. 2020 ¹⁷	Hospitalized	99	51.4 (41.8)	NA	63/73 (86)
Chen et al. 2020 ¹³	Death	113	113 (69.1- 168.4)	NA	59/68 (60)
	Recovered	161	26.2 (8.7- 55.4)		21/45 (14)

Gao et al. 2020 ¹²	Severe	15	39.4 (27.7)	0.011	NA
	Mild	28	18.8 (22.2)		
Guan et al. 2020 ¹⁸	Severe	173	NA	NA	110/135 (81.5)
	Non-severe	926	NA		371/658 (56.4)
Jin et al. 2020 ¹⁹	Severe (GI symptoms)	74	15.7 (4.8-23.9)	0.003	NA
	Non-severe (no- GI symptoms)	577	7.9 (2.6-19.6)		
Liu et al. 2020 ²⁰	Severe	13	62.9 (42.4-86.6)	NA	NA
	Mild	27	7.6 (3.1-57.3)		
Luo et al. 2020 ¹⁵	Died	84	100 (60.7-179.4)	0.000	NA
	Recovered	214	9.6 (5-37.9)		

Mo et al. 2020 ²¹	Severe	85	46 (22-106)	0.001	NA
	Mild	70	23 (10-47)		
Shang et al. 2020 ²²	Severe	139	43.1 (9.8-97.3)	<0.001	NA
	Non-severe	304	10 (2.9-27.1)		
Shi et al. 2020 ²³	Hospitalized	81	47.6 (41.8)	NA	NA
Wang et al. 2020 ³	Severe	16	43.8 (12.3-101.9)	0.000	NA
	Non-severe	193	12.1 (0.1-91.4)		
Young et al. 2020 ²⁴	Severe	6	65.6 (47.5-97.5)	NA	NA
	Non-severe	18	11.1 (0.9-19.1)		

Data are presented as mean (SD) or medians (IQR). Severe: patients admitted to the intensive care unit (ICU). GI: Gastrointestinal. NA: data was not available. P-value indicates the mean or median difference of CRP levels between the severe and non-severe group.



Commentary

HERV-W envelope expression in blood leukocytes as a marker of disease severity of COVID-19



Marta Garcia-Montojo, Avindra Nath*

Section of Infections of the Nervous System, National Institute of Neurological Disorders and Stroke, National Institutes of Health, Bethesda, MD, USA

ARTICLE INFO

Article History:

Received 13 April 2021

Accepted 13 April 2021

Available online 13 May 2021

We are currently in the midst of a pandemic, caused by SARS-CoV-2, that has shaken the entire social and economic fabric of society. Within less than a year it spread across the entire globe and has spared no country, society, race or age group. Even several world leaders have been infected. While we have made great progress towards developing effective vaccines, to date we do not have any effective anti-viral agents. This desperate situation has called for desperate measures. For example, hydroxychloroquine was initially used for treating the infection based on minimal in vitro data, resulting in world-wide shortages of the drug, only for subsequent clinical trials to show that it was ineffective in treating the infection. It has become clear however, that in the early phases of the infection particularly in hospitalized patients, anti-inflammatory measures such as the use of corticosteroids can be helpful. All the same, potent immunosuppression can be detrimental to the host since this is what is necessary for the ultimate recovery of the patient. Hence better methods are necessary that would modulate the immune system more precisely to prevent organ damage and yet preserve the antiviral effects.

The current study by Balestrieri et al. in *EBioMedicine*, studied 30 hospitalized patients infected with SARS-CoV-2 with a wide range of severity of illnesses. They were classified as asymptomatic, presymptomatic, mild, moderate or severe. 24/30 patients were males. They determined the expression of the envelope protein of an endogenous retrovirus family W (HERV-W), in blood leukocytes and compared it to other immune markers and the clinical status of the individuals [1]. The expression of HERV-W envelope protein has been previously implicated in certain autoimmune diseases, such as multiple sclerosis (MS), chronic inflammatory demyelinating polyneuropathy and type 1 diabetes. Increased levels of HERV-W transcripts have also been found in schizophrenia and bipolar disorder [2].

HERVs are retroviral elements derived from retroviruses that infected the human ancestral genome millions of years ago and were incorporated into the chromosomal DNA. Over the years they have become highly mutated; however, several of these genes still have an open reading frame (ORF). Even though there are 22 complete HERV-W families in the human genome, an ORF for the envelope protein is only present in chromosome 7q21.2 [3,4]. The expression of this protein is tightly regulated. It is highly expressed in the human placenta in syncytiotrophoblasts where it is critical for syncytial formation. For this reason, the protein is also called syncytin [5]. However, the protein is epigenetically silenced in the fetus and in adulthood. Reactivation of the gene following thymic development can result in an inflammatory or an autoimmune response. Some viral and bacterial infections have been shown to increase the expression of HERV-W env.

The authors of the present study found that HERV-W envelope can also be activated in patients with COVID-19. They found activation of this protein in circulating T lymphocytes. The highest activation was found in CD4 and CD8 lymphocytes with lower levels in B cells and monocytes. Previous studies have identified expression of HERV-W in patients with multiple sclerosis in monocytes, NK cells and B cells and in T cells [6,7]. Increased expression of HERV-W, especially in monocytes, was previously described in acute infections, and importantly, it is associated with an activated phenotype of leukocytes and occurs early upon antigenic stimulation [7].

It is remarkable that exposure of leukocytes in vitro to the SARS-CoV-2 spike protein resulted in a potent and sustained expression of HERV-W envelope. The expression of HERV-W transcripts in leukocytes of patients with COVID-19 correlated with the expression of several proinflammatory cytokines such as IL-6, IL-17 and TNF- α as well as chemokines CCL-2 and CXCL6. These molecules are associated with severe forms of COVID-19 and are poor prognostic markers. In line with this observation, the expression of HERV-W envelope transcripts in leukocytes and protein in CD4 lymphocytes was associated with severe respiratory illness and systemic markers of disease severity. This is important since acute respiratory distress syndrome with COVID-19 is thought to be mediated by an over-aggressive immune response. Further, the antiviral responses to SARS-CoV-2 are primarily mediated by CD4 lymphocytes and not by CD8 cells which may be functionally impaired in some patients [8]. Hence it would be important to determine the effect of HERV-W envelope expression on the functional properties of CD4 lymphocytes.

A previous study identified three different immunophenotypes of hospitalized COVID-19 patients. Immunophenotype 1 showed robust

DOI of original article: [http://dx.doi.org/10.1016/j.ebiom.2021.103341](https://doi.org/10.1016/j.ebiom.2021.103341).

* Corresponding author.

E-mail address: natha@ninds.nih.gov (A. Nath).

CD4 T cell activation, paucity of cT_{FH} cells with exhausted CD8 T cells. This phenotype was associated with more severe disease. Immunophenotype 2 showed more traditional effector CD8 T cells subsets, less CD4 T cell activation and immunophenotype 3 showed lack of T or B cell activation showing an inability to mount an immune response to the virus [9]. The current study found a correlation between HERV-W envelope expression and T cell exhaustion markers suggesting that it might be a driver of immunophenotype 1. Further studies are needed to determine the mechanism of interactions between HERV-W and these molecules. While in vitro studies can provide some insight, human *in vivo* studies will be necessary since HERV-W expression is specific for humans.

A major question that needs to be answered is, what are the therapeutic implications of these observations? A humanized IgG4 monoclonal antibody to HERV-W envelope, GNbAC1, has already been developed and clinical studies have been conducted in patients with multiple sclerosis and type 1 diabetes. Hence the safety profile is known at least in the context of these phase 1 and 2 studies where the antibody seemed remarkably safe [10]. This might represent an excellent opportunity to conduct a randomized controlled clinical study in patients with COVID-19 to determine if it may provide any benefit to hospitalized patients who are severely ill.

Declaration of Competing Interest

The authors have no conflicts of interest to disclose

Acknowledgments

Supported by funding from the Division of Intramural Research, National Institute of Neurological Disorders and Stroke, National Institutes of Health ([NS003130](#))

Contributions

Both authors wrote the commentary.

References

- [1] Balestrieri E, Minutolo A, Petrone V, et al. Evidence of the pathogenic HERV-W envelope expression in T lymphocytes in association with the respiratory outcome of COVID-19 patients. *EBioMedicine* 2021. doi: [10.1016/j.ebiom.2021.103341](#).
- [2] Kury P, Nath A, Creange A, et al. Human endogenous retroviruses diseases. *Trends Mol Med* 2018;24(4):379–94.
- [3] Voisset C, Cecile O, Bedin F, et al. Chromosomal distribution and coding capacity of the human endogenous retrovirus HERV-W family. *AIDS Res and Hum Retrovir* 2000;16(8):731–40.
- [4] Kim HS, Kim DS, Huh JW, et al. Molecular characterization of the HERV-W envelope gene in humans and primates: expression, FISH, phylogeny, and evolution. *Mol Cells* 2008;26(1):53–60.
- [5] Blond JL, Lavillette D, Cheynet V, et al. An envelope glycoprotein of the human endogenous retrovirus HERV-W is expressed in the human placenta and fuses cells expressing the type D mammalian retrovirus receptor. *J Virol* 2020;74(7):3321–9.
- [6] Mameli G, Poddighe L, Mei A, et al. Expression and activation by Epstein Barr virus of human endogenous retroviruses-W in blood cells and astrocytes: inference for multiple sclerosis. *PLoS ONE* 2012;7(9):e44991.
- [7] Garcia-Montojo M, Rodriguez-Martinez E, Ramos-Mozo P, et al. Syncytin-1/HERV-W envelope is an early activation marker of leukocytes and is upregulated in multiple sclerosis patients. *Eur J Immunol* 2020;50(5):685–94.
- [8] Grifoni A, Weiskopf D, Ramirez SI, et al. Targets of T cell responses to SARS-CoV-2 coronavirus in humans with COVID-19 disease and unexposed individuals. *Cell* 2020;181:1489–501.e15.
- [9] Mathew D, Giles JR, Baxter AE, et al. Deep immune profiling of COVID-19 patients reveals distinct immunotypes with therapeutic implications. *Science* 2020;369(6508):eabc8511.
- [10] Kornmann G, Curtin F. Temelimumab, an IgG4 Anti-Human endogenous retrovirus monoclonal antibody: an early development safety review. *Drug Saf* 2020 Dec;43(12):1287–96.



Silvia Spoto ORCID iD: 0000-0002-8799-4997

Massimo Ciccozzi ORCID iD: 0000-0003-3866-9239

Silvia Angeletti ORCID iD: 0000-0002-7393-8732

High value of Mid-regional proAdrenomedullin in COVID-19: a marker of widespread endothelial damage, disease severity and mortality.

Running head: MR-proADM in COVID-19

Silvia Spoto, MD^{a*}, Felice E. Agrò, MD^b, Federica Sambuco, MD^c, Francesco Travaglino, MD^c, Emanuele Valeriani, MD^a, Marta Fogolari, MD^d, Fabio Mangiacapra, PhD^e, Sebastiano Costantino, MD^a, Massimo Ciccozzi, PhD^f, Silvia Angeletti, MD^d

^a*Diagnostic and Therapeutic Medicine Department, University Campus Bio-Medico of Rome, Italy* ^b*Department of Anesthesia, Intensive Care and Pain Management, University Campus Bio-Medico of Rome, Italy*

^c*Emergency Department University Campus Bio-Medico of Rome, Italy*

^d*Unit of Clinical Laboratory Science, University Campus Bio-Medico of Rome, Italy*

^e*Unit of Cardiovascular Science, University Campus Bio-Medico of Rome, Italy*

^f*Unit of Medical Statistics and Molecular Epidemiology, University Campus Bio-Medico of Rome, Rome, Italy*

* Corresponding Author: Silvia Spoto MD, Diagnostic and Therapeutic Medicine Department

This article has been accepted for publication and undergone full peer review but has not been through the copyediting, typesetting, pagination and proofreading process, which may lead to differences between this version and the Version of Record. Please cite this article as doi: 10.1002/jmv.26676.

University Campus Bio-Medico of Rome, Italy.

++3906225418824

e-mail: s.spoto@unicampus.it

Abstract word count: 189

Text word count: 2463

ABSTRACT

The widespread endothelial damage due to severe acute respiratory syndrome Coronavirus 2 (SARS-CoV2) may lead to a disruption of the adrenomedullin (ADM) system responsible for vascular leakage, increased inflammatory status, and microvascular alteration with multi-organs dysfunction. The aim of this study was to evaluate the role of Mid-regional proAdrenomedullin (MR-proADM) as a marker of SARS CoV2-related widespread endothelial damage, clinically identified by organs damage, disease severity and mortality. Patients with SARS-CoV2 infection has been prospectively enrolled and demographic characteristic, clinical and laboratory data has been evaluated. In the overall population, 58% developed acute respiratory distress syndrome (ARDS), 23.3% of patients died, 6.5% acute cardiac injury, 1.4% of patients developed acute ischemic stroke, 21.2% acute kidney injury, 11.8% acute liver damage, and 5.4% septic shock. The best MR-proADM cut-off values for ARDS development and mortality prediction were 3.04 nmol/L and 2 nmol/L, respectively. Patients presenting with MR-proADM values \geq 2 nmol/L showed a significantly higher mortality risk. In conclusion, MR-proADM values \geq 2 nmol/l identify those patients with high mortality risk related to a multiorgan dysfunction syndrome. These patients must be carefully evaluated and considered for an intensive therapeutic approach.

Keywords: acute respiratory distress syndrome, adrenomedullin, COVID-19, multiple organ dysfunction syndrome, SARS virus

Data availability Statement

The data that support the findings of this study are available from the corresponding author upon reasonable request.

INTRODUCTION

The Coronavirus disease 2019 (COVID-19), caused by the severe acute respiratory distress syndrome *Coronavirus 2* (SARS-CoV2), was responsible for an unprecedent threat to global health. (1) The clinical manifestations of the disease range from asymptomatic cases to severe pneumonia with high mortality rates (4 to 13%), mainly in the case of acute respiratory distress syndrome (ARDS) development.(2)

Trying to stratify disease severity, the World Health Organization classified patients in four classes (mild to critical) basing on clinical and radiological characteristics.(3) The use of biomarkers, however, may help clinicians identifying those patients with a severe disease and a higher risk of death.(4, 5) Up to date, no markers of endothelial damage in COVID-19 have been validated in clinical practice.

Adrenomedullin (ADM), a 6 kDa protein with a 22 minutes half-life, is produced by endothelial and vascular smooth muscle cells due to volume overload to maintain endothelial barrier function, freely diffuses through the blood and interstitium, and binds to specific widespread receptors, mainly located in cardiovascular and pulmonary tissues.(6, 7) The leading function of ADM is the vasodilatation in both vascular resistance and capacitance vessels resulting in a blood flow increase. ADM further reduce vasoconstriction through an inhibition of the renin-angiotensin-aldosterone

system and maintains endothelial integrity reducing vascular permeability.(7) A disruption of ADM system results in vascular leakage that represents the first step of inflammation and of coagulation cascade activation.(8, 9)

As derived from ADM in a 1:1 ratio, Mid-Regional proAdrenomedullin (MR-proADM) values directly reflect the effects of its less stable and easily detectable precursor and has been recently introduced in clinical practice as a prognostic marker in patients with bacterial infection.(10) A significant relation between MR-proADM values and bacterial pneumonia severity index score, indeed, has been highlighted.(11) Healthy individuals showed MR-proADM values of about 0.33 nmol/L.(10) MR-proADM values of 0.8 nmol/L, conversely, are diagnostic of bacterial infection with higher values indicative of a higher infection severity -from 1.2 to 1.9 and 3.7 nmol/L in localized infections, sepsis or septic shock, respectively-(12) In patients with sepsis and septic shock, MR-proADM values more than 3.4 and 4.3 nmol/L, respectively, were significantly associated with 90-day mortality.(13)

Despite the vast majority of studies evaluated the role of MR-proADM in bacterial infections leading to sepsis, scant evidence is available in patients with viral infections without any information on COVID-19.(12, 14-16)

Knowing that COVID-19 related damage resemble the alteration occurring during sepsis, however, a disruption of ADM pathway during SARS-CoV2 infection may be hypothesized.(8, 9, 17)

The aim of this study was to evaluate the role of MR-proADM as a marker of SARS-CoV2 related widespread endothelial damage, clinically identified by organs damage, disease severity and mortality.

MATERIALS AND METHODS

This study has been approved by the Ethical Committee of the University Campus Bio-Medico of Rome and all patients provided informed consent before the enrollment within the study.

Patient selection and characteristics

All patients hospitalized for SARS-CoV2 infection at COVID Center of the Campus Bio-Medico of Rome University, were prospectively included between 1st April and 30th June 2020. The COVID Center included both Medicine Department and Intensive Care Unit (ICU). Pregnancy and lack of informed consent represented exclusion criteria.

The following data were collected at inclusion: demographic characteristics (age and gender); onset symptoms; relevant comorbidities; immune status (active malignancy or other causes of immunosuppression); concomitant antimicrobial, antiviral, or immunosuppressive treatments administration; clinical presentation. Furthermore, all patients received a complete physical examination including body temperature, blood pressure, heart and respiratory rate, cardiac, pulmonary, abdominal, and neurological evaluation. Laboratory values at inclusion comprehended complete blood counts, MR-proADM, C-reactive protein (CRP), ferritin, procalcitonin (PCT), coagulation (D-Dimer, international normalized ratio, activated partial thromboplastin time), liver (aspartate aminotransferase, alanine aminotransferase, albumin, bilirubin) and kidney (creatinine) functionality tests, serum lactate, arterial blood gas examination.

All patients received standard of care basing on disease severity and comprehending oxygen support, anticoagulant therapy, hydroxychloroquine, and tocilizumab whether indicated.

Laboratory values measurement

Diagnosis of COVID-19 was confirmed by a reverse transcription polymerase chain reaction test on a nasopharyngeal and/or endotracheal aspirate swab detecting spike protein (S) and envelope (E) genes for SARS-CoV2. MR-proADM and PCT plasma concentrations were measured by an automated Kryptor analyzer, using a time-resolved amplified cryptate emission (TRACE) technology assay (Kryptor PCT; Brahms AG; Hennigsdorf, Germany), with commercially available immunoluminometric assays (Brahms).(12, 18-20)

Clinical outcomes and definitions

Primary outcome was ARDS development and 30-day mortality. Secondary outcomes were acute cardiac injury, transient ischemic attack/stroke, acute kidney injury, acute liver failure, and septic shock development. ARDS was defined according to the Berlin definition; acute cardiac injury when there was a rise and/or fall of cardiac troponin values with at least one value above the 99th percentile of the upper reference limit; transient ischemic stroke as a brief episodes of neurological dysfunction resulting from focal cerebral ischemia not associated with permanent cerebral infarction; acute ischemic stroke as an episode of neurological dysfunction caused by focal cerebral, spinal, or retinal infarction; acute kidney injury diagnosed by KDIGO criteria as an increase in serum creatinine by ≥ 0.3 mg/dl within 48 h, ≥ 1.5 times from baseline within 7 days, or urine volume < 0.5 ml/kg/h for 6 h; acute liver damage as elevation of serum transaminases ($> 2 \times$ upper normal values); shock as persisting hypotension despite volume resuscitation, requiring vasopressors to maintain mean arterial pressure ≥ 65 mmHg and serum lactate level > 2 mmol/L.(21-26)

All included patients were followed until death or 30-day follow-up, whichever came first.

Statistical Analysis

Continuous variables were expressed as mean (standard deviation) or median (interquartile ranges), according to data distribution, and were compared using the Student's t-test or the Mann-Whitney U test; categorical variables were expressed as counts and percentages and compared using the Chi square or Fisher's exact tests, as appropriate.

Receiver operating characteristic (ROC) analysis has been performed among independent variables associated with SARS-CoV2 infection to define the cutoff point for MR-proADM, CRP, Ferritin, PCT values, and sequential organ failure assessment (SOFA) score in predicting ARDS and mortality, and the accuracy of MR-proADM, CRP, Ferritin, and PCT values in patients with SARS-CoV2 infection.

ROC curves and areas under the curve (AUC) values has been calculated for all markers including a group of 50 healthy individuals evaluated at Campus Bio-Medico University of Rome.

Pretest odds, posttest odds, and the consequent posttest probability have been computed to investigate whether combination of MR-proADM, PCT, and SOFA score improves post-test probability.

Kaplan-Meier curves were created to estimate the overall survival and compared using the log-rank test. To evaluate whether the value of MR-proADM influenced mortality rates, a Cox regression model was fitted using age and sex as covariates and the adjusted hazard ratios were calculated.

Data have been analyzed using Med-Calc 11.6.1.0 statistical package (MedCalc Software, Mariakerke, Belgium) and R (version 3.6.3, R Core Development Team, Vienna, Austria).(27)

P values < 0.05 were considered statistically significant.

RESULTS

Patients Characteristics

A total of 69 patients has been included in the primary analysis. The main patient characteristics are shown in Table 1. The median age was 78.0 years and 53.6% of patients were male. Cardiovascular (68.1%) and chronic pulmonary disease (33.3%) represented the most frequent comorbidities. The median SOFA score was 2 (IQR, 1-7), 56.5% of patients has been admitted to medical ward while the 43.5% to ICU. Median hospital stay was 17 days.

In the overall population, 58% (40/69 patients) developed ARDS, 23.2% (16/69) of patients died, 6.5% (3/46) acute cardiac injury, 1.4% (1/69) of patients developed acute ischemic stroke, 21.2% (14/66) acute kidney injury, 11.8% (8/68) acute liver damage, and 5.4% (3/56) septic shock. At the end of follow-up, all remaining 53 patients have been discharged.

Laboratory markers values in SARS-CoV2 infection

Median MR-proADM, CRP, ferritin, and PCT values were 1.49 nmol/l (IQR, 0.67-2.26), 4.24 mg/dL (IQR, 1.06-10.13), 413.00 ng/mL (IQR 125.5-1016.5), and 0.06 ng/mL (IQR, 0.03-0.41), respectively (Supplementary Table 1).

AUCs values resulting from ROC curve analysis for MRproADM, CRP, PCT, and ferritin in patients with SARS-CoV2 infection are showed in Supplementary Table 2. ROC curves and AUC values resulted statistically significant for all variable, but PCT (Supplementary Figure 1, Supplementary Table 2).

The best cut-off values for MR-proADM, CRP, ferritin, and PCT in patients with SARS-CoV2 infection were 1.00 nmol/L, 0.48 mg/dL, 115.58 ng/mL, and 0.26 ng/ml, respectively (Supplementary Table 2).

ROC curves comparison between the different variables has been reported in Supplementary Table 3 and schematized in Supplementary Figure 1. AUC value for MR-proADM (0.78) was significantly higher than PCT (0.55; $p < 0.0001$), smaller than CRP (0.91, $p < 0.0001$) and similar than ferritin (0.86, $p = 0.051$). AUC value of CRP was significantly higher than MR-proADM and PCT ($p < 0.0001$) and similar than ferritin ($p = 0.67$). Finally, AUC value of ferritin was significantly higher only than PCT ($p < 0.0001$).

ARDS prediction during SARS-CoV2 infection

Median values with interquartile ranges and Mann-Whitney's comparison for MR-proADM, CRP, ferritin and SOFA score for patients with or without ARDS development during follow-up are reported in Supplementary Table 4. All these variables resulted significantly higher in patients with ARDS.

ROC curves and AUC values resulted statistically significant for all considered variables despite only CRP presented significantly higher AUC values than MR-proADM ($p=0.030$) (Figure 1A, Supplementary Figure 2, and Supplementary Table 5 and 6). Furthermore, the best cut-off for ARDS development prediction were 3.04 nmol/L for MR-proADM, 3.88 mg/dL for CRP, 165.58 ng/mL for ferritin, and 1 for SOFA, respectively.

30-day mortality prediction during SARS-CoV2 infection

Median values with interquartile ranges and Mann-Whitney's comparison for MR-proADM and SOFA score in survivors and non survivors at 30-day follow-up are reported in Supplementary Table 7.

ROC curve and AUC values for MR-proADM and SOFA score resulted statistically significant ($p<0.0001$) without differences between the variables (Figure 1B, Supplementary Figure 3, and Supplementary Table 8 and 9). The best cut-off for 30-day mortality prediction were ≥ 2 nmol/L for MR-proADM, 2.91 mg/dl for CRP, 635.86 ng/ml for ferritin, and ≥ 3 for SOFA score.

Patients presenting with MR-proADM values ≥ 2 nmol/L, indeed, showed a significantly higher mortality risk than patients with MR-proADM values < 2 nmol/L (adjusted hazard ratio 12.34; 95% CI, 2.66 to 57.28; Fig 2 and Supplementary Table 10).

DISCUSSION

The results of this study showed that MR-proADM may be used as a marker of organ damage, disease severity, and mortality in patients with COVID-19. Patients who developed ARDS, the most frequent complication, presented higher MR-proADM values than patients without acute respiratory involvement. Furthermore, MR-proADM values ≥ 2 nmol/L were associated with a significantly higher mortality risk.

COVID-19 represents a systemic disease causing widespread endothelial damage with multiple organ dysfunction syndrome, in severe cases.(2) The role of endothelial cells in organ failure development during infections has been recently evaluated.(9) Coating the blood vessels and representing the interface between blood and parenchymal cells, vascular endothelial cell lining is responsible for organ function. The effects of

endothelial cell lining are also supported by the glycocalyx that controls hemostasis, leukocyte and platelet adhesion, the transmission of shear stress to the endothelium, and anti-inflammatory defenses. A disruption of this system may occur during sepsis and result in organ dysfunction, mainly affecting the hemostatic, pulmonary, kidney, and liver systems.(9, 28) Whether these alterations in endothelial cell lining is adaptive or maladaptive depends on both disease extension and time from disease onset. A localized vasodilatation, indeed, allows leukocytes to reach the site of infection while the activation of coagulation helps in restrain the widespread of infection. At more advanced stages, these alterations lead to a septic phenotype, resulting in a systemic reduction of vascular tone, increase in vascular permeability, alterations in microvascular perfusion, and hemostatic alteration up to disseminated intravascular coagulopathy.(9) Furthermore, vascular endothelial damage along with blood hypercoagulability are well known risk factors for venous thromboembolism.(29, 30)

Being responsible for endothelial integrity, an alteration of ADM system during sepsis causes vascular leakage and organ dysfunction (Figure 3).(31) Recent observational studies confirmed these pathological data showing as high values of ADM and of its more stable product MR-proADM are significantly associated with organ failure, disease severity and a worse prognosis.(12, 16, 32, 33)

The widespread endothelial and pulmonary damage related to SARS-CoV2 infection may cause a relevant disruption of the ADM system, mainly in severe cases. The receptors and binding sites for ADM, indeed, were mostly represented within the cardiovascular and lung tissue.(7) Our results confirm these hypothesis and showed as MR-proADM, identifying those patients with a higher risk of ARDS development and with a widespread organ involvement, may be listed among other evaluated prognostic markers.(34)

Furthermore, the role of ADM in COVID-19 related organ damage may suggest the use of new therapeutic agents, such as monoclonal antibody. Adrecizumab, a humanized, monoclonal, non-neutralizing ADM-binding antibody has been evaluated in patients with sepsis and acute heart failure in order to improve vascular integrity, tissue congestion, and thereby clinical outcomes.(7, 35)

CONCLUSION

MR-proADM values ≥ 2 nmol/l identify those patients with high mortality risk related to a multiple organ dysfunction syndrome. These patients must be carefully evaluated and considered for an intensive therapeutic approach. Further studies in larger populations will be warranted to confirm these data.

Author Contributions

S.S. led the study design, data collection, data analysis, data interpretation, and manuscript writing; F.E.A., F.S., and F.T. assisted with data collection and analysis of the validation dataset; E.V. and M.F. assisted with computer queries, data analysis and manuscript preparation; F.M. assisted with data collection and analysis of the validation dataset; M.C. assisted with data collection and analysis of the development dataset as well as study design, data interpretation and manuscript writing; S.C. and S.A. assisted with chart review and data analysis and supervised all aspects of the investigation, as well as assisting with study design, data interpretation and manuscript writing.

List of abbreviations: ADM, adrenomedullin; ARDS, acute respiratory distress syndrome; AUC, areas under the curve; COVID-19, Coronavirus disease 2019; CRP, C-reactive protein; MODS, multiple organ dysfunction syndrome; MR-proADM, MidRegional-proAdrenomedullin; PCT, procalcitonin; ROC, receiver operating

characteristic; SARS-CoV2, severe acute respiratory distress syndrome *Coronavirus 2*; SOFA, sequential organ failure assessment.

Acknowledgments: we thank Stefano Spoto for his help in collecting clinical data.

Conflict of interest: none

Funding: none

References

1. Benvenuto D, Giovanetti M, Ciccozzi A, Spoto S, Angeletti S, Ciccozzi M. The 2019-new coronavirus epidemic: Evidence for virus evolution. *J Med Virol.* 2020;92(4):455-9.
2. Potere N, Valeriani E, Candeloro M, Tana M, Porreca E, Abbate A, et al. Acute complications and mortality in hospitalized patients with coronavirus disease 2019: a systematic review and meta-analysis. *Crit Care.* 2020;24(1):389.
3. World Health Organization. Clinical management of severe acute respiratory infection (SARI) when COVID-19 disease is suspected: Interim guidance. Accessed: March 2020. WHO REFERENCE NUMBER: WHO/2019-nCoV/clinical/2020.4 2020 [
4. Lippi G, Favaloro EJ. D-dimer is Associated with Severity of Coronavirus Disease 2019: A Pooled Analysis. *Thromb Haemost.* 2020;120(5):876-8.
5. Lippi G, Plebani M, Henry BM. Thrombocytopenia is associated with severe coronavirus disease 2019 (COVID-19) infections: A meta-analysis. *Clin Chim Acta.* 2020;506:145-8.

6. Dschietzig T, Azad HA, Asswad L, Bohme C, Bartsch C, Baumann G, et al. The adrenomedullin receptor acts as clearance receptor in pulmonary circulation. *Biochem Biophys Res Commun.* 2002;294(2):315-8.
7. Voors AA, Kremer D, Geven C, Ter Maaten JM, Struck J, Bergmann A, et al. Adrenomedullin in heart failure: pathophysiology and therapeutic application. *Eur J Heart Fail.* 2019;21(2):163-71.
8. Wilson DC, Schefold JC, Baldira J, Spinetti T, Saeed K, Elke G. Adrenomedullin in COVID-19 induced endotheliitis. *Crit Care.* 2020;24(1):411.
9. Ince C, Mayeux PR, Nguyen T, Gomez H, Kellum JA, Ospina-Tascon GA, et al. The Endothelium in Sepsis. *Shock.* 2016;45(3):259-70.
10. Morgenthaler NG, Struck J, Alonso C, Bergmann A. Measurement of midregional proadrenomedullin in plasma with an immunoluminometric assay. *Clin Chem.* 2005;51(10):1823-9.
11. Spoto S, Legramante JM, Minieri M, Fogolari M, Terrinoni A, Valeriani E, et al. How biomarkers can improve pneumonia diagnosis and prognosis: procalcitonin and mid-regional-pro-adrenomedullin. *Biomark Med.* 2020;14(7):549-62.
12. Angeletti S, Spoto S, Fogolari M, Cortigiani M, Fioravanti M, De Florio L, et al. Diagnostic and prognostic role of procalcitonin (PCT) and MR-pro-Adrenomedullin (MR-proADM) in bacterial infections. *APMIS.* 2015;123(9):740-8.
13. Spoto S, Fogolari M, De Florio L, Minieri M, Vicino G, Legramante J, et al. Procalcitonin and MR-proAdrenomedullin combination in the etiological diagnosis and prognosis of sepsis and septic shock. *Microb Pathog.* 2019;137:103763.

14. Valenzuela Sanchez F, Valenzuela Mendez B, Rodríguez Gutierrez J, Bohollo de Austria R, Rubio Quiñones J, Puget Martínez L, et al. Initial levels of mr-proadrenomedullin: a predictor of severity in patients with influenza a virus pneumonia. *Intensive Care Med Exp.* 2015;3:A832.
15. Michels M, Djamiatun K, Faradz SM, Koenders MM, de Mast Q, van der Ven AJ. High plasma mid-regional pro-adrenomedullin levels in children with severe dengue virus infections. *J Clin Virol.* 2011;50(1):8-12.
16. Elke G, Bloos F, Wilson DC, Brunkhorst FM, Briegel J, Reinhart K, et al. The use of mid-regional proadrenomedullin to identify disease severity and treatment response to sepsis - a secondary analysis of a large randomised controlled trial. *Crit Care.* 2018;22(1):79.
17. Talero E, Di Paola R, Mazzon E, Esposito E, Motilva V, Cuzzocrea S. Anti-inflammatory effects of adrenomedullin on acute lung injury induced by Carrageenan in mice. *Mediators Inflamm.* 2012;2012:717851.
18. Angeletti S, Dicuonzo G, Fioravanti M, De Cesaris M, Fogolari M, Lo Presti A, et al. Procalcitonin, MR-Proadrenomedullin, and Cytokines Measurement in Sepsis Diagnosis: Advantages from Test Combination. *Dis Markers.* 2015;2015:951532.
19. Angeletti S, Ciccozzi M, Fogolari M, Spoto S, Lo Presti A, Costantino S, et al. Procalcitonin and MR-proAdrenomedullin combined score in the diagnosis and prognosis of systemic and localized bacterial infections. *J Infect.* 2016;72(3):395-8.
20. Spoto S, Celli E, de Cesaris M, Locorriere L, Mazzaroppi S, Nobile E, et al. Procalcitonin and MR-Proadrenomedullin Combination with SOFA and qSOFA Scores for Sepsis Diagnosis and Prognosis: A Diagnostic Algorithm. *Shock.* 2018;50(1):44-52.

21. Force ADT, Ranieri VM, Rubenfeld GD, Thompson BT, Ferguson ND, Caldwell E, et al. Acute respiratory distress syndrome: the Berlin Definition. *JAMA*. 2012;307(23):2526-33.
22. Rhodes A, Evans LE, Alhazzani W, Levy MM, Antonelli M, Ferrer R, et al. Surviving Sepsis Campaign: International Guidelines for Management of Sepsis and Septic Shock: 2016. *Crit Care Med*. 2017;45(3):486-552.
23. Summary of Recommendation Statements. *Kidney Int Suppl* (2011). 2012;2(1):8-12.
24. Thygesen K, Alpert JS, Jaffe AS, Chaitman BR, Bax JJ, Morrow DA, et al. Fourth universal definition of myocardial infarction (2018). *Eur Heart J*. 2019;40(3):237-69.
25. Sacco RL, Kasner SE, Broderick JP, Caplan LR, Connors JJ, Culebras A, et al. An updated definition of stroke for the 21st century: a statement for healthcare professionals from the American Heart Association/American Stroke Association. *Stroke*. 2013;44(7):2064-89.
26. Easton JD, Saver JL, Albers GW, Alberts MJ, Chaturvedi S, Feldmann E, et al. Definition and evaluation of transient ischemic attack: a scientific statement for healthcare professionals from the American Heart Association/American Stroke Association Stroke Council; Council on Cardiovascular Surgery and Anesthesia; Council on Cardiovascular Radiology and Intervention; Council on Cardiovascular Nursing; and the Interdisciplinary Council on Peripheral Vascular Disease. The American Academy of Neurology affirms the value of this statement as an educational tool for neurologists. *Stroke*. 2009;40(6):2276-93.

27. R Core Team (2019). R: A language and environment for statistical computing. R Foundation for Statistical Computing, Vienna, Austria. URL <https://www.R-project.org/2019>).
28. Cheung KCP, Fanti S, Mauro C, Wang G, Nair AS, Fu H, et al. Preservation of microvascular barrier function requires CD31 receptor-induced metabolic reprogramming. *Nat Commun.* 2020;11(1):3595.
29. Anderson FA, Jr., Spencer FA. Risk factors for venous thromboembolism. *Circulation.* 2003;107(23 Suppl 1):I9-16.
30. Porfidia A, Valeriani E, Pola R, Porreca E, Rutjes AWS, Di Nisio M. Venous thromboembolism in patients with COVID-19: Systematic review and meta-analysis. *Thromb Res.* 2020;196:67-74.
31. Koyama T, Ochoa-Callejero L, Sakurai T, Kamiyoshi A, Ichikawa-Shindo Y, Iinuma N, et al. Vascular endothelial adrenomedullin-RAMP2 system is essential for vascular integrity and organ homeostasis. *Circulation.* 2013;127(7):842-53.
32. Angeletti S, Fogolari M, Morolla D, Capone F, Costantino S, Spoto S, et al. Role of Neutrophil Gelatinase-Associated Lipocalin in the Diagnosis and Early Treatment of Acute Kidney Injury in a Case Series of Patients with Acute Decompensated Heart Failure: A Case Series. *Cardiol Res Pract.* 2016;2016:3708210.
33. Viaggi B, Poole D, Tujjar O, Marchiani S, Ognibene A, Finazzi S. Mid regional pro-adrenomedullin for the prediction of organ failure in infection. Results from a single centre study. *PLoS One.* 2018;13(8):e0201491.

34. Tian W, Jiang W, Yao J, Nicholson CJ, Li RH, Sigurslid HH, et al. Predictors of mortality in hospitalized COVID-19 patients: A systematic review and meta-analysis. *J Med Virol.* 2020.
35. Geven C, Bergmann A, Kox M, Pickkers P. Vascular Effects of Adrenomedullin and the Anti-Adrenomedullin Antibody Adrecizumab in Sepsis. *Shock.* 2018;50(2):132-40.

Table 1 Characteristics of the study population

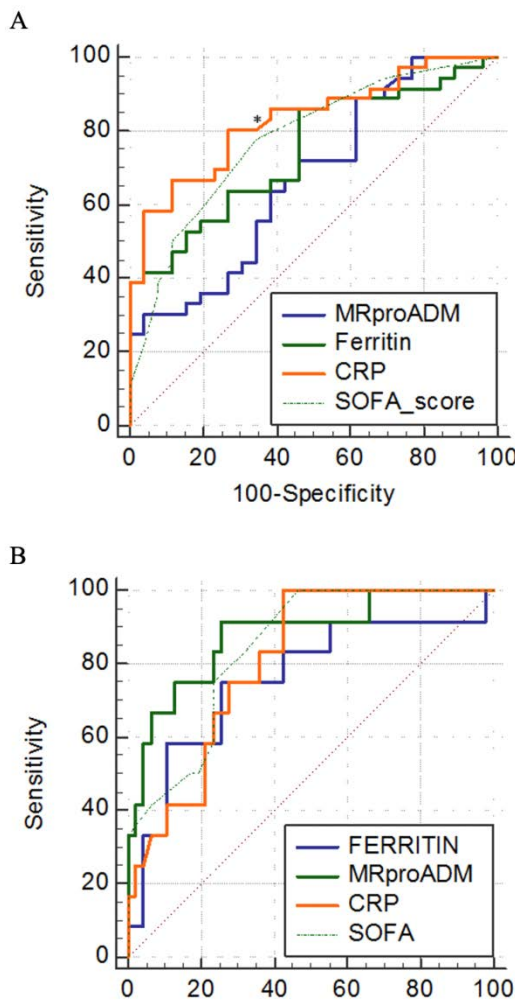
Variables	Overall	MR-proADM < 2	MR-proADM ≥ 2	
	n=69	n=43	n=21	
Median age, years (IQR)	78.00 (61.00-84.00)	72.00 (57.50-83.00)	81.00 (78.00-86.00)	0.085
Male sex, n (%)	37 (53.6)	22 (51.2)	12 (57.1)	0.854
Comorbidities, n (%)				
Cardiovascular	47 (68.1)	24 (60.0)	18 (94.7)	0.014
Chronic pulmonary disease	23 (33.3)	11 (27.5)	8 (42.1)	0.410
Chronic liver disease	4 (5.8)	3 (7.5)	0	0.544
Kidney disease	13 (18.8)	3 (7.5)	9 (50.0)	0.001
Diabetes mellitus	19 (27.5)	10 (25.0)	7 (38.9)	0.445
Blood hypertension	38 (55.1)	21 (52.5)	13 (72.2)	0.262
Active cancer	7 (10.1)	3 (7.5)	2 (11.8)	0.629
Symptoms at onset, n (%)				
Fever	27 (39.1)	17 (48.6)	8 (42.1)	0.866

Cough	15 (21.7)	13 (35.1)	2 (10.5)	0.099
Dyspnea	26 (37.7)	10 (27.0)	13 (68.4)	0.007
Pharyngodynbia	3 (4.3)	3 (8.1)	0	0.516
Gastrointestinal	11 (15.9)	6 (16.2)	3 (15.8)	1.000
Neurological	4 (5.8)	1 (2.7)	2 (10.5)	0.263
Arthro-myalgia	5 (7.2)	5 (13.5)	0	0.155
Anosmia	69 (100.0)	37 (100.0)	19 (100.0)	NA
Laboratory values, median (IQR)				
MR-proADM	1.49 (0.67-2.26)	0.91 (0.51-1.49)	4.19 (2.28-5.95)	<0.001
CRP	4.24 (1.06-10.13)	2.71 (0.51-6.24)	6.80 (4.99-14.07)	0.001
Ferritin	413.0 (125.5-1016.5)	245.5 (119.0-457.5)	777.5 (449.8-2009.0)	<0.001
PCT	0.06 (0.03-0.41)	0.04 (0.03-0.06)	0.72 (0.09-6.83)	<0.001
AST	27.50 (20.00-46.25)	25.00 (20.00-33.25)	46.00 (31.00-78.00)	0.002
ALT	17.00 (9.75-31.00)	16.50 (9.25-29.75)	17.00 (10.00-49.00)	0.682
Bilirubin	0.50 (0.40-0.80)	0.50 (0.40-0.70)	0.60 (0.40-0.90)	0.422
Creatinine	0.94 (0.70-1.50)	0.86 (0.66-1.01)	1.08 (0.99-3.68)	<0.001
PaO ₂ /FiO ₂	332.50 (237.00-383.25)	347.50 (281.75-390.00)	267.00 (197.00-381.00)	0.147
Prognostic score and Outcomes				
ICU admission, n (%)	30 (43.5)	13 (30.2)	13 (61.9)	0.031
Hospital discharge, n (%)	53 (76.8)	41 (95.3)	9 (42.9)	<0.001
Median hospital stays, days (IQR)	17.00 (9.00-32.00)	16.00 (10.00-25.00)	23.50 (13.25-44.25)	0.054

SOFA (median [IQR])	2.00 (1.00-7.00)	1.00 (1.00-3.00)	7.00 (3.00-8.00)	<0.001
ARDS, n (%)	40 (58.0)	22 (51.2)	15 (71.4)	0.203
Acute cardiac injury, n (%)*	3 (6.5)	0	3 (14.3)	0.108
Stroke	1 (1.4)	0	1 (1.4)	0.108
Acute kidney injury, n (%)*	14 (21.2)	1 (3.3)	10 (32.3)	0.009
Acute liver damage, n (%)*	8 (11.8)	2 (6.2)	6 (19.4)	0.237
Septic shock, n (%)*	3 (5.4)	0	2 (13.3)	0.082
Death, n (%)	16 (23.2)	2 (4.7)	12 (57.1)	<0.001

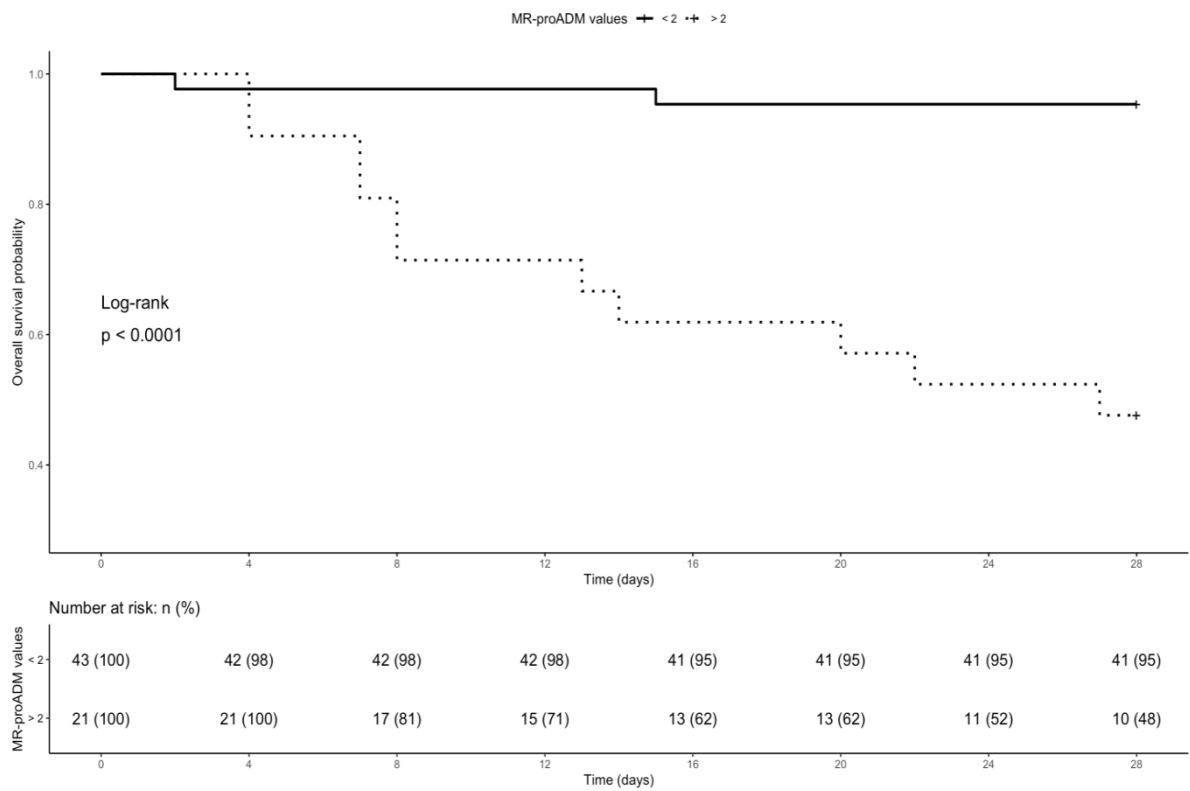
*These outcomes are not available for all included patients (please refer to the text).

ARDS, acute respiratory distress syndrome; CRP, C-reactive protein; ICU, Intensive Care Unit; IQR, interquartile range; MR-proADM, Mid-regional proAdrenomedullin; PCT, procalcitonin; SOFA, sequential organ failure assessment.

Titles and legends of figures

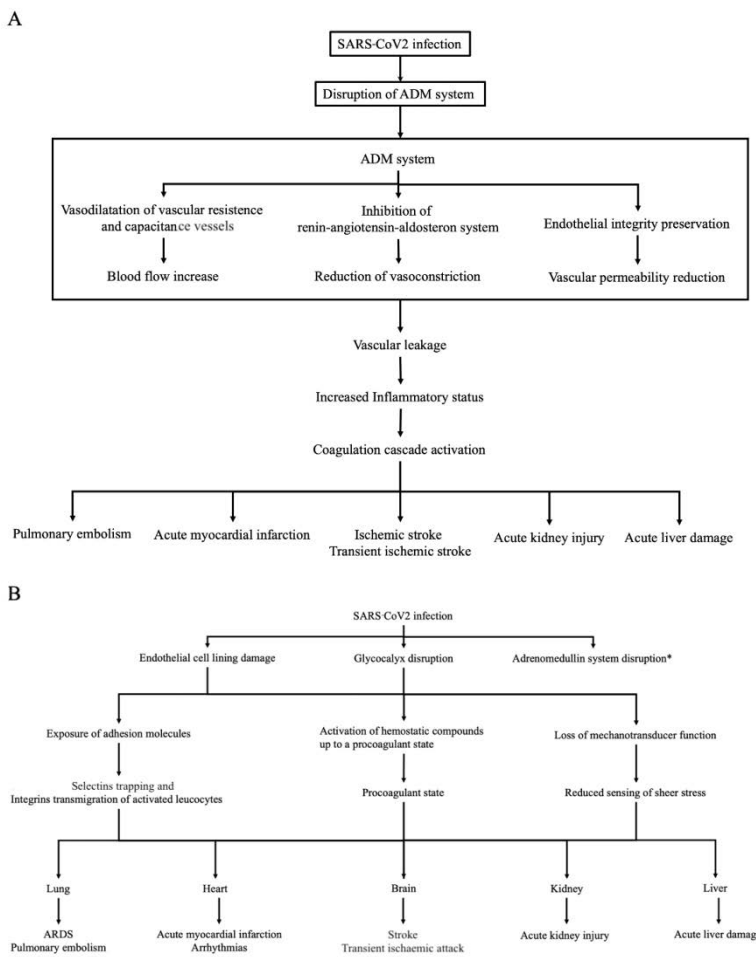
Title Figure 1 ROC curves for ARDS development (A) and mortality (B) in SARS-CoV2 infection.

Legend Figure 1 ARDS, acute respiratory distress syndrome; ROC, Receiver operating characteristic; SARS-CoV2, severe acute respiratory syndrome-Coronavirus 2.



Title Figure 2 Kaplan-Meier curves in patients with MR-proADM values $<$ or ≥ 2 nmol/L.

Legend Figure 2 MR-proADM, Mid-Regional proAdrenomedullin.



Title Figure 3 Adrenomedullin system disruption (A) and widespread endothelial damage (B) in SARS-CoV2 infection.

Legend Figure 3 ADM, adrenomedullin; ARDS, Acute respiratory distress syndrome; SARS-CoV2, severe acute respiratory syndrome-Coronavirus 2.

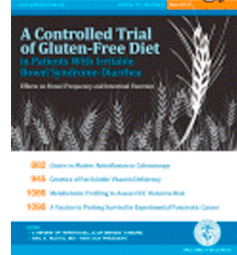
* see panel A

Journal Pre-proof

Hyperlipasemia and potential pancreatic injury patterns in COVID-19: A marker of severity or innocent bystander?

Hemant Goyal, MD FACP PGDCA (MBA), Sonali Sachdeva, MBBS, Abhilash Perisetti, MD FACP, Rupinder Mann, MD, Sumant Inamdar, MD, MPH, Benjamin Tharian, MD MRCP FACP FRACP

Gastroenterology



PII: S0016-5085(20)35326-9
DOI: <https://doi.org/10.1053/j.gastro.2020.10.037>
Reference: YGAST 63847

To appear in: *Gastroenterology*
Accepted Date: 23 October 2020

Please cite this article as: Goyal H, Sachdeva S, Perisetti A, Mann R, Inamdar S, Tharian B, Hyperlipasemia and potential pancreatic injury patterns in COVID-19: A marker of severity or innocent bystander?, *Gastroenterology* (2020), doi: <https://doi.org/10.1053/j.gastro.2020.10.037>.

This is a PDF file of an article that has undergone enhancements after acceptance, such as the addition of a cover page and metadata, and formatting for readability, but it is not yet the definitive version of record. This version will undergo additional copyediting, typesetting and review before it is published in its final form, but we are providing this version to give early visibility of the article. Please note that, during the production process, errors may be discovered which could affect the content, and all legal disclaimers that apply to the journal pertain.

© 2020 by the AGA Institute

Hyperlipasemia and potential pancreatic injury patterns in COVID-19: A marker of severity or innocent bystander?

Running head: Hyperlipasemia in COVID-19

Hemant Goyal, Sonali Sachdeva, Abhilash Perisetti, Rupinder Mann, Suman Inamdar, Benjamin Tharian

Names of authors with affiliations

1) Hemant Goyal, MD FACP PGDCA (MBA)

¹The Wright Center for Graduate Medical Education

501 S. Washington Avenue

Scranton, PA 18503 USA

Office: 570.591.5175

Email: doc.hemant@yahoo.com

²Clinical Assistant Professor of Medicine

Mercer University School of Medicine

Macon, GA USA 31207

2) Sonali Sachdeva, MBBS

Department of anesthesiology and intensive care

Maulana Azad Medical College

New Delhi, India

Email: sonalisachdeva1993@gmail.com

3) Abhilash Perisetti, MD FACP

Department of Gastroenterology and Hepatology

The University of Arkansas for Medical Sciences,

Little Rock, AR, USA

Email: abhilash.perisetti@gmail.com

4) Rupinder Mann, MD

Department of Internal Medicine,
Saint Agnes Medical Center,
1303 E Herndon Ave, Fresno, CA 93730, USA
Email: rupindrmann@yahoo.com

5) Suman Inamdar MD, MPH

Assistant Professor of Medicine
Program director- Advanced Endoscopy Fellowship
University of Arkansas for Medical Sciences
Little Rock, AR, USA
Email: Sinamdar@uams.edu

6) Benjamin Tharian, MD MRCP FACP FRACP

Associate Professor of Medicine
Director of General and Advanced Endoscopy
University of Arkansas for Medical Sciences
Little Rock, AR, USA
Email: Btharian@uams.edu

Word count: 880

Author contributions:

Conception and design: Hemant Goyal
Statistical analysis: Hemant Goyal, Sonali Sachdeva
First draft: Sonali Sachdeva
Critical revision and editing: All authors

Final approval: All authors

Funding: None

Conflict of Interest and Ethical statement:

This manuscript, as submitted or its essence in another version is not under consideration for publication elsewhere and will not be published elsewhere while under review by *Gastroenterology*. All authors have made substantive contributions to the study, and all authors endorse the data and conclusions. All authors have no commercial associations or sources of support that might pose a conflict of interest.

Corresponding author:

Hemant Goyal, MD FACP PGDCA (MBA)
The Wright Center for Graduate Medical Education
501 S. Washington Avenue
Scranton, PA 18505
Office: 570.591.5175
Email: doc.hemant@yahoo.com

Hyperlipasemia and potential pancreatic injury patterns in COVID-19: A marker of severity or innocent bystander?

Introduction

Coronavirus disease 2019 (COVID-19) is caused by Severe Acute Respiratory Syndrome (SARS-CoV-2). Gastrointestinal symptoms are increasingly being reported in COVID-19¹. Data on the involvement of the pancreas in COVID-19 has been emerging, and multiple case reports of SARS-CoV-2-induced acute pancreatitis have been published in the literature². The angiotensin-converting enzyme-2 (ACE-2) is the target receptor of SARS-CoV-2 and is expressed abundantly by both the exocrine and endocrine pancreatic tissues ³. The presence of ACE-2 in the pancreas could make it susceptible to SARS-CoV-2 resulting in interstitial leakage of pancreatic lipase, adipose tissue lipolysis, and potentially toxic fatty acid-induced damage. These changes can at least contribute to cytokine storm, multiorgan dysfunction, and COVID-19 morbidity ⁴. Due to its non-specificity, lipase could be elevated in a myriad of conditions such as infections, renal dysfunction, medication-related, gastrointestinal, and hepatobiliary disease ⁵. Given this, it is critical to evaluate the prevalence of hyperlipasemia in COVID-19 and predict clinical outcomes.

Methods

We conducted a systematic search using PubMed, Embase, Ovid, and Google Scholar databases from December 1st, 2019 to October 9th, 2020, to evaluate hyperlipasemia in COVID-19 patients. The following search terms were used- 'COVID-19', 'SARS-CoV-2', 'lipase,' 'pancreatic injury,' 'pancreas.' The articles with relevant data on the prevalence of hyperlipasemia and its effect on COVID-19 severity were examined. All adult patients with nasopharyngeal RT-PCR positive for SARS-CoV-2 were included in the analysis. Severe COVID-19 was defined as clinical deterioration resulting in adverse clinical outcomes such as admission to the intensive care unit (ICU), need for mechanical ventilation, or death. Hyperlipasemia was defined as any elevation in the lipase levels above the upper limit of the normal (ULN) reference level. The definition of hyperlipasemia varied among the

studies because of differences in the range of lipase levels, as was the definition of severe COVID-19.

The OpenMeta[Analyst] software was used to estimate the pooled prevalence of lipase elevations among COVID-19 patients and the pooled odds ratio (OR) for severe COVID-19 among this subset of patients. Results were reported with a 95% confidence interval (CI), and a p-value of <0.05 was considered statistically significant. Heterogeneity was assessed using the I^2 test, and $I^2 > 50\%$ was taken as a measure of moderate inter-study variation.

Results

The initial search yielded 52 articles. After excluding duplicates and reviews articles, seven studies (6 retrospective observational studies and one prospective observational study) were included in the pooled analysis. A flow chart depicting the study screening and selection process is represented in Supplemental Figure 1.

Data on the point-prevalence of hyperlipasemia was available in all seven studies, whereas only 4 reported clinical outcomes, ICU admission status, and need for mechanical ventilation, or death. The normal range of serum lipase levels differed among studies. While four studies had an average upper limit of 50-60 U/L; two had a higher cut-off (>300 U/L) for lipase levels. Data about 756 COVID-19 patients were reported in these studies, out of which 92 patients had hyperlipasemia. All were single center experiences, except one. Two studies reported severe COVID-19 as patients needing ICU admission, one study with a need for mechanical ventilation, and only one study used a combination of all three as severe COVID-19. Supplemental Table 1 outlines the baseline characteristics of the included studies.

The results of this pooled analysis are shown in Figure 1 (A & B). Among 756 COVID-19 patients with available lipase levels, the pooled prevalence of hyperlipasemia was 11.7% (95% CI: 0.094-0.140, P=0.001), and $I^2 = 0\%$. The pooled OR for severe COVID-19 in these patients was 3.143 (95% CI: 1.543-6.400, P=0.003); mild inter-study heterogeneity was observed ($I^2 = 27\%$).

Discussion

Based on the result of our pooled analysis, hyperlipasemia was found to be in 11.7% of patients affected by SARS-CoV-2. COVID-19 patients with hyperlipasemia are at a ~3-fold higher risk of poor clinical outcomes, including the need for ICU admission, mechanical ventilation, or death.

Although multiple mechanisms have been proposed for pancreatic injury in COVID-19, the exact etiology remains unclear. Some of the mechanisms include direct pancreatic tissue damage by SARS-CoV-2 and intense inflammatory response (interleukin [IL]-1 β , IL-6, and tumor necrosis factors) with cytokine storm mediated tissue injury. Furthermore, studies showed COVID-19 patients with pancreatic injury had a higher prevalence of severe illness on admission, lower levels of CD3+, CD4+ T cells, and higher levels of aspartate aminotransferase, γ -glutamyl transferase, creatinine, lactate dehydrogenase, and erythrocyte sedimentation rate⁶.

Limitations of this study include a modest sample size of 756 COVID-19 patients, of which 92 patients had elevated serum lipase levels. The degree of hyperlipasemia was not uniform across all studies. Potential confounders such as age, comorbidities, and medication use could alter the results of this study. Furthermore, a lack of high-quality randomized controlled trials with adjustment of potential confounders is a notable limitation. Given the inclusion of observational studies, selection bias, information bias, and confounding bias are possible. The prevalence of hyperlipasemia could be underestimated due to a lack of testing and non-reporting of the data in many patients.

Severe pancreatic injury resulting in acute pancreatitis may not be a common event in COVID-19. As evidenced by lipase elevation, mild to moderate pancreatic injury is a clinically significant finding in these patients. Future prospective studies are warranted to ascertain the exact impact of lipase elevation in COVID-19 and guide management strategies for these patients.

REFERENCES

1. Aziz M, et al. Taste Changes (Dysgeusia) in COVID-19: A Systematic Review and Meta-analysis. *Gastroenterology* 2020;159:1132-1133.
2. Aloysius MM, et al. COVID-19 presenting as acute pancreatitis. *Pancreatology* 2020;20:1026-1027.
3. Liu F, Long X, Zhang B, Zhang W, Chen X, Zhang Z. ACE2 Expression in Pancreas May Cause Pancreatic Damage After SARS-CoV-2 Infection. *Clin Gastroenterol Hepatol*. 2020;18:2128-2130.e2.
4. Hegyi P, Szakács Z, Sahin-Tóth M. Lipotoxicity and cytokine storm in severe acute pancreatitis and COVID-19. *Gastroenterology* 2020;159:824-827.
5. Hameed AM, et al. Significant elevations of serum lipase not caused by pancreatitis: a systematic review. *HPB (Oxford)* 2015;17:99-112.
6. Wang F, Wang H, Fan J, Zhang Y, et al. Pancreatic Injury Patterns in Patients With Coronavirus Disease 19 Pneumonia. *Gastroenterology*. 2020;159:367-370.

Journal Pre-proof

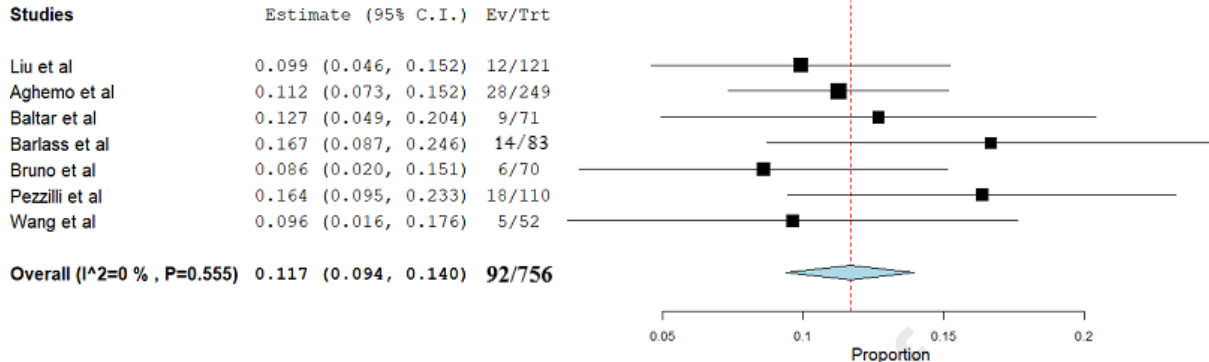


Figure 1-A: Pooled Incidence Rate of Hyperlipasemia in COVID-19 patients

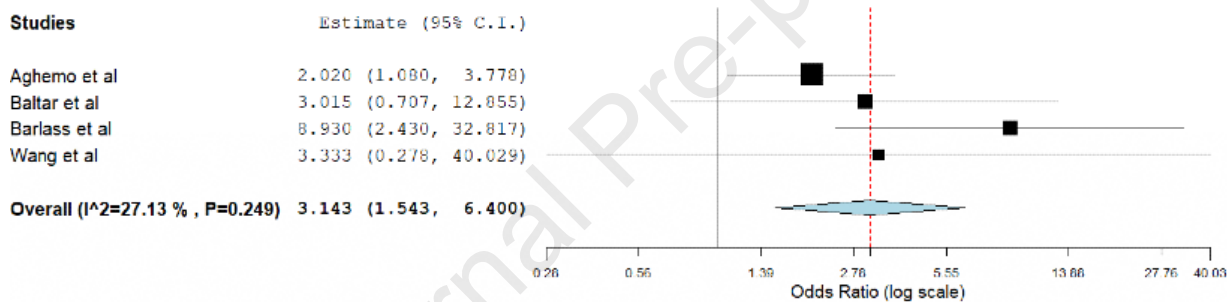


Figure 1-B: Pooled Odds Ratio of Severe COVID-19 in patients with hyperlipasemia



Lactate dehydrogenase levels predict coronavirus disease 2019 (COVID-19) severity and mortality: A pooled analysis

Brandon Michael Henry, MD ^{a,*}, Gaurav Aggarwal, MD ^b, Johnny Wong ^c, Stefanie Benoit, MD ^{d,e}, Jens Vikse ^f, Mario Plebani ^g, Giuseppe Lippi, MD ^h

^a Cardiac Intensive Care Unit, The Heart Institute, Cincinnati Children's Hospital Medical Center, Cincinnati, OH, USA

^b Department of Medicine, Jersey City Medical Center, Jersey City, NJ, USA

^c College of Medicine, SUNY Downstate Health Sciences University, New York, USA

^d Division of Nephrology and Hypertension, Cincinnati Children's Hospital Medical Center, OH, USA

^e Department of Pediatrics, College of Medicine, University of Cincinnati, OH, USA

^f Department of Clinical Immunology, Stavanger University Hospital, Stavanger, Norway

^g Department of Lab Medicine, University Hospital, Padova, Italy

^h Section of Clinical Biochemistry, Department of Neuroscience, Biomedicine and Movement, University of Verona, Verona, Italy

ARTICLE INFO

Article history:

Received 20 April 2020

Received in revised form 20 May 2020

Accepted 20 May 2020

Keywords:

Lactate dehydrogenase

COVID-19

Coronavirus

ABSTRACT

Coronavirus disease 2019 (COVID-19) infection has now reached a pandemic state, affecting more than a million patients worldwide. Predictors of disease outcomes in these patients need to be urgently assessed to decrease morbidity and societal burden. Lactate dehydrogenase (LDH) has been associated with worse outcomes in patients with viral infections. In this pooled analysis of 9 published studies ($n = 1532$ COVID-19 patients), we evaluated the association between elevated LDH levels measured at earliest time point in hospitalization and disease outcomes in patients with COVID-19. Elevated LDH levels were associated with a ~6-fold increase in odds of developing severe disease and a ~16-fold increase in odds of mortality in patients with COVID-19. Larger studies are needed to confirm these findings.

© 2020 Elsevier Inc. All rights reserved.

1. Introduction

The current pandemic of coronavirus disease 2019 (COVID-19) originally emerged from China, but has since then infected >1 million patients worldwide, with over 400,000 cases in the US alone [1]. This condition is associated with high morbidity, leading to significant strain on healthcare infrastructure and resources. The associated fatality rate is also higher than other respiratory viral infections. Hence, it is necessary to urgently identify reliable predictors of disease severity and mortality for careful allocation of healthcare resources and to enable earlier clinical intervention and monitoring to improve clinical outcomes.

Various biomarkers are currently under investigation for their role in determination of prognosis in patients with COVID-19. Lactate dehydrogenase (LDH) is one such biomarker of interest, especially since elevated LDH levels have been associated with worse outcomes in patients with other viral infections in the past [2–4]. Early data in COVID-19 patients has suggested significant differences in LDH levels between patients and without severe disease [5]. Hence, we performed

a pooled analysis of the published literature to explore the possible association between increased LDH values and odds of disease severity and mortality in COVID-19 patients.

2. Methods

2.1. Search design

A comprehensive search of literature on online databases Medline (PubMed interface), Web of Science, EMBASE and Scopus, using no language restriction, was conducted with the search terms “lactate dehydrogenase” OR “LDH” AND “COVID-19” OR “coronavirus 2019” OR “SARS-CoV-2” until April 3, 2020. References of all identified studies were investigated to determine other eligible studies. The reporting of this study was performed in compliance with the PRISMA guidelines (Preferred reporting items for systematic reviews and meta-analyses). The PRISMA Checklist is shown in Supplement 1.

2.2. Selection and data collection

All resulting documents were assessed by title, abstract, and full text for observational studies reporting frequency data on LDH values at

* Corresponding author at: Cardiac Intensive Care Unit, The Heart Institute, Cincinnati Children's Hospital Medical Center, 3333 Burnet Avenue, Cincinnati, OH 45229, USA.

E-mail address: Brandon.henry@cchmc.org (B.M. Henry).

admission or earliest time point in hospitalization in COVID-19 patients with or without severe disease or in non-survivors and survivors by two independent reviewers. "Severe disease" was clinically defined as patients requiring life support, meeting criteria for acute respiratory distress syndrome (ARDS), need for mechanical ventilation, or intensive care unit (ICU) admission. An acceptable study level definition of elevated LDH with an upper limit cut-off in the range of 240–255 U/L was required. Studies fitting the criteria were included in a pooled analysis. Studies with a higher than 255 U/L cut-off for abnormality were excluded to avoid biasing the analysis via threshold effect. Additional data was sought from study authors when appropriate.

2.3. Statistical analysis

Pooled analysis was performed with MetaXL, software version 5.3 (EpiGear International Pty Ltd., Sunrise Beach, Australia), using a random effects model to estimate the odds ratio (OR) and 95% confidence interval (95% CI) of elevated LDH levels in association with severe versus non-severe COVID-19 and non-survival vs survival. A leave-one-out sensitivity analysis was performed to determine sources of heterogeneity amongst studies. We also performed a meta-regression analysis to assess the impact of age on association of elevated LDH levels with

disease severity and mortality. When unavailable, mean and standard deviation of LDH levels were extrapolated from sample size, median and interquartile range (IQR), according to Hozo et al. [6]. Publication bias analysis was performed using funnel plot analysis. The study was carried out in accordance with the declaration of Helsinki and with the terms of local legislation.

3. Results

3.1. Study identification and characteristics of studies

A total of 289 studies were initially found, out of which 208 were excluded due to repetition. Another 63 were removed as they did not report LDH values. 18 studies were left, out of which 9 were removed because they were review articles or editorials. Nine studies (four case-control studies and five retrospective cohort studies) with 1532 patients, were finally used in the pooled analysis [7–15]. One study by Wu et al. reported cohorts of both severity and mortality [13]. All studies were from China and all reported LDH values were measured at time of admission or earliest time point after hospitalization. The PRISMA flow diagram is demonstrated in Fig. 1. The characteristics of included studies are presented in Table 1. Five studies did not report LDH values for all included patients; the study level samples used are presented in Table 1.

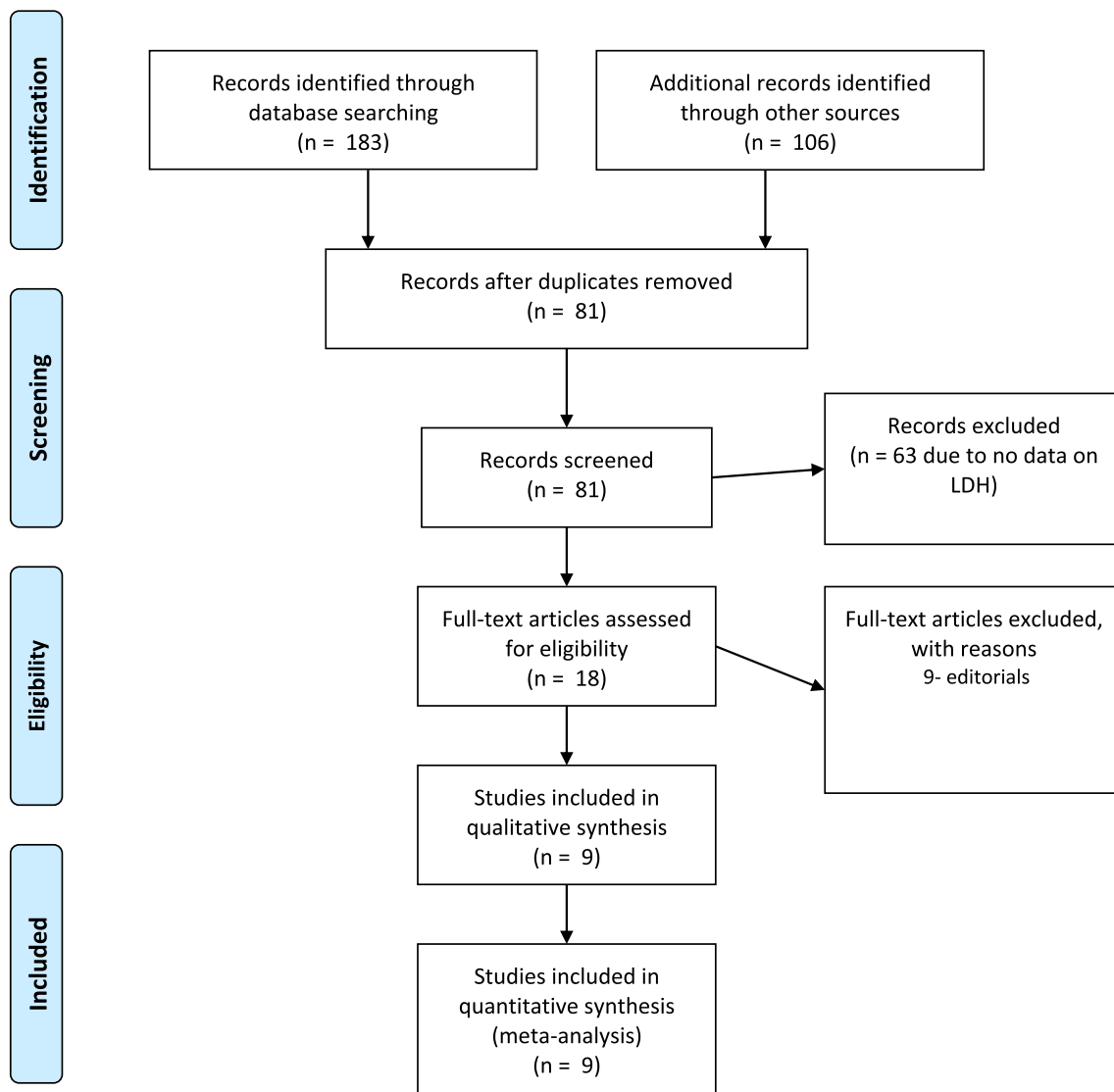


Fig. 1. PRISMA Flow diagram.

Table 1

Characteristics of included studies.

Study	Setting	Sample size	Outcomes	Severe patients			Non-severe patients		
				n (%)	Age (yrs)*	Elevated LDH (%)	n (%)	Age (yrs)*	Elevated LDH (%)
Guan W et al. 2020	China	675	Admission to ICU, MV	44 (6.5%)	63 (53–71)	31 (70.5%)	631 (93.5%)	46 (35–57)	246 (39.0%)
Huang C et al. 2020	China	40	ICU Care	13 (32.5%)	49 (41–61)	12 (92.3%)	27 (67.5)	49 (41–58)	17 (63.0%)
Liu Y et al. 2020	China	12	Respiratory Failure, MV	6 (50.0%)	64 (63–65)	5 (83.3%)	6 (50.0%)	44 (35–55)	6 (100.0%)
Ruan Q et al. 2020	China	60	Death	60 (42.3%)	67 (15–81)	57 (95.0%)	82 (57.7%)	50 (44–81)	48 (58.5%)
Wan S et al. 2020	China	135	Respiratory Distress, Admission to ICU	40 (29.6%)	56 (52–73)	30 (75.0%)	95 (70.4%)	44 (33–49)	28 (29.5%)
Wang Z et al. 2020	China	61	SpO ₂ < 90%	12 (19.7%)	70.5 (62–77)	10 (83.3%)	49 (80.3%)	37 (32–51)	15 (30.6%)
Wu C et al. 2020	China	188	Admission to ICU	48 (25.5%)	NR	46 (95.8%)	140 (74.5%)	46.97 ± 11.2	80 (57.1%)
Wu C et al. 2020	China	188	Death	43 (22.9%)	NR	41 (95.3%)	145 (77.1%)	46.97 ± 11.2	85 (58.6%)
Zhang G et al. 2020	China	95	Admission to ICU, MV	25 (26.3%)	52 (38–63)	25 (100.0%)	70 (73.7%)	49 (41–56)	49 (70.0%)
Zhou F et al. 2020	China	184	Death	54 (29.3%)	69 (63–76)	53 (98.1%)	130 (70.7%)	52 (45–58)	70 (53.8%)

* Age data presented as median (IQR) or mean (SD). MV — Mechanical Ventilation, ICU — Intensive Care Unit, NR — Not reported.

3.2. Pooled analysis of disease severity

Seven studies compared elevated LDH values in severe vs. non-severe cases in a total of 1206 patients, 188 (15.6%) of whom had severe disease outcome [7–9,11–14]. A total of 600 patients (49.8%) presented with elevated LDH values, with 159 severe patients (84.6%) having elevated LDH vs 441 patients (43.3%) in non-severe group. The LDH cutoff in the included studies ranged from 240 to 253.2 U/L. Findings of our pooled analysis are shown in Fig. 2. Elevated LDH values were found to be associated with an increased odds of severe COVID-19 outcome in all but 2 individual studies [8,9]. Pooled analysis showed about ~6.5-fold increase in odds of developing severe COVID-19 disease (OR: 6.53 [95% CI: 3.47–12.28], $I^2 = 31\%$, Cochran's Q, $p = 0.19$). A leave-one-out sensitivity study did not find any significant differences in association, however, analysis with exclusion of Guan et al. showed a substantially reduced heterogeneity (OR: 8.54 [95% CI: 4.33–16.87], $I^2 = 9.3\%$, $p = 0.36$). LDH was associated with significantly increased odds of severe COVID-19 in both case-control studies (OR: 7.76 [95% CI: 3.64–16.53], $I^2 = 0\%$, Cochran's Q, $p = 0.75$) and retrospective cohort studies (OR: 5.77 [95% CI: 1.82–18.29], $I^2 = 59\%$, Cochran's Q, $p =$

0.06). The results of meta-regression analysis demonstrated no impact of age on the association of elevated LDH levels and disease severity in patients with COVID-19 (correlation coefficient = 0.0027, [95% CI −0.12–0.11], $p = 0.96$, Fig. 3). Funnel plot analysis indicate some asymmetry amongst studies suggestive of publication bias, however, limited studies exclude firm conclusions (Fig. 4).

3.3. Pooled analysis of mortality

Three studies compared elevated LDH values with survival and non-survival in 514 patients, 157 (30.5%) of whom were non-survivors [10,13,15]. A total of 354 patients (68.9%) had elevated LDH values, of which 151 non-survivors (96.2%) had elevated LDH vs. 203 patients (56.9%) in the survivor group. The LDH cutoff in the included studies ranged from 245 to 253.2 U/L. Elevated LDH value was also found to be associated with significantly increased odds of mortality, displaying over 16-fold increased odds compared to patients with LDH below the cutoff value (OR: 16.64 [95% CI: 7.07–39.13], $I^2 = 0\%$, Cochran's Q, $p = 0.67$) (Fig. 2). Sensitivity analysis noted no difference amongst studies. Limited number of studies prevented a meta-regression analysis.

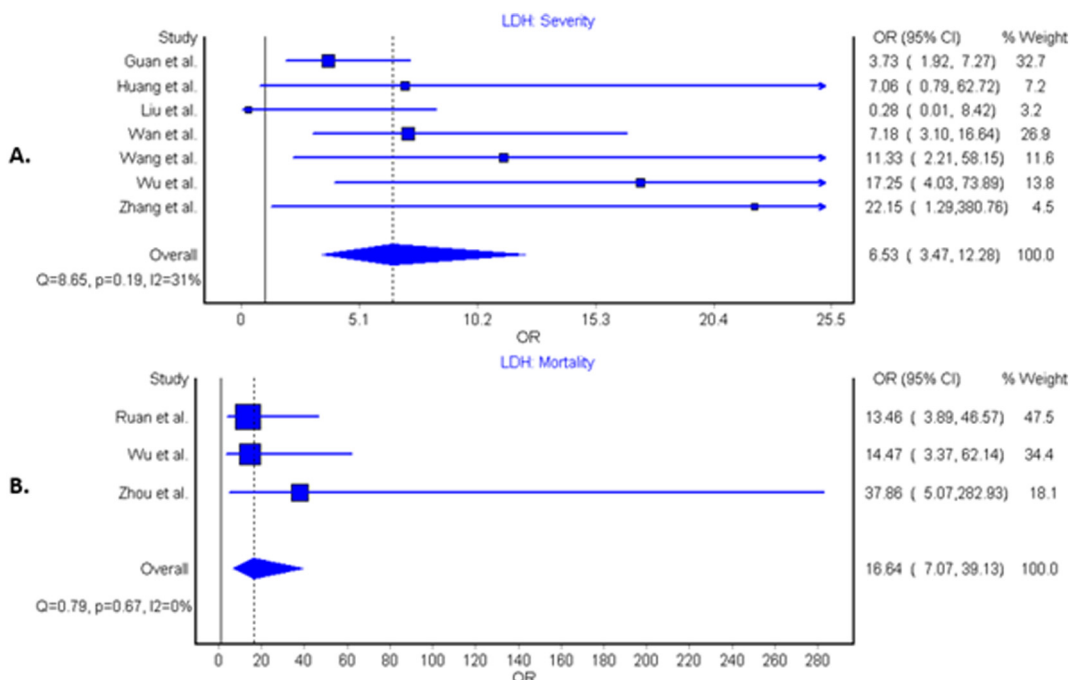


Fig. 2. Forest plots demonstrating association of elevated lactate dehydrogenase levels with disease severity (panel A) and mortality (panel B) in patients with coronavirus disease 2019 infection.

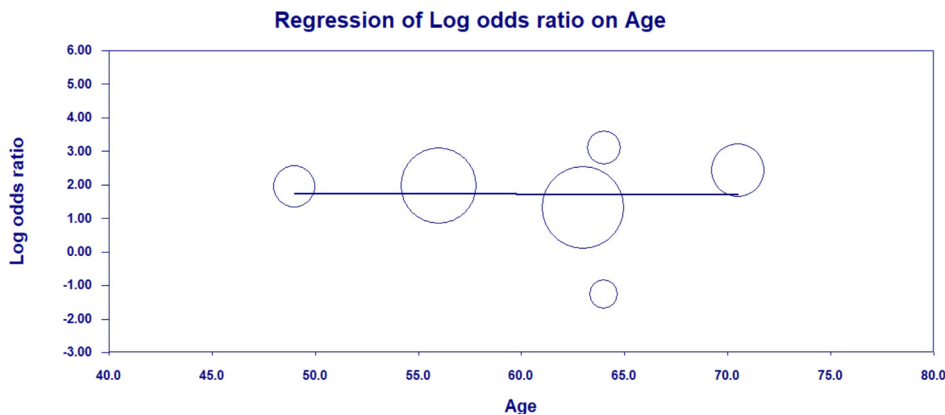


Fig. 3. Meta-regression plot showing no impact of age on association of elevated LDH levels and severity of disease in patients with COVID-19 infection.

4. Discussion

The results of our pooled analysis demonstrate an association between elevated LDH values and worse outcomes in patients with COVID-19. Specifically, there was a >6-fold increase in odds of severe disease and a >16-fold increase in odds of mortality in patients with elevated LDH. Furthermore, in all the three studies reporting mortality as an outcome, elevated LDH levels were found in >95% of non-survivors compared to <60% of survivors.

LDH is an intracellular enzyme found in cells in almost all organ systems, which catalyzes the interconversion of pyruvate and lactate, with concomitant interconversion of NADH and NAD⁺ [16]. The enzyme is composed by two major subunits (i.e., A and B), and is present in humans in five separate isozymes (LDH-1 in cardiomyocytes, LDH-2 in reticuloendothelial system, LDH-3 in pneumocytes, LDH-4 in kidneys and pancreas, and LDH-5 in liver and striated muscle). Although LDH has been traditionally used as a marker of cardiac damage since the 1960s, abnormal values can result from multiple organ injury and decreased oxygenation with upregulation of the glycolytic pathway. The acidic extracellular pH due to increased lactate from infection and tissue injury triggers the activation of metalloproteases and enhances macrophage mediated angiogenesis [17].

Severe infections may cause cytokine-mediated tissue damage and LDH release [17]. Since LDH is present in lung tissue (isozyme 3), patients with severe COVID-19 infections can be expected to release greater amounts of LDH in the circulation, as a severe form of interstitial

pneumonia, often evolving into acute respiratory distress syndrome, is the hallmark of the disease. However, the contribution of the different LDH isoenzymes to the LDH elevation observed in COVID-19 has not been determined. Additionally, LDH levels are elevated in thrombotic microangiopathy, which is associated with renal failure and myocardial injury [18–20]. Elevated d-dimer levels and thrombocytopenia in patients with severe COVID-19 have also been reported, which suggests a hypercoagulable state may be contributing to severity of illness and mortality [21,22].

Multiple studies have found LDH to be a predictor of worse outcomes in hospitalized patients [2,23]. Many of the prognosticators and therapies currently being studied for COVID-19 are based on experience with the previous coronavirus outbreak, Severe Acute Respiratory Syndrome (SARS), or with other viral respiratory infections. LDH levels were also found to be elevated in patients with Middle East Respiratory Syndrome (MERS) [24]. Elevated LDH levels seem to reflect that the multiple organ injury and failure may play a more prominent role in this pathology in influencing the clinical outcomes in patients with COVID-19.

Our study has some limitations, such as the small number of studies with limited sample sizes. There was heterogeneity in the LDH data, likely due to the poor standardization of analytical methods and poor description in "Material and Methods" section of the analytical performances, including different methods of measurement. To account for heterogeneity amongst studies, we performed sensitivity analysis. We also performed funnel plot analysis to assess for publication bias. Finally, all the studies were from China and hence the findings may not be

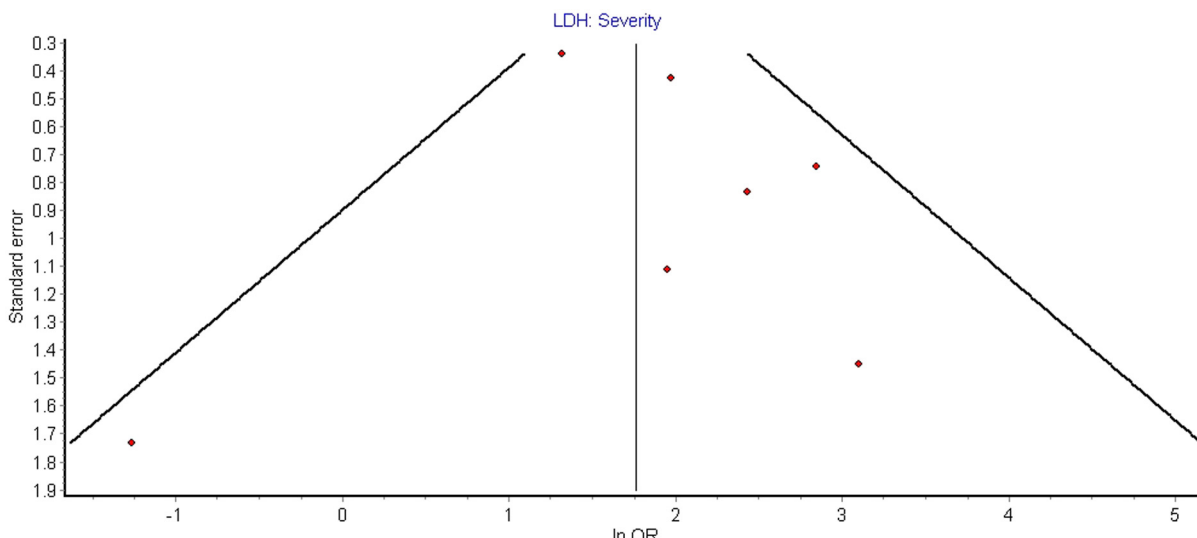


Fig. 4. Funnel plot demonstrating publication bias for studies evaluating association of elevated LDH levels and severity of disease in patients with COVID-19 infection.

applicable to other populations. Larger studies from other countries are needed to confirm our findings. In the meantime, we suggest that LDH level may be used as an important tool in determining prognosis in patients with COVID-19. Since LDH measurement is based on a colorimetric method, quick processing of multiple samples can be done using computer automation which may help in quick triage of COVID-19 patients [25].

5. Conclusion

In our pooled analysis, elevated LDH values were associated with 6-fold increased odds of severe COVID-19 disease. More importantly, elevated LDH was associated with a >16-fold increase in odds of mortality. As such, patients' LDH should be closely monitored for any of signs of disease progression or decompensation. Since the LDH levels used in the study were at admission or earliest time during hospitalization, admission LDH levels could be considered for inclusion in future risk stratification models for COVID-19 severity and mortality. Larger studies are needed to confirm these findings.

Supplementary data to this article can be found online at <https://doi.org/10.1016/j.ajem.2020.05.073>.

CRediT authorship contribution statement

Brandon Michael Henry: Conceptualization, Methodology, Investigation, Writing - review & editing, Supervision. **Gaurav Aggarwal:** Writing - original draft, Investigation, Data curation. **Johnny Wong:** Methodology, Software. **Stefanie Benoit:** Conceptualization, Writing - review & editing. **Jens Vikse:** Conceptualization, Writing - review & editing. **Mario Plebani:** Conceptualization, Writing - review & editing. **Giuseppe Lippi:** Conceptualization, Writing - review & editing.

Acknowledgement

None.

Funding

None.

Disclosure

None.

References

- [1] World Health Organization. Coronavirus disease 2019 (COVID-19) pandemic. <https://www.who.int/emergencies/diseases/novel-coronavirus-2019/>; 2020. [Accessed 12 April 2020].
- [2] Chen CY, Lee CH, Liu CY, Wang JH, Wang LM, Perng RP. Clinical features and outcomes of severe acute respiratory syndrome and predictive factors for acute respiratory distress syndrome. *J Chin Med Assoc.* 2005;68(1):4–10.

- [3] Chiang CH, Shih JF, Su WJ, Perng RP. Eight-month prospective study of 14 patients with hospital-acquired severe acute respiratory syndrome. *Mayo Clin Proc.* 2004; 79(11):1372–9.
- [4] Tao RJ, Luo XL, Xu W, et al. Viral infection in community acquired pneumonia patients with fever: a prospective observational study. *J Thorac Dis.* 2018;10(7): 4387–95.
- [5] Henry B, De Olivera MHS, S. B, M. P, G. L Hematologic, biochemical and immune marker abnormalities associated with severe illness and mortality in coronavirus disease 2019 (COVID 19): a meta-analysis. *Clin Chem Lab Med.* 2020.
- [6] Hozo SP, Djulbegovic B, Hozo I. Estimating the mean and variance from the median, range, and the size of a sample. *BMC Med Res Methodol.* 2005;5:13.
- [7] Guan WJ, Ni ZY, Hu Y, et al. Clinical characteristics of coronavirus disease 2019 in China. *N Engl J Med.* 2020;382:1708–20.
- [8] Huang C, Wang Y, Li X, et al. Clinical features of patients infected with 2019 novel coronavirus in Wuhan, China. *Lancet.* 2020;395(10223):497–506.
- [9] Liu Y, Yang Y, Zhang C, et al. Clinical and biochemical indexes from 2019-nCoV infected patients linked to viral loads and lung injury. *Sci China Life Sci.* 2020;63(3): 364–74.
- [10] Ruan Q, Yang K, Wang W, Jiang L, Song J. Clinical predictors of mortality due to COVID-19 based on an analysis of data of 150 patients from Wuhan, China. *Intensive Care Med.* May 2020;46(5):846–8.
- [11] Wan S, Xiang Y, Fang W, et al. Clinical features and treatment of COVID-19 patients in Northeast Chongqing. *J Med Virol.* 2020. <https://doi.org/10.1002/jmv.25783> [Epub ahead of print March 21, 2020].
- [12] Wang Z, Yang B, Li Q, Wen L, Zhang R. Clinical features of 69 cases with coronavirus disease 2019 in Wuhan, China. *Clin Infect Dis.* 2020;cia272. <https://doi.org/10.1093/cid/cia272>.
- [13] Wu C, Hu X, Song J, et al. Heart injury signs are associated with higher and earlier mortality in coronavirus disease 2019 (COVID-19) medRxiv ; 2020 2020.2022.20028589.
- [14] Zhang G, Zhang J, Wang B, Zhu X, Wang Q, Qiu S. Analysis of clinical characteristics and laboratory findings of 95 cases of 2019 novel coronavirus pneumonia in Wuhan, China: a retrospective analysis. *Respir Res.* 2020;21(1):74.
- [15] Zhou F, Yu T, Du R, et al. Clinical course and risk factors for mortality of adult inpatients with COVID-19 in Wuhan, China: a retrospective cohort study. *Lancet.* 2020; 395(10229):1054–62.
- [16] Hsu PP, Sabatini DM. Cancer cell metabolism: Warburg and beyond. *Cell.* 2008;134 (5):703–7.
- [17] Martinez-Outschoorn UE, Prisco M, Ertel A, et al. Ketones and lactate increase cancer cell "stemness," driving recurrence, metastasis and poor clinical outcome in breast cancer: achieving personalized medicine via metabolo-genomics. *Cell Cycle.* 2011; 10(8):1271–86.
- [18] Kaplan B, Meier-Kriesche HU. Death after graft loss: an important late study endpoint in kidney transplantation. *Am J Transplant.* 2002;2(10):970–4.
- [19] Patschan D, Witzke O, Duhrsen U, Erbel R, Philipp T, Herget-Rosenthal S. Acute myocardial infarction in thrombotic microangiopathies – clinical characteristics, risk factors and outcome. *Nephrol Dial Transplant.* 2006;21(6):1549–54.
- [20] Zhang T, Chen H, Liang S, et al. A non-invasive laboratory panel as a diagnostic and prognostic biomarker for thrombotic microangiopathy: development and application in a Chinese cohort study. *PLoS One.* 2014;9(11):e111992.
- [21] Lippi G, Favaloro EJ. D-dimer is associated with severity of coronavirus disease 2019: a pooled analysis. *Thromb Haemost.* May 2020;120(5):876–8.
- [22] Lippi G, Plebani M, Henry BM. Thrombocytopenia is associated with severe coronavirus disease 2019 (COVID-19) infections: a meta-analysis. *Clin Chim Acta.* 2020; 506:145–8.
- [23] Erez A, Shental O, Tchebiner JZ, et al. Diagnostic and prognostic value of very high serum lactate dehydrogenase in admitted medical patients. *Isr Med Assoc J.* 2014; 16(7):439–43.
- [24] Assiri A, Al-Tawfiq JA, Al-Rabeeah AA, et al. Epidemiological, demographic, and clinical characteristics of 47 cases of Middle East respiratory syndrome coronavirus disease from Saudi Arabia: a descriptive study. *Lancet Infect Dis.* 2013;13(9):752–61.
- [25] Kjeld M. An automated colorimetric method for the estimation of lactate dehydrogenase activity in serum. *Scand J Clin Lab Invest.* 1972;29(4):421–5.

Cite as: E. R. Mann *et al.*, *Sci. Immunol.* 10.1126/sciimmunol.eabd6197 (2020).

CORONAVIRUS

Longitudinal immune profiling reveals key myeloid signatures associated with COVID-19

Elizabeth R. Mann,^{1,2*} Madhvi Menon,^{1*} Sean Blandin Knight,^{1,3*} Joanne E. Konkel,^{1*} Christopher Jagger,¹ Tovah N. Shaw,¹ Siddharth Krishnan,¹ Magnus Rattray,⁴ Andrew Ustianowski,^{5,1} Nawar Diar Bakerly,³ Paul Dark,⁶ Graham Lord,¹ Angela Simpson,⁷ Timothy Felton,⁷ Ling-Pei Ho,⁸ NIHR Respiratory TRC,⁹ Marc Feldmann,⁹ CIRCO,¹⁰ John R. Grainger,^{1*}† Tracy Hussell^{1*}†

¹Lydia Becker Institute of Immunology and Inflammation, Division of Infection, Immunity & Respiratory Medicine, School of Biological Sciences, Faculty of Biology, Medicine and Health, University of Manchester, Manchester Academic Health Science Centre, Room 2.16, Core Technology Facility, 46 Grafton Street, Manchester, M13 9PL, UK.

²Maternal and Fetal Health Centre, Division of Developmental Biology, School of Medical Sciences, Faculty of Biology, Medicine and Health, The University of Manchester, 5th Floor St. Mary's Hospital, Oxford Road, Manchester M13 9WL, UK. ³Respiratory Department, Salford Royal NHS Foundation Trust, Stott Lane, M6 8HD, UK. ⁴Division of Informatics, Imaging and Data Sciences, Faculty of Biology, Medicine and Health, University of Manchester, M13 9PL, UK. ⁵Regional Infectious Diseases Unit, North

Manchester General Hospital, Manchester, UK. ⁶Intensive Care Department, Salford Royal NHS Foundation Trust, Stott Lane, M6 8HD, UK. ⁷Division of Infection, Immunity and Respiratory Medicine, Manchester NIHR BRC, Education and Research Centre, Wythenshawe Hospital, UK. ⁸MRC Human Immunology Unit, Weatherall Institute of Molecular Medicine, University of Oxford. ⁹Kennedy Institute of Rheumatology, Botnar Research Centre, Nuffield Department of Orthopaedics, Rheumatology and Musculoskeletal Science, Windmill Rd, Headington, Oxford, OX3 7LD, UK

*Contributed equally

†The members of the NIHR Respiratory Translational Research Collaboration (TRC) collaborative group are listed at the end of the Acknowledgments.

¶The members of the Coronavirus Immune Response and Clinical Outcomes (CIRCO) collaborative group can be found at the end of the Acknowledgments.

†Joint corresponding authors. Email: tracy.hussell@manchester.ac.uk; john.grainger-2@manchester.ac.uk

COVID-19 pathogenesis is associated with an exaggerated immune response. However, the specific cellular mediators and inflammatory components driving diverse clinical disease outcomes remain poorly understood. We undertook longitudinal immune profiling on both whole blood and peripheral blood mononuclear cells (PBMCs) of hospitalized patients during the peak of the COVID-19 pandemic in the UK. Here, we report key immune signatures present shortly after hospital admission that were associated with the severity of COVID-19. Immune signatures were related to shifts in neutrophil to T cell ratio, elevated serum IL-6, MCP-1 and IP-10, and most strikingly, modulation of CD14⁺ monocyte phenotype and function. Modified features of CD14⁺ monocytes included poor induction of the prostaglandin-producing enzyme, COX-2, as well as enhanced expression of the cell cycle marker K-67. Longitudinal analysis revealed reversion of some immune features back to the healthy median level in patients with a good eventual outcome. These findings identify previously unappreciated alterations in the innate immune compartment of COVID-19 patients and lend support to the idea that therapeutic strategies targeting release of myeloid cells from bone marrow should be considered in this disease. Moreover, they demonstrate that features of an exaggerated immune response are present early after hospital admission suggesting immune-modulating therapies would be most beneficial at early timepoints.

INTRODUCTION

Severe acute respiratory syndrome coronavirus 2 (SARS-CoV-2) infection can result in the clinical syndrome COVID-19 (1) that, to date, has resulted in over 20 million confirmed cases and in excess of 733,000 attributable deaths worldwide. As such, a large number of clinical trials have been established to evaluate anti-viral and immune modulatory strategies aimed at improving clinical outcome for this globally-devastating virus.

SARS-CoV-2 is a single stranded, positive sense RNA virus that enters cells via human angiotensin-converting enzyme 2

(ACE2) (2). Ordinarily, diverse immune mechanisms exist to detect every stage of viral replication and protect the host from viral challenge. Pattern recognition receptors of the innate immune system recognize viral antigen and virus-induced damage, increasing bone marrow hematopoiesis, the release of myeloid cells including neutrophils and monocytes, and the production of a plethora of cytokines and chemokines (3). If inflammatory mediator release is not controlled in duration and amplitude then “emergency haematopoiesis” leads to bystander tissue damage and a cytokine storm that manifests as organ dysfunction. Initial studies suggest

cytokine storm occurs in COVID-19 (4). Indeed, neutrophilia and lymphopenia (resulting in an increased neutrophil to lymphocyte ratio), increased systemic interleukin-6 (IL-6) and C-reactive protein (CRP), correlate with incidence of intensive care admission and mortality (5). However, detailed understanding of cellular and molecular inflammatory mediators across the COVID-19 disease trajectory would support the development of better clinical interventions.

We carried out the Coronavirus Immune Response and Clinical Outcomes (CIRCO) study at four hospitals in Greater Manchester, UK, which was designed to examine the kinetics of the immune response in COVID-19 patients, as well as to identify early indicators of disease severity. Understanding the specific elements and kinetics of the immune response is critical to gain insight into immune phenotypes associated with disease progression, identify potential biomarkers that predict clinical outcomes and determine at which stage of the disease immune modulation may be most effective (4).

Here, by analyzing fresh blood samples immediately without prior storage we outline unappreciated immune abnormalities present within COVID-19 patients. Assessment of inflammatory mediators within the blood demonstrated these immune properties were most dysregulated in patients with severe COVID-19 prior to admission to intensive care, indicating immune modulating therapies should be considered early after admission. Furthermore, our study demonstrated profound alterations in the myeloid cells of COVID-19 patients. Our data demonstrate that monocytes from COVID-19 patients displayed elevated levels of the cell cycle marker Ki-67 but reduced expression of the prostaglandin-generating enzyme COX-2, with both these features being predominant in severe COVID-19 patients. These findings not only identify possible immune biomarkers for patient stratification but potential mechanisms of immune dysfunction contributing to the immunopathology of COVID-19.

RESULTS

CIRCO patient clinical characteristics

In total, 73 patients were recruited and 49 were stratified for maximum disease severity (Fig. 1A). Six patients were excluded due to: an alternative diagnosis (2 patients); indeterminate imaging findings with negative result in the SARS-CoV-2 nasopharyngeal test (2 patients); or diagnosis of a confounding acute illness (2 patients). Two patients could not be stratified for disease severity due to insufficient clinical observation data and a further 16 were not stratified because recruitment occurred more than 7 days after admission. The median time from patient-reported symptom onset to hospital admission was 7 days. The overall median age was 61 and 63% were male. The most frequent co-morbidities were diabetes, ischemic heart disease, hypertension, asthma and chronic obstructive pulmonary disease (COPD) (Table 1). The

majority (86%) of patients tested positive for SARS-CoV-2 via nasopharyngeal RT-PCR. In 14% of patients, symptoms and radiographic features were highly suggestive of COVID-19, but nasopharyngeal test was negative for the virus and thus a clinical diagnosis was made; these patients are clearly indicated in all graphs (white triangles). Patient disease severity was defined as mild (less than 28% FiO₂), moderate (28–60% FiO₂) or severe (above 60% FiO₂, or admission to intensive care) (Fig. 1B). Death occurred in 50% of severe cases of COVID-19 and only one of the ten patients with severe disease was categorized as severe upon admission.

Broad shifts in the innate and adaptive immune compartments in COVID-19 patients

Based on blood cell counts by the hospital laboratory at admission, no significant differences in total white blood cells, neutrophils, monocytes or lymphocytes were observed between groups of COVID-19 patients that went on to progress to mild, moderate or severe disease (Fig. S1A). However, as reported previously (6, 7), a trend was evident toward a higher neutrophil to lymphocyte ratio (NLR) at hospital admission in those patients whose outcome eventually was severe (Fig. S1B). This suggested that a more in-depth immune profiling could aid in patient stratification prior to escalation of the disease.

Thus, we further explored alterations in the innate and adaptive immune compartments using high dimensional flow cytometry on white blood cells from freshly lysed whole blood (see Fig. S1C for gating strategy). Initially, we examined the first blood sample taken at the time of patient recruitment to the study (this was typically 2–3 days after hospital admission and was not greater than 7 days). At this recruitment time point, alterations to the characteristics and relative abundance of diverse immune cell types was observed. Uniform manifold approximation and projection (UMAP) visualization outlined alterations between patients and healthy controls in the characteristics of neutrophils and monocytes, dramatic increases in the frequency of neutrophils and decreased T cells, B cells and basophils. Cellular changes were exaggerated with disease severity (Fig. 2A). In a subset of infected individuals CD16^{low} granulocytes were present (Fig. 2A); these cells can be associated with altered immune cell output from the bone marrow (8). This global picture of alterations to innate and adaptive immune cells was confirmed by manual flow cytometric gating (Fig. 2B and Fig. S1, C and D). In addition to these alterations, examining cell frequencies within isolated peripheral blood mononuclear cells (PBMCs) revealed a decrease in the frequency of plasmacytoid dendritic cells (pDCs) in COVID-19 patients, that was enhanced with elevated disease severity (Fig. S1E). There were no changes observed in frequencies of CD56⁺ NK cells (Fig. S1E).

Given the dramatic alterations in neutrophil and T cell

frequencies at the time of recruitment (Fig. 2B), we next examined their profile longitudinally over the course of hospitalization. To do this we used the first day of patient-reported symptom onset as a common reference point to align patient disease trajectories. This revealed that in the majority of patients, irrespective of final severity, neutrophil frequencies, although initially extremely high, decreased prior to hospital discharge while T cell frequencies reciprocally increased (Fig. 2C and 2D). In contrast, CD14⁺ monocytes and B cells showed no obvious trends during the hospital stay (Fig. 2C and D). These data highlight the importance of examining neutrophil to lymphocyte ratio in COVID-19 patients (6, 7), but, along with other studies (9), indicate that assessment of neutrophil to T cell ratio may provide a more stringent disease insight. Notably, in two severe patients with poor outcome, T cell frequencies were extremely low and neutrophil frequencies high even after entry into an intensive care unit (ICU) (Fig. 2C; white and pink crossed squares and Fig. 2D, red triangles); indicating that rebalancing of neutrophil to T cell ratio is crucial to recovery.

Defined soluble mediators are associated with severe disease

Broad changes in circulating immune cells in other viral infections are associated with alterations to circulating inflammatory mediators, such as cytokines and chemokines. These are potent modifiers of bone marrow output, immune cell survival and cell-recruitment to the inflamed lung. We used multiplex bead array to assess soluble inflammatory mediators in serum from patients at recruitment to the study. Of the 13 mediators analyzed in serum IL-6, IL-10, monocyte-chemoattractant protein-1 (MCP-1) and interferon gamma-induced protein 10 (IP-10) were significantly increased in COVID-19 patients and tracked with disease severity (Fig. S2A). No significant changes in other cytokines or chemokines measured, including IFN- γ , IL-1 β , IL-8 and TNF- α were observed in COVID-19 patients (Fig. S2B).

Interestingly, longitudinal analysis (examined as above from the day of reported disease onset) of IL-6, MCP-1 and IP-10 in mild and severe patients revealed that the highest levels of these cytokines and chemokines occurred early in the disease trajectory at recruitment to the study (Fig. S2C). Indeed, there was a significant decrease in IL-6 and IP-10 in patients upon recovery (Fig. S2D). There was a dramatic reduction in IL-6, IP-10 and MCP-1 upon admission of severe patients into ICU from the ward (Fig. S2E), although this finding is based on just 3 patients. This may be due to the treatment modalities employed in intensive care, such as sedation, that can have immunomodulatory effects (10), and will be important to investigate further. Interestingly, the patient whose health declined rapidly following admission, and ultimately died from the disease, displayed a dramatic rebound in IL-6 and MCP-1 levels after 2 days on ICU (Fig. S2,

D and E; red triangles).

Activation of adaptive immune cells in COVID-19 patients

To build on our basic assessment of cell populations outlined in Fig. 2, we next investigated alterations to specific T and B cell populations by flow cytometrically analyzing isolated peripheral blood mononuclear cells (PBMCs). Within the T cell compartment, we noted no dramatic alterations in CD4⁺ or CD8⁺ T cell frequencies (Fig. 3A and B). However, a slight decrease in CD4⁺ T cells was observed in severe COVID-19 patients (Fig. 3B). Both T cell subsets showed signs of activation in COVID-19 patients and this was more apparent in CD8⁺ T cells. Of note, the degree of T cell activation did not track with disease severity and was highly variable amongst patients (Fig. S3, A to D). Despite this, COVID-19 patients exhibited decreased frequencies of naive but elevated frequencies of effector TEMRA and HLA-DR⁺CD38⁺ CD8⁺ T cells (Fig. S3, A to C). CD8⁺ T cell subsets remained remarkably stable over the hospitalized disease course (Fig. S3E).

Interestingly, in 34/43 COVID-19 patients, higher perforin expression was observed in CD8⁺ T cells compared to healthy individuals (Fig. 3C and Fig. S3F), implying CD8⁺ T cells in COVID-19 patients had activated a cytotoxic program. Perforin expression in CD8⁺ T cells did not significantly track with disease severity (Fig. 3D), but a positive correlation was observed between the frequency of perforin⁺CD8⁺ T cells and clinical measurements of the inflammatory marker C-reactive protein (CRP) (Fig. 3E). This indicates increased frequencies of circulating perforin⁺ CD8⁺ T cells are more prevalent in highly inflamed patients. However, perforin⁺CD8⁺ T cells were found to increase over time in mild and most moderate COVID-19 patients, with highest levels immediately prior to discharge (Fig. S3, G to H), suggesting the higher frequencies seen in severe patients are not necessarily detrimental. This enhancement over time in mild and moderate patients suggests the higher frequencies seen in severe patients are not necessarily detrimental. Overall, these data demonstrate heterogeneous T cell activation in COVID-19 patients, but a consistent cytotoxic profile in the CD8⁺ T cell compartment.

Similar to the trend in whole blood (Fig. 2B), B cell frequency was reduced in PBMCs of COVID-19 patients. Decreases were particularly striking in severe patients compared to those with mild and moderate disease (Fig. 3F) and persisted with time (Fig. S4A). Although reduced in frequency, B cells displayed increased expression of Ki-67 (indicative of proliferation), which positively correlated with CRP levels (Fig. 3G). When examining B cell subsets, we observed an expansion of antibody-secreting plasmablasts (CD27^{hi}CD38^{hi}CD24⁻), that positively correlated with IgG expression by B cells (Fig. 3H and I). Further, we observed a decrease in unswitched memory (CD27⁺IgD⁺IgM⁺) B cells but no global differences in frequencies of other B cell subsets

(Fig. S4B). Of note, the differences in B cell subsets did not track with disease severity (Fig. S4C). The only subpopulation of B cells dramatically expanded in patients with severe COVID-19, compared to patients with mild and moderate disease, was double negative (DN) B cells (CD27-IgD⁻) (Fig. 3J). This subset was relatively stable throughout patient hospitalization and associated with a worse disease trajectory (Fig. S4D). DN B cells have previously been associated with an exhausted phenotype in patients with HIV (11), suggesting that patients with severe COVID-19 may have an impaired capacity to generate an effective B cell response.

Altered monocyte phenotype and function is a feature of COVID-19

COVID-19 research to date has primarily focused on T and B cells, although recent publications have highlighted alterations to monocyte phenotype (12). Monocytes can contribute significantly to inflammatory disease directly or via differentiation to macrophages and dendritic cells (13, 14). When released into the blood stream, monocytes will be affected by circulating cytokines and chemokines, including MCP-1, which we define as raised early in COVID-19 sera (Fig. S2A). In COVID-19 patients, we observed an expansion of intermediate CD14⁺CD16⁺ monocytes that tended to be highest in patients with a mild disease outcome (Fig. S5, A and B). Enhanced expression of CD64, the high affinity Fc receptor for monomeric IgG (FcγRI), was apparent on classical CD14⁺ monocytes (Fig. 4A) and again was most evident in mild disease.

We next examined monocyte activation by stimulating with lipopolysaccharide (LPS); stimulation frequencies of viable cells were high (greater than 90%) and similar in COVID-19 patients and healthy controls. Following stratification for final disease severity, TNF- α was enhanced in patients with mild disease (Fig. 4B and Fig. S5C). In contrast, IL-1 β production was lower in monocytes from COVID-19 patients compared to monocytes from healthy individuals (Fig. S5D), although this was not related to disease severity. These data highlight that monocytes from COVID-19 patients exhibit a modified cytokine profile upon activation. As well as cytokines, monocytes are major producers of lipid mediators, such as prostaglandins (15) and so we also examined cyclooxygenase-2 (COX-2) expression (a rate-limiting enzyme in prostaglandin synthesis). Notably, in LPS-stimulated monocytes a reduction in COX-2 was evident in all COVID-19 patients and was most apparent in those with severe disease (Fig. 4, C to E). Accordingly, expression of COX-2 in stimulated monocytes was inversely correlated to systemic levels of the cytokine MCP-1 (Fig. S5E), which were highest in severe COVID-19 patients (Fig. S2A).

One possible reason that monocytes in COVID-19 patients display altered functionality in the periphery is due to inflammation-induced emergency myelopoiesis (3). This process

occurs during infection where hematopoietic stem cells and myeloid progenitors expand in the bone marrow in order to provide more cells to combat viral infection. However, if egress is too fast then monocytes exit in an altered state. For example, unusually high expression of the cell cycle marker Ki-67 is observed in peripheral monocytes during H1N1 influenza (16) and Ebola virus (17) infection. We therefore, investigated expression of the proliferation marker Ki-67 in COVID-19. A striking increase in Ki-67⁺ monocytes (<5% in monocytes from most healthy controls) was evident in COVID-19 patients, but was most dramatic in patients with severe disease (Fig. 4, F and G). Ki-67 expression strongly correlated with CRP levels (Fig. 4H), and with systemic levels of the cytokines IL-6, MCP-1, IP-10 and IL-10 (Fig. S5F), cytokines that were enhanced in COVID-19 patients and tracked with severity (Fig. S2A). Enhancement of Ki-67 expression was also observed in unstimulated monocytes from COVID-19 patients (Fig. S5G).

We next assessed how monocyte alterations varied over the patients' hospital stay and noted that patients with mild COVID-19 had consistently higher TNF- α and COX-2 expression in LPS-activated monocytes compared to patients with severe disease (Fig. 4, I and J). Indeed, COX-2 remained low in severe patients throughout intensive care but levels were restored upon recovery in mild patients (Fig. 4L). IL-1 β was consistently low over time in both severity groups with no significant differences in monocyte production of IL-1 β between the first and last measured time points from mild or severe patients (Fig. S5H). Ki-67 expression, however, was highest at recruitment and decreased in patients (back down to levels seen in healthy controls) during the progression of disease, independent of severity category or final outcome (Fig. 4, K and L). Thus, defined alterations to monocyte function, specifically to TNF- α and COX-2, are maintained across the disease time-course and levels of expression are associated with severity. Taken together, these findings highlight alterations to monocyte phenotype and function as key features of disease progression and severity in COVID-19.

DISCUSSION

Respiratory viruses continue to cause devastating global disease. This detailed, prospective, observational analysis of COVID-19 patients of varying severity and outcome, in real time, has revealed specific immunological features that track with disease severity, providing important information concerning pathogenesis that should influence clinical trials and therapeutics. Of particular importance, increased expression of the cell cycle marker Ki-67 in blood monocytes, reduced expression of COX-2, and a high neutrophil to T cell ratio are early predictors of disease severity that could be used to stratify patients upon admission for therapeutics. Critically, the majority of aberrant immune parameters studied reverted in

patients with good outcome. Unexpectedly, multiple aspects of inflammation that were high upon admission, diminished as patients progressed in severity and were admitted to intensive care. In particular, levels of IP-10 and Ki-67 expression by monocytes were reduced after admission to intensive care, even in patients who did not recover. These data indicate that treating patients early after hospitalization is likely to be most beneficial, while cytokine levels and immune functions are disrupted.

Though other studies have focused on defects in adaptive immunity in COVID-19 pathogenesis (18), we demonstrate here considerable abnormalities in the innate immune system, in particular within myeloid cells. Profound neutrophilia exists in severe COVID-19, supportive of a role for neutrophils in acute respiratory distress syndrome (19, 20) and in line with the excess neutrophils seen in the autopsied lungs of patients that died from COVID-19 (21). Neutrophils assist in the clearance of pathogens through phagocytosis, oxidative burst and by liberating traps (neutrophil extracellular traps or NETs) that capture pathogens. The latter two functions, however, can also promote inflammation and are associated with many of the features seen in COVID-19 (22). Indeed, elevated neutrophil products have been identified in the sera of COVID-19 patients and correlate with clinical parameters such as C-reactive protein, D-dimer, and lactate dehydrogenase (23).

Altered monocyte phenotypes were also seen in COVID-19 patients, with patient blood monocytes expressing the cell cycle marker Ki-67 (up to 98%); a feature not observed in health. This likely represents either early or enhanced release of monocytes from the bone marrow due to systemic inflammatory signals and is similar to that described in pandemic H1N1 influenza (16) and Ebola virus infections (17). Equally remarkable was the reduced expression of COX-2 in monocytes in patients with severe disease, which was evident across their disease trajectory. COX-2 facilitates the production of prostanoids including prostaglandin E2 (PGE2), and other viruses are known to target this pathway to enhance viral replication (24). However, its reduction in monocytes in response to viral lung infection has not previously been reported. Reduced COX-2 alongside high IL-6 and IP-10, as seen here in severe COVID-19 patients, is an immune profile associated with pathology in idiopathic pulmonary fibrosis (IPF) (25). Therefore, our data indicate a possible fibrotic signature in patients with severe disease, supporting studies observing an unusual pattern of fibrosis in the lungs of COVID-19 patients.

Our data concur with several features of COVID-19 studied in Wuhan, China, as well as with more recent studies from across the globe (26, 27) and are also corroborated by single cell RNA sequencing of bronchoalveolar lavage cells at a single time point (28). Similarities include elevated CRP and IL-

6 in patients at the time of hospitalization who eventually died (29) and increased IP-10 in those who later developed severe disease (30). IP-10 is an interferon-inducible chemokine that facilitates directed migration of many immune cells (31) and is elevated in other coronavirus infections including MERS-CoV and SARS-CoV (32), as well as in Influenza virus of swine origin (H1N1) (33, 34). The heightened levels of monocyte-chemoattractant protein 1 (MCP-1) upon admission further indicate dysregulation of monocyte function and migration in patients with severe disease. Importantly, IL-6, IP-10 and MCP-1 levels are generally the highest around the time of hospital admission but are reduced rapidly as patients are admitted to intensive care, which may well signify exhaustion of the immune cells producing these mediators.

Examining cells of the adaptive immune system, we identified lymphopenia which is now a well-established hallmark of COVID-19 patients (35–38). Despite this being a key feature of COVID-19, the drivers of loss of T and B cell numbers in peripheral blood remain obscure and could equally reflect either cell death and/or elevated trafficking to the site of inflammation. Focusing on T cells, the phenotype and function of circulating T cells remain an issue with conflicting reports within the literature. Consistent with previous reports, our data show modest increases in T cell activation (27, 39, 40), primarily driven by a substantial heterogeneity between patients. Despite this, the frequencies of T cells with activated phenotypes remained stable across the disease trajectory, implying most changes to these adaptive mediators could have occurred prior to hospitalization. Importantly our data highlight activation of a cytotoxic program in CD8⁺ T cells, evidenced by perforin expression, which would support effective viral clearance that has previously been suggested (41). Focusing on B cells, patients with severe COVID-19 displayed a dramatic expansion of CD27 IgD⁻ double negative (DN) B cells. This is in agreement with a recent study reporting lupus-like hallmarks of extrafollicular B cell activation in critically unwell COVID-19 patients (42). DN B cells are also associated with immune senescence as a result of excessive immune activation, and an exhausted phenotype is observed in patients with HIV (11). Further studies evaluating the functional capacity of expanded DN B cells will be critical to understand their contribution to severe COVID-19.

There are, of course, limitations to any study of samples during a viral pandemic for which there is no vaccine. However, we believe that these do not diminish the importance of the major findings from our study. A longitudinal analysis in real time for phenotypic, functional and soluble markers naturally limits the number of patients interrogated. In-depth analysis of smaller cohorts however, is necessary to gain insight into mechanism and is of interest to the pharmaceutical industry. It takes time to recruit the appropriate number of control subjects of the approximate gender and age of COVID

patients and also with the span of comorbidities associated with the greatest risk from SARS-CoV-2. The majority of our controls were drawn from frontline workers, who produced remarkably similar results to each other. The only other potential limitation is that patients may not accurately define the onset of symptoms. As data are plotted per patient, however, this does not affect the interpretation of the results.

There are clinical implications of our data. Using non-steroidal anti-inflammatory drugs (NSAIDs) remains controversial (43) and our study would suggest they may not be desirable, as this may compound the already low COX-2 (44). Since most of the pathogenic mechanisms involve myeloid cells, neutrophils and monocytes, it would be advantageous to reduce their influx to the lung once lung pathology is established. Relevant strategies include inhibition of the complement anaphylatoxin C5a (45) or IL-8 (CXCL8), which are strong chemoattractants for many immune cells, including neutrophils. Antagonism of CXCR2 that mobilizes neutrophil and monocyte from the bone marrow, neutrophil elastase inhibitors and inhibition of G-CSF, IL-23 and IL-17 that promote neutrophil survival, are also options (46). Anti-IL-6, IL-1RA and anti-TNF- α agents are already being investigated for COVID-19 treatment and are relevant to neutrophils, which express the requisite cytokine receptors. Furthermore, JAK inhibitors are currently in clinical trials and may also reduce neutrophil levels (47). Targeting toxic products of neutrophils such as S100A1/A2, HMGB1 and free radicals, but also the formation of NETs, could be beneficial (21).

In summary, this is a key longitudinal study immune profiling COVID-19 patients that places equal emphasis on innate and adaptive immunity. We identify substantial alterations in the myeloid compartment in COVID-19 patients that have not previously been reported. It would appear that comparable innate immune features have been evident in past pandemics with similar or even different viruses and so focusing immune modulation strategies on neutrophils and monocytes is an urgent priority.

MATERIALS AND METHODS

Study design

Between 29th March and 7th May, 2020, adults requiring hospital admission with suspected COVID-19 were recruited from 4 hospitals in the Greater Manchester area. Our research objective was to undertake an observational study to (1) examine the kinetics of the immune response in COVID-19 patients and (2) identify early indicators of disease severity. Informed consent was obtained for each patient. Peripheral blood samples were collected at Manchester University Foundation Trust (MFT), Salford Royal NHS Foundation Trust (SRFT) and Pennine Acute NHS Trust (PAT) under the framework of the Manchester Allergy, Respiratory and Thoracic Surgery (ManARTS) Biobank (study no M2020-88) for

MFT or the Northern Care Alliance Research Collection (NCARC) tissue biobank (study no. NCA-009) for SRFT and PAT (REC reference 15/NW/0409 for ManARTS and 18/WA/0368 for NCARC). Clinical information was extracted from written/electronic medical records. Patients were included if they tested positive for SARS-CoV-2 by reverse-transcriptase-polymerase-chain-reaction (RT-PCR) on nasopharyngeal/oropharyngeal swabs or sputum. Patients with negative nasopharyngeal RT-PCR results were also included if there was a high clinical suspicion of COVID-19, the radiological findings supported the diagnosis and there was no other explanation for symptoms. Patients were excluded if an alternative diagnosis was reached, where indeterminate imaging findings were combined with negative SARS-CoV-2 nasopharyngeal (NP) test or there was another confounding acute illness not directly related to COVID-19. The severity of disease was scored each day, based on degree of respiratory failure (Fig. 1B). Patients were not stratified for disease severity if there was no available clinical observation data or patients were recruited more than 7 days after hospital admission. Where severity of disease changed during admission, the highest disease severity score was selected for classification. The first available time point was used for all cross-sectional comparisons between mild, moderate and severe disease. Peripheral blood samples were collected as soon after admission as possible and at 1-2 day intervals thereafter. For longitudinal analysis we elected to correlate clinical data with immune parameters directly, rather than using the WHO ordinal scale on account of the small range of values this affords our inpatient cohort, which our study would not be powered to discern. Healthy blood samples were obtained from frontline workers at Manchester University and NHS Trusts (age range 28-69; median age=44.5 years; 42.5% males). Samples from healthy donors were examined alongside patient samples.

Isolation of PBMCs and serum

Whole venous blood was collected in tubes containing EDTA or serum gel clotting activator (Starstedt). Peripheral blood mononuclear cells (PBMCs) were isolated by density gradient centrifugation using Ficoll-Paque Plus (GE Healthcare) and 50 ml SepMate tubes (STEMCELL technologies) according to the manufacturer's protocol. Serum was separated by centrifuging serum tubes at 2000 \times g at 4°C for 20 min.

Whole blood lysis

Red blood cell lysis was carried out using 10x volume of distilled water for 10 s followed by addition of 10x PBS to re-establish a 1x PBS solution and stop lysis. Cells were centrifuged at 500 \times g for 5 min and lysis repeated if necessary.

Flow cytometry

White blood cells from lysed whole blood and isolated PBMCs separated by density gradient centrifugation were

stained immediately on receipt. The following antibodies were used: BDCA-2 (clone 201A), CCR7 (clone G043H7), CD11b (clone ICRF44), CD11c (clone 3.9 or Bu15), CD123 (clone 6H6), CD14 (clone 63D3), CD16 (clone 3G8), CD19 (clone H1B19), CD24 (clone M1/69 or ML5), CD27 (clone M-T271), CD3 (clone OKT3 or UCHT1), CD38 (clone HIT2), CD4 (clone SK3), CD45 (clone 2D1), CD45RA (clone HI100), CD56 (clone MEM-188), CD62L (clone DREG-56), CD8 (clone SK1), HLA-DR (clone L234), ICOS (clone C398.4A), IgD (clone IA6-2), IgM (clone MHM-88), IgG (clone M1310G05), Ki-67 (clone Ki-67 or 11F6), PD-1 (clone EH12.2H7), perforin (clone dG9), CD66b (clone G10F5), CD64 (clone 10.1), IL-1 β (clone H1b-98) and TNF- α (clone MAAb11), all from Biolegend; and COX-2 (clone AS67) from BD Biosciences. PBMCs were also stimulated in vitro for 3 hours with 10 ng/ml LPS in the presence of 10 μ g/ml brefeldin A to allow accumulation and analysis of intracellular proteins by flow cytometry. Cells were cultured in RPMI containing 10% fetal calf serum, L-Glutamine, Non-essential Amino Acids, HEPES and penicillin plus streptomycin (Gibco). For surface stains samples were fixed with BD Cytofix (BD Biosciences) prior to acquisition and for intracellular stains (Ki-67, COX-2, TNF- α and IL-1 β) the Foxp3/Transcription Factor Staining Buffer Set (eBioscience) was used. All samples were acquired on a LSRIFortessa flow cytometer (BD Biosciences) and analyzed using FlowJo (TreeStar).

LEGENDplex

Thirteen different mediators associated with anti-viral responses were measured in serum using LEGENDplex assays (BioLegend, San Diego, USA) according to the manufacturer's instructions.

Statistics

Results are presented as individual data points with medians. Statistical analysis was performed using Prism 8 Software (GraphPad). Normality tests were performed on all datasets. Groups were compared using an unpaired *t*-test (normal distribution) or Mann-Whitney test (failing normality testing) for healthy individuals versus COVID-19 patients. Paired *t*-test (normal distribution) or Wilcoxon matched-pairs signed rank test (failing normality testing) was used for longitudinal data where first and last time points were examined. One-way ANOVA with Holm-Sidak post-hoc testing (normal distribution) or Kruskal-Wallis test with Dunn's post-hoc testing (failing normality testing) was used for multiple group comparisons. Correlations were assessed with Pearson correlation coefficient (normal distribution) or Spearman's rank correlation coefficient test (failing normality testing) for separate parameters within the COVID-19 patient group. Information on tests used is detailed in figure legends. In all cases, a *p*-value of ≤ 0.05 was considered significant. ns, not significant; **p* < 0.05, ***p* < 0.01, ****p* < 0.001.

SUPPLEMENTARY MATERIALS

immunology.scienmag.org/cgi/content/full/5/51/eabd6197/DC1

Figure S1. Immune cell types in COVID-19 patients.

Figure S2. Serum cytokines and chemokines in COVID-19 patients.

Figure S3. T cell activation in COVID-19 patients.

Figure S4. B cell subsets in COVID-19 patients.

Figure S5. Monocytes in COVID-19 patients.

Table S1. Raw data file (Excel spreadsheet).

REFERENCES AND NOTES

- M. Z. Tay, C. M. Poh, L. Rénia, P. A. MacAry, L. F. P. Ng, The trinity of COVID-19: Immunity, inflammation and intervention. *Nat. Rev. Immunol.* **20**, 363–374 (2020). [doi:10.1038/s41577-020-0311-8](https://doi.org/10.1038/s41577-020-0311-8) Medline
- P. Zhou, X.-L. Yang, X.-G. Wang, B. Hu, L. Zhang, W. Zhang, H.-R. Si, Y. Zhu, B. Li, C.-L. Huang, H.-D. Chen, J. Chen, Y. Luo, H. Guo, R.-D. Jiang, M.-Q. Liu, Y. Chen, X.-R. Shen, X. Wang, X.-S. Zheng, K. Zhao, Q.-J. Chen, F. Deng, L.-L. Liu, B. Yan, F.-X. Zhan, Y.-Y. Wang, G.-F. Xiao, Z.-L. Shi, A pneumonia outbreak associated with a new coronavirus of probable bat origin. *Nature* **579**, 270–273 (2020). [doi:10.1038/s41586-020-2012-7](https://doi.org/10.1038/s41586-020-2012-7) Medline
- S. Boettcher, M. G. Manz, Regulation of Inflammation- and Infection-Driven Hematopoiesis. *Trends Immunol.* **38**, 345–357 (2017). [doi:10.1016/j.it.2017.01.004](https://doi.org/10.1016/j.it.2017.01.004) Medline
- P. Mehta, D. F. McAuley, M. Brown, E. Sanchez, R. S. Tattersall, J. J. Manson; HLH Across Speciality Collaboration, UK, COVID-19: Consider cytokine storm syndromes and immunosuppression. *Lancet* **395**, 1033–1034 (2020). [doi:10.1016/S0140-6736\(20\)30628-0](https://doi.org/10.1016/S0140-6736(20)30628-0) Medline
- F. Wu, S. Zhao, B. Yu, Y.-M. Chen, W. Wang, Z.-G. Song, Y. Hu, Z.-W. Tao, J.-H. Tian, Y.-Y. Pei, M.-L. Yuan, Y.-L. Zhang, F.-H. Dai, Y. Liu, Q.-M. Wang, J.-J. Zheng, L. Xu, E. C. Holmes, Y.-Z. Zhang, A new coronavirus associated with human respiratory disease in China. *Nature* **579**, 265–269 (2020). [doi:10.1038/s41586-020-2008-3](https://doi.org/10.1038/s41586-020-2008-3) Medline
- E. Terpos, I. Ntanasis-Stathopoulos, I. Elalamy, E. Kastritis, T. N. Sergentanis, M. Politou, T. Psaltopoulou, G. Gerotziafas, M. A. Dimopoulos, Hematological findings and complications of COVID-19. *Am. J. Hematol.* **95**, 834–847 (2020). [doi:10.1002/ajhb.25829](https://doi.org/10.1002/ajhb.25829) Medline
- J. Fu, J. Kong, W. Wang, M. Wu, L. Yao, Z. Wang, J. Jin, D. Wu, X. Yu, The clinical implication of dynamic neutrophil to lymphocyte ratio and D-dimer in COVID-19: A retrospective study in Suzhou China. *Thromb. Res.* **192**, 3–8 (2020). [doi:10.1016/j.thromres.2020.05.006](https://doi.org/10.1016/j.thromres.2020.05.006) Medline
- Y. Orr, J. M. Taylor, P. G. Bannon, C. Geczy, L. Kritharides, Circulating CD10-/CD16low neutrophils provide a quantitative index of active bone marrow neutrophil release. *Br. J. Haematol.* **131**, 508–519 (2005). [doi:10.1111/j.1365-2141.2005.05794.x](https://doi.org/10.1111/j.1365-2141.2005.05794.x) Medline
- J. Liu, Y. Liu, P. Xiang, L. Pu, H. Xiong, C. Li, M. Zhang, J. Tan, Y. Xu, R. Song, M. Song, L. Wang, W. Zhang, B. Han, L. Yang, X. Wang, G. Zhou, T. Zhang, B. Li, Y. Wang, Z. Chen, X. Wang, Neutrophil-to-lymphocyte ratio predicts critical illness patients with 2019 coronavirus disease in the early stage. *J. Transl. Med.* **18**, 206 (2020). [doi:10.1186/s12967-020-02374-0](https://doi.org/10.1186/s12967-020-02374-0) Medline
- M. A. Smith, M. Hibino, B. A. Falcione, K. M. Eichinger, R. Patel, K. M. Empey, Immunosuppressive aspects of analgesics and sedatives used in mechanically ventilated patients: An underappreciated risk factor for the development of ventilator-associated pneumonia in critically ill patients. *Ann. Pharmacother.* **48**, 77–85 (2014). [doi:10.1177/1060028013510698](https://doi.org/10.1177/1060028013510698) Medline
- S. Rinaldi, S. Pallikkuth, V. K. George, L. R. de Armas, R. Pahwa, C. M. Sanchez, M. F. Pallin, L. Pan, N. Cotugno, G. Dickinson, A. Rodriguez, M. Fischl, M. Alcaide, L. Gonzalez, P. Palma, S. Pahwa, Paradoxical aging in HIV: Immune senescence of B Cells is most prominent in young age. *Aging (Albany NY)* **9**, 1307–1325 (2017). [doi:10.18632/aging.101229](https://doi.org/10.18632/aging.101229) Medline
- E. J. Giannarellos-Bourboulis, M. G. Netea, N. Rovina, K. Akinosoglou, A. Antoniadou, N. Antonakos, G. Damoraki, T. Gkavogianni, M.-E. Adam, P. Katsaounou, M. Ntaganou, M. Kyriakopoulou, G. Dimopoulos, I. Koutsodimitropoulos, D. Velissaris, P. Koufaryris, A. Karageorgos, K. Katrini, V. Lekakis, M. Lupsie, A. Kotsaki, G. Renieris, D. Theodoulou, V. Panou, E. Koukaki, N. Koulouris, C. Gogos, A. Koutsoukou, Complex immune dysregulation in COVID-19

- patients with severe respiratory failure. *Cell Host Microbe* **27**, 992–1000.e3 (2020). doi:10.1016/j.chom.2020.04.009 Medline
13. M. Guilliams, A. Mildner, S. Yona, Developmental and Functional Heterogeneity of Monocytes. *Immunity* **49**, 595–613 (2018). doi:10.1016/j.jimmuni.2018.10.005 Medline
14. M. Merad, J. C. Martin, Pathological inflammation in patients with COVID-19: A key role for monocytes and macrophages. *Nat. Rev. Immunol.* **20**, 355–362 (2020). doi:10.1038/s41577-020-0331-4 Medline
15. J. I. Kurland, R. Bockman, Prostaglandin E production by human blood monocytes and mouse peritoneal macrophages. *J. Exp. Med.* **147**, 952–957 (1978). doi:10.1084/jem.147.3.952 Medline
16. S. L. Cole, J. Dunning, W. L. Kok, K. H. Benam, A. Benlahrech, E. Repapi, F. O. Martinez, L. Drumright, T. J. Powell, M. Bennett, R. Elderfield, C. Thomas, T. Dong, J. McCauley, F. Y. Liew, S. Taylor, M. Zambon, W. Barclay, V. Cerundolo, P. J. Openshaw, A. J. McMichael, L.-P. Ho; MOSAIC investigators, M1-like monocytes are a major immunological determinant of severity in previously healthy adults with life-threatening influenza. *JCI Insight* **2**, e91868 (2017). doi:10.1172/jci.insight.91868 Medline
17. A. K. McElroy, R. S. Akondy, D. R. McIlwain, H. Chen, Z. Bjornson-Hooper, N. Mukherjee, A. K. Mehta, G. Nolan, S. T. Nichol, C. F. Spiropoulou, Immunologic timeline of Ebola virus disease and recovery in humans. *JCI Insight* **5**, e137260 (2020). doi:10.1172/jci.insight.137260 Medline
18. A. Grifoni, D. Weiskopf, S. I. Ramirez, J. Mateus, J. M. Dan, C. R. Moderbacher, S. A. Rawlings, A. Sutherland, L. Premkumar, R. S. Jadi, D. Marrama, A. M. de Silva, A. Frazier, A. F. Carlin, J. A. Greenbaum, B. Peters, F. Krammer, D. M. Smith, S. Crotty, A. Sette, Targets of T cell responses to SARS-CoV-2 coronavirus in humans with COVID-19 Disease and unexposed individuals. *Cell* **181**, 1489–1501.e15 (2020). doi:10.1016/j.cell.2020.05.015 Medline
19. V. Brinkmann, U. Reichard, C. Goosmann, B. Fauler, Y. Uhlemann, D. S. Weiss, Y. Weinrauch, A. Zychlinsky, Neutrophil extracellular traps kill bacteria. *Science* **303**, 1532–1535 (2004). doi:10.1126/science.1092385 Medline
20. M. Ojima, N. Yamamoto, T. Hirose, S. Hamaguchi, O. Tasaki, T. Kojima, K. Tomono, H. Ogura, T. Shimazu, Serial change of neutrophil extracellular traps in tracheal aspirate of patients with acute respiratory distress syndrome: Report of three cases. *J. Intensive Care* **8**, 25 (2020). doi:10.1186/s40560-020-00444-5 Medline
21. B. J. Barnes, J. M. Adrover, A. Baxter-Stoltzfus, A. Borczuk, J. Cools-Lartigue, J. M. Crawford, J. DaBler-Plenker, P. Guerci, C. Huynh, J. S. Knight, M. Loda, M. R. Looney, F. McAllister, R. Rayes, S. Renaud, S. Rousseau, S. Salvatore, R. E. Schwartz, J. D. Spicer, C. C. Yost, A. Weber, Y. Zuo, M. Egeblad, Targeting potential drivers of COVID-19: Neutrophil extracellular traps. *J. Exp. Med.* **217**, e20200652 (2020). doi:10.1084/jem.20200652 Medline
22. N. Chen, M. Zhou, X. Dong, J. Qu, F. Gong, Y. Han, Y. Qiu, J. Wang, Y. Liu, Y. Wei, J. Xia, T. Yu, X. Zhang, L. Zhang, Epidemiological and clinical characteristics of 99 cases of 2019 novel coronavirus pneumonia in Wuhan, China: A descriptive study. *Lancet* **395**, 507–513 (2020). doi:10.1016/S0140-6736(20)30211-7 Medline
23. Y. Zuo, S. Yalavarthi, H. Shi, K. Gockman, M. Zuo, J. A. Madison, C. Blair, A. Weber, B. J. Barnes, M. Egeblad, R. J. Woods, Y. Kanthi, J. S. Knight, Neutrophil extracellular traps in COVID-19. *JCI Insight* **5**, e138999 (2020). Medline
24. X. Yan, Q. Hao, Y. Mu, K. A. Timani, L. Ye, Y. Zhu, J. Wu, Nucleocapsid protein of SARS-CoV activates the expression of cyclooxygenase-2 by binding directly to regulatory elements for nuclear factor-kappa B and CCAAT/enhancer binding protein. *Int. J. Biochem. Cell Biol.* **38**, 1417–1428 (2006). doi:10.1016/j.biocel.2006.02.003 Medline
25. W. R. Coward, C. A. Feghali-Bostwick, G. Jenkins, A. J. Knox, L. Pang, A central role for G9a and EZH2 in the epigenetic silencing of cyclooxygenase-2 in idiopathic pulmonary fibrosis. *FASEB J.* **28**, 3183–3196 (2014). doi:10.1096/fj.13-241760 Medline
26. C. Lucas, P. Wong, J. Klein, T. B. R. Castro, J. Silva, M. Sundaram, M. K. Ellingson, T. Mao, J. E. Oh, B. Israelow, T. Takahashi, M. Tokuyama, P. Lu, A. Venkataraman, A. Park, S. Mohanty, H. Wang, A. L. Wyllie, C. B. F. Vogels, R. Earnest, S. Lapidus, I. M. Ott, A. J. Moore, M. C. Muenker, J. B. Fournier, M. Campbell, C. D. Odio, A. Casanova-Massana, R. Herbst, A. C. Shaw, R. Medzhitov, W. L. Schulz, N. D. Grubaugh, C. Dela Cruz, S. Farhadian, A. I. Ko, S. B. Ormer, A. Iwasaki; Yale IMPACT Team, Longitudinal analyses reveal immunological misfiring in severe COVID-19. *Nature* **584**, 463–469 (2020). doi:10.1038/s41586-020-2588-y Medline
27. J. Hadadj, N. Yatim, L. Barnabei, A. Corneau, J. Boussier, N. Smith, H. Péré, B. Charbit, V. Bondet, C. Chenevier-Gobeaux, P. Breillat, N. Carlier, R. Gauzit, C. Morbieu, F. Pène, N. Marin, N. Roche, T.-A. Szwebel, S. H. Merkling, J.-M. Treliuyer, D. Veyer, L. Mouthon, C. Blanc, P.-L. Tharaux, F. Rozenberg, A. Fischer, D. Duffy, F. Rieux-Laucat, S. Kernéis, B. Terrier, Impaired type I interferon activity and inflammatory responses in severe COVID-19 patients. *Science* **369**, 718–724 (2020). doi:10.1126/science.abc6027 Medline
28. M. Liao, Y. Liu, J. Yuan, Y. Wen, G. Xu, J. Zhao, L. Cheng, J. Li, X. Wang, F. Wang, L. Liu, I. Amit, S. Zhang, Z. Zhang, Single-cell landscape of bronchoalveolar immune cells in patients with COVID-19. *Nat. Med.* **26**, 842–844 (2020). doi:10.1038/s41591-020-0901-9 Medline
29. Q. Ruan, K. Yang, W. Wang, L. Jiang, J. Song, Clinical predictors of mortality due to COVID-19 based on an analysis of data of 150 patients from Wuhan, China. *Intensive Care Med.* **46**, 846–848 (2020). doi:10.1007/s00134-020-05991-x Medline
30. C. Huang, Y. Wang, X. Li, L. Ren, J. Zhao, Y. Hu, L. Zhang, G. Fan, J. Xu, X. Gu, Z. Cheng, T. Yu, J. Xia, Y. Wei, W. Wu, X. Xie, W. Yin, H. Li, M. Liu, Y. Xiao, H. Gao, L. Guo, J. Xie, G. Wang, R. Jiang, Z. Gao, Q. Jin, J. Wang, B. Cao, Clinical features of patients infected with 2019 novel coronavirus in Wuhan, China. *Lancet* **395**, 497–506 (2020). doi:10.1016/S0140-6736(20)30183-5 Medline
31. C. Agostini, M. Facco, M. Siviero, D. Carollo, S. Galvan, A. M. Cattelan, R. Zambello, L. Trentin, G. Semenzato, CXCR chemokines IP-10 and mig expression and direct migration of pulmonary CD8+/CXCR3+ T cells in the lungs of patients with HIV infection and T-cell alveolitis. *Am. J. Respir. Crit. Care Med.* **162**, 1466–1473 (2000). doi:10.1164/ajrccm.162.4.2003130 Medline
32. J. Zhou, H. Chu, C. Li, B. H.-Y. Wong, Z.-S. Cheng, V. K.-M. Poon, T. Sun, C. C.-Y. Lau, K. K.-Y. Wong, J. Y.-W. Chan, J. F.-W. Chan, K. K.-W. To, K.-H. Chan, B.-J. Zheng, K.-Y. Yuen, Active replication of Middle East respiratory syndrome coronavirus and aberrant induction of inflammatory cytokines and chemokines in human macrophages: Implications for pathogenesis. *J. Infect. Dis.* **209**, 1331–1342 (2014). doi:10.1093/infdis/jit504 Medline
33. K. K. To, I. F. Hung, I. W. Li, K. L. Lee, C. K. Koo, W. W. Yan, R. Liu, K. Y. Ho, K. H. Chu, C. L. Watt, W. K. Luk, K. Y. Lai, F. L. Chow, T. Mok, T. Buckley, J. F. Chan, S. S. Wong, B. Zheng, H. Chen, C. C. Lau, H. Tse, V. C. Cheng, K. H. Chan, K. Y. Yuen, Delayed clearance of viral load and marked cytokine activation in severe cases of pandemic H1N1 2009 influenza virus infection. *Clin. Infect. Dis.* **50**, 850–859 (2010). doi:10.1086/650581 Medline
34. J. F. Bermejo-Martín, I. Martín-Loeches, J. Rello, A. Antón, R. Almansa, L. Xu, G. López-Campos, T. Pumarola, L. Ran, P. Ramírez, D. Banner, D. C. Ng, L. Socias, A. Loza, D. Andaluz, E. Maravi, M. J. Gómez-Sánchez, M. Gordón, M. C. Gallegos, V. Fernández, S. Aldunate, C. León, P. Merino, J. Blanco, F. Martín-Sánchez, L. Rico, D. Varillas, V. Iglesias, M. A. Marcos, F. Gandía, F. Bobillo, B. Nogueira, S. Rojo, S. Resino, C. Castro, R. Ortiz de Lejarazu, D. Kelvin, Host adaptive immunity deficiency in severe pandemic influenza. *Crit. Care* **14**, R167 (2010). doi:10.1186/cc9259 Medline
35. J. Liu, S. Li, J. Liu, B. Liang, X. Wang, H. Wang, W. Li, Q. Tong, J. Yi, L. Zhao, L. Xiong, C. Guo, J. Tian, J. Luo, J. Yao, R. Pang, H. Shen, C. Peng, T. Liu, Q. Zhang, J. Wu, L. Xu, S. Lu, B. Wang, Z. Weng, C. Han, H. Zhu, R. Zhou, H. Zhou, X. Chen, P. Ye, B. Zhu, L. Wang, W. Zhou, S. He, Y. He, S. Jie, P. Wei, J. Zhang, Y. Lu, W. Wang, L. Zhang, L. Li, F. Zhou, J. Wang, U. Dittmer, M. Lu, Y. Hu, D. Yang, X. Zheng, Longitudinal characteristics of lymphocyte responses and cytokine profiles in the peripheral blood of SARS-CoV-2 infected patients. *EBioMedicine* **55**, 102763 (2020). doi:10.1016/j.ebiom.2020.102763 Medline
36. F. A. Lagunas-Rangel, Neutrophil-to-lymphocyte ratio and lymphocyte-to-C-reactive protein ratio in patients with severe coronavirus disease 2019 (COVID-19): A meta-analysis. *J. Med. Virol.* (2020). doi:10.1002/jmv.25819 Medline
37. C. Qin, L. Zhou, Z. Hu, S. Zhang, S. Yang, Y. Tao, C. Xie, K. Ma, K. Shang, W. Wang, D.-S. Tian, Dysregulation of immune response in patients with coronavirus 2019 (COVID-19) in Wuhan, China. *Clin. Infect. Dis.* **71**, 762–768 (2020). doi:10.1093/cid/ciaa248 Medline
38. G. Chen, D. Wu, W. Guo, Y. Cao, D. Huang, H. Wang, T. Wang, X. Zhang, H. Chen, H. Yu, X. Zhang, M. Zhang, S. Wu, J. Song, T. Chen, M. Han, S. Li, X. Luo, J. Zhao, Q. Ning, Clinical and immunological features of severe and moderate coronavirus disease 2019. *J. Clin. Invest.* **130**, 2620–2629 (2020). doi:10.1172/JCI137244 Medline

39. A. G. Laing, A. Lorenc, I. Del Molino Del Barrio, A. Das, M. Fish, L. Monin, M. Muñoz-Ruiz, D. R. McKenzie, T. S. Hayday, I. Francos-Quijorna, S. Kamdar, M. Joseph, D. Davies, R. Davis, A. Jennings, I. Zlatarev, P. Vantourout, Y. Wu, V. Sofra, F. Cano, M. Greco, E. Theodoridis, J. Freedman, S. Gee, J. Nuo En Chan, S. Ryan, E. Bugallo-Blanco, P. Peterson, K. Kisand, L. Haljasmägi, L. Martinez, B. Merrick, K. Bisnauthsing, K. Brooks, M. Ibrahim, J. Mason, F. Lopez Gomez, K. Babalola, S. Abdul-Jawad, J. Cason, C. Mant, K. J. Doores, J. Seow, C. Graham, F. Di Rosa, J. Edgeworth, M. Shankar-Hari, A. C. Hayday, A consensus Covid-19 immune signature combines immuno-protection with discrete sepsis-like traits associated with poor prognosis. *medRxiv* (2020); www.medrxiv.org/content/10.1101/2020.06.08.20125112v1.
40. D. Mathew, J. R. Giles, A. E. Baxter, D. A. Oldridge, A. R. Greenplate, J. E. Wu, C. Alanio, L. Kuri-Cervantes, M. B. Pampena, K. D'Andrea, S. Manne, Z. Chen, Y. J. Huang, J. P. Reilly, A. R. Weisman, C. A. G. Ittner, O. Kuthuru, J. Dougherty, K. Nzingha, N. Han, J. Kim, A. Pattekar, E. C. Goodwin, E. M. Anderson, M. E. Weirick, S. Gouma, C. P. Arevalo, M. J. Bolton, F. Chen, S. F. Lacey, H. Ramage, S. Cherry, S. E. Hensley, S. A. Apostolidis, A. C. Huang, L. A. Vella, M. R. Betts, N. J. Meyer, E. J. Wherry; UPenn COVID Processing Unit, Deep immune profiling of COVID-19 patients reveals distinct immunotypes with therapeutic implications. *Science* **369**, eabc8511 (2020). doi:[10.1126/science.abc8511](https://doi.org/10.1126/science.abc8511) Medline
41. H. Y. Zheng, M. Zhang, C.-X. Yang, N. Zhang, X.-C. Wang, X.-P. Yang, X.-Q. Dong, Y.-T. Zheng, Elevated exhaustion levels and reduced functional diversity of T cells in peripheral blood may predict severe progression in COVID-19 patients. *Cell. Mol. Immunol.* **17**, 541–543 (2020). doi:[10.1038/s41423-020-0401-3](https://doi.org/10.1038/s41423-020-0401-3) Medline
42. M. R. Woodruff, R. Ramorell, K. Cashman, D. Nguyen, A. Saini, N. Haddad, A. Ley, S. Kyu, J. C. Howell, T. Ozturk, S. Lee, W. Chen, J. Estrada, A. Morrison-Porter, A. Derrico, F. Anam, M. Sharma, H. Wu, S. Le, S. Jenks, C. M. Tipton, W. Hu, F. E.-H. Lee, I. Sanz, Dominant extrafollicular B cell responses in severe COVID-19 disease correlate with robust viral-specific antibody production but poor clinical outcomes. *medRxiv*, (2020); <http://www.medrxiv.org/content/10.1101/2020.04.29.20083717v2>.
43. G. A. FitzGerald, Misguided drug advice for COVID-19. *Science* **367**, 1434 (2020). Medline
44. T. H. Page, J. J. O. Turner, A. C. Brown, E. M. Timms, J. J. Inglis, F. M. Brennan, B. M. J. Foxwell, K. P. Ray, M. Feldmann, Nonsteroidal anti-inflammatory drugs increase TNF production in rheumatoid synovial membrane cultures and whole blood. *J. Immunol.* **185**, 3694–3701 (2010). doi:[10.4049/jimmunol.1000906](https://doi.org/10.4049/jimmunol.1000906) Medline
45. A. M. Risitano, D. C. Mastellos, M. Huber-Lang, D. Yancopoulou, C. Garlanda, F. Ciceri, J. D. Lambris, Complement as a target in COVID-19? *Nat. Rev. Immunol.* **20**, 343–344 (2020). doi:[10.1038/s41577-020-0320-7](https://doi.org/10.1038/s41577-020-0320-7) Medline
46. T. Németh, M. Sperandio, A. Mócsai, Neutrophils as emerging therapeutic targets. *Nat. Rev. Drug Discov.* **19**, 253–275 (2020). doi:[10.1038/s41573-019-0054-z](https://doi.org/10.1038/s41573-019-0054-z) Medline
47. J. J. O'Shea, D. M. Schwartz, A. V. Villarino, M. Gadina, I. B. McInnes, A. Laurence, The JAK-STAT pathway: Impact on human disease and therapeutic intervention. *Annu. Rev. Med.* **66**, 311–328 (2015). doi:[10.1146/annurev-med-051113-024537](https://doi.org/10.1146/annurev-med-051113-024537) Medline
- which helped support some CIRCO members), The Wellcome Trust/Royal Society (ERM, 206206/Z/17/Z), the Lister Institute (JEK) and BBSRC (JEK BB/M025977/1, TNS BB/SO1103X/1). The Oxford and Manchester NIHR BRC provided support for study design and sample collection. **Competing Interests:** GL is Co-founder and Scientific Advisory Board Member of Gritstone Oncology Inc., which is a public company that develops therapeutic vaccines (primarily for the treatment of cancer). MR has a paid consultancy with AstraZeneca. The other authors declare that they have no competing interests. **Author Contributions:** ERM, MM, SBK, JEK, CJ, TS, JRG and TH designed the study and performed: tissue processing, data collection, data analysis, data interpretation and manuscript writing. SK and MR performed data analysis and generated the figures. AU, NDB, PD, AS, and TF performed sample collection and biobanking. AU, AS, and TF contributed to data interpretation, presentation of clinical data and paper construction. L-PH, RTRC, GL, CIRCO and MF contributed to study design, patient consent and sample collection, and manuscript preparation. CIRCO performed tissue processing, data collection, and data analysis. **Data and Materials Availability:** All data needed to evaluate the conclusions in the paper are present in the paper or the Supplementary Materials. This work is licensed under a Creative Commons Attribution 4.0 International (CC BY 4.0) license, which permits unrestricted use, distribution, and reproduction in any medium, provided the original work is properly cited. To view a copy of this license, visit <https://creativecommons.org/licenses/by/4.0/>. This license does not apply to figures/photos/artwork or other content included in the article that is credited to a third party; obtain authorization from the rights holder before using such material. The members of the NIHR Respiratory Translational Research Collaboration (TRC) collaborative group are: Alex Horsley (Manchester BRC), Tim Harrison (Nottingham BRC), Joanna Porter (UCL BRC), Ratko Djukanovic (Southampton BRC), Stefan Marciniak (Cambridge BRC), Chris Brightling (Leicester BRC), Ling-Pei Ho (Oxford BRC), Lorcan McGarvey (Queen's University Belfast), and Jane Davies (Imperial BRC). The members of the CIRCO collaborative group are: Rohan Ahmed, Halima Ali Shuwa, Miriam Avery, Katharine Birchall, Oliver Brand, Evelyn Charsley, Alistair Chinery, Christine Chew, Richard Clark, Emma Connolly, Karen Connolly, Simon Dawson, Laura Durrans, Hannah Durrington, Jasmine Egan, Claire Fox, Helen Francis, Miriam Franklin, Susannah Glasgow, Nicola Godfrey, Kathryn J. Gray, Seamus Grundy, Jacinta Guerin, Pamela Hackney, Mudassar Iqbal, Chantelle Hayes, Emma Hardy, Jade Harris, Anu John, Bethany Jolly, Verena Kästele, Saba Khan, Gabriella Lindberg, Sylvia Lui, Lesley Lowe, Alex G. Mathioudakis, Flora A. McClure, Joanne Mitchell, Clare Moizer, Katrina Moore, David J. Morgan, Stuart Moss, Syed Murtuza Baker, Rob Oliver, Grace Padden, Christina Parkinson, Laurence Pearmain, Mike Phuycharoen, Ananya Saha, Barbora Salcman, Nicholas A. Scott, Seema Sharma, Jane Shaw, Joanne Shaw, Elizabeth Shepley, Lara Smith, Simon Stephan, Ruth Stephens, Gael Tavernier, Rhys Tudge, Louis Wareing, Roanna Warren, Thomas Williams, Lisa Willmore, and Mehwish Younas.

Submitted 2 July 2020

Accepted 14 September 2020

Published First Release 17 September 2020

10.1126/sciimmunol.abd6197

Acknowledgments: This report is independent research supported by the North West Lung Centre Charity and National Institute for Health Research Clinical Research Facility at Manchester University NHS Foundation Trust. The views expressed in this publication are those of the author(s) and not necessarily those of the NHS, the North West Lung Centre Charity, National Institute for Health Research or the Department of Health. The authors would like to acknowledge the Manchester Allergy, Respiratory and Thoracic Surgery Biobank, the Northern Care Alliance Research Collection tissue bank and the North West Lung Centre Charity for supporting this project. In addition, we would like to thank the Immunology community within the Lydia Becker Institute of Immunology and Inflammation, the core flow cytometry facility at the University of Manchester, the Manchester COVID-19 Rapid Response Group and the study participants for their contribution. **Funding:** This work was supported by The Kennedy Trust for Rheumatology Research who provided a Rapid Response Award for costs associated with the laboratory analysis of the immune response in COVID-19 patients to JRG, The Wellcome Trust (TH, 202865/Z/16/Z; 106898/A/15/Z)

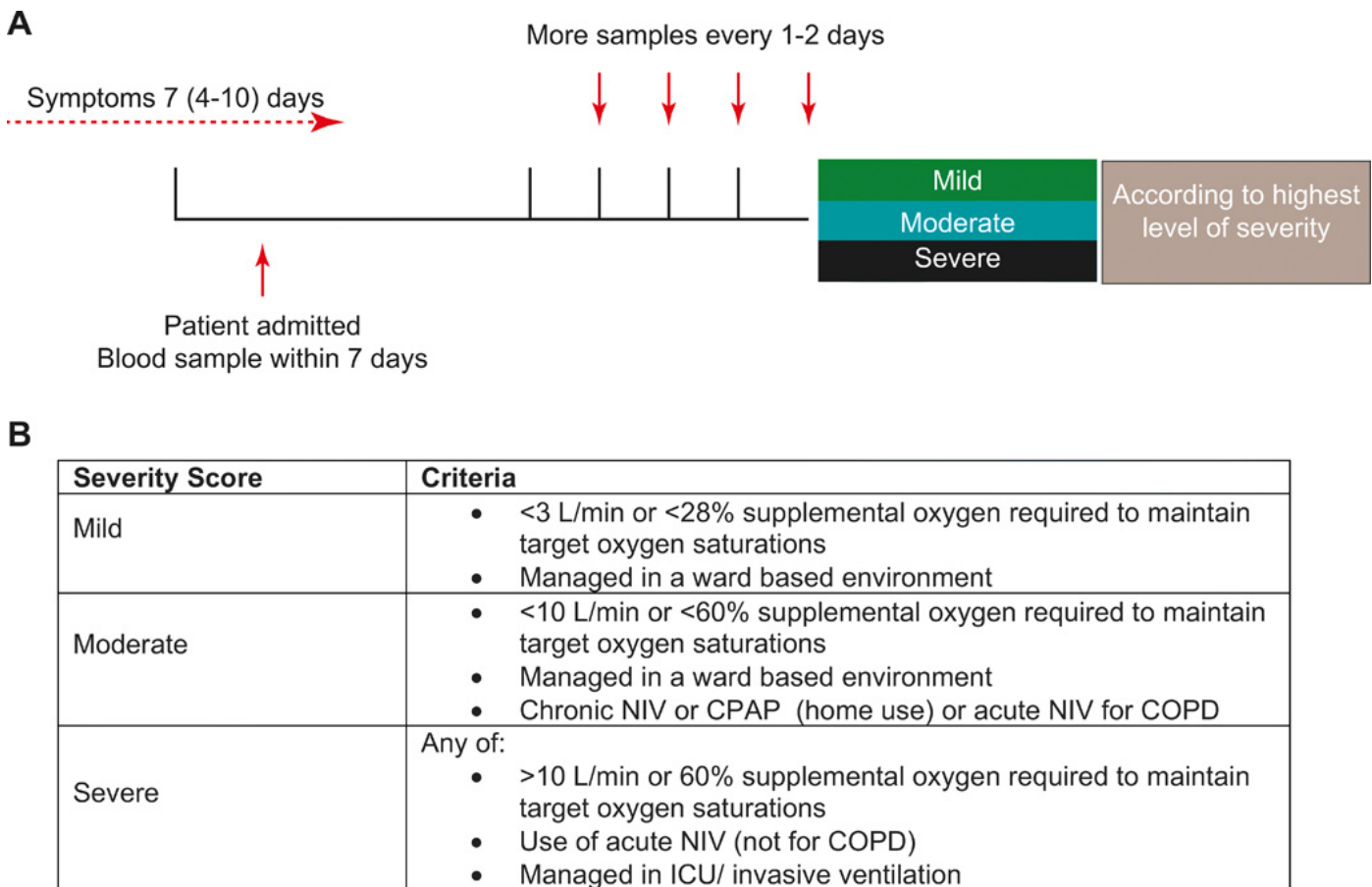


Fig. 1. Patient recruitment and categorization. (A) Patients were recruited to the study as close to admission as possible and within 7 days. Peripheral blood samples were collected on recruitment and at intervals thereafter. Samples were analyzed immediately and results stratified based on their ultimate disease severity. (B) Criteria for patient stratification. NIV, non-invasive ventilation; CPAP, continuous positive airway pressure; ICU, intensive care unit.

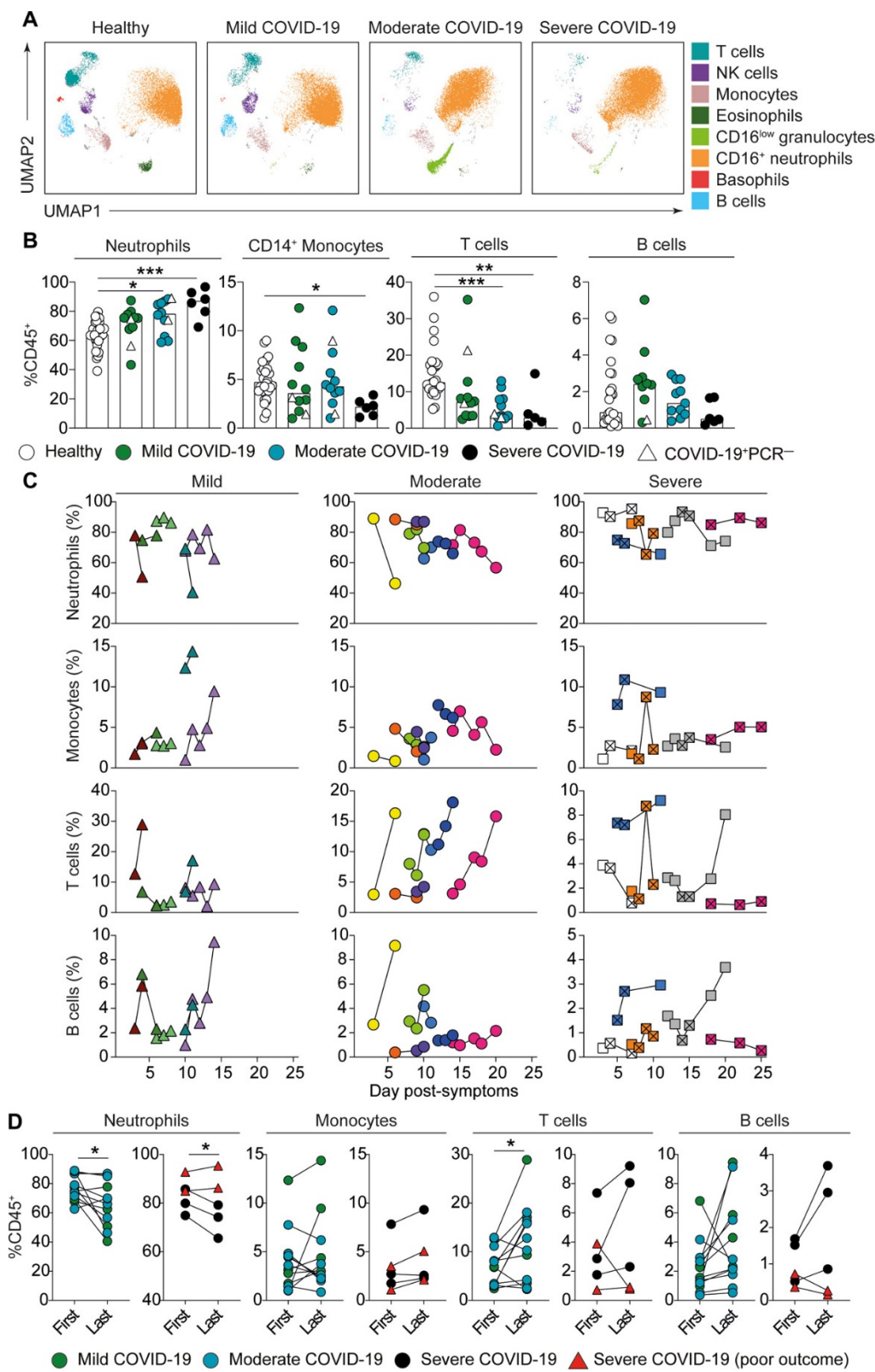


Fig. 2. Whole blood immune profile of COVID-19 patients.

(A) Uniform Manifold Approximation and Projection (UMAP) of flow cytometry panel broadly visualizing white cells in whole blood. Representative images for healthy individuals, mild, moderate and severe patients are shown. Key indicates cells identified on the image. (B) Graphs show neutrophil (CD16^{hi}CD11b^{hi}), CD14⁺ monocyte, CD3⁺ T cell, and CD19⁺ B cell frequencies in whole blood samples of healthy individuals ($n=28$) and recruitment samples from COVID-19 patients with mild ($n=12$), moderate ($n=13$) and severe ($n=6$) disease. (C) Longitudinal time course of (top row) neutrophils (CD16^{hi}CD11b^{hi}), (2nd row) CD14⁺ monocytes, (3rd row) CD3⁺ T cells and (bottom row) B cells segregated by disease severity. Individual patients are shown as different colors and shapes with lines connecting data from the same patient. Crossed squares for severe patients are time points in intensive care unit (ICU). X axis values represent the number of days since reported onset of symptoms. (D) Graphs showing frequencies of neutrophils (CD16^{hi}CD11b^{hi}), monocytes, T cells and B cells at the first and last time points in (left) mild/moderate patients (green and blue circles) and (right) severe patients (black circles). Red triangles represent severe patients that had poor outcome (deceased or long-term ICU) and are not included in the statistical test. Graphs show individual patient data with the bar representing median values. In all graphs, open triangles represent SARS-CoV-2 PCR negative patients. Kruskal Wallis with Dunn's post-hoc test; 2B Neutrophils, T cells and B cells. One-way ANOVA with Holm-Sidak post-hoc test: 2B Monocytes. Paired t-test; 2D all except monocyte graph detailing mild and moderate patients which was tested using Wilcoxon matched-pairs signed rank test. (* $P<0.05$, ** $P<0.01$, *** $P<0.001$, **** $P<0.0001$).

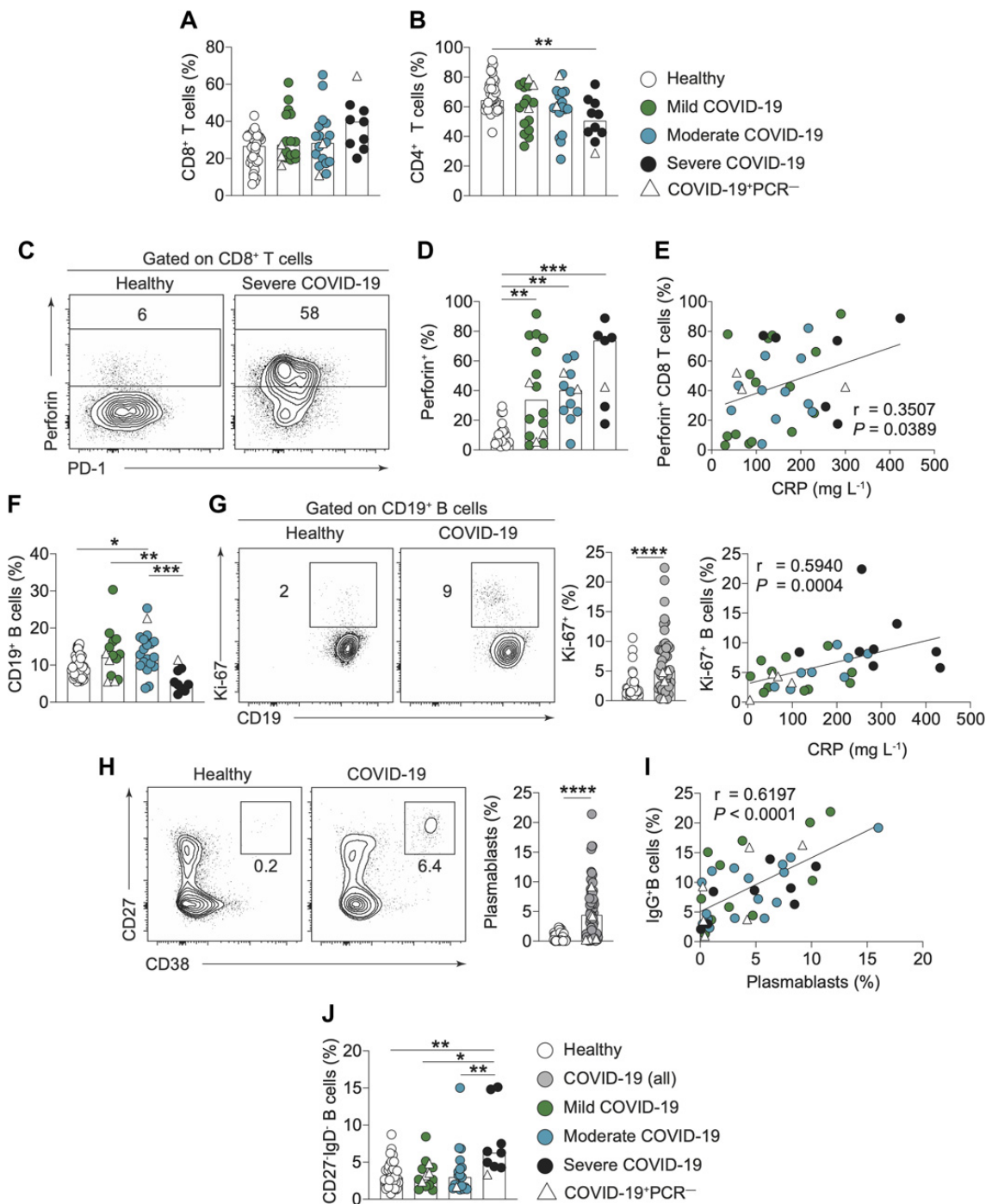
included in the statistical test. Graphs show individual patient data with the bar representing median values. In all graphs, open triangles represent SARS-CoV-2 PCR negative patients. Kruskal Wallis with Dunn's post-hoc test; 2B Neutrophils, T cells and B cells. One-way ANOVA with Holm-Sidak post-hoc test: 2B Monocytes. Paired t-test; 2D all except monocyte graph detailing mild and moderate patients which was tested using Wilcoxon matched-pairs signed rank test. (* $P<0.05$, ** $P<0.01$, *** $P<0.001$, **** $P<0.0001$).

Fig. 3. Altered phenotype of T and B cells in COVID-19 patients. (A,B) Graphs show frequencies of (A) CD8⁺ and (B) CD4⁺ T cells in freshly isolated PBMCs of healthy individuals ($n=36$) and recruitment samples from COVID-19 patients with mild ($n=17$), moderate ($n=18$) and severe ($n=9-10$) disease. (C,D)

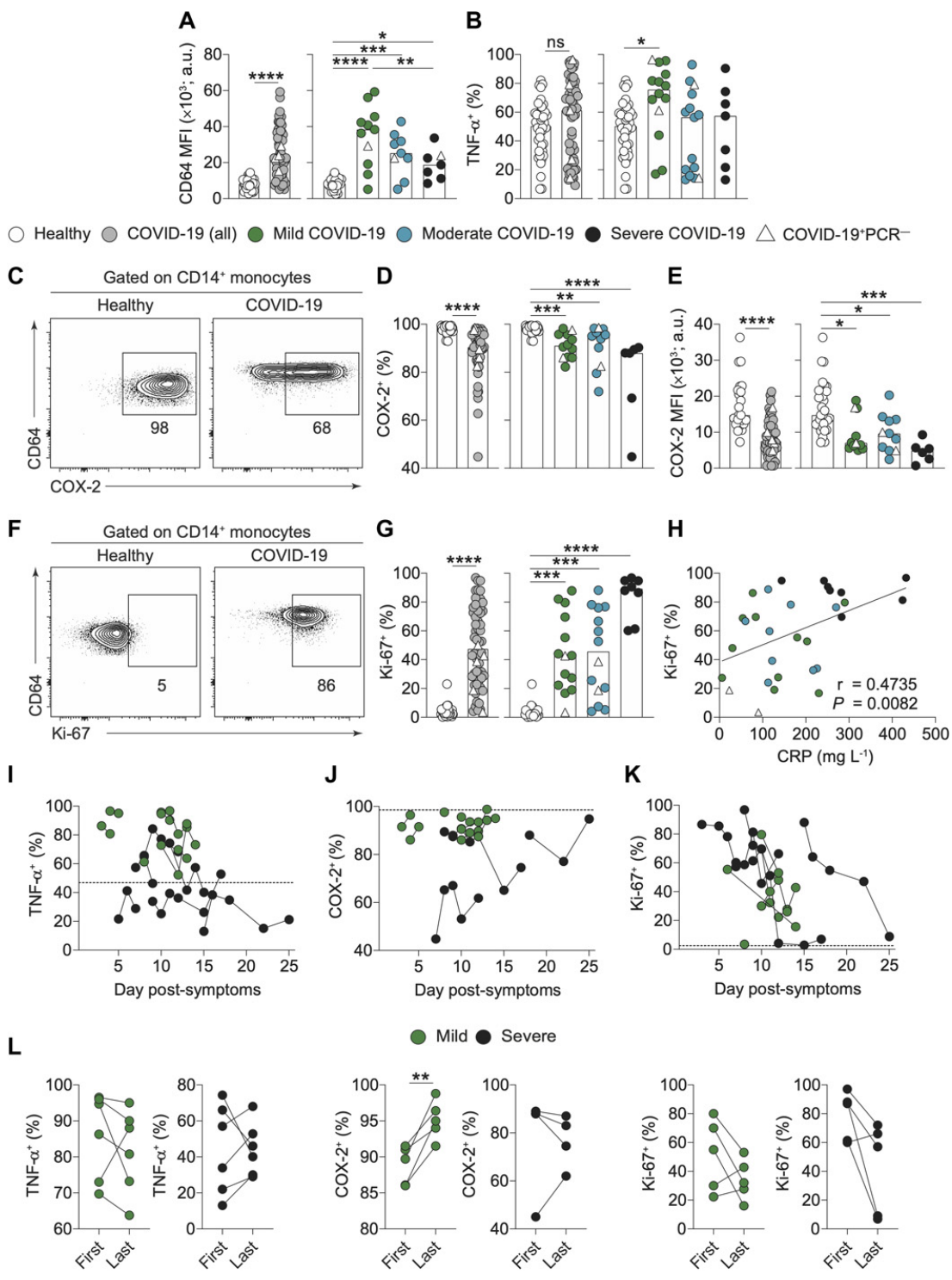
Representative flow cytometry plots and graph showing frequency of CD8⁺ T cells which are positive for perforin in healthy individuals ($n=21$) and COVID-19 patients with mild ($n=16$), moderate ($n=12$) and severe ($n=7$) disease. (E) Graph showing correlation of perforin⁺ CD8⁺ T cell frequency with C-reactive protein (CRP) in COVID-19 patients.

(F) Graphs show frequencies of CD19⁺ B cells in freshly isolated PBMCs of healthy individuals ($n=43$) and recruitment samples from COVID-19 patients with mild ($n=14$), moderate ($n=19$) and severe ($n=9$) disease. (G) Representative flow cytometry plots and cumulative data show

Downloaded from <http://immunology.science.org/> by guest on September 18, 2020



Ki-67 expression by B cells in healthy individuals ($n=39$) and COVID-19 patients ($n=45$). Correlation graph shows correlation of Ki-67⁺ B cells with C-reactive protein (CRP). (H) Representative flow cytometry plots and cumulative data show frequency of CD27^{hi}CD38^{hi} plasmablasts in healthy individuals ($n=42$) and COVID-19 patients ($n=66$). (I) Correlation graph shows correlation of plasmablasts and IgG⁺ B cell frequencies. (J) Graph shows frequencies of double negative (CD27⁻IgD⁻) B cells in freshly prepared PBMC of healthy individuals ($n=42$) and recruitment samples from COVID-19 patients with mild ($n=14$), moderate ($n=19$) and severe ($n=9$) disease. Graphs show individual patient data with the bar representing median values. In all graphs, open triangles represent SARS-CoV-2 PCR negative patients. Mann-Whitney U test; 3G, 3H. Kruskal Wallis with Dunn's post-hoc test; 3A, 3D, 3F, 3J. One-way ANOVA with Holm-Sidak post-hoc test: 3B. Spearman ranked coefficient correlation test; 3E, 3G, 3I. (* $P < 0.05$, ** $P < 0.01$, *** $P < 0.001$, **** $P < 0.0001$).



individuals (n=37) and total COVID-19 patients (n=60). COVID-19 patients were also stratified into mild (n=14), moderate (n=14) and severe (n=8) disease. (H) Correlation of Ki-67 (% of monocytes expressing Ki-67) with CRP in COVID-19 patients. (I-K) Longitudinal time course of frequencies of CD14⁺ monocytes that are positive for (I) TNF- α , (J) COX2 and (K) Ki-67 following LPS stimulation in mild (green shapes, n=6-7) and severe (black shapes, n=4-6) COVID-19 patients with lines connecting data from the same patient. On all graphs x axis values represent the number of days since onset of symptoms and the dotted line represents the median value from healthy individuals. (L) Graphs showing frequencies of monocytes which are TNF- α ⁺, COX-2 and Ki-67⁺ following LPS stimulation at the first and last time points in (left) mild patients (green circles) and (right) severe patients (black circles). Graphs show individual patient data with the bar representing median values. In all graphs, open triangles represent SARS-CoV-2 PCR negative patients. Mann-Whitney U test; 4A, 4B, 4D, 4E, 4G. Kruskal Wallis with Dunn's post-hoc test; 4B, 4D, 4E, 4G. One-way ANOVA with Holm-Sidak post-hoc test: 4A. Spearman ranked coefficient correlation test; 4H. Paired t-test; 4L. (*P<0.05, **P<0.01, ***P<0.001, ****P<0.0001).

Fig. 4. Dysregulation of circulating monocytes in COVID-19. (A) Graphs show levels of CD64 expression as assessed by mean fluorescence intensity (MFI) on CD14⁺ classical monocytes in freshly prepared PBMC of healthy individuals (n=25) and recruitment samples from all COVID-19 patients (n=58). COVID-19 patients were also stratified into mild (n=12), moderate (n=10) and severe (n=8) disease. (B) Graphs show frequencies of TNF- α ⁺ CD14⁺ monocytes following LPS stimulation of freshly prepared PBMC from healthy individuals (n=41) and COVID-19 patients (n=59). COVID-19 patients were also stratified into mild (n=14), moderate (n=15) and severe (n=7) disease. (C) Representative FACS plots demonstrating intracellular COX2 expression by CD14⁺ monocytes from healthy individuals and COVID-19 patients. (D, E) Graphs showing (D) frequencies of COX-2⁺ CD14⁺ monocytes and (E) COX-2 expression level as determined by MFI in CD14⁺ monocytes following LPS stimulation of freshly prepared PBMC from healthy individuals (n=33) and total COVID-19 patients (n=51). COVID-19 patients were also stratified into mild (n=12), moderate (n=11) and severe (n=6) disease. (F) Representative FACS plots demonstrating intracellular Ki-67 staining by CD14⁺ monocytes. (G) Graphs show frequencies of Ki-67⁺ CD14⁺ monocytes following LPS stimulation of freshly prepared PBMC from healthy

Table 1. Clinical characteristics. Data are listed as median (IQR) ^m, where m is the number of missing data points, n (%), or n/N (%), where N is the total number with available data. PE, pulmonary embolism; AKI, Acute kidney injury. ^aAdmission observations. Representative participants from each severity cohort were used in cross-sectional or longitudinal analysis.

	All patients (49)	Mild (18)	Moderate (21)	Severe (10)
Age	61 (51–71)	61.5 (45–72.5)	59 (51–68)	66 (52–72.5)
Sex				
Male	31 (63.3%)	11 (61.1%)	13 (62%)	7 (70%)
Female	18 (36.7%)	7 (38.9%)	8 (38%)	3 (30%)
BMI	27.5 (24.9–30) ⁴	27.1 (23.6–30) ¹	28.3 (25.7–30) ²	26.5 (24.9–30.4) ¹
Co-morbidity				
Diabetes	8/49 (16.3%)	3/18 (16.7%)	2/21 (9.5%)	3/10 (30%)
Ischemic heart disease	5/49 (10.2%)	2/18 (11.1%)	1/21 (4.8%)	2/10 (20%)
Hypertension	14/49 (28.6%)	5/18 (27.8%)	7/21 (33.3%)	2/10 (20%)
Chronic Obstructive Pulmonary Disease	9/49 (18.4%)	4/18 (22.2%)	4/21 (19.1%)	1/10 (10%)
Asthma	5/49 (10.2%)	2/18 (11.1%)	3/21 (14.3%)	0/10 (0%)
Malignancy	3/49 (6.1%)	0/18 (0%)	1/21 (4.8%)	2/10, (20%)
Presentation				
Illness onset to admission (days)	7 (4–10) ⁴	7 (4–8) ¹	7.5 (2.8–10.8) ³	5.5 (4–9.5)
Dyspnea	29/41 (70.7%)	8/16 (50%)	14/16 (87.5%)	7/9 (77.8%)
Cough	30/41 (73.2%)	11/16 (68.8%)	12/16 (75%)	7/9 (77.8%)
Fever	28/41 (68.3%)	10/16 (62.5%)	9/16 (56.3%)	9/9 (100%)
Diarrhea/ Vomiting	14/41 (34.2%)	3/16 (18.8%)	7/16 (43.8%)	4/9 (44.4%)
Myalgia	10/40 (25%)	4/15 (26.7%)	3/16 (18.8%)	3/9 (33.3%)
Fatigue	10/38 (26.3%)	3/14 (21.4%)	5/15 (33.3%)	2/9 (22.2%)
Day recruited	2 (2–3)	3 (2–4.5)	2 (2–3)	2 (2–3)
Number of timepoints	2 (1–4)	2 (1 – 2)	3 (2–3)	4.5 (2–5)
Respiratory rate ^a	20 (18–25) ¹⁰	20 (17–24) ⁵	21 (18–26) ³	21.5 (17.8–24) ²
Temperature ^a	37.5 (36.9–38.4) ¹⁰	37.1 (36.5–37.4) ⁵	37.7 (37.1–38.8) ³	38 (37.7–39.2) ²
Systolic blood pressure ^a	125 (117–136) ¹⁰	122 (117–126) ⁵	126 (118–136) ³	137.5 (114.5–156.3) ²
Chest Radiograph Findings				
Bilateral opacification	41/47 (87.2%)	11/16 (68.8%)	20/21 (95.2%)	10/10 (100%)
Unilateral opacification	3/47 (6.4%)	2/16 (12.5%)	1/21 (4.8%)	0/10 (0%)
No abnormality	3/47 (6.4%)	3/16 (18.8%)	0/21 (0%)	0/10 (0%)
COVID Nasopharyngeal Test				
Positive	42 (86%)	15 (83.3%)	18 (85.7%)	9 (90%)
Negative	7 (14%)	3 (16.7%)	3 (14.3%)	1 (10%)
Differential full blood count at admission				
White blood cell count ($\times 10^9/L$)	6.9 (5.7–9.8)	6.7 (4.7–7.5)	7.1 (6.3–10)	7.3 (5.7–10)
Lymphocytes ($\times 10^9/L$)	1.1 (0.8–1.4)	1.2 (0.8–1.3)	1.3 (0.8–1.5)	0.9 (0.8–1.1)
Neutrophils ($\times 10^9/L$)	5.1 (3.8–7.4)	4.7 (3.2–5.7)	5.3 (4.5–7.7)	6.3 (4.2–8.6)
Monocytes ($\times 10^9/L$)	0.4 (0.2–0.7)	0.4 (0.2–0.6)	0.5 (0.3–0.7)	0.3 (0.2–0.5)
Platelets ($\times 10^9/L$)	244 (188–367) ²	241 (188–316) ²	269 (195–366)	204 (155–412)
Highest acute phase response/Liver function tests				
C-Reactive protein (CRP) (mg/L)	127 (75–226)	88 (38–166)	120 (75–201)	269 (244–296)
Alanine aminotransferase (U/L)	48 (27–87) ¹⁶	57 (28–75) ⁹	35 (25–79) ⁵	49 (37–105) ²
Alkaline phosphatase (U/L)	78 (63–96) ¹⁶	79 (63–82) ⁹	72 (63–90) ⁵	110 (71–172) ²
Bilirubin ($\mu\text{mol}/L$)	11 (7–15) ¹⁶	10 (8–14) ⁹	9 (7–13) ⁵	13 (10–21) ²
Complications				
PE	5/49 (10.2%)	1/18 (5.6%)	4/21 (19.1%)	0/10 (0%)
AKI	3/49 (6.1%)	0/18 (0%)	2/21 (9.5%)	1/10 (10%)
Mortality	6/49 (12.2%)	1/18 (5.6%)	0/21 (0%)	5/10 (50%)

Longitudinal immune profiling reveals key myeloid signatures associated with COVID-19

Elizabeth R. Mann, Madhvi Menon, Sean Blandin Knight, Joanne E. Konkel, Christopher Jagger, Tovah N. Shaw, Siddharth Krishnan, Magnus Rattray, Andrew Ustianowski, Nawar Diar Bakerly, Paul Dark, Graham Lord, Angela Simpson, Timothy Felton, Ling-Pei Ho, NIHR Respiratory TRC,, Marc Feldmann, CIRCO,, John R. Grainger and Tracy Hussell

Sci. Immunol. **5**, eabd6197.
DOI: 10.1126/scimmunol.abd6197

ARTICLE TOOLS

<http://immunology.science.org/content/5/51/eabd6197>

SUPPLEMENTARY MATERIALS

<http://immunology.science.org/content/suppl/2020/09/16/5.51.eabd6197.DC1>

REFERENCES

This article cites 45 articles, 6 of which you can access for free
<http://immunology.science.org/content/5/51/eabd6197#BIBL>

PERMISSIONS

<http://www.sciencemag.org/help/reprints-and-permissions>

Use of this article is subject to the [Terms of Service](#)

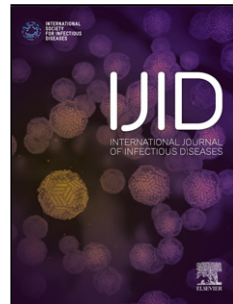
Science Immunology (ISSN 2470-9468) is published by the American Association for the Advancement of Science, 1200 New York Avenue NW, Washington, DC 20005. The title *Science Immunology* is a registered trademark of AAAS.

Copyright © 2020, American Association for the Advancement of Science

Journal Pre-proof

Mild versus severe COVID-19: laboratory markers

Thirumalaisamy P. Velavan Christian G. Meyer



PII: S1201-9712(20)30277-0

DOI: <https://doi.org/doi:10.1016/j.ijid.2020.04.061>

Reference: IJID 4149

To appear in: *International Journal of Infectious Diseases*

Received Date: 5 April 2020

Revised Date: 15 April 2020

Accepted Date: 22 April 2020

Please cite this article as: Velavan TP, Meyer CG, Mild versus severe COVID-19: laboratory markers, *International Journal of Infectious Diseases* (2020), doi: <https://doi.org/10.1016/j.ijid.2020.04.061>

This is a PDF file of an article that has undergone enhancements after acceptance, such as the addition of a cover page and metadata, and formatting for readability, but it is not yet the definitive version of record. This version will undergo additional copyediting, typesetting and review before it is published in its final form, but we are providing this version to give early visibility of the article. Please note that, during the production process, errors may be discovered which could affect the content, and all legal disclaimers that apply to the journal pertain.

© 2020 Published by Elsevier.

1 **Mild versus severe COVID-19: laboratory markers**

2

3 Thirumalaisamy P. Velavan^{1,2,3,4*#}, Christian G. Meyer^{1,2,3*}

4

5 ¹ Institute of Tropical Medicine, Universitätsklinikum Tübingen, Germany.6 ² Vietnamese German Center for Medical Research, Hanoi, Vietnam.7 ³ Faculty of Medicine, Duy Tan University, Da Nang, Vietnam.8 ⁴Fondation Congolaise pour la Recherche Médicale, Brazzaville, Congo

9

10 [#] Correspondence:11 Prof. Dr. T.P. Velavan, Institute of Tropical Medicine, Universitätsklinikum Tübingen,
12 Germany. Tel.: +49-7071-2985981; Email: velavan@medizin.uni-tuebingen.de

13

14 *Both authors contributed equally

15

16 Key words: Laboratory markers; COVID-19, Mild and severe COVID-19; Biomarkers

17

18 Words:1480 (Including tables)

19

20

21

22

23

24

25

26

27

28

29 **Abstract:**

30 The number of COVID-19 patients is increasing dramatically worldwide and treatment in
31 intensive care units (ICU) has become a major challenge, the early recognition of severe
32 forms of is absolutely essential for timely triaging of patients. While the clinical status, in
33 particular Peripheral oxygen saturation (SpO₂) levels and concurrent comorbidities of
34 COVID-19 patients largely determines the need of their admittance to ICUs, several
35 laboratory parameters may facilitate the assessment of disease severity. In hospitalized
36 patients, clinicians should consider low lymphocyte count as well as the serum levels of
37 CRP, D-dimers, ferritin and IL-6 which may be used in risk stratification to predict severe and
38 fatal COVID-19. The more several or all of these parameters are altered, the more likely it is
39 that the course of the disease will be unfavourable.

40

41

42

43

44 **Highlights**

- 45 • several laboratory parameters may facilitate the assessment of COVID-19 severity
46 • discriminating mild from severe COVID-19 disease.
47 • Cumulative data from clinical characteristics of COVID-19 patients
48 • low lymphocyte count as well as the serum levels of CRP, D-dimers, ferritin and IL-6.

49

50

51

52

53

54

55

56

57

58
59
60
61

62 As the number of COVID-19 patients is increasing dramatically worldwide and treatment in
63 intensive care units (ICU) has become a major challenge, the early recognition of severe
64 forms of COVID-19 is absolutely essential for timely triaging of patients. SARS-CoV-2
65 infection, especially in older patients and those with pre-existing illness, progress to severe
66 disease with critical respiratory symptoms and significant pulmonary changes visible by
67 imaging techniques. The changes include ground glass opacities, patchy consolidation,
68 alveolar exudates and interlobular involvement, ultimately prognosticating deterioration [1].
69 Further to recognized risk factors such as old age and underlying comorbidities, in particular
70 cardiovascular diseases, diabetes, respiratory diseases and other conditions [2], several
71 markers have been identified that modulate the course of COVID-19. Here we summarize
72 laboratory markers that might be useful in indicating progression from mild to severe disease
73 ([Table 1](#)).

74

75 COVID-19 patients admitted to ICUs had higher concentrations of proinflammatory cytokines
76 and, importantly, increased secretion of those T-helper-2 (Th2) cytokines suppressing
77 inflammation [1]. Given the high levels of cytokines induced by SARS-CoV-2, treatment to
78 reduce inflammation-related lung damage is critical. Any intervention to reduce inflammation
79 will, however, affect negatively the viral clearance. Among the various inflammatory cytokine
80 and chemokine levels assessed in several studies, tumour necrosis factor alpha (TNF- α),
81 interferon- γ -induced protein 10 (IP-10), monocyte chemoattractant protein 1 (MCP-1),
82 chemokine (C-C motif) ligand 3 (CCL-3) and distinct interleukins (IL) (IL-2, IL-6, IL-7, IL-10)
83 were significantly associated with disease severity and particularly observed among cases
84 admitted to ICUs. IL-1 and IL-8 were not associated with severity ([Table 1](#)). Apparently, the

85 serum levels of some interleukins bear the potential to discriminate between mild and severe
86 disease and possibly may be used as prognostic markers.

87

88 Among haematological parameters, lymphopenia is clearly associated with disease severity;
89 patients who died from COVID-19 had significantly lower lymphocyte counts than survivors.
90 In fact, repletion of lymphocytes may be an important factor for recovery [3]. Other blood
91 cells, including white blood cells, neutrophils, eosinophils, platelets and CD8 cell counts were
92 partly only predictors in discriminating mild from severe COVID-19 ([Table1](#)); their
93 significance is still ambiguous. Granulocyte colony stimulating factor (G-CSF) was elevated
94 in ICU patients and significantly associated with the severity of disease ([Table1](#)).

95

96 Patients with severe COVID-19 appear to have signs of liver dysfunction more frequently
97 than those with milder disease. An increase in alanine aminotransferase (ALT), aspartate
98 aminotransferase (AST) and total bilirubin levels has been observed among many ICU
99 patients [4] ([Table 1](#)). Infection of liver cells with SARS-CoV-2 cannot be excluded, as 2-10%
100 of patients with COVID-19 have diarrhoea and viral RNA has been detected in both stool and
101 blood samples, which implies the possibility of hepatic virus presence [5]. It is also likely that
102 any immune-mediated inflammation, in particular cytokine storm, but also pneumonia-
103 associated hypoxia, may lead to liver damage in critically ill COVID-19 patients [4]. C-
104 reactive protein (CRP) levels are increased in COVID-19 patients and it has been shown that
105 survivors had median CRP values of approximately 40 mg/L, while non-survivors had
106 median values of 125 mg/L, indicating a strong correlation with disease severity and
107 prognosis [6] ([Table 1](#)). Other predictors of poor outcome include the serum levels of ferritin
108 and lactate dehydrogenase (LDH). Elevated ferritin levels due to secondary hemophagocytic
109 lymphohistiocytosis (sHLH) and cytokine storm syndrome have been reported in severe
110 COVID-19 patients. Based on body temperature, organomegaly, blood cell cytopenia,
111 triglycerides, fibrinogen as well as AST and ferritin levels, a predictive H-score was proposed
112 to estimate the risk of developing secondary hemophagocytic lymphohistiocytosis [7].

113

114 Correlations of abnormal coagulation parameters with poor prognosis were observed (Table
115 1). Non-survivors showed significantly higher levels of plasma D-dimers and fibrin
116 degradation products, increased prothrombin times and activated partial thromboplastin
117 times compared to survivors [8]. Coagulopathy and overt disseminated intravascular
118 coagulation appear to be associated with high mortality rates. Among the coagulation
119 parameters, D-dimer elevation >1 ug/L was the strongest independent predictor of mortality
120 [2]. Elevated cardiac troponin I levels indicating heart injury are also predictive of mortality in
121 critically ill patients [9;10].

122

123 The haematological and coagulation parameters summarized here as well as increased
124 inflammatory reactions caused by various cytokines and liver enzymes are a globally
125 observed phenomenon in COVID-19 patients. While the clinical status, in particular SpO₂
126 levels and concurrent comorbidities of COVID-19 patients largely determines the need of
127 their admittance to ICUs, several laboratory parameters may facilitate the assessment of
128 disease severity and rational triaging. The more several or all of these parameters are
129 altered, the more likely it is that the course of the disease will be unfavourable. In
130 hospitalized patients, clinicians should consider low lymphocyte count as well as the serum
131 levels of CRP, D-dimers, ferritin and IL-6 which may be used in risk stratification to predict
132 severe and fatal COVID-19. In order to further support clinical decision making, large
133 datasets and sound metanalyses are now urgently required.

134

135 Acknowledgements

136 All authors have an academic interest and contributed equally. TPV is a member of the Pan
137 African Network for Rapid Research, Response, and Preparedness for Infectious Diseases
138 Epidemics consortium (PANDORA-ID-NET).

139

140 **Conflict of interest:** All authors disclose no conflict of interest.

141

142 **Funding Source:** European and Developing Countries Clinical Trials Partnership (EDCTP)
143 Pan African Network for Rapid Research, Response, and Preparedness for Infectious
144 Diseases Epidemics consortium (PANDORA-ID-NET- EDCTP grant ID: RIA2016E-1609).

Journal Pre-proof

145
146**Table 1: Haematological, Cytokines, Liver enzymes and Coagulation parameters in mild vs. severe COVID19 patients**

Haematological parameters	COVID-19 cases/cases (n)	Interpretation	Reference
White blood cell count (WBC)	15 mild, 9 severe, 5 critical cases	normal or ↓ in 23/29	[11]
	41 cases (13 ICU cases)	↑ in ICU cases	[1]
	43 (28 mild, 15 severe)	normal in all cases	[13]
	1994 cases (meta-analysis)	↓ in 29% of cases	[15]
	54 cases	normal in cases	[16]
Neutrophil count	41 cases (13 ICU cases)	↑ in ICU cases	[1]
	201 cases	↑ in ARDS cases	[17]
	12 cases	↓ in most cases	[18]
Lymphocyte count	Familial cluster, 6 cases	↓ in 2 of 3 cases >60 years	[19]
	15 mild, 9 severe, 5 critical cases	↓ in 20/29	[11]
	41 cases (13 ICU cases)	↓ in ICU cases	[1]
	140 cases	↓ in most cases	[20]
	43; 28 mild, 15 severe cases	normal in cases	[13]
	1994 cases (meta-analysis)	↓ in most cases	[15]
	54 cases	↓ in most cases	[16]
	12 cases	↓ in most cases	[18]
	30 cases	↓ in 40% cases	[21]
	70 mild, 85 severe cases	↓ in all cases	[14]
Eosinophil count	140 cases	↓ in most cases	[20]
Thrombocyte count	Familial cluster, 6 cases	↓ in 2 of 3 cases >60 yrs.	[19]
	70 mild, 85 severe cases	normal; slightly lower in severe cases	[14]
Granulocyte-colony stimulating factor (G-CSF)	41 cases (13 ICU cases)	↑ in ICU cases	[1]
CD8 cell count	12 cases	↓ in most cases	[18]

147
148

Cytokines	COVID-19 cases (n)	Interpretation	Reference

Tumour necrosis factor alpha (TNF-alpha)	41 cases (13 ICU cases)	↑ in ICU cases	[1]
Interferon-γ induced protein 10 (IP-10),	41 cases (13 ICU cases)	↑ in ICU cases	[1]
Monocyte chemoattractant protein 1 (MCP-1)	41 cases (13 ICU cases)	↑ in ICU cases	[1]
Chemokine (C-C Motif) Ligand 3 (CCL-3)	41 cases (13 ICU cases)	↑ in ICU cases	[1]
Interleukin-1 (IL-1)	15 mild, 9 severe, 5 critical cases	normal in all cases	[11]
Interleukin-2 (IL-2)	41 cases (13 ICU cases)	↑ in ICU cases	[1]
Interleukin-2 receptor (IL-2R)	15 mild, 9 severe, 5 critical cases	↑, >critical >severe >mild	[11]
Interleukin-6 (IL-6)	15 mild, 9 severe, 5 critical cases 69 cases, mortality 7,5% 150 cases 43; 28 mild, 15 severe cases 70 mild, 85 severe cases	↑ according to severity >critical >severe >mild ↑ in the patient group with SpO ₂ <90% ↑ in non-survivors ↑ in severe cases ↑; higher in severe cases	[11] [12] [7] [13] [14]
Interleukin-7 (IL-7)	41 cases (13 ICU cases)	↑ in ICU cases	[1]
Interleukin-8 (IL-8)	15 mild, 9 severe, 5 critical cases	normal in all cases	[11]
Interleukin-10 (IL-10)	15 mild, 9 severe, 5 critical cases 69 cases, mortality 7,5% 41 cases (13 ICU cases)	normal in all cases ↑ in the patient group with SpO ₂ <90% ↑ in ICU cases	[11] [12] [1]

149

Liver enzymes/biomarkers	COVID-19 cases/cases (n)	Interpretation	Reference
Albumin	15 mild, 9 severe, 5 critical cases	↓ in 15/29	[11]
	41 cases (13 ICU cases)	↓ in ICU cases	[1]
	12 cases	↓ in most cases	[18]
	70 mild, 85 severe cases	↓ in all cases	[14]
Alanine aminotransferase (ALT)	15 mild, 9 severe, 5 critical cases	-	[11]
	41 cases (13 ICU cases)	↑ in ICU cases	[1]
Aspartate aminotransferase (AST)	15 mild, 9 severe, 5 critical cases	-	[11]
Total bilirubin	41 cases (13 ICU cases)	↑ in ICU cases	[1]
	15 mild, 9 severe, 5 critical cases	- normal in all cases	[11]
Glucose	43; 28 mild, 15 severe cases	↑ in severe cases	[13]
Serum creatinine	126 mild, 24 severe cases	↑ in severe cases	[11]

Lactate dehydrogenase (LDH)	Familial cluster, 6 cases	↑ in the 3 cases >60 yrs.	[19]
	15 mild, 9 severe, 5 critical cases	↑ in 20/29	[11]
	69 cases, mortality 7,5%	↑ in the patient group with SpO ₂ <90%	[12]
	41 cases (13 ICU cases)	↑ in ICU cases	[1]
	201 cases	↑ in ARDS cases	[17]
	1994 cases (meta-analysis)	↑ in 28% of cases	[15]
	54 cases	↑ in most cases	[16]
	12 cases	↑ in all cases	[18]
	70 mild, 85 severe cases	↑ in severe cases	[14]
C-reactive protein (CRP)	Familial cluster, 6 cases	↑ in the 3 cases >60 yrs.	[19]
	126 mild, 24 severe cases	higher in severe cases	[22]
	15 mild, 9 severe, 5 critical cases	↑ in 27/29	[11]
	69 cases, mortality 7,5%	↑ in cases with SpO ₂ <90%	[12]
	140 cases	↑ in severe cases	[20]
	43; 28 mild, 15 severe cases	↑ in severe cases	[13]
	1994 cases (meta-analysis)	↑ in 44% of cases	[15]
	54 cases	↑ in most cases	[16]
	12 cases	↑ in most cases	[18]
Procalcitonin (PCT)	70 mild, 85 severe cases	↑ in all cases, higher in severe cases	[14]
	140 cases	↑ in severe cases	[20]
Ferritin	70 mild, 85 severe cases	↑ in all cases	[14]
	150	↑ in non-survivors	[7]
NT-proBNP	126 mild, 24 severe cases	↑ in severe cases	[22]
Cardiac troponin I	126 mild, 24 severe cases	↑ in severe cases	[22]
Cardiac troponin I (meta-analysis)	218 mild, 123 severe cases	↑ in severe cases	[9]
	138 hospitalized severe cases	↑ in severe cases	[10]
Angiotensin II level	12 cases	↑ in cases	[18]

150

Coagulation parameters	COVID-19 cases/cases (n)	Interpretation	Reference
d-dimers	191 cases, 91 with comorbidities	↑ in non-survivors	[2]

	94 cases	↑ in cases vs. controls	[23]
	201 cases	↑ in ARDS cases	[17]
	140 cases	↑ in severe cases	[20]
	43; 28 mild, 15 severe cases	↑ in severe cases	[13]
	30 cases	↑ in 17% of cases	[21]
	70 mild, 85 severe cases	normal; slightly higher in severe cases	[14]
	183 cases; 21 non-survivors	↑ in all cases, higher in non-survivors	[8]
Antithrombin (AT)	94 cases	↓ in cases vs. controls	[23]
Prothrombin time (PT)	94 cases	↓ in cases vs. controls	[23]
	41 cases (13 ICU cases)	↑ in ICU cases	[1]
	183 cases; 21 non-survivors	↑ in non-survivors	[8]
Activated partial thromboplastin time (APTT)	183 cases; 21 non-survivors	↑ in non-survivors	[8]
Thrombin clotting time (TCT)	94 cases	shorter in critical cases vs. controls	[23]
	43; 28 mild, 15 severe cases	↑ in severe cases	[13]
Fibrin degradation products (FDP)	94 cases	↑ in cases vs. controls	[23]
	183 cases; 21 non-survivors	↑ in non-survivors	[8]
Fibrinogen	94 cases	↑ in cases vs. controls	[23]
	43; 28 mild, 15 severe cases	↑ in severe cases	[13]
	183 cases; 21 non-survivors	↑ in all cases, higher in non-survivors	[8]

151

152 **ARDS:** acute respiratory distress syndrome; **ICU:** Intensive care unit; **ARDS:** acute respiratory distress syndrome; **CD8:** cluster of differentiation 8153 **SpO₂:** Peripheral oxygen saturation; **NT-proBNP:** N-terminal pro b-type natriuretic peptide

154

155

156

157

158

159
160

Reference List

- 161 1. Huang C, Wang Y, Li X *et al.* Clinical features of patients infected with 2019 novel
162 coronavirus in Wuhan, China. Lancet 2020; 395:497-506.
- 163 2. Zhou F, Yu T, Du R *et al.* Clinical course and risk factors for mortality of adult
164 inpatients with COVID-19 in Wuhan, China: a retrospective cohort study. Lancet
165 2020.
- 166 3. Henry BM. COVID-19, ECMO, and lymphopenia: a word of caution. Lancet
167 Respir.Med. 2020.
- 168 4. Zhang C, Shi L, Wang FS. Liver injury in COVID-19: management and challenges.
169 Lancet Gastroenterol.Hepatol. 2020.
- 170 5. Yeo C, Kaushal S, Yeo D. Enteric involvement of coronaviruses: is faecal-oral
171 transmission of SARS-CoV-2 possible? Lancet Gastroenterol.Hepatol. 2020; 5:335-7.
- 172 6. Ruan Q, Yang K, Wang W, Jiang L, Song J. Clinical predictors of mortality due to
173 COVID-19 based on an analysis of data of 150 patients from Wuhan, China. Intensive
174 Care Med. 2020.
- 175 7. Mehta P, McAuley DF, Brown M, Sanchez E, Tattersall RS, Manson JJ. COVID-19:
176 consider cytokine storm syndromes and immunosuppression. Lancet 2020.
- 177 8. Tang N, Li D, Wang X, Sun Z. Abnormal coagulation parameters are associated with
178 poor prognosis in patients with novel coronavirus pneumonia. J.Thromb.Haemost.
179 2020.
- 180 9. Lippi G, Lavie CJ, Sanchis-Gomar F. Cardiac troponin I in patients with coronavirus
181 disease 2019 (COVID-19): Evidence from a meta-analysis. Prog.Cardiovasc.Dis.
182 2020.
- 183 10. Wang D, Hu B, Hu C *et al.* Clinical Characteristics of 138 Hospitalized Patients With
184 2019 Novel Coronavirus-Infected Pneumonia in Wuhan, China. JAMA 2020.
- 185 11. Chen L, Liu HG, Liu W *et al.* [Analysis of clinical features of 29 patients with 2019
186 novel coronavirus pneumonia]. Zhonghua Jie.He.He.Hu Xi.Za Zhi. 2020; 43:203-8.
- 187 12. Wang Z, Yang B, Li Q, Wen L, Zhang R. Clinical Features of 69 Cases with
188 Coronavirus Disease 2019 in Wuhan, China. Clin.Infect.Dis. 2020.
- 189 13. Gao Y, Li T, Han M *et al.* Diagnostic Utility of Clinical Laboratory Data
190 Determinations for Patients with the Severe COVID-19. J.Med.Viro. 2020.
- 191 14. Mo P, Xing Y, Xiao Y *et al.* Clinical characteristics of refractory COVID-19
192 pneumonia in Wuhan, China. Clin.Infect.Dis. 2020.
- 193 15. Li LQ, Huang T, Wang YQ *et al.* 2019 novel coronavirus patients' clinical
194 characteristics, discharge rate and fatality rate of meta-analysis. J.Med.Viro. 2020.

- 195 16. Li YY, Wang WN, Lei Y *et al.* [Comparison of the clinical characteristics between
196 RNA positive and negative patients clinically diagnosed with 2019 novel coronavirus
197 pneumonia]. Zhonghua Jie.He.He.Hu Xi.Za Zhi. 2020; 43:E023.
- 198 17. Wu C, Chen X, Cai Y *et al.* Risk Factors Associated With Acute Respiratory Distress
199 Syndrome and Death in Patients With Coronavirus Disease 2019 Pneumonia in
200 Wuhan, China. JAMA Intern.Med. 2020.
- 201 18. Liu Y, Yang Y, Zhang C *et al.* Clinical and biochemical indexes from 2019-nCoV
202 infected patients linked to viral loads and lung injury. Sci.China Life Sci. 2020;
203 63:364-74.
- 204 19. Chan JF, Yuan S, Kok KH *et al.* A familial cluster of pneumonia associated with the
205 2019 novel coronavirus indicating person-to-person transmission: a study of a family
206 cluster. Lancet 2020; 395:514-23.
- 207 20. Zhang JJ, Dong X, Cao YY *et al.* Clinical characteristics of 140 patients infected with
208 SARS-CoV-2 in Wuhan, China. Allergy 2020.
- 209 21. Liu M, He P, Liu HG *et al.* [Clinical characteristics of 30 medical workers infected
210 with new coronavirus pneumonia]. Zhonghua Jie.He.He.Hu Xi.Za Zhi. 2020; 43:E016.
- 211 22. Chen C, Chen C, Yan JT, Zhou N, Zhao JP, Wang DW. [Analysis of myocardial
212 injury in patients with COVID-19 and association between concomitant
213 cardiovascular diseases and severity of COVID-19]. Zhonghua Xin.Xue.Guan.Bing.Za
214 Zhi. 2020; 48:E008.
- 215 23. Han H, Yang L, Liu R *et al.* Prominent changes in blood coagulation of patients with
216 SARS-CoV-2 infection. Clin.Chem.Lab Med. 2020.
- 217
- 218

Review

Prognostic Value of Cardiovascular Biomarkers in COVID-19: A Review

Maryam Aboughdir ^{1,2,†}, Thomas Kirwin ^{1,3,†}, Ashiq Abdul Khader ¹ and Brian Wang ^{1,*}

¹ Department of Medicine, Imperial College London, London W12 0NN, UK; m.aboughdir@gmail.com (M.A.); tkirwin05@gmail.com (T.K.); asa415@ic.ac.uk (A.A.K.)

² Department of Medicine, St. George's University of London, London SW17 0RE, UK

³ College of Medical and Dental Sciences, University of Birmingham, Birmingham B15 2TT, UK

* Correspondence: brian.wang15@imperial.ac.uk; Tel.: +44-79-2006-8530

† These authors contributed equally to this work.

Received: 8 April 2020; Accepted: 9 May 2020; Published: 11 May 2020



Abstract: In early December 2019, the coronavirus disease (COVID-19) caused by severe acute respiratory syndrome coronavirus 2 (SARS-CoV-2) first emerged in Wuhan, China. As of May 10th, 2020, a total of over 4 million COVID-19 cases and 280,000 deaths have been reported globally, reflecting the raised infectivity and severity of this virus. Amongst hospitalised COVID-19 patients, there is a high prevalence of established cardiovascular disease (CVD). There is evidence showing that COVID-19 may exacerbate cardiovascular risk factors and preexisting CVD or may lead to cardiovascular complications. With intensive care units operating at maximum capacity and such staggering mortality rates reported, it is imperative during this time-sensitive COVID-19 outbreak to identify patients with an increased risk of adverse outcomes and/or myocardial injury. Preliminary findings from COVID-19 studies have shown the association of biomarkers of acute cardiac injury and coagulation with worse prognosis. While these biomarkers are recognised for CVD, there is emerging prospect that they may aid prognosis in COVID-19, especially in patients with cardiovascular comorbidities or risk factors that predispose to worse outcomes. Consequently, the aim of this review is to identify cardiovascular prognostic factors associated with morbidity and mortality in COVID-19 and to highlight considerations for incorporating laboratory testing of biomarkers of cardiovascular performance in COVID-19 to optimise outcomes.

Keywords: COVID-19; coronavirus; cardiovascular disease; SARS-CoV-2

1. Introduction

In early December 2019, the coronavirus disease (COVID-19) caused by severe acute respiratory syndrome coronavirus 2 (SARS-CoV-2) first emerged in Wuhan, China [1]. On January 31st, 2020, the World Health Organisation declared COVID-19 a public health emergency of international concern, and on March 11th, 2020, it was finally characterised as a pandemic [2]. As of May 10th 2020, a total of over 4 million COVID-19 cases and 280,000 deaths have been reported globally, reflecting the raised infectivity and severity of this virus, yet the lack of widespread testing availability means these figures are likely even higher than reported [3]. It is therefore important to predict the risk of morbidity and mortality, especially in vulnerable patients.

SARS-CoV-2 is an enveloped, non-segmented, single-stranded, positive-sense RNA virus belonging to the Coronaviridae family [4]. SARS-CoV-2 is a zoonotic virus not too dissimilar to the SARS-CoV outbreak of 2002 and the Middle East respiratory syndrome coronavirus of 2012 [5–8]. This novel coronavirus enters cells via binding of the viral surface spike protein to the angiotensin-converting enzyme (ACE) 2 protein [9]. ACE2 is highly expressed in lung alveolar

cells, providing the route of entry for the virus [10]. In addition, ACE2 is also widely present in the myocardium, which has raised concerns due to the possibility of direct viral infection of the cardiovascular system [10].

Although COVID-19 patients present primarily with symptoms of respiratory disease and therefore follow a pneumonia-like treatment plan, it is essential that the cardiovascular system is not ignored and to recognise those presenting with early signs of acute myocardial injury. Of the patients hospitalised for COVID-19 thus far, the prevalence of cardiovascular comorbidities has been staggering. Based on early reports, patients with cardiovascular disease (CVD) may represent 25% of those in an intensive care unit (ICU) plus those with hypertension accounting for 58% of patients [11]. Additionally, Zhou et al. found that myocardial injury, defined by raised serum cardiac troponin I (cTnI) levels, in COVID-19 patients was associated with over 50% mortality rate [12]. Furthermore, heart failure was prevalent in 23% of patients presenting with COVID-19, which was also more prevalent amongst patients who died compared to those who survived (51.9% vs. 11.7%) [12]. This demonstrates how essential it is to recognise those presenting with early signs of acute myocardial injury and to initiate a more intensive treatment plan.

Based on these observations, several theories surrounding the interplay between the pathophysiology of COVID-19 and the cardiovascular system have been postulated [13,14]. Namely, COVID-19 may exacerbate cardiovascular risk factors and preexisting CVD or may increase susceptibility for the development of new cardiovascular complications. Alternatively, CVD or myocardial injury may predispose to worse outcomes in COVID-19 patients, which is reflected by a number of studies whereby established CVD is associated with more severe COVID-19, leading to higher morbidity and mortality.

With such staggering mortality rates reported, it is fundamental during this time-sensitive COVID-19 outbreak to identify patients with an increased risk of adverse CVD outcomes and/or myocardial injury. One may achieve this through laboratory investigations of biomarkers such as cTnI, brain natriuretic peptide (BNP), D-dimers, and fibrinogen—all of which reflect cardiovascular function and are used as diagnostic tools in addition to assessing the risk of CVD in patients [15–18]. While these biomarkers are recognised for CVD, there is an emerging prospect that they may aid prognosis in COVID-19, especially in patients with cardiovascular comorbidities or risk factors that predispose to worse outcomes. This is crucial as the speed of deterioration of many COVID-19 patients means any early biomarkers indicative of severe morbidity or mortality may then help prevent this rapid deterioration. Consequently, the aim of this review is to identify cardiovascular prognostic factors associated with morbidity and mortality in COVID-19 and to highlight considerations by summarising the evidence for utilising laboratory testing of biomarkers of cardiovascular performance in COVID-19 to optimise outcomes.

2. Biomarkers of Myocardial Injury in COVID-19

COVID-19 patients at risk of serious illness and ICU admission tend to be older and to present with similar comorbidities, including heart failure, hypertension, and coronary artery disease [12,19,20]. In a meta-analysis of 8 studies (46,248 COVID-19 patients in total), CVD was reported as the third most prevalent comorbidity in COVID-19 patients (5%, 95% CI 4%–7%), and patients with severe COVID-19 symptoms had a higher risk of CVD (OR 3.42, 95% CI 1.88–6.22) [21]. Whilst these results were limited by significant heterogeneity due to variations in the severity of COVID-19 patients and follow-up period, a similarly high prevalence of CVD in COVID-19 patients (15%) was observed in the study by Huang and colleagues [1,21]. Notably, Yang and Jin state that COVID-19 patients with established CVD are susceptible to more adverse complications—these patients are therefore also at a greater risk of myocardial injury, which mainly manifests as elevated serum cTnI levels [22].

cTnI is a gold-standard necrotic biomarker for myocardial risk assessment worldwide [15]. It is released virtually exclusively in the myocardium in the presence of myocardial injury irrespective of the mechanism of insult [15]. Other biomarkers of myocardial injury that are of diagnostic value

include creatine kinase-myocardial band (CK-MB) and BNP, which may provide insight into the severity of symptoms in COVID-19. Although they are already established for CVD, results from emerging studies, as discussed below, elucidate the potential role of these biomarkers, particularly cTnI and cardiac troponin T (cTnT), as predictors of prognosis in COVID-19 patients, as shown in Table 1.

The predictive potential of troponin proteins for severe morbidity in COVID-19 patients has been demonstrated. For instance, Huang et al. reported a substantial elevation of cTnI ($>28 \text{ pg/mL}$) in 5 out of 41 (12%) COVID-19 patients [1]. All 5 then developed acute myocardial injury, and 4 out of the 5 were admitted into an ICU—this allows the conceptualisation of cTnI as a prognostic tool in other diseases such as COVID-19 [1]. In addition, a meta-analysis of 4 studies with 341 COVID-19 patients reported a significantly higher cTnI mean difference in patients with more severe COVID-19 symptoms compared with patients with non-severe COVID-19 presentation (25.6 ng/L, 95% CI 6.8–44.5 ng/L), although heterogeneity was relatively high, posing a limitation similar to the previously mentioned meta-analysis [23]. Nevertheless, Shi et al. also identified that 82 out of 416 (19.7%) COVID-19 patients presented with myocardial injury, diagnosed by significantly raised serum cTnI levels [19]. Amongst these patients, there was a significantly higher mortality rate of 51.2% compared to a 4.5% mortality rate in those with normal cTnI levels and no myocardial injury, signifying the serious nature of myocardial injury in COVID-19 patients [19]. Importantly, it demonstrates the potential value of cTnI in foreshadowing the outcomes of COVID-19 patients.

The possible role of cTnT in COVID-19 prognosis is also exemplified by Guo et al., who reported the elevation of cTnT levels in 52 out of 187 (27.8%) hospitalised COVID-19 patients, all of whom developed myocardial injury [20]. In those 52 patients, mortality was a staggering 59.6% compared to 8.9% in those patients with normal serum cTnT levels [20]. Whilst COVID-19 patients with raised cTnT levels and established CVD had an alarming mortality rate of 69.4%, those with raised serum cTnT levels but no history of CVD still had a relatively high mortality rate of 37.5% [20]. This indicates the prognostic value of detecting elevated cTnT levels in all COVID-19 patients, irrespective of the presence of underlying CVD. Conversely, patients with normal serum cTnT levels and established CVD had a much lower mortality rate of 13.3% compared to the 59.6% rate in patients with elevated cTnT levels [20].

Interestingly, Guo et al. also observed a significant positive linear correlation between serum cTnT and plasma C-reactive protein ($p < 0.001$), suggesting a link between the severity of inflammation observed in COVID-19 and myocardial injury [20]. Indeed, several myocarditis autopsy findings of inflammatory mononuclear infiltrate in myocardial tissue have been reported in patients with high viral load—these studies also further explore the changes in cardiac inflammatory markers during COVID-19 manifestation [24–26]. It is therefore plausible that, through these inflammatory changes, there is an increased risk of myocardial injury, which manifests as elevated serum cTnT levels and consequently leads to more severe symptoms.

Whilst cTnI and cTnT have demonstrated remarkable potential in predicting COVID-19 outcomes, BNP too has shown some prospect in the prognosis of COVID-19. Guo and colleagues found that raised cTnT levels were significantly associated with elevated serum BNP levels ($p < 0.001$) [20]. They reported that, alongside the gradual elevation of serum cTnT levels, BNP levels likewise progressively increased in COVID-19 patients whose health deteriorated, contrasting the low and stable serum BNP levels in successfully discharged patients [20]. Similarly, a case report presented the cardiac involvement in deterioration of a COVID-19 patient without preexisting CVD, whereby serum levels of BNP (5647 pg/mL), cTnT (0.24 ng/mL), and CK-MB (20.3 ng/mL) were all elevated—this patient was then admitted to the ICU with myocarditis [27]. Moreover, Shi et al. report significantly raised BNP levels in COVID-19 patients with myocardial injury compared to those without (1689 pg/mL vs. 139 pg/mL, $p < 0.001$)—these patients consequently also had a high mortality rate of 51.2% [19]. As such, the aforementioned findings in these studies are groundbreaking as they reflect the prospect of routinely measuring serum BNP levels in COVID-19 patients at admission to reduce mortality and to prevent deterioration where possible.

In addition to cTnI and BNP, CK-MB may similarly hold prognostic value in COVID-19. In the study by Wang et al., 36 out of 138 (26.1%) COVID-19 patients were admitted to the ICU with severe symptoms, all of whom had significantly elevated serum cTnI and CK-MB levels ($p = 0.004$ and $p < 0.001$, respectively) compared to non-ICU patients [11]. Perhaps this implies that patients with more severe COVID-19 symptoms have adverse outcomes of acute myocardial injury—reflected by the elevation in CK-MB and cTnI levels. Likewise, this study provides insight into the value of CK-MB, along with cTnI, in categorising COVID-19 patients with an increased risk of adverse outcomes and admission to ICU for health deterioration. The value of CK-MB and cTnI in COVID-19 is also exemplified in the study by Zhou et al., whereby a significant association between elevated CK-MB and cTnI levels and in-hospital death was illustrated ($p = 0.043$ and $p < 0.0001$, respectively) [12]. Similarly, Wan et al. found that creatine kinase was significantly higher in COVID-19 patients with severe symptoms compared to those with mild symptoms ($p = 0.0016$) [28]. These studies demonstrate the benefit of utilising CK-MB in determining the patients that require urgent intervention.

Although BNP and CK-MB have evidently demonstrated some prognostic value in COVID-19, it is important to highlight that, in all studies measuring BNP or CK-MB, cTnI was also measured and it provided the same, if not a clearer, link between myocardial injury and COVID-19 outcomes. Additionally, contrasting findings are reported between studies regarding creatine kinase levels and severe COVID-19 presentation. For instance, whilst Wan et al. found creatine kinase to be significantly elevated in COVID-19 patients with severe symptoms, Huang et al. found no significant difference in serum creatine kinase levels between ICU and non-ICU patients ($p = 0.31$) [1,28]. Therefore, more studies that clearly illustrate a conclusive link between CK-MB and BNP and COVID-19 outcomes will provide a better understanding of their prognostic role. It is through the lack of evidence in the literature that one, therefore, postulates cTnI may be a preferred option compared to CK-MB and BNP, mainly due to its high sensitivity in detecting worsening prognosis and myocardial injury in COVID-19 patients.

It is worth noting that raised serum cTnI levels are similarly associated with a higher risk of mortality in other diseases such as pneumonia (odds ratio = 9.5), sepsis (odds ratio = 1.92), chronic obstructive pulmonary disease (hazard ratio = 4.5), and acute respiratory distress syndrome (hazard ratio = 1.6) [29–32]. Hence, one may logically also predict a correlation between elevated serum cTnI levels and a higher risk of mortality in COVID-19 patients. Studies have clearly illustrated a significant difference in serum cTnI levels between COVID-19 patients who survived and those who died. cTnI levels provide novel insight into a multi-faceted prognostic use of cTnI in other diseases than CVD as it has proven to be a reliable marker of mortality in the previously discussed studies. During a crisis such as the current COVID-19 pandemic, measuring serum cTnI levels may enable healthcare professionals to predict prognosis and to therefore avoid worsening outcomes in vulnerable patients by identifying them at an earlier stage and by providing them with an intensive treatment plan which tackles both the myocardial injury and COVID-19.

Table 1. A table highlighting the biomarkers of myocardial injury that may have prognostic value in the coronavirus disease (COVID-19).

Cardiac Biomarker	Definition	Association with COVID-19	Prognostic Potential	References
cTn	cTnI and cTnT are gold-standard necrotic biomarkers for myocardial injury irrespective of the mechanism of insult [15].	Raised cTnI/cTnT is associated with <ul style="list-style-type: none"> Acute myocardial injury ICU admission In-hospital death Severity of inflammation in COVID-19 	+++	[1,19,20,23]

Table 1. *Cont.*

Cardiac Biomarker	Definition	Association with COVID-19	Prognostic Potential	References
BNP	BNP is a predictor of adverse outcome following acute myocardial injury. BNP concentrations increase immediately following myocardial injury, with the extent of increasing correlating with the injury size [16,33].	Raised BNP is associated with <ul style="list-style-type: none"> • Acute myocardial injury • ICU admission • In-hospital death 	++	[1,20,27]
CK-MB	CK-MB is a biomarker of myocardial damage and reperfusion. Raised CK-MB levels are correlated with injury size and are predictors of poor prognosis [34–36].	Raised CK-MB is associated with <ul style="list-style-type: none"> • Acute myocardial injury • ICU admission • In-hospital death 	+	[1,11,12,28]

Raised cTnI/cTnT, BNP, and CK-MB levels are all associated with deteriorating clinical parameters in COVID-19 patients. Prognostic potential as judged by the authors on association with clinical findings and the quality of the literature in support of this. cTn cardiac troponin, cTnI cardiac troponin I, cTnT cardiac troponin T, BNP brain natriuretic peptide, CK-MB creatine kinase-myocardial band, ICU intensive care unit.

3. Vascular biomarkers

3.1. Markers of Coagulation

It has been clear from early reports in China that abnormal coagulation is associated with poor prognosis in COVID-19 patients. Tang et al. clearly illustrated this by retrospectively analysing the coagulation parameters of 183 hospitalised COVID-19 patients [37]. Strikingly, 70.14% of non-survivors matched the diagnostic criteria for disseminated intravascular coagulation (DIC) in later stages of the disease (according to the criteria described by the International Society on Thrombosis and Haemostasis) [38]. This contrasts with only one (0.6%) survivor meeting the criteria. Hence, abnormal coagulation is a principal factor involved in the deterioration and high mortality seen in COVID-19. However, it is less clear if coagulation parameters, as seen in Table 2, could be used to stratify patients on admission, thus highlighting those more likely to develop severe disease in order to prompt swift intensive treatment.

Thus far, D-dimer has demonstrated promise in its ability to hold prognostic value in COVID-19 patients. Wang et al. conducted a retrospective single-centre case series including 138 patients with confirmed COVID-19 [11]. Those who were eventually admitted to ICU had significantly increased D-dimer levels (median D-dimer 414 mg/L vs. 166 mg/L, $p < 0.0001$) on admission compared to those who avoided intensive treatment [11]. This finding was substantiated by a smaller retrospective cohort study that found D-dimer levels were four times the upper limit of normal in patients subsequently admitted to the ICU, a level much higher than non-ICU patients (median D-dimer level 2.4 mg/L vs. 0.5 mg/L, $p = 0.0042$, reference range < 0.5 mg/L) [1]. Remarkably, a multi-centre retrospective cohort study of 191 patients demonstrated that, even after multi-variant analysis, an increased D-dimer on admission was highly associated with in-hospital death (OR 18.42, $p = 0.003$) [12]. Furthermore, 81% of those who did not survive had a D-dimer > 1 μ g/mL on admission compared to just 24% of those who survived [12]. This striking evidence greatly supports the prognostic ability of D-dimer. However, those still hospitalised at the end of the study were excluded; thus, only those who had died or been discharged during the study period were counted. Therefore, this may have exaggerated the difference between the groups as only those with more severe disease at an earlier stage would be included in the analysis of those who died.

Nonetheless, in addition to D-dimer being raised on admission, numerous studies from China have demonstrated that, in non-survivors, D-dimer continues to rise throughout the clinical course of the disease [11,37]. This is compared to a low and stable D-dimer in those who survived. Importantly,

an increased D-dimer was highly associated with acute myocardial injury, diagnosed via a raised cTnI, which as mentioned previously has been correlated with an increased risk of in-hospital death [20]. Therefore, it is reasonable to suggest that D-dimer has prognostic value when taken on admission and could also be used to highlight patients who are deteriorating. However, the practicalities of such an implementation would need to be considered. For example, whilst Wan et al. found that a raised D-dimer was associated with a more severe disease, the median D-dimer level in the severe cases was still within the normal range on admission [28]. This could present a barrier in confidently triaging patients on their D-dimer level if it is still below the cutoff. Although, in this study of 135 patients, there was only one fatality, a death rate much lower than previously reported. Therefore, the raised yet normal D-dimer could be explained by a relatively well cohort.

Prothrombin time (PT) may also hold some predictive value in COVID-19 patients. Contrasting evidence has surfaced concerning the association of an extended PT with admission to ICU. Whilst a smaller retrospective cohort study found that those who were admitted to ICU had a significantly longer PT on admission (median PT 12.2 s vs. 10.7 s, $p = 0.012$), Wang et al. reported no significant difference [1,11]. Although, of the 138 patients included in Wang et al.'s analysis, a large proportion was still hospitalised and not discharged (61.6%) [11]. Therefore, patients who were not admitted to ICU may have deteriorated and subsequently required intensive care; thus, comparing patients by ICU admission may be unreliable in this cohort. Nevertheless, there is good evidence to support that a prolonged PT is associated with in-hospital death. A large multi-centre retrospective cohort study found that a PT over 16 s was greatly associated with in-hospital death (OR 4.62, $p = 0.019$), whilst Tang et al. found that PT time was significantly increased in non-survivors (median PT 15.5 s vs. 13.6 s, $p < 0.001$) [12]. Tang et al. also demonstrated that, from admission, PT continued to rise in those who did not survive, supporting its association with in-hospital death [37]. Like D-dimer, an increased PT was also associated with acute cardiac injury, implying that abnormal coagulation parameters on admission are associated with myocardial injury [20]. However, as previously discussed, the pathology of this injury, whether infarction or myocarditis, is still unclear.

Similar trends have also been noted in platelet counts. There was no difference in the platelet counts on admission of those admitted to ICU [1,11]. However, a reduced platelet count was associated with in-hospital death and cardiac injury. Zhou et al. reported a much lower platelet count in those who died (median platelet count, $165.5 \times 10^9/\text{L}$ vs. $220.0 \times 10^9/\text{L}$, $p < 0.001$) with 20% of non-survivors having a platelet count less than $100 \times 10^9/\text{L}$ on admission compared to just 1% of those who survived [12]. In addition, those with raised cTnI on admission had a significantly lower platelet count compared to those without cardiac injury (median platelet count, $172 \times 10^3/\mu\text{L}$ vs. $216 \times 10^3/\mu\text{L}$, $p < 0.001$). This further illustrates that abnormal coagulation is associated with cardiac injury in hospitalised COVID-19 patients [19].

Lastly, a study of 183 patients found that fibrinogen degradation products (FDP) were also significantly raised on admission in patients that did not survive (median FDP $7.6 \mu\text{g/mL}$ vs. $4.0 \mu\text{g/mL}$, $p < 0.001$) [37]. Whilst fibrinogen levels showed no significant difference on admission, it was significantly lower in non-survivors in late hospitalisation [37]. This suggests that a decreasing fibrinogen level is associated with the progression of the disease; thus, it may aid in the identification of deteriorating patients.

In light of the striking rate of DIC in patients who did not survive, it has been suggested that the use of heparin in COVID-19 may be beneficial. Therefore, Tang et al. conducted a retrospective analysis of COVID-19 patients and found that the use of low molecular weight heparin was associated with improved prognosis in severe COVID-19 cases with a markedly elevated D-dimer [39]. This further supports the pivotal role that abnormal coagulation plays in the deterioration of COVID-19 patients and how coagulation parameters may help in determining the prognosis of patients. Furthermore, it demonstrates that a raised D-dimer may also aid treatment optimisation in severe cases of COVID-19.

Evidently, coagulation parameters have demonstrated their prognostic potential in COVID-19 patients. However, in all studies that demonstrated an association between COVID-19 and coagulation

markers, D-Dimer consistently provided the clearest link to ICU admission and in-hospital death. Additionally, as seen in Table 2, it has been the most widely studied biomarker and thus may be the most reliable in predicting the outcome in COVID-19 patients.

3.2. Angiotensin II

As previously mentioned, SARS-CoV-2 uses the ACE2 receptor for entry into target cells, found commonly in the lungs, heart, and vessels [10]. ACE converts angiotensin I to angiotensin II, which can then activate the angiotensin II receptor type 1 [40]. Angiotensin II has profound effects not limited to the cardiovascular system, including vasoconstriction; the release of pro-inflammatory cytokines, such as IL-6; as well as pro-oxidative effects [41–43]. Numerous studies have demonstrated that the use of ACE inhibitors (ACEIs) and angiotensin II receptor I blockers (ARBs) lead to an increase in expression of the ACE 2 receptor [40]. This has sparked debate surrounding the use of ACEI/ARBs due to potentially enhancing the risk of infection by increasing the entry way, ACE2.

Interestingly, it has been revealed recently that the plasma levels of Angiotensin II were raised in infected patients compared to that of healthy controls [26]. This may be in part explained by the reduction of ACE2 due to the binding and internalisation of the enzyme caused by the virus. Moreover, the level of angiotensin II in COVID-19 patients was strongly associated with viral load and lung injury, suggesting that COVID-19 was causing an imbalance in the renin–angiotensin system [26]. This implies that angiotensin II may be a mediator of the disease, leading to pulmonary vasoconstriction and inflammatory or oxidative organ damage. Therefore, it would be not unreasonable to suggest that the use of an ACEI or ARB may be beneficial in the treatment of COVID-19. Whilst there have been no other studies to date to our knowledge, this suggests that angiotensin II could be used as a biomarker to stratify patients as those with higher angiotensin II would have increased risk of organ failure, thus requiring more intensive treatment. Furthermore, this could provide an explanation for the increased risk of myocardial injury whilst hospitalised with COVID-19. The powerful vasoconstrictive effects of angiotensin II may increase the demand on the heart whilst potentially inducing oxidative damage. This risk of myocardial injury may then be further increased by the coagulative state mentioned previously. However, further studies are essential to support these findings, especially when considering the small sample size of patients in the study.

Table 2. A table highlighting the vascular biomarkers that may have prognostic value in COVID-19.

Vascular Biomarker	Definition	Association with COVID-19	Prognostic Potential	References
D-Dimer	D-dimer is a marker of fibrinolysis. Increased D-Dimer levels are associated with, but not limited to, venous thromboembolism, inflammation, and pregnancy. It is relatively nonspecific [17,44].	Increased D-Dimer is associated with <ul style="list-style-type: none"> • ICU admission • In-hospital death • Acute myocardial injury 	+++	[1,11,12,20,28,37]
PT	PT is used to evaluate the extrinsic and common pathways of coagulation. It is the time taken for plasma to clot after adding thromboplastin. PT is increased in DIC and can be a sign of liver disease or vitamin K deficiency [45].	Increased PT is associated with <ul style="list-style-type: none"> • In-hospital death • Acute myocardial injury • Potentially associated with ICU admission 	++	[1,11,12,20,37]
Platelet Count	Number of platelets in a volume of blood: Decreased in many conditions, namely DIC, anaemia, and marrow failure [46].	Reduced platelet count is associated with <ul style="list-style-type: none"> • In-hospital death • Acute myocardial injury 	++	[11,12,19]

Table 2. *Cont.*

Vascular Biomarker	Definition	Association with COVID-19	Prognostic Potential	References
Fibrinogen	Fibrinogen is an acute phase protein involved in platelet aggregation and is decreased acutely by consumption due to DIC or chronically due to hepatic impairment [18].	Decreasing fibrinogen levels correlates with deteriorating clinical parameters in COVID-19 patients.	+	[37]
FDP	FDP are fragments released following plasmin-mediated degradation of fibrinogen/fibrin and raised in inflammatory and thrombotic conditions [18].	Raised FDP is associated with in-hospital death in COVID-19 patients.	+	[37]
Angiotensin II	Angiotensin II is a circulating hormone involved in the renin–angiotensin system. It is a regulator of blood pressure through vasoconstriction and sympathetic nervous stimulation [41].	Angiotensin II is raised in infected patients compared to control. Raised plasma levels of Angiotensin II associated with • Viral load • Lung injury	+	[24]

Raised levels of D-dimers, Prothrombin time (PT), fibrinogen degradation products (FDP), and angiotensin II and reduced platelet count and fibrinogen levels are all associated with deteriorating clinical parameters in COVID-19 patients. Prognostic potential is judged by the authors on association with clinical findings and the quality of the literature in support of this. PT, prothrombin time; FDP, fibrinogen degradation products; DIC, disseminated intravascular coagulation; ICU, intensive care unit.

4. Concluding Remarks

Biomarkers of acute myocardial injury have evidently revealed their potential in predicting worsening prognosis for COVID-19 patients with and without myocardial injury. cTnI provides remarkable prognostic value for patients at increased risk of worsening outcomes and in-hospital mortality, though studies have also shown the association of raised CK-MB and BNP levels with more severe symptoms of COVID-19. Raised serum cTnT and cTnI levels show a clear correlation with deteriorating health and increased mortality in patients with established CVD or cardiovascular risk factors and even in those presenting without a history of CVD. As a result, detecting elevated serum cTnT or cTnI levels on admission as a routine procedure may be invaluable to reduce mortality and severe COVID-19 patients during a time when ICUs are operating at maximum capacity. Additionally, it may allow healthcare professionals to initiate intensive treatment in those vulnerable patients before COVID-19 symptoms worsen.

Collectively, the evidence presented suggests a common coagulation activation in patients that die from COVID-19. D-dimer has demonstrated predictive value for both ICU treatment and in-hospital death when taken on admission. Furthermore, FDP, PT, and platelets when taken on admission may also highlight those more likely to die in hospital. Therefore, the measurement of coagulation parameters on admission may help in the assignment of scarce ICU beds. The continued activation of coagulation throughout the clinical course of non-survivors, evidenced by an increasing D-dimer level and PT plus a decreasing fibrinogen level, may help identify deteriorating patients that require extra support or palliative care. Furthermore, plasma levels of angiotensin II may offer a novel method of predicting disease severity. Also, the pathogenic role of angiotensin II in COVID-19 and the potential use of ACE/ARBs needs to be more clearly elucidated.

Nonetheless, when considering the prognostic potential of these biomarkers, it is poignant to contemplate whether they are causative in the deterioration of COVID-19 or simply a consequence of disease progression. Additionally, the mechanism concerning the abnormal biomarker levels should be elucidated. For instance, many of the markers of coagulation are raised in inflammatory or hepatic diseases and, thus, are nonspecific (Table 2). Hence, whilst it is clear that the body is in a pro-coagulative

phase, the cause of this is unclear. Further investigation into the role of these biomarkers may permit insight into the pathogenesis of SARS-CoV-2.

Similarly, the exact pathology of myocardial injury in COVID-19 is unknown, although this review has highlighted possible mechanisms to be explored. Firstly, the high association with abnormal coagulation may suggest a causative link. Alternatively, a common trigger, such as angiotensin II, might instigate both coagulation activation and myocardial injury. Nevertheless, more studies are required to elucidate the specific mechanism of myocardial injury and its association with severe inflammation in COVID-19, along with the subsequent detrimental symptoms that often lead to mortality in vulnerable patients.

When reviewing the literature published thus far on COVID-19, the requirement for multi-centre studies with larger cohorts and clinical power is abundantly clear. Furthermore, due to the high demand for research to published, numerous papers included in the review comprise of patients still not discharged from hospital. Consequently, the data has incomplete endpoints, thus reducing the potential clinical translation of their findings. Moreover, the evidence presented only concerns patients presenting to hospital, and further studies in outpatient, primary care, or community settings are required to get a full overview of the clinical severity and cardiovascular impact.

Whilst these cardiovascular biomarkers present excellent prognostic potential, the implementation of their use should be considered. These are routine blood tests done for many well-resourced hospitals; hence, minimal change in practice would be necessary to swiftly implement their use. However, for countries or hospitals with less clinical resources, implementation may be challenging. Furthermore, those less equipped are those most likely to benefit from a prognostic test that would aid in the assignment of scarce resources. Therefore, the development of a rapid tests which could quickly determine an increase in prominent biomarkers may be extremely beneficial. If this was distributed to countries or hospitals less equipped to treat COVID-19, it could greatly support the global battle against this pandemic.

Author Contributions: Writing—original draft preparation, M.A. and T.K.; writing—review and editing, A.A.K. and B.W; supervision, B.W. All authors have read and agreed to the published version of the manuscript.

Funding: This research received no external funding

Conflicts of Interest: The authors declare no conflict of interest.

Abbreviations

ACE	Angiotensin-converting enzyme
ACEI	Angiotensin-converting enzyme 2 inhibitor
ARB	Angiotensin II receptor I blocker
BNP	Brain natriuretic peptide
CK-MB	Creatine kinase-myocardial band
COVID-19	Coronavirus disease
cTnI	Cardiac troponin I
cTnT	Cardiac troponin T
CVD	Cardiovascular disease
DIC	Disseminated intravascular coagulation
FDP	Fibrinogen degradation products
ICU	Intensive care unit
PT	Prothrombin time
SARS-CoV-2	Severe acute respiratory syndrome virus 2

References

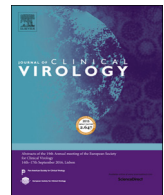
1. Huang, C.; Wang, Y.; Li, X.; Ren, L.; Zhao, J.; Hu, Y.; Zhang, L.; Fan, G.; Xu, J.; Gu, X.; et al. Clinical features of patients infected with 2019 novel coronavirus in Wuhan, China. *Lancet* **2020**, *395*, 497–506. [[CrossRef](#)]
2. Ghebreyesus, T.A. WHO Director-General's Opening Remarks at the Media Briefing on COVID-19-11 March 2020; WHO: Geneva, Switzerland, 2020.
3. Dong, E.; Du, H.; Gardner, L. An interactive web-based dashboard to track COVID-19 in real time. *Lancet Infect. Dis.* **2020**, *20*, 533–534. [[CrossRef](#)]
4. Su, S.; Wong, G.; Shi, W.; Liu, J.; Lai, A.C.K.; Zhou, J.; Liu, W.; Bi, Y.; Gao, G.F. Epidemiology, Genetic Recombination, and Pathogenesis of Coronaviruses. *Trends Microbiol.* **2016**, *24*, 490–502. [[CrossRef](#)]
5. Lee, N.; Hui, D.; Wu, A.; Chan, P.; Cameron, P.; Joynt, G.M.; Ahuja, A.; Yung, M.Y.; Leung, C.B.; To, K.F.; et al. A major outbreak of severe acute respiratory syndrome in Hong Kong. *N. Engl. J. Med.* **2003**, *348*, 1986–1994. [[CrossRef](#)]
6. Mousavizadeh, L.; Ghasemi, S. Genotype and phenotype of COVID-19: Their roles in pathogenesis. *J. Microbiol. Immunol. Infect.* **2020**, in press. [[CrossRef](#)] [[PubMed](#)]
7. de Groot, R.J.; Baker, S.C.; Baric, R.S.; Brown, C.S.; Drosten, C.; Enjuanes, L.; Fouchier, R.A.M.; Galiano, M.; Gorbatenya, A.E.; Memish, Z.A.; et al. Middle East Respiratory Syndrome Coronavirus (MERS-CoV): Announcement of the Coronavirus Study Group. *J. Virol.* **2013**, *87*, 7790–7792. [[CrossRef](#)] [[PubMed](#)]
8. van Boheemen, S.; de Graaf, M.; Lauber, C.; Bestebroer, T.M.; Raj, V.S.; Zaki, A.M.; Osterhaus, A.D.M.E.; Haagmans, B.L.; Gorbatenya, A.E.; Snijder, E.J.; et al. Genomic characterization of a newly discovered coronavirus associated with acute respiratory distress syndrome in humans. *MBio* **2012**, *3*, 12. [[CrossRef](#)]
9. Hoffmann, M.; Kleine-Weber, H.; Schroeder, S.; Krüger, N.; Herrler, T.; Erichsen, S.; Schiergens, T.S.; Herrler, G.; Wu, N.H.; Nitsche, A.; et al. SARS-CoV-2 Cell Entry Depends on ACE2 and TMPRSS2 and Is Blocked by a Clinically Proven Protease Inhibitor. *Cell* **2020**, *181*, 271–280. [[CrossRef](#)] [[PubMed](#)]
10. Junyi, G.; Zheng, H.; Li, L.; Jiagao, L. Coronavirus Disease 2019 (COVID-19) and Cardiovascular Disease: A Viewpoint on the Potential Influence of Angiotensin-Converting Enzyme Inhibitors/Angiotensin Receptor Blockers on Onset and Severity of Severe Acute Respiratory Syndrome Coronavirus 2 Infec. *J. Am. Heart Assoc.* **2020**, *9*, e016219. [[CrossRef](#)]
11. Wang, D.; Hu, B.; Hu, C.; Zhu, F.; Liu, X.; Zhang, J.; Wang, B.; Xiang, H.; Cheng, Z.; Xiong, Y.; et al. Clinical Characteristics of 138 Hospitalized Patients with 2019 Novel Coronavirus-Infected Pneumonia in Wuhan, China. *JAMA J. Am. Med. Assoc.* **2020**. [[CrossRef](#)]
12. Zhou, F.; Yu, T.; Du, R.; Fan, G.; Liu, Y.; Liu, Z.; Xiang, J.; Wang, Y.; Song, B.; Gu, X.; et al. Clinical course and risk factors for mortality of adult inpatients with COVID-19 in Wuhan, China: A retrospective cohort study. *Lancet* **2020**, *395*, 1054–1062. [[CrossRef](#)]
13. Clerkin, K.J.; Fried, J.A.; Raikhelkar, J.; Sayer, G.; Griffin, J.M.; Masoumi, A.; Jain, S.S.; Burkhoff, D.; Kumaraiah, D.; Rabbani, L.; et al. Coronavirus Disease 2019 (COVID-19) and Cardiovascular Disease. *Circulation* **2020**. [[CrossRef](#)] [[PubMed](#)]
14. Zheng, Y.Y.; Ma, Y.T.; Zhang, J.Y.; Xie, X. COVID-19 and the cardiovascular system. *Nat. Rev. Cardiol.* **2020**, *17*, 259–260. [[CrossRef](#)] [[PubMed](#)]
15. Gohar, A.; Chong, J.P.C.; Liew, O.W.; den Ruijter, H.; de Kleijn, D.P.V.; Sim, D.; Yeo, D.P.S.; Ong, H.Y.; Jaufeerally, F.; Leong, G.K.T.; et al. The prognostic value of highly sensitive cardiac troponin assays for adverse events in men and women with stable heart failure and a preserved vs. reduced ejection fraction. *Eur. J. Heart Fail.* **2017**, *19*, 1638–1647. [[CrossRef](#)]
16. Heeschen, C.; Hamm, C.W.; Mitrovic, V.; Lantelme, N.H.; White, H.D. N-terminal pro-B-type natriuretic peptide levels for dynamic risk stratification of patients with acute coronary syndromes. *Circulation* **2004**, *110*, 3206–3212. [[CrossRef](#)]
17. Chopra, N.; Doddamreddy, P.; Grewal, H.; Kumar, P.C. An elevated D-dimer value: A burden on our patients and hospitals. *Int. J. Gen. Med.* **2012**, *5*, 87–92. [[CrossRef](#)]
18. Boral, B.M.; Williams, D.J.; Boral, L.I. Disseminated intravascular coagulation. *Am. J. Clin. Pathol.* **2016**, *146*, 670–680. [[CrossRef](#)]
19. Shi, S.; Qin, M.; Shen, B.; Cai, Y.; Liu, T.; Yang, F.; Gong, W.; Liu, X.; Liang, J.; Zhao, Q.; et al. Association of Cardiac Injury with Mortality in Hospitalized Patients with COVID-19 in Wuhan, China. *JAMA Cardiol.* **2020**. [[CrossRef](#)]

20. Guo, T.; Fan, Y.; Chen, M.; Wu, X.; Zhang, L.; He, T.; Wang, H.; Wan, J.; Wang, X.; Lu, Z. Cardiovascular Implications of Fatal Outcomes of Patients with Coronavirus Disease 2019 (COVID-19). *JAMA Cardiol.* **2020**. [[CrossRef](#)]
21. Yang, J.; Zheng, Y.; Gou, X.; Pu, K.; Chen, Z.; Guo, Q.; Ji, R.; Wang, H.; Wang, Y.; Zhou, Y. Prevalence of comorbidities in the novel Wuhan coronavirus (COVID-19) infection: A systematic review and meta-analysis. *Int. J. Infect. Dis.* **2020**, *94*, 91–95. [[CrossRef](#)]
22. Yang, C.; Jin, Z. An Acute Respiratory Infection Runs Into the Most Common Noncommunicable Epidemic—COVID-19 and Cardiovascular Diseases. *JAMA Cardiol.* **2020**. [[CrossRef](#)] [[PubMed](#)]
23. Lippi, G.; Lavie, C.J.; Sanchis-Gomar, F. Cardiac troponin I in patients with coronavirus disease 2019 (COVID-19): Evidence from a meta-analysis. *Prog. Cardiovasc. Dis.* **2020**. [[CrossRef](#)] [[PubMed](#)]
24. Liu, K.; Fang, Y.-Y.; Deng, Y.; Liu, W.; Wang, M.-F.; Ma, J.-P.; Xiao, W.; Wang, Y.-N.; Zhong, M.-H.; Li, C.-H.; et al. Clinical characteristics of novel coronavirus cases in tertiary hospitals in Hubei Province. *Chin. Med. J.* **2020**, *133*, 1025–1031. [[CrossRef](#)]
25. Xu, Z.; Shi, L.; Wang, Y.; Zhang, J.; Huang, L.; Zhang, C.; Liu, S.; Zhao, P.; Liu, H.; Zhu, L.; et al. Pathological findings of COVID-19 associated with acute respiratory distress syndrome. *Lancet Respir. Med.* **2020**, *8*, 420–422. [[CrossRef](#)]
26. Liu, Y.; Yang, Y.; Zhang, C.; Huang, F.; Wang, F.; Yuan, J.; Wang, Z.; Li, J.; Li, J.; Feng, C.; et al. Clinical and biochemical indexes from 2019-nCoV infected patients linked to viral loads and lung injury. *Sci. China Life Sci.* **2020**, *63*, 364–374. [[CrossRef](#)]
27. Inciardi, R.M.; Lupi, L.; Zaccone, G.; Italia, L.; Raffo, M.; Tomasoni, D.; Cani, D.S.; Cerini, M.; Farina, D.; Gavazzi, E.; et al. Cardiac Involvement in a Patient with Coronavirus Disease 2019 (COVID-19). *JAMA Cardiol.* **2020**. [[CrossRef](#)]
28. Wan, S.; Xiang, Y.; Fang, W.; Zheng, Y.; Li, B.; Hu, Y.; Lang, C.; Huang, D.; Sun, Q.; Xiong, Y.; et al. Clinical Features and Treatment of COVID-19 Patients in Northeast Chongqing. *J. Med. Virol.* **2020**. [[CrossRef](#)]
29. Vestjens, S.M.T.; Spoorenberg, S.M.C.; Rijkers, G.T.; Grutters, J.C.; Ten Berg, J.M.; Noordzij, P.G.; van de Garde, E.M.W.; Bos, W.J.W.; Biesma, D.H.; Endeman, H.; et al. High-sensitivity cardiac troponin T predicts mortality after hospitalization for community-acquired pneumonia. *Respirology* **2017**. [[CrossRef](#)]
30. Bessière, F.; Khenifer, S.; Dubourg, J.; Durieu, I.; Lega, J.C. Prognostic value of troponins in sepsis: A meta-analysis. *Intensive Care Med.* **2013**, *39*, 1181–1189. [[CrossRef](#)]
31. Høiseth, A.D.; Neukamm, A.; Karlsson, B.D.; Omland, T.; Brekke, P.H.; Søyseth, V. Elevated high-sensitivity cardiac troponin T is associated with increased mortality after acute exacerbation of chronic obstructive pulmonary disease. *Thorax* **2011**, *66*, 775–781. [[CrossRef](#)]
32. Metkus, T.S.; Guallar, E.; Sokoll, L.; Morrow, D.; Tomaselli, G.; Brower, R.; Schulman, S.; Korley, F.K. Prevalence and prognostic association of circulating troponin in the acute respiratory distress syndrome. *Crit. Care Med.* **2017**, *45*, 1709–1717. [[CrossRef](#)] [[PubMed](#)]
33. Omland, T. Clinical and laboratory diagnostics of cardiovascular disease: Focus on natriuretic peptides and cardiac ischemia. *Scand. J. Clin. Lab. Investigig. Suppl.* **2005**, *240*, 18–24. [[CrossRef](#)] [[PubMed](#)]
34. Mastro, F.; Guida, P.; Scarscia, G.; Rotunno, C.; Amorese, L.; Carrozzo, A.; Capone, G.; Paparella, D. Cardiac troponin i and creatine kinase-MB release after different cardiac surgeries. *J. Cardiovasc. Med.* **2015**, *16*, 456–464. [[CrossRef](#)] [[PubMed](#)]
35. Lopes, R.D.; Lokhnygina, Y.; Hasselblad, V.; Newby, K.L.; Yow, E.; Granger, C.B.; Armstrong, P.W.; Hochman, J.S.; Mills, J.S.; Ruzyllo, W.; et al. Methods of creatine kinase-MB analysis to predict mortality in patients with myocardial infarction treated with reperfusion therapy. *Trials* **2013**, *14*, 123. [[CrossRef](#)]
36. Wu Alan, H.B.; Feng, Y.J.; Contois, J.H.; Pervaiz, S. Comparison of myoglobin, creatine kinase-MB, and cardiac troponin I for diagnosis of acute myocardial infarction. *Ann. Clin. Lab. Sci.* **1996**, *110*, 70–77.
37. Tang, N.; Li, D.; Wang, X.; Sun, Z. Abnormal coagulation parameters are associated with poor prognosis in patients with novel coronavirus pneumonia. *J. Thromb. Haemost.* **2020**, *18*, 844–847. [[CrossRef](#)]
38. Taylor, F.; Toh, C.-H.; Hoots, K.; Wada, H.; Levi, M. Towards Definition, Clinical and Laboratory Criteria, and a Scoring System for Disseminated Intravascular Coagulation. *Thromb. Haemost.* **2001**, *86*, 1327–1330. [[CrossRef](#)]
39. Tang, N.; Bai, H.; Chen, X.; Gong, J.; Li, D.; Sun, Z. Anticoagulant treatment is associated with decreased mortality in severe coronavirus disease 2019 patients with coagulopathy. *J. Thromb. Haemost.* **2020**, *18*, 1094–1099. [[CrossRef](#)]

40. Bavishi, C.; Maddox, T.M.; Messerli, F.H. Coronavirus Disease 2019 (COVID-19) Infection and Renin Angiotensin System Blockers. *JAMA Cardiol.* **2020**. [[CrossRef](#)]
41. Fyhrquist, F.; Metsarinne, K.; Tikkanen, I. Role of angiotensin II in blood pressure regulation and in the pathophysiology of cardiovascular disorders. *J. Hum. Hypertens.* **1995**, *9* (Suppl. 5), 19–24.
42. Dandona, P.; Dhindsa, S.; Ghanim, H.; Chaudhuri, A. Angiotensin II and inflammation: The effect of angiotensin-converting enzyme inhibition and angiotensin II receptor blockade. *J. Hum. Hypertens.* **2007**, *21*, 20–27. [[CrossRef](#)] [[PubMed](#)]
43. Wen, H. Oxidative stress-mediated effects of angiotensin II in the cardiovascular system. *World J. Hypertens.* **2012**, *2*, 34–44. [[CrossRef](#)] [[PubMed](#)]
44. Wells, P.S.; Anderson, D.R.; Rodger, M.; Forgie, M.; Kearon, C.; Dreyer, J.; Kovacs, G.; Mitchell, M.; Lewandowski, B.; Kovacs, M.J. Evaluation of D-dimer in the diagnosis of suspected deep-vein thrombosis. *N. Engl. J. Med.* **2003**, *349*, 1227–1235. [[CrossRef](#)] [[PubMed](#)]
45. Kamal, A.H.; Tefferi, A.; Pruthi, R.K. How to interpret and pursue an abnormal prothrombin time, activated partial thromboplastin time, and bleeding time in adults. *Mayo Clin. Proc.* **2007**, *82*, 864–873. [[CrossRef](#)] [[PubMed](#)]
46. Smock, K.J.; Perkins, S.L. Thrombocytopenia: An update. *Int. J. Lab. Hematol.* **2014**, *36*, 269–278. [[CrossRef](#)]



© 2020 by the authors. Licensee MDPI, Basel, Switzerland. This article is an open access article distributed under the terms and conditions of the Creative Commons Attribution (CC BY) license (<http://creativecommons.org/licenses/by/4.0/>).



Prognostic value of interleukin-6, C-reactive protein, and procalcitonin in patients with COVID-19

Fang Liu¹, Lin Li¹, MengDa Xu, Juan Wu, Ding Luo, YuSi Zhu, BiXi Li, XiaoYang Song, Xiang Zhou^{*}

Department of Anesthesiology, General Hospital of Central Theater Command of PLA, Wuhan, China



ARTICLE INFO

Keywords:
COVID-19
Interleukin-6
C-reactive protein
Procalcitonin
Prognosis

ABSTRACT

Background: The inflammatory response plays a critical role in coronavirus disease 2019 (COVID-19), and inflammatory cytokine storm increases the severity of COVID-19.

Objective: To investigate the ability of interleukin-6 (IL-6), C-reactive protein (CRP), and procalcitonin (PCT) to predict mild and severe cases of COVID-19.

Study design: This retrospective cohort study included 140 patients diagnosed with COVID-19 from January 18, 2020, to March 12, 2020. The study population was divided into two groups according to disease severity: a mild group (MG) ($n = 107$) and a severe group (SG) ($n = 33$). Data on demographic characteristics, baseline clinical characteristics, and the levels of IL-6, CRP, and PCT on admission were collected.

Results: Among the 140 patients, the levels of IL-6, CRP, and PCT increased in 95 (67.9 %), 91 (65.0 %), and 8 (5.7 %) patients on admission, respectively. The proportion of patients with increased IL-6, CRP, and PCT levels was significantly higher in the SG than in the MG. Cox proportional hazard model showed that IL-6 and CRP could be used as independent factors to predict the severity of COVID-19. Furthermore, patients with $\text{IL-6} > 32.1 \text{ pg/mL}$ or $\text{CRP} > 41.8 \text{ mg/L}$ were more likely to have severe complications.

Conclusion: The serum levels of IL-6 and CRP can effectively assess disease severity and predict outcome in patients with COVID-19.

1. Background

Coronavirus disease 2019 (COVID-19) is highly infectious and contagious. The first COVID-19 epidemic occurred in Wuhan, China, in December 2019 [1,2]. The epidemic was declared to be a public health emergency of international concern by the World Health Organization on January 30, 2020. The clinical manifestations change rapidly, and severe cases can lead to hypoxia, multiple organ dysfunction, and death. However, no reliable indicators are yet available to predict disease severity and progression. The objective of this study is to identify specific serological indicators that can be used for diagnosis and guidance of treatment decisions.

2. Objective

To investigate the ability of IL-6, CRP, and PCT to predict mild and severe cases of COVID-19.

3. Study design

3.1. Methods and definitions

The General Hospital of Central Theater Command of People's Liberation Army was designated to treat COVID-19 patients. This single-center, retrospective observational study was approved by the institutional Research Ethics Committee (Process No. 2020-008-1). A total of 141 cases of COVID-19 were confirmed in this hospital between January 18, 2020, and March 12, 2020. All patients were confirmed positively by SARS-CoV-2 nucleic acid RT-PCR (Ct value ≤ 38.0 , BGI, Shenzhen, China) using specimens derived from oropharyngeal swabs or sputum, prior to or during the hospitalization. All patients were monitored via the electronic health information system, and clinical data were collected until March 12, 2020, the last follow-up date. Patients with severe disease were categorized based on the seventh edition of the Chinese National Health Commission [3] and should meet any of the following criteria: 1) shortness of breath, respiratory rate

* Corresponding author.

E-mail address: zhouxiang188483@126.com (X. Zhou).

¹ These authors contributed equally to this work and should be considered as co-first authors.

≥30 beats per min; 2) oxygen saturation ≤93 % at rest; 3) arterial oxygen partial pressure (PaO_2)/oxygen concentration (FiO_2) ≤300 mmHg (1 mmHg = 0.133 K Pa); and 4) lung images showing obvious progress of lesion size > 50 % within 24–48 h. The patients with mild disease should meet the following criteria: 1) mild clinical symptoms or 2) mild or no lesions on imaging findings.

3.2. Data collection

Data on demographic characteristics, underlying comorbidities, symptoms, physical and radiological findings, and laboratory tests were collected from electronic and paper medical records. Hospitalization time, hospital discharge time, and time from disease onset to hospitalization were also recorded. Body temperature was measured using an infrared thermometer, and fever was defined as temperature ≥37.3 °C. Venous blood samples were collected after 12 h fasting in the morning one day after admission and were analyzed within 2 h. All data were checked by two physicians.

3.3. Statistical analysis

Statistical Package for the Social Sciences software version 25.0 (IBM, Chicago, IL) was used for statistical analysis. Continuous and categorical variables were presented as median (IQR) and n (%), respectively. Mann-Whitney U test, χ^2 test, or Fisher's exact test was used to compare continuous and categorical variables.

The predictive value of serum IL-6, CRP, and PCT was evaluated by measuring the area under the receiver operating characteristic curve (AUROC). The optimal threshold value was obtained by calculating the Youden index. Kaplan-Meier curves were constructed for analyzing survival data. A multivariate Cox proportional risk model was used to determine predictive factors for disease risk.

4. Results

4.1. Demographic data and initial clinical signs and symptoms

A total of 140 patients with COVID-19 were included in this study (one patient was excluded because of massive gastrointestinal hemorrhage). In the study population, 107 patients were assigned to a mild group (MG) and 33 patients were allocated to a severe group (SG). There was no significant difference in the male to female ratio between the two groups. The median age was 65.5 years (range, 23–96). The average age was significantly higher in the SG than in the MG ($P < 0.0001$, Table 1). Overall, the most common initial symptoms were fever (64.3 %) and cough (45.0 %), followed by fatigue, muscle soreness, and chest tightness (Table 1). Most patients had comorbidities, including hypertension (45 %), heart disease (25 %), diabetes (24.3 %), and respiratory diseases (11.4 %). The number of comorbidities was significantly higher in patients in the SG (Table 1). Demographic characteristics are shown in Table 1.

4.2. Serum levels of IL-6, CRP, and PCT varied between mild and severe cases

The levels of IL-6, CRP, and PCT increased in 95 (67.9 %), 91 (65.0 %), and 8 (5.7 %) patients on admission, respectively. The proportion of patients with increased levels of IL-6, CRP, and PCT was significantly higher in the SG ($P < 0.001$, $p < 0.001$, and $p = 0.025$ for IL-6, CRP, and PCT, respectively) (Table 2 and Fig. 1). The AUROC of these parameters ranged between 0.8 and 0.9 (IL-6, 0.808; CRP, 0.858; and PCT, 0.812), indicating a high diagnostic value for clinical severity (Fig. 2). Furthermore, the sensitivity, specificity, and positive and negative predictive values of these inflammatory markers were calculated to obtain the optimal threshold value, which corresponded to 32.1 pg/mL, 41.8 mg/L, and 0.07 ng/mL for IL-6, CRP, and PCT, respectively

(Table 3).

4.3. Serum levels of IL-6, CRP, and PCT can distinguish between severe and mild cases

We hypothesized that patients with higher levels of IL-6, CRP, or PCT were more likely to have severe disease. Patients were reclassified into two groups according to the optimal threshold of these indicators. Kaplan-Meier survival curves showed that patients with IL-6, CRP, or PCT higher than the optimal threshold had a significantly higher probability of developing severe disease (log-rank, $P < 0.0001$, Fig. 3).

The multivariate Cox model showed that IL-6 ($P < 0.001$), CRP ($P < 0.001$), and PCT ($P = 0.002$) could be used as independent factors to predict the severity of COVID-19. The patients with IL-6 > 32.1 pg/mL, CRP > 41.8 mg/L, or PCT > 0.07 ng/mL were more likely to have severe complications (HR, 2.375; 95 % CI, 1.058–5.329; $P < 0.001$ for IL-6; HR, 4.394; 95 % CI, 1.924–10.033; $P < 0.001$ for CRP; HR, 4.908; 95 % CI, 1.797–13.402; $P = 0.002$ for PCT) (Table 4).

5. Discussion

The inflammatory response plays a critical role in COVID-19, and inflammatory cytokine storm increases the severity of COVID-19 [4,5]. Wan et al. [6] found that cytokine storm is crucial to the progression of COVID-19 and can lead to severe complications and death. The fifth edition of "Diagnosis and Treatment of COVID-19" [7] recommends monitoring the cytokine levels to improve treatment efficacy and reduce mortality. The seventh edition of this guideline [3] points out that peripheral blood inflammatory factors such as IL-6 may increase during COVID-19 infection.

The levels of IL-6, CRP, and PCT increased significantly in 67.9 %, 65.0 %, and 5.7 % of patients on admission, respectively. The proportion of patients with increased levels of IL-6, CRP, and PCT was significantly higher in the SG than in the MG, which is consistent with the concept of "cytokine storm" proposed by Professor Li Lanjuan, who demonstrated that inflammatory factors played a crucial role in the progression from mild to severe disease.

Cox proportional hazard model analysis showed that IL-6, CRP, and PCT could be used as independent factors to predict the severity of COVID-19. IL-6 is a multifunctional cytokine that transmits cell signaling and regulates immune cells. This factor has a strong proinflammatory effect with multiple biological functions and plays an important role in inflammation, tumor, and hematological diseases [8,9]. IL-6 is the primary trigger for cytokine storms. Yang et al. [4] pointed out that peripheral blood IL-6 levels could be used as an independent factor to predict the progression of COVID-19, which is consistent with the results of this study; therefore, the role of IL-6 in this disease deserves special attention.

CRP is a non-specific acute-phase protein induced by IL-6 in the liver and a sensitive biomarker of inflammation, infection, and tissue damage [10]. CRP expression level is usually low but increases rapidly and significantly during acute inflammatory responses [11,12]. The elevation of CRP in isolation or in combination with other markers may reveal bacterial or viral infections. Our study explored the relationship between CRP and COVID-19 and found that patients with CRP > 41.8 mg/L were more likely to develop severe disease.

PCT is a glycoprotein without hormonal activity and the precursor of calcitonin [13,14]. Serum PCT levels are usually low or undetectable [15]. PCT levels are increased by bacterial infections and relatively low with viral infections and, therefore, can be used to distinguish between bacterial and viral infections [16]. The higher PCT levels in the SG suggest that severe COVID-19 patients may have concomitant bacterial infections. It should be noted that the optimal cut-off value of PCT was 0.07 ng/mL and did not exceed the normal range (0–0.5 ng/mL), and this result may be due to the small sample size (eight patients).

Table 1

Demographic data and initial clinical signs and symptoms in the study cohort.

	Total n = 140	Mild group n = 107	Severe group n = 33	X ² /Z	p-value
Age	65.5 (54.3–73.0)	62.0 (52.0–69.0)	77.0 (65.5–87.5)		
Sex	Female Male	91 (65.0 %) 49 (35.0 %)	66 (61.7 %) 41 (38.3 %)	25 (75.8 %) 8 (24.2 %)	2.196 0.138
Time from onset to hospitalization (days)	8.0 (4.0–13.8)	8.0 (4.0–14.0)	8.0 (3.5–10.5)	-0.497	0.619
Hospitalization time	19.0 (13.0–29.0)	18.0 (13.0–28.0)	21.0 (12.0–30.5)	-0.469	0.639
Comorbidities	Cardiopathy Respiratory disease Hypertension Diabetes	35 (25.0 %) 16 (11.4 %) 63 (45 %) 34 (24.3 %)	22 (20.6 %) 12 (11.2 %) 41 (38.3 %) 22 (20.6 %)	13 (39.4 %) 4 (12.1 %) 22 (66.7 %) 12 (36.4 %)	4.771 0.000 8.190 3.425
Treatments	Antiviral drugs Antibiotics	131 (93.6 %) 128 (91.4 %)	99 (92.5 %) 95 (88.8 %)	32 (97.0 %) 33 (100 %)	0.255 2.743
Clinical symptoms	Fever Cough Diarrhea Fatigue Loss of appetite Myalgia Dyspnea Chest tightness Nausea Dizziness Headache Abdominal pain	90 (64.3 %) 63 (45.0 %) 5 (3.6 %) 21 (15.0 %) 9 (6.4 %) 13 (9.3 %) 9 (6.4 %) 14 (10.0 %) 3 (2.1 %) 4 (2.9 %) 2 (1.4 %) 3 (2.1 %)	69 (64.5 %) 46 (43.0 %) 4 (3.7 %) 11 (10.3 %) 5 (4.7 %) 9 (8.4 %) 3 (2.8 %) 6 (5.6 %) 0 3 (2.8 %) 2 (1.9 %) 2 (1.9 %)	21 (63.6 %) 17 (51.5 %) 1 (3.0 %) 10 (30.3 %) 4 (12.1 %) 4 (12.1 %) 6 (18.2 %) 8 (24.2 %) 3 (9.1 %) 1 (3.0 %) 0 1 (3.0 %)	0.008 0.741 0.000 6.438 1.253 0.089 7.524 7.771 0.012 1.000 1.000 0.557

Data are median (IQR), n (%), or n/N (%). P-values were calculated using the Mann-Whitney U test, χ^2 test, or Fisher's exact test.**Table 2**

Serum levels of IL-6, CRP, and PCT in patients with COVID-2019.

	Total n = 140	Mild group n = 107	Severe group n = 33	X ² /Z	p-value
IL-6 (pg/mL)					
> 7.0	95 (67.9 %)	63 (58.9 %)	32 (97.0 %)	16.778	< 0.0001
0–7.0	45 (32.1 %)	44 (41.1 %)	1 (3.0 %)		
CRP (mg/L)					
> 8.0	91 (65.0 %)	60 (56.1 %)	31 (93.9 %)	15.895	< 0.0001
0–8.0	49 (35.0 %)	47 (43.9 %)	2 (6.1 %)		
PCT (ng/mL)					
> 0.5	8 (5.7 %)	3 (2.8 %)	5 (15.2 %)	5.030	0.025
0–0.5	132 (94.3 %)	104 (97.2 %)	28 (84.8 %)		

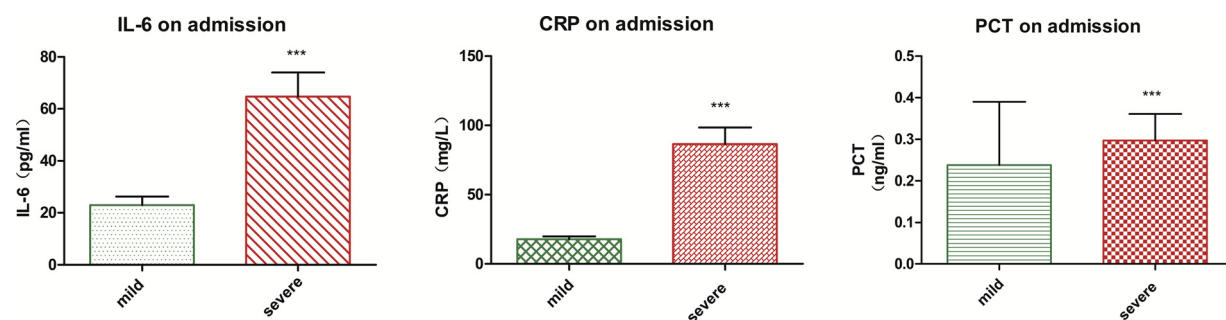
IL-6, interleukin 6; CRP, C-reactive protein; PCT, procalcitonin. Data are presented as median (IQR), n (%), or n/N (%). P-values were calculated using the Mann-Whitney U test, or χ^2 test.

Fig. 1. Serum levels of IL-6, CRP, and PCT in patients with COVID-2019 ***P < 0.0001.

Therefore, the validity of PCT as an independent factor to predict the severity of COVID-19 needs to be further studied using a larger sample size.

This study has limitations. First, the number of cases was small because of the single-center design of the study. Second, clinical data were limited.

In conclusion, the serum levels of IL-6 and CRP have a significant correlation with the severity of COVID-19 and can be used as independent factors to predict disease risk. However, the validity of PCT

needs to be further investigated.

CRediT authorship contribution statement

Fang Liu: Data curation, Writing - original draft. **Lin Li:** Data curation, Writing - original draft. **MengDa Xu:** Data curation, Writing - original draft. **Juan Wu:** Writing - original draft. **Ding Luo:** Data curation. **YuSi Zhu:** Data curation. **BiXi Li:** Data curation. **XiaoYang Song:** Supervision. **Xiang Zhou:** Conceptualization, Methodology,

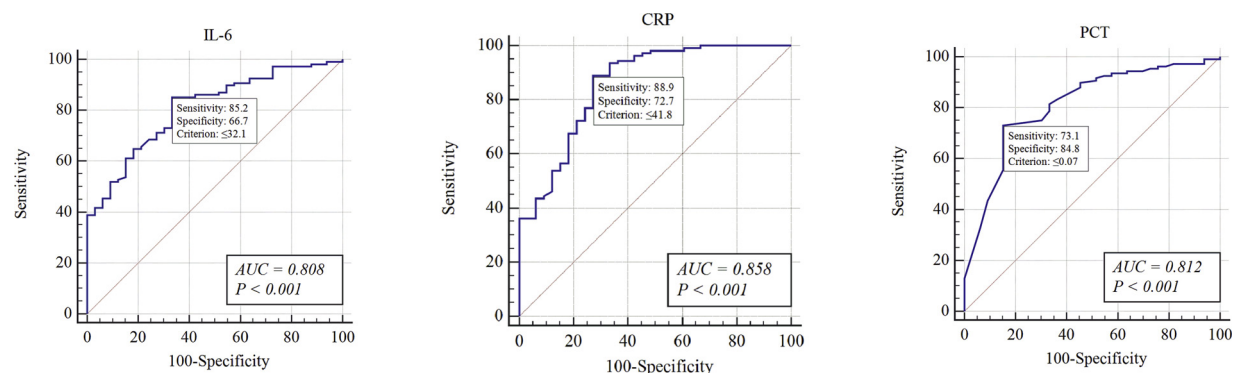


Fig. 2. Receiver operating characteristic curve of interleukin-6 (IL-6), C-reactive protein (CRP), and procalcitonin (PCT) in patients with COVID-2019 on admission.

Table 3

Area under the receiver operating characteristic curve and optimal cut-off values of IL-6, CRP, and PCT.

Variables	Assessment of validity							
	AUC	Optimal cut-off value	Sensitivity	Specificity	Predictive value		Likelihood ratio	
					Positive	Negative	Positive	Negative
IL-6	0.808	32.1 pg/mL	85.19 %	66.67 %	57.89 %	89.21 %	2.55	0.22
CRP	0.858	41.8 mg/L	88.89 %	72.73 %	66.67 %	91.35 %	3.25	0.15
PCT	0.812	0.07 ng/mL	73.15 %	84.85 %	49.12 %	93.98 %	4.82	0.31

AUC, area under the curve.

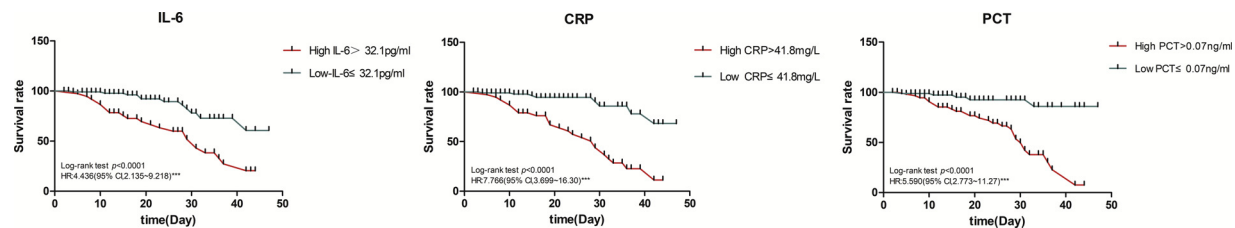


Fig. 3. Survival according to the levels of interleukin-6 (IL-6), C-reactive protein (CRP), and procalcitonin (PCT).

Table 4

Univariate and multivariate Cox model analysis of IL-6, CRP, and PCT.

Variables	Univariate			Multivariate		
	HR	95 % CI	P-value	HR	95 % CI	P-value
IL-6	3.918	1.890–8.119	< 0.0001	2.375	1.058–5.329	< 0.0001
Age	1.056	1.030–1.083	< 0.0001	1.042	1.015–1.070	0.002
Cardiopathy	2.497	1.238–5.037	0.011	–	–	–
Diabetes	1.752	0.862–3.564	0.122	–	–	–
Hypertension	2.244	1.085–4.639	0.029	–	–	–
Polypnea	4.593	1.839–11.474	0.001	–	–	–
CRP	6.503	3.008–14.059	< 0.0001	4.394	1.924–10.033	< 0.0001
Age	1.056	1.030–1.083	< 0.0001	1.037	1.010–1.064	0.007
Hypertension	2.244	1.085–4.639	0.029	–	–	–
Polypnea	4.593	1.839–11.474	0.001	–	–	–
PCT	7.386	2.833–19.257	< 0.0001	4.908	1.797–13.402	0.002
Age	1.056	1.030–1.083	< 0.0001	1.037	1.012–1.064	0.004
Cardiopathy	2.497	1.238–5.037	0.011	–	–	–
Diabetes	1.752	0.862–3.564	0.122	–	–	–
Hypertension	2.244	1.085–4.639	0.029	–	–	–
Polypnea	4.593	1.839–11.474	0.001	–	–	–

HR, hazard ratio.

Writing - review & editing.

Declaration of Competing Interest

We declare that we have no financial and personal relationships

with other people or organizations that can inappropriately influence our work, there is no professional or other personal interest of any nature or kind in any product, service and/or company that could be construed as influencing the position presented in, or the review of, the manuscript entitled, "Prognostic value of interleukin-6, C-reactive

protein, and procalcitonin in patients with COVID-19".

Acknowledgment

This project was supported by the National Natural Science Foundation of China (81901932) and Medjaden Academy & Research Foundation for Young Scientists (COVID-19-MJA20200329). We thank all the medical staff of General hospital of central theater command of PLA for their hard work and great efforts in the outbreak of COVID-19.

References

- [1] C. Huang, Y. Wang, X. Li, L. Ren, J. Zhao, Y. Hu, L. Zhang, G. Fan, J. Xu, X. Gu, Z. Cheng, T. Yu, J. Xia, Y. Wei, W. Wei, X. Xie, W. Yin, H. Lin, M. Liu, Y. Xiao, H. Gao, L. Guo, J. Xie, G. Wang, R. Jiang, Z. Gao, Q. Jin, J. Wang, B. Cao, Clinical features of patients infected with 2019 novel coronavirus in Wuhan, China, *Lancet* 395 (2020) 497–506, [https://doi.org/10.1016/S0140-6736\(20\)30183-5](https://doi.org/10.1016/S0140-6736(20)30183-5).
- [2] D. Wang, B. Hu, C. Hu, F. Zhu, X. Liu, J. Zhang, B. Wang, H. Xiang, Z. Cheng, Y. Xiong, Y. Zhao, Y. Li, X. Wang, Z. Peng, Clinical characteristics of 138 hospitalized patients with 2019 novel coronavirus-infected pneumonia in Wuhan, China, *JAMA* 323 (2020) 1061–1069, <https://doi.org/10.1001/jama.2020.1585>.
- [3] National Health and Health Commission of the People's Republic of China. Diagnosis and Treatment of Pneumonia of New Coronavirus Infection (Trial Version 7). (2020-03-03), <http://www.nhc.gov.cn/yzygj/s7653p/202003/46c9294a7dfe4cef80dc7f5912eb1989.shtml>.
- [4] P.H. Yang, Y.B. Ding, Z. Xu, R. Pu, P. Li, J. Yan, J.L. Liu, F.P. Meng, L. Huang, L. Shi, T.J. Jiang, E.Q. Qin, M. Zhao, D.W. Zhang, P. Zhao, L.X. Yu, Z.H. Wang, Z.X. Hong, Z.H. Xiao, Q. Xi, D.X. Zhao, P. Yu, C.Z. Zhu, Z. Chen, S.G. Zhang, J.S. Ji, G.W. Cao, F.S. Wang, Epidemiological and clinical features of COVID-19 patients with and without pneumonia in Beijing, China, *Medrxiv* (2020), <https://doi.org/10.1101/2020.02.28.20028068>.
- [5] A. Zumla, D.S. Hui, E.I. Azhar, Z.A. Memish, M. Maeurer, Reducing mortality from 2019-nCoV: host-directed therapies should be an option, *Lancet* 395 (2020) e35–e36, [https://doi.org/10.1016/S0140-6736\(20\)30305-6](https://doi.org/10.1016/S0140-6736(20)30305-6).
- [6] S.X. Wan, Q.J. Yi, S.B. Fan, J.L. Lv, X.X. Zhang, L. Guo, C.H. Lang, Q. Xiao, K.H. Xiao, Z.J. Yi, M. Qiang, J.L. Xiang, B.S. Zhang, Y.P. Chen, Characteristics of lymphocyte subsets and cytokines in peripheral blood of 123 hospitalized patients with 2019 novel coronavirus pneumonia (NCP), *medRxiv* (2020), <https://doi.org/10.1101/2020.02.10.20021832>.
- [7] National Health and Health Commission of the People's Republic of China. Diagnosis and Treatment of Pneumonia of New Coronavirus Infection (Trial Version 5). (2020-02-21), <http://www.nhc.gov.cn/jkj/s3578/202002/dc7f3a7326e249c0bad0155960094b0b.shtml>.
- [8] T. Kojii, K. Michael, IL-6 and related cytokines as the critical lynchpins between inflammation and cancer, *Semin. Immunol.* 26 (2014) 54–74, <https://doi.org/10.1016/j.smim.2014.01.001>.
- [9] H.S. Lai, W.H. Lin, S.L. Lai, H.Y. Lin, W.M. Hsu, C.H. Chou, P.H. Lee, Interleukin-6 mediates angiotensinogen gene expression during liver regeneration, *PLoS One* 8 (2013) e67868, <https://doi.org/10.1371/journal.pone.0067868>.
- [10] M.B. Pepys, G.M. Hirschfield, C-reactive protein: a critical update, *J. Clin. Invest.* 111 (2013) 1805–1812, <https://doi.org/10.1172/JCI18921>.
- [11] E. Mooiweer, B. Luijk, M.J. Bonten, M.B. Ekkelenkamp, C-Reactive protein levels but not CRP dynamics predict mortality in patients with pneumococcal pneumonia, *J. Infect.* 62 (2011) 314–316, <https://doi.org/10.1016/j.jinf.2011.01.012>.
- [12] W.H. Hahn, J.H. Song, H. Kim, S. Park, Is procalcitonin to C-reactive protein ratio useful for the detection of late onset neonatal sepsis? *J. Matern. Fetal. Neonatal. Med.* 31 (2018) 822–826, <https://doi.org/10.1080/14767058.2017.1297410>.
- [13] K. Saeed, A.P. Dale, E. Leung, T. Cusack, F. Mohamed, G. Lockyer, S. Arnaudov, A. Wade, B. Moran, G. Lewis, M. Dryden, T. Cecil, J.A. Cepeda, Procalcitonin levels predict infectious complications and response to treatment in patients undergoing cytoreductive surgery for peritoneal malignancy, *Eur. J. Surg. Oncol.* 42 (2016) 234–243, <https://doi.org/10.1016/j.ejso.2015.10.004>.
- [14] J.J. Choi, M.W. McCarthy, Novel applications for serum procalcitonin testing in clinical practice, *Expert Rev. Mol. Diagn.* 18 (2018) 27–34, <https://doi.org/10.1080/14737159.2018.1407244>.
- [15] L.F. Zhang, X.H. Zhang, Serum sTREM-1, PCT, CRP, Lac as biomarkers for death risk within 28 days in patients with severe sepsis, *Open Life Sci.* 13 (2018) 42–47, <https://doi.org/10.1515/biol-2018-0006>.
- [16] A. Rodríguez, L.F. Reyes, J. Monclou, B. Suberviola, M. Bodí, G. Sirgo, J. Solé-Violán, J. Guardiola, D. Barahona, E. Díaz, I. Martín-Loeches, M.I. Restrepo, Relationship between acute kidney injury and serum procalcitonin (PCT) concentration in critically ill patients with influenza infection, *Med. Intensiva.* 42 (2018) 399–408, <https://doi.org/10.1016/j.medin.2017.12.004>.

ARTICLE



<https://doi.org/10.1038/s41467-021-23494-1>

OPEN

SARS-CoV-2 RNAemia and proteomic trajectories inform prognostication in COVID-19 patients admitted to intensive care

Clemens Gutmann^{1,16}, Kaloyan Takov^{1,16}, Sean A. Burnap^{1,16}, Bhawana Singh^{1,16}, Hashim Ali^{1,16}, Konstantinos Theofilatos¹, Ella Reed¹, Maria Hasman¹, Adam Nabeebaccus^{1,2}, Matthew Fish^{1,3,4}, Mark JW. McPhail^{2,5,6}, Kevin O'Gallagher^{1,2}, Lukas E. Schmidt¹, Christian Cassel¹, Marieke Rienks¹, Xiaoke Yin¹, Georg Auzinger², Salvatore Napoli⁵, Salma F. Mujib⁶, Francesca Trovato^{2,5,6}, Barnaby Sanderson^{1,4}, Blair Merrick^{1,7}, Umar Niazi^{1,8}, Mansoor Saqi⁸, Konstantina Dimitrakopoulou⁸, Rafael Fernández-Leiro^{1,9}, Silke Braun^{1,10}, Romy Kronstein-Wiedemann¹¹, Katie J. Doores^{1,3}, Jonathan D. Edgeworth^{3,7}, Ajay M. Shah^{1,2}, Stefan R. Bornstein^{1,12,13}, Torsten Tonn^{1,11,14}, Adrian C. Hayday^{1,3,15}, Mauro Giacca¹, Manu Shankar-Hari^{1,3,4,✉} & Manuel Mayr^{1,12,✉}

Prognostic characteristics inform risk stratification in intensive care unit (ICU) patients with coronavirus disease 2019 (COVID-19). We obtained blood samples ($n = 474$) from hospitalized COVID-19 patients ($n = 123$), non-COVID-19 ICU sepsis patients ($n = 25$) and healthy controls ($n = 30$). Severe acute respiratory syndrome coronavirus 2 (SARS-CoV-2) RNA was detected in plasma or serum (RNAemia) of COVID-19 ICU patients when neutralizing antibody response was low. RNAemia is associated with higher 28-day ICU mortality (hazard ratio [HR], 1.84 [95% CI, 1.22–2.77] adjusted for age and sex). RNAemia is comparable in performance to the best protein predictors. Mannose binding lectin 2 and pentraxin-3 (PTX3), two activators of the complement pathway of the innate immune system, are positively associated with mortality. Machine learning identified 'Age, RNAemia' and 'Age, PTX3' as the best binary signatures associated with 28-day ICU mortality. In longitudinal comparisons, COVID-19 ICU patients have a distinct proteomic trajectory associated with mortality, with recovery of many liver-derived proteins indicating survival. Finally, proteins of the complement system and galectin-3-binding protein (LGALS3BP) are identified as interaction partners of SARS-CoV-2 spike glycoprotein. LGALS3BP overexpression inhibits spike-pseudoparticle uptake and spike-induced cell-cell fusion in vitro.

A full list of author affiliations appears at the end of the paper.

Coronavirus disease 2019 (COVID-19) caused by the severe acute respiratory syndrome coronavirus 2 (SARS-CoV-2; a single-stranded RNA virus) poses an unprecedented challenge to health care systems globally. It is increasingly apparent that conventional prognostic scores for patients admitted to intensive care units (ICUs) such as the Acute Physiology and Chronic Health Evaluation (APACHE II) score¹ and Sequential Organ Failure Assessment (SOFA) score², are unsuitable for outcome prediction in COVID-19 ICU patients^{3–6}.

In this context, circulating SARS-CoV-2 RNA (RNAemia) has been highlighted as a promising prognostic marker in hospitalized COVID-19 patients, as it is associated with disease severity⁷ and mortality^{8–10}, with an estimated prevalence of 10% (95% CI: 5–18%, random-effects model)⁷. Further, we hypothesized that the acute and profound alterations in the innate and adaptive immune system in COVID-19 patients^{3,11–13}, especially in RNAemic patients^{14–18}, will be accompanied by marked changes in the circulating proteome and interactome that will highlight mechanistically relevant signatures and trajectories when compared to non-COVID-19 sepsis and healthy controls. Thus far, proteomics studies have focused on the determination of protein markers of COVID-19 severity^{19–22}, often with healthy individuals as a comparator, but have not assessed the longitudinal relationship between proteomic changes, RNAemia, and 28-day ICU mortality.

In this study, we assessed RNAemia, antibody response against SARS-CoV-2, and proteomic profiles in serial blood samples from COVID-19 patients admitted to two ICUs. Controls included hospitalized, non-ICU patients with and without COVID-19 as well as SARS-CoV-2-negative ICU sepsis patients. Sepsis is defined as organ dysfunction caused by a dysregulated host response to infection^{23,24}. As SARS-CoV-2 infection causes organ

dysfunction (pulmonary and extrapulmonary)^{25,26} and there is overlap in immunological changes between SARS-CoV-2 infection and sepsis^{11,27}, this formed the rationale for using SARS-CoV-2-negative ICU sepsis patients as additional comparators. We compared the associations of RNAemia and protein measurements with 28-day ICU mortality, including established protein markers of acute respiratory distress syndrome (ARDS), i.e., the receptor for advanced glycation end-products (RAGE)^{28–30}, and prognosis in ICU patients with sepsis, i.e., pentraxin-3 (PTX3)^{31–34}. In the context of RNAemia, we explored the plasma protein interactions with the SARS-CoV-2 spike glycoprotein, identifying galectin-3-binding protein (LGALS3BP) as a novel binding partner with antiviral activities.

Results

Demographics and clinical characteristics of COVID-19 patients. 474 blood samples were available for analysis (Fig. 1, Supplementary Fig. 1): 295 longitudinal samples from ICU patients with COVID-19 admitted to two university hospitals (GSTT; $n = 62$ and KCH; $n = 16$) and samples from hospitalized, non-ICU COVID-19 patients for comparison ($n = 45$); ICU and non-ICU patients without COVID-19 served as controls ($n = 55$). The baseline clinical characteristics of all COVID-19 ICU patients are shown in Supplementary Table 1. The primary outcome measure was defined as mortality 28 days after ICU admission. As expected³⁵, non-survivors (23%) were older than survivors ($P = 0.0004$). COVID-19 patients admitted to ICU were predominantly males (72%). All other characteristics, including common comorbidities, the time from symptom onset to ICU admission, APACHE II score, and SOFA score, were similar between ICU survivors and non-survivors. The mortality rate in COVID-19 ICU patients was twice as high as in hospitalized,

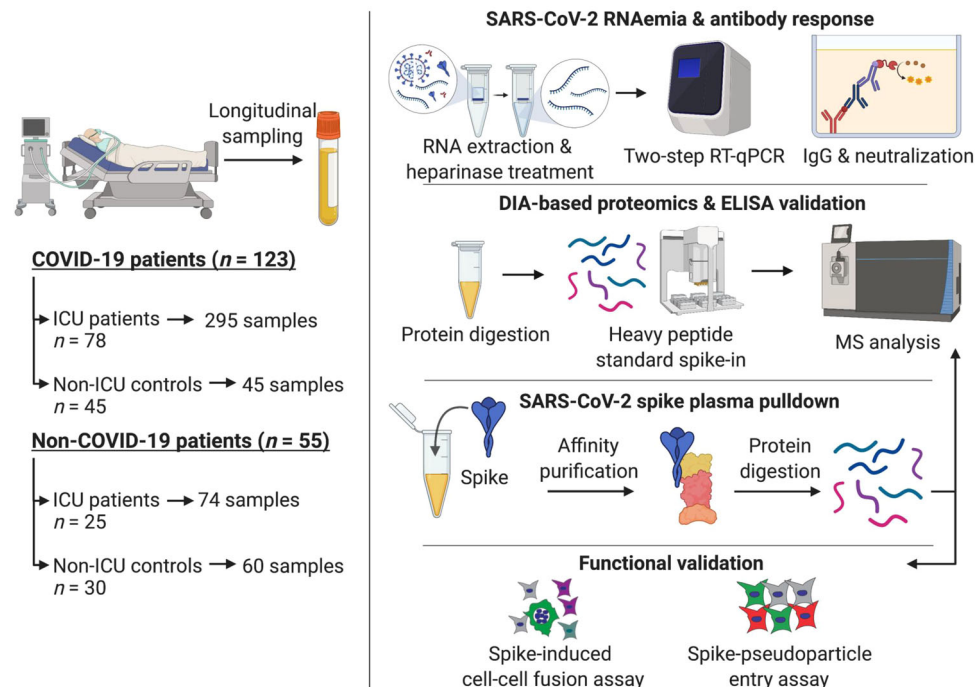


Fig. 1 Schematic of study design. Plasma and serum samples were obtained from multiple patient cohorts across two UK-based university hospitals, including 123 COVID-19 patients: 78 SARS-CoV-2 positive patients in ICU were sampled at multiple time points over a 2-week period and compared to hospitalized non-ICU SARS-CoV-2 positive patients ($n = 45$). We used non-COVID-19 ICU patients ($n = 25$) and patients before undergoing elective cardiac surgery ($n = 30$) as controls. Patient samples were assessed for SARS-CoV-2 RNAemia, antibody responses, and protein changes in the circulation by data-independent acquisition (DIA) mass spectrometry (MS) analysis. Plasma protein interactions with SARS-CoV-2 spike glycoprotein were determined using a pulldown assay followed by data-dependent acquisition (DDA) MS analysis. Functional effects of LGALS3BP were assessed in two assays: SARS-CoV-2 spike-mediated cell-cell fusion (syncytia formation) and cell entry through SARS-CoV-2 spike pseudoparticle assays.

non-ICU COVID-19 patients (23% vs. 11%; Supplementary Table 2).

Frequency of SARS-CoV-2 RNAemia and association with mortality in COVID-19 ICU patients. The presence of circulating viral RNA was analyzed by reverse transcription-quantitative polymerase chain reaction (RT-qPCR). Serum (GSTT; $n = 62$) and plasma (KCH; $n = 16$) samples were collected within 24 h of admission to ICU with COVID-19 and thereafter during week 1, week 2, and again before discharge. Out of 78, 18 (23%) COVID-19 ICU patients had detectable RNAemia within the first 6 days of admission to ICU (Supplementary Table 1). RNAemia was more common early after symptom onset (Supplementary Fig. 2). RNAemia within 6 days of admission to ICU was detectable in 56% of non-survivors but only in 13% of survivors ($P = 0.0006$, Supplementary Table 1). RNAemia was associated with a higher risk of 28-day mortality (hazard ratio [HR], 2.05 [95% CI: 1.38–3.04]), that was comparable to age (2.89 [1.66–5.03] Fig. 2a) and maintained after correction for age and sex (HR, 1.84 [95% CI: 1.22–2.77], Fig. 2b). In comparison, only 2 out of 45 (4%) non-ICU COVID-19 patients tested positive for RNAemia upon hospitalization (Supplementary Table 2). General demographics and baseline clinical characteristics of COVID-19 patients with and without RNAemia in the first 6 days of admission to ICU are presented in Supplementary Table 3. Hypertension ($r = 0.33$, $P = 0.003$), bilirubin ($r = 0.32$, $P = 0.005$), respiration rate ($r = 0.27$, $P = 0.018$), and elevated potassium levels ($r = 0.26$, $P = 0.023$) were positively correlated to RNAemia, while monocyte counts were inversely correlated ($r = -0.23$, $P = 0.047$, Fig. 2c). Hierarchical clustering analysis of all clinical variables and RNAemia is presented in Supplementary Fig. 3. To confirm the specificity of our RT-qPCR assay, we measured SARS-CoV-2 RNAemia in 134 plasma samples from 55 non-COVID-19 patients, all of which tested negative (Supplementary Table 4).

Humoral immune response during SARS-CoV-2 RNAemia. In COVID-19 ICU patients with detailed information on the days, post-onset of symptoms (POS, $n = 70$), IgG antibodies to the S1 domain of SARS-CoV-2 spike glycoprotein and SARS-CoV-2 neutralizing capacity were measured by ELISA and Surrogate Virus Neutralization Test³⁶, respectively. The latter test evaluates the inhibition of binding of the receptor-binding domain (RBD) of SARS-CoV-2 spike to ACE2. COVID-19 ICU patients who tested positive ($n = 15$) or negative ($n = 55$) for RNAemia within the first six days in ICU showed no difference in their strong IgG response to SARS-CoV-2 S1 or in their neutralization capacity (Fig. 2d). However, when individual samples ($n = 232$) were compared, RNAemia positive samples ($n = 29$) had lower anti-SARS-CoV-2 spike IgG levels and lower SARS-CoV-2 neutralization capacity (Fig. 2e).

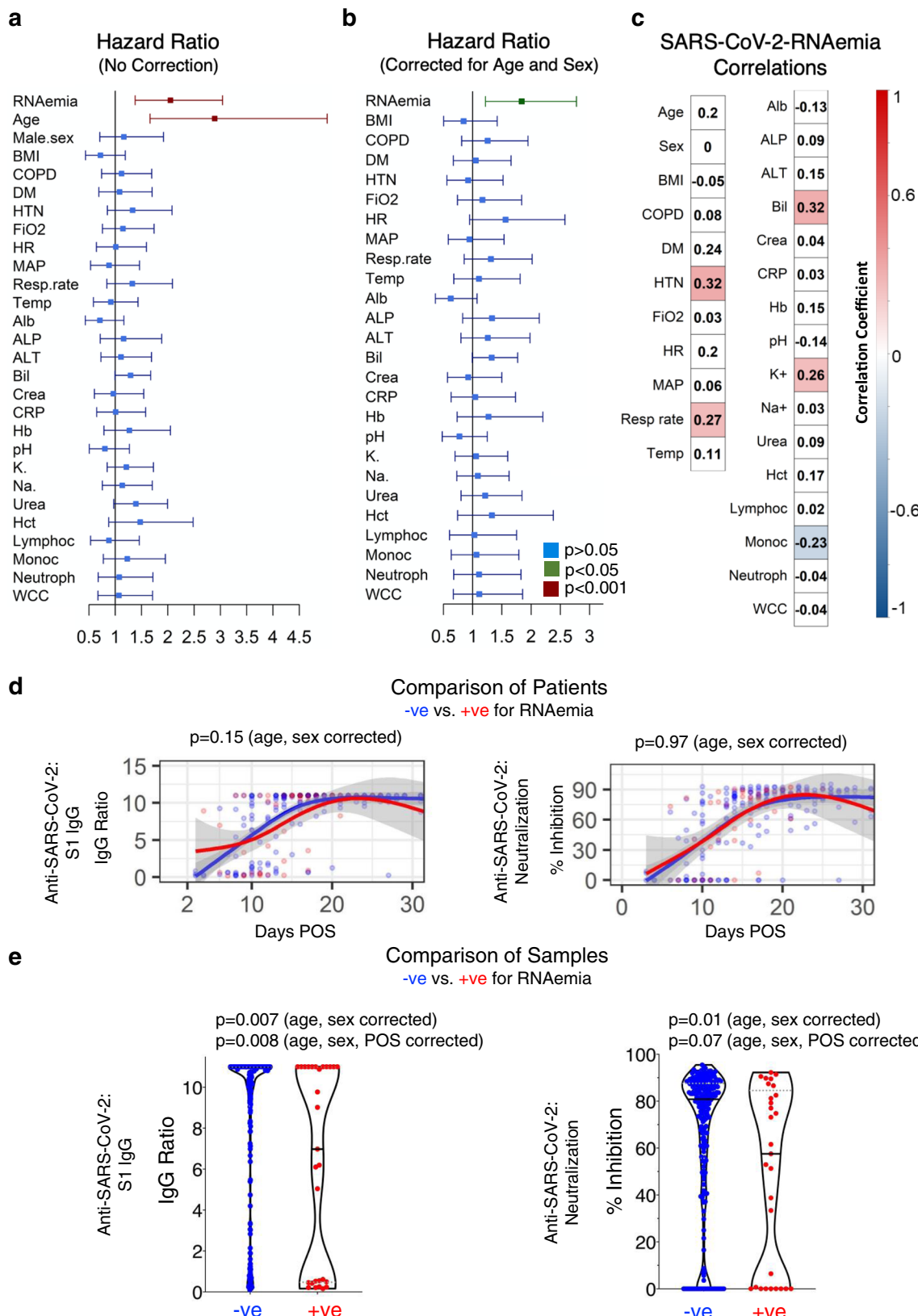
Plasma proteome alterations in COVID-19 ICU patients. To capture the host response of COVID-19 ICU patients, we interrogated their plasma proteome. Baseline plasma samples from COVID-19 ICU patients (KCH cohort, $n = 12$) were compared to plasma samples from COVID-19-negative sepsis ICU patients (sepsis, $n = 12$) and patients prior to undergoing elective cardiac surgery (controls, $n = 30$) (Supplementary Table 4). The plasma proteome was quantified by a data-independent acquisition-mass spectrometry (DIA-MS) approach, using authentic heavy peptide standards representing 500 proteins³⁷, revealing 100 significantly altered proteins across the three patient groups ($q < 0.05$) (Fig. 3a). Hierarchical cluster analysis highlighted a cluster of 47 plasma proteins enriched in COVID-19, including members of the

complement cascade, as well as proteins involved in platelet degranulation, the acute phase response, and coagulation (Fig. 3a, b).

Of the 100 circulating proteins altered across control, sepsis ICU, and COVID-19 ICU patients, 29 overlapped with previous proteomic reports identifying markers of COVID-19 severity^{19,20} (Supplementary Fig. 4). However, only a few were associated with 28-day mortality, as determined through DIA-MS analysis of baseline serum samples obtained from a larger COVID-19 ICU patient cohort (GSTT, $n = 62$) (Fig. 3c). Complement factor B (CFB), carboxypeptidase N (CPN1), and alpha-1-antichymotrypsin (SERPINA3) were all negatively associated with outcome but none of these three associations remained significant after correcting for multiple testing. An independent, publicly available dataset utilizing proximity-extension assays in plasma (Olink Explore 1536, $n = 264$ survivors, $n = 42$ non-survivors, Fig. 4a, Supplementary Table 5)³⁸ also confirmed the lack of outcome association for three other proteins identified as markers of COVID-19 severity in previous proteomics studies^{19,20}: lipopolysaccharide-binding protein, CD14, and inter-alpha-trypsin inhibitor heavy chain H3 (ITIH3) (Fig. 3c).

Protein changes that emerged as significantly associated with mortality in ICU patients but have not been previously linked to the severity of COVID-19, included an elevation of mannose binding lectin 2 (MBL2) and reductions in protein C (PROC), plasminogen (PLG), coagulation factor 7 (F7) and vitamin D-binding protein (GC) (Fig. 3d). A correlation matrix of clinical variables and proteins associated with COVID-19 severity (Fig. 3c) and outcome (Fig. 3c, d) measured in serum of the GSTT cohort is presented in Supplementary Fig. 5.

Predictors of 28-day mortality in COVID-19 patients identified by machine learning. Next, we compared the predictive performance of RNAemia against protein markers and clinical characteristics for 28-day mortality in ICU patients. In the external validation cohort of hospitalized COVID-19 patients described above ($n = 264$ survivors; $n = 42$ non-survivors)³⁸, PROC and F7 were the only proteins associated with 28-day mortality in our DIA-MS data (Fig. 3c, d) that were also measured by Olink proximity-extension assays³⁸. Reduced PROC and F7 were confirmed to be associated with 28-day mortality (Fig. 4a, Supplementary Table 5)³⁸. MBL2 was not part of the Olink panel (Explore 1536) but MBL2 is known to form complexes with PTX3³⁹. Interestingly, PTX3 emerged as one of the proteins most strongly associated with mortality among 1472 unique proteins measured in the external validation, outperforming most measured cytokines and chemokines, showing a larger fold change than PROC or F7 (Fig. 4a, Supplementary Table 5)³⁸. PTX3, a protein we and others have previously highlighted as a prognostic marker in ICU patients with sepsis^{31–34}, also positively associated with COVID-19 mortality in our ICU cohort when measured by ELISA (Fig. 4b). In contrast, RAGE, an established protein marker of ARDS^{28–30}, remained unaffected by SARS-CoV-2 RNAemia and mortality (Fig. 4c, Supplementary Fig. 6a). PTX3 forms multimers that accumulated in the high molecular weight fraction after high-performance size-exclusion chromatography of plasma (Fig. 4d). PTX3 multimers correlated to neutrophil-related proteins such as S100A8/A9, defensin (DEFA1), and SERPINA3 as well as to monocyte/macrophage-related markers such as CD14⁴⁰ (Fig. 4e). A machine learning-based approach was adopted to determine the best prognostic markers (Supplementary Fig. 7). Based on statistical significance ($P < 0.05$, Fig. 4b, Supplementary Table 1), age, RNAemia, urea, and PTX3 were shortlisted as singleton markers. In non-survivors, PTX3 was elevated (median circulating levels, 4.93 ng/ml [IQR: 2.78–6.20])



compared to survivors (median circulating levels, 2.16 ng/ml [IQR: 1.41–3.64], $P = 0.018$, adjusted for age and sex) (Fig. 4b). Although RNAemia surfaced as the best singleton predictor, its sensitivity was low (Supplementary Table 6). Age was the next best singleton predictor, however, its positive predictive value (PPV) of 44% demonstrates low probability confidence in

predicting mortality. When binary combinations were analyzed, two signatures emerged with comparable classification performance: “Age, RNAemia” and “Age, PTX3” (Supplementary Table 6). Although the triplet combination of age, FiO_2 , and RNAemia achieved a ROC of ~86% with a sensitivity of 72.22% and a specificity of 88.33% (Supplementary Table 6), the gain in

Fig. 2 SARS-CoV-2 RNAemia and the humoral immune response. **a** Unadjusted hazard ratios with 95% confidence interval (CI) based on two ICU patient cohorts ($n = 60$ survivors and $n = 18$ non-survivors, KCH and GSTT). Green indicates P value < 0.05 , maroon indicates P value < 0.001 and blue indicates P value > 0.05 . **b**, Hazard ratios with 95% CI after adjustment for age and sex ($n = 60$ survivors and $n = 18$ non-survivors, KCH and GSTT). **c** Association of SARS-CoV-2 RNAemia with binary variables (Cohen's Kappa correlation) and continuous variables (point-biserial correlation). Red indicates positive and blue negative correlation with P value < 0.05 . Abbreviations: Alb albumin, ALP alkaline phosphatase, ALT alanine aminotransferase, Bil bilirubin, COPD chronic obstructive pulmonary disease, Crea creatinine, CRP C-reactive protein, DM diabetes, Hct hematocrit, Hb hemoglobin, HR heart rate, HTN hypertension, Lymphoc lymphocytes, MAP mean arterial pressure, Monoc monocytes, Neutroph neutrophils, K⁺ potassium, Resp. rate respiratory rate, Na⁺ sodium, Temp body temperature, WCC white cell count. **d** Anti-SARS-CoV-2 spike IgG and anti-SARS-CoV-2 neutralization response based on days post-onset of symptoms (POS) in patients who tested positive (red) or negative (blue) for plasma/serum SARS-CoV-2 RNA within the first 6 ICU days (261 samples from $n = 55$ RNAemia negative and $n = 15$ RNAemia positive patients). Lines show fitted generalized additive models (GAM) with gray bands indicating the 95% CI, correcting for age and sex. **e** Anti-SARS-CoV-2 spike IgG levels and anti-SARS-CoV-2 neutralization capacity in individual samples negative (232 samples) or positive (29 samples) for SARS-CoV-2 RNA ($n = 70$ patients). Lines inside violin plots show median (continuous line) and interquartile range (dotted lines). Significance was determined through a Mann-Whitney U test. P values are corrected for age, sex, and days POS. All statistical analyses are two-tailed.

PPV was nominal with no uplift in specificity when compared to "Age, RNAemia", suggesting the binary combination to be an optimal signature to choose. The technical validation of our "Age, RNAemia" model was undertaken using a permutation test for statistical significance of the classifier performance (Supplementary Fig. 8a); and stability of feature importance in an alternate machine learning feature ranking model, i.e., random forest with resampling (Supplementary Fig. 8b). Kaplan-Meier plots (Fig. 5) also illustrate that the binary combinations "Age, RNAemia" ($P < 0.0001$) and "Age, PTX3" ($P < 0.0001$) provide improved stratification.

Longitudinal protein associations with SARS-CoV-2 RNAemia and clinical improvement. To explore whether the association of RNAemia with 28-day mortality may reflect distinct pathological processes, we identified proteins that associate with RNAemia at baseline (Fig. 6a) and over time (Fig. 6b). Nine proteins were significantly associated with RNAemia at baseline which included an increase in plasma protease C1 inhibitor (SERPING1) and complement component C4A (C4A); paralleled by a reduction in VE-cadherin (CDH5) and CFH-related protein 1 (CFHR1) (Fig. 6a). A correlation matrix of clinical variables and proteins associated with RNAemia or outcome is presented in Supplementary Fig. 5. In longitudinal serum samples from the GSTT cohort (baseline, week 1 and week 2; $n = 47$), a greater increase of polymeric immunoglobulin receptor (PIGR) was observed in RNAemia positive, compared to RNAemia negative ICU patients (Fig. 6b). In contrast, plasma kallikrein (KLKB1) levels significantly increased over time but tended to be higher in RNAemia negative ICU patients (Fig. 6b).

Hierarchical cluster analysis upon significantly changing serum proteins over the two-week period (baseline, week 1 and week 2, $n = 47$) revealed four distinct protein clusters (Fig. 6c), which were annotated by gene ontology enrichment analysis. Alterations in PIGR correlated closely with neutrophil degranulation proteins such as S100A8 and S100A9 (Fig. 6c, Cluster 2), while KLKB1 kinetics followed members of the coagulation system such as F11 and SERPIND1 (Fig. 6c, Cluster 4). A comparison of the trajectories of individual proteins between patients who survived and died is shown in Supplementary Fig. 9. The most pronounced changes were observed among proteins constituting cluster 3 ($P = 0.003$) and cluster 4 ($P < 0.001$) (Fig. 6c). L-selectin levels (cluster 3) declined over time but were higher in patients who survived (Supplementary Fig. 9). In contrast, the recovery of many liver-derived proteins was suppressed in patients who died (cluster 4), including apolipoproteins linked to lipid metabolism (i.e., ApoB, ApoC1, and ApoE), biotinidase, complement factor H (CFH), and kininogen (Supplementary Fig. 9). Significant

correlations between proteins constituting these clusters and clinical variables are depicted in Supplementary Fig. 5.

LGALS3BP is enriched in COVID-19 and binds to SARS-CoV-2 spike glycoprotein. To further explore potential mechanistic links between RNAemia and circulating proteins, we searched for binding partners of the SARS-CoV-2 spike glycoprotein. The SARS-CoV-2 spike glycoprotein is the largest protein in the viral envelope, responsible for cell entry, and is the main target of neutralizing antibodies⁴¹. A magnetic affinity pulldown of a His-tagged SARS-CoV-2 spike glycoprotein mixed with plasma from COVID-19 ICU patients was coupled with proteomics to determine interaction partners. Proteomics analysis identified 28 spike-binding proteins after excluding contaminants and non-specific binders (Fig. 7a, b, Supplementary Table 7). Eight of them were immunoglobulins (Fig. 7a) and five were members of the complement system, which are known to directly interact with antigen-bound antibodies (i.e., C1 complement complex, Fig. 7b, Supplementary Table 7). Additional interaction partners included complement component 4-binding proteins alpha and beta (C4BPA and C4BPB), CPN1 (among the proteins associated with 28-day mortality, Fig. 3c), and galectin-3-binding protein (LGALS3BP). Apart from apolipoprotein D (APOD), LGALS3BP was the only protein to be retrieved to a greater extent with spike glycoprotein from plasma of COVID-19 ICU patients compared to COVID-19-negative plasma (Fig. 7c, Supplementary Table 8).

LGALS3BP was markedly elevated in COVID-19 patients as discovered by DIA-MS and confirmed by ELISA, but unchanged between control and sepsis patients without COVID-19 (Fig. 7d). Strikingly, LGALS3BP was among the most elevated proteins when compared to sepsis ICU patients (Fig. 7e). Of the proteins revealed to bind spike, only LGALS3BP and members of the complement cascade were also specifically elevated in COVID-19 ICU patients. LGALS3BP abundance in COVID-19 patients closely correlated with proteins and regulators of the complement cascade (C6, C9, C4BPA, and C4BPB) (Fig. 7f, Supplementary Fig. 10). While LGALS3BP rises with COVID-19 severity²⁰, LGALS3BP levels were not predictive for 28-day mortality and declined over time (Fig. 3c, Supplementary Fig. 11). We, therefore, explored the functional effects of LGALS3BP in cell-based assays.

LGALS3BP impairs SARS-CoV-2 spike-mediated cell-cell fusion and spike-pseudoparticle entry in vitro. SARS-CoV-2 spike induces cell-cell fusion (syncytia formation) when spike, ectopically expressed on the membrane of host cells, binds to ACE2 receptors of adjacent cells^{42–45}. To test the effect of LGALS3BP on spike-mediated syncytia formation, HEK293-ACE2

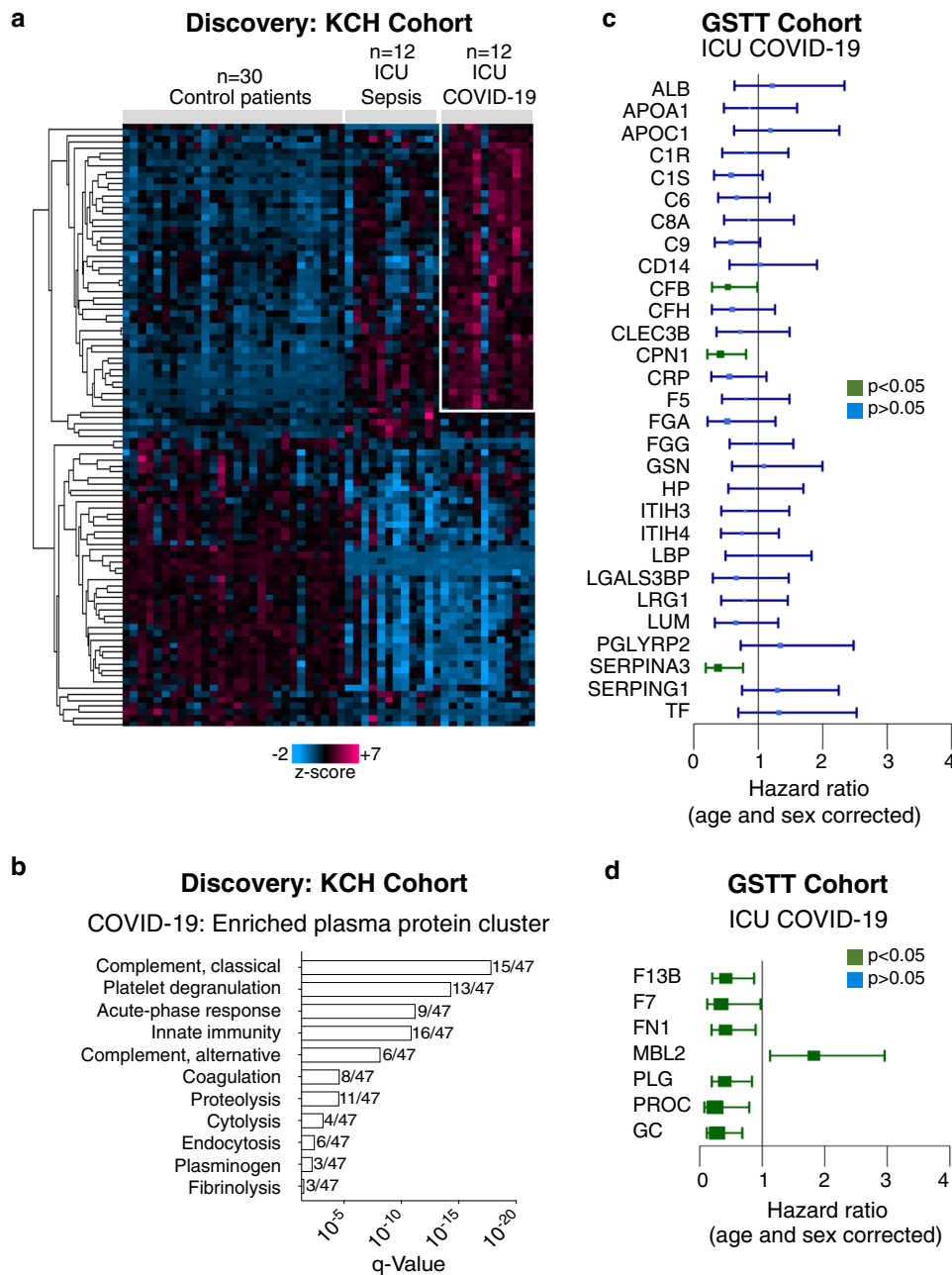


Fig. 3 COVID-19 circulating proteome signature and associations with 28-day mortality. **a** Plasma proteome profiling was conducted using a data-independent acquisition-mass spectrometry (DIA-MS) approach with spiked standards for 500 proteins. Hierarchical cluster analysis was conducted upon significantly changing plasma proteins across control patients before elective cardiac surgery ($n = 30$), ICU patients with sepsis ($n = 12$), and ICU patients with COVID-19 ($n = 12$, KCH). The heatmap highlights 47 proteins enriched in COVID-19. Kruskal-Wallis, Benjamini-Hochberg correction $q < 0.05$. **b** Gene ontology enrichment analysis was conducted upon these 47 proteins and significantly enriched pathways are represented. **c** Twenty-nine common proteins cross-referenced against two published proteomic studies, exploring protein markers of COVID-19 severity. The ability of these 29 proteins to predict 28-day mortality was explored in an independent ICU patient cohort ($n = 62$ patients, GSTT) by DIA-MS, and hazard ratios with 95% CI are shown. **d** Proteomic analysis by DIA-MS conducted upon the serum samples of the GSTT COVID-19 ICU cohort returned additional candidates that predict 28-day mortality as shown on hazard ratio plots with 95% CI ($n = 62$ patients, GSTT). Significance was determined through the Mann-Whitney U test, correcting for age and sex and applying the Benjamini-Hochberg procedure. All statistical analyses are two-tailed.

and Vero cells were transfected with an LGALS3BP-coding plasmid, followed by transfection of a SARS-CoV-2 spike-coding plasmid 24 h later. Small interfering RNA (siRNA)-mediated knockdown of ACE2 served as a positive control (siACE2), while transfection of siNT1 (non-targeting control siRNA), pcDNA3 (plasmid backbone) and pmCherry (plasmid coding for mCherry) served as negative controls (Fig. 8a). As expected, siACE2 significantly reduced spike-mediated cell-cell fusion compared with

siNT1 (Fig. 8b-d). Strikingly, LGALS3BP overexpression also significantly reduced cell-cell fusion compared with pcDNA3 and pmCherry. This reduction in cell-cell fusion was dose-dependent with increasing amounts of LGALS3BP plasmid (Supplementary Fig. 12a-c). To rule out an effect of LGALS3BP on green fluorescent protein (GFP) expression, we co-transfected a GFP-coding plasmid demonstrating that the LGALS3BP-coding plasmid had no effect (Supplementary Fig. 12d, e). Overexpression of LGALS3BP

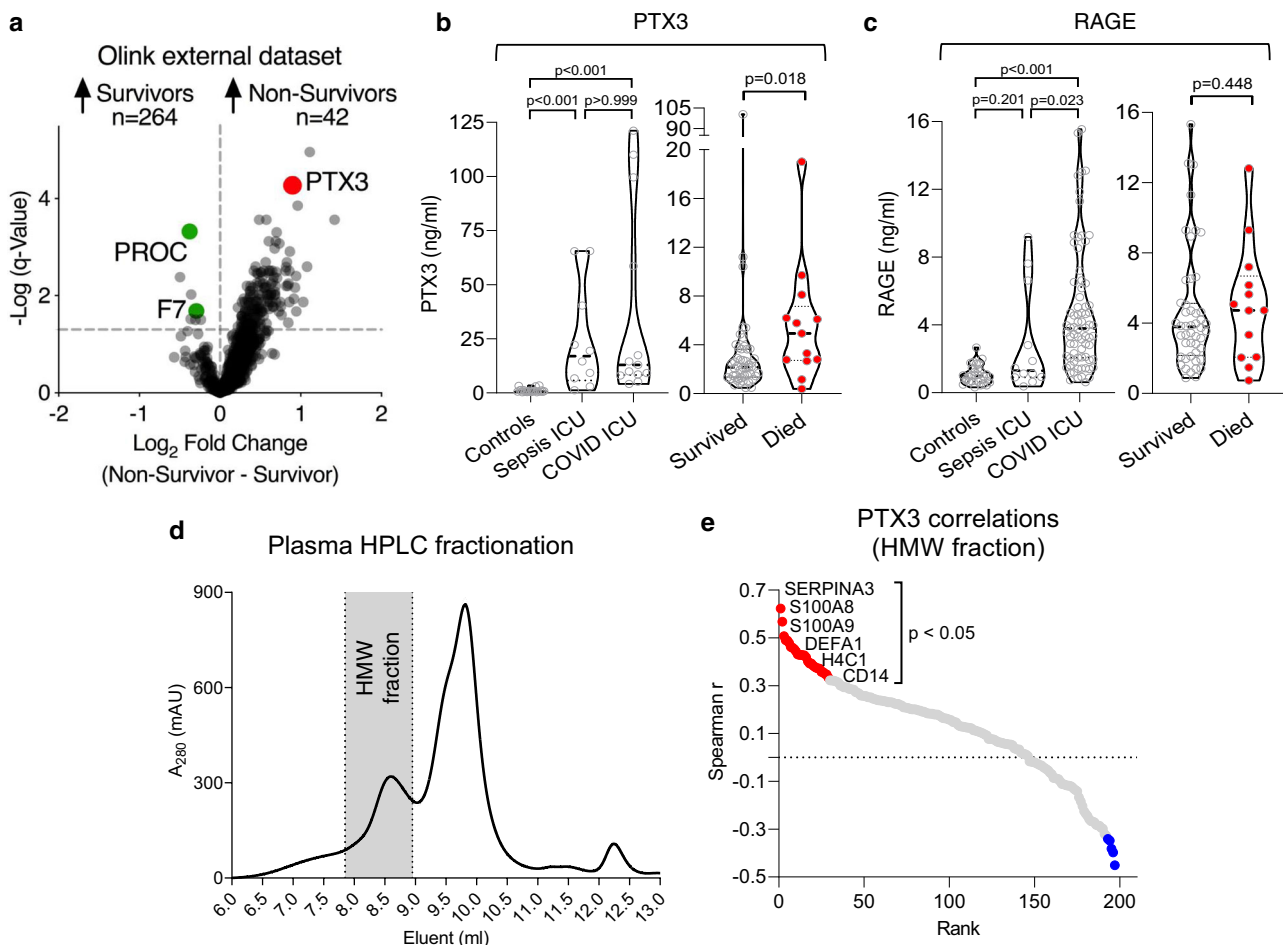


Fig. 4 External protein marker validation and PTX3 selection. **a** PTX3 was among the proteins most strongly associated with poor outcome among 1472 unique plasma proteins (Data provided by the MGH Emergency Department COVID-19 Cohort (Filbin, Goldberg, Hacohen) with Olink Proteomics)³⁸. Of the 10 proteins we found to be associated with outcome in our DIA-MS data (Fig. 3c, d), PROC and F7 were the only proteins also measured in the external validation data, confirming an inverse association with mortality. The log2FC (adjusted for categorical age) was higher for PTX3: 0.8, adjusted P value = 0.00044 compared with PROC: -0.4, adjusted P value = 0.0006 and F7: -0.3, adjusted P value = 0.03. **b** PTX3 measurements by ELISA (KCH and GSTT samples for COVID-19-ICU cohorts in left and right panel, respectively). **c** ELISA measurements for RAGE, as an established marker for ARDS. **d** High-performance liquid chromatography (HPLC) fractionation of plasma ($n = 35$ time points from 13 patients, KCH). PTX3-containing high molecular weight (HMW) fraction is shaded in gray. A₂₈₀ denotes the absorbance of the eluent at 280 nm. **e** Proteomics analysis of the HMW fraction. Significant Spearman correlations of PTX3 with neutrophil- and macrophage-related proteins. All statistical analyses are two-tailed.

and knockdown of ACE2 was verified by immunoblotting in HEK293-ACE2 cells (Supplementary Fig. 12f).

Next, we tested whether LGALS3BP affects the entry of pseudoparticles carrying the spike protein in addition to a GFP reporter, which is an established model of the SARS-CoV-2 entry pathway⁴⁶. For this purpose, we transfected HEK293-ACE2 with an LGALS3BP-coding plasmid followed by the addition of pseudoparticles 24 h later (carrying spike or vesicular stomatitis virus G (VSV-G) protein as a control). siACE2 served as a positive control, while transfection of siNT1 and pcDNA3 served as negative controls (Fig. 8e). As expected, siACE2 significantly reduced cellular uptake of spike-pseudoparticles compared with siNT1 (Fig. 8f, g), while uptake of VSV-G particles remained unaffected (Fig. 8f, h). Strikingly, LGALS3BP overexpression also significantly reduced uptake of spike-pseudoparticles compared with pcDNA3 (Fig. 8f, g), while VSV-G uptake remained unaffected (Fig. 8f, h). In contrast, we did not observe a significant reduction in spike-pseudoparticle uptake when spike-pseudoparticles were pre-incubated with the supernatant from LGALS3BP-expressing cells (Supplementary Fig. 13a–c).

Discussion

The main findings of our study include a 23% prevalence of SARS-CoV-2 RNAemia in ICU patients with COVID-19, an independent association of SARS-CoV-2 RNAemia with risk of 28-day mortality, and a proteomic trajectory characterized by four distinct protein clusters which mirrored the clinical status. Furthermore, we performed pulldown experiments with SARS-CoV-2 spike glycoprotein identifying LGALS3BP and complement system proteins as potential interaction partners. We highlight that overexpression of LGALS3BP impaired SARS-CoV-2 spike glycoprotein-induced syncytia formation and spike-pseudoparticle transduction efficiency.

SARS-CoV-2 RNAemia was observed in 23% of COVID-19 ICU patients within the first six days of admission to ICU, which is more frequent than its estimated prevalence (10% [95% CI: 5–18%, random-effects model]⁷). Likely explanations include: first, the fact that RNAemia is expected to be more common in ICU patients due to disease severity⁷. Second, we optimized detection by performing a two-step RT-qPCR protocol rather than the one-step RT-qPCR protocol used in previous studies in

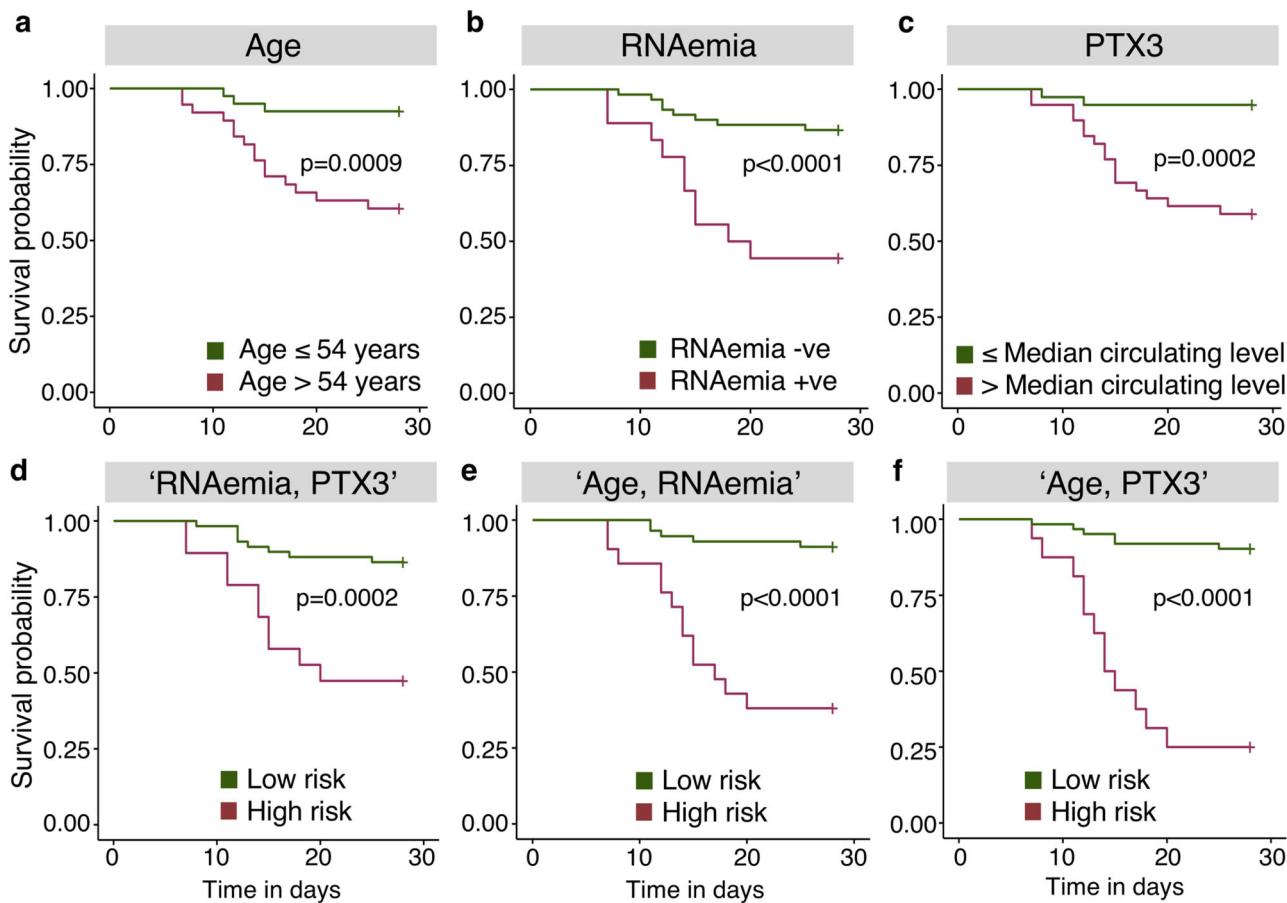


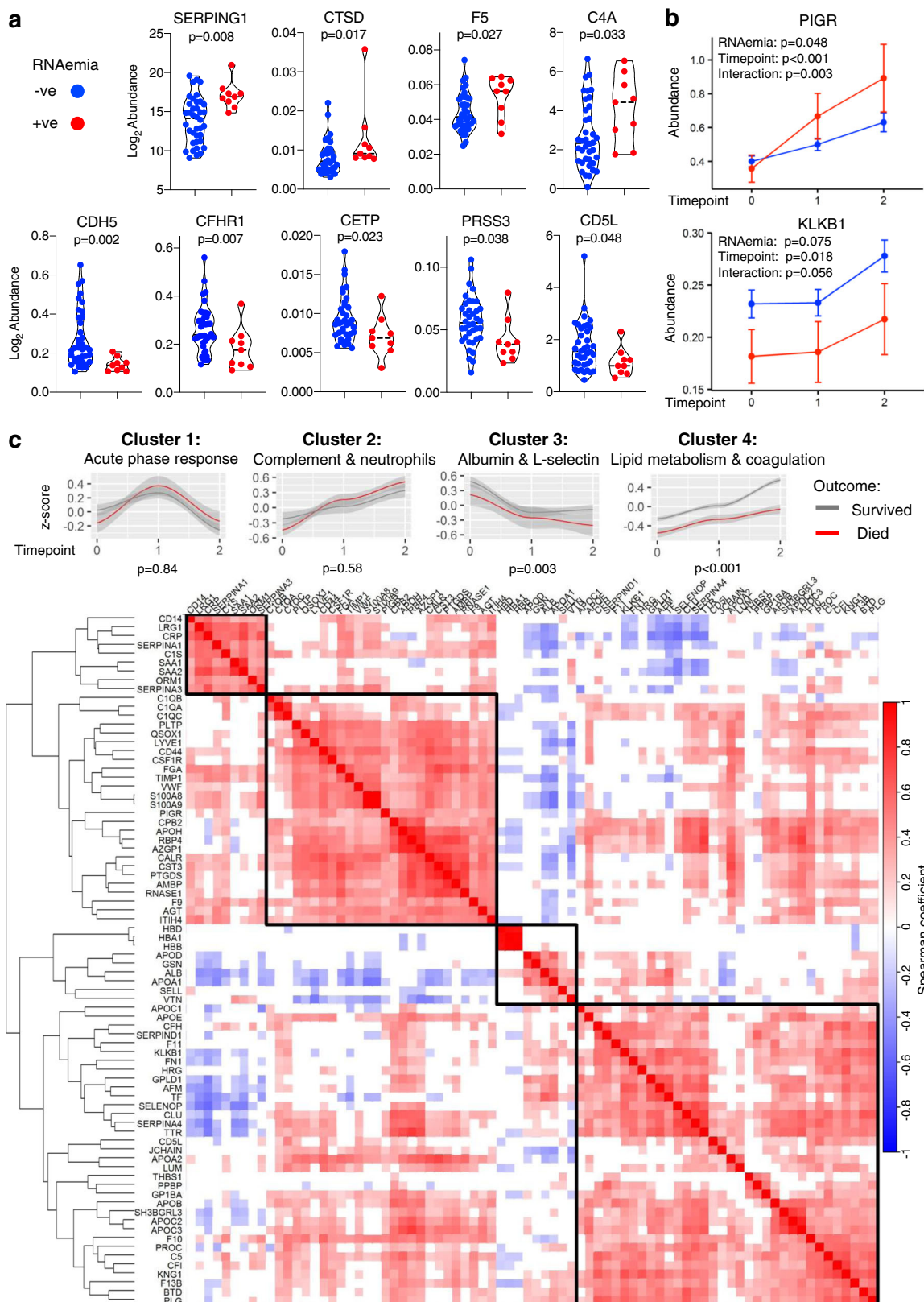
Fig. 5 SARS-CoV-2 mortality prediction using machine learning. **a** Kaplan-Meier plot for age (using the median age of 54 years). **b** Kaplan-Meier plot for SARS-CoV-2 RNAemia. As a single predictor, RNAemia provides the best stratification for survival. **c** Kaplan-Meier plot for PTX3 using the median levels of serum or plasma. **d–f** Kaplan-Meier plots for “RNAemia, PTX3”, “Age, RNAemia”, and “Age, PTX3” combined using support vector machine with radial basis function kernel (SVM RBF), a non-linear machine learning model. The machine learning model selected binary combinations of “Age, RNAemia” and “Age, PTX3” as the best predictors. Kaplan-Meier analysis is two-tailed. Nonsurvivors: $n = 18$; survivors: $n = 60$.

which RNAemia has been assessed thus far. Third, RNAemia was more frequent closer to the onset of symptoms⁷ and when humoral response against SARS-CoV-2 was low. The latter observation was maintained after correcting for time since onset of symptoms. Thus, this is not a mere reflection of low humoral response in early sampling points. Using droplet digital PCR¹⁵, RNAemia might become even more frequent but the clinical relevance of very low levels of RNAemia is unclear.

RNAemia within 6 days of ICU admission was strongly associated with 28-day mortality, which is a well-defined outcome measure in clinical trials^{5,47}. Thus far, studies on RNAemia included predominantly non-ICU patients and associated RNAemia with disease severity⁷. Few studies also reported on the ability of RNAemia to predict mortality^{8–10} but none of these studies specifically focused on ICU patients in which RNAemia is likely to be most informative. Our study focused on COVID-19 ICU patients ($n = 78$) with 28-day mortality as an outcome and included hospitalized, non-ICU COVID-19 patients ($n = 45$) as well as non-COVID-19 patients ($n = 55$). In comparison to RNAemia as assessed in our study (HR, 1.84 [95% CI: 1.22–2.77] adjusted for age and sex), the mortality risk conferred by increased nasopharyngeal SARS-CoV-2 RNA levels was found to be small (HR, 1.07 [95% CI: 1.03–1.11], $n = 1145$)⁴⁸. Correlation between nasopharyngeal and plasma viral load was previously found to be of moderate strength ($r = 0.32$)⁹, suggesting that the viral load in the nasopharyngeal compartment only accounts for a minor part ($r^2 = 10.2\%$)⁹ of the plasma variation. Thus, other

pathological processes are likely to contribute to RNAemia, independent of viral load. RNAemia could be a consequence of severe disease and might reflect the extent of viral dissemination. Notably, serum levels of CDH5, an endothelial-specific surface protein, differed between RNAemia positive versus negative ICU patients. RNAemia was also inversely associated with monocyte counts. A decrease in monocyte counts in COVID-19 patients has been attributed to extravasation and recruitment to lungs^{11,49}.

Similar to previous studies on RNAemia, the proteomic studies published to date focused on hospitalized COVID-19 patients. Proteome changes were associated with disease severity and healthy individuals were often used as controls^{19–22}. In our study we highlight that few of the plasma protein changes associated with disease severity also predict outcome in ICU patients who are already critically ill, and included pre-pandemic sepsis ICU patients as an additional control. An argument could be made for using ARDS controls, due to similarities between non-COVID-19 ARDS and COVID-19 ARDS that we have previously reported^{3,50}. However, in addition to our rationale for non-COVID-19 sepsis controls highlighted earlier, all sepsis patients used as controls were mechanically ventilated⁵¹; would meet the consensus definitions of ARDS⁵²; and could have been enrolled in clinical trials of ARDS⁵³, since the most common etiology of ARDS is infection. The validation of the trajectory of differentially expressed proteins in COVID-19 and their association with outcome was done in serum samples of the larger GSTT COVID-19 ICU cohort ($n = 62$). The Olink measurements in the external



validation cohort were performed in plasma (Fig. 4a). Validation in plasma and in serum ensures that the protein changes are independent of the sample type, which is important for the clinical applicability of findings. The Olink platform covered two (of ten) proteins (PROC, F7) associated with 28-day mortality

measured by our DIA-MS approach, highlighting the complementarity of these different proteomics methods⁵⁴.

Our proteomics data reveal that complement activation is a core component of the overreaction of the immune system in response to COVID-19 (Fig. 3b), with elevated MBL2 being a predictor of

Fig. 6 Circulating protein changes associated with SARS-CoV-2 RNAemia over time. **a** DIA-MS analysis upon serum samples from the GSTT COVID-19 ICU cohort was used to determine proteins that associate with the presence of SARS-CoV-2 RNAemia at baseline ($n=9$ positive, $n=38$ negative). Proteins that were significantly associated with RNAemia at baseline are individually represented as violin plots. Significance was determined through the Limma linear model analysis using Benjamini and Hochberg's FDR correction. **b** Proteins with significantly different trajectories over time (baseline, week 1—time point 1, week 2—time point 2) between RNAemia positive and negative patients ($n=9$ positive patients, $n=38$ negative patients with samples in each of the three-time points, totaling $n=141$ samples). PIGR polymeric immunoglobulin receptor, KLKB1 kallikrein B1. The median and 95% CI of the median is shown. Unadjusted for multiple comparisons. **c** Serial serum samples from COVID-19 ICU patients (GSTT, baseline, week 1 and week 2, $n=10$ nonsurvivors, $n=37$ survivors with samples in each time point, totaling 141 samples) were analyzed by DIA-MS to determine protein changes over time in ICU. The heat map represents a hierarchical cluster analysis conducted upon a Spearman correlation network of significantly changing proteins over time in ICU, applying row-wise corrections for multiple testing using the Benjamini-Hochberg FDR correction. Comparison of the trajectories of protein clusters in COVID-19 ICU patients based on 28-day mortality is also shown. Gene ontology enrichment analysis was used to determine functional pathways associated with the distinct protein clusters identified. Listed are the protein clusters that show a significant change between 28-day survivors (gray) and nonsurvivors (red)—and having significant interaction with time points (baseline, week 1—time point 1, week 2—time point 2). Lines show nonlinear regression curves with gray bands indicating the 95% CI. P values represent the significance of the outcome term in a fitted GAM model when correcting for age and sex. All statistical analyses are two-tailed.

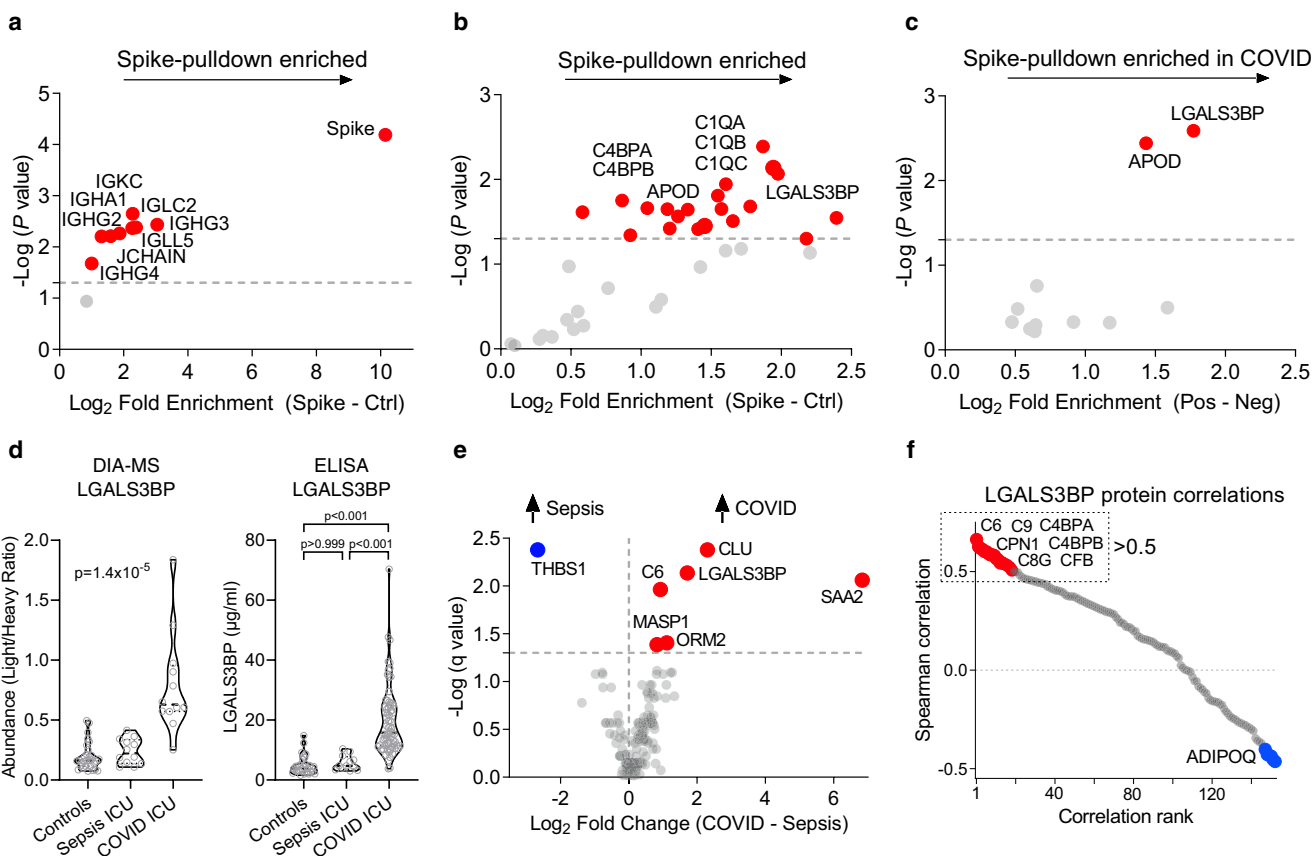


Fig. 7 LGALS3BP interacts with SARS-CoV-2 spike glycoprotein. **a** Magnetic bead-based affinity isolation of binding partners using His-tagged SARS-CoV-2 spike glycoprotein as a bait for proteins in SARS-CoV-2-positive patient plasma ($n=8$). Volcano plot depicting significantly enriched constant chains of immunoglobulins. **b** Volcano plot depicting significantly enriched non-immunoglobulin proteins ($n=8$). **c** Comparison of SARS-CoV-2 spike glycoprotein pulldown using plasma from COVID-19 ICU patients ($n=8$) and non-COVID-19 patients ($n=3$). Significance was determined by paired Student's t tests for (a) and (b) and unpaired Student's t tests for (c). **d** LGALS3BP levels across three patient cohorts as determined by DIA-MS or ELISA: control patients before undergoing elective cardiac surgery ($n=30$), pre-pandemic sepsis ICU patients ($n=12$) and COVID-19 ICU patients ($n=74$). Kruskal-Wallis and Dunn's multiple comparisons tests were used to determine statistical significance. **e** Volcano plot representing protein changes between baseline plasma samples from patients in ICU with either sepsis ($n=12$) or COVID-19 ($n=12$). Significance was determined through the Mann-Whitney U test with Benjamini-Hochberg's FDR correction. **f** Plasma proteins correlating to LGALS3BP after age and sex corrections in COVID-19 ICU patients ($n=12$) are highlighted by a Spearman correlation matrix across the proteomic dataset. Proteins with a Spearman correlation coefficient greater than 0.5 were used for gene ontology pathway enrichment analysis (Supplementary Fig. 10). All statistical analyses are two-tailed.

28-day ICU mortality (Fig. 3d). Systemic complement activation has been associated with respiratory failure in hospitalized COVID-19 patients⁵⁵, and complement deficiencies appear to have protective effects on COVID-19-associated morbidity and mortality⁵⁶. Similarly, C3 deficient mice developed less respiratory

dysfunction following SARS-CoV infection⁵⁷. It was recently reported⁵⁸ that circulating complement factors are high before seroconversion, while markers of systemic complement activation decrease after seroconversion, although this particular study did not include patients admitted to ICU with life-threatening

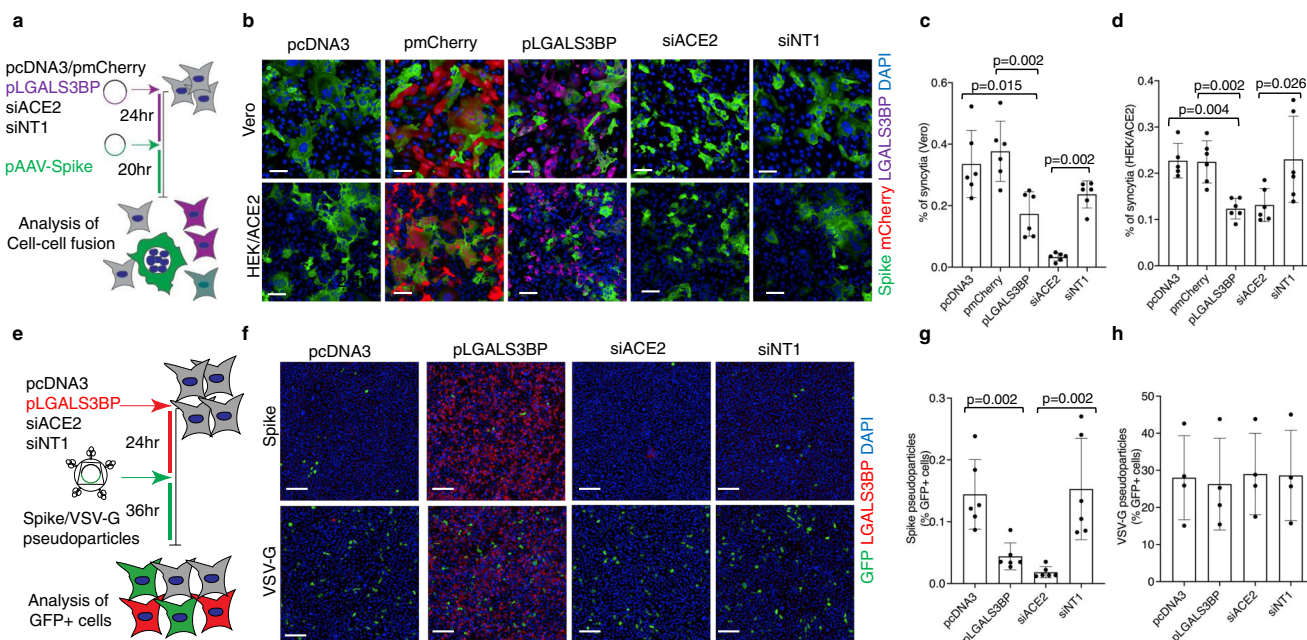


Fig. 8 LGALS3BP overexpression impairs SARS-CoV-2 spike-mediated syncytia formation and cellular uptake of SARS-CoV-2 spike-pseudoparticles. **a** Schematic representation of the SARS-CoV-2 spike-mediated cell-cell fusion assay. **b–d** Vero and HEK293-ACE2 cells were transfected either with pcDNA3 (plasmid backbone), pmCherry (plasmid coding mCherry), pLGALS3BP (plasmid coding LGALS3BP), siACE2 (siRNA targeting ACE2), or siNT1 (non-targeting siRNA), followed by transfection of pAAV-Spike (plasmid coding SARS-CoV-2 spike) 24 h later. After 20 h, cells were stained with anti-LGALS3BP (violet), anti-Spike (green), and DAPI for nuclei (blue). Representative images are shown in **b**, and quantifications are shown in **c** for Vero cells and in **d** for HEK293-ACE2 cells. Data (mean ± standard deviation; $n = 6$; Mann-Whitney U test) are plotted as the percentage of fused cells (syncytia) normalized to the total number of cells. Scale bars in **b** represent 100 μ m. **e** Schematic representation of the SARS-CoV-2 spike/VSV-G pseudoparticle transduction assay. **f–h** HEK293-ACE2 cells were transfected either with pcDNA3, pLGALS3BP, siACE2, or siNT1, followed by the addition of spike- or VSV-G pseudoparticles carrying a GFP reporter 24 h later. After 36 h, cells were stained with anti-LGALS3BP (red), anti-GFP (green), and DAPI for nuclei (blue). Representative images are shown in **f** and quantifications are shown in **g** for spike-pseudoparticles (mean ± standard deviation; $n = 6$; Mann-Whitney U test) and in **h** for VSV-G pseudoparticles (mean ± standard deviation; $n = 3$). Data are plotted as the percentage of GFP-positive cells normalized to the total number of cells. Scale bars in **f** represent 200 μ m. All statistical analyses are two-tailed.

COVID-19⁵⁸. Interestingly, patients with RNAemia (Fig. 6a) showed dysregulation in several components of the complement (SERPING1, C4A, and CFHR1), the coagulation (F5) and the kinin-kallikrein system (KLKB1). Combined activation of these pathways is a hallmark of thromboinflammation^{59,60}.

Viral envelope glycoproteins are known to be an important trigger of the contact pathway of coagulation⁵⁹ and the complement system⁶¹. MBL2 binds to glycoproteins on the viral surface^{62,63} and is a key molecule for the lectin pathway of complement activation in the circulation⁶⁴. MBL2 levels were markedly elevated in COVID-19 ICU patients who died. High levels of MBL2 have previously been associated with lectin pathway-mediated tissue damage^{65,66}. Furthermore, we found MASP1, the downstream mediator of MBL2, to be increased in plasma from COVID-19 ICU patients compared with sepsis patients. Moreover, PTX3 is important for activation (through MBL2 and C1q)³⁹ and regulation (through CFH and C4BPB)^{67,68} of the complement system^{64,69}. The MBL2/PTX3 complex can directly activate the complement system independent of antigen-antibody complexes. Consistent with our previous results on PTX3 in sepsis patients^{31,70}, PTX3 also emerged as a strong predictor for mortality in COVID-19 ICU patients. This is in agreement with other studies^{38,40,71} reporting strong associations of PTX3 with COVID-19 mortality⁷¹. PTX3 is released from neutrophils upon activation^{70,72}, is abundant in macrophages⁴⁰, but also highly expressed in lung and adipose tissue (www.gtexportal.org/home/gene/LGALS3BP). While anti-SARS-CoV-2 antibody levels were similar in COVID-19 ICU patients who survived and died, MBL2 and PTX3 were associated with poor outcome

pointing towards the importance of antibody-independent mechanisms of complement activation in COVID-19. Clinical trials with complement inhibitors are currently ongoing for COVID-19⁵⁹.

Besides members of the complement system, we demonstrate that LGALS3BP is a novel binding partner of SARS-CoV-2 spike glycoprotein. However, the direct interaction between LGALS3BP and SARS-CoV-2 spike remains to be confirmed as pulldown assays cannot rule out indirect binding to the bait protein. Interestingly, the N-terminal domain of the SARS-CoV-2 spike glycoprotein is highly homologous to human galectin-3⁷³, which may explain the interaction we observed with LGALS3BP. The presence of this 13-strand beta-sheet domain is not unique to the SARS-CoV-2 spike as it is also present in the spike glycoproteins of other members of the *Betacoronavirus* genus⁷⁴. It has been proposed that this galectin domain was acquired from host cells and provided the virus with another cell attachment mechanism in its arsenal thus presenting an evolutionary advantage⁷⁵. Thus, it has been suggested that galectin-3 inhibitors may be useful in the treatment of COVID-19^{73,76}. LGALS3BP is prominently expressed in the lung⁷⁷, but also adipose tissue (www.gtexportal.org/home/gene/LGALS3BP) and possesses antiviral activity⁷⁸. The rise in circulating LGALS3BP is not observed in non-COVID-19 sepsis ICU patients, highlighting the specificity for viral over bacterial infections. LGALS3BP directly interacts with adeno-associated viruses, inducing viral particle aggregation and impairment of transduction⁷⁹. LGALS3BP also reduces the infectivity of human immunodeficiency virus (HIV) particles⁸⁰. The antiviral effect on HIV is mediated predominantly through

intracellular effects⁸⁰. Similarly, the supernatant from LGALS3BP-overexpressing cells did not inhibit SARS-CoV-2 spike-pseudoparticle entry. However, LGALS3BP overexpression reduced spike-mediated syncytia formation, and decreased spike-pseudoparticle entry, which are two functional readouts that we have recently used for drug discovery in COVID-19⁴⁵. Thus, LGALS3BP may impede SARS-CoV-2 also through extracellular effects. LGALS3BP may be bound to the extracellular surface of the plasma membrane, similarly to other secreted proteins such as fibroblast growth factor-2⁸¹ and HIV-1 tat protein⁸². The possibility of LGALS3BP binding to carbohydrates on the extracellular surface could explain its antiviral effects⁸³.

In summary, we report that RNAemia in COVID-19 ICU patients is associated with a higher risk of death, an observation that could potentially be a disease-specific enrichment biomarker⁸⁴ for antiviral medications, given the lack of benefit of these drugs in unselected ICU patients with COVID-19⁸⁵. Proteomics analyses of blood samples from ICU patients with COVID-19 uncovered protein trajectories that mirror the recently reported immune trajectory in COVID-19 and add further granularity to COVID-19 biology, in particular with regard to complement activators of the innate immune system (MBL2/PTX3) being associated with mortality; and recovery of several liver-derived proteins being linked to survival⁸⁶. Finally, our observation that LGALS3BP is a novel interaction partner of the SARS-CoV-2 spike glycoprotein has potential therapeutic implications.

Methods

Study design and recruitment. An overview of the study design is presented in Supplementary Fig. 1. COVID-19 cohorts: COVID-19-positive patients, as confirmed by RT-qPCR of nasopharyngeal samples, who were admitted to the ICUs of Guy's and St Thomas' NHS Foundation Trust (GSTT) and King's College Hospital (KCH) between March 12, 2020, and July 1, 2020, were recruited for an observational cohort study with serial blood sampling and analysis of clinical outcomes. The primary outcome measure was defined as mortality 28 days after ICU admission. Serial blood sampling was performed within 24 h of admission to ICU and thereafter three measurements were taken during week 1, week 2, and again before discharge. In addition, we obtained plasma samples from COVID-19 patients upon hospitalization at GSTT (non-ICU COVID-19 cohort). Non-COVID-19 comparator cohorts: Plasma was collected from patients enrolled at the same time in the same KCH ICU as our COVID-19 ICU cohort but who repeatedly tested negative for nasopharyngeal SARS-CoV-2 (intra-pandemic, non-COVID-19 ICU cohort). Serial blood sampling of these samples was performed identically to our COVID-19 cohort. Additionally, pre-pandemic plasma samples from patients recruited at GSTT prior to the COVID-19 pandemic were available as controls. Firstly, this included serial plasma samples from sepsis ICU patients (pre-pandemic, non-COVID-19 ICU sepsis cohort) recruited between October 16, 2019, and February 26, 2020, collected upon admission and at three-time points thereafter. Sepsis was defined according to Sepsis-3 definitions (infection with organ dysfunction defined using SOFA score 2 or more points). The eligibility criteria for this cohort and the study protocol have been reported before⁵¹. Secondly, plasma samples from patients before elective cardiac surgery (pre-pandemic, non-COVID-19 control cohort) recruited between July 8, 2019, and September 9, 2019. The study was approved by an institutional review board (REC19/NW/0750 for all patients recruited at KCH; REC19/SC/0187 for patients recruited at GSTT of the COVID-19 ICU cohort, the pre-pandemic sepsis ICU cohort, the pre-pandemic control cohort; REC19/SC/0232 for patients recruited at GSTT of the non-ICU COVID-19 cohort). Written informed consent was obtained directly from patients (if mentally competent), or from the next of kin or professional consultee. The consent procedure was then completed with retrospective consent if the patient regained capacity.

Inactivation of serum and plasma. Plasma was collected in EDTA BD Vacutainer™ tubes (BD, 362799), whereas serum was collected in silica BD Vacutainer™ tubes (BD, 367820) and left to clot for 15 min. Plasma and serum tubes were then centrifuged at 2000×g for 15 min. Infectious samples were then transferred to a containment level 3 facility for safe inactivation. Samples destined for RNA extraction were inactivated by the addition of 100 µL of serum or plasma to 500 µL QIAzol (Qiagen, 79306), followed by 40 s of vortexing and 5 min incubation at room temperature. Samples destined for protein analysis were inactivated by the addition of 1% (v/v) Triton X-100 (Sigma, T8787) and 1% (v/v) tributyl phosphate (Sigma, 00675), followed by 15 s of vortexing and 4 h incubation at room

temperature. Heat treatment was not performed to avoid protein precipitation. All samples were then frozen at -80 °C until further processing.

High-performance liquid chromatography fractionation of plasma. High-performance size-exclusion chromatography of the KCH plasma samples ($n = 35$, from 13 patients) was performed using a TSKgel® G5000PW_{XL} column (hydroxylated methacrylate, 10 µm particle size, 100 nm mean pore size; Tosoh Bioscience, 0008023) equipped with a TSKgel® PW_{XL} guard column (hydroxylated methacrylate, 12 µm particle size, mixed pore size; Tosoh Bioscience, 0008033). Totally, 20 µL plasma was fractionated with PBS as a mobile phase at a flow rate of 0.6 ml/min. The high molecular weight (HMW) fraction (7.86–8.96 ml eluent) was denatured, reduced, alkylated, digested, and DDA-MS was performed.

RNA extraction and heparinase treatment. Total RNA was extracted using the miRNeasy Mini kit (Qiagen, 217004) according to the manufacturer's recommendations. Total RNA was eluted in 30 µL of nuclease-free H₂O by centrifugation at 8500×g for 1 min at 4 °C. To overcome the confounding effect of heparin on qPCR^{87,88}, RNA was treated with heparinase⁸⁹. Briefly, 8 µL of RNA was added to 2 µL of heparinase 1 from Flavobacterium (Sigma, H2519), 0.4 µL RNase inhibitor (Ribo Lock 40 U/µL, ThermoFisher, EO0381) and 5.6 µL of heparinase buffer (pH 7.5) and incubated at 25 °C for 3 h.

Reverse transcription-quantitative polymerase chain reaction (RT-qPCR). For detection of SARS-CoV-2 RNA we performed a two-step RT-qPCR using the LunaScript® RT SuperMix Kit (NEB, E3010) and the Luna Universal Probe qPCR Master Mix (NEB, M3004) according to the manufacturer's recommendations, apart from reducing the total qPCR reaction volume to 5 µL and loading a cDNA dilution of 1:4 instead of 1:8 when performing the qPCR reaction. Primer/probe sequences targeting the SARS-CoV-2 nucleocapsid (N) gene (N1 and N2) were predesigned by Integrated DNA Technologies (IDT, 10006821, 10006822, 10006823, 10006824, 10006825, and 10006826) according to the protocol for the detection of SARS-CoV-2 of the United States Centers for Disease Control and Prevention (US CDC), using 5' FAM/ZEN™/3' Iowa Black™ FQ probes (Supplementary Table 9). The qPCR reaction concentration for probe (125 nM), forward (500 nM) and reverse primers (500 nM) were used according to the US CDC protocol. A plasmid positive control (2019-nCoV_N Positive Control plasmid, IDT, 10006625) was measured on each qPCR plate. Reactions were loaded using a Bravo Automated Liquid Handling Platform (Agilent). qPCR was performed on a ViiA7 Real-Time PCR System (Applied Biosystems). Samples were considered positive for SARS-CoV-2 if the cycle quantification (Cq) value of either N1 or N2 was below 40. The abundance of SARS-CoV-2 RNA in patients who tested positive had a mean Cq of 34.4; range: 29.8–37.6. As reported before⁹⁰, N1 primers returned lower Cq values (higher abundance) than N2 primers (Supplementary Fig. 14).

Measurement of anti-SARS-CoV-2 antibodies. IgG antibodies against the SARS-CoV-2 spike S1 domain were measured by ELISA (Anti-SARS-CoV-2 IgG ELISA, Euroimmun, EI 2606-9601G) according to the manufacturer's recommendations. Since no international reference serum for anti-SARS-CoV-2 antibodies exists, calibration was performed in ratios, giving relative antibody quantification. Neutralizing antibodies against SARS-CoV-2 were measured using a Surrogate Virus Neutralization Test (SARS-CoV-2 sVNT Kit, GenScript, L00847)³⁶ according to the manufacturer's recommendations. This ELISA-based kit detects antibodies that are able to block the interaction between the SARS-CoV-2 spike RBD and the angiotensin-converting enzyme (ACE2) cell receptor. For technical validation of sVNT measurements in a subset of samples (38 samples from 16 ICU patients), neutralization potency was measured using HIV-1 (human immunodeficiency virus-1) based virus particles, pseudotyped with SARS-CoV-2 spike protein in a HeLa cell line stably expressing the ACE2 receptor¹³. Briefly, serial dilutions of serum samples were prepared with Dulbecco's Modified Eagle Medium (DMEM) containing 10% fetal bovine serum (FBS) and 1% penicillin-streptomycin; and incubated with pseudotyped virus for 1 h at 37 °C in 96-well plates. The HeLa cells stably expressing the ACE2 receptor (provided by J. Voss, Scripps Research) were then added (12,500 cells per 50 µL per well) and the plates were incubated for 72 h. Infection levels were assessed in lysed cells with the Bright-Glo luciferase kit (Promega), using a Victor X3 Multilabel Reader (Perkin Elmer). Measurements were performed in duplicate and duplicates were used to calculate the ID₅₀. In this technical validation, a significant positive correlation was obtained for values returned by both assays ($r = 0.81$, $P < 0.0001$).

In-solution protein digestion. Totally, 10 µL of inactivated serum or plasma were denatured by the addition of urea (final concentration 7.2 M) and reduced using dithiothreitol (final concentration 5 mM) for 1 h at 37 °C and shaking at 180 rpm. Reduced proteins were cooled down to room temperature before being alkylated in the dark for 1 h using iodoacetamide (final concentration 25 mM). An aliquot equivalent to 40 µg of alkylated protein was added to a 0.1 M triethylammonium bicarbonate solution (pH 8.2) and digested for 18 h at 37 °C, shaking at 180 rpm using 1.6 µg of Trypsin/LysC (Promega, V5072). Digested peptide solutions were acidified using trifluoroacetic acid (TFA, final concentration 1%).

Peptide clean-up and stable isotope-labelled standard (SIS) spike-in. Peptide clean-up was achieved using a Bravo AssayMAP Liquid Handling Platform (Agilent). After conditioning and equilibration of the resin, acidified peptide solutions were loaded onto AssayMAP C18 Cartridges (Agilent, 5190-6532), washed using 1% acetonitrile (ACN), 0.1% TFA (aq) and eluted using 70% ACN, 0.1% TFA (aq). Eluted peptides were vacuum centrifuged (Thermo Scientific, Savant SPD131DDA) to dry and resuspended in 40 µL of 2% ACN, 0.05% TFA (aq). For clinical cohort analysis, 6 µL of cleaned peptide solution was added to two injection equivalents of PQ500 SIS mix (Biognosys, Ki-3019-96) using a Bravo Liquid Handling Platform (Agilent).

DIA-MS analysis. Peptides were analyzed using a high-performance liquid chromatography (HPLC)-MS assembly consisting of an UltiMate 3000 HPLC system (Thermo Scientific) which was equipped with a capillary flow selector and coupled via an EASY-Spray NG Source (Thermo Scientific) to an Orbitrap Fusion Lumos Tribrid mass spectrometer (Thermo Scientific). To generate DIA data for serum samples (GSTT COVID-19 ICU cohort) and plasma samples (KCH COVID-19 ICU cohort, the pre-pandemic sepsis ICU cohort and the pre-pandemic control patients before elective cardiac surgery), peptides were injected onto a C18 trap cartridge (Thermo Scientific, 160454) at a flow rate of 25 µL/min for 1 min, using 0.1% formic acid (FA, aq). The initial capillary flow rate was reduced from 3 to 1.2 µL/min in 1 min at 1% B. Peptides were then eluted from the trap cartridge and separated on an analytical column (Thermo Scientific, ES806A, at 50 °C) using the following gradient: 1–11 min, 1–5% B; 11–32 min, 5–18% B; 32–52 min, 18–40% B; 52–52.1 min, 40–99% B; 52.1–58 min, 99% B. The flow rate was increased to 3 µL/min and the column was washed using the following gradient: 58–58.1 min, 99–1% B; 58.1–59.9 min, 1–99% B; 59.9–60 min, 99–1% B. Finally, the column was equilibrated at 1% B for 6 min. In all HPLC-DIA-MS analyses, mobile phase A was 0.1% FA (aq) and mobile phase B was 80% ACN, 0.1% FA (aq). Precursor MS1 spectra were acquired using Orbitrap detection (resolution 60000 at 200 m/z, scan range 329–1201 m/z). Quadrupole isolation was used to sequentially scan 30 precursor m/z windows of variable width (Supplementary Table 10). Per isolation window, semi-targeted Orbitrap MS2 spectra (resolution 30000 at 200 m/z) were collected following higher-energy C-trap dissociation.

MS database search for DIA-MS analysis. PQ500 SIS-spiked DIA data from all serum and plasma samples of the GSTT COVID-19 ICU cohort, the KCH COVID-19 ICU cohort, the non-COVID-19 sepsis ICU cohort and the control patients before elective cardiac surgery were analyzed in Spectronaut v14 (Biognosys AG), using the provided PQ500 analysis plug-in. MS1 and MS2 mass tolerance strategies were set to dynamic. Retention time calibration was achieved using the spiked iRT peptides included in the PQ500 SIS mix. Precursor and protein Q-value cutoff was set to 0.01. Quantification was conducted at an MS2 level using peak areas and individual runs were normalized using the global strategy set to the median. All peptides for reported proteins were manually checked to ensure accurate peak integration across all samples. Peptides with a Q-value of more than 0.01 or a signal to noise ratio of less than 5 were marked as missing. Peptides with more than 30% missing values across all samples were filtered out and the remaining missing values were imputed using the K nearest neighbours (KNN) algorithm ($K = 5$)⁹¹. Spearman correlations of peptides belonging to the same protein were computed. In case more than two peptides per protein were detected, peptides were filtered if their correlation with the remaining peptides was less than $r = 0.4$. In case two peptides per protein were detected, the most abundant peptide was kept even when correlation was less than $r = 0.4$. Final protein abundance was calculated by summing up the quantified peptide abundances. Final quantitative comparisons were conducted using the light/heavy peptide abundance ratio. For validation of our DIA-MS data, we correlated levels to clinical measurements of albumin ($n = 49$, $r = 0.68$, $P < 0.05$) and C-reactive protein ($n = 49$, $r = 0.83$, $P < 0.05$) as examples of high and medium-abundant proteins.

Enzyme-linked immunosorbent assay (ELISA). ELISAs for receptor for advanced glycation end-products (RAGE; R&D Systems, DRG00), galectin-3-binding protein (LGALS3BP; R&D Systems, DGBP30B), and pentraxin-3 (PTX3; Abcam, ab214570) were performed according to the manufacturer's instructions.

SARS-CoV-2 spike protein pulldown. His-tagged recombinant SARS-CoV-2 spike glycoprotein (RP-87680, ThermoFisher) was added to 1:2 PBS-diluted plasma from COVID-19 ICU patients ($n = 8$) or non-COVID-19 controls ($n = 3$) at 200 ng/µL and incubated overnight at 4°C with intermittent mixing. His-tagged spike was then isolated by means of metal affinity magnetic beads (Dynabeads His-Tag Isolation and Pulldown, 10103D, ThermoFisher) and eluted in imidazole-containing phosphate buffer. Proteins in the pulldown isolates were denatured, reduced, alkylated and precipitated, as described above. Proteins interacting non-specifically with the solid phase were determined by incubating plasma samples with magnetic beads without the addition of His-tagged spike. Pulldown of His-tagged spike without the addition of plasma was performed as an additional control. Spike pulldown protein digestion followed the same protocol outlined above.

Data-dependent acquisition (DDA)-MS analysis. Proteins from the spike pulldown experiments were subject to in-solution tryptic digestion and C18 clean-up as described above. Tryptic peptides were analyzed by LC-MS/MS. An UltiMate 3000 HPLC system (Thermo Scientific) with a nanoflow selector was coupled via an EASY-Spray Source (Thermo Scientific) to a Q Exactive HF mass spectrometer (Thermo Scientific, 160454) at a flow rate of 25 µL/min for 1 min, using 0.1% FA (aq). Peptides were eluted from the trap cartridge and separated on an analytical column (EASY-Spray C18 column, 75 µm × 50 cm, Thermo Scientific, ES803A, at 45 °C) at a flow rate of 0.25 µL/min using the following gradient: 0–1 min, 1% B; 1–6 min, 1–6% B; 6–40 min, 6–18% B; 40–70 min, 18–35% B; 70–80 min, 35–45% B; 80–81 min, 45–99% B; 81–89.8 min, 99% B; 89.8–90 min, 99–1% B; 90–120 min, 1% B. Mobile phase A was 0.1% FA (aq) and mobile phase B was 80% ACN, 0.1% FA (aq). Precursor MS1 spectra were acquired using Orbitrap detection (resolution 60,000 at 200 m/z, scan range 350–1600). Data-dependent MS2 spectra of the most abundant precursor ions were obtained after higher-energy C-trap dissociation and Orbitrap detection (resolution 15,000 at 200 m/z) with TopN mode (loop count 15) and dynamic exclusion (duration 40 s) enabled.

MS database search for DDA-MS analysis. Proteome Discoverer software (version 2.3.0.523, Thermo Scientific) was used to search raw SARS-CoV-2 spike glycoprotein pulldown data files against a human database (UniProtKB/Swiss-Prot version 2020_01, 20,365 protein entries) supplemented with SARS-CoV-2 spike glycoprotein (1 protein entry) using Mascot (version 2.6.0, Matrix Science). The mass tolerance was set at 10 ppm for precursor ions and 0.02 Da for fragment ions. Trypsin was used as the digestion enzyme with up to two missed cleavages being allowed. Carbamidomethylation of cysteines and oxidation of methionine residues were chosen as fixed and variable modifications, respectively.

Cell culture. HEK293T cells (ATCC CRL-3216) were cultured in Dulbecco's modified Eagle medium (DMEM) with 1 g/L glucose (Life Technologies) supplemented with 10% FBS (Life Technologies) plus a final concentration of 100 IU/ml penicillin and 100 µg/ml streptomycin, or without antibiotics where required for transfections. Vero (WHO) Clone 118 cells (ECACC 88020401) were cultured in Dulbecco's modified Eagle medium (DMEM, Life Technologies) with 1 g/L glucose (Life Technologies) supplemented with 10% heat-inactivated FBS (Life Technologies) plus a final concentration of 100 IU/ml penicillin and 100 µg/ml streptomycin, or without antibiotics where required for transfection. Cells were incubated at 37 °C, 5% CO₂.

Plasmids. Human ACE2-coding plasmid (Addgene, 1786), pLVTHM/GFP (Addgene, 12247), psPAX2 (Addgene, 12260), pMD2.G (Addgene, 12259) were obtained from Addgene and pCMV6-LGALS3BP (OriGene, RC204918) from ORIGENE. pcDNA3, pAAV-CMV-GFP and pAAV-mCherry were obtained from L. Zentilin (Molecular Medicine Lab, International Centre for Genetic Engineering and Biotechnology, Trieste, Italy). The SARS-CoV-2 spike coding sequence (NCBI accession number NC_045512.2) was codon-optimized and synthesized with a V-5 tag at the C-terminus and then cloned into the pZac 2.1 AAV (pAAV-Spike) vector under the control of a cytomegalovirus promoter. The last 19 amino acids at the C-terminus of the SARS-CoV-2 spike protein contain an endoplasmic reticulum retention sequence, which reduces the yield of spike-pseudoparticle production. For pseudoparticle production, a pAAV-Spike-d19-V5 expression vector was generated, deleting the 19 amino acid endoplasmic reticulum retention signal through PCR amplification (primer sequences are listed in Supplementary Table 9), and cloned into the pAAV-Spike-V5 vector. The construct was verified by sequencing.

Antibodies. Antibodies against the following proteins were used: ACE2 (Abcam, ab15348), LGALS3BP (Abcam, ab217572), SARS-CoV-2 spike protein (GeneTex GTx632604), V5-488 (Thermo Fisher Scientific, 377500A488), α-tubulin (Sigma-Aldrich T5168), mouse-HRP (Abcam ab6789) and rabbit-HRP (Abcam ab205718).

Small interfering RNA and SARS-CoV-2-spike coding plasmid transfections. siRNAs (siACE2, M-005755-00-0005; siNT1, non-targeting siRNA) were reverse transfected in 96 well plates, with the transfection reagent (Lipofectamine RNAi-MAX, Life Technologies) and siRNAs (25 nM) diluted in Opti-MEM (Life Technologies) after 5 min of incubation at room temperature. The transfection mixes were incubated for 30 min at room temperature and then added to the 96-well plates (CellCarrierUltra 96, Perkin Elmer). Reverse transfection of plasmids (pcDNA3, pmCherry, pLGALS3BP) was performed in 96-well plates, using a different amount for each plasmid. Totally, 25 ng to 100 ng of plasmids were diluted in 25 µL of Opti-MEM (Life Technologies) and mixed with the transfection reagent (FuGENE HD, Promega) using a ratio of 1 µg pDNA: 3 µL FuGeneHD. The transfection mixes were incubated for 25 min at room temperature and added to the 96-well plates (CellCarrierUltra 96, Perkin Elmer). After 30 min, 6.5 × 10³ Vero cells or 8 × 10³ HEK293-ACE2 cells were seeded in each well. 24 h after transfection, 75 ng of either pEC117-Spike-V5 or pCMV-EGFP expression plasmids were transfected using a standard forward transfection protocol. After 24 h, cells were fixed in 4% PFA and processed for immunofluorescence.

Pseudoparticle production and transduction. An HIV-1-based replication-deficient lentiviral system was used to produce VSV-G and SARS-CoV-2 spike pseudotyped particles⁹². The particles were produced in HEK293T cells by cotransfected 10 µg PLVTHM(GFP) plasmid, 5 µg psPAX2 (packing vector) and 5 µg pMD2.G (VSV-G pseudotyped particles) or pAAV-SΔc19 (Spike pseudotyped particles) using FugeneHD (Promega) transfection reagent in a ratio of 1 µg pDNA: 3 µl FugeneHD⁹². Viral supernatants were collected 48 h after transfection and centrifuged at 2105×g for 10 min at 4 °C. The supernatants were then filtered with a 0.45 µm pore size filter, aliquoted and stored at -80 °C. For pseudoparticle transduction, 24 h before transduction, both siRNAs and plasmids were transfected into the HEK293 cell expressing ACE2 by using a reverse transfection protocol. 24 h after transfection, equal amounts of VSV-G or Spike pseudoparticles were added to each treatment. After 36 h, cells were fixed, nuclei were labelled with Hoechst and assessed for pseudoparticle transduction efficiency based on GFP expression.

Immunofluorescence. After fixation in 4% PFA for 10 min at room temperature, cells were washed two times in 100 µL/well (96-well plate) of 1× PBS and then permeabilized in same volumes of 0.1% Triton X100 (Sigma-Aldrich 1086431000) for 10 min at room temperature. Cells were then washed two times with 1× PBS and blocked in 2% bovine serum albumin (BSA) for 1 h at room temperature. After blocking, 45 µL/well (96-well plate) of diluted primary antibody (1:500 in 1% BSA SARS-CoV-2 spike antibody or V5-488, and Flag/LGALS3BP antibody were added to each well and incubated overnight at 4 °C. Cells were then washed two times in 1× PBS, the 1× PBS was removed and 45 µL/well of diluted (1:500 in 1% BSA) secondary antibodies were added to each well and incubated 2 h at room temperature. Cells were then washed two times in 1× PBS. Nuclear staining was performed by Hoechst 33342 (1:5000) according to manufacturer's instruction.

Image acquisition and analysis of syncytia and pseudoparticle entry. Syncytia: Image acquisition was performed using the Operetta CLS high content screening microscope (Perkin Elmer) with a Zeiss 20× (NA = 0.80) objective, a total of 25 fields were acquired per wavelength, well and replicate (~10,000–15,000 cells per well and replicate). Images were subsequently analyzed, using the Harmony software (version 4.9, PerkinElmer). Images were first flatfield-corrected and nuclei were segmented using the "Find Nuclei" analysis module (Harmony software, version 4.9, PerkinElmer). The thresholds for image segmentation were adjusted according to the signal to background ratio. The splitting coefficient was set in order to avoid splitting of overlapping nuclei (fused cells). The intensity of the green fluorescence (spike/GFP) was calculated using the 'Calculate Intensity Properties' module (Harmony software, version 4.9, PerkinElmer). All cells that scored a nuclear area greater than 4 times the average area of a single nucleus and simultaneously showed a green signal (spike) in the cytoplasm were considered as syncytia. In the case of manual quantification of syncytia, >3 fused nuclei were counted as syncytia, when the cytoplasm showed a green signal (spike). Data are expressed as the percentage of fused cells by calculating the average number of fused cells normalized to the total number of cells per well. Pseudoparticle entry: Mean intensities of the segmented nucleus in the DAPI channel and the Hoechst channel for each nucleus across all fields were extracted. Each assay plate included siACE2 (siRNA targeting ACE2) as a positive control as well as pcDNA3 and siNT1 (non-targeting siRNA) as negative controls. Briefly, nuclei were segmented based on Hoechst staining, and cells were then classified as positive or negative depending on the GFP signal. Data are expressed as the percentage of GFP-positive cells by calculating the average number of GFP-positive cells normalized to the total number of cells per well.

Western blotting. After 48 h of transfection with siRNAs or plasmids, supernatants were collected, and cell debris was removed by centrifugation. HEK293 cell membranes were isolated using the Mem-PERTM Plus Membrane Protein Extraction Kit (Thermo Fisher, 89842), according to the manufacturer's instructions. Equal amounts of total cellular proteins (15–20 µg), as measured by BCA assay (Thermo Fisher, 23227), were resolved by electrophoresis in 4–20% gradient polyacrylamide gels (Mini-PROTEAN, BiOrad) and transferred to nitrocellulose/PVDF membranes (GE Healthcare). Membranes were blocked at room temperature for 60 min with PBST (PBS + 0.1% Tween-20) containing 5% skim milk powder (Cell signalling, 9999). Blots were then incubated (4 °C, overnight) with primary antibodies against ACE2 (diluted 1:1000), LGALS3BP (diluted 1:1000) and α-tubulin (diluted 1:10,000). Blots were then washed three times (8 min each) with PBST. For standard Western blotting detection, blots were incubated with either an anti-rabbit HRP-conjugated antibody (1:5000) or an anti-mouse HRP-conjugated antibody (1:10,000) for 1 h at room temperature. After washing three times at room temperature with PBST (10 min each), blots were developed with Enhanced Chemiluminescence (ECL, Amersham).

Machine learning. Machine learning was deployed to identify a prognostic classifier for COVID-19 ICU patients based on 27 clinical variables, RNAemia, as well as ELISA measurements of candidates selected from the literature (PTX3^{31–34}, RAGE^{28–30}, and LGALS3BP). To ascertain the translational value of our machine learning results, we did not include our DIA MS-based data. The RNAemia feature was defined as a binary feature that takes a true value when RNAemia was present

within six days upon admission to ICU. Feature selection was undertaken using an ensemble approach - feature filter for singleton variables followed by a wrapper method to evaluate binary and triplet combinations of these shortlisted singleton features (Supplementary Fig. 7). Mann-Whitney U test of statistical significance (*P* value < 0.05) was used as feature selection criterium for singleton markers (Fig. 4b, Supplementary Table 1). Binary and triplet combinatorial feature search was performed using wrapper feature selection⁹³ with support vector machine (SVM) classifier using radial basis function (RBF) kernel. Feature combinations were evaluated using the average of sensitivity, PPV and area under the receiver operating characteristic curve (ROC AUC) metrics. Although the F1-score, i.e., the harmonic mean of sensitivity and precision (PPV), is a commonly used evaluation metric for imbalanced data, the drawback is that F1-score does not reflect the correct classification of the majority class, i.e., true negatives. Combining ROC AUC along with sensitivity and PPV addresses this limitation of standalone usage of the F1-score. SVM uses hyperplane (decision surface) leveraging only a percentage of training samples (support vectors), thus offering high generalization ability attributed to its near impervious characteristic to new samples⁹⁴. Combinations were restricted to a maximum of triplets to enhance the ease of clinical implementation and avoid the risk of overfitting. In addition, tenfold cross-validation along with leave-one-out validation was used to avoid overfitting and test model generalization. The SVM Synthetic Minority Oversampling Technique was used to prevent the learning bias of SVM RBF towards the majority class³⁵. Tuning of the SVM RBF external parameter i.e., C was performed using grid search. The Scikit-learn default i.e., "scale" was used for the SVM RBF gamma parameter⁹⁶. A permutation test was performed to evaluate the null hypothesis that the classifier performance is by chance i.e., input variables and outcome labels are independent⁹⁷. Hence, rejection of the null hypothesis implies that the classifier has found a real class structure (pattern) in the data. For technical validation of our "Age, RNAemia" model based on SVM RBF, we employed a permutation test for statistical significance of the classifier performance; and stability of feature importance in an alternate machine learning feature ranking model, i.e., Random forest with resampling. Age and RNAemia were ranked among the top five most important features based on mean importance across 100 resampling cycles of sensitivity analysis. A permutation test with 50 permutes i.e., repeating the classification procedure after random permuting of the outcome labels returned a significant *P* value (Supplementary Fig. 8). The implementation of machine learning was done using Scikit-learn 0.23.2 python package⁹⁶.

Statistical analysis. All statistical analyses were two-tailed. Shapiro-Wilk normality test was extensively applied in proteomics and clinical data and some features were found to be not normally distributed. For this reason, nonparametric methods were used throughout the manuscript for differential expression analysis and correlation analysis. Mann-Whitney U significance test was used for continuous variables and Fisher exact test for binary variables in Supplementary Tables 1, 3 and 4. Statistical comparisons on MS and ELISA data were performed applying the nonparametric Mann-Whitney U test on the preprocessed data removing the residuals of age and sex from fitted linear models. Spike pulldown data were analyzed by paired or unpaired Student's t-tests as appropriate, because of the low sample size which makes the use of nonparametric tests not suitable. Timepoint comparisons were performed using the nonparametric Kruskal-Wallis test. Linear mixed models analysis was performed to further evaluate the combinatorial effect of time and RNAemia, and time and outcome respectively in the expression of significant proteins, correcting in all cases for age and sex. Correlations between continuous variables were analyzed using Spearman correlation. Correlations between categorical and continuous variables were examined using point-biserial correlation. Correlations between categorical variables were examined using Cohen's Kappa correlation. Anti-SARS-CoV-2 antibody data and trajectories of protein clusters were fitted using Generalized Alternative Models (GAM), with *P* values reporting the effect of RNAemia or mortality in the model because the trajectories of the antibody data have been demonstrated to be nonlinear and the same was observed for the protein clusters. Survival analysis was performed using Cox regression and Kaplan-Meier plots leveraging the R "survival" package. As two groups, i.e., low and high risk were being compared, no adjustments for multiple comparisons were performed in the Kaplan-Meier analysis. All features were scaled to a mean of zero and a standard deviation of one. Proteins quantified by MS and clinical features with missing values ≥30% were dropped and not used for data analysis. This resulted in two clinical variables being dropped, i.e., eosinophils and basophils. The remaining features were imputed, as applicable, using KNN based imputation with *K* = 5 (Supplementary Table 11)⁹¹. To validate DIA-MS findings, a publicly available proximity-extension assay proteomics-based dataset was analyzed (Data provided by the MGH Emergency Department COVID-19 Cohort (Filbin, Goldberg, Hacohen) with Olink Proteomics)³⁸. Differential expression analysis of proteins in survivors and non-survivors 28-days after hospitalization within the Olink dataset³⁸ was achieved through the Ebayes method of the limma package since RQ values of Olink measurements were normally distributed. Benjamini-Hochberg's FDR corrected *q*-values were calculated to correct for multiple testing in all parts of the analysis: differential expression, correlation, survival. Statistical analysis and associated figures were generated with R programming environment (version 4.02), Python

programming environment (version 3.8.6) and GraphPad software (version 8.4.3). Schematic diagrams were created with Biorender.com.

Reporting summary. Further information on research design is available in the Nature Research Reporting Summary linked to this article.

Data availability

The authors declare that the data supporting the findings of this study are available within the article and its Supplementary Data. The mass spectrometry proteomics data have been deposited to the ProteomeXchange Consortium via the PRIDE partner repository with the dataset identifiers PXD024026 and PXD024089 (<https://www.ebi.ac.uk/pride/>). We used the following human protein database: UniProtKB/Swiss-Prot version 2020_01, 20,365 protein entries (<https://www.uniprot.org>).

The external validation data was provided by the MGH Emergency Department COVID-19 Cohort (Filbin, Goldberg, Hacohen) with Olink Proteomics³⁸ (https://info.olink.com/mgh-covid-study-overview-page?utm_campaign=Broad%2520%2520Explore%2520Covid%2520Study&utm_source=research-gate&utm_medium=MGH%2520post). Source data are provided with this paper.

Received: 5 November 2020; Accepted: 28 April 2021;

Published online: 07 June 2021

References

1. Knaus, W. A., Draper, E. A., Wagner, D. P. & Zimmerman, J. E. APACHE II: a severity of disease classification system. *Crit. Care Med.* **13**, 818–829 (1985).
2. Vincent, J. L. et al. The S. O. F. A. (Sepsis-related Organ Failure Assessment) score to describe organ dysfunction/failure. On behalf of the Working Group on Sepsis-Related Problems of the European Society of Intensive Care Medicine. *Intensive Care Med.* **22**, 707–710 (1996).
3. Sinha, P. et al. Prevalence of phenotypes of acute respiratory distress syndrome in critically ill patients with COVID-19: a prospective observational study. *Lancet Respir. Med.* **8**, 1209–1218 (2020).
4. Zou, X. et al. Acute physiology and chronic health evaluation II score as a predictor of hospital mortality in patients of coronavirus disease 2019. *Crit. Care Med.* **48**, e657–e665 (2020).
5. Intensive Care National Audit And Research Centre. *ICNARC Report on COVID-19 in Critical Care 31 July 2020.* (2020).
6. Gupta, R. K. et al. Systematic evaluation and external validation of 22 prognostic models among hospitalised adults with COVID-19: an observational cohort study. *Eur. Respir. J.* <https://doi.org/10.1183/13993003.03498-2020> (2020).
7. Andersson, M. I. et al. SARS-CoV-2 RNA detected in blood products from patients with COVID-19 is not associated with infectious virus. *Wellcome Open Res* **5**, 181 (2020).
8. Xu, D. et al. Relationship between serum SARS-CoV-2 nucleic acid(RNAemia) and organ damage in COVID-19 patients: a cohort study. *Clin. Infect. Dis.* <https://doi.org/10.1093/cid/ciaa1085> (2020).
9. Fajnzylber, J. et al. SARS-CoV-2 viral load is associated with increased disease severity and mortality. *Nat. Commun.* **11**, 5493 (2020).
10. Prebensen, C. et al. Severe acute respiratory syndrome coronavirus 2 RNA in plasma is associated with intensive care unit admission and mortality in patients hospitalized with coronavirus disease 2019. *Clin. Infect. Dis.* <https://doi.org/10.1093/cid/ciaa1338> (2020).
11. Laing, A. G. et al. A dynamic COVID-19 immune signature includes associations with poor prognosis. *Nat. Med.* <https://doi.org/10.1038/s41591-020-1038-6> (2020).
12. Carter, M. J. et al. Peripheral immunophenotypes in children with multisystem inflammatory syndrome associated with SARS-CoV-2 infection. *Nat. Med.* <https://doi.org/10.1038/s41591-020-1054-6> (2020).
13. Seow, J. et al. Longitudinal observation and decline of neutralizing antibody responses in the three months following SARS-CoV-2 infection in humans. *Nat. Microbiol.* <https://doi.org/10.1038/s41564-020-00813-8> (2020).
14. Chen, X. et al. Detectable coronavirus 2 viral load (RNAemia) is closely correlated with drastically elevated interleukin 6 level in critically ill patients with coronavirus disease 2019. *Clin. Infect. Dis.* <https://doi.org/10.1093/cid/ciaa449> (2020).
15. Bermejo-Martin, J. F. et al. Viral RNA load in plasma is associated with critical illness and a dysregulated host response in COVID-19. *Crit. Care* **24**, 691 (2020).
16. Veras, F. P. et al. SARS-CoV-2-triggered neutrophil extracellular traps mediate COVID-19 pathology. *J. Exp. Med.* **217**, e20201129 (2020).
17. Zaid, Y. et al. Platelets can associate with SARS-CoV-2 RNA and are hyperactivated in COVID-19. *Circ. Res.* <https://doi.org/10.1161/CIRCRESAHA.120.317703> (2020).
18. Zhang, S. et al. SARS-CoV-2 binds platelet ACE2 to enhance thrombosis in COVID-19. *J. Hematol. Oncol.* **13**, 120 (2020).
19. Shen, B. et al. Proteomic and metabolomic characterization of COVID-19 patient sera. *Cell* **182**, 59–72.e15 (2020).
20. Messner, C. B. et al. Ultra-high-throughput clinical proteomics reveals classifiers of COVID-19 infection. *Cell Syst.* **11**, 11–24.e4 (2020).
21. Overmyer, K. A. et al. Large-scale multi-omic analysis of COVID-19 severity. *Cell Syst.* <https://doi.org/10.1016/J.CEL.S.2020.10.003> (2020).
22. Di, B. et al. Identification and validation of predictive factors for progression to severe COVID-19 pneumonia by proteomics. *Signal Transduct. Target. Ther.* **5**, 217 (2020).
23. Singer, M. et al. The third international consensus definitions for sepsis and septic shock (Sepsis-3). *J. Am. Med. Assoc.* **315**, 801 (2016).
24. Shankar-Hari, M. et al. Developing a new definition and assessing new clinical criteria for septic shock: for the Third International Consensus definitions for sepsis and septic shock (Sepsis-3). *J. Am. Med. Assoc.* **315**, 775–787 (2016).
25. Wilson, J. K. & Shankar-Hari, M. Immunological subpopulations within critically ill COVID-19 patients. *Chest* <https://doi.org/10.1016/j.chest.2021.01.023> (2021).
26. Gupta, A. et al. Extrapulmonary manifestations of COVID-19. *Nat. Med.* **26**, 1017–1032 (2020).
27. Shankar-Hari, M. et al. Early PREdiction of sepsis using leukocyte surface biomarkers: the EXPRES-sepsis cohort study. *Intensive Care Med.* **44**, 1836–1848 (2018).
28. Jones, T. K. et al. Plasma sRAGE acts as a genetically regulated causal intermediate in sepsis-associated acute respiratory distress syndrome. *Am. J. Respir. Crit. Care Med.* **201**, 47–56 (2020).
29. Jabaudon, M. et al. Plasma sRAGE is independently associated with increased mortality in ARDS: a meta-analysis of individual patient data. *Intensive Care Med.* **44**, 1388–1399 (2018).
30. Jabaudon, M. et al. Soluble form of the receptor for advanced glycation end products is a marker of acute lung injury but not of severe sepsis in critically ill patients. *Crit. Care Med.* **39**, 480–488 (2011).
31. Cuello, F. et al. Redox state of pentraxin 3 as a novel biomarker for resolution of inflammation and survival in sepsis. *Mol. Cell. Proteom.* **13**, 2545–2557 (2014).
32. Mauri, T. et al. Persisting high levels of plasma pentraxin 3 over the first days after severe sepsis and septic shock onset are associated with mortality. *Intensive Care Med.* **36**, 621–629 (2010).
33. Muller, B. et al. Circulating levels of the long pentraxin PTX3 correlate with severity of infection in critically ill patients. *Crit. Care Med.* **29**, 1404–1407 (2001).
34. Porte, R. et al. The long pentraxin PTX3 as a humoral innate immunity functional player and biomarker of infections and sepsis. *Front. Immunol.* **10**, 794 (2019).
35. Williamson, E. J. et al. Factors associated with COVID-19-related death using OpenSAFEly. *Nature* <https://doi.org/10.1038/s41586-020-2521-4> (2020).
36. von Rhein, C. et al. Comparison of potency assays to assess SARS-CoV-2 neutralizing antibody capacity in COVID-19 convalescent plasma. *J. Virol. Methods* **114031** (2020). <https://doi.org/10.1016/J.JVIROMET.2020.114031>
37. Dupuis, N., Muller, S., Treiber, T. & Escher, C. Evaluation of PQ500, a 500-plasma protein blood panel in NSCLC subjects using high-throughput MRM mass spectrometry. *J. Clin. Oncol.* **37**, 110–110 (2019).
38. Filbin, M. R. et al. Longitudinal proteomic analysis of plasma from patients with severe COVID-19 reveal patient survival-associated signatures, tissue-specific cell death, and cell-cell interactions. *Cell Reports Med.* **100287** (2021).
39. Ma, Y. J. et al. Heterocomplexes of mannose-binding lectin and the pentraxins PTX3 or serum amyloid P component trigger cross-activation of the complement system. *J. Biol. Chem.* **286**, 3405–3417 (2011).
40. Brunetta, E. et al. Macrophage expression and prognostic significance of the long pentraxin PTX3 in COVID-19. *Nat. Immunol.* **22**, 19–24 (2021).
41. Ou, X. et al. Characterization of spike glycoprotein of SARS-CoV-2 on virus entry and its immune cross-reactivity with SARS-CoV. *Nat. Commun.* **11**, 1620 (2020).
42. Xia, S. et al. Inhibition of SARS-CoV-2 (previously 2019-nCoV) infection by a highly potent pan-coronavirus fusion inhibitor targeting its spike protein that harbors a high capacity to mediate membrane fusion. *Cell Res.* **30**, 343–355 (2020).
43. Buchrieser, J. et al. Syncytia formation by SARS-CoV-2-infected cells. *EMBO J.* **39**, e106267 (2020).
44. Bussani, R. et al. Persistence of viral RNA, pneumocyte syncytia and thrombosis are hallmarks of advanced COVID-19 pathology. *EBioMedicine* **61**, 103104 (2020).
45. Braga, L. et al. Drugs that inhibit TMEM16 proteins block SARS-CoV-2 spike-induced syncytia. *Nature* <https://doi.org/10.1038/s41586-021-03491-6> (2021).
46. Lu, M. et al. Real-time conformational dynamics of SARS-CoV-2 spikes on virus particles. *Cell Host Microbe* **28**, 880–891.e8 (2020).

47. Vincent, J.-L. Endpoints in sepsis trials: More than just 28-day mortality? *Crit. Care Med.* **32**, S209–S213 (2004).
48. Pujadas, E. et al. SARS-CoV-2 viral load predicts COVID-19 mortality. *Lancet Respir. Med.* **8**, e70 (2020).
49. Sánchez-Cerrillo, I. et al. COVID-19 severity associates with pulmonary redistribution of CD1c+ DC and inflammatory transitional and nonclassical monocytes. *J. Clin. Investig.* <https://doi.org/10.1172/JCI140335> (2020).
50. Camporta, L. et al. Outcomes in mechanically ventilated patients with hypoxaemic respiratory failure caused by COVID-19. *Br. J. Anaesth.* **125**, e480–e483 (2020).
51. Fish, M. et al. Cellular and molecular mechanisms of IMMunE dysfunction and Recovery from SEpsis-related critical illness in adults: an observational cohort study (IMMERSE) protocol paper. *J. Intensive Care Soc.* <https://doi.org/10.1177/1751143720966286> (2020).
52. ARDS Definition Task Force, R. et al. Acute respiratory distress syndrome: the Berlin Definition. *J. Am. Med. Assoc.* **307**, 2526–2533 (2012).
53. Saha, R. et al. Impact of differences in acute respiratory distress syndrome randomised controlled trial inclusion and exclusion criteria: systematic review and meta-analysis. *Br. J. Anaesth.* <https://doi.org/10.1016/j.bja.2021.02.027> (2021).
54. Joshi, A., Rienks, M., Theofilatos, K. & Mayr, M. Systems biology in cardiovascular disease: a multiomics approach. *Nat. Rev. Cardiol.* <https://doi.org/10.1038/s41569-020-00477-1> (2020).
55. Holter, J. C. et al. Systemic complement activation is associated with respiratory failure in COVID-19 hospitalized patients. *Proc. Natl Acad. Sci. USA* **117**, 25018–25025 (2020).
56. Ramlall, V. et al. Immune complement and coagulation dysfunction in adverse outcomes of SARS-CoV-2 infection. *Nat. Med.* <https://doi.org/10.1038/s41591-020-1021-2> (2020).
57. Gralinski, L. E. et al. Complement activation contributes to severe acute respiratory syndrome coronavirus pathogenesis. *MBio* **9**, e01753-18 (2018).
58. Galbraith, M. D. et al. Seroconversion stages COVID19 into distinct pathophysiological states. *Elife* **10**, e65508 (2021).
59. Risitano, A. M. et al. Complement as a target in COVID-19? *Nat. Rev. Immunol.* **20**, 343–344 (2020).
60. Song, W.-C. & FitzGerald, G. A. COVID-19, microangiopathy, hemostatic activation, and complement. *J. Clin. Investig.* **130**, 3950–3953 (2020).
61. Yu, J. et al. Direct activation of the alternative complement pathway by SARS-CoV-2 spike proteins is blocked by factor D inhibition. *Blood* **136**, 2080–2089 (2020).
62. Zhou, Y. et al. A single asparagine-linked glycosylation site of the severe acute respiratory syndrome coronavirus spike glycoprotein facilitates inhibition by mannose-binding lectin through multiple mechanisms. *J. Virol.* **84**, 8753–8764 (2010).
63. Ip, W. K. E. et al. Mannose-binding lectin in severe acute respiratory syndrome coronavirus infection. *J. Infect. Dis.* **191**, 1697–1704 (2005).
64. Polycarpou, A. et al. Rationale for targeting complement in COVID-19. *EMBO Mol. Med.* **12**, e12642 (2020).
65. Jordan, J. E., Montalto, M. C. & Stahl, G. L. Inhibition of mannose-binding lectin reduces postischemic myocardial reperfusion injury. *Circulation* **104**, 1413–1418 (2001).
66. Schafranski, M. D., Stier, A., Nishihara, R. & Messias-Reason, I. J. T. Significantly increased levels of mannose-binding lectin (MBL) in rheumatic heart disease: a beneficial role for MBL deficiency. *Clin. Exp. Immunol.* **138**, 521–525 (2004).
67. Deban, L. et al. Binding of the long pentraxin PTX3 to factor H: interacting domains and function in the regulation of complement activation. *J. Immunol.* **181**, 8433–8440 (2008).
68. Braunschweig, A. & Józsi, M. Human pentraxin 3 binds to the complement regulator C4b-binding protein. *PLoS ONE* **6**, e23991 (2011).
69. Ma, Y. J. & Garred, P. Pentraxins in complement activation and regulation. *Front. Immunol.* **9**, 3046 (2018).
70. Burnap, S. A. et al. A proteomics-based assessment of inflammation signatures in endotoxemia. *Mol. Cell. Proteomics* <https://doi.org/10.1074/mcp.RA120.002305> (2020).
71. Gisby, J. et al. Longitudinal proteomic profiling of dialysis patients with COVID-19 reveals markers of severity and predictors of death. *Elife* **10**, e64827 (2021).
72. Jaillon, S. et al. The humoral pattern recognition receptor PTX3 is stored in neutrophil granules and localizes in extracellular traps. *J. Exp. Med.* **204**, 793–804 (2007).
73. Caniglia, J. L., Asuthkar, S., Tsung, A. J., Guda, M. R. & Velpula, K. K. Immunopathology of galectin-3: an increasingly promising target in COVID-19. *F1000Research* **9**, 1078 (2020).
74. Peng, G. et al. Crystal structure of bovine coronavirus spike protein lectin domain. *J. Biol. Chem.* **287**, 41931–41938 (2012).
75. Li, F. Receptor recognition mechanisms of coronaviruses: a decade of structural studies. *J. Virol.* **89**, 1954–1964 (2015).
76. Sethi, A., Sanam, S., Munagalasetty, S., Jayanthi, S. & Alvala, M. Understanding the role of galectin inhibitors as potential candidates for SARS-CoV-2 spike protein: *in silico* studies. *RSC Adv.* **10**, 29873–29884 (2020).
77. Ullrich, A. et al. The secreted tumor-associated antigen 90K is a potent immune stimulator. *J. Biol. Chem.* **269**, 18401–18407 (1994).
78. Loimaranta, V., Hepojoki, J., Laaksoaho, O. & Pulliainen, A. T. Galectin-3-binding protein: a multitask glycoprotein with innate immunity functions in viral and bacterial infections. *J. Leukoc. Biol.* **104**, 777–786 (2018).
79. Denard, J. et al. Human galectin 3 binding protein interacts with recombinant adeno-associated virus type 6. *J. Virol.* **86**, 6620–6631 (2012).
80. Wang, Q., Zhang, X., Han, Y., Wang, X. & Gao, G. M2BP inhibits HIV-1 virion production in a vimentin filaments-dependent manner. *Sci. Rep.* **6**, 32736 (2016).
81. Chu, C. C., Rahimi, N., Forsten-Williams, K. & Nugent, M. A. Heparan sulfate proteoglycans function as receptors for fibroblast growth factor-2 activation of extracellular signal-regulated kinases 1 and 2. *Circ. Res.* **94**, 316–323 (2004).
82. Chang, H. C., Samaniego, F., Nair, B. C., Buonaguro, L. & Ensoli, B. HIV-1 Tat protein exits from cells via a leaderless secretory pathway and binds to extracellular matrix-associated heparan sulfate proteoglycans through its basic region. *AIDS* **11**, 1421–1431 (1997).
83. Filbin, M. R. et al. Longitudinal proteomic analysis of plasma from patients with severe COVID-19 reveal patient survival-associated signatures, tissue-specific cell death, and cell-cell interactions. *Cell Reports Med.* **100287**, <https://doi.org/10.1016/j.xcrm.2021.100287> (2021).
84. Shankar-Hari, M. & Rubenfeld, G. D. Population enrichment for critical care trials: phenotypes and differential outcomes. *Curr. Opin. Crit. Care* **25**, 489–497 (2019).
85. Rochwerg, B. et al. A living WHO guideline on drugs for covid-19. *Br. Med. J.* **370**, m3379 (2020).
86. Liu, C. et al. Time-resolved systems immunology reveals a late juncture linked to fatal COVID-19. *Cell* **184**, 1836–1857.e22 (2021).
87. Ding, M. et al. An optimized sensitive method for quantitation of DNA/RNA viruses in heparinized and cyropreserved plasma. *J. Virol. Methods* **176**, 1–8 (2011).
88. Kaudewitz, D. et al. Impact of intravenous heparin on quantification of circulating microRNAs in patients with coronary artery disease. *Thromb. Haemost.* **110**, 609–615 (2013).
89. Schulte, C. et al. Comparative analysis of circulating noncoding RNAs versus protein biomarkers in the detection of myocardial injury. *Circ. Res.* **125**, 328–340 (2019).
90. Vogels, C. B. F. et al. Analytical sensitivity and efficiency comparisons of SARS-CoV-2 RT-qPCR primer-probe sets. *Nat. Microbiol.* <https://doi.org/10.1038/s41564-020-0761-6> (2020).
91. Troyanskaya, O. et al. Missing value estimation methods for DNA microarrays. *Bioinformatics* **17**, 520–525 (2001).
92. Ali, H. et al. Cellular TRIM33 restrains HIV-1 infection by targeting viral integrase for proteasomal degradation. *Nat. Commun.* **10**, 926 (2019).
93. Saeys, Y., Inza, I. & Larrañaga, P. A review of feature selection techniques in bioinformatics. *Bioinformatics* **23**, 2507–2517 (2007).
94. Cortes, C. & Vapnik, V. Support-vector networks. *Mach. Learn.* **20**, 273–297 (1995).
95. Chawla, N. V., Bowyer, K. W., Hall, L. O. & Kegelmeyer, W. P. SMOTE: synthetic minority over-sampling technique. *J. Artif. Intell. Res.* **16**, 321–357 (2002).
96. Pedregosa, F. et al. Scikit-learn: machine learning in Python. *J. Mach. Learn. Res.* **12**, 2825–2830 (2011).
97. Ojala, M. & Garriga, G. C. Permutation tests for studying classifier performance. *J. Mach. Learn. Res.* **11**, 1833–1863 (2010).

Acknowledgements

We thank Dr. Victor Corman for his assistance and helpful comments.

Financial support

M.M. and A.M.S. are British Heart Foundation (BHF) Chair Holders with BHF program grant support (CH/16/3/32406, RG/16/14/32397, and CH/1999001/11735, RE/18/2/34213, respectively). C.G., E.R., and B.S. are funded by BHF PhD studentships (FS/18/60/34181, FS/17/65/33481, and FS/19/58/34895). M.H. is funded by an interdisciplinary PhD studentship from King's BHF Centre of Research Excellence. M.F. is funded by a National Institute of Academic Anesthesia BJA-RCOA PhD Fellowship WKRO-2018-0047. M.J.W.M. is grateful to the Biomedical Research Centre at Guy's and St. Thomas' NHS Foundation Trust for support. K.O.G. is supported by a UK Medical Research Council Clinical Research Training Fellowship (MR/R017751/1). B.M. was supported by an NIHR Academic Clinical Fellowship in Combined Infection Training. K.J.D. was supported by a King's Together Rapid COVID-19 Call award, by an MRC Discovery Award (MC/PC/15068), Huo Family Foundation and the Fondation Dormeur, Vaduz. The NIHR Collaboration for Leadership in Applied Health Research and Care South

London at King's College Hospital NHS Foundation Trust, awarded to J.D.E. who is also supported by a charitable donation from the Lower Green Foundation. R.F.L. is funded by a Spanish Ministry of Economy and Competitiveness Grant BFU2017-87316. M.G. is supported by the European Research Council (ERC) Advanced Grant 787971 "CuRE" and by Program Grant RG/19/11/34633 from the BHF. M.M.'s research was made possible through the support of the BIRAX Ageing Initiative and funding from the EU Horizon 2020 research and innovation program under the Marie Skłodowska-Curie grant agreement No. 813716 (TRAIN-HEART), the Leducq Foundation (18CVD02), the excellence initiative VASCage (Centre for Promoting Vascular Health in the Ageing Community, project number 868624) of the Austrian Research Promotion Agency FFG (COMET program—Competence Centers for Excellent Technologies) funded by the Austrian Ministry for Transport, Innovation and Technology; the Austrian Ministry for Digital and Economic Affairs; and the federal states Tyrol (via Standortagentur), Salzburg, and Vienna (via Vienna Business Agency), two BHF project grant supports (PG/17/48/32956 and SP/17/10/33219) and the BHF Centre for Vascular Regeneration with Edinburgh/Bristol (RM/17/3/33381). M.M. and S.R.B. acknowledge support as visiting professors as part of the Transcampus TU Dresden King's College London Initiative. The work of A.C.H. is supported by a Cancer ImmunoTherapy Accelerator award from CRUK; the Wellcome Trust (106292/Z/14/Z); the Rosetrees Trust; King's Together Seed Fund; The John Black Charitable Foundation; Royal Society Grant IES/R3/170319 and the Francis Crick Institute, which receives core funding from Cancer Research UK (FC001093), the MRC (FC001093) and the Wellcome Trust (FC001093). M.S.H. is supported by the National Institute for Health Research Clinician Scientist Award (CS-2016-16-011). The research was funded/supported by the National Institute for Health Research (NIHR) Biomedical Research Centre based at Guy's and St Thomas' NHS Foundation Trust and King's College London. The views expressed are those of the author(s) and not necessarily those of the NHS, the NIHR or the Department of Health.

Author contributions

C.G., K.T., S.A.B., B.S., K.Th., E.R., L.E.S., M.R., X.Y., S.B., J.D.E., A.M.S., S.R.B., T.T., A. C.H., M.G., M.S.H., and M.M. contributed to the study design, data interpretation, and writing of the paper. C.G., K.T., S.A.B., B.S., H.A., K.Th., M.H., L.E.S., C.C., U.N., M.S., K.D., R.F.L., R.K.W., K.J.D. contributed to the laboratory data generation and analysis. A.N., M.F., M.J.W.M., K.O.G., G.A., S.N., S.F.M., F.T., B.Sa., B.M., and M.S.H. contributed to the participant recruitment, sample collection, sample processing, and clinical data collection. All authors reviewed the paper.

Competing interests

King's College London has filed and licensed a patent application with regard to using PTX3 as a biomarker in sepsis. King's College London has filed a patent application on the methods used to detect SARS-CoV-2 Spike protein-induced syncytia as described in this paper. A.C.H. is a board member and equity holder in ImmunoQure, A.G., and Gamma Delta Therapeutics, and is an equity holder in Adapte Biotherapeutics.

Additional information

Supplementary information The online version contains supplementary material available at <https://doi.org/10.1038/s41467-021-23494-1>.

Correspondence and requests for materials should be addressed to M.S-H. or M.M.

Peer review information *Nature Communications* thanks Ariel Jaitovich, Jochen Schwenk and the other, anonymous, reviewer(s) for their contribution to the peer review of this work. Peer reviewer reports are available.

Reprints and permission information is available at <http://www.nature.com/reprints>

Publisher's note Springer Nature remains neutral with regard to jurisdictional claims in published maps and institutional affiliations.



Open Access This article is licensed under a Creative Commons Attribution 4.0 International License, which permits use, sharing, adaptation, distribution and reproduction in any medium or format, as long as you give appropriate credit to the original author(s) and the source, provide a link to the Creative Commons license, and indicate if changes were made. The images or other third party material in this article are included in the article's Creative Commons license, unless indicated otherwise in a credit line to the material. If material is not included in the article's Creative Commons license and your intended use is not permitted by statutory regulation or exceeds the permitted use, you will need to obtain permission directly from the copyright holder. To view a copy of this license, visit <http://creativecommons.org/licenses/by/4.0/>.

© The Author(s) 2021

¹King's College London British Heart Foundation Centre, School of Cardiovascular Medicine and Sciences, London, UK. ²King's College Hospital NHS Foundation Trust, London, UK. ³Peter Gorer Department of Immunobiology, School of Immunology and Microbial Sciences, King's College London, London, UK. ⁴Department of Intensive Care Medicine, Guy's and St Thomas' NHS Foundation Trust, London, UK. ⁵Department of Inflammation Biology, School of Immunology and Microbial Sciences, Faculty of Life Sciences and Medicine, King's College London, London, UK. ⁶Institute of Liver Studies, King's College Hospital, London, UK. ⁷Clinical Infection and Diagnostics Research group, Department of Infection, Guy's and St Thomas' NHS Foundation Trust, London, UK. ⁸NIHR Biomedical Research Centre, Guy's and St Thomas' NHS Foundation Trust and King's College London, London, UK. ⁹Structural Biology Programme, Spanish National Cancer Research Centre (CNIO), Madrid, Spain. ¹⁰Medical Clinic I, University Hospital Carl Gustav Carus, Technical University Dresden, Dresden, Germany. ¹¹Experimental Transfusion Medicine, Faculty of Medicine Carl Gustav Carus, Technical University Dresden, Dresden, Germany. ¹²Department of Internal Medicine III, University Hospital Carl Gustav Carus, Technical University Dresden, Dresden, Germany. ¹³Department of Diabetes, School of Life Course Science and Medicine, King's College London, London, UK. ¹⁴Institute for Transfusion Medicine, German Red Cross Blood Donation Service North East, Dresden, Germany. ¹⁵The Francis Crick Institute, London, UK. ¹⁶These authors contributed equally: Clemens Gutmann, Kaloyan Takov, Sean A. Burnap, Bhawana Singh, Hashim Ali. email: manu.shankar-hari@kcl.ac.uk; manuel.mayr@kcl.ac.uk



OPEN

Serum S100B protein as a marker of severity in Covid-19 patients

Antonio Aceti¹, Lory Marika Margarucci², Elena Scaramucci¹, Massimiliano Orsini³, Gerardo Salerno¹, Gabriele Di Sante^{4,5}, Gianluca Gianfranceschi², Rosa Di Liddo⁶, Federica Valeriani², Francesco Ria^{4,5}, Maurizio Simmaco¹, Pier Paolo Parnigotto^{6,7}, Matteo Vitali⁸, Vincenzo Romano Spica^{2,11} & Fabrizio Michetti^{9,10,11}

SARS-CoV-2 infection shows a wide-ranging clinical severity, requiring prognostic markers. We focused on S100B, a calcium-binding protein present in biological fluids, being a reliable biomarker in disorders having inflammatory processes as common basis and RAGE as main receptor. Since Covid-19 is characterized by a potent inflammatory response also involving RAGE, we tested if S100B serum levels were related to disease severity. Serum samples ($n = 74$) were collected from hospitalized SARS-CoV-2 positive patients admitted to Covid center. Illness severity was established by admission clinical criteria and Covid risk score. Treatment protocols followed WHO guidelines available at the time. Circulating S100B was determined by ELISA assay. Statistical analysis used Pearson's χ^2 test, t-Test, and ANOVA, ANCOVA, Linear Regression. S100B was detected in serum from Covid-19 patients, significantly correlating with disease severity as shown both by the level of intensity of care ($p < 0.006$) as well by the value of Covid score (Multiple R-squared: 0.3751); the correlation between Covid-Score and S100B was 0.61 ($p < 0.01$). S100B concentration was associated with inflammation markers (Ferritin, C-Reactive Protein, Procalcitonin), and organ damage markers (Alanine Aminotransferase, Creatinine). Serum S100B plays a role in Covid-19 and can represent a marker of clinical severity in Sars-CoV-2 infected patients.

Evaluation of Covid-19 severity and possible outcomes is limited by clinical heterogeneity and lack of specific markers^{1–3}. Several laboratory parameters are considered in clinical practice, but the identification of novel indicators in blood specimens is a key issue for understanding the underlying biological mechanisms and improving prognostic accuracy^{4–9}. As a candidate marker we focused on the S100B protein, which is regarded to be involved in inflammatory processes as a Danger-Associated Molecular Patterns (DAMP) molecule^{10,11}. S100B is a small acidic calcium-binding protein, originally isolated in the nervous system, where it is concentrated in astrocytes, being also present in oligodendrocytes, Schwann cells, enteric glial cells, and some neuron subpopulations^{12,13}. It is also present in definite non-neuronal cell types, including dendritic cells, certain lymphocyte subpopulations, chondrocytes, Langerhans cells, melanocytes, adrenal medulla satellite cells, Leydig cells, skeletal muscle satellite cells, and adipocytes, which intriguingly constitute a site of concentration for the protein comparable to the nervous tissue¹⁰. S100B can be detected in biological fluids (cerebrospinal fluid, peripheral blood, urine, saliva, feces) in particular conditions^{10,12,14}. Besides, the protein has been shown to be actively released and interact with target cells through the multiligand transmembrane immunoglobulin-like Receptor for Advanced Glycation Endproducts (RAGE) which is able to initiate an intracellular signaling cascade¹⁵ and was associated to several

¹Sant'Andrea Hospital A.O.U., Sapienza University of Rome, Via di Grottarossa 1035, 00189 Rome, Italy. ²Department of Movement, Human and Health Sciences, Laboratory of Epidemiology and Biotechnologies, University of Rome "Foro Italico", Piazza Lauro De Bosis 6, 00135 Rome, Italy. ³Istituto Zooprofilattico Sperimentale Delle Venezie, Viale dell'Università 10, 35020 Legnaro, Padua, Italy. ⁴Department of Translational Medicine and Surgery, Section of General Pathology, Università Cattolica del Sacro Cuore, Largo Francesco Vito 1, 00168 Rome, Italy. ⁵Fondazione Policlinico Universitario A. Gemelli - IRCCS, Largo A. Gemelli 1-8, 00168 Rome, Italy. ⁶Department of Pharmaceutical and Pharmacological Sciences, University of Padua, Via Marzolo 5, 35131 Padua, Italy. ⁷Foundation for Biology and Regenerative Medicine, Tissue Engineering and Signaling (T.E.S.) Onlus, Via De Sanctis 10, 35030 Caselle di Selvazzano Dentro, Padua, Italy. ⁸Department of Public Health and Infectious Diseases, Sapienza University of Rome, Piazzale Aldo Moro, 5, 00185 Rome, Italy. ⁹Department of Neuroscience, Università Cattolica del Sacro Cuore, Largo Francesco Vito 1, 00168 Rome, Italy. ¹⁰IRCCS San Raffaele Scientific Institute, Università Vita-Salute San Raffaele, Via Olgettina, 58, 20132 Milan, Italy. ¹¹These authors contributed equally: Vincenzo Romano Spica and Fabrizio Michetti. email: vincenzo.romanospica@uniroma4.it

Participants	All (n=74)	HIC ^a (n=19)	LIC ^b (n=55)	p value
Characteristics				
Median age (IQR)—years	66 (32–89)	63 (35–85)	66 (32–89)	0.66
Female – number (%)	25 (49)	9 (64)	16 (43)	
Period from hospitalization to blood sample collection—days (SD)	18.0 ± 18.0	19.5 ± 17.8	17.6 ± 18.3	0.72
Period from blood sample collection to hospital discharge—days (SD)	13.2 ± 11.5	14.0 ± 11.8	13.0 ± 11.5	0.79
Serum data				
S100B—ng/mL (SD)	2.39 ± 6.04	8.80 ± 10.24	0.62 ± 2.10	0.006
White Blood Cell count per mm ³ (SD)	7.21 ± 3.01	7.78 ± 4.56	7.05 ± 2.45	0.55
Lymphocyte count per mm ³ (SD)	1.49 ± 0.73	1.41 ± 0.85	1.51 ± 0.69	0.67
Alanine Aminotransferase—IU/L (SD)	29.8 ± 26.2	39.4 ± 43.0	27.2 ± 18.9	0.28
Creatinine—mg/dL (SD)	0.96 ± 0.57	0.89 ± 0.45	0.98 ± 0.60	0.52
d-Dimer—ng/mL (SD)	583 ± 514	810 ± 585	520 ± 479	0.08
Prothrombin—seconds (SD)	13.7 ± 2.0	13.9 ± 1.9	13.6 ± 2.1	0.62
Ferritin—mg/L (SD)	782 ± 914	1212 ± 1387	663 ± 705	0.16
Procalcitonin—ng/mL (SD)	334 ± 583	586 ± 1192	265 ± 197	0.30
C Reactive Protein—mg/dL (SD)	6.00 ± 7.60	6.27 ± 8.34	5.92 ± 7.46	0.88

Table 1. Overview of patients included in the study and their serum data. ^aHigh Intensity Care ward. ^bLow Intensity Care ward.

pathological conditions, reasonably referred to inflammatory processes¹². Based on these findings, S100B is considered a reliable biomarker for a variety of neural and non-neural pathological conditions, even displaying a predictive role^{14–17}.

Indeed, S100B appears to share similar characteristics to DAMPs molecules, including the interaction with RAGE and, once released in the microenvironment, the active participation to the inflammatory tissue reaction to damage^{10,18}. Interestingly, the S100B-RAGE axes has been shown to participate in pulmonary inflammatory processes^{19,20}.

Thus, in the light of the notion that SARS CoV-2 infection can induce a severe acute respiratory syndrome with a complex pattern of clinical manifestations characterized by a potent inflammatory response^{18,21–23} we tested the possibility that S100B could be present in detectable amounts in serum of Covid-19 patients, as well as the possible relationship between severity of the disease and increase in S100B serum levels.

Results

S100B is present in serum of Covid patients, correlating with disease severity. S100B was detected at concentrations over the LOD in the serum of 19 patients out of 74 (25.7%), ranging from 0.25 to 29.46 ng/mL. Results obtained by non-parametric Wilcox test showed a positive significant association ($p < 0.001$) between S100B serum concentrations and the severity of the disease as measured based on HIC or LIC wards where the Covid-19 patients were hospitalized. S100B levels showed a higher mean value in HIC than in LIC (8.80 ± 10.24 and 0.62 ± 2.10 ng/mL, respectively; $p < 0.006$), as reported in Table 1 and Fig. 1.

No statistically significant differences were observed for other variable and in particular among the groups for age, gender and number of days of hospitalization to the date of blood sampling. The Wilcox test showed no statistically significant differences between S100B levels and gender.

Finally, the number of patients positive for serum S100B was significantly higher in HIC ($p < 0.01$). This result was confirmed by both Welch-ANOVA model ($p < 0.01$) and Games-Howell test ($p < 0.01$). The incremental trend of S100B vs clinical severity measured by Covid-score was statistically significant. Figure 2 shows the distribution of S100B concentration and Covid Score in all patients (A) and the subgroup of patient where S100B was detected in the serum (B). Most patients admitted in LIC ward show a presence of S100B below the LOD, even if with different values of Covid Score (A). Additional information is reported in supplementary material (Figs. S1 and S2). When considering only those samples over the LOD, a hypothetical trendline was extrapolated (B), suggesting a theoretical distribution. Both trendlines show significant correlations between S100B and the score for evaluating clinical risk (multiple R-squared 0.4369 and 0.3751, respectively), supporting a putative role of S100B as a marker for clinical severity.

S100B correlates with several blood markers. A positive and significant correlation was observed between S100B and Ferritin concentrations ($p < 0.01$, 74 Observations), as well as for other parameters (Table 2), and in particular PCT ($p < 0.01$), d-Dimer ($p < 0.05$) and CRP ($p < 0.1$). The ANCOVA model displayed the marginal effects of the CRP and the hospitalization ward (HIC as corner point) variables on the S100B levels, showing a positive and statistically significant relation ($p < 0.05$ and $p < 0.01$, respectively). Similar results were found for PCT ($p < 0.01$) and ALT ($p < 0.01$). In order to estimate the marginal effects of the measured parameters, a stepwise selection procedure was carried out, showing ALT and PCT variables as the best predictors of the S100B levels. A further linear regression was used to verify the single and interactive effects of CRP, ALT, PCT variables, showing a significant interaction with ALT and PCT ($p < 0.001$) and a correlation with CRP (Fig. 3). The whole

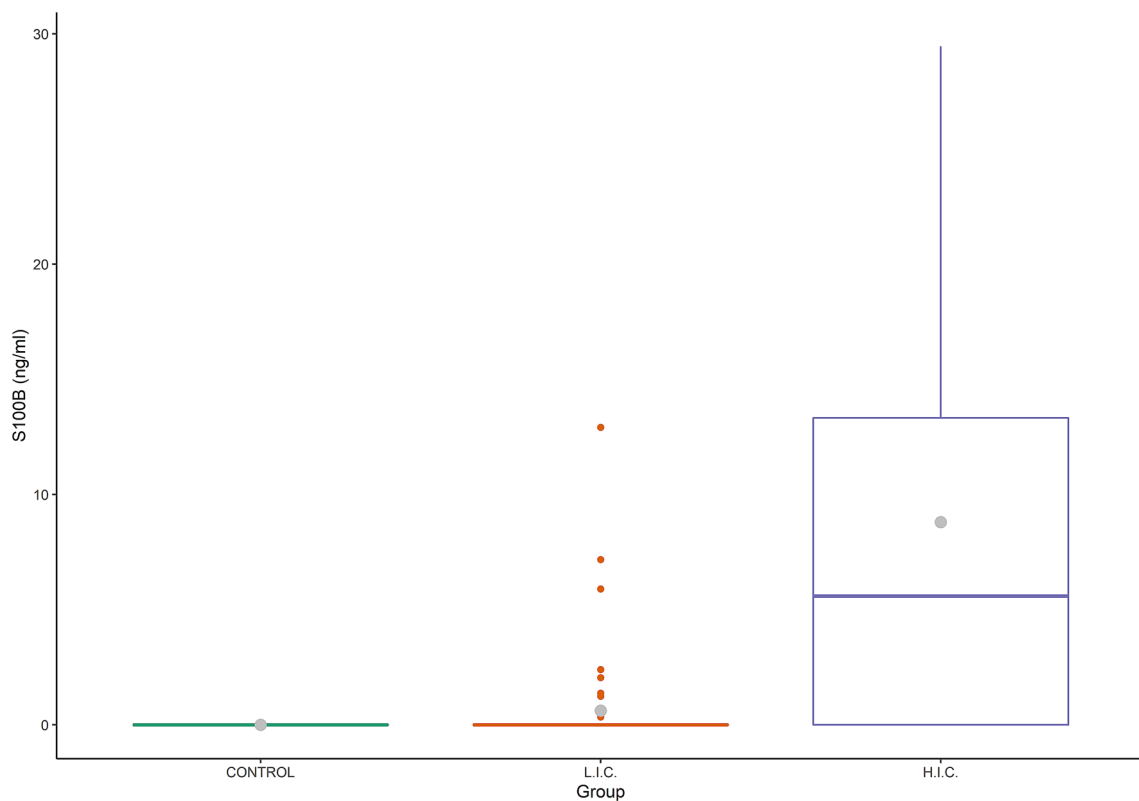


Figure 1. Detection of S100B in Covid patients and controls. Box plot showing the distribution of S100B in Covid ($n=74$) patients with different clinical severity of disease. Also data from controls ($n=5$ healthy individuals: negative for SARS-CoV-2 detection by PCR and negative by serologic test) are included. Grey dot: mean value, Line: median value; HIC: High Intensity Care; LIC: Low Intensity Care.

of the results suggests that both S100B presence and levels correlate with the severity of the disease, the trend of CRP and Ferritin values and inflammatory status, as well as with other key parameters of Covid-19 severity, such as PCT, d-Dimer, ALT. Moreover, we observed a significant correlation between S100B and CRE levels ($p<0.01$) in the subgroup of patients with high levels of ALT (>40 IU/L, $n=19$)¹⁸, thus suggesting the possibility of an independent association with a liver and/or kidney damage.

Discussion

In this study, we investigated the levels of circulating S100B in serum of patients affected by SARS-CoV-2 virus at various stages of the disease. S100B serum concentrations resulted correlated with the severity of the disease, as indicated by clinical/laboratory parameters. The major part of data at present available on the S100B protein as a biomarker and pathogenic factor deals with disorders primarily related to the nervous system whereas disorders primarily related to other systems having been essentially disregarded¹²: thus, present results appear to enlarge the field of investigation on this protein and its potentials in Covid-19 and, more in general, infectious diseases. Indeed, the discrete distribution of S100B in definite extra-neuronal cell types offers the basis for a functional/pathogenic role of the protein in extra-neuronal tissues, which at present has not been exhaustively investigated.

This study was performed during the epidemic peak, with the advantage of collecting homogeneous data from the same outbreak but with all the restrictions present while managing the emergency, including the limits in sample size and in the number of additional clinical or laboratory parameters to be assessed. However, the acquired data were stressed by an accurate statistical analysis, strongly reporting a role for S100B in Covid-19.

The increased levels of S100B are reasonably related to inflammatory processes, as also supported by its significant correlation with CRP, which is known to be a recognized inflammatory hallmark²⁴. S100B is known to participate in inflammatory processes^{25,26} which are also known to be raised during SARS-CoV-2 disease^{19,21}. Interestingly, in this respect we observed that S100B levels are correlated with indicators of distress involving non-neuronal districts, such as ALT, d-Dimer, PCT, suggesting, in this case, a wider and systemic valence for S100B as a putative biomarker.

The source of increased serum S100B in SARS-CoV-2 patients remains to be identified. Since information indicating a prevalent involvement of the nervous system in pathogenic processes of SARS-CoV-2 at present is lacking²⁷, it seems unlikely that in this case the protein is primarily released from this tissue, which at present is regarded to be the natural source of the protein in biological fluids in the major part of pathological conditions already known. Among the cell types which are known to express and putatively release the protein, adipocytes, dendritic and lymphoid cell types²⁸⁻³¹ appear to be putative sources for serum S100B in this disease. Adipocytes are known to secrete inflammatory cytokines which play a recognized role in crosstalk with the immune

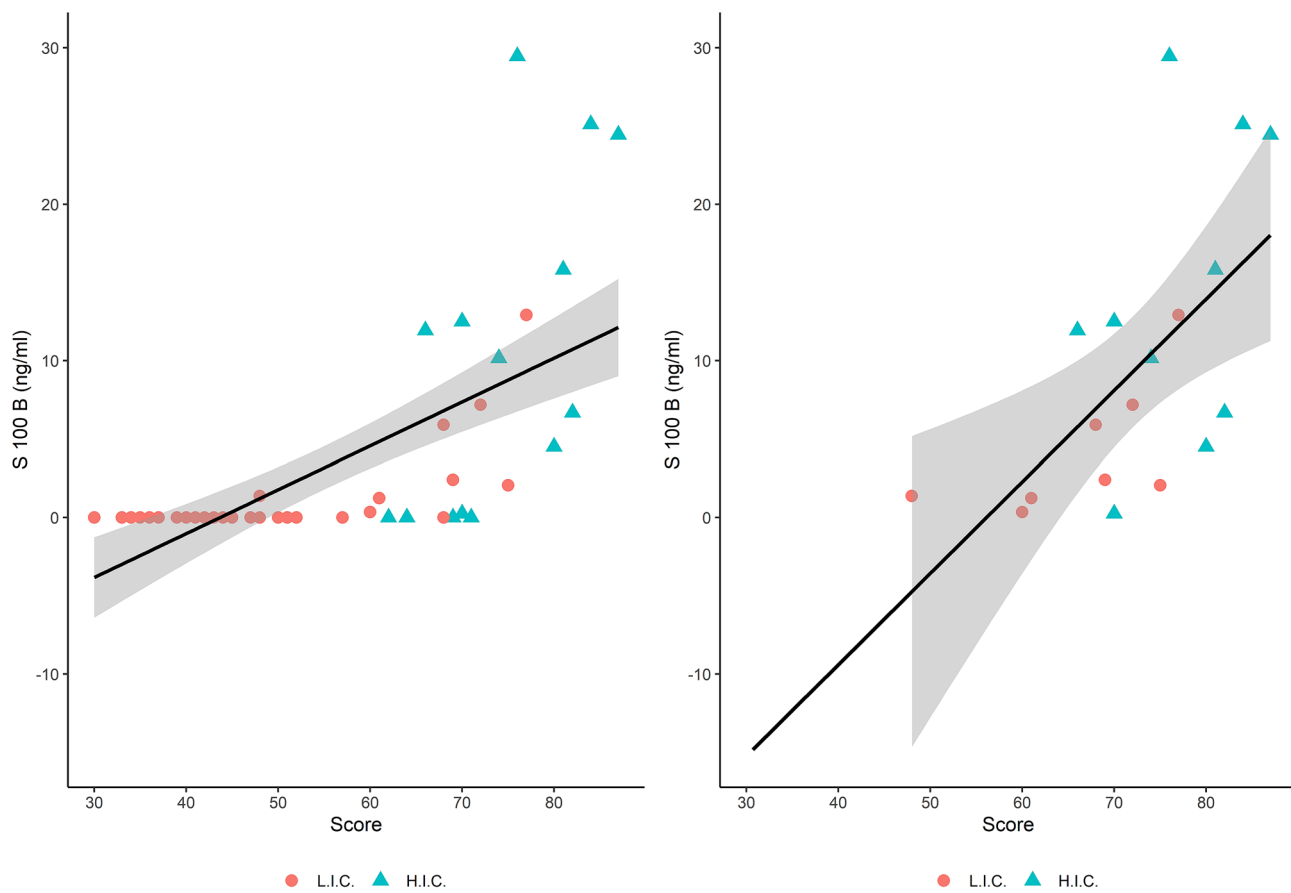


Figure 2. Relationship between Covid-Score and concentration of S100B. The scatterplot shows a positive correlation between S100B concentration (ng/mL) and clinical severity of the disease as represented by Covid-score. Analysis considering all samples (A) or only those with S100B detected in serum (B), from both HIC and LIC wards. Most of the samples with a concentration of S100B below the LOD belongs to the group hospitalized in the LIC wards (A). When considering only patients with S100B over the LOD and from both wards (B), the regression equation was $Y = 0.584X - 32.778$. Figure A is reported as a comparison respect to figure B to highlight the distribution of S100B levels below the LOD and the independent linear regression curves are reported in supplementary materials (S1). The hospitalization ward is indicated for each patient (Red Dots: Low Intensity Care (LIC); Blue Triangles: High Intensive Care (HIC)). The linear regression lines and their confidence intervals (95%) are showed by the gray areas. The correlation between Covid-Score and S100B is equal to 0.66 ($p < 0.001$) (A) and 0.61 ($p < 0.01$) (B).

system, which at present are known to be especially relevant in processes leading to obesity^{32,33}. Since the role(s) of molecules secreted by this intriguing cell type, including S100B, is at present largely unknown, this finding might add a novel element deserving interest. In the case of dendritic and lymphoid cell types, their role in inflammatory processes is widely known^{34,35}, so that the mechanistic involvement of S100B in their function would merely increase the breadth of knowledge in this respect. It is interesting to note that, under pulmonary inflammation, S100B has been reported to be upregulated in bronchiolar epithelial cells and airway dendritic cells^{36,37}. Moreover, as shown in alveolar cell types, S100B can stimulate the secretion of pro-inflammatory cytokines, that are commonly involved in lung inflammation, following a similar process suspected to be present also in Covid-19^{19–22,36,37}.

Additional studies will be needed in order to define the source of serum S100B in patients affected by SARS-CoV-2, but the finding of increased serum levels of the protein, correlated with the gravity of the disease and inflammatory processes, offers a novel biomarker potentially useful to monitor the disease. In addition, in the light of growing evidence candidating S100B as an active factor in inflammatory processes¹², the present findings may even propose the protein as a therapeutic target to counteract the potent inflammatory processes characterizing this infectious disease.

In conclusion, increased serum levels of S100B correlate with the severity of Covid-19 and inflammatory processes, offering a novel biomarker potentially beneficial in monitoring the disease course and prognosis. In the light of growing evidence candidating S100B as an active factor in inflammatory processes driven by DAMP and RAGE, the present findings propose this protein as a severity marker and its cellular pathways as candidate targets to unravel pathogenetic mechanisms and counteract the potent inflammatory processes characterizing SARS-CoV-2 infection.

	S100B^a	WBC^b	LYM^c	ALT^d	CRE^e	d-Dimer^f	PT^g	FERR^h	PCTⁱ	CRP^j	age^k	days before^l	days after^m	Covid scoreⁿ
	n = 74	n = 74	n = 74	n = 74	n = 74	n = 74	n = 74	n = 69	n = 74	n = 74	n = 74	n = 74	n = 71	n = 56
S100B ^a		0.05	0.03	0.36	0.1	0.21	-0.06	0.32	0.53	0.2	-0.14	-0.07	-0.03	0.66
n = 74		0.7	0.805	0.002**	0.402	0.073 ⁺	0.599	0.007**	0.001***	0.082 ⁺	0.245	0.557	0.83	0.001***
WBC ^b	0.05	-	0.13	-0.09	0.22	0.12	0.15	0.3	0.14	0.07	0.06	-0.12	0.07	-0.08
n = 74	0.7	-	0.266	0.441	0.06 ⁺	0.324	0.188	0.011*	0.223	0.542	0.595	0.303	0.54	0.579
LYM ^c	0.03	0.13	-	-0.17	-0.04	-0.21	-0.1	-0.15	0.04	-0.23	-0.2	-0.11	-0.28	-0.004
n = 74	0.805	0.266	-	0.138	0.717	0.067 ⁺	0.385	0.209	0.723	0.046*	0.096 ⁺	0.331	0.02*	0.974
ALT ^d	0.36	-0.09	-0.17	-	-0.11	0.32	-0.09	-0.02	0.12	0.31	-0.23	-0.13	0.03	0.11
n = 74	0.002**	0.441	0.138	-	0.347	0.006**	0.452	0.866	0.299	0.008**	0.048*	0.279	0.84	0.432
CRE ^e	0.1	0.22	-0.04	-0.11	-	-0.03	0.21	-0.13	0.29	-0.05	0.2	0.02	0.03	-0.09
n = 74	0.402	0.06 ⁺	0.717	0.347	-	0.822	0.073 ⁺	0.276	0.013*	0.701	0.09 ⁺	0.895	0.83	0.506
d-Dimer ^f	0.21	0.12	-0.21	0.32	-0.03	-	0.08	0.32	0.15	0.26	-0.01	-0.15	0.02	0.21
n = 74	0.073 ⁺	0.324	0.067 ⁺	0.006**	0.822	-	0.509	0.008**	0.197	0.026*	0.921	0.19	0.89	0.117
PT ^g	-0.06	0.15	-0.1	-0.09	0.21	0.08	-	0.05	-0.03	-0.07	0.03	0.23	0.23	-0.07
n = 74	0.599	0.188	0.385	0.452	0.073 ⁺	0.509	-	0.678	0.791	0.539	0.805	0.049*	0.05*	0.612
FERR ^h	0.32	0.3	-0.15	-0.02	-0.13	0.32	0.05	-	0.12	0.24	0.09	-0.1	-0.04	0.38
n = 69	0.007**	0.011*	0.209	0.866	0.276	0.008**	0.678	-	0.333	0.043*	0.447	0.435	0.76	0.005***
PCT ⁱ	0.53	0.14	0.04	0.12	0.29	0.15	-0.03	0.12	-	0.23	-0.05	-0.16	0.02	0.28
n = 74	0.000***	0.223	0.723	0.299	0.013*	0.197	0.791	0.333	-	0.048*	0.693	0.177	0.89	0.04*
CRP ^j	0.2	0.07	-0.23	0.31	-0.05	0.26	-0.07	0.24	0.23	-	0.07	-0.05	0.15	0.04
n = 74	0.082 ⁺	0.542	0.046*	0.008***	0.701	0.026*	0.539	0.043*	0.048*	-	0.538	0.661	0.2	0.766
age ^k	-0.14	0.06	-0.2	-0.23	0.2	-0.01	0.03	0.09	-0.05	0.07	-	0.26	0.24	-0.06
n = 74	0.245	0.595	0.096 ⁺	0.048	0.09 ⁺	0.921	0.805	0.447	0.693	0.538	-	0.026*	0.05 ⁺	0.63
days before ^l	-0.07	-0.12	-0.11	-0.13	0.02	-0.15	0.23	-0.1	-0.16	-0.05	0.26	-	0.75	0.11
n = 74	0.557	0.303	-0.2	0.279	0.895	0.19	0.049*	0.435	0.177	0.661	0.026*	-	0.001***	0.422
days after ^m	-0.03	0.07	0.096	0.03	0.03	0.02	0.23	-0.04	0.02	0.15	0.24	0.75	-	0.05
n = 71	0.83	0.54	0.02*	0.84	0.83	0.89	0.05 ⁺	0.76	0.89	0.2	0.05 ⁺	0.001***	-	0.72
Covid score ⁿ	0.66	-0.08	-0.004	0.11	-0.09	0.21	-0.07	0.38	0.28	0.04	-0.06	0.11	0.05	-
n = 56	0.001***	0.579	0.974	0.432	0.506	0.117	0.612	0.005***	0.04*	0.766	0.63	0.422	0.72	-

Table 2. Correlation matrix: Pearson correlation coefficients and relative *p* values. Statistically significant results are highlighted in bold. *n* number of patients. ^aS100B protein, ng/mL. ^bWhite Blood Cell count per mm³. ^cLymphocyte count per mm³. ^dAlanine Aminotransferase—IU/L. ^eCreatinine—mg/dL. ^fd-Dimer—ng/mL. ^gProthrombin—seconds. ^hFerritin—mg/L. ⁱProcalcitonin—ng/mL. ^jC Reactive Protein—mg/dL. ^kPatients' age—years. ^lPeriod from hospitalization to blood sample collection—days. ^mPeriod from blood sample collection to hospital discharge—days. ⁿCovid score—%. ⁺*p* < 0.1; ^{*}*p* < 0.05; ^{**}*p* < 0.01; ^{***}*p* < 0.001.

Methods

Dataset. 74 serum samples from patients with confirmed SARS-CoV-2 infection hospitalized in an academic Covid hospital in Rome, Italy, were collected during the epidemic pick (from January 29th to May 6th, 2020). The inclusion criteria were Covid-19 diagnosis and age (≥ 18 y.o.), while exclusion criteria were concomitant or pre-existing neurological disorders, cardiovascular diseases, diabetes and cancer. According to WHO clinical criteria at admission time, patients were hospitalized in High (HIC) and Low Intensity Care (LIC) wards, respectively. Severity of Covid-19 at the time of blood sampling was quantified using a Covid-score, attributing a value ranging from 0 to 100%^{4-7,9}. Main variables incorporated in the Covid-score included: older age, male sex, comorbidities, respiratory rate, oxygenation, radiographic severity, higher neutrophils, higher CRP and lower albumin at presentation, predicted critical care admission and mortality; in particular: age > 50 , male, oxygen saturation $< 93\%$, radiological severity score > 3 , neutrophil count $> 8.0 \times 10^9/\text{L}$, CRP $> 40 \text{ mg/L}$, albumin $< 34 \text{ g/L}$, creatinine $> 100 \mu\text{mol/L}$, comorbidity and chronic lung disease, ALT $> 40 \text{ IU/L}$; Creatinine $> 100 \mu\text{mol/L}$; D-dimer $> 0.5 \mu\text{g/L}$; Prothrombin-time $> 16 \text{ s}$; Ferritin $> 300 \mu\text{g/L}$; Procalcitonin $> 0.1 \text{ ng/mL}$.

Namely, patients recovered in HIC (*n* = 16) presented: severe pneumonia (fever or suspected respiratory infection, plus one of the following: respiratory rate > 30 breaths/min; severe respiratory distress or SpO₂ $\leq 93\%$ on room air); and LIC (*n* = 58) comprehended a group spanning from uncomplicated disease to pneumonia but without signs of severe pneumonia. In both groups, all patients received treatment in accordance with the guidelines available at the time of the study¹. Time of hospitalization ranged from 7 to 85 days (average: 29.97). Table 1 shows patients' characteristics together with data obtained on serum samples. Patients were balanced with respect to gender (female = 49%), their age ranging from 32 to 89 (median: 66.0). Serum samples from healthy subjects (*n* = 5) negative for SARS-CoV-2 detection by PCR and negative by serologic test were used as controls for the ELISA test.

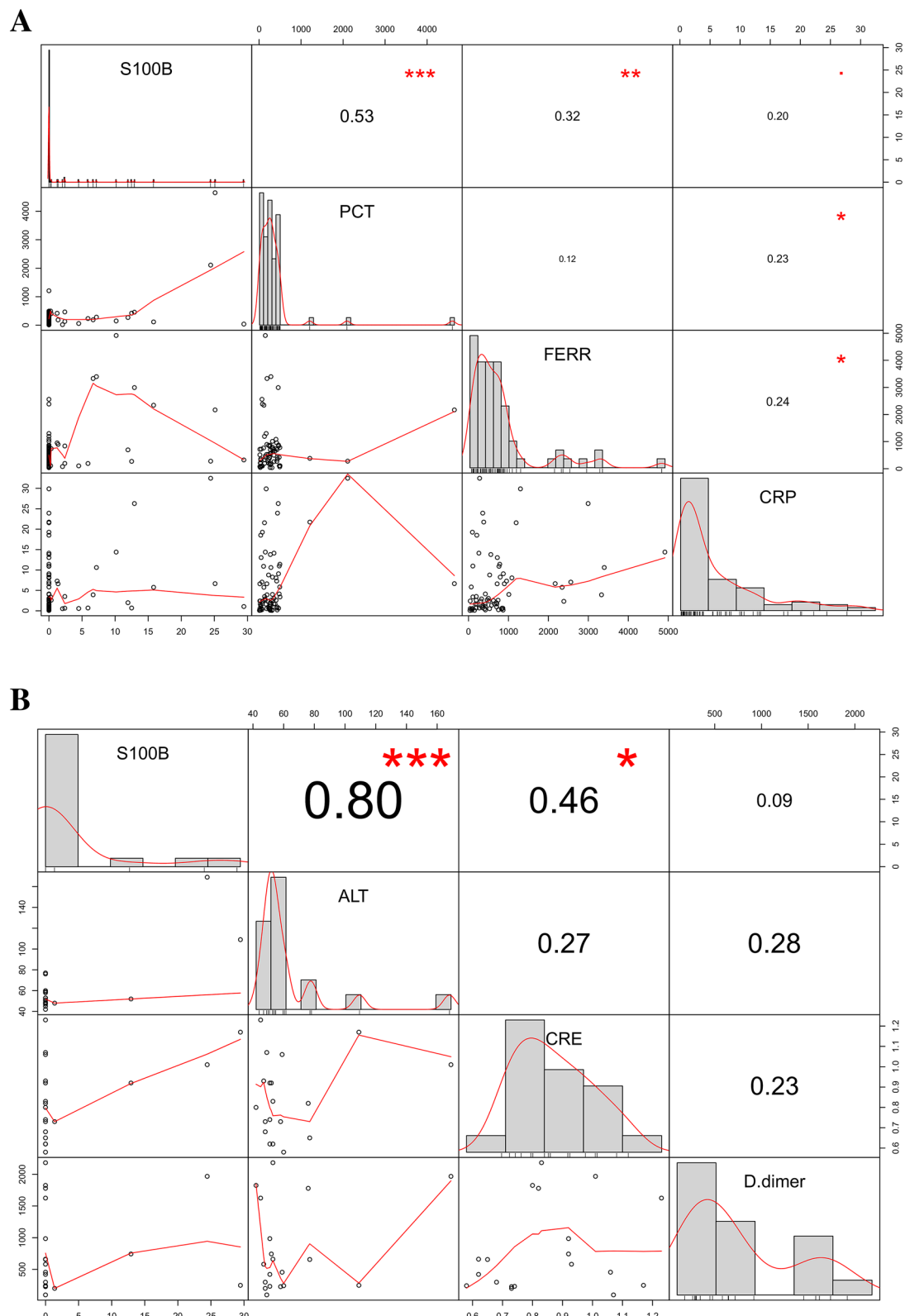


Figure 3. Correlation of S100B with other blood markers. **(A)** Correlation of S100B versus inflammatory markers. S100B significantly correlates with PCT, FERR, CRP. Scatterplots of pairwise variable are shown. Values in the middle of boxes are referred to the Pearson Correlation. PCT: Procalcitonin; FERR: Ferritin, CRP: C-Reactive Protein. Red Stars and dots are referred to the p-values ($^{***}p < 0.0001$; $^{**}p < 0.001$; $^*p < 0.01$; $^+p < 0.1$). **(B)** Correlation of S100B versus Organ Damage markers. S100B significantly correlates with ALT and CRE (subgroup of patients showing ALT > 40 IU/L). Scatterplots of pairwise variable are shown. Values in the middle of boxes are referred to the Pearson Correlation. ALT: Alanine Aminotransferase; CRE: Creatinine; d-Dimer: d-Dimer. Values in the middle of boxes are referred to the Pearson Correlation. Red Stars and dots are referred to the p values ($^{***}p < 0.0001$; $^{**}p < 0.001$; $^*p < 0.01$; $^+p < 0.1$).

Ethics. The project protocol involved the rapid recruitment of patient-participants during the pandemic pick and no additional project-related procedures (we used only material from routine venipunctures). Anonymity was assured by the hospital privacy protocol and written consent obtained by each of recruited participants. The study was approved by the Sant'Andrea University Hospital Ethical Committee/Institutional Review Board (N. 5773/2020).

Laboratory Tests. The serum S100B concentrations were measured by adapting the enzyme-linked immunosorbent assay (ELISA) kit following manufacturer protocols (S100B ELISA Kit, Abcam, England). Samples resulting below the detection limit of the test (LOD, equal to 0.1 ng/mL) were considered negative and assigned a value of 0 ng/mL. From the same serum, a panel of consolidated blood markers was also assessed, including White Blood Cell count (WBC), Lymphocytes (LYM), Alanine Aminotransferase (ALT), Creatinine (CRE), d-Dimer, Prothrombin (PT), Ferritin (FERR), Procalcitonin (PCT), C Reactive Protein (CRP).

Statistical analysis. Continuous variables were S100B serum concentration (ng/mL), WBC (count per mm³), LYM (count per mm³), ALT (IU/L), CRE (mg/dL), d-Dimer (ng/mL), PT (seconds), FERR (ng/mL), PCT (pg/mL), CRP (mg/dL), period from hospitalization to blood sample collection (days), period from sample collection to hospital discharge (days), severity of the disease (Covid score), age (years). Categorical variables were gender (male = 0, female = 1), S100B protein in detectable amount (below LOD = 0 and over LOD = 1), hospitalization ward (LIC = 0 and HIC = 1). Relations between continuous variables were compared by Pearson's correlation. Pearson's χ^2 test was used to compare the frequencies of the categorical variables and non parametric test Wilcoxon or Kruskal were used to compare the two groups under the non-normality assumption. Linear models (ANOVA, ANCOVA, and Linear Regression) were performed to evaluate the effect of variables observed on concentration of S100B. Whenever the test of homogeneity of variance was not satisfied, the ANOVA results were substituted by those from Welch ANOVA. Tukey test were performed to evaluate the difference of means between groups. If equal variance assumption is violated during the ANOVA process, pairwise comparison was based on the Games-Howell statistics. Stepwise regression was performed to obtain the model with the best predictors. All analyses were considered statistically significant at a p value of less than 0.05, if not differently indicated. All data were analyzed using the R environment for statistical computing (Version 4.0.1).

Received: 25 July 2020; Accepted: 15 October 2020

Published online: 29 October 2020

References

- WHO. Clinical management of severe acute respiratory infection (SARI) when COVID-19 disease is suspected: interim guidance, 13 March 2020 [Online]. Available from: <https://apps.who.int/iris/handle/10665/331446>. Accessed 24 March 2002.
- Guan, W. et al. Clinical characteristics of coronavirus disease 2019 in China. *N Engl J Med* **382**, 1708–1720 (2020).
- Zhao, D. et al. A comparative study on the clinical features of Coronavirus 2019 (COVID-19) pneumonia with other pneumonias. *Clin. Infect. Dis.* 2020 Mar 12. <https://doi.org/10.1093/cid/ciaa247> [Epub ahead of print].
- Galloway, J. B. et al. A clinical risk score to identify patients with COVID-19 at high risk of critical care admission or death: an observational cohort study. *J. Infect.* **81**, 282–288 (2020).
- Xiao, L. et al. Development and validation of the HNC-LL score for predicting the severity of coronavirus disease 2019. *EBioMedicine* **57**, 102880 (2020).
- Ji, D. et al. Prediction for progression risk in patients with COVID-19 pneumonia: The CALL Score. *Clin. Infect. Dis.* 2020 Apr 9. <https://doi.org/10.1093/cid/ciaa414> [Epub ahead of print].
- Bhargava, A. et al. Predictors for Severe COVID-19 Infection. *Clin. Infect. Dis.* 2020 May 30. <https://doi.org/10.1093/cid/ciaa674> [Epub ahead of print].
- Liu, R. et al. The value of urine biochemical parameters in the prediction of the severity of coronavirus disease 2019. *Clin Chem Lab Med* **58**, 1121–1124 (2020).
- Wynants, L. et al. Prediction models for diagnosis and prognosis of Covid-19 infection: systematic review and critical appraisal. *Br Med J* **369**, m1328 (2020).
- Gong, T., Liu, L., Jiang, W. & Zhou, R. DAMP-sensing receptors in sterile inflammation and inflammatory diseases. *Nat Rev Immunol* **20**, 95–112 (2020).
- Yang, D., Han, Z. & Oppenheim, J. J. Alarms and immunity. *Immunol Rev* **280**, 41–56 (2017).
- Michetti, F. et al. The S100B story: from biomarker to active factor in neural injury. *J Neurochem* **148**, 168–187 (2019).
- Lippi, G. & Cervellin, G. Protein S100B: from cancer diagnostics to the evaluation of mild traumatic brain injury. *Clin Chem Lab Med* **54**, 703–705 (2016).
- Michetti, F., Massaro, A., Russo, G. & Rigon, G. The S-100 antigen in cerebrospinal fluid as a possible index of cell injury in the nervous system. *J Neurol Sci* **44**, 259–263 (1980).
- Kato, K., Kimura, S., Semba, R., Suzuki, F. & Nakajima, T. Increase in S-100 protein levels in blood plasma by epinephrine. *J Biochem* **94**, 1009–1011 (1983).
- Gazzolo, D. et al. Increased urinary S100B protein as an early indicator of intraventricular hemorrhage in preterm infants: correlation with the grade of hemorrhage. *Clin Chem* **47**, 1836–1838 (2001).
- Di Liddo, R. et al. S100B as a new fecal biomarker of inflammatory bowel diseases. *Eur Rev Med Pharmacol Sci* **24**, 323–332 (2020).
- Cheng, C. et al. Expression profiling of endogenous secretory receptor for advanced glycation end products in human organs. *Mod Pathol* **18**, 1385–1396 (2005).
- Merad, M. & Martin, J. C. Pathological inflammation in patients with COVID-19: a key role for monocytes and macrophages. *Nat Rev Immunol* **20**, 355–362 (2020).
- Rojas, A., Gonzalez, I. & Morales, M. A. SARS-CoV-2-mediated inflammatory response in lungs: should we look at RAGE?. *Inflamm Res* **69**, 641–643 (2020).
- Tay, M. Z., Poh, C. M., Rénia, L., MacAry, P. A. & Ng, L. F. P. The trinity of COVID-19: immunity, inflammation and intervention. *Nat Rev Immunol* **20**, 363–374 (2020).

22. Song, J. *et al.* Immunological and inflammatory profiles in mild and severe cases of COVID-19. *Nat Commun* **11**, 3410 (2020).
23. Prati, D. *et al.* Updated definitions of healthy ranges for serum alanine aminotransferase levels. *Ann Intern Med* **137**, 1–10 (2002).
24. Sproston, N. R. & Ashworth, J. J. Role of C-reactive protein at sites of inflammation and infection. *Front Immunol* **9**, 754 (2018).
25. Sorci, G. *et al.* S100B Protein, a damage-associated molecular pattern protein in the brain and heart, and beyond. *Cardiovasc Psychiatry Neurol* **2010**, 656481 (2010).
26. Zhu, L. *et al.* S100B regulates inflammatory response during osteoarthritis via fibroblast growth factor receptor 1 signalling. *Mol Med Rep* **18**, 4855–4864 (2018).
27. Frontera, J. *et al.* Global consortium study of neurological dysfunction in COVID-19 (GCS-NeuroCOVID): study design and rationale. *Neurocrit Care* 2020 May 22. <https://doi.org/10.1007/s12028-020-00995-3> [Epub ahead of print].
28. Michetti, F., Dell'Anna, E., Tiberio, G. & Cocchia, D. Immunochemical and immunocytochemical study of S-100 protein in rat adipocytes. *Brain Res* **262**, 352–356 (1983).
29. Cocchia, D., Tiberio, G., Santarelli, R. & Michetti, F. S-100 protein in “follicular dendritic” cells or rat lymphoid organs. An immunochemical and immunocytochemical study. *Cell Tissue Res.* 1983; **230**:95–103.
30. Steiner, J. *et al.* Human CD8(+) T cells and NK cells express and secrete S100B upon stimulation. *Brain Behav Immun* **25**, 1233–1241 (2011).
31. Miki, Y. *et al.* Morphologic, flow cytometric, functional, and molecular analyses of S100B positive lymphocytes, unique cytotoxic lymphocytes containing S100B protein. *Eur J Haematol* **90**, 99–110 (2013).
32. Engin, A. B. Adipocyte-macrophage cross-talk in obesity. *Adv Exp Med Biol* **960**, 327–343 (2017).
33. Maurizi, G., Della Guardia, L., Maurizi, A. & Poloni, A. Adipocytes properties and crosstalk with immune system in obesity-related inflammation. *J Cell Physiol* **233**, 88–97 (2018).
34. Sonnenberg, G. F. & Artis, D. Innate lymphoid cells in the initiation, regulation and resolution of inflammation. *Nat Med* **21**, 698–708 (2015).
35. Qian, C. & Cao, X. Dendritic cells in the regulation of immunity and inflammation. *Semin Immunol* **35**, 3–11 (2018).
36. Sorci, G. *et al.* The danger signal S100B integrates pathogen- and danger-sensing pathways to restrain inflammation. *PLoS Pathog* **7**, e1001315 (2011).
37. Piazza, O. *et al.* S100B induces the release of pro-inflammatory cytokines in alveolar type I-like cells. *Int J Immunopathol Pharmacol* **26**, 383–391 (2013).

Acknowledgements

The authors thank Dr. Gianluca Gianfranceschi for the technical support and Tiziana Zilli for the library support; The study was partially supported by Nando-Elsa Peretti Foundation Project (grant assigned to F.M.; NaEPF 2019-041), by Fondazione per la Ricerca Scientifica Termale grant: “Development of innovative strategies for thermal water treatments: nanotechnologies & perspectives for hygiene” (CUP H81I18000070008) and by the Foundation for Biology and Regenerative Medicine, Tissue Engineering and Signaling T.E.S (PPP).

Author contributions

A.A., V.R.S. and F.M. designed the experiments. A.A., E.S., and M.S. collected clinical data. E.S., G.S., G.G., F.V. and M.S. performed laboratory analysis. L.M.M., M.O. and F.V. analysed data. A.A., M.O., G.D.S., R.D.L., F.R., P.P.P., M.V., V.R.S. and F.M. interpreted the results. M.O., M.V., V.R.S. and F.M. wrote the Article. M.V., V.R.S. and F.M. edited and revised the Article.

Competing interests

The authors declare no competing interests.

Additional information

Supplementary information is available for this paper at <https://doi.org/10.1038/s41598-020-75618-0>.

Correspondence and requests for materials should be addressed to V.R.S.

Reprints and permissions information is available at www.nature.com/reprints.

Publisher's note Springer Nature remains neutral with regard to jurisdictional claims in published maps and institutional affiliations.



Open Access This article is licensed under a Creative Commons Attribution 4.0 International License, which permits use, sharing, adaptation, distribution and reproduction in any medium or format, as long as you give appropriate credit to the original author(s) and the source, provide a link to the Creative Commons licence, and indicate if changes were made. The images or other third party material in this article are included in the article's Creative Commons licence, unless indicated otherwise in a credit line to the material. If material is not included in the article's Creative Commons licence and your intended use is not permitted by statutory regulation or exceeds the permitted use, you will need to obtain permission directly from the copyright holder. To view a copy of this licence, visit <http://creativecommons.org/licenses/by/4.0/>.

© The Author(s) 2020



Review

The Role of P-Selectin in COVID-19 Coagulopathy: An Updated Review

Chiara Agrati, Alessandra Sacchi, Eleonora Tartaglia, Alessandra Vergori , Roberta Gagliardini, Alessandra Scarabello and Michele Bibas *

National Institute for Infectious Diseases “Lazzaro Spallanzani” I.R.C.C.S., Via Portuense 292, 00146 Rome, Italy; chiara.agrati@inmi.it (C.A.); alessandra.sacchi@inmi.it (A.S.); eleonora.tartaglia@inmi.it (E.T.); alessandra.vergori@inmi.it (A.V.); roberta.gagliardini@inmi.it (R.G.); alessandra.scarabello@inmi.it (A.S.)

* Correspondence: michele.bibas@inmi.it

Abstract: In severe COVID-19, which is characterized by blood clots and neutrophil-platelet aggregates in the circulating blood and different tissues, an increased incidence of cardiovascular complications and venous thrombotic events has been reported. The inflammatory storm that characterizes severe infections may act as a driver capable of profoundly disrupting the complex interplay between platelets, endothelium, and leukocytes, thus contributing to the definition of COVID-19-associated coagulopathy. In this frame, P-selectin represents a key molecule expressed on endothelial cells and on activated platelets, and contributes to endothelial activation, leucocyte recruitment, rolling, and tissue migration. Briefly, we describe the current state of knowledge about P-selectin involvement in COVID-19 pathogenesis, its possible use as a severity marker and as a target for host-directed therapeutic intervention.



Citation: Agrati, C.; Sacchi, A.; Tartaglia, E.; Vergori, A.; Gagliardini, R.; Scarabello, A.; Bibas, M. The Role of P-Selectin in COVID-19

Coagulopathy: An Updated Review.
Int. J. Mol. Sci. **2021**, *22*, 7942.
<https://doi.org/10.3390/ijms22157942>

Academic Editor: Nicola Pozzi

Received: 28 June 2021
Accepted: 21 July 2021
Published: 26 July 2021

Publisher’s Note: MDPI stays neutral with regard to jurisdictional claims in published maps and institutional affiliations.



Copyright: © 2021 by the authors. Licensee MDPI, Basel, Switzerland. This article is an open access article distributed under the terms and conditions of the Creative Commons Attribution (CC BY) license (<https://creativecommons.org/licenses/by/4.0/>).

1. Introduction

The severe acute respiratory syndrome coronavirus 2 (SARS-CoV-2) causes coronavirus disease 2019 (COVID-19), which can present with a wide range of manifestations, including pneumonia and acute respiratory distress syndrome (ARDS) [1]. COVID-19 has a very different clinical spectrum, ranging from asymptomatic or paucisymptomatic (in up to 45 percent of people) to severe diseases necessitating intensive care unit admission (ICU). As seen in patients with COVID-19 and post-mortem samples from those who died after SARS-CoV-2 infection, SARS-CoV-2 infection causes a pro-thrombotic condition manifested mainly by microthrombosis [2]. Excessive pulmonary immunothrombosis, an intrinsic route of innate immunity induced by pathogens and wounded cells to prevent the spread and survival of invading pathogens, is connected to patients with severe COVID-19 who have an extremely high risk of thrombosis [3]. Excessive stimulation of the immunothrombosis process causes thromboinflammation, a condition in which inflammation and thrombosis coexist within the microvessels in response to damaging stimuli. Immunothrombosis is defined by the production of microthrombi in tiny capillaries, in which endothelial cells exposed to microorganisms adopt a pro-adhesive phenotype. Neutrophils and monocytes are primarily responsible for this process [4]. The fast-paced nature of this discipline needs the integration of existing biology data with COVID-19 clinical findings in order to better understand the disease’s etiology and contribute to the development of new possible therapeutics. In this review, we summarize the current published studies that show the role of P-selectin in COVID-19 associated coagulopathy.

2. Selectins

The selectins are a family of calcium-dependent (C-type) lectins best known for mediating immune cell adherence to the endothelium, allowing immune cells to enter

secondary lymphoid organs and inflammatory sites. The selectin family consists of three members, each called for their expression patterns: P-selectin, E-selectin, and L-selectin, which are expressed on platelets, endothelial cells, and leukocytes, respectively [5]. Only P-selectin was the subject of our investigation.

P-selectin is a type-1 transmembrane protein encoded by the SELP gene in humans. P-selectin is found on chromosome 1q21-q24, spans > 50 kb, and has 17 exons. Megakaryocytes (platelet precursors) and endothelial cells express P-selectin on a constant basis [6]. Two different processes are involved in the induction of P-selectin expression. First, megakaryocytes and endothelial cells produce P-selectin, which is then deposited in platelet alpha granules and endothelial cell Weibel-Palade bodies. When a cell is exposed to an activating stimulus like thrombin, P-selectin is rapidly translocated to the cell surface, eliminating the requirement for transcription or translation. Within minutes after activation, P-selectin is transported to the exterior plasma membrane. This increase in P-selectin expression is very temporary, as the protein is quickly internalized and destroyed or recycled within the cell. TNF also increases the transcription of P-selectin [6]. P-selectin binds to heparan sulfate and fucoidans, but its principal ligand is P-selectin glycoprotein ligand-1 (PSGL-1), which is expressed on practically all leukocytes. PSGL-1 is found on a variety of hematological cells, including neutrophils, eosinophils, lymphocytes, and monocytes, where it promotes cell tethering and adhesion [7]. P-selectin is involved in the initial attachment and rolling of platelets and leukocytes to inflamed and injured regions. PSGL-1 signaling in leukocytes and platelets, as well as GPIb signaling in platelets, play important roles in hemostasis and thrombosis. The VWF receptor, glycoprotein (GP) Iba, has also been demonstrated to be a counter-receptor for P-selectin, suggesting that platelet rolling on P-selectin may be facilitated [8]. Platelet and leukocyte activity, in this case, are strikingly similar, both cell types must slow down (roll) before firmly adhering to the site of injury/inflammation. The fact that the adhesion molecules that cause initial adhesion in both leukocytes and platelets are kept in the same organelle and are thus always released jointly demonstrates how closely hemostatic and inflammatory responses are linked [9]. Furthermore, soluble P-selectin (sP-sel) is detected in the circulation as a monomer, indicating that sP-sel must dimerize to activate signaling in leukocytes, according to *in vitro* investigations. As a result, when sP-sel dimerizes or is identified as a dimer on the surface of platelet-derived microparticles, it can activate leukocytes, making it not only a helpful biomarker but also a direct contributor to vascular disease [10].

3. P-Selectin in Human Diseases

P-selectin levels in the plasma have been found to be elevated in a number of human illnesses. Endothelial cells in Sickle Cell Disease (SCD) express P-selectin on a long-term basis [11]. P-selectin upregulation in endothelial cells and platelets contributes to cell-cell interactions implicated in the development of vaso-occlusion and sickle cell pain crises [12]. P-selectin levels in the blood have been found to be elevated in a variety of acute and chronic cardiovascular diseases, including peripheral arterial disease, coronary artery disease, hypertension, and acute myocardial infarction [13–17]. P-selectin is also involved in atherosclerosis [18], as well as hypercholesterolemia [19,20]. In patients with symptomatic internal carotid artery stenosis, elevated levels were found, with further increases in acute ischemic stroke [21]. When compared to healthy controls, P-selectin levels were found to be 2- to 2.5-fold higher in patients on the first day following cerebral ischemia. P-selectin levels continued to drop steadily from the second day onwards, eventually returning to normal 90 days following the stroke [22]. Increased prothrombotic activity, impaired fibrinolysis, diminished endothelial thromboresistance, and platelet hyperreactivity with overall hypercoagulability are common in diabetic patients. Many investigations have found that patients with diabetes mellitus have a greater median plasma level of circulating P-selectin, as well as enhanced P-selectin expression on platelets [23]. This activation, it should be noted, was not linked to improved glycemic control with increased insulin therapy [24]. P-selectin may be responsible for increased platelet activation in deep venous

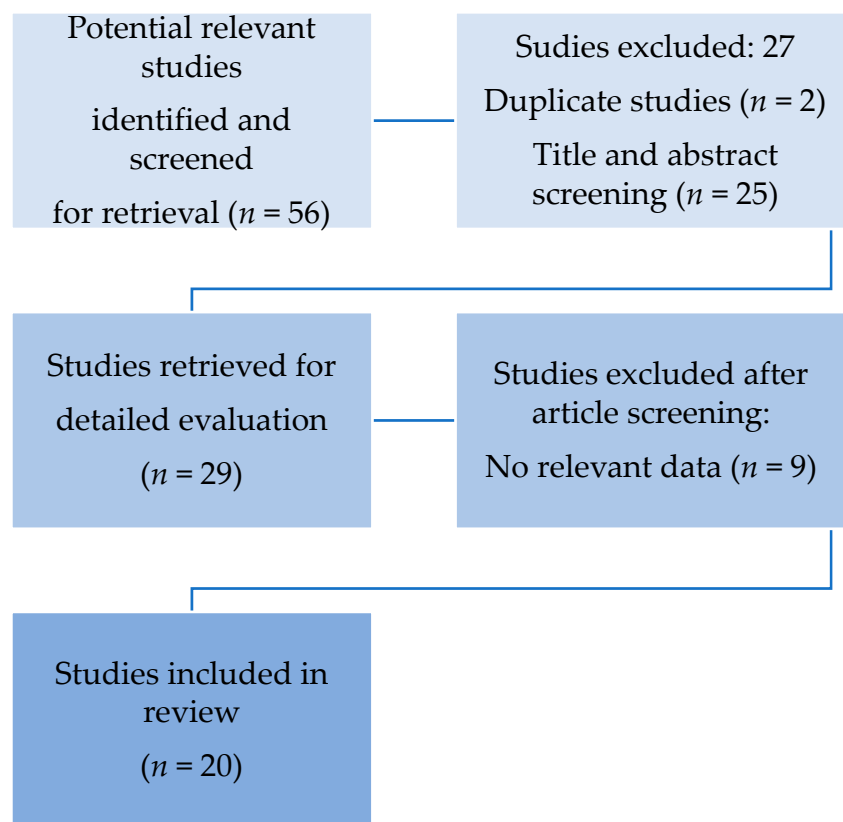
thrombosis (DVT), in addition to its effect on arterial thrombosis. Furthermore, it may play a role in the diagnosis of DVT, according to a meta-analysis report that included eleven trials [25]. P-selectin may play a predictive role in the diagnosis of DVT in cancer patients, according to other researchers [26]. In venous thrombosis, higher levels of sP-selectin were discovered than in advanced-stage cancer patients, leading to the hypothesis that, despite an increase in sP-selectin in patients with metastatic cancer, their values rise in acute DVT [27]. Thrombotic consumptive diseases, such as disseminated intravascular coagulation, thrombotic thrombocytopenic purpura, and heparin-induced thrombocytopenia, also have higher levels of P-selectin [28–30]. Oncology is one area where P-selectin's role has been demonstrated convincingly in both experimental and clinical research. P-selectin is one of the most well-studied platelet-tumor interaction mediators. Heparin inhibits tumor cell spread in vivo by inhibiting the P-selectin-mediated platelet-tumor interaction [31]. One possible explanation is that P-selectin is required for the creation of the platelet cloak that surrounds circulating tumor cells and protects tumor cells from NK cell attack [32]. While P- and L-selectins have been found to have a synergistic effect on tumor cell systemic dissemination in vivo, heparin's inhibitory influence on this process is related to the blockage of P-selectin function [33]. Furthermore, P-selectin's cytoplasmic domain appears to facilitate platelet infiltration into tumors by binding to talin-1, inducing talin1-mediated activation of αIIbb3 integrin and hence platelet recruitment into tumors [34]. Previous research has found that enhanced P-selectin expression occurs during viral infections, including influenza [35]. Increased P-selectin expression enhances platelet-leukocyte aggregation formation via P-selectin glycoprotein ligand-1 (PSGL-1). Platelet-leukocyte aggregates (PLA) production has been described as a highly sensitive measure of platelet activation in vivo during viral illnesses [36]. Several investigations have found that patients living with HIV have higher levels of P-selectin than people who are not infected. This backs up the observation that adult HIV-infected patients have higher levels of platelet activation [37]. Importantly, these levels were found to persist in follow-up investigations after 3 to 24 months of effective ART [38]. Despite the fact that ART reduced platelet activation in individuals who did not receive protease inhibitors (PIs), platelet activation levels in those on PI-based therapy persisted despite successful ART [39–41]. High plasma soluble P-selectin concentrations at baseline were connected to reduced FEV1 and RV/TLC, a sign of severe air trapping in asthma patients [42]. Severe obstructive sleep apnea was also linked to higher plasma P-selectin levels, which were correlated to illness severity measures such as the apnea-hypopnea index, oxygen desaturation index, and respiratory disturbance index [43,44].

4. Methodology

To give the most thorough background information on P-selectin in COVID-19, we did an exhaustive literature search utilizing PubMed/Medline, EMBASE, and Google Scholar to find publications published in English between January 2020 and June 2021. The main search terms used were “P-selectin” or “sP-selectin” and “COVID-19” or “SARS-CoV-2”

5. Search Strategy

The search procedure used in this systematic review is visualized in Figure 1. All publications were reviewed by two separate reviewers (CA and MB) on the basis of title, abstract, and full-text level. The systematic review covered all papers on the function of P-selectin in the pathophysiology of COVID-19. Titles and abstracts chosen by one of the reviewers were included in the full-text screening process. Final articles that matched our study topic were withheld after rigorous reading and review of each selected full-text. Both independent reviewers also searched the reference lists of the selected full-text articles for supplemental papers. The same two reviewers went through the same selection process for these new articles. Articles written in languages other than English were not included in the study. All study designs were considered, with the exception of editorials, single-case reports, and reviews. Observational studies were mostly chosen.

**Figure 1.** Search strategy.

6. Results

Our initial search rendered 56 articles. After reviewing the full-text articles, 20 studies were selected, and data from 936 cases were analyzed. (Table 1)

Table 1. Studies on P-selectin in COVID-19 patients.

AUTHOR	COVID-19 pts	Age Median (Range)	Gender M/F	Moderate COVID-19+ (n)	Severe non-ICU COVID-19+ (n)	Severe ICU COVID-19+ (n)	Main Findings
Goshua [45]	68	62 (20–93)	27/41	-	higher than HC (n = 20)	higher than non-ICU (n = 48)	Association with critical illness and death
Hottz [46]	41	57 (47–64)	19/22	-	-	higher than controls (n = 35)	Association with critical illness and death
Campo [47]	54	65 (57–73)	40/14	-	higher than HC (n = 17)	higher than non-ICU (n = 37)	Association with critical illness and death
Vassiliou [48]	38	65(51–78)	31/7	-		higher than non-ICU (n = 38)	Association with critical illness and death
Barrett [49]	100	65	61/39		higher than HC (n = 100)		Association with critical illness and death
Agrati [50]	46	67 (50–80)	34/12	-	higher than HC (n = 19)	no differences with non-ICU (n = 27)	Higher P-Sel regardless ICU admission
Manne [51]	41	55 (33–77)	19/22	-	higher than HC (n = 24)	no differences with non-ICU (n = 17)	Higher P-Sel regardless ICU admission

Table 1. *Cont.*

AUTHOR	COVID-19 pts	Age Median (Range)	Gender M/F	Moderate COVID-19+ (n)	Severe non-ICU COVID-19+ (n)	Severe ICU COVID-19+ (n)	Main Findings
Shen [52]	62	66 (60–71)	32/30	-	higher than HC (n = 37)	higher than non-ICU (n = 25)	Higher values in COVID-19+ ICU patients.
Petito [53]	36	70.6 (36–60)	20/16	-	higher than HC (n = 17)	higher than non-ICU (n = 19)	Higher values in COVID-19+ ICU patients
Comer [54]	54	63 (47–84)	34/20	-	higher than HC (n = 20)	higher than non-ICU (n = 34)	Higher values in COVID-19+ ICU patients
Fraser [55]	10	61 (54.8–67)	3/7	-	-	higher than HC (n = 10)	Higher values in COVID-19+ ICU patients
Karsli [56]	80	-	-	-	higher than HC (n = 50)	higher than non-ICU (n = 35)	Higher values in COVID-19+ ICU patients
Taus [57]	37	61.8 (47–94)	18/19	-	higher than HC (n = 37)	-	P-Sel higher than controls
Chao [58]	15	71 (53–80)	5/10	higher than HC (n = 5)	-	-	P-Sel higher than controls
Canzano [59]	46	72 (58–84)	28/18	-	higher than HC (n = 46)	-	P-Sel higher than controls
Bongiovanni [60]	8	51.4 (39–64)	5/3	-	higher than HC (n = 8)	-	P-Sel higher than controls
Venter [61]	30	53.1 (38–69)	-	lower than HC (n = 30)	-	-	Study reporting a lower P-Sel level in COVID-19+
Clark [62]	79	67 (54–75)	43/34	-	Similar to Controls (n = 79)	-	Study reporting a similar P-Sel level In COVID-19+ and Controls
Bertolin [63]	60	52 (37–68)	31/29	Similar to Controls (n = 60)	-	-	Study reporting a similar P-Sel level In COVID-19+ and Controls
Spadaro [64]	31	67 (55–75)	26/5	-	-	31 lower value than COVID-19- ARDS (n = 31)	P-Sel lower than ARDS controls, but higher than normal value

Abbreviation: P-sel = P-selectin; med= median; ICU = intensive care unit; (n) = number of patients in each class.

Five studies have associated P-selectin levels with critical illness and death [45–49]. Goshua et al. [45] found P-selectin and other platelet and endothelial markers significantly elevated in intensive care unit (ICU) patients compared with controls, and also significantly higher in ICU patients than in non-ICU patients. Mortality was significantly correlated with the elevation of those markers. Hottz et al. [46], evaluating the P-selectin values within 72 h from ICU admission, demonstrated an increased level of those patients compared with healthy control and asymptomatic or mildly ill infected patients. Patients' poor outcomes, including the need for mechanical ventilation and in-hospital mortality, were predicted by P-selectin levels above the control group median and platelet-dependent TF expression in monocytes upon admission. Patients with severe COVID-19 syndrome had increased platelet activation and platelet-monocyte aggregation formation, however, patients with mild self-limiting COVID-19 disease did not. Although P-selectin was the predominant adhesion molecule enabling platelet-monocyte aggregation formation in this scenario, platelet-induced TF expression needed both P-selectin and integrin αIIb/b3 signaling. Pre-

treatment with aspirin and clopidogrel did not inhibit platelet-induced TF in monocytes, which was interesting. After adjusting for confounding factors, Campo et al. [47], discovered that P-selectin values were greater and had a different pattern over time in patients who died versus those who survived. P-selectin levels that were higher were likewise linked to myocardial damage. This study backs up previous findings that COVID-19 is linked to changes in platelet activation and aggregation, and that there are no variations in platelet aggregation values between ICU and non-ICU COVID-19 patients. P-selectin and sCD40L values, on the other hand, were influenced by COVID-19 severity, with P-selectin and sCD40L levels being higher in ICU patients.

In order to predict death, Vassiliou et al. [48] looked at patterns of several endothelium-related indicators in critically ill COVID-19 patients on ICU admission. COVID-19 critically sick patients who would not survive had higher ICU entry levels of sP-sel and other endothelial markers. Non-survivors had a cumulative theoretical predictive score of 4.1, compared to 1.4 for survivors, based on biomarkers. They did not find greater levels of sP-sel in severely ill COVID-19 patients in this cohort when compared to patients hospitalized in the ward. This is most likely related to the fact that markers were tested on admission rather than during hospitalization. Barrett et al. [49], following adjustment for age, sex, race/ethnicity, antiplatelet therapy, platelet count, and chronic obstructive pulmonary disease, TxB2, P-selectin, sCD40L were independently associated with the risk of thrombosis or death.

Two studies reported no difference in P-selectin levels in ICU and non-ICU groups [50,51]. Compared to normal reference values and contextually sampled healthy donors, Agrati et al. [50] found a greater P-selectin plasma concentration in patients with COVID-19, regardless of ICU admission. Furthermore, after platelet removal in HD, data revealed a large reduction in P-selectin, implying that the majority of this molecule was stuck in the platelets. In contrast, both ICU and non-ICU COVID-19 patients had equal amounts of P-selectin with and without platelets, implying that COVID-19 caused these molecules to be released from active platelets/cells. In both groups, platelet counts were found to be comparable. ICU patients had a considerably lower lymphocyte count, demonstrating the link between lymphocytopenia and illness severity. P-selectin was found to be considerably higher in all COVID-19 patients compared to healthy donors, according to Manne et al. [51]. In terms of P-selectin expression, there was no difference between ICU and non-ICU COVID-19 patients. Surprisingly, mRNA from the SARS-CoV-2 N1 gene was found in platelets from two of the 25 COVID-19 patients, suggesting that platelets may take up SARS-CoV-2 mRNA without requiring ACE2. P-selectin expression was higher in COVID-19 patients' resting platelets and when they were activated. COVID-19 patients had considerably higher circulating platelet-neutrophil, -monocyte, and -T-cell aggregates than healthy donors. Platelets from COVID-19 patients also aggregated more quickly and distributed more widely by fibrinogen and collagen. [51] Five studies found higher values in COVID-19 ICU patients compared with severe non-ICU COVID-19 patients [52–56]. SARS-CoV-2 interacts with platelets and megakaryocytes via an ACE2-independent mechanism, according to Shen et al. [52], and may influence alternative receptor expression linked with COVID-19 coagulation abnormalities. Increased P-selectin translocation on platelet surfaces revealed a direct contact between SARS-CoV-2 and human platelets. A higher value of P-selectin in ICU patients compared with severe COVID-19 non-ICU patients was reported. [52]

In individuals with COVID-19, circulating platelets and neutrophils are highly stimulated, according to Petito et al. [53]. Patients with COVID-19 have considerably higher levels of soluble P-selectin and neutrophil-derived microparticles (PMN-MPs), suggesting that they could be used as simple platelet and neutrophil activation indicators in SARS-CoV-2 infection. Even though the majority of the cases were modest, they discovered significant platelet and neutrophil activity. Platelet and neutrophil activation indicators, on the other hand, were linked to the severity of COVID-19. Furthermore, platelet and neutrophil activity returned to normal in COVID-19 individuals. Plasma from COVID-19 patients activated platelets and neutrophils, resulting in neutrophil extracellular traps (NETs) formation, implying that inflammatory mediators, most likely cytokines, generated

during the SARS-CoV-2 infection are responsible for the in vivo platelet and neutrophil activation seen in COVID-19 patients [53].

The hyperactive platelet pattern was verified by Comer et al. [54]. When compared to controls, the circulating levels of the platelet activation markers PF4 and sP-sel were significantly higher in COVID-19-positive individuals. While circulating levels of PF4 did not differ between severe and non-severe COVID-19 individuals, the severe COVID-19 group had greater sP-sel. Fraser et al. [55] used a machine learning system for thrombosis profiling (using P-selectin value) in ICU, predicting severity and mortality of COVID-19. Three thrombotic factors and five endothelial cell damage markers were evaluated in plasma from COVID19⁺ and COVID19⁻ ICU patients, as well as age and sex-matched healthy control subjects. COVID-19⁺ patients had higher vWF than healthy control participants, but more crucially, in the plasma of COVID-19⁺ patients, sP-sel was considerably raised by ICU day 3 and remained persistently elevated in plasma until ICU day 7. COVID-19⁺ patients had exacerbated and chronic endothelium damage, as evidenced by raised sP-sel. Karsli et al. [56] focused on the diagnostic and predictive relevance of serum soluble sP-Sel levels in COVID-19 illness and found that patients with mild-to-moderate and severe pneumonia had greater serum sP-Sel levels than those with no pneumonia. At the cut-off level of 4.125 ng/ml, sP-Sel levels were reported to be 97.5 percent sensitive and 80 percent specific in the diagnosis of COVID-19. Patients with an inflammatory reaction had higher sP-Sel levels than the control group, and their risk of endotheliopathy and thrombosis was higher.

Four studies were only able to report higher values of P-selectin in COVID-19 patients than healthy controls, confirming the pro-thrombotic platelet phenotype, in SARS-CoV-2 infected patients [57–60]. Taus et al. [57], have addressed COVI-19 induced changes in platelet subpopulations as well as exploring the role of platelet in driving thromboinflammation through the release of inflammatory cytokines. After carefully selecting patients without concurrent conditions known to affect platelet function, the study found that patients with COVID-19 had increased basal expression of P-selectin on platelets, which was unaltered upon further agonist stimulation, suggesting a procoagulant platelet status that could not be enhanced. Using paired analysis, Chao et al. [58], evaluated platelet and leukocyte activation in consecutive samples from a patient cohort throughout the acute and convalescent phases of COVID-19. The baseline CD62P surface expression levels in this sample of primarily mild and moderate COVID-19 patients were similar in the acute and convalescent phases. During the acute phase, platelet populations were much more susceptible to conventional platelet agonists, ADP and thrombin, than during the convalescent phase. According to the researchers, platelet activation was an early response to mild or moderate COVID-19, and it was not exclusively associated with a severe disease.

Canzano et al. [59], found a substantial increase in platelet P-selectin expression (10-fold higher than in healthy subjects). Surprisingly, they discovered a negative relationship between circulating PLA and levels of IL-6, CRP, and D-dimer.

Bongiovanni et al. [60] also studied the expression of activation indicators and transmembrane receptors in platelets from hospitalized stable COVID-19 patients who did not have any pre-existing diseases and were not on any anticoagulants or antiplatelet drugs (except prophylactic low-molecular-weight heparin during hospitalization). They limited the measurements to stable COVID-19 patients who did not require assisted ventilation or extracorporeal perfusion, which could cause platelet activity unrelated to the condition. In comparison to controls, they found significantly greater levels of the platelet activation marker P-Selectin. Furthermore, compared to controls, COVID-19 patients had faster platelet aggregation and greater spreading of fibrinogen and collagen.

COVID-19 patients have a lower P-selectin concentration than control samples, according to Venter et al. [61]. However, compared to the results of other investigations, the concentrations of sP-sel in controls were substantially greater. The platelet physiology disruption in COVID-19 individuals was profound. COVID-19 samples were substan-

tially more hypercoagulable and viscous than healthy controls, according to TEG® and viscometry data.

In a retrospective cohort analysis of 79 hospitalized COVID-19 patients, Clark et al. [62] looked at platelet reactivity. They were unable to add healthy controls for comparison during the early stages of the pandemic, which hampered this study. As an alternative, they included hospitalized individuals who tested negative for COVID-19 but were diagnosed with something else. Based on P-selectin activation, there was no difference in platelet reactivity between the COVID-19 positive and negative control groups of hospitalized patients.

Patients hospitalized with non-severe COVID-19 have lower platelet reactivity than healthy controls, according to Bertolin et al. [63]. The findings of platelet hyporesponsiveness could be attributed to platelets being significantly stimulated *in vivo* during COVID-19, leading to subsequent refractoriness to new agonists administered during ex vivo platelet function testing, according to the author. There was no difference in P-selectin levels between non-severe COVID-19 patients and healthy controls. In a single-center prospective analysis, Spadaro et al. [64] sought to describe significant differences between COVID-19-related and traditional ARDS. Because they only involved patients who required mechanical ventilation, the findings could not be applied to mild or moderate COVID-19. P-selectin levels were greater in classical ARDS patients than in COVID-19 ARDS patients in those patients. The most severe forms of COVID-19 ARDS are characterized by the predominance of “endothelial” injury over “alveolar” injury, as evidenced by higher levels of Ang-2 and ICAM-1 in non-survivors compared to survivors. COVID-19 ARDS and classical ARDS both had a similar loss in gas exchange but different biomarker expression, suggesting different pathological pathways.

7. Discussion

The existing literature on the role of P-selectin in COVID-19 patients suggests that it could be a valuable biomarker for predicting clinical outcomes in COVID-19 patients. However, the paucity and inconsistency of existing evidence, the absence of standardized methodologies for biomarker testing and assessment, and the lack of prospective validation in relevant patient populations all may restrict the clinical relevance of P-selectin as a biomarker. The pathophysiological mechanism underlying COVID-19 patients’ increased rate of thromboembolic events is unknown. Upregulation of P-selectin on injured endothelial cells and activated platelets, on the other hand, contributes to a pro-thrombotic state that leads to immunothrombosis and thromboinflammation.

Based on our current understanding of the processes of thrombocytopenia and endotheliopathy, which are highlighted in this P-selectin review, drugs targeting platelet activation and death, as well as increasing endothelial cell health, could be useful in treating COVID-19 patients. Although aspirin is only suggested in COVID-19 antithrombosis reviews as a treatment for acute arterial thrombotic complications, prophylactic antiplatelet agents are now being included in therapeutic algorithms for the management of COVID-19 patients, and many clinical trials on the prophylactic use of antiplatelet agents have been proposed or are currently underway.

Dipyridamole (DIP) is an antiplatelet drug that works by inhibiting phosphodiesterase (PDE) and increasing intracellular cAMP/cGMP levels. DIP supplementation was related to significantly lower D-dimer concentrations, greater lymphocyte, and platelet recovery in the circulation, and markedly improved clinical outcomes in a proof-of-concept experiment including 31 patients with COVID-19 compared to control patients [65]. Dipyridamole’s effectiveness in hospitalized COVID-19 patients is being studied in randomized clinical studies. Three small randomized clinical trials are evaluating dipyridamole 100 mg four times a day and a combination of dipyridamole extended-release 200 mg twice daily and aspirin 25 mg twice daily. (TOLD, ClinicalTrials.gov Identifier: NCT04424901; DICER ClinicalTrials.gov Identifier: NCT04391179; and ATTAC-19 ClinicalTrials.gov Identifier: NCT04410328). The primary objectives included reductions in D-dimer levels (for the first

two trials) and improvements in the COVID-19 WHO ordinal scale (a scale that ranks the severity of sickness from 0 [not infected] to 8 [death])(ATTAC-19).

Aspirin is an inexpensive, widely available treatment that inhibits the COX-1 enzyme, which is essential for the formation of thromboxane A2 and pro-inflammatory prostaglandins, irreversibly at low dosages. Aspirin has been demonstrated to prevent both arterial and venous thrombotic events in SARS-CoV-2 infected individuals and to abolish in-vitro hyperactivity in platelets [51,66]. While the effects of aspirin on clinical outcomes of community-acquired pneumonia patients have been investigated, providing preliminary results on its potential usefulness in lowering mortality, data regarding the efficacy of antiplatelet drugs in COVID-19 is scarce. Chow et al. [67] studied 420 COVID-19 patients. Of these, 314 (76.3%) were aspirin-free and 98 (23.7%) were on aspirin within 24 h of admission or 7 days prior to admission. After adjusting for eight confounding variables, aspirin use was found to be associated with a 46% lower risk of mechanical ventilation, a 43% lower risk of ICU admission, and a 47% lower risk of in-hospital mortality, with no differences in major bleeding thrombosis between aspirin users and non-users [67]. The small sample study and the retrospective nature of the study do not allow for definite conclusions. Further, allocation to aspirin was not associated with reduced mortality or, among those not on invasive mechanical ventilation at baseline, the risk of progressing to the composite endpoint of invasive mechanical ventilation or death in the only large published (medRxiv) randomized trial (RECOVERY) [68], which included over 14,000 patients and over 2000 deaths. However, being assigned to aspirin was linked to a slight increase in the chance of being discharged alive from the hospital after 28 days. As expected, aspirin treatment was linked to a higher risk of severe bleeding and a lower risk of thromboembolic consequences, with roughly six more patients experiencing a major bleeding event and six fewer experiencing a thromboembolic event for every 1000 patients treated with aspirin [68]. Furthermore, any potential benefit of antithrombotic treatments in COVID-19 patients may be contingent on treatment initiation timing, particularly if thrombi have already been formed by the time of admission. The apparent absence of effect in the INSPIRATION and REMAP-CAP/ACTIV-4a/ATTACC severe illness cohorts, in this opinion, shows that these patients may have passed the phase when therapeutic anticoagulation could be beneficial [69,70]. Inclacumab, which is in Phase 3, and Crizanlizumab, which has been approved by the FDA and EMA, are anti-P-selectin monoclonal antibodies that have been developed for human use. The latter, a humanized IgG2 kappa monoclonal antibody that blocks leucocyte and platelet adhesion to the artery wall, is used to avoid vaso-occlusive crises and reduce hyperinflammation in adults and juveniles patients with sickle cell disease [71]. A clinical trial (CRITICAL ClinicalTrials.gov Identifier: NCT04435184) to assess the efficacy and safety of Crizanlizumab in hospitalized adult patients with moderate COVID-19 was just completed and results are pending.

8. Conclusions

Due to the increased risk of morbid sequelae in COVID-19 patients, more large-scale prospective trials to examine the usefulness of P-selectin as a platelet and endothelial activation marker, to stratify risk, and for unfavorable prognostic outcomes are urgently needed. This type of study offers the potential to disclose the mechanisms driving platelet activation and endothelial injury, as well as to identify specific treatments aimed at minimizing endothelial activation and lowering the risk of thrombosis.

Author Contributions: Conceptualization, C.A. and M.B.; methodology, M.B.; formal analysis, M.B.; writing—original draft preparation, M.B.; writing—review and editing, C.A. and M.B.; funding acquisition, C.A., A.S. (Alessandra Sacchi), E.T., A.V., R.G., A.S. (Alessandra Scarabello) and M.B. All authors have read and agreed to the published version of the manuscript.

Funding: This research was funded by the Italian Ministry of Health (Line 1 Ricerca Corrente, COVID-2020-12371817, COVID-2020-12371735).

Conflicts of Interest: The authors declare no conflict of interest.

References

- Nishiga, M.; Wang, D.W.; Han, Y.; Lewis, D.B.; Wu, J.C. COVID-19 and cardiovascular disease: From basic mechanisms to clinical perspectives. *Nat. Rev. Cardiol.* **2020**, *17*, 543–558. [[CrossRef](#)]
- Bonaventura, A.; Vecchié, A.; Dagna, L.; Martinod, K.; Dixon, D.L.; Van, T.B.W.; Dentali, F.; Montecucco, F.; Massberg, S.; Levi, M.; et al. Endothelial dysfunction and immunothrombosis as key pathogenic mechanisms in COVID. *Nat. Rev. Immunol.* **2021**, *21*, 319–329. [[CrossRef](#)]
- Stark, K.; Massberg, S. Interplay between inflammation and thrombosis in cardiovascular pathology. *Nat. Rev. Cardiol.* **2021**, *6*, 1–17. [[CrossRef](#)]
- Gu, S.X.; Tyagi, T.; Jain, K.; Gu, V.W.; Lee, S.H.; Hwa, J.M.; Kwan, J.M.; Krause, D.S.; Lee, A.I.; Halene, S.; et al. Thrombocytopathy and endotheliopathy: Crucial contributors to COVID-19 thromboinflammation. *Nat. Rev. Cardiol.* **2021**, *18*, 194–209. [[CrossRef](#)] [[PubMed](#)]
- Smith, B.A.H.; Bertozzi, C.R. The clinical impact of glycobiology: Targeting selectins, Siglecs and mammalian glycans. *Nat. Rev. Drug. Discov.* **2021**, *20*, 217–243. [[CrossRef](#)]
- Tvaroška, I.; Selvaraj, C.; Koča, J. Selectins-The Two Dr. Jekyll and Mr. Hyde Faces of Adhesion Molecules-A Review. *Molecules* **2020**, *19*, 2835. [[CrossRef](#)]
- Grobler, C.; Maphumulo, S.C.; Grobbelaar, L.M.; Bredenkamp, J.C.; Laubscher, G.J.; Lourens, P.J.; Steenkamp, J.; Kell, D.B.; Pretorius, E. Covid-19: The Rollercoaster of Fibrin(Ogen), D-Dimer, Von Willebrand Factor, P-Selectin and Their Interactions with Endothelial Cells, Platelets and Erythrocytes. *Int. J. Mol. Sci.* **2020**, *21*, 5168. [[CrossRef](#)]
- Polgar, J.; Matuskova, J.; Wagner, D.D. The P-selectin, tissue factor, coagulation triad. *J. Thromb. Haemost.* **2005**, *3*, 1590–1596. [[CrossRef](#)] [[PubMed](#)]
- Furie, B. P-selectin and blood coagulation: It's not only about inflammation any more. *Arterioscler. Thromb. Vasc. Biol.* **2005**, *25*, 877–878. [[CrossRef](#)]
- Furie, B.; Furie, B.C. Role of platelet P-selectin and microparticle PSGL-1 in thrombus formation. *Trends. Mol. Med.* **2004**, *10*, 171–178. [[CrossRef](#)] [[PubMed](#)]
- Kato, G.J.; Piel, F.B.; Reid, C.D.; Gaston, M.H.; Ohene-Frempong, K.; Krishnamurti, L.; Smith, W.R.; Panepinto, J.A.; Weatherall, D.J.; Costa, F.F.; et al. Sickle cell disease. *Nat. Rev. Dis. Primers.* **2018**, *15*, 18010. [[CrossRef](#)]
- Karki, N.R.; Kutlar, A. P-Selectin Blockade in the Treatment of Painful Vaso-Occlusive Crises in Sickle Cell Disease: A Spotlight on Crizanlizumab. *J. Pain. Res.* **2021**, *30*, 849–856. [[CrossRef](#)] [[PubMed](#)]
- Song, C.; Wu, G.; Chang, S.; Bie, L. Plasma P-selectin level is associated with severity of coronary heart disease in Chinese Han population. *J. Int. Med. Res.* **2020**, *48*, 300060519896437. [[CrossRef](#)]
- Hoel, H.; Pettersen, E.M.; Høiseth, L.Ø.; Mathiesen, I.; Seternes, A.; Seljeflot, I.; Hisdal, J. Effects of intermittent negative pressure treatment on circulating vascular biomarkers in patients with intermittent claudication. *Vasc. Med.* **2021**, *13*, 1358863X211007933. [[CrossRef](#)]
- Shen, L.; Yang, T.; Xia, K.; Yan, Z.; Tan, J.; Li, L.; Qin, Y.; Shi, W. P-selectin (CD62P) and soluble TREM-like transcript-1 (sTLT-1) are associated with coronary artery disease: A case control study. *Cardiovasc. Disord.* **2020**, *24*, 387. [[CrossRef](#)]
- Barale, C.; Russo, I. Influence of Cardiometabolic Risk Factors on Platelet Function. *Int. J. Mol. Sci.* **2020**, *17*, 623. [[CrossRef](#)]
- Hally, K.E.; Parker, O.M.; Brunton-O'Sullivan, M.M.; Harding, S.A.; Larsen, P.D. Linking Neutrophil Extracellular Traps and Platelet Activation: A Composite Biomarker Score for Predicting Outcomes after Acute Myocardial Infarction. *Thromb. Haemost.* **2021**, *13*, 1728763. [[CrossRef](#)]
- Nguyen, S.D.; Korhonen, E.A.; Lorey, M.B.; Hakanpää, L.; Mäyränpää, M.I.; Kovanen, P.T.; Saharinen, P.; Alitalo, K.; Öörni, K. Lysophosphatidylcholine in phospholipase A₂-modified LDL triggers secretion of angiopoietin 2. *Atherosclerosis* **2021**, *327*, 87–99. [[CrossRef](#)]
- Collado, A.; Domingo, E.; Marquesm, P.; Perello, E.; Martínez-Hervás, S.; Piqueras, L.; Ascaso, J.F.; Real, J.T.; Sanz, M.J. Oral Unsaturated Fat Load Impairs Postprandial Systemic Inflammation in Primary Hypercholesterolemia Patients. *Front. Pharmacol.* **2021**, *20*, 656244. [[CrossRef](#)]
- Chan, L.W.; Luo, X.P.; Ni, H.C.; Shi, H.M.; Liu, L.; Wen, Z.C.; Gu, X.Y.; Qiao, J.; Li, J. High levels of LDL-C combined with low levels of HDL-C further increase platelet activation in hypercholesterolemic patients. *Braz. J. Med. Biol. Res.* **2015**, *48*, 167–173. [[CrossRef](#)]
- Appleton, J.P.; Richardson, C.; Dovlatova, N.; May, J.; Sprigg, N.; Heptinstall, S.; Bath, P.M. Remote platelet function testing using P-selectin expression in patients with recent cerebral ischaemia on clopidogrel. *Stroke Vasc. Neurol.* **2021**, *6*, 103–108. [[CrossRef](#)]
- Atkinson, C.; Zhu, H.; Qiao, F.; Varela, J.C.; Yu, J.; Song, H.; Kindy, M.S.; Tomlinson, S. Complement-dependent P-selectin expression and injury following ischemic stroke. *J. Immunol.* **2006**, *175*, 7266–7274. [[CrossRef](#)] [[PubMed](#)]
- Moin, A.S.M.; Al-Qaissi, A.; Sathyapalan, T.; Atkin, S.L.; Butler, A.E. Platelet Protein-Related Abnormalities in Response to Acute Hypoglycemia in Type 2 Diabetes. *Front. Endocrinol. (Lausanne)* **2021**, *30*, 651009. [[CrossRef](#)] [[PubMed](#)]
- Palella, E.; Cimino, R.; Pullano, S.A.; Fiorillo, A.S.; Gulletta, E.; Brunetti, A.; Foti, D.P.; Greco, M. Laboratory Parameters of Hemostasis, Adhesion Molecules, and Inflammation in Type 2 Diabetes Mellitus: Correlation with Glycemic Control. *Int. J. Environ. Res. Public Health* **2020**, *17*, 300. [[CrossRef](#)] [[PubMed](#)]
- Antonopoulos, C.N.; Sfyroeras, G.S.; Kakisis, J.D.; Moulakakis, K.G.; Liapis, C.D. The role of soluble P selectin in the diagnosis of venous thromboembolism. *Thromb. Res.* **2014**, *133*, 17–24. [[CrossRef](#)]

26. Ay, C.; Dunkler, D.; Marosi, C.; Chiriac, A.L.; Vormittag, R.; Simanek, R.; Quehenberger, P.; Zielinski, C.; Pabinger, I. Prediction of venous thromboembolism in cancer patients. *Blood* **2010**, *116*, 5377–5382. [[CrossRef](#)]
27. Sánchez-López, V.; Gao, L.; Ferrer-Galván, M.; Arellano-Orden, E.; Elías-Hernández, T.; Jara-Palomares, L.; Asensio-Cruz, M.I.; Castro-Pérez, M.J.; Rodríguez-Martorell, F.J.; Lobo-Beristain, J.L.; et al. Differential biomarker profiles between unprovoked venous thromboembolism and cancer. *Ann. Med.* **2020**, *52*, 310–320. [[CrossRef](#)]
28. Laursen, M.A.; Larsen, J.B.; Larsen, K.M.; Hvas, A.M. Platelet function in patients with septic shock. *Thromb. Res.* **2020**, *185*, 33–42. [[CrossRef](#)]
29. Widemann, A.; Pasero, C.; Arnaud, L.; Poullin, P.; Loundou, A.D.; Choukroun, G.; Sanderson, F.; Lacroix, R.; Sabatier, F.; Coppo, P.; et al. Circulating endothelial cells and progenitors as prognostic factors during autoimmune thrombotic thrombocytopenic purpura: Results of a prospective multicenter French study. *J. Thromb. Haemost.* **2014**, *12*, 1601–1609. [[CrossRef](#)]
30. Campello, E.; Radu, C.M.; Duner, E.; Lombardi, A.M.; Spiezia, L.; Bendo, R.; Ferrari, S.; Simioni, P.; Fabris, F. Activated Platelet-Derived and Leukocyte-Derived Circulating Microparticles and the Risk of Thrombosis in Heparin-Induced Thrombocytopenia: A Role for PF4-Bearing Microparticles? *Cytometry B Clin. Cytom.* **2018**, *94*, 334–341. [[CrossRef](#)]
31. Fabricius, H.Å.; Starzeneck, S.; Lange, T. The Role of Platelet Cell Surface P-Selectin for the Direct Platelet-Tumor Cell Contact During Metastasis Formation in Human Tumors. *Front. Oncol.* **2021**, *15*, 642761. [[CrossRef](#)]
32. Schlesinger, M. Role of platelets and platelet receptors in cancer metastasis. *J. Hematol. Oncol.* **2018**, *11*, 125. [[CrossRef](#)]
33. Kappelmayer, J.; Nagy, B., Jr. The Interaction of Selectins and PSGL-1 as a Key Component in Thrombus Formation and Cancer Progression. *Biomed. Res. Int.* **2017**, *2017*, 6138145. [[CrossRef](#)]
34. Qi, C.; Wei, B.; Zhou, W. P-selectin-mediated platelet adhesion promotes tumor growth. *Oncotarget* **2015**, *6*, 6584–6596. [[CrossRef](#)]
35. Tavares, L.P.; Teixeira, M.M.; Garcia, C.C. The inflammatory response triggered by Influenza virus: A two edged sword. *Inflamm. Res.* **2017**, *66*, 283–302. [[CrossRef](#)]
36. Finsterbusch, M.; Schrottmaier, W.C.; Kral-Pointner, J.B.; Salzmann, M.; Assinger, A. Measuring and interpreting platelet-leukocyte aggregates. *Platelets* **2018**, *29*, 677–685. [[CrossRef](#)] [[PubMed](#)]
37. Nkambule, B.B.; Mxinwa, V.; Mkandla, Z.; Mutize, T.; Mokgalaboni, K.; Nyambuya, T.M.; Dludla, P.V. Platelet activation in adult HIV-infected patients on antiretroviral therapy: A systematic review and meta-analysis. *BMC. Med.* **2020**, *18*, 357. [[CrossRef](#)] [[PubMed](#)]
38. Agrati, C.; Mazzotta, V.; Pinnetti, C.; Biava, G.; Bibas, M. Venous thromboembolism in people living with HIV infection (PWH). *Transl. Res.* **2021**, *227*, 89–99. [[CrossRef](#)] [[PubMed](#)]
39. O'Halloran, J.A.; Dunne, E.; Gurwith, M.; Lambert, J.S.; Sheehan, G.J.; Feeney, E.R.; Pozniak, A.; Reiss, P.; Kenny, D.; Mallon, P. The effect of initiation of antiretroviral therapy on monocyte, endothelial and platelet function in HIV-1 infection. *HIV Med.* **2015**, *16*, 608–619. [[CrossRef](#)]
40. O'Brien, M.P.; Hunt, P.W.; Kitch, D.W.; Klingman, K.; Stein, J.H.; Funderburg, N.T.; Berger, J.S.; Tebas, P.; Clagett, B.; Moisi, D.; et al. A Randomized Placebo Controlled Trial of Aspirin Effects on Immune Activation in Chronically Human Immunodeficiency Virus-Infected Adults on Virologically Suppressive Antiretroviral Therapy. *Open. Forum. Infect. Dis.* **2017**, *4*, 278. [[CrossRef](#)]
41. Bibas, M.; Biavam, G.; Antinori, A. HIV-Associated Venous Thromboembolism. *Infect. Dis.* **2011**, *3*, e2011030. [[CrossRef](#)]
42. Johansson, M.W.; Grill, B.M.; Barreto, K.T.; Favour, M.C.; Schira, H.M.; Swanson, C.M.; Lee, K.E.; Sorkness, R.L.; Mosher, D.F.; Denlinger, L.C.; et al. Plasma P-Selectin Is Inversely Associated with Lung Function and Corticosteroid Responsiveness in Asthma. *Int. Arch. Allergy Immunol.* **2020**, *181*, 879–887. [[CrossRef](#)] [[PubMed](#)]
43. Horváth, P.; Lázár, Z.; Gálffy, G.; Puskás, R.; Kunos, L.; Losonczy, G.; Mészáros, M.; Tárnoki, Á.D.; Tárnoki, D.L.; Bikov, A. Circulating P-Selectin Glycoprotein Ligand 1 and P-Selectin Levels in Obstructive Sleep Apnea Patients. *Lung* **2020**, *198*, 173–179. [[CrossRef](#)]
44. Zhu, D.; Xu, Z.; Liu, T.; Li, Y. Soluble P-selectin levels in patients with obstructive sleep apnea: A systematic review and meta-analysis. *Eur. Arch. Otorhinolaryngol.* **2021**. [[CrossRef](#)]
45. Goshua, G.; Pine, A.B.; Meizlish, M.L.; Chang, C.H.; Zhang, H.; Bahel, P.; Baluha, A.; Bar, N.; Bona, R.D.; Burns, A.J.; et al. Endotheliopathy in COVID-19-associated coagulopathy: Evidence from a single-centre, cross-sectional study. *Lancet Haematol.* **2020**, *7*, 575–582. [[CrossRef](#)]
46. Hottz, E.D.; Azevedo-Quintanilha, I.G.; Palhinha, L.; Teixeira, L.; Barreto, E.A.; Pão, C.R.R.; Righy, C.; Franco, S.; Souza, T.M.L.; Kurtz, P.; et al. Platelet activation and platelet-monocyte aggregate formation trigger tissue factor expression in patients with severe COVID-19. *Blood* **2020**, *136*, 1330–1341. [[CrossRef](#)] [[PubMed](#)]
47. Campo, G.; Contoli, M.; Fogagnolo, A.; Vieceli, D.S.F.; Zucchetti, O.; Ronzoni, L.; Verri, M.; Fortini, F.; Pavasini, R.; Morandi, L.; et al. Over time relationship between platelet reactivity, myocardial injury and mortality in patients with SARS-CoV-2-associated respiratory failure. *Platelets* **2020**, *3*, 1–8. [[CrossRef](#)]
48. Vassiliou, A.G.; Keskinidou, C.; Jahaj, E.; Gallos, P.; Dimopoulos, I.; Kotanidou, A.; Orfanos, S.E. ICU Admission Levels of Endothelial Biomarkers as Predictors of Mortality in Critically Ill COVID-19 Patients. *Cells* **2021**, *10*, 186. [[CrossRef](#)]
49. Barrett, T.J.; Lee, A.H.; Xia, Y.; Lin, L.H.; Black, M.; Cotzia, P.; Hochman, J.; Berger, J.S. Platelet and Vascular Biomarkers Associate With Thrombosis and Death in Coronavirus Disease. *Circ. Res.* **2020**, *127*, 945–947. [[CrossRef](#)]
50. Agrati, C.; Bordoni, V.; Sacchi, A.; Petrosillo, N.; Nicastri, E.; Del, N.F.; D'Offizi, G.; Palmieri, F.; Marchioni, L.; Capobianchi, M.R.; et al. Elevated P-Selectin in Severe Covid-19: Considerations for Therapeutic Options. *Mediterr. J. Hematol. Infect. Dis.* **2021**, *13*, e2021016. [[CrossRef](#)] [[PubMed](#)]

51. Manne, B.K.; Denorme, F.; Middleton, E.A.; Portier, I.; Rowley, J.W.; Stubben, C.; Petrey, A.C.; Tolley, N.D.; Guo, L.; Cody, M.; et al. Platelet gene expression and function in patients with COVID-19. *Blood* **2020**, *136*, 1317–1329. [CrossRef]
52. Shen, S.; Zhang, J.; Fang, Y.; Lu, S.; Wu, J.; Zheng, X.; Deng, F. SARS-CoV-2 interacts with platelets and megakaryocytes via ACE2-independent mechanism. *J. Hematol. Oncol.* **2021**, *14*, 72. [CrossRef]
53. Petito, E.; Falcinelli, E.; Paliani, U.; Cesari, E.; Vaudo, G.; Sebastiani, M.; Cerotto, V.; Guglielmini, G.; Gori, F.; Malvestiti, M.; et al. Association of Neutrophil Activation, More Than Platelet Activation, With Thrombotic Complications in Coronavirus Disease. *J. Infect. Dis.* **2021**, *223*, 933–944. [CrossRef]
54. Comer, S.P.; Cullinan, S.; Szklanna, P.B.; Weiss, L.; Cullen, S.; Kelliher, S.; Smolenski, A.; Murphy, C.; Altaie, H.; Curran, J.; et al. COVID-19 induces a hyperactive phenotype in circulating platelets. *PLoS. Biol.* **2021**, *19*, e3001109. [CrossRef]
55. Fraser, D.D.; Patterson, E.K.; Slessarev, M.; Gill, S.E.; Martin, C.; Daley, M.; Miller, M.R.; Patel, M.A.; Dos Santos, C.C.; Bosma, K.J.; et al. Endothelial Injury and Glycocalyx Degradation in Critically Ill Coronavirus Disease 2019 Patients: Implications for Microvascular Platelet Aggregation. *Crit. Care Explor.* **2020**, *2*, e0194. [CrossRef]
56. Karsli, E.; Sabirli, R.; Altintas, E.; Canacik, O.; Sabirli, G.T.; Kaymaz, B.; Kurt, Ö.; Koseler, A. Soluble P-selectin as a potential diagnostic and prognostic biomarker for COVID-19 disease: A case-control study. *Life Sci.* **2021**, *277*, 119634. [CrossRef]
57. Taus, F.; Salvagno, G.; Canè, S.; Fava, C.; Mazzaferri, F.; Carrara, E.; Petrova, V.; Barouni, R.M.; Dima, F.; Dalbeni, A.; et al. Platelets Promote Thromboinflammation in SARS-CoV-2 Pneumonia. *Arterioscler. Thromb. Vasc. Biol.* **2020**, *40*, 2975–2989. [CrossRef]
58. Chao, Y.; Rebetz, J.; Bläckberg, A.; Hovold, G.; Sunnerhagen, T.; Rasmussen, M.; Semple, J.W.; Shannon, O. Distinct phenotypes of platelet, monocyte, and neutrophil activation occur during the acute and convalescent phase of COVID. *Platelets* **2021**, *17*, 1–11. [CrossRef]
59. Canzano, P.; Brambilla, M.; Porro, B.; Cosentino, N.; Tortorici, E.; Vicini, S.; Poggio, P.; Cascella, A.; Pengo, M.F.; Veglia, F.; et al. Platelet and Endothelial Activation as Potential Mechanisms Behind the Thrombotic Complications of COVID-19 Patients. *JACC Basic. Transl. Sci.* **2021**, *6*, 202–218. [CrossRef] [PubMed]
60. Bongiovanni, D.; Klug, M.; Lazareva, O.; Weidlich, S.; Biasi, M.; Ursu, S.; Warth, S.; Buske, C.; Lukas, M.; Spinner, C.D.; et al. SARS-CoV-2 infection is associated with a pro-thrombotic platelet phenotype. *Cell Death Dis.* **2021**, *12*, 50. [CrossRef]
61. Venter, C.; Bezuidenhout, J.A.; Laubscher, G.J.; Lourens, P.J.; Steenkamp, J.; Kell, D.B.; Pretorius, E. Erythrocyte, Platelet, Serum Ferritin, and P-Selectin Pathophysiology Implicated in Severe Hypercoagulation and Vascular Complications in COVID. *Int. J. Mol. Sci.* **2020**, *21*, 8234. [CrossRef]
62. Clark, C.C.; Jukema, B.N.; Barendrecht, A.D.; Spanjaard, J.S.; Jorritsma, N.K.N.; Smits, S.; de Maat, S.; Seinen, C.W.; Verhoef, S.; Parr, N.M.J.; et al. Thrombotic Events in COVID-19 Are Associated With a Lower Use of Prophylactic Anticoagulation Before Hospitalization and Followed by Decreases in Platelet Reactivity. *Front. Med. (Lausanne)* **2021**, *8*, 650129. [CrossRef]
63. Bertolin, A.J.; Dalçóquio, T.F.; Salsoso, R.; Furtado, R.H.D.M.; Kalil-Filho, R.; Hajjar, L.A.; Siciliano, R.F.; Kallás, E.G.; Baracioli, L.M.; Lima, F.G.; et al. Platelet Reactivity and Coagulation Markers in Patients with COVID-19. *Adv. Ther.* **2021**, *38*, 3911–3923. [CrossRef]
64. Spadaro, S.; Fogagnolo, A.; Campo, G.; Zucchetti, O.; Verri, M.; Ottaviani, I.; Tunstall, T.; Grasso, S.; Scaramuzzo, V.; Murgolo, F.; et al. Markers of endothelial and epithelial pulmonary injury in mechanically ventilated COVID-19 ICU patients. *Crit. Care* **2021**, *25*, 74. [CrossRef]
65. Liu, X.; Li, Z.; Liu, S.; Sun, J.; Chen, Z.; Jiang, M.; Zhang, Q.; Wei, Y.; Wang, X.; Huang, Y.Y.; et al. Potential therapeutic effects of dipyridamole in the severely ill patients with COVID-19. *Acta Pharm. Sin. B* **2020**, *10*, 1205–1215. [CrossRef]
66. Antithrombotic Trialists' (ATT) Collaboration; Baigent, C.; Blackwell, L.; Collins, R.; Emberson, J.; Godwin, J.; Peto, R.; Buring, J.; Hennekens, C.; Kearney, P.; et al. Aspirin in the primary and secondary prevention of vascular disease: Collaborative meta-analysis of individual participant data from randomised trials. *Lancet* **2009**, *373*, 1849–1860. [CrossRef] [PubMed]
67. Chow, J.H.; Khanna, A.K.; Kethireddy, S.; Yamane, D.; Levine, A.; Jackson, A.M.; McCurdy, M.T.; Tabatabai, A.; Kumar, G.; Park, P.; et al. Aspirin Use Is Associated With Decreased Mechanical Ventilation, Intensive Care Unit Admission, and In-Hospital Mortality in Hospitalized Patients With Coronavirus Disease. *Anesth. Analg.* **2021**, *132*, 930–941. [CrossRef] [PubMed]
68. RECOVERY Collaborative Group; Peter, W.H.; Guilherme, P.A.; Natalie, S.; Jonathan, R.E.; Mark, C.; Enti, S.; Leon, P.; Nigel, J.B.; Simon, T.; et al. Aspirin in patients admitted to hospital with COVID-19 (RECOVERY): A randomised, controlled, open-label platform trial. *Health Sci.* **2021**, *8*, 21258132. [CrossRef]
69. Patrick, R.L.; Ewan, C.G.; Jeffrey, S.B.; Matthew, D.N.; Bryan, J.M.; Jose, C.N.; Michelle, N.G.; Marc, C.; Robert, S.R.; Harmony, R.R. Therapeutic Anticoagulation in Non-Critically Ill Patients with Covid-19. *Health Sci.* **2021**, *5*, 21256846. [CrossRef]
70. Sadeghipour, P.; Talasaz, A.H.; Rashidi, F.; Sharif-Kashani, B.; Beigmohammadi, M.T.; Farrokhpour, M.; Sezavar, S.H.; Payandemehr, P.; Dabbagh, A.; Moghadam, K.G.; et al. Effect of Intermediate-Dose vs Standard-Dose Prophylactic Anticoagulation on Thrombotic Events, Extracorporeal Membrane Oxygenation Treatment, or Mortality Among Patients With COVID-19 Admitted to the Intensive Care Unit: The INSPIRATION Randomized Clinical Trial. *JAMA* **2021**, *325*, 1620–1630. [PubMed]
71. Blair, H.A. Crizanlizumab: First Approval. *Drugs* **2020**, *80*, 79–84. [CrossRef]



The potential role of neopterin in Covid-19: a new perspective

Hayder M. Al-kuraishy¹ · Ali I. Al-Gareeb¹ · Khalid J. Alzahrani² · Natália Cruz-Martins^{3,4,5} · Gaber El-Saber Batiha⁶

Received: 1 April 2021 / Accepted: 19 July 2021

© The Author(s), under exclusive licence to Springer Science+Business Media, LLC, part of Springer Nature 2021

Abstract

Neopterin (NPT) is a member of pteridines group, synthesized by macrophages when stimulated by interferon gamma (INF- γ). NPT is regarded as a macrophage stimulation indicator, marker of cellular immune activation and T helper 1 (Th1) type 1 immune response. Here, we aimed to provide a view point on the NPT features and role in Covid-19. Serum NPT level is regarded as an independent prognostic factor for Covid-19 severity, with levels starting to increase from the 3rd day of SARS-CoV-2 infection, being associated with severe dyspnea, longer hospitalization period and complications. Also, early raise of NPT reflects monocytes/macrophages activation before antibody immune response, despite the NPT level may also remain high in Covid-19 patients or at the end of incubation period before the onset of clinical symptoms. On the other hand, NPT attenuates the activity of macrophage foam cells and is linked to endothelial inflammation through inhibition of adhesion molecules and monocytes migration. However, NPT also exerts anti-inflammatory and antioxidant effects by suppressing NF- κ B signaling and NLRP3 inflammasomes. NPT can be viewed as a protective compensatory mechanism to counterpoise hyper-inflammation, oxidative stress, and associated organ damage.

Keywords Neopterin · SARS-CoV-2 infection · Covid-19 severity

Background

Coronavirus disease 2019 (Covid-19) is a global pandemic infectious disease caused by the severe acute respiratory syndrome coronavirus 2 (SARS-CoV-2), having its entry through interaction with angiotensin converting enzyme 2 (ACE2) receptors, which expressed mainly in lung type II alveolar cells [1]. Moreover, the SARS-CoV-2 entry into target cells is facilitated by cellular transmembrane protein serine (TMPRSS2) through proteolytic cleaving of spike

protein [2]. As a consequence, the SARS-CoV-2 binding to the ACE2 receptors expressed in lung alveolar cells, along with macrophages and endothelial cells leads to down-regulation of these receptors with induction a momentous dysregulation of renin-angiotensin system (RAS) [3]. Dysfunctional RAS with high angiotensin II (AngII) has been linked to acute lung injury (ALI) through intensification of inflammatory changes and lung vascular permeability [4]. Moreover, SARS-CoV-2 triggers a local immune response, through recruiting monocytes and macrophages to the site

✉ Natália Cruz-Martins
ncmartins@med.up.pt

Gaber El-Saber Batiha
gaberbatiha@gmail.com

Hayder M. Al-kuraishy
Hayderm36@yahoo.com

Ali I. Al-Gareeb
Dr.alialgareeb78@yahoo.com

Khalid J. Alzahrani
Ak.jamaan@tu.edu.sa

¹ Department of Clinical Pharmacology and Medicine, College of Medicine, ALmustansiriya University, Baghdad, Iraq

² Department of Clinical Laboratories Sciences, College of Applied Medical Sciences, Taif University, P.O. Box 11099, Taif 21944, Saudi Arabia

³ Faculty of Medicine, University of Porto, Alameda Prof. Hernâni Monteiro, 4200-319 Porto, Portugal

⁴ Institute for Research and Innovation in Health (i3S), University of Porto, 4200-135 Porto, Portugal

⁵ Instituto de Investigação e Formação Avançada em Ciências e Tecnologias da Saúde, CESPU, Rua Central de Gandra, 1317, 4585-116 Gandra, Portugal

⁶ Department of Pharmacology and Therapeutics, Faculty of Veterinary Medicine, Damanhour University, Damanhour 22511, AlBeheira, Egypt

of infection with activation of cellular immune response [5]. However, an abnormal immune response and high viral replication may cause pyroptosis (inflammatory program cell death) through induction of IL-1 β release [6]. Likewise, severe SARS-CoV-2 and abnormal immune response may propagate to induce the development of cytokine storm (CS) [7]. At molecular level, SARS-CoV-2 infection is thoroughly analogous to that of SARS-CoV with strong inflammatory response-induced ALI, and acute respiratory distress syndrome (ARDS) [8]. In this sense, the disease severity is not solely linked to viral infection but also to an exaggerated immune response, as evident in previous SARS-CoV and Middle East Respiratory Syndrome coronavirus (MERS-CoV) [9]. In the previous pandemic (SARS-CoV, in 2003) an exaggerated immune response was observed, where high neopterin (NPT) serum levels were linked to disease severity and poor clinical course [10]. In this sense, here we provide a critical view on the NPT features and its role in Covid-19.

Characteristics and role of neopterin

Neopterin (NPT) is a member of a chemical group named as pteridines, synthesized by macrophages from dihydro-NPT when stimulated by interferon gamma (INF- γ). NPT is regarded as an indicator of macrophage stimulation, marker of cellular immune activation and T helper 1 (Th1) type 1 immune response. NPT is quietly differed from biopterins, which are pterin derivative act as cofactor for endogenous enzymes mainly amino acid hydroxylase for synthesis of different molecules such as nitric oxide [11]. Briefly, NPT is an oxidized form of dihydroneopterin during antioxidant reactions, where high NPT levels in serum and other biological fluids is linked to an elevated production of reactive oxygen species (ROS) and induction of oxidative stress (OS) during intense activation of cellular immunity [12].

Different studies have shown that high NPT serum level is linked to diverse infectious diseases and immunological disorders, including autoimmune diseases [13], malignancy [14], and viral infections, like rubella, cytomegalovirus, hepatitis C, and dengue fever [15]. Also, Omma et al. [16] observed that NPT serum level is correlated with disease severity. However, El-Lebedy et al., [17] showed that NPT serum level is not correlated with the disease' severity in patients with rheumatoid arthritis. Indeed, various types of viral infections are able to activate the formation and release of INF- γ from infected cells, where INF- γ stimulates macrophages to produce and release of NPT. Therefore, NPT concentrations reflect an underlying cell-mediated immune activation [18].

Macrophages have a crucial role in innate immune response during viral infections. Two types of monocyte-derived macrophages are developed: classically activated

macrophages (M1) and alternatively activated macrophages (M2). M1 macrophages have pro-inflammatory role, are stimulated by tumor necrosis alpha (TNF- α), INF- γ , and pathogen-associated molecular patterns (PAMPs), while M2 macrophages have anti-inflammatory role and activated by IL-13 and IL-4 [19]. Specifically, NPT serum level is correlated with activation of M1 macrophages and associated hyper-inflammation-induced tissue damage [20]. Moreover, T cells through TNF- α , natural killer (NK) cells through interferon gamma (INF- γ) and viral infections through pathogen-associated molecular patterns (PAMPs) activate classical macrophage (M1) for the release of neopterin (NPT), which inhibit release of adhesion molecules [21]. As a consequence, a high release of NPT leads to the negative feedback inhibition of macrophage activity with macrophage polarization' induction from pro-inflammatory M1 to the anti-inflammatory M2 type [22].

On the other hand, NPT has a protective effect against plaque generation in patients with carotid atherosclerosis through inhibition of vascular cell adhesion molecule-1 (VCAM-1), intercellular adhesion molecule-1 (ICAM-1), and monocyte chemotactic protein-1 (MCP-1) to endothelial cells. Likewise, NPT derivatives improve endothelial function via activation of nitric oxide (NO) synthase. Tetrahydrobiopterin is regarded as derivative of NPT also act as a cofactor for endothelial nitric oxide synthase (eNOS) suppresses vascular injury and improve endothelial function [23]. Similarly, Shira et al. [24] observed that NPT might be conceived as a new therapeutic line in the management of ischemic heart disease and atherosclerosis through suppressing inflammation-induced endothelial dysfunction and atherogenesis. Indeed, it has been stated that elevated NPT in paraquat-induced ALI might be a compensatory mechanism due to development of OS and reduction of antioxidant capacity [25]. Therefore, there is a strong controversy regarding the potential role of NPT in cardio-pulmonary disorders. The net-effect of NPT is shown in Fig. 1.

Role of neopterin in Covid-19

At present, different studies have tried to address the critical role of NPT in Covid-19 severity and clinical outcomes. In a retrospective study with 115 hospitalized patients with severe Covid-19, Bellmann-Weiler et al. [26] illustrated that NPT serum levels above 45 nmol/L at time of admission predict both severity and the need for mechanical ventilation at intensive care unit (ICU), since high NPT serum levels reflect exaggerated T cells activations-induced ALI and ARDS in SARS-CoV-2 pneumonia [27]. Similarly, Robertson et al. [28] showed that NPT serum levels are regarded as an independent prognostic factor for Covid-19 severity. Besides, in SARS patients, the NPT level started to increase

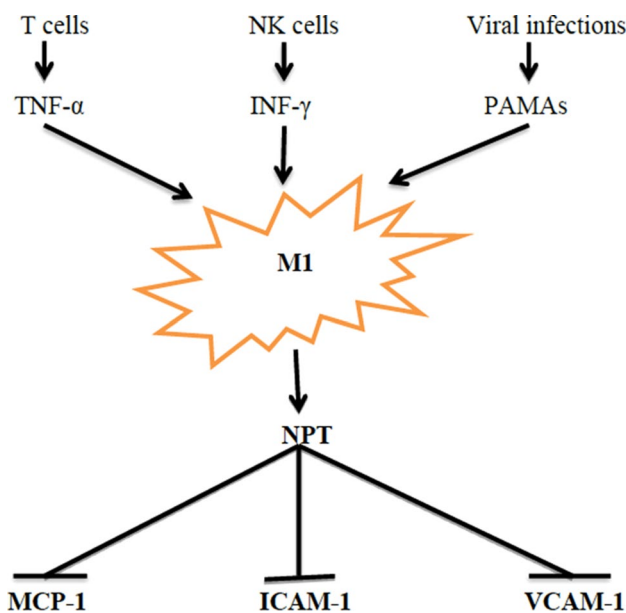


Fig. 1 Activation of neopterin release and inhibition of adhesion molecules: T cells through tumor necrosis alpha (TNF- α), natural killer (NK) cells through interferon gamma (INF- γ) and viral infections through pathogen-associated molecular patterns (PAMPs) activate macrophage (M1) for release of neopterin (NPT), which inhibit release of adhesion molecules, monocyte chemoattractant protein-1 (MCP-1), intracellular adhesion molecule-1(ICAM-1), and vascular cell adhesion molecule-1 (VCAM-1)

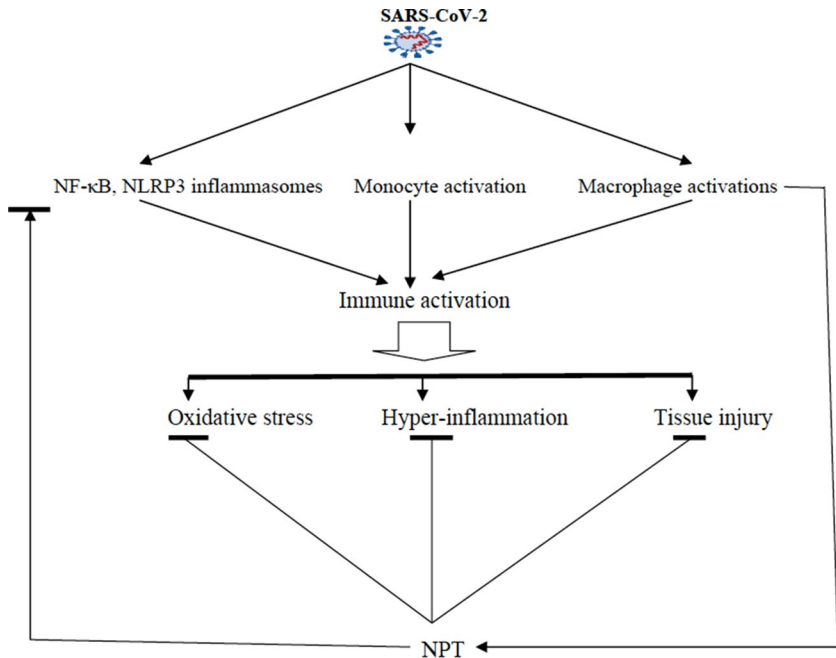
from the 3rd day of infection and was linked to severe dyspnea, longer hospitalization period and associated complications. Thus, early increase of NPT reflects monocytes/macrophages activation before antibody immune response [10]. In a prospective study, Ozge et al. [29] confirmed that NPT serum level has higher sensitivity (100%) and specificity (76%) in severe Covid-19 patients compared to mild ones. Thus, NPT serum level can be a helpful biomarker to recognize Covid-19 patients at an elevated risk of a deteriorated outcome. In addition, it has been reported that NPT serum level may be a diagnostic biomarker in viral infections of lower respiratory tract as it increased more than 10 nmol/L in 96% of patients. Also, NPT serum level can be able to differentiate a viral infection of lower respiratory tract from that of bacterial one, being stated an increase two times higher in case of viral when compared to bacterial infection. Also, in viral infections, elevation of NPT serum level is associated with high CRP as compared with bacterial infection, in which C-reactive protein (CRP) is slightly increased [30, 31]. In addition to this, NPT serum level is correlated with viral load, infectivity, and mortality in infected patients with HIV [32], hepatitis C and B [33]. Indeed, NPT level in cerebrospinal fluid (CSF) is elevated in patients with severe SARS-CoV-2 infection with neurological disorders suggesting a remarkable pattern of CSF inflammation and central

nervous system (CNS) pathobiology in Covid-19-induced brain injury [34].

Despite these findings confirmed strong associations between NPT serum level and Covid-19 severity, none of studies follow NPT level at the end course of Covid-19 severity. The NPT level may remain high in patients with Covid-19 or elevated at the end of incubation period before the onset of clinical symptoms, but none of the studies follow NPT level at the end course of Covid-19 severity [35, 36]. In addition, severe cases of Covid-19 have been linked to a high-risk of acute kidney injury (AKI) in about 50% of cases [37]. In AKI, NPT level is correlated with elevated blood urea and serum creatinine levels [38]. Furthermore, the correlation between NPT level and blood urea and/or serum creatinine levels was not evaluated in most studies that concern NPT level in Covid-19. Therefore, linking NPT level with Covid-19 severity seems to be a compensatory protective mechanism against SARS-CoV-2 rather than a causal factor. In fact, during viral infection, macrophages synthesize dihydro-NPT upon IFN- γ activation, which oxidized to form NPT. Therefore, NPT is an oxidized form of dihydro-NPT during macrophage-induced inflammatory changes and OS. Free radicals, ROS and other oxidants agents during OS increase conversion of 7,8-dihydro-NPT to NPT. Therefore, measurement of total NPT (NPT plus dihydro-NPT) is a more accurate measure than NPT alone in assessment of macrophage activity [15]. It has been shown that the generated 7,8-dihydro-NPT during macrophages activation exert antioxidant activity against local oxidizing inflammatory environment [39]. Undeniably, NPT is not always a reflex of the disease activity and severity, as shown by a systematic review and meta-analysis, illustrating that NPT level has no any role or substantial effect on disease activity and severity of RA [40].

Nonetheless, most studies that confirmed the potential benefit of NPT as a biomarker of Covid-19 severity did not discuss why it increases and do it exert harmful or protective effects during the clinical course in Covid-19 patients. It has been revealed that SARS-CoV-2 infection leads to endotheliitis which provoke the release of pro-inflammatory cytokines [41]. As a consequence, endothelial inflammation activates the production of IL-6 and adhesion molecules, like ICAM-1, MCP-1, and VCAM-1 that encourage T cells and monocyte adhesions and infiltrations into vascular neointima with secretion of TNF- α [42]. Yan et al. [43] illustrated that NPT attenuates the activity of macrophage foam cells and is linked with endothelial inflammation through inhibition of adhesion molecules and monocytes migration. Therefore, high NPT levels in Covid-19 patients can display a protective effect to counteract the SARS-CoV-2-induced endotheliitis and endothelial dysfunctions. Into the bargain, SARS-CoV-2 infection is associated with macrophage activation with acquisition of pro-inflammatory phenotype

Fig. 2 The potential role of neopterin in SARS-CoV-2 infection: Neopterin (NPT) inhibits tissue injury, hyperinflammation and oxidative stress that are induced by SARS-CoV-2-mediated immune activation



(M1) and activation of NF- κ B and nod-like receptor pyrin 3 (NLRP3) inflammasomes leading to hyper-inflammatory status [44]. Different studies have shown that NPT exert anti-inflammatory effects through suppressing NF- κ B signaling and NLRP3 inflammasomes [22]. The inhibitory effect of NPT on the NLRP3 inflammasomes is mediated through activation of anti-inflammatory IL-10 and nuclear translocation of transcription factor-2 (Nrf-2). As well, a prolonged NPT effect accelerates the development of M2 over M1 leading to an anti-inflammatory status to counterbalance the M1-mediated pro-inflammatory response [45].

On the other hand, SARS-CoV-2 infection-induced complications are linked to OS induction, resulting from an overproduction of ROS from neutrophils and activated monocytes/macrophages axis [46]. Laforge et al. [47] illustrated that ROS and OS in SARS-CoV-2 infection led to high neutrophil–lymphocyte ratio, dysfunction of red blood cell, thrombosis, and tissue damage. Thus, antioxidants, like vitamins C, D and E may attenuate Covid-19 severity through modulation of glutathione level, immune response and tissue oxygenations [48]. It has been documented that NPT and 7,8-dihydro-NPT have antioxidant effects comparable to that of melatonin [49]. Similarly, high NPT level reflects a poor endogenous antioxidant capacity and deregulated immune response [50]; herein, NPT may attenuate Covid-19-associated inflammatory and OS-derived disorders as well as tissue damage (Fig. 2).

Furthermore, the NPT level is also increased in patients with type 2 diabetes mellitus (T2DM) [51], cardiovascular disorders [52] and in elderly [53] due to OS and depletion of antioxidant capacity. In a recent study, old age patients

with T2DM and cardiovascular disorders were regarded as high-risk group for Covid-19 severity [54]. In this sense, NPT level in those risk groups with Covid-19 should be reevaluated, despite high NPT level in patients with Covid-19 seems to be a protective compensatory mechanism to counterbalance the hyper-inflammatory response, OS, and associated organ damage through its anti-inflammatory and antioxidant effects. Furthermore, the development of NPT agonist agents either drugs or analogues of phytomedicine may be of a great value in the management of Covid-19.

Conclusion

An elevated NPT serum level in Covid-19 patients is regarded as a protective compensatory mechanism to counterpoise the hyper-inflammatory response, OS, and associated organ damage through its anti-inflammatory and antioxidant effects. Thus, prospective and randomized, controlled clinical trials should be warranted to confirm and reevaluate the association between serum NPT level and Covid-19 severity mainly in high-risk patients.

Acknowledgements This work was supported by Taif University Researchers Supporting Program (Project Number: TURSP-2020/128), Taif University, Saudi Arabia.

Author contributions Study design: HMAK, GESB; Investigation: HMAK, AIAG, KJA; Supervision: GESB; Validation: NCM, GESB; Writing—original draft: HMAK, AIAG; Writing—review and editing: NCM, GESB.

Data availability Data sharing not applicable to this article as no datasets were generated or analyzed during the current study.

Declarations

Conflict of interest The authors declare that there are no conflict of interest.

References

- Al-Kuraishy HM, Al-Naimi MS, Lungnier CM, Al-Gareeb AI (2020) Macrolides and COVID-19: an optimum premise. *Biomed Biotechnol Res J* 4(3):189
- Al-Kuraishy HM, Hussien NR, Al-Naimi MS, Al-Buhadily AK, Al-Gareeb AI, Lungnier C (2020) Renin-Angiotensin system and fibrinolytic pathway in COVID-19: one-way skepticism. *Biomed Biotechnol Res J* 4(5):33
- Al-Kuraishy HM, Al-Gareeb AI, Qusty N, Cruz-Martins N, Batisha GE (2021) Sequential doxycycline and colchicine combination therapy in Covid-19: the salutary effects. *Pulm Pharmacol Ther* 67:102008
- Al-Kuraishy HM, Al-Niemi MS, Hussain NR, Al-Gareeb AI, Al-Harchan NA, Al-Kurashi AH (2020) The potential role of renin angiotensin system (RAS) and dipeptidyl peptidase-4 (DPP-4) in COVID-19: navigating the uncharted. In: Kibel A (ed) Selected chapters from the reninangiotensin system. IntechOpen, London, pp 151–165
- Al-Kuraishy HM, Al-Gareeb AI, Alblihed M, Cruz-Martins N, Batisha GE (2021) COVID-19 and risk of acute ischemic stroke and acute lung injury in patients with type II diabetes mellitus: the anti-inflammatory role of metformin. *Front Med* 8:110
- Lugnier C, Al-Kuraishy HM, Rousseau E (2021) PDE4 inhibition as a therapeutic strategy for improvement of pulmonary dysfunctions in Covid-19 and cigarette smoking. *Biochem Pharmacol* 185:114431
- Al-Kuraishy HM, Al-Gareeb AI, Cruz-Martins N, Batisha GE (2021) Hyperbilirubinemia in Gilbert syndrome attenuates Covid-19 induced-metabolic disturbances: a case-report study. *Front Cardiovasc Med* 8:71
- Al-kuraishy HM, Al-Gareeb AI, Alqarni M, Cruz-Martins N, Batisha GE (2021) Pleiotropic effects of tetracyclines in the management of COVID-19: emerging perspectives. *Front Pharmacol* 12:136
- Zou L, Dai L, Zhang Y, Fu W, Gao Y, Zhang Z, Zhang Z (2020) Clinical characteristics and risk factors for disease severity and death in patients with Coronavirus disease 2019 in Wuhan, China. *Front Med* 7:532
- Zheng B, Cao KY, Chan CP, Choi JW, Leung W, Leung M, Duan ZH, Gao Y, Wang M, Di B, Hollidt JM (2005) Serum neopterin for early assessment of severity of severe acute respiratory syndrome. *Clin Immunol* 116(1):18–26
- Michałak Ł, Bulska M, Strząbała K, Szcześniak P (2017) Neopterin as a marker of cellular immunological response. *Postepy Hig Med Dosw* 71(1):727–736
- Goyal N, Kashyap B, Singh NP, Kaur IR (2017) Neopterin and oxidative stress markers in the diagnosis of extrapulmonary tuberculosis. *Biomarkers* 22(7):648–653
- Arshadi D, Nikbin B, Shakiba Y, Kiani A, Jamshidi AR, Boroushaki MT (2013) Plasma level of neopterin as a marker of disease activity in treated rheumatoid arthritis patients: association with gender, disease activity and anti-CCP antibody. *Int Immunopharmacol* 17(3):763–767
- Melichar B, Spisarová M, Bartoušková M, Krčmová LK, Javoršká L, Študentová H (2017) Neopterin as a biomarker of immune response in cancer patients. *Ann Transl Med* 5(13):280
- Koç DÖ, Özhan Y, Acar ET, Bireroğlu N, Aslan F, Keğin M, Sipahi H (2020) Serum neopterin levels and IDO activity as possible markers for presence and progression of hepatitis B. *Pteridines* 31(1):91–99
- Omra A, Colak S, Can Sandikci S, Yucel C, Erden A, Sertoglu E, Ozgurtas T (2019) Serum neopterin and ischemia modified albumin levels are associated with the disease activity of adult immunoglobulin a vasculitis (Henoch-Schönlein purpura). *Int J Rheum Dis* 22(10):1920–1925
- El-Lebedy D, Hussein J, Ashmawy I, Mohammed AM (2017) Serum level of neopterin is not a marker of disease activity in treated rheumatoid arthritis patients. *Clin Rheumatol* 36(9):1975–1979
- Pizzini A, Kurz K, Santifaller J, Tschartschenthaler C, Theurl I, Fuchs D, Weiss G, Bellmann-Weiler R (2019) Assessment of neopterin and indoleamine 2, 3-dioxygenase activity in patients with seasonal influenza: a pilot study. *Influenza Other Respir Viruses* 13(6):603–609
- Orecchioni M, Ghosheh Y, Pramod AB, Ley K (2019) Macrophage polarization: different gene signatures in M1 (LPS+) vs. classically and M2 (LPS-) vs. alternatively activated macrophages. *Front Immunol* 10:1084
- Prebble H, Cross S, Marks E, Healy J, Searle E, Aamir R, Butler A, Roake J, Hock B, Anderson N, Gieseg SP (2018) Induced macrophage activation in live excised atherosclerotic plaque. *Immunobiology* 223(8–9):526–535
- Watanabe T (2020) Neopterin derivatives—a novel therapeutic target rather than biomarker for atherosclerosis and related diseases. *Vasa*. <https://doi.org/10.1024/0301-1526/a000903>
- de Paula MR, Ghisoni K, Lim CK, Aguiar AS Jr, Guillemin GJ, Latini A (2018) Neopterin preconditioning prevents inflammatory activation in mammalian astrocytes. *Free Radic Biol Med* 115:371–382
- Farghaly HS, Metwalley KA, Raafat DM, Saeid GM, Gabri MF, Algohary M (2021) Association between vascular endothelial dysfunction and the inflammatory marker neopterin in patients with classic congenital adrenal hyperplasia. *Atherosclerosis*. <https://doi.org/10.1016/j.atherosclerosis.2021.05.017>
- Shirai R, Sato K, Yamashita T, Yamaguchi M, Okano T, Watanabe-Kominato K, Watanabe R, Matsuyama TA, Ishibashi-Ueda H, Koba S, Kobayashi Y (2018) Neopterin counters vascular inflammation and atherosclerosis. *J Am Heart Assoc* 7(3):e007359
- Toygar M, Aydin I, Agilli M, Aydin FN, Oztosun M, Gul H, Macit E, Karslioglu Y, Topal T, Uysal B, Honca M (2015) The relation between oxidative stress, inflammation, and neopterin in the paraquat-induced lung toxicity. *Hum Exp Toxicol* 34(2):198–204
- Bellmann-Weiler R, Lässer L, Burkert F, Seiwald S, Fritzsche G, Wildner S, Schroll A, Koppelstätter S, Kurz K, Griesmacher A, Weiss G (2021) Neopterin predicts disease severity in hospitalized patients with COVID-19. InOpen forum infectious diseases, vol 1. Oxford University Press, Oxford, p ofaa521
- Peng Y, Mentzer AJ, Liu G, Yao X, Yin Z, Dong D, Dejnirattisai W, Rostron T, Supasa P, Liu C, Lopez-Camacho C (2020) Broad and strong memory CD4+ and CD8+ T cells induced by SARS-CoV-2 in UK convalescent individuals following COVID-19. *Nat Immunol* 21(11):1336–1345
- Robertson J, Gostner JM, Nilsson S, Andersson LM, Fuchs D, Gisslen M (2020) Serum neopterin levels in relation to mild and severe COVID-19. *BMC Infect Dis* 20(1):1–6
- Ozger HS, Dizbay M, Corbacioglu SK, Aysert P, Demirbas Z, Tunçcan OG, Hizel K, Bozdayı G, Caglar K (2020) The prognostic role of neopterin in COVID-19 patients. *J Med Virol* 93(3):1520–1525

30. Ip M, Rainer TH, Lee N, Chan C, Chau SS, Leung W, Leung MF, Tam TK, Antonio GE, Lui G, Lau TK (2007) Value of serum procalcitonin, neopterin, and C-reactive protein in differentiating bacterial from viral etiologies in patients presenting with lower respiratory tract infections. *Diagn Microbiol Infect Dis* 59(2):131–136
31. Coster D, Wasserman A, Fisher E, Rogowski O, Zeltser D, Shapira I, Bernstein D, Meilik A, Raykhshtat E, Halpern P, Berliner S (2019) Using the kinetics of C-reactive protein response to improve the differential diagnosis between acute bacterial and viral infections. *Infection* 2019:1–8
32. Wirleitner B, Schroecksnadel K, Winkler C, Fuchs D (2005) Neopterin in HIV-1 infection. *Mol Immunol* 42(2):183–194
33. Abdelaziz HG, El-Tantawy TM, Attia HA, Hamed MM (2020) Neopterin as a predictor of response to pegylated interferon therapy in Egyptian patients with chronic hepatitis C virus. *Asian J Res Biochem* 6:43–52
34. Edén A, Kanberg N, Gostner J, Fuchs D, Hagberg L, Andersson LM, Lindh M, Price RW, Zetterberg H, Gisslén M (2020) CSF biomarkers in patients With COVID-19 and neurologic symptoms: a case series. *Neurology* 96(2):e294–e300
35. Eisenhut M (2013) Neopterin in diagnosis and monitoring of infectious diseases. *J Biomark.* <https://doi.org/10.1155/2013/196432>
36. Zhou F, Yu T, Du R, Fan G, Liu Y, Liu Z, Xiang J, Wang Y, Song B, Gu X, Guan L (2020) Clinical course and risk factors for mortality of adult inpatients with COVID-19 in Wuhan, China: a retrospective cohort study. *Lancet* 395:1054–1062
37. Hirsch JS, Ng JH, Ross DW, Sharma P, Shah HH, Barnett RL, Hazzan AD, Fishbane S, Jhaveri KD, Abate M, Andrade HP (2020) Acute kidney injury in patients hospitalized with COVID-19. *Kidney Int* 98(1):209–218
38. Enger TB, Pleym H, Stenseth R, Greiff G, Wahba A, Videm V (2017) A preoperative multimarker approach to evaluate acute kidney injury after cardiac surgery. *J Cardiothorac Vasc Anesth* 31(3):837–846
39. Giesege SP, Amit Z, Yang YT, Shchepetkina A, Katouah H (2010) Oxidant production, oxLDL uptake, and CD36 levels in human monocyte-derived macrophages are downregulated by the macrophage-generated antioxidant 7, 8-dihydronoopterin. *Antioxid Redox Signal* 13(10):1525–1534
40. Hejrati A, Taghadosi M, Alizadeh-Navaei R, Hosseinzadeh S, Bashash D, Esmaili M, Zafari P (2020) Neopterin serum level does not reflect the disease activity in rheumatoid arthritis: a systematic review and meta-analysis. *IUBMB Life* 72(12):2563–2571
41. Thacker VV, Sharma K, Dhar N, Mancini GF, Sordet-Dessimoz J, McKinney JD (2020) Rapid endothelial infection, endothelialitis and vascular damage characterise SARS-CoV-2 infection in a human lung-on-chip model. *bioRxiv*. <https://doi.org/10.1101/2020.08.10.243220>
42. Chistiakov DA, Melnichenko AA, Myasoedova VA, Grechko AV, Orekhov AN (2017) Mechanisms of foam cell formation in atherosclerosis. *J Mol Med* 95(11):1153–1165
43. Yan JQ, Tan CZ, Wu JH, Zhang DC, Chen JL, Zeng BY, Jiang YP, Nie J, Liu W, Liu Q, Dai H (2013) Neopterin negatively regulates expression of ABCA1 and ABCG1 by the LXR α signaling pathway in THP-1 macrophage-derived foam cells. *Mol Cell Biochem* 379(1):123–131
44. van den Berg DF, Te Velde AA (2020) Severe COVID-19: NLRP3 inflammasome dysregulated. *Front Immunol* 11:1580
45. Yang CA, Huang ST, Chiang BL (2015) Sex-dependent differential activation of NLRP3 and AIM2 inflammasomes in SLE macrophages. *Rheumatology* 54(2):324–331
46. Schönrich G, Raftery MJ, Samstag Y (2020) Devilishly radical NETwork in COVID-19: oxidative stress, neutrophil extracellular traps (NETs), and T cell suppression. *Adv Biol Regul* 77:100741
47. Laforge M, Elbim C, Frère C, Hémadi M, Massaad C, Nuss P, Benoliel JJ, Becker C (2020) Tissue damage from neutrophil-induced oxidative stress in COVID-19. *Nat Rev Immunol* 20(9):515–516
48. Qin M, Cao Z, Wen J, Yu Q, Liu C, Wang F, Zhang J, Yang F, Li Y, Fishbein G, Yan S (2020) An antioxidant enzyme therapeutic for COVID-19. *Adv Mater* 32(43):2004901
49. Girgin G, Sabuncuoğlu S, Ünal AZ, Baydar T (2017) Assessment of antioxidant and cytotoxic activity of known antioxidants compared to neopterin. *Multidiscip Digit Publ Inst Proc* 1(10):1071
50. Murr C, Winklhofer-Roob BM, Schroecksnadel K, Maritschnegg M, Mangge H, Böhm BO, Winkelmann BR, März W, Fuchs D (2009) Inverse association between serum concentrations of neopterin and antioxidants in patients with and without angiographic coronary artery disease. *Atherosclerosis* 202(2):543–549
51. Rasheed HA, Al-Kuraishy HM, Al-Gareeb AI, Hussien NR, Al-Nami MS (2019) Effects of diabetic pharmacotherapy on prolactin hormone in patients with type 2 diabetes mellitus: bane or boon. *J Adv Pharm Technol Res* 10(4):163
52. Al-Kuraishy HM, Al-Gareeb AI, Al-Buhadilly AK (2018) Rosuvastatin improves vaspin serum levels in obese patients with acute coronary syndrome. *Diseases* 6(1):9
53. Abdul-Hadi M, Hussien N, Rasheed H, Al-Kuraishy H, Al-Gareeb A (2020) Subclinical hypothyroidism and erectile dysfunction: the potential nexus. *Urol Sci* 31(2):56
54. Al-kuraishy H, Al-Gareeb AI, Guerreiro SG, Cruz-Martins N, Batiha GE (2021) COVID-19 in relation to hyperglycemia and diabetes mellitus. *Front Cardiovasc Med* 8:335

Publisher's Note Springer Nature remains neutral with regard to jurisdictional claims in published maps and institutional affiliations.



COVID-19

The role of C-reactive protein as a prognostic marker in COVID-19

Dominic Stringer,¹ Philip Braude,² Phyto K Myint,³ Louis Evans,⁴ Jemima T Collins,⁵ Alessia Verduri,⁶ Terry J Quinn,⁷ Arturo Vilches-Moraga,⁸ Michael J Stechman,⁹ Lyndsay Pearce,¹⁰ Susan Moug,¹¹ Kathryn McCarthy,¹² Jonathan Hewitt¹³ and Ben Carter^{1*}; COPE Study Collaborators

¹Department of Biostatistics and Health Informatics, Institute of Psychiatry, Psychology & Neuroscience, King's College London, London, UK, ²North Bristol NHS Trust, UK, ³Institute of Applied Health Sciences, University of Aberdeen, ⁴Ysbyty Gwynedd, Bangor, ⁵Ysbyty Ystrad Fawr, Aneurin Bevan University Health Board, ⁶Hospital of Modena Policlinico, Italy, ⁷Institute of Cardiovascular and Medical Sciences, University of Glasgow, ⁸Department of Ageing and Complex Medicine, Salford Royal NHS Foundation Trust, Salford, University of Manchester, Manchester, UK, ⁹Department of Surgery, University Hospital of Wales, Cardiff, ¹⁰Department of Colorectal Surgery, Salford Royal NHS Foundation Trust, Manchester, UK, ¹¹Department of Surgery, Royal Alexandra Hospital, Paisley, UK, ¹²Department of Surgery, North Bristol NHS Trust, Bristol, UK, and ¹³Cardiff University and Aneurin Bevan University Health Board

*Corresponding author. Department of Biostatistics and Health Informatics, Institute of Psychiatry, Psychology & Neuroscience, King's College, London, De Crespigny Park, London SE5 8AF, UK. E-mail: ben.carter@kcl.ac.uk

Received 22 October 2020; Editorial decision 8 January 2021; Accepted 25 January 2021

Abstract

Background: C-reactive protein (CRP) is a non-specific acute phase reactant elevated in infection or inflammation. Higher levels indicate more severe infection and have been used as an indicator of COVID-19 disease severity. However, the evidence for CRP as a prognostic marker is yet to be determined. The aim of this study is to examine the CRP response in patients hospitalized with COVID-19 and to determine the utility of CRP on admission for predicting inpatient mortality.

Methods: Data were collected between 27 February and 10 June 2020, incorporating two cohorts: the COPE (COVID-19 in Older People) study of 1564 adult patients with a diagnosis of COVID-19 admitted to 11 hospital sites (test cohort) and a later validation cohort of 271 patients. Admission CRP was investigated, and finite mixture models were fit to assess the likely underlying distribution. Further, different prognostic thresholds of CRP were analysed in a time-to-mortality Cox regression to determine a cut-off. Bootstrapping was used to compare model performance [Harrell's C statistic and Akaike information criterion (AIC)].

Results: The test and validation cohort distribution of CRP was not affected by age, and mixture models indicated a bimodal distribution. A threshold cut-off of CRP ≥ 40 mg/L performed well to predict mortality (and performed similarly to treating CRP as a linear variable).

Conclusions: The distributional characteristics of CRP indicated an optimal cut-off of ≥ 40 mg/L was associated with mortality. This threshold may assist clinicians in using CRP as an early trigger for enhanced observation, treatment decisions and advanced care planning.

Key words: CRP, COVID-19, bimodal, trimodal, mortality, prognostic marker, mixture model

Key Messages

- C-reactive protein (CRP) has been used inconsistently both in patient management and as a prognostic marker during COVID-19.
- Admission elevated CRP for patients with COVID-19 was associated with increased inpatient mortality and was indicative of disease severity at admission.
- The distribution of CRP at admission was found to be bimodally distributed, and a CRP ≥ 40 mg/L was the optimal threshold of increased risk of mortality.
- Admission CRP ≥ 40 mg/L may be used by treating clinicians as an early warning for enhanced care and patient-centred decision making.

Introduction

Elevated levels of serum C-reactive protein (CRP) have been observed in patients with COVID-19 and used to assist with triage, diagnostics and prognostication.^{1,2} CRP is a non-specific acute phase protein that is produced by hepatocytes and elevated in acute infection or inflammation.³ Secretion begins 4–10 h after an inflammatory insult and peaks at 48 h, with a short half-life of 19 h. Crucially, it may be elevated before a patients' vital signs are affected or leukocytes are raised.³ The profile of this biomarker has made CRP useful and routinely available in clinical medicine for diagnostics.

CRP can be used to assist with differentiation between viral and bacterial infections, for example, influenza produces a mean CRP level of 25.65 mg/L [95% confidence interval (CI) 18.88 to 32.41 mg/L] versus bacterial pneumonia which produces a mean CRP level of 135.96 mg/L (95% CI 99.38 to 172.54 mg/L).⁴ In COVID-19, a CRP level of ≥ 4 mg/L has been shown to be useful for triaging suspected cases when comparing polymerase chain reaction (PCR)-positive patients versus negative controls who have presented to a fever clinic with respiratory symptoms or a high temperature [odds ratio (OR) 4.75; 95% CI 3.28 to 6.88].⁵

However, debate remains over the utility of CRP as a prognostic marker for patients admitted to hospital with COVID-19. In a recent systematic review, 10 of the 22 included COVID-19 prognostic models treated CRP either as a factor or covariate.⁶ Most these studies used CRP with a binary threshold; proposed values to predict inpatient mortality varied from ≥ 10 mg/L to ≥ 76 mg/L. In addition to a binary threshold, CRP has been examined in a trichotomized model with the

two thresholds at ≥ 40 mg/L and ≥ 100 mg/L.⁷ A lower cut-off of ≥ 20.44 mg/L was used as a threshold for related lung injury,⁸ and >32.5 mg/L was found to offer 80% predictive power for a person needing mechanical ventilation.⁹ The studies adjusted for admission CRP as a covariate to account for baseline disease severity have assumed a linear or natural logarithm transformation [$\ln(\text{CRP})$] relationship with outcome.^{10,11} Although using CRP in a continuous manner may offer an improved understanding of the contribution of CRP within each analysis, it does not allow CRP to be used by clinical teams to guide management of patients with COVID-19.

Whilst CRP has been argued as an important marker of disease progression in COVID-19,⁶ its distribution has never been explored to understand whether distinct patterns exist in a heterogeneous population. The use of CRP as a biomarker in COVID-19 may present a quick and accessible tool in clinical management, trigger longer periods of enhanced observation, provide information around likely disease progression and assist with early therapeutic, ventilation and palliative care discussions.

The aim of this study is to examine the distribution of CRP at hospital admission, and objectives are to: (i) assess CRP as a prognostic bimodal or trimodal distribution; (ii) propose and compare the categorization of CRP as a prognostic marker to either a linear or a log-linear measure of CRP.

Methods

Permission to conduct this study was granted in the UK by the Health Research Authority (20/HRA/1898) and in Italy by the ethics committee of University Hospital of Modena

Policlinico (369/2020/OSS/AOUMO). Written consent was not required from participants as per ethical review.

Study design

This observational study used two cohorts at different time points to examine the contribution of CRP to clinical outcomes. This study has been reported in accordance with the STROBE statement.¹²

Settings

Thirteen hospital sites participated, 12 from the UK and one from Italy. All were acute hospitals directly admitting patients with suspected or confirmed COVID-19.

Participants

Original cohort (cohort 1)

Participants in Cohort 1 were included as part of the COPE study (COVID in Older People study) as reported in the paper by Hewitt *et al.*^{13,14} Briefly, this was a European multicentre observational study recruiting 1564 hospitalized adults between 27 February and 28 April 2020 with either SARS-CoV-2 viral polymerase chain reaction (PCR) confirmed disease (95.9%) or clinically diagnosed (4.1%) COVID-19. Any patient aged 18 years or older admitted to the participating hospitals with a diagnosis of COVID-19 was included. The study found frailty was associated with longer hospital stay, and a better predictor of mortality as an inpatient, and at Day 7, than age or comorbidity alone.

Validation cohort (cohort 2)

Cohort 2 consisted of an additional 271 patients recruited between 29 April and 10 June 2020 from a combination of six of Cohort 1's hospitals plus two additional recruiting hospitals. All patients were SARS-CoV-2 viral PCR-positive.

Variables

A prognostic threshold for CRP was needed within the COPE protocol (March 2020). The limited literature available early in the pandemic included a case series of 73 patients with COVID-19 presenting with a mean CRP level of 51.4 mg/L [standard deviation (SD) 41.8].¹ Based on this paper, and proposed by the clinical experience of the authors who delivered acute care, a dichotomous threshold was chosen with <40 mg/L (lower admission CRP), and ≥40 mg/L (CRP-elevated, indicating increased disease severity¹⁴).

Data sources

CRP was measured at hospital admission and transcribed from patients' medical records. There was no attempt to standardize the CRP assay between sites. A standardized case reporting form was used for all hospital sites. Data were transferred to King's College London in anonymous format for statistical analysis.

Graphical data analysis

Using the test cohort, the distribution of CRP was examined graphically and stratified by age. Finite bivariate and trivariate Gaussian mixture models were fit to CRP, representing two and three latent classes, respectively. The theoretical distribution from these models was compared with the empirical data and the threshold between the two and three classes was examined. The normality assumptions were assessed visually.

Statistical analysis

Primary analysis: mixture modelling analysis

The empirical data from the test cohort were fit to a Gaussian mixture model with one, two or three components using an expectation-maximization algorithm (to refine the starting values) then maximum likelihood estimation (Stata routine '*fmm*'). The models were compared using the Akaike information criterion (AIC) and the thresholds were determined by the posterior probability of belonging to the two or three class models.

Secondary analysis: prognostic modelling analysis

To assess differing thresholds for CRP as a prognostic factor of outcome, a series of mixed-effects multivariable Cox proportional hazards models for time to mortality were fit, in a method consistent with the COPE study primary analysis.¹³ The model was adjusted for elevated CRP using a level of ≥40 mg/L, in addition to: patient age group (<65, 65–79, ≥80 years old), sex, diabetes (yes/no), hypertension (yes/no), coronary artery disease (yes/no) and kidney disease [estimated glomerular filtration rate (eGFR) <60 ml/min/1.73m²]. Dichotomized thresholds of CRP were compared within a range of 10 mg/L to 100 mg/L in 5-mg/L intervals (≥10 mg/L, ≥15 mg/L, etc). Model performance was evaluated and compared using Harrell's C and the AIC.¹⁵ We compared the dichotomized thresholds against linear CRP and Ln(CRP) (as CRP is known to be skewed) as benchmarks of performance. This method was chosen as dichotomizing results can lead to a loss of information, resulting in a lower predictive power compared with using a continuous measure.¹⁶ Bootstrapping was

used to construct 95% percent confidence intervals for differences in model performance between the best-fitting models. Bootstrapping was stratified by site with 1000 replications for each comparison. A complete case analysis was used in all cases due to negligible missing data (<4%).

Validation cohort (cohort 2)

To provide an indication of whether the original results from Cohort 1 were likely to be replicable to a wider group of patients with COVID-19, the analysis was repeated on an independent validation sample (Cohort 2). Using the validation cohort, two-class and three-class mixture models were estimated using the empirical data without restriction. On evidence of overfitting, to assess the additional benefit of a very elevated category for CRP, the validation cohort was fitted using a three-class mixture model, with the class-two mean fixed using the validation cohort two-class mixture model mean.

Comparison of the prognostic effect of CRP

Using a mixed-effect multivariable Cox regression, the effect of elevated CRP will be reported using a adjusted hazards ratio (aHR), alongside the respective 95% confidence interval (95% CI), for a linear CRP, $\ln(\text{CRP})$.

Results

The study included 1835 patients across Cohorts 1 and 2, who were drawn from 12 hospitals in the UK and one from Italy. Of the total study participants, 26.4% ($n=484$) died in-hospital, varying between sites from 13.3% to 42.9%. A comparison for those who died in hospital was carried out in [Table 1](#), split into Cohort 1 ($n=1564$) and Cohort 2 ($n=271$). In Cohort 1, 27.2% died and the median CRP level for those who died was 115 mg/L (interquartile range: 63 mg/L–191 mg/L) compared with 69 mg/L (29 mg/L–140 mg/L) among those who survived. For patients with $\text{CRP} \geq 40 \text{ mg/L}$, mortality was 31.9% compared with 15.0% for patients with $\text{CRP} < 40 \text{ mg/L}$. Median follow-up time (time to mortality or discharge) was 13 days (6–22 days).

Cohort 2 experienced 21.8% mortality. Among those who died, median CRP level was 86 mg/L (48 mg/L–173.5 mg/L) compared with 53 mg/L (16 mg/L–109 mg/L) among those who survived. For patients with $\text{CRP} \geq 40 \text{ mg/L}$, mortality was 28.6% compared with 10.4% for patients with $\text{CRP} < 40 \text{ mg/L}$. The median follow-up time (time to death or discharge) was 10 days (5–18 days).

Results of cohort 1 ($n = 1564$)

Distribution of CRP

On graphical examination of the distribution of $\ln(\text{CRP})$, it exhibited negative skew, with two ‘peaks’ suggestive of a bimodal distribution, see [Figure 1](#), Plot (i), and [Figure S1](#), available as [Supplementary data](#) at *IJE* online, Plots (i, ii). The distribution of $\ln(\text{CRP})$ was observed in age-stratified groups of <65, 65–79, and ≥80 years. On inspection, there was no difference between the distribution age-stratified or the complete dataset.

Primary analysis: mixture modelling analysis

Following the two suggested peaks in the examination of the $\ln(\text{CRP})$ distribution, a two-latent class finite mixture model was fitted. It appeared to graphically fit the data when examined against the empirical distribution in [Figure 1](#), Plot (i). This was supported by a comparison with the one-class (or null) model, which displayed a higher AIC (4739 compared with 4524). The simple threshold at which the predicted probability of belonging to a two-class model being greater than one-class was 38 mg/L. This will be implemented as $\geq 40 \text{ mg/L}$ herein, to account for the imprecision of the measurement of CRP and also for ease of recall in a busy clinical setting.

The three-class finite mixture model fit slightly better than the two-class finite mixture model (AIC of 4484), with probability of class-one membership highest between range 0–14 mg/L, class-two between 15–120 mg/L and class-three for values of $\text{CRP} \geq 120 \text{ mg/L}$, see [Figure 1](#), Plot (iii).

The primary analysis proposed a single optimal threshold of $\text{CRP} \geq 40 \text{ mg/L}$ to indicate elevated CRP.

Secondary analysis: prognostic modelling

The time-to-mortality analysis included 1502 participants (96%) in the complete case population. A cut-off of $\geq 65 \text{ mg/L}$ appeared to fit best in the sample on all measures (Harrell’s C statistic of 0.7068, AIC of 5124) ([Table 2](#)) after fitting different binary categorizations of CRP in a Cox model for time to mortality. Differences in measures of goodness of fit were small, especially between cut-offs in the range of $\geq 40 \text{ mg/L}$ to $\geq 90 \text{ mg/L}$. CRP as a continuous $\ln(\text{CRP})$ measure performed considerably better (Harrell’s C statistic of 0.7157, AIC of 5001) and with little improvement on this using a linear scale (Harrell’s C statistic of 0.7040, AIC of 5024). Regarding bootstrapped differences in the measures of goodness of fit between a cut-off of $\geq 40 \text{ mg/L}$ and the marginally better performing cut-off of $\geq 65 \text{ mg/L}$, no difference in performance was

Table 1 Descriptive characteristics for Cohort 1 and 2 samples with comparison by in-hospital mortality

	Cohort 1 (Original)			Cohort 2 (Validation)		
	All patients (n = 1564)	Dead (n = 425)	Alive (n = 1139)	All patients (n = 271)	Dead (n = 59)	Alive (n = 212)
Sites						
Hospital A	115 (7.4%)	15 (13.0%)	100 (87.0%)	25 (9.2%)	4 (16.0%)	21 (84.0%)
Hospital B	50 (3.2%)	14 (28.0%)	36 (72.0%)	0 (0%)	0 (0%)	0 (0%)
Hospital C	153 (9.8%)	34 (22.2%)	119 (77.8%)	0 (0%)	0 (0%)	0 (0%)
Hospital D	43 (2.7%)	10 (23.3%)	33 (76.7%)	9 (3.3%)	0 (0.0%)	9 (100.0%)
Hospital E	123 (7.9%)	15 (12.2%)	108 (87.8%)	58 (21.4%)	9 (15.5%)	49 (84.5%)
Hospital F	154 (9.8%)	23 (14.9%)	131 (85.1%)	15 (5.5%)	4 (26.7%)	11 (73.3%)
Hospital G	112 (7.2%)	36 (32.1%)	76 (67.9%)	0 (0%)	0 (0%)	0 (0%)
Hospital H	246 (15.7%)	108 (43.9%)	138 (56.1%)	0 (0%)	0 (0%)	0 (0%)
Hospital I	380 (24.3%)	126 (33.2%)	254 (66.8%)	62 (22.9%)	12 (19.4%)	50 (80.7%)
Hospital J	179 (11.5%)	43 (24.0%)	136 (76.0%)	13 (4.8%)	3 (23.1%)	10 (76.9%)
Hospital K	9 (0.6%)	1 (11.1%)	8 (88.9%)	4 (1.5%)	1 (25.0%)	3 (75.0%)
Hospital L	0 (0%)	0 (0%)	0 (0%)	57 (21.0%)	14 (24.6%)	43 (75.4%)
Hospital M	0 (0%)	0 (0%)	0 (0%)	28 (10.3%)	12 (42.9%)	16 (57.1%)
Age, years						
<65	488 (31.2%)	55 (11.3%)	433 (88.7%)	61 (22.5%)	6 (9.8%)	55 (90.2%)
65–79	535 (34.2%)	168 (31.4%)	367 (68.6%)	85 (31.4%)	14 (16.5%)	71 (83.5%)
≥80	541 (34.6%)	202 (37.3%)	339 (62.7%)	124 (45.8%)	38 (30.7%)	86 (69.4%)
Missing	0 (0.0%)	0 (0.0%)	0 (0.0%)	1 (0.4%)	1 (100.0%)	0 (0.0%)
Sex						
Female	661 (42.3%)	170 (25.7%)	491 (74.3%)	134 (49.5%)	29 (21.6%)	105 (78.4%)
Male	903 (57.7%)	255 (28.2%)	648 (71.8%)	136 (50.2%)	30 (22.1%)	106 (77.9%)
Missing	0 (0%)	0 (0%)	0 (0%)	0 (0%)	0 (0%)	1 (100.0%)
Smoking status						
Never smokers	814 (52.0%)	205 (25.2%)	609 (74.8%)	132 (48.7%)	24 (18.2%)	108 (81.8%)
Ex-smokers	603 (38.6%)	185 (30.7%)	418 (69.3%)	91 (33.6%)	25 (27.5%)	66 (72.5%)
Current smokers	121 (7.7%)	26 (21.5%)	95 (78.5%)	18 (6.6%)	2 (11.1%)	16 (88.9%)
Missing	26 (1.7%)	9 (34.6%)	17 (65.4%)	30 (11.1%)	8 (26.7%)	22 (73.3%)
Diabetes						
No	1144 (73.1%)	295 (25.8%)	849 (74.2%)	204 (75.3%)	41 (20.1%)	163 (79.9%)
Yes	415 (26.5%)	128 (30.8%)	287 (69.2%)	66 (24.4%)	18 (27.3%)	48 (72.7%)
Missing	5 (0.3%)	2 (40.0%)	3 (60.0%)	1 (0.4%)	0 (0.0%)	1 (100.0%)
Hypertension						
No	755 (48.3%)	184 (24.4%)	571 (75.6%)	126 (46.5%)	22 (17.5%)	104 (82.5%)
Yes	804 (51.4%)	238 (29.6%)	566 (70.4%)	145 (53.5%)	37 (25.5%)	108 (74.5%)
Missing	5 (0.3%)	3 (60.0%)	2 (40.0%)	0 (0%)	0 (0%)	0 (0%)
Coronary artery disease						
No	1214 (77.6%)	290 (23.9%)	924 (76.1%)	220 (81.8%)	43 (19.6%)	177 (80.5%)
Yes	345 (22.1%)	132 (38.3%)	213 (61.7%)	51 (18.8%)	16 (31.4%)	35 (68.6%)
Missing	5 (0.3%)	3 (60.0%)	2 (40.0%)	0 (0%)	0 (0%)	0 (0%)
Increased C-reactive protein (≥40 mg/L)						
No	439 (28.1%)	66 (15.0%)	373 (85.0%)	96 (35.4%)	10 (10.4%)	86 (89.6%)
Yes	1125 (71.9%)	359 (31.9%)	766 (68.1%)	161 (59.4%)	46 (28.6%)	115 (71.4%)
Missing	32 (2.0%)	12 (37.5%)	20 (62.5%)	14 (5.2%)	3 (21.4%)	11 (78.6%)
Impaired renal function (eGFR^a <60 mL/min per 1.73 m²)						
No	980 (63.7%)	202 (20.6%)	778 (79.4%)	132 (48.7%)	20 (15.2%)	112 (84.9%)
Yes	570 (36.4%)	217 (38.1%)	353 (61.9%)	81 (29.9%)	25 (30.9%)	56 (69.1%)
Missing	14 (0.9%)	6 (42.9%)	8 (57.1%)	58 (21.4%)	14 (24.1%)	44 (75.9%)
Clinical Frailty Scale (1–9)						
1: Very fit	91 (5.8%)	7 (7.7%)	84 (92.3%)	11 (4.1%)	1 (9.1%)	10 (90.9%)
2: Fit	197 (12.6%)	22 (11.2%)	175 (88.8%)	22 (8.1%)	1 (4.6%)	21 (95.5%)

Downloaded from https://academic.oup.com/ije/article/50/2/420/6156754 by guest on 25 May 2021

(Continued)

Table 1 Continued

	Cohort 1 (Original)			Cohort 2 (Validation)		
	All patients (n = 1564)	Dead (n = 425)	Alive (n = 1139)	All patients (n = 271)	Dead (n = 59)	Alive (n = 212)
3: Managing well	287 (18.4%)	55 (19.2%)	232 (80.8%)	37 (13.7%)	7 (18.9%)	30 (81.1%)
4: Vulnerable	185 (11.8%)	52 (28.1%)	133 (71.9%)	25 (9.2%)	5 (20.0%)	20 (80.0%)
5: Mildly frail	182 (11.6%)	50 (27.5%)	132 (72.5%)	38 (14.0%)	6 (15.8%)	32 (84.2%)
6: Moderately frail	251 (16.0%)	84 (33.5%)	167 (66.5%)	51 (18.8%)	11 (21.6%)	40 (78.4%)
7: Severely frail	260 (16.6%)	96 (36.9%)	164 (63.1%)	61 (22.5%)	20 (32.8%)	41 (67.2%)
8: Very severely frail	79 (5.1%)	44 (55.7%)	35 (44.3%)	5 (1.9%)	3 (60.0%)	2 (40.0%)
9: Terminally ill	27 (1.7%)	12 (44.4%)	15 (55.6%)	4 (1.5%)	1 (25.0%)	3 (75.0%)
Missing	5 (0.3%)	3 (60.0%)	2 (40.0%)	17 (6.3%)	4 (23.5%)	13 (76.5%)
Median CRP ^b (mg/L) (lower and upper quartile)	80.5 (36–154)	115 (63–191)	69 (29–140)	65 (20–117)	86 (48–173.5)	53 (16–109)

^aEstimated glomerular filtration rate.^bC-reactive protein.

seen with 95% CI for all measures (Table 3). There was evidence that cut-offs of both ≥ 40 mg/L and ≥ 65 mg/L outperformed a cut-off of ≥ 10 mg/L, the upper limit of the normal range for CRP.¹⁷ It should be noted that $\text{Ln}(\text{CRP})$ was the optimal parameterization compared with either ≥ 40 mg/L (-135.1 AIC, bootstrapped 95% CI -210.4 to -65.1) or ≥ 65 mg/L (-123.5 AIC, bootstrapped 95% CI -197.6 to -55.8).

Results of cohort 2 (n = 271)

Distribution of CRP

Cohort 2 included 271 new patients from eight hospital sites: 85 (31.4%) were fully independent, recruited from two new hospital sites; 186 were pseudo-independent, being newly recruited patients from original hospital sites in Cohort 1. There was no difference in the demographics, comorbidities and distribution of CRP seen in Cohort 2 and Cohort 1 (Table 1).

Fitting finite mixture models

The empirical distribution of the Cohort 2 $\text{Ln}(\text{CRP})$ appeared, graphically, to have a reasonably similar pattern to Cohort 1, see Figure 1, Plot (ii). The two-class finite mixture model gave a consistent threshold (CRP ≥ 41 mg/L). The unrestricted three-class finite mixture model exhibited likely overfitting to the data on examination of the distributions. Inconclusive evidence for the additional second cut-off was found with the class three distribution entirely contained within class two, with a large variance. There was no additional benefit for fixing the central distribution mean and allowing the mixture proportion to vary, but this can be seen graphically in Figure 1, Plot (iv). The

simple threshold between class one and class two was ≥ 41 mg/L.

The time-to-mortality analysis included 208 of the participants (77%) with complete data. Fitting different binary categorizations of CRP in a Cox model for time to mortality gave a CRP cut-off of ≥ 40 mg/L as the best fitting model (Harrell's C statistic of 0.7187, AIC of 424), outperforming the $\text{Ln}(\text{CRP})$ model (Harrell's C statistic of 0.7014, AIC of 427), see Table 2. There was no evidence of difference in performance between cut-offs of ≥ 65 mg/L and ≥ 40 mg/L, nor between ≥ 40 mg/L and $\text{Ln}(\text{CRP})$ on examination of bootstrapped 95% CI in Supplementary Table S1, available as Supplementary data at IJE online.

The prognostic effect of elevated CRP with prognostic properties

The aHRs for CRP ≥ 40 mg/L were 2.58 (95% CI 1.95 to 3.41) and 2.61 (95% CI 0.54 to 4.63) for Cohorts 1 and 2 and the estimate of CRP appeared stable (Supplementary Table S2, available as Supplementary data at IJE online). For comparison CRP ≥ 65 mg/L, the aHR was consistent in Cohort 1 (aHR = 2.48; 95% CI 1.96 to 3.14) but appeared unstable in Cohort 2 (aHR = 1.61; 95% CI 0.84 to 3.09). Using a cut-off of ≥ 40 , the sensitivity, specificity, positive predictive value and negative predictive value were 0.84; 0.33; 0.32; and 0.85 for Cohort 1 and 0.82, 0.43, 0.29 and 0.90 for Cohort 2, respectively.

Discussion

Key results

CRP reasonably followed a bimodal distribution using data from two independent cohorts. There was inconclusive evidence of a trimodal distribution; although the AIC

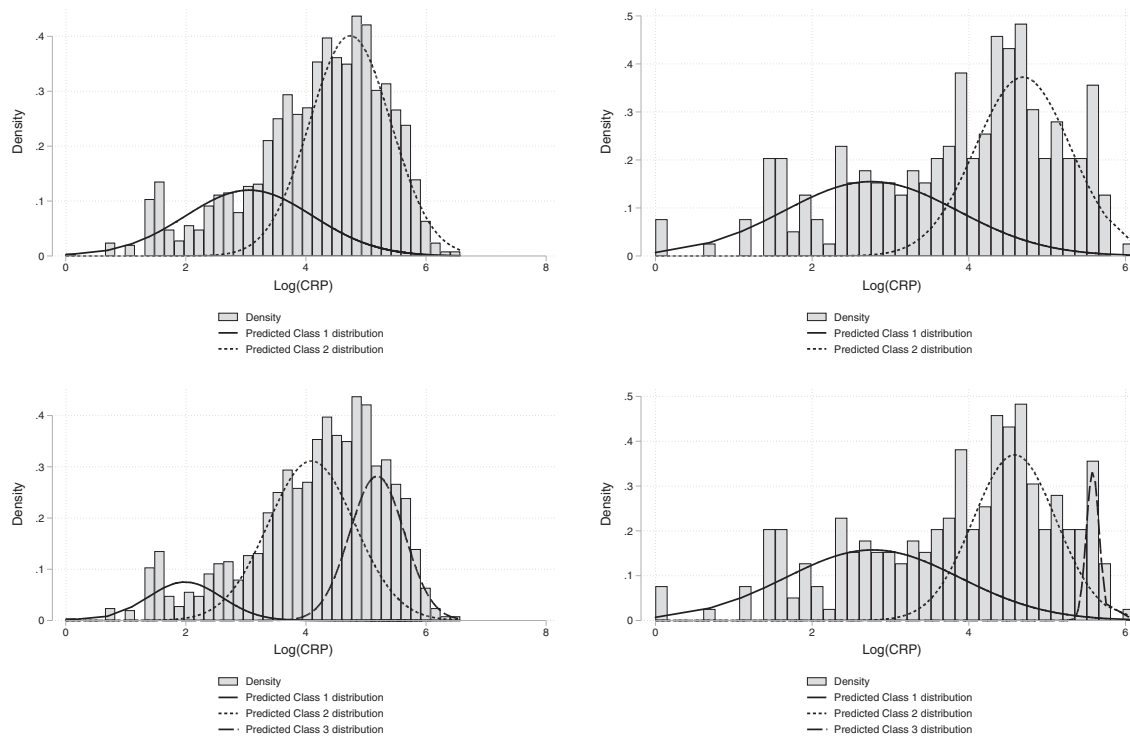


Figure 1 Distribution of C-reactive protein (CRP) in the original cohort (left panel) and the validation cohort (right panel), overlaid predicted distributions from a two-class (upper row), compared with three-class (lower row) finite mixture models

metric suggested it fit better, on graphical examination there appeared to be overfitting.

In an analysis of 1835 patients across 13 hospital sites using a binary cut-off for CRP as a prognostic factor of COVID-19, inpatient death appeared to have similar predictive power compared with treating it as a linear or $\ln(\text{CRP})$. In addition, a cut-off value to indicate disease severity is simpler to use in a clinical setting than a linear predictor. These findings support the use of a simple binary threshold for CRP in daily clinical medicine. These results are well aligned with many published analyses in COVID-19 which have already employed a binary cut-off.^{4,18–20}

The bimodal distribution of CRP may reflect the presence of a latent class influence. Candidate variables for this latent class may include confounders that were not fully controlled for: chronic inflammatory conditions, genomic variation of the virus, genetic susceptibility of populations or other binary exposures such as Bacillus Calmette-Guérin (BCG) vaccination status.^{21–23}

The association of higher CRP with worse outcomes may be due to the severity of the disease consistent with the ‘cytokine storm’ theory of COVID-19, where the innate immune system is activated releasing TNF-alpha, IL-6 and IL-1. Elshazli *et al.* found CRP to be a valid biomarker of death from COVID-19 when examining a range of haematological and immunological markers. IL-6 was found

to be most predictive ($OR = 13.87$) of death, and CRP the next best marker ($OR = 7.09$).²⁴ However, IL-6 is not routinely available to clinicians, but being linked to CRP as a trigger for its transcription makes CRP a better candidate tool for front-line hospital usage.²⁵ In the same Elshazli paper, a threshold level of 38.2 mg/L was demonstrated to have the best sensitivity and specificity, which fits well with our findings; this was also found within a recent Cochrane Diagnostic Test Accuracy review.²⁶ In addition, an elevated CRP may not be attributable to COVID-19 alone and may represent concomitant pathology such as secondary bacterial pneumonia. Although co-infection is well known in other viral respiratory illnesses, the rate in COVID-19 has been found to be far less, being present in around 5.9% of the general COVID-19 hospital population and 8.1% of those with critical illness.¹⁸

The data presented here support a single threshold, and whilst there was argument for competing cut-offs of ≥ 40 , ≥ 65 or greater, the single cut-off is consistent with other studies.^{8,24} In addition, it would be clearer and safer to offer a conservative approach using the lower value of CRP, as a higher threshold may falsely reassure clinicians.

There is a need for simple tests to aid clinical management, as the behaviour of CRP in COVID-19 may provide useful immediate risk stratification as to who may have a poor outcome. The threshold of $\text{CRP} \geq 40$ offered a high

Table 2 Performance of different cut-offs/parametrizations of C-reactive protein (CRP) in a Cox model for time to mortality

CRP (mg/L) parametrization	Cohort 1 (Original)			Cohort 2 (Validation)		
	N below cut-off (%)	Harrell's C statistic	AIC	N below cut off (%)	Harrell's C statistic	AIC
Null (CRP not included)	NA	0.6592	5224.41	NA	0.6816	428.58
CRP ≥ 10	132 (8.6%)	0.6697	5174.10	39 (15.2%)	0.6811	430.58
CRP ≥ 15	190 (12.4%)	0.6797	5159.14	56 (21.8%)	0.6995	429.22
CRP ≥ 20	230 (15.0%)	0.6858	5148.08	66 (25.7%)	0.7024	426.59
CRP ≥ 25	279 (18.2%)	0.6930	5144.01	75 (29.2%)	0.7055	427.83
CRP ≥ 30	326 (21.3%)	0.6953	5143.46	83 (32.3%)	0.7044	427.44
CRP ≥ 35	381 (24.9%)	0.6963	5141.06	91 (35.4%)	0.7145	425.61
CRP ≥ 40	439 (28.7%)	0.7024	5136.10	96 (37.4%)	0.7187	424.35
CRP ≥ 45	486 (31.7%)	0.7055	5132.53	103 (40.1%)	0.7015	427.18
CRP ≥ 50	530 (34.6%)	0.7059	5126.61	111 (43.2%)	0.6974	428.68
CRP ≥ 55	569 (37.1%)	0.7025	5130.50	120 (46.7%)	0.6900	428.85
CRP ≥ 60	605 (39.5%)	0.7064	5127.69	125 (48.6%)	0.6926	428.16
CRP ≥ 65	648 (42.3%)	0.7068	5124.45	129 (50.2%)	0.6867	428.47
CRP ≥ 70	687 (44.8%)	0.7033	5131.22	135 (52.5%)	0.6895	428.32
CRP ≥ 75	727 (47.5%)	0.7006	5131.79	139 (54.1%)	0.6879	428.87
CRP ≥ 80	766 (50.0%)	0.7005	5133.82	145 (56.4%)	0.6853	429.49
CRP ≥ 85	804 (52.5%)	0.7021	5135.11	155 (60.3%)	0.6887	429.16
CRP ≥ 90	834 (54.4%)	0.7001	5138.43	161 (62.6%)	0.6816	430.34
CRP ≥ 95	863 (56.3%)	0.6975	5142.08	169 (65.8%)	0.6828	429.98
CRP ≥ 100	887 (57.9%)	0.7010	5137.48	173 (67.3%)	0.6890	429.69
CRP (linear)	NA	0.7040	5024.81	NA	0.6992	426.42
log(CRP)	NA	0.7157	5001.00	NA	0.7014	426.51

Number of cases defined as not elevated CRP.

NA, not available.

negative predictive value, so patients presenting with a low CRP are unlikely to exhibit disease progression, and high sensitivity analysis which might lead to opening discussions with patients and their carers about the possible course of the disease. This may assist with early resource planning around the potential for critical care support, and may help guide rapid safe discharge from acute hospitals.⁵ Although the results within this paper give a population-based cut-off, any interpretation and management plan must be made on an individual patient basis, with clinicians using CRP in context of clinical history, examination and investigation and noting that the threshold offered a low positive predictive value. Beyond clinical predictive value, this model may be useful for monitoring the outcomes of treatments, for example in a trial of tocilizumab, CRP monitoring was used as a marker of efficacy.²⁶

Strengths and limitations

This was a large study that included participants admitted to 13 hospital sites. The demographics, case mix and

mortality are similar to other larger studies reported within the UK, increasing the findings' generalizability.²⁰ We have also shown good replication between the two UK-wide cohorts. However, caution should be given to the threshold reported for CRP, as studies identifying optimal cut-offs may be subject to selection bias and may not be replicable.²⁷ Using a threshold of ≥ 40 offered a high sensitivity and negative predictive value but low positive predictive value.

A limitation of this study is that due to the urgent nature of research data collection in a pandemic, disease severity on admission was only assessed using CRP without collection of circulating lymphocytes, interleukin-6, procalcitonin, serum lactate and viral load, all of which may also contribute to disease severity.²⁸

Interpretation

A simple threshold ≥ 40 mg/L should be used within clinical practice to guide disease severity and likely disease progression. Future studies should analyse using this simple threshold.

Table 3 Bootstrapped differences in model performance of Cox model for time to mortality for different C-reactive protein (CRP) parameterizations using Cohort 1 (Original Cohort)

Model comparison	Difference in	Coefficient	Bias	Standard error	95% CI	
≥ 10 compared with ≥ 40	Harrell's C statistic	-0.033	0.003	0.007	-0.044	-0.016
	AIC ⁺	38.002	-0.326	12.591	14.250	64.258
$\geq 65^a$ compared with ≥ 40	Harrell's C statistic	0.004	0.002	0.007	-0.006	0.020
	AIC	-11.655	0.260	11.400	-32.978	11.775
Linear CRP compared with ≥ 40	Harrell's C statistic	0.002	0.003	0.008	-0.010	0.020
	AIC	-111.289	102.784	15.212	-41.031	19.531
$\text{Ln}_{(\text{CRP})}$ compared with ≥ 40	Harrell's C statistic	0.013	0.002	0.006	0.004	0.028
	AIC	-135.105	-0.857	37.105	-210.386	-65.123
≥ 10 compared with $\geq 65^a$	Harrell's C statistic	-0.037	0.001	0.010	-0.058	-0.018
	AIC	49.657	-0.585	15.262	21.293	79.554
Linear CRP compared with $\geq 65^a$	Harrell's C statistic	-0.003	0.001	0.007	-0.016	0.012
	AIC	-99.633	102.470	13.781	-25.825	29.435
$\text{Log}_{(\text{CRP})}$ compared with $\geq 65^a$	Harrell's C statistic	0.009	0.000	0.006	-0.002	0.021
	AIC	-123.450	-1.117	36.286	-197.611	-55.831
Linear CRP compared with ≥ 10	Harrell's C statistic	0.034	0.000	0.010	0.018	0.056
	AIC	-149.291	103.429	15.581	-77.820	-18.453
$\text{Log}_{(\text{CRP})}$ compared with ≥ 10	Harrell's C statistic	0.046	-0.001	0.009	0.028	0.063
	AIC	-173.107	-0.531	38.325	-253.435	-99.153
$\text{Log}_{(\text{CRP})}$ compared with Linear CRP	Harrell's C statistic	0.012	-0.001	0.004	0.003	0.019
	AIC	-23.816	0.618	9.527	-41.730	-4.322

^aA threshold of ≥ 65 has been included as a comparison with ≥ 40 .

Generalizability

The impact of these findings support the routine assessment of serum CRP as an adjunct in the early diagnosis and assessment of illness severity of hospitalized patients with COVID-19. We recommend that CRP ≥ 40 mg/L on admission may indicate an increased risk of disease progression and death, and warrants an enhanced level of discussion and clinical support.

Conclusions

We have demonstrated that CRP follows a bimodal distribution in hospitalized patients with COVID-19. This requires further exploration to discover the latent class effect of unobserved factors influencing the distribution of CRP. A CRP of ≥ 40 mg/L on admission to hospital should be seen as a reliable indicator of disease severity and increased risk of death. We recommend clinicians use this cut-off as a prognostic indicator only, in conjunction with an individualized clinical assessment, frailty assessment and incorporating a person's wishes and values, to make early decisions about enhanced observation, critical care support and advanced care planning.

Supplementary data

Supplementary data are available at *IJE* online.

Data availability

Data are available on request from the corresponding author after submission of a statistical analysis plan, after approval from the COPE Study Investigators.

Funding

This study received no specific funding. The study was partially supported through the NIHR Maudsley Biomedical Research Centre at the South London and Maudsley NHS Foundation Trust in partnership with King's College London (B.C.).

Cope Study Collaborators

Aberdeen University: Dr Eilidh Bruce, Dr Alice Einarsson; Glasgow Royal Infirmary: Dr Aine McGovern; Inverclyde Royal Infirmary: Carly Bisset, Ross Alexander; Italy (University Hospital of Modena Policlinico): Professor Giovanni Guaraldi; King's College London: Caroline Murphy, Joanna Kelly, Dr Roxanna Short; North Bristol Trust: Tarik El Jichi Mutasem, Sandeep Singh, Dolcie Paxton, Will Harris, Dr James Hesford, Dr Mark Holloway, Dr Emma Mitchel, Dr Frances Rickard; Royal Alexandra Hospital, Paisley: Norman Galbraith, Emma Bhatti, Jenny Edwards, Siobhan Duffy, Dr Fenella Barlow-Pay; Salford Royal Infirmary: Madeline Garcia, Shefali Sangani, Thomas Kneen, Thomas Lee, Angeline Price;

Ysbyt Yystad Fawr: Dr Charlotte Davey, Ms Sheila Jones, Kiah Lunstone, Alice Cavenagh, Charlotte Silver, Thomas Telford, Rebecca Simmons.

Author contributions

Concept of the study (B.C., P.B.); developed the protocol (B.C., D.S., P.B.); collected the data (P.B., P.M., L.E., J.C., V.A., T.Q., A.V., M.S., L.P., J.H., S.M., K.Mc.); analysed the data (D.S., B.C.); interpreted the findings (D.S., B.C., P.B.); drafted the initial manuscript (D.S., P.B., B.C.); all authors approved the final manuscript. B.C. is the guarantor of the study findings.

Conflict of interest

None declared.

References

- Chen N, Zhou M, Dong X et al. Epidemiological and clinical characteristics of 99 cases of 2019 novel coronavirus pneumonia in Wuhan, China: a descriptive study. *Lancet* 2020;395:507–13.
- Liu F, Li L, Xu M et al. Prognostic value of interleukin-6, C-reactive protein, and procalcitonin in patients with COVID-19. *J Clin Virol* 2020;127:104370.
- Pepys MB, Hirschfield GM. C-reactive protein: a critical update. *J Clin Invest* 2003;111:1805–12.
- Haran JP, Beaudoin FL, Suner S, Lu S. C-reactive protein as predictor of bacterial infection among patients with an influenza-like illness. *Am J Emerg Med* 2013;31:137–44.
- Li Q, Ding X, Xia G et al. Eosinopenia and elevated C-reactive protein facilitate triage of COVID-19 patients in fever clinic: a retrospective case-control study. *EclinMed* 2020;23:100375.
- Gupta RK, Michael Marks M, Samuels THA et al. Systematic evaluation and external validation of 22 prognostic models among hospitalized adults with COVID-19: An observational cohort study. *Eur Respir J* 2020;56:2003498.
- Osuafor CN, Davidson C, Mackett AJ. Clinical features and inpatient trajectories of older inpatients with COVID-19: a retrospective observational study. *Geriatrics (Basel)* 2020;6:1.
- Chen W, Zheng KI, Liu S, Yan Z, Xu C, Qiao Z. Plasma CRP level is positively associated with the severity of COVID-19. *Am Clin Microbiol Antimicrob* 2020;19:18.
- Herold T, Jurinovic V, Arnreich C et al. Elevated levels of IL-6 and CRP predict the need for mechanical ventilation in COVID-19. *J Allergy Clin Immunol* 2020;146:128–36.e4.
- Hamer M, Gale CR, Kivimäki M, Batty GD. Overweight, obesity, and risk of hospitalization for COVID-19: A community-based cohort study of adults in the United Kingdom. *Proc Natl Acad Sci U SA* 2020;117:21011–13.
- Shang W, Dong J, Ren Y et al. The value of clinical parameters in predicting the severity of COVID-19. *J Med Virol* 2020;92: 2188–92.
- Elm E, von Altman DG, Egger M et al.; for the STROBE Initiative. The Strengthening the Reporting of Observational Studies in Epidemiology (STROBE) statement: guidelines for reporting observational studies. *PLoS Med* 2007;4:e296.
- Hewitt J, Carter B, Vilches-Moraga A et al. The effect of frailty on survival in patients with COVID-19 (COPE): a multicentre, European, observational cohort study. *Lancet Public Health* 2020. [https://www.thelancet.com/journals/lanpub/article/PIIS2468-2667\(20\)30146-8/abstract](https://www.thelancet.com/journals/lanpub/article/PIIS2468-2667(20)30146-8/abstract) (9 July 2020, date last accessed).
- Price A, Barlow-Pay F, Duffy S et al. A study protocol for COPE study: COVID-19 in Older PEople – the influence of frailty and multimorbidity on survival. A multi-centre, European observational study. *BMJ Open* 2020;10:e040569.
- Harrell FE, Calif RM, Pryor DB, Lee KL, Rosati RA. Evaluating the yield of medical tests. *JAMA* 1982;247:2543–46.
- Akaike H. A new look at the statistical model identification. *IEEE Trans Automat Contr* 1974;19:716–23.
- Ali N. Elevated level of C-reactive protein may be an early marker to predict risk for severity of COVID-19. *J Med Virol* 2020;92:2409–11.
- Langford BJ, So M, Raybardhan S et al. Bacterial co-infection and secondary infection in patients with COVID-19: a living rapid review and meta-analysis. *Clin Microbiol Infect* 2020. [https://www.clinicalmicrobiologyandinfection.com/article/S1198-743X\(20\)30423-7/abstract](https://www.clinicalmicrobiologyandinfection.com/article/S1198-743X(20)30423-7/abstract) (1 September 2020, date last accessed).
- Vasileva D, Badawi A. C-reactive protein as a biomarker of severe H1N1 influenza. *Inflamm Res* 2019;68:39–46.
- Docherty AB, Harrison EM, Green CA et al. Features of 20 133 UK patients in hospital with covid-19 using the ISARIC WHO Clinical Characterisation Protocol: prospective observational cohort study. *BMJ* 2020. <https://www.bmjjournals.org/content/369/bmj.m1985> (1 September 2020, date last accessed).
- Wu T-L, Tsao K-C, Chang CP-Y, Li C-N, Sun C-F, Wu JT. Development of ELISA on microplate for serum C-reactive protein and establishment of age-dependent normal reference range. *Clin Chim Acta* 2002;322:163–68.
- Ferreira GD, Simões JA, Senaratna C et al. Physiological markers and multimorbidity. *J Comorb* 2018;8:2235042X1880698.
- Toyoshima Y, Nemoto K, Matsumoto S, Nakamura Y, Kiyotani K. SARS-CoV-2 genomic variations associated with mortality rate of COVID-19. *J Hum Genet* 2020;65:1075–78.
- Elshazli RM, Toraih EA, Elgaml A et al. Diagnostic and prognostic value of hematological and immunological markers in COVID-19 infection: a meta-analysis of 6320 patients. *PloS One* 2020;15:e0238160.
- Markanday A. Acute phase reactants in infections: evidence-based review and a guide for clinicians. *Open Forum Infect Dis* 2015;2. <https://www.ncbi.nlm.nih.gov/pmc/articles/PMC4525013/> (16 September 2020, date last accessed).
- Luo P, Liu Y, Qiu L, Liu X, Liu D, Li J. Tocilizumab treatment in COVID-19: a single center experience. *J Med Virol* 2020;92: 814–18.
- Hölländer N, Sauerbrei W, Schumacher M. Confidence intervals for the effect of a prognostic factor after selection of an ‘optimal’ cutpoint. *Stat Med* 2004;23:1701–13.
- Tan L, Kang X, Ji X et al. Validation of predictors of disease severity and outcomes in COVID-19 patients: a descriptive and retrospective study. *Med N Y N* 2020. <https://www.ncbi.nlm.nih.gov/pmc/articles/PMC7235581/> (18 September 2020, date last accessed).



COVID-19

The role of C-reactive protein as a prognostic marker in COVID-19

Dominic Stringer,¹ Philip Braude,² Phyto K Myint,³ Louis Evans,⁴ Jemima T Collins,⁵ Alessia Verduri,⁶ Terry J Quinn,⁷ Arturo Vilches-Moraga,⁸ Michael J Stechman,⁹ Lyndsay Pearce,¹⁰ Susan Moug,¹¹ Kathryn McCarthy,¹² Jonathan Hewitt¹³ and Ben Carter^{1*}; COPE Study Collaborators

¹Department of Biostatistics and Health Informatics, Institute of Psychiatry, Psychology & Neuroscience, King's College London, London, UK, ²North Bristol NHS Trust, UK, ³Institute of Applied Health Sciences, University of Aberdeen, ⁴Ysbyty Gwynedd, Bangor, ⁵Ysbyty Ystrad Fawr, Aneurin Bevan University Health Board, ⁶Hospital of Modena Policlinico, Italy, ⁷Institute of Cardiovascular and Medical Sciences, University of Glasgow, ⁸Department of Ageing and Complex Medicine, Salford Royal NHS Foundation Trust, Salford, University of Manchester, Manchester, UK, ⁹Department of Surgery, University Hospital of Wales, Cardiff, ¹⁰Department of Colorectal Surgery, Salford Royal NHS Foundation Trust, Manchester, UK, ¹¹Department of Surgery, Royal Alexandra Hospital, Paisley, UK, ¹²Department of Surgery, North Bristol NHS Trust, Bristol, UK, and ¹³Cardiff University and Aneurin Bevan University Health Board

*Corresponding author. Department of Biostatistics and Health Informatics, Institute of Psychiatry, Psychology & Neuroscience, King's College, London, De Crespigny Park, London SE5 8AF, UK. E-mail: ben.carter@kcl.ac.uk

Received 22 October 2020; Editorial decision 8 January 2021; Accepted 25 January 2021

Abstract

Background: C-reactive protein (CRP) is a non-specific acute phase reactant elevated in infection or inflammation. Higher levels indicate more severe infection and have been used as an indicator of COVID-19 disease severity. However, the evidence for CRP as a prognostic marker is yet to be determined. The aim of this study is to examine the CRP response in patients hospitalized with COVID-19 and to determine the utility of CRP on admission for predicting inpatient mortality.

Methods: Data were collected between 27 February and 10 June 2020, incorporating two cohorts: the COPE (COVID-19 in Older People) study of 1564 adult patients with a diagnosis of COVID-19 admitted to 11 hospital sites (test cohort) and a later validation cohort of 271 patients. Admission CRP was investigated, and finite mixture models were fit to assess the likely underlying distribution. Further, different prognostic thresholds of CRP were analysed in a time-to-mortality Cox regression to determine a cut-off. Bootstrapping was used to compare model performance [Harrell's C statistic and Akaike information criterion (AIC)].

Results: The test and validation cohort distribution of CRP was not affected by age, and mixture models indicated a bimodal distribution. A threshold cut-off of CRP ≥ 40 mg/L performed well to predict mortality (and performed similarly to treating CRP as a linear variable).

Conclusions: The distributional characteristics of CRP indicated an optimal cut-off of ≥ 40 mg/L was associated with mortality. This threshold may assist clinicians in using CRP as an early trigger for enhanced observation, treatment decisions and advanced care planning.

Key words: CRP, COVID-19, bimodal, trimodal, mortality, prognostic marker, mixture model

Key Messages

- C-reactive protein (CRP) has been used inconsistently both in patient management and as a prognostic marker during COVID-19.
- Admission elevated CRP for patients with COVID-19 was associated with increased inpatient mortality and was indicative of disease severity at admission.
- The distribution of CRP at admission was found to be bimodally distributed, and a CRP ≥ 40 mg/L was the optimal threshold of increased risk of mortality.
- Admission CRP ≥ 40 mg/L may be used by treating clinicians as an early warning for enhanced care and patient-centred decision making.

Introduction

Elevated levels of serum C-reactive protein (CRP) have been observed in patients with COVID-19 and used to assist with triage, diagnostics and prognostication.^{1,2} CRP is a non-specific acute phase protein that is produced by hepatocytes and elevated in acute infection or inflammation.³ Secretion begins 4–10 h after an inflammatory insult and peaks at 48 h, with a short half-life of 19 h. Crucially, it may be elevated before a patients' vital signs are affected or leukocytes are raised.³ The profile of this biomarker has made CRP useful and routinely available in clinical medicine for diagnostics.

CRP can be used to assist with differentiation between viral and bacterial infections, for example, influenza produces a mean CRP level of 25.65 mg/L [95% confidence interval (CI) 18.88 to 32.41 mg/L] versus bacterial pneumonia which produces a mean CRP level of 135.96 mg/L (95% CI 99.38 to 172.54 mg/L).⁴ In COVID-19, a CRP level of ≥ 4 mg/L has been shown to be useful for triaging suspected cases when comparing polymerase chain reaction (PCR)-positive patients versus negative controls who have presented to a fever clinic with respiratory symptoms or a high temperature [odds ratio (OR) 4.75; 95% CI 3.28 to 6.88].⁵

However, debate remains over the utility of CRP as a prognostic marker for patients admitted to hospital with COVID-19. In a recent systematic review, 10 of the 22 included COVID-19 prognostic models treated CRP either as a factor or covariate.⁶ Most these studies used CRP with a binary threshold; proposed values to predict inpatient mortality varied from ≥ 10 mg/L to ≥ 76 mg/L. In addition to a binary threshold, CRP has been examined in a trichotomized model with the

two thresholds at ≥ 40 mg/L and ≥ 100 mg/L.⁷ A lower cut-off of ≥ 20.44 mg/L was used as a threshold for related lung injury,⁸ and >32.5 mg/L was found to offer 80% predictive power for a person needing mechanical ventilation.⁹ The studies adjusted for admission CRP as a covariate to account for baseline disease severity have assumed a linear or natural logarithm transformation [$\ln(\text{CRP})$] relationship with outcome.^{10,11} Although using CRP in a continuous manner may offer an improved understanding of the contribution of CRP within each analysis, it does not allow CRP to be used by clinical teams to guide management of patients with COVID-19.

Whilst CRP has been argued as an important marker of disease progression in COVID-19,⁶ its distribution has never been explored to understand whether distinct patterns exist in a heterogeneous population. The use of CRP as a biomarker in COVID-19 may present a quick and accessible tool in clinical management, trigger longer periods of enhanced observation, provide information around likely disease progression and assist with early therapeutic, ventilation and palliative care discussions.

The aim of this study is to examine the distribution of CRP at hospital admission, and objectives are to: (i) assess CRP as a prognostic bimodal or trimodal distribution; (ii) propose and compare the categorization of CRP as a prognostic marker to either a linear or a log-linear measure of CRP.

Methods

Permission to conduct this study was granted in the UK by the Health Research Authority (20/HRA/1898) and in Italy by the ethics committee of University Hospital of Modena

Policlinico (369/2020/OSS/AOUMO). Written consent was not required from participants as per ethical review.

Study design

This observational study used two cohorts at different time points to examine the contribution of CRP to clinical outcomes. This study has been reported in accordance with the STROBE statement.¹²

Settings

Thirteen hospital sites participated, 12 from the UK and one from Italy. All were acute hospitals directly admitting patients with suspected or confirmed COVID-19.

Participants

Original cohort (cohort 1)

Participants in Cohort 1 were included as part of the COPE study (COVID in Older People study) as reported in the paper by Hewitt *et al.*^{13,14} Briefly, this was a European multicentre observational study recruiting 1564 hospitalized adults between 27 February and 28 April 2020 with either SARS-CoV-2 viral polymerase chain reaction (PCR) confirmed disease (95.9%) or clinically diagnosed (4.1%) COVID-19. Any patient aged 18 years or older admitted to the participating hospitals with a diagnosis of COVID-19 was included. The study found frailty was associated with longer hospital stay, and a better predictor of mortality as an inpatient, and at Day 7, than age or comorbidity alone.

Validation cohort (cohort 2)

Cohort 2 consisted of an additional 271 patients recruited between 29 April and 10 June 2020 from a combination of six of Cohort 1's hospitals plus two additional recruiting hospitals. All patients were SARS-CoV-2 viral PCR-positive.

Variables

A prognostic threshold for CRP was needed within the COPE protocol (March 2020). The limited literature available early in the pandemic included a case series of 73 patients with COVID-19 presenting with a mean CRP level of 51.4 mg/L [standard deviation (SD) 41.8].¹ Based on this paper, and proposed by the clinical experience of the authors who delivered acute care, a dichotomous threshold was chosen with <40 mg/L (lower admission CRP), and ≥40 mg/L (CRP-elevated, indicating increased disease severity¹⁴).

Data sources

CRP was measured at hospital admission and transcribed from patients' medical records. There was no attempt to standardize the CRP assay between sites. A standardized case reporting form was used for all hospital sites. Data were transferred to King's College London in anonymous format for statistical analysis.

Graphical data analysis

Using the test cohort, the distribution of CRP was examined graphically and stratified by age. Finite bivariate and trivariate Gaussian mixture models were fit to CRP, representing two and three latent classes, respectively. The theoretical distribution from these models was compared with the empirical data and the threshold between the two and three classes was examined. The normality assumptions were assessed visually.

Statistical analysis

Primary analysis: mixture modelling analysis

The empirical data from the test cohort were fit to a Gaussian mixture model with one, two or three components using an expectation-maximization algorithm (to refine the starting values) then maximum likelihood estimation (Stata routine '*fmm*'). The models were compared using the Akaike information criterion (AIC) and the thresholds were determined by the posterior probability of belonging to the two or three class models.

Secondary analysis: prognostic modelling analysis

To assess differing thresholds for CRP as a prognostic factor of outcome, a series of mixed-effects multivariable Cox proportional hazards models for time to mortality were fit, in a method consistent with the COPE study primary analysis.¹³ The model was adjusted for elevated CRP using a level of ≥40 mg/L, in addition to: patient age group (<65, 65–79, ≥80 years old), sex, diabetes (yes/no), hypertension (yes/no), coronary artery disease (yes/no) and kidney disease [estimated glomerular filtration rate (eGFR) <60 ml/min/1.73m²]. Dichotomized thresholds of CRP were compared within a range of 10 mg/L to 100 mg/L in 5-mg/L intervals (≥ 10 mg/L, ≥ 15 mg/L, etc). Model performance was evaluated and compared using Harrell's C and the AIC.¹⁵ We compared the dichotomized thresholds against linear CRP and $\ln(\text{CRP})$ (as CRP is known to be skewed) as benchmarks of performance. This method was chosen as dichotomizing results can lead to a loss of information, resulting in a lower predictive power compared with using a continuous measure.¹⁶ Bootstrapping was

used to construct 95% percent confidence intervals for differences in model performance between the best-fitting models. Bootstrapping was stratified by site with 1000 replications for each comparison. A complete case analysis was used in all cases due to negligible missing data (<4%).

Validation cohort (cohort 2)

To provide an indication of whether the original results from Cohort 1 were likely to be replicable to a wider group of patients with COVID-19, the analysis was repeated on an independent validation sample (Cohort 2). Using the validation cohort, two-class and three-class mixture models were estimated using the empirical data without restriction. On evidence of overfitting, to assess the additional benefit of a very elevated category for CRP, the validation cohort was fitted using a three-class mixture model, with the class-two mean fixed using the validation cohort two-class mixture model mean.

Comparison of the prognostic effect of CRP

Using a mixed-effect multivariable Cox regression, the effect of elevated CRP will be reported using a adjusted hazards ratio (aHR), alongside the respective 95% confidence interval (95% CI), for a linear CRP, $\ln(\text{CRP})$.

Results

The study included 1835 patients across Cohorts 1 and 2, who were drawn from 12 hospitals in the UK and one from Italy. Of the total study participants, 26.4% ($n=484$) died in-hospital, varying between sites from 13.3% to 42.9%. A comparison for those who died in hospital was carried out in [Table 1](#), split into Cohort 1 ($n=1564$) and Cohort 2 ($n=271$). In Cohort 1, 27.2% died and the median CRP level for those who died was 115 mg/L (interquartile range: 63 mg/L–191 mg/L) compared with 69 mg/L (29 mg/L–140 mg/L) among those who survived. For patients with $\text{CRP} \geq 40 \text{ mg/L}$, mortality was 31.9% compared with 15.0% for patients with $\text{CRP} < 40 \text{ mg/L}$. Median follow-up time (time to mortality or discharge) was 13 days (6–22 days).

Cohort 2 experienced 21.8% mortality. Among those who died, median CRP level was 86 mg/L (48 mg/L–173.5 mg/L) compared with 53 mg/L (16 mg/L–109 mg/L) among those who survived. For patients with $\text{CRP} \geq 40 \text{ mg/L}$, mortality was 28.6% compared with 10.4% for patients with $\text{CRP} < 40 \text{ mg/L}$. The median follow-up time (time to death or discharge) was 10 days (5–18 days).

Results of cohort 1 ($n = 1564$)

Distribution of CRP

On graphical examination of the distribution of $\ln(\text{CRP})$, it exhibited negative skew, with two ‘peaks’ suggestive of a bimodal distribution, see [Figure 1](#), Plot (i), and [Figure S1](#), available as [Supplementary data](#) at *IJE* online, Plots (i, ii). The distribution of $\ln(\text{CRP})$ was observed in age-stratified groups of <65, 65–79, and ≥80 years. On inspection, there was no difference between the distribution age-stratified or the complete dataset.

Primary analysis: mixture modelling analysis

Following the two suggested peaks in the examination of the $\ln(\text{CRP})$ distribution, a two-latent class finite mixture model was fitted. It appeared to graphically fit the data when examined against the empirical distribution in [Figure 1](#), Plot (i). This was supported by a comparison with the one-class (or null) model, which displayed a higher AIC (4739 compared with 4524). The simple threshold at which the predicted probability of belonging to a two-class model being greater than one-class was 38 mg/L. This will be implemented as $\geq 40 \text{ mg/L}$ herein, to account for the imprecision of the measurement of CRP and also for ease of recall in a busy clinical setting.

The three-class finite mixture model fit slightly better than the two-class finite mixture model (AIC of 4484), with probability of class-one membership highest between range 0–14 mg/L, class-two between 15–120 mg/L and class-three for values of $\text{CRP} \geq 120 \text{ mg/L}$, see [Figure 1](#), Plot (iii).

The primary analysis proposed a single optimal threshold of $\text{CRP} \geq 40 \text{ mg/L}$ to indicate elevated CRP.

Secondary analysis: prognostic modelling

The time-to-mortality analysis included 1502 participants (96%) in the complete case population. A cut-off of $\geq 65 \text{ mg/L}$ appeared to fit best in the sample on all measures (Harrell’s C statistic of 0.7068, AIC of 5124) ([Table 2](#)) after fitting different binary categorizations of CRP in a Cox model for time to mortality. Differences in measures of goodness of fit were small, especially between cut-offs in the range of $\geq 40 \text{ mg/L}$ to $\geq 90 \text{ mg/L}$. CRP as a continuous $\ln(\text{CRP})$ measure performed considerably better (Harrell’s C statistic of 0.7157, AIC of 5001) and with little improvement on this using a linear scale (Harrell’s C statistic of 0.7040, AIC of 5024). Regarding bootstrapped differences in the measures of goodness of fit between a cut-off of $\geq 40 \text{ mg/L}$ and the marginally better performing cut-off of $\geq 65 \text{ mg/L}$, no difference in performance was

Table 1 Descriptive characteristics for Cohort 1 and 2 samples with comparison by in-hospital mortality

	Cohort 1 (Original)			Cohort 2 (Validation)		
	All patients (n = 1564)	Dead (n = 425)	Alive (n = 1139)	All patients (n = 271)	Dead (n = 59)	Alive (n = 212)
Sites						
Hospital A	115 (7.4%)	15 (13.0%)	100 (87.0%)	25 (9.2%)	4 (16.0%)	21 (84.0%)
Hospital B	50 (3.2%)	14 (28.0%)	36 (72.0%)	0 (0%)	0 (0%)	0 (0%)
Hospital C	153 (9.8%)	34 (22.2%)	119 (77.8%)	0 (0%)	0 (0%)	0 (0%)
Hospital D	43 (2.7%)	10 (23.3%)	33 (76.7%)	9 (3.3%)	0 (0.0%)	9 (100.0%)
Hospital E	123 (7.9%)	15 (12.2%)	108 (87.8%)	58 (21.4%)	9 (15.5%)	49 (84.5%)
Hospital F	154 (9.8%)	23 (14.9%)	131 (85.1%)	15 (5.5%)	4 (26.7%)	11 (73.3%)
Hospital G	112 (7.2%)	36 (32.1%)	76 (67.9%)	0 (0%)	0 (0%)	0 (0%)
Hospital H	246 (15.7%)	108 (43.9%)	138 (56.1%)	0 (0%)	0 (0%)	0 (0%)
Hospital I	380 (24.3%)	126 (33.2%)	254 (66.8%)	62 (22.9%)	12 (19.4%)	50 (80.7%)
Hospital J	179 (11.5%)	43 (24.0%)	136 (76.0%)	13 (4.8%)	3 (23.1%)	10 (76.9%)
Hospital K	9 (0.6%)	1 (11.1%)	8 (88.9%)	4 (1.5%)	1 (25.0%)	3 (75.0%)
Hospital L	0 (0%)	0 (0%)	0 (0%)	57 (21.0%)	14 (24.6%)	43 (75.4%)
Hospital M	0 (0%)	0 (0%)	0 (0%)	28 (10.3%)	12 (42.9%)	16 (57.1%)
Age, years						
<65	488 (31.2%)	55 (11.3%)	433 (88.7%)	61 (22.5%)	6 (9.8%)	55 (90.2%)
65–79	535 (34.2%)	168 (31.4%)	367 (68.6%)	85 (31.4%)	14 (16.5%)	71 (83.5%)
≥80	541 (34.6%)	202 (37.3%)	339 (62.7%)	124 (45.8%)	38 (30.7%)	86 (69.4%)
Missing	0 (0.0%)	0 (0.0%)	0 (0.0%)	1 (0.4%)	1 (100.0%)	0 (0.0%)
Sex						
Female	661 (42.3%)	170 (25.7%)	491 (74.3%)	134 (49.5%)	29 (21.6%)	105 (78.4%)
Male	903 (57.7%)	255 (28.2%)	648 (71.8%)	136 (50.2%)	30 (22.1%)	106 (77.9%)
Missing	0 (0%)	0 (0%)	0 (0%)	0 (0%)	0 (0%)	1 (100.0%)
Smoking status						
Never smokers	814 (52.0%)	205 (25.2%)	609 (74.8%)	132 (48.7%)	24 (18.2%)	108 (81.8%)
Ex-smokers	603 (38.6%)	185 (30.7%)	418 (69.3%)	91 (33.6%)	25 (27.5%)	66 (72.5%)
Current smokers	121 (7.7%)	26 (21.5%)	95 (78.5%)	18 (6.6%)	2 (11.1%)	16 (88.9%)
Missing	26 (1.7%)	9 (34.6%)	17 (65.4%)	30 (11.1%)	8 (26.7%)	22 (73.3%)
Diabetes						
No	1144 (73.1%)	295 (25.8%)	849 (74.2%)	204 (75.3%)	41 (20.1%)	163 (79.9%)
Yes	415 (26.5%)	128 (30.8%)	287 (69.2%)	66 (24.4%)	18 (27.3%)	48 (72.7%)
Missing	5 (0.3%)	2 (40.0%)	3 (60.0%)	1 (0.4%)	0 (0.0%)	1 (100.0%)
Hypertension						
No	755 (48.3%)	184 (24.4%)	571 (75.6%)	126 (46.5%)	22 (17.5%)	104 (82.5%)
Yes	804 (51.4%)	238 (29.6%)	566 (70.4%)	145 (53.5%)	37 (25.5%)	108 (74.5%)
Missing	5 (0.3%)	3 (60.0%)	2 (40.0%)	0 (0%)	0 (0%)	0 (0%)
Coronary artery disease						
No	1214 (77.6%)	290 (23.9%)	924 (76.1%)	220 (81.8%)	43 (19.6%)	177 (80.5%)
Yes	345 (22.1%)	132 (38.3%)	213 (61.7%)	51 (18.8%)	16 (31.4%)	35 (68.6%)
Missing	5 (0.3%)	3 (60.0%)	2 (40.0%)	0 (0%)	0 (0%)	0 (0%)
Increased C-reactive protein (≥40 mg/L)						
No	439 (28.1%)	66 (15.0%)	373 (85.0%)	96 (35.4%)	10 (10.4%)	86 (89.6%)
Yes	1125 (71.9%)	359 (31.9%)	766 (68.1%)	161 (59.4%)	46 (28.6%)	115 (71.4%)
Missing	32 (2.0%)	12 (37.5%)	20 (62.5%)	14 (5.2%)	3 (21.4%)	11 (78.6%)
Impaired renal function (eGFR^a <60 mL/min per 1.73 m²)						
No	980 (63.7%)	202 (20.6%)	778 (79.4%)	132 (48.7%)	20 (15.2%)	112 (84.9%)
Yes	570 (36.4%)	217 (38.1%)	353 (61.9%)	81 (29.9%)	25 (30.9%)	56 (69.1%)
Missing	14 (0.9%)	6 (42.9%)	8 (57.1%)	58 (21.4%)	14 (24.1%)	44 (75.9%)
Clinical Frailty Scale (1–9)						
1: Very fit	91 (5.8%)	7 (7.7%)	84 (92.3%)	11 (4.1%)	1 (9.1%)	10 (90.9%)
2: Fit	197 (12.6%)	22 (11.2%)	175 (88.8%)	22 (8.1%)	1 (4.6%)	21 (95.5%)

Downloaded from https://academic.oup.com/ije/article/50/2/420/6156754 by guest on 25 May 2021

(Continued)

Table 1 Continued

	Cohort 1 (Original)			Cohort 2 (Validation)		
	All patients (n = 1564)	Dead (n = 425)	Alive (n = 1139)	All patients (n = 271)	Dead (n = 59)	Alive (n = 212)
3: Managing well	287 (18.4%)	55 (19.2%)	232 (80.8%)	37 (13.7%)	7 (18.9%)	30 (81.1%)
4: Vulnerable	185 (11.8%)	52 (28.1%)	133 (71.9%)	25 (9.2%)	5 (20.0%)	20 (80.0%)
5: Mildly frail	182 (11.6%)	50 (27.5%)	132 (72.5%)	38 (14.0%)	6 (15.8%)	32 (84.2%)
6: Moderately frail	251 (16.0%)	84 (33.5%)	167 (66.5%)	51 (18.8%)	11 (21.6%)	40 (78.4%)
7: Severely frail	260 (16.6%)	96 (36.9%)	164 (63.1%)	61 (22.5%)	20 (32.8%)	41 (67.2%)
8: Very severely frail	79 (5.1%)	44 (55.7%)	35 (44.3%)	5 (1.9%)	3 (60.0%)	2 (40.0%)
9: Terminally ill	27 (1.7%)	12 (44.4%)	15 (55.6%)	4 (1.5%)	1 (25.0%)	3 (75.0%)
Missing	5 (0.3%)	3 (60.0%)	2 (40.0%)	17 (6.3%)	4 (23.5%)	13 (76.5%)
Median CRP ^b (mg/L) (lower and upper quartile)	80.5 (36–154)	115 (63–191)	69 (29–140)	65 (20–117)	86 (48–173.5)	53 (16–109)

^aEstimated glomerular filtration rate.^bC-reactive protein.

seen with 95% CI for all measures (Table 3). There was evidence that cut-offs of both ≥ 40 mg/L and ≥ 65 mg/L outperformed a cut-off of ≥ 10 mg/L, the upper limit of the normal range for CRP.¹⁷ It should be noted that $\text{Ln}(\text{CRP})$ was the optimal parameterization compared with either ≥ 40 mg/L (-135.1 AIC, bootstrapped 95% CI -210.4 to -65.1) or ≥ 65 mg/L (-123.5 AIC, bootstrapped 95% CI -197.6 to -55.8).

Results of cohort 2 (n = 271)

Distribution of CRP

Cohort 2 included 271 new patients from eight hospital sites: 85 (31.4%) were fully independent, recruited from two new hospital sites; 186 were pseudo-independent, being newly recruited patients from original hospital sites in Cohort 1. There was no difference in the demographics, comorbidities and distribution of CRP seen in Cohort 2 and Cohort 1 (Table 1).

Fitting finite mixture models

The empirical distribution of the Cohort 2 $\text{Ln}(\text{CRP})$ appeared, graphically, to have a reasonably similar pattern to Cohort 1, see Figure 1, Plot (ii). The two-class finite mixture model gave a consistent threshold (CRP ≥ 41 mg/L). The unrestricted three-class finite mixture model exhibited likely overfitting to the data on examination of the distributions. Inconclusive evidence for the additional second cut-off was found with the class three distribution entirely contained within class two, with a large variance. There was no additional benefit for fixing the central distribution mean and allowing the mixture proportion to vary, but this can be seen graphically in Figure 1, Plot (iv). The

simple threshold between class one and class two was ≥ 41 mg/L.

The time-to-mortality analysis included 208 of the participants (77%) with complete data. Fitting different binary categorizations of CRP in a Cox model for time to mortality gave a CRP cut-off of ≥ 40 mg/L as the best fitting model (Harrell's C statistic of 0.7187, AIC of 424), outperforming the $\text{Ln}(\text{CRP})$ model (Harrell's C statistic of 0.7014, AIC of 427), see Table 2. There was no evidence of difference in performance between cut-offs of ≥ 65 mg/L and ≥ 40 mg/L, nor between ≥ 40 mg/L and $\text{Ln}(\text{CRP})$ on examination of bootstrapped 95% CI in Supplementary Table S1, available as Supplementary data at IJE online.

The prognostic effect of elevated CRP with prognostic properties

The aHRs for CRP ≥ 40 mg/L were 2.58 (95% CI 1.95 to 3.41) and 2.61 (95% CI 0.54 to 4.63) for Cohorts 1 and 2 and the estimate of CRP appeared stable (Supplementary Table S2, available as Supplementary data at IJE online). For comparison CRP ≥ 65 mg/L, the aHR was consistent in Cohort 1 (aHR = 2.48; 95% CI 1.96 to 3.14) but appeared unstable in Cohort 2 (aHR = 1.61; 95% CI 0.84 to 3.09). Using a cut-off of ≥ 40 , the sensitivity, specificity, positive predictive value and negative predictive value were 0.84; 0.33; 0.32; and 0.85 for Cohort 1 and 0.82, 0.43, 0.29 and 0.90 for Cohort 2, respectively.

Discussion

Key results

CRP reasonably followed a bimodal distribution using data from two independent cohorts. There was inconclusive evidence of a trimodal distribution; although the AIC

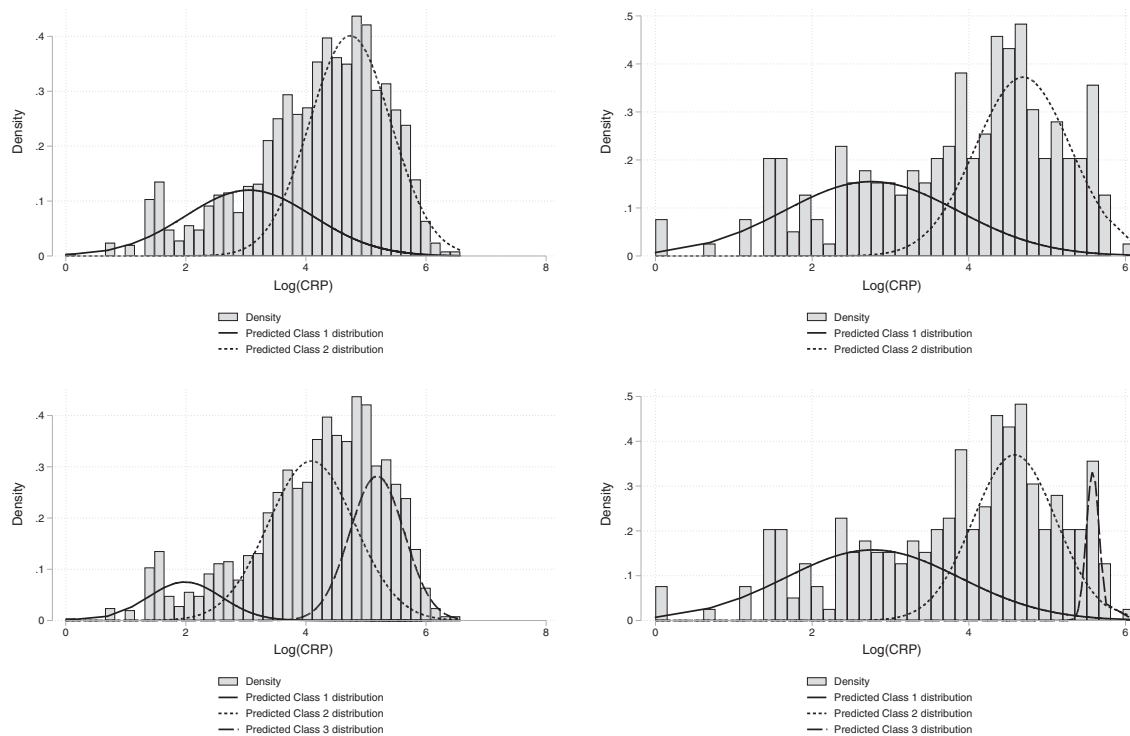


Figure 1 Distribution of C-reactive protein (CRP) in the original cohort (left panel) and the validation cohort (right panel), overlaid predicted distributions from a two-class (upper row), compared with three-class (lower row) finite mixture models

metric suggested it fit better, on graphical examination there appeared to be overfitting.

In an analysis of 1835 patients across 13 hospital sites using a binary cut-off for CRP as a prognostic factor of COVID-19, inpatient death appeared to have similar predictive power compared with treating it as a linear or $\ln(\text{CRP})$. In addition, a cut-off value to indicate disease severity is simpler to use in a clinical setting than a linear predictor. These findings support the use of a simple binary threshold for CRP in daily clinical medicine. These results are well aligned with many published analyses in COVID-19 which have already employed a binary cut-off.^{4,18–20}

The bimodal distribution of CRP may reflect the presence of a latent class influence. Candidate variables for this latent class may include confounders that were not fully controlled for: chronic inflammatory conditions, genomic variation of the virus, genetic susceptibility of populations or other binary exposures such as Bacillus Calmette-Guérin (BCG) vaccination status.^{21–23}

The association of higher CRP with worse outcomes may be due to the severity of the disease consistent with the ‘cytokine storm’ theory of COVID-19, where the innate immune system is activated releasing TNF-alpha, IL-6 and IL-1. Elshazli *et al.* found CRP to be a valid biomarker of death from COVID-19 when examining a range of haematological and immunological markers. IL-6 was found

to be most predictive ($OR = 13.87$) of death, and CRP the next best marker ($OR = 7.09$).²⁴ However, IL-6 is not routinely available to clinicians, but being linked to CRP as a trigger for its transcription makes CRP a better candidate tool for front-line hospital usage.²⁵ In the same Elshazli paper, a threshold level of 38.2 mg/L was demonstrated to have the best sensitivity and specificity, which fits well with our findings; this was also found within a recent Cochrane Diagnostic Test Accuracy review.²⁶ In addition, an elevated CRP may not be attributable to COVID-19 alone and may represent concomitant pathology such as secondary bacterial pneumonia. Although co-infection is well known in other viral respiratory illnesses, the rate in COVID-19 has been found to be far less, being present in around 5.9% of the general COVID-19 hospital population and 8.1% of those with critical illness.¹⁸

The data presented here support a single threshold, and whilst there was argument for competing cut-offs of ≥ 40 , ≥ 65 or greater, the single cut-off is consistent with other studies.^{8,24} In addition, it would be clearer and safer to offer a conservative approach using the lower value of CRP, as a higher threshold may falsely reassure clinicians.

There is a need for simple tests to aid clinical management, as the behaviour of CRP in COVID-19 may provide useful immediate risk stratification as to who may have a poor outcome. The threshold of $\text{CRP} \geq 40$ offered a high

Table 2 Performance of different cut-offs/parametrizations of C-reactive protein (CRP) in a Cox model for time to mortality

CRP (mg/L) parametrization	Cohort 1 (Original)			Cohort 2 (Validation)		
	N below cut-off (%)	Harrell's C statistic	AIC	N below cut off (%)	Harrell's C statistic	AIC
Null (CRP not included)	NA	0.6592	5224.41	NA	0.6816	428.58
CRP ≥ 10	132 (8.6%)	0.6697	5174.10	39 (15.2%)	0.6811	430.58
CRP ≥ 15	190 (12.4%)	0.6797	5159.14	56 (21.8%)	0.6995	429.22
CRP ≥ 20	230 (15.0%)	0.6858	5148.08	66 (25.7%)	0.7024	426.59
CRP ≥ 25	279 (18.2%)	0.6930	5144.01	75 (29.2%)	0.7055	427.83
CRP ≥ 30	326 (21.3%)	0.6953	5143.46	83 (32.3%)	0.7044	427.44
CRP ≥ 35	381 (24.9%)	0.6963	5141.06	91 (35.4%)	0.7145	425.61
CRP ≥ 40	439 (28.7%)	0.7024	5136.10	96 (37.4%)	0.7187	424.35
CRP ≥ 45	486 (31.7%)	0.7055	5132.53	103 (40.1%)	0.7015	427.18
CRP ≥ 50	530 (34.6%)	0.7059	5126.61	111 (43.2%)	0.6974	428.68
CRP ≥ 55	569 (37.1%)	0.7025	5130.50	120 (46.7%)	0.6900	428.85
CRP ≥ 60	605 (39.5%)	0.7064	5127.69	125 (48.6%)	0.6926	428.16
CRP ≥ 65	648 (42.3%)	0.7068	5124.45	129 (50.2%)	0.6867	428.47
CRP ≥ 70	687 (44.8%)	0.7033	5131.22	135 (52.5%)	0.6895	428.32
CRP ≥ 75	727 (47.5%)	0.7006	5131.79	139 (54.1%)	0.6879	428.87
CRP ≥ 80	766 (50.0%)	0.7005	5133.82	145 (56.4%)	0.6853	429.49
CRP ≥ 85	804 (52.5%)	0.7021	5135.11	155 (60.3%)	0.6887	429.16
CRP ≥ 90	834 (54.4%)	0.7001	5138.43	161 (62.6%)	0.6816	430.34
CRP ≥ 95	863 (56.3%)	0.6975	5142.08	169 (65.8%)	0.6828	429.98
CRP ≥ 100	887 (57.9%)	0.7010	5137.48	173 (67.3%)	0.6890	429.69
CRP (linear)	NA	0.7040	5024.81	NA	0.6992	426.42
log(CRP)	NA	0.7157	5001.00	NA	0.7014	426.51

Number of cases defined as not elevated CRP.

NA, not available.

negative predictive value, so patients presenting with a low CRP are unlikely to exhibit disease progression, and high sensitivity analysis which might lead to opening discussions with patients and their carers about the possible course of the disease. This may assist with early resource planning around the potential for critical care support, and may help guide rapid safe discharge from acute hospitals.⁵ Although the results within this paper give a population-based cut-off, any interpretation and management plan must be made on an individual patient basis, with clinicians using CRP in context of clinical history, examination and investigation and noting that the threshold offered a low positive predictive value. Beyond clinical predictive value, this model may be useful for monitoring the outcomes of treatments, for example in a trial of tocilizumab, CRP monitoring was used as a marker of efficacy.²⁶

Strengths and limitations

This was a large study that included participants admitted to 13 hospital sites. The demographics, case mix and

mortality are similar to other larger studies reported within the UK, increasing the findings' generalizability.²⁰ We have also shown good replication between the two UK-wide cohorts. However, caution should be given to the threshold reported for CRP, as studies identifying optimal cut-offs may be subject to selection bias and may not be replicable.²⁷ Using a threshold of ≥ 40 offered a high sensitivity and negative predictive value but low positive predictive value.

A limitation of this study is that due to the urgent nature of research data collection in a pandemic, disease severity on admission was only assessed using CRP without collection of circulating lymphocytes, interleukin-6, procalcitonin, serum lactate and viral load, all of which may also contribute to disease severity.²⁸

Interpretation

A simple threshold ≥ 40 mg/L should be used within clinical practice to guide disease severity and likely disease progression. Future studies should analyse using this simple threshold.

Table 3 Bootstrapped differences in model performance of Cox model for time to mortality for different C-reactive protein (CRP) parameterizations using Cohort 1 (Original Cohort)

Model comparison	Difference in	Coefficient	Bias	Standard error	95% CI	
≥ 10 compared with ≥ 40	Harrell's C statistic	-0.033	0.003	0.007	-0.044	-0.016
	AIC ⁺	38.002	-0.326	12.591	14.250	64.258
$\geq 65^a$ compared with ≥ 40	Harrell's C statistic	0.004	0.002	0.007	-0.006	0.020
	AIC	-11.655	0.260	11.400	-32.978	11.775
Linear CRP compared with ≥ 40	Harrell's C statistic	0.002	0.003	0.008	-0.010	0.020
	AIC	-111.289	102.784	15.212	-41.031	19.531
$\text{Ln}_{(\text{CRP})}$ compared with ≥ 40	Harrell's C statistic	0.013	0.002	0.006	0.004	0.028
	AIC	-135.105	-0.857	37.105	-210.386	-65.123
≥ 10 compared with $\geq 65^a$	Harrell's C statistic	-0.037	0.001	0.010	-0.058	-0.018
	AIC	49.657	-0.585	15.262	21.293	79.554
Linear CRP compared with $\geq 65^a$	Harrell's C statistic	-0.003	0.001	0.007	-0.016	0.012
	AIC	-99.633	102.470	13.781	-25.825	29.435
$\text{Log}_{(\text{CRP})}$ compared with $\geq 65^a$	Harrell's C statistic	0.009	0.000	0.006	-0.002	0.021
	AIC	-123.450	-1.117	36.286	-197.611	-55.831
Linear CRP compared with ≥ 10	Harrell's C statistic	0.034	0.000	0.010	0.018	0.056
	AIC	-149.291	103.429	15.581	-77.820	-18.453
$\text{Log}_{(\text{CRP})}$ compared with ≥ 10	Harrell's C statistic	0.046	-0.001	0.009	0.028	0.063
	AIC	-173.107	-0.531	38.325	-253.435	-99.153
$\text{Log}_{(\text{CRP})}$ compared with Linear CRP	Harrell's C statistic	0.012	-0.001	0.004	0.003	0.019
	AIC	-23.816	0.618	9.527	-41.730	-4.322

^aA threshold of ≥ 65 has been included as a comparison with ≥ 40 .

Generalizability

The impact of these findings support the routine assessment of serum CRP as an adjunct in the early diagnosis and assessment of illness severity of hospitalized patients with COVID-19. We recommend that CRP ≥ 40 mg/L on admission may indicate an increased risk of disease progression and death, and warrants an enhanced level of discussion and clinical support.

Conclusions

We have demonstrated that CRP follows a bimodal distribution in hospitalized patients with COVID-19. This requires further exploration to discover the latent class effect of unobserved factors influencing the distribution of CRP. A CRP of ≥ 40 mg/L on admission to hospital should be seen as a reliable indicator of disease severity and increased risk of death. We recommend clinicians use this cut-off as a prognostic indicator only, in conjunction with an individualized clinical assessment, frailty assessment and incorporating a person's wishes and values, to make early decisions about enhanced observation, critical care support and advanced care planning.

Supplementary data

Supplementary data are available at *IJE* online.

Data availability

Data are available on request from the corresponding author after submission of a statistical analysis plan, after approval from the COPE Study Investigators.

Funding

This study received no specific funding. The study was partially supported through the NIHR Maudsley Biomedical Research Centre at the South London and Maudsley NHS Foundation Trust in partnership with King's College London (B.C.).

Cope Study Collaborators

Aberdeen University: Dr Eilidh Bruce, Dr Alice Einarsson; Glasgow Royal Infirmary: Dr Aine McGovern; Inverclyde Royal Infirmary: Carly Bisset, Ross Alexander; Italy (University Hospital of Modena Policlinico): Professor Giovanni Guaraldi; King's College London: Caroline Murphy, Joanna Kelly, Dr Roxanna Short; North Bristol Trust: Tarik El Jichi Mutasem, Sandeep Singh, Dolcie Paxton, Will Harris, Dr James Hesford, Dr Mark Holloway, Dr Emma Mitchel, Dr Frances Rickard; Royal Alexandra Hospital, Paisley: Norman Galbraith, Emma Bhatti, Jenny Edwards, Siobhan Duffy, Dr Fenella Barlow-Pay; Salford Royal Infirmary: Madeline Garcia, Shefali Sangani, Thomas Kneen, Thomas Lee, Angeline Price;

Ysbyt Yystad Fawr: Dr Charlotte Davey, Ms Sheila Jones, Kiah Lunstone, Alice Cavenagh, Charlotte Silver, Thomas Telford, Rebecca Simmons.

Author contributions

Concept of the study (B.C., P.B.); developed the protocol (B.C., D.S., P.B.); collected the data (P.B., P.M., L.E., J.C., V.A., T.Q., A.V., M.S., L.P., J.H., S.M., K.Mc.); analysed the data (D.S., B.C.); interpreted the findings (D.S., B.C., P.B.); drafted the initial manuscript (D.S., P.B., B.C.); all authors approved the final manuscript. B.C. is the guarantor of the study findings.

Conflict of interest

None declared.

References

- Chen N, Zhou M, Dong X et al. Epidemiological and clinical characteristics of 99 cases of 2019 novel coronavirus pneumonia in Wuhan, China: a descriptive study. *Lancet* 2020;395:507–13.
- Liu F, Li L, Xu M et al. Prognostic value of interleukin-6, C-reactive protein, and procalcitonin in patients with COVID-19. *J Clin Virol* 2020;127:104370.
- Pepys MB, Hirschfield GM. C-reactive protein: a critical update. *J Clin Invest* 2003;111:1805–12.
- Haran JP, Beaudoin FL, Suner S, Lu S. C-reactive protein as predictor of bacterial infection among patients with an influenza-like illness. *Am J Emerg Med* 2013;31:137–44.
- Li Q, Ding X, Xia G et al. Eosinopenia and elevated C-reactive protein facilitate triage of COVID-19 patients in fever clinic: a retrospective case-control study. *EclinMed* 2020;23:100375.
- Gupta RK, Michael Marks M, Samuels THA et al. Systematic evaluation and external validation of 22 prognostic models among hospitalized adults with COVID-19: An observational cohort study. *Eur Respir J* 2020;56:2003498.
- Osuafor CN, Davidson C, Mackett AJ. Clinical features and inpatient trajectories of older inpatients with COVID-19: a retrospective observational study. *Geriatrics (Basel)* 2020;6:1.
- Chen W, Zheng KI, Liu S, Yan Z, Xu C, Qiao Z. Plasma CRP level is positively associated with the severity of COVID-19. *Am Clin Microbiol Antimicrob* 2020;19:18.
- Herold T, Jurinovic V, Arnreich C et al. Elevated levels of IL-6 and CRP predict the need for mechanical ventilation in COVID-19. *J Allergy Clin Immunol* 2020;146:128–36.e4.
- Hamer M, Gale CR, Kivimäki M, Batty GD. Overweight, obesity, and risk of hospitalization for COVID-19: A community-based cohort study of adults in the United Kingdom. *Proc Natl Acad Sci U SA* 2020;117:21011–13.
- Shang W, Dong J, Ren Y et al. The value of clinical parameters in predicting the severity of COVID-19. *J Med Virol* 2020;92: 2188–92.
- Elm E, von Altman DG, Egger M et al.; for the STROBE Initiative. The Strengthening the Reporting of Observational Studies in Epidemiology (STROBE) statement: guidelines for reporting observational studies. *PLoS Med* 2007;4:e296.
- Hewitt J, Carter B, Vilches-Moraga A et al. The effect of frailty on survival in patients with COVID-19 (COPE): a multicentre, European, observational cohort study. *Lancet Public Health* 2020. [https://www.thelancet.com/journals/lanpub/article/PIIS2468-2667\(20\)30146-8/abstract](https://www.thelancet.com/journals/lanpub/article/PIIS2468-2667(20)30146-8/abstract) (9 July 2020, date last accessed).
- Price A, Barlow-Pay F, Duffy S et al. A study protocol for COPE study: COVID-19 in Older PEople – the influence of frailty and multimorbidity on survival. A multi-centre, European observational study. *BMJ Open* 2020;10:e040569.
- Harrell FE, Calif RM, Pryor DB, Lee KL, Rosati RA. Evaluating the yield of medical tests. *JAMA* 1982;247:2543–46.
- Akaike H. A new look at the statistical model identification. *IEEE Trans Automat Contr* 1974;19:716–23.
- Ali N. Elevated level of C-reactive protein may be an early marker to predict risk for severity of COVID-19. *J Med Virol* 2020;92:2409–11.
- Langford BJ, So M, Raybardhan S et al. Bacterial co-infection and secondary infection in patients with COVID-19: a living rapid review and meta-analysis. *Clin Microbiol Infect* 2020. [https://www.clinicalmicrobiologyandinfection.com/article/S1198-743X\(20\)30423-7/abstract](https://www.clinicalmicrobiologyandinfection.com/article/S1198-743X(20)30423-7/abstract) (1 September 2020, date last accessed).
- Vasileva D, Badawi A. C-reactive protein as a biomarker of severe H1N1 influenza. *Inflamm Res* 2019;68:39–46.
- Docherty AB, Harrison EM, Green CA et al. Features of 20 133 UK patients in hospital with covid-19 using the ISARIC WHO Clinical Characterisation Protocol: prospective observational cohort study. *BMJ* 2020. <https://www.bmjjournals.org/content/369/bmj.m1985> (1 September 2020, date last accessed).
- Wu T-L, Tsao K-C, Chang CP-Y, Li C-N, Sun C-F, Wu JT. Development of ELISA on microplate for serum C-reactive protein and establishment of age-dependent normal reference range. *Clin Chim Acta* 2002;322:163–68.
- Ferreira GD, Simões JA, Senaratna C et al. Physiological markers and multimorbidity. *J Comorb* 2018;8:2235042X1880698.
- Toyoshima Y, Nemoto K, Matsumoto S, Nakamura Y, Kiyotani K. SARS-CoV-2 genomic variations associated with mortality rate of COVID-19. *J Hum Genet* 2020;65:1075–78.
- Elshazli RM, Toraih EA, Elgaml A et al. Diagnostic and prognostic value of hematological and immunological markers in COVID-19 infection: a meta-analysis of 6320 patients. *PloS One* 2020;15:e0238160.
- Markanday A. Acute phase reactants in infections: evidence-based review and a guide for clinicians. *Open Forum Infect Dis* 2015;2. <https://www.ncbi.nlm.nih.gov/pmc/articles/PMC4525013/> (16 September 2020, date last accessed).
- Luo P, Liu Y, Qiu L, Liu X, Liu D, Li J. Tocilizumab treatment in COVID-19: a single center experience. *J Med Virol* 2020;92: 814–18.
- Hölländer N, Sauerbrei W, Schumacher M. Confidence intervals for the effect of a prognostic factor after selection of an ‘optimal’ cutpoint. *Stat Med* 2004;23:1701–13.
- Tan L, Kang X, Ji X et al. Validation of predictors of disease severity and outcomes in COVID-19 patients: a descriptive and retrospective study. *Med N Y N* 2020. <https://www.ncbi.nlm.nih.gov/pmc/articles/PMC7235581/> (18 September 2020, date last accessed).

RESEARCH LETTER

Open Access



YKL-40 as a new promising prognostic marker of severity in COVID infection

Lauranne Schoneveld¹, Aurélie Ladang¹, Monique Henket², Anne-Noëlle Frix², Etienne Cavalier^{1*}& Julien Guiot^{2†} on behalf of the COVID-19 clinical investigators of the CHU de Liège

Keywords: COVID-19, SARS-CoV-2, YKL-40, Chitinase 3-like 1, Interstitial lung disease

The severe acute respiratory syndrome coronavirus 2 (SARS-CoV-2) is responsible for a disease named COVID-19, which may be associated with common symptoms or lead patients to intensive care unit (ICU) or death. The severity of the disease is mainly driven by diffuse interstitial lung diseases (ILD). YKL-40 has a pro-mitogenic action on pulmonary fibroblasts, increases the activity of macrophages and is associated with inflammatory disorders, arteriosclerosis and endothelial dysfunction. In ILD, YKL-40 has been described to be associated with the severity of lung diseases and with the risk of death [1–6]. Yet, in COVID-19 infection, YKL-40 serum levels could therefore be of interest for diagnosis and prognosis since it is at the cross-link between vascular and epithelial lung damage, which are typical characteristics of COVID-19 infection. By closing the gap between those two pathological characteristics, we thought that YKL-40 could be of interest a specific biomarker of severe COVID-19 infection.

We thus retrospectively compared serum levels of YKL-40 in a cohort of 103 patients infected by SARS-CoV-2 hospitalized between March 1 and April 29, 2020, with a group of 58 appariated healthy subjects (HS), 26 patients suffering from chronic obstructive pulmonary disease (COPD) and 53 from non-COVID ILD. Measurement of YKL-40 was taken with the MicroVue™ YKL-40 enzyme immunoassay kit during the 3 first days of admission and

retrospectively analyzed and correlated the results with clinical data [ICU admission, acute renal failure (ARF) or multiple organ failure (MOF)].

Median age of COVID-19 positive patients was 69 yo with a male predominance (67%). A significant proportion of the cohort ($n=103$) experienced ICU admission (30%), ARF (32%) and MOF (28%).

COVID-19 patients who were admitted in ICU had statistically higher CRP, creatinine, LDH and YKL-40 ($p<0.05$) (Table 1). The lymphocyte count was not statistically lower ($p=0.059$) and D-dimers were not higher ($p=0.1297$) compared to the other group.

COVID-19 patients exhibited higher serum levels of YKL-40 than HS, COPD and ILD ($p<0.0001$ for all groups) (Fig. 1). Median serum level of YKL-40 was 206 ng/ml (95–431) in the COVID-19 group, 46 ng/ml (34–67) in the HS subgroup, whereas they were of 60 ng/ml (41–73) in the COPD and 73 ng/ml (42–91) in the ILD groups, respectively.

Patients suffering from more severe diseases had significantly higher YKL-40 values than those who did not experience ICU admission, MOF or ARF ($p<0.05$, $p<0.05$, $p<0.001$, respectively). Patients infected by COVID-19 suffering from prior chronic renal failure and chronic cardiopathy were exhibiting an increased serum level of YKL-40 ($p<0.0001$ and $p<0.001$, respectively). Death was not statistically correlated to levels of YKL-40 within the COVID-19 patient group ($p=0.12$).

The area under the ROC curve (AUC) for the discrimination of patients admitted or not to the ICU in association with the levels of YKL-40, the age and the percentage of lesions visible on the thoracic scanner

*Correspondence: etienne.cavalier@chuliege.be

†Etienne Cavalier and Julien Guiot have contributed equally to this work

¹ Department of Clinical Chemistry, University of Liege, CHU de Liège, Domaine Universitaire du Sart-Tilman, B35, 4000 Liège, Belgium
Full list of author information is available at the end of the article



© The Author(s) 2021. **Open Access** This article is licensed under a Creative Commons Attribution 4.0 International License, which permits use, sharing, adaptation, distribution and reproduction in any medium or format, as long as you give appropriate credit to the original author(s) and the source, provide a link to the Creative Commons licence, and indicate if changes were made. The images or other third party material in this article are included in the article's Creative Commons licence, unless indicated otherwise in a credit line to the material. If material is not included in the article's Creative Commons licence and your intended use is not permitted by statutory regulation or exceeds the permitted use, you will need to obtain permission directly from the copyright holder. To view a copy of this licence, visit <http://creativecommons.org/licenses/by/4.0/>. The Creative Commons Public Domain Dedication waiver (<http://creativecommons.org/publicdomain/zero/1.0/>) applies to the data made available in this article, unless otherwise stated in a credit line to the data.

Table 1 Comparison between COVID-19 patients admitted to intensive care or not

Variables	ICU, No (n=72)	ICU, Yes (n=31)	p value
Age (year)	71 (58–82)	65 (59–69)	<0.05
Gender M/F	44/28	22/9	NS
Height (cm)	169 (162–176)	175 (169–180)	<0.05
Weight (kg)	71 (63–84)	96 (80–105)	<0.0001
BMI (kg/m ²)	25 (22–29)	31 (27–34)	<0.0001
Abnormal lung lesions (%)	20 (10–35)	40 (30–50)	<0.001
SpO ₂ (%)	93 (89–96)	88 (75–90)	<0.0001
Death, No/Yes (%)	92.8/7.2	89.3/10.7	NS
Shock or organ failure, No/Yes (%)	91.3/8.7	26.7/73.3	<0.0001
Cardiopathy, No/Yes (%)	85.5/14.5	75/25	NS
ARF, No/Yes (%)	79.7/20.3	40/60	<0.001
CRF, No/Yes (%)	85.5/14.5	96.7/3.3	NS
Diabetes, No/Yes (%)	85.5/14.5	62.1/37.9	<0.05
Red blood cells (× 10e6/μl)	4.29±0.79	4.48±0.85	NS
Hematocrit (%)	38±7	39±7	NS
Hemoglobin (g/dl)	13±2	14±2	NS
Globular volume (fl)	89±8	89±7	NS
Reticulocytes (%)	0.97 (0.72–1.15)	1 (0.57–1.04)	NS
Reticulocytes (× 10 ³ /μl)	39 (29–50)	39 (24–51)	NS
Leucocytes (× 10e3/μl)	6.15 (4.63–8.03)	7.87 (4.91–13.54)	<0.05
Blood neutrophils (%)	73±12	78±17	<0.05
Blood lymphocytes (%)	15 (10–24)	10 (5–20)	<0.05
Blood monocytes (%)	0.2 (0–0.9)	0 (0–0.1)	<0.01
Blood eosinophils (%)	7.73±4.36	5.63±3.32	NS
Blood basophils (%)	0.2 (0.2–0.4)	0.2 (0.1–0.3)	NS
Blood neutrophils (10 ³ /μl)	4.54 (3.07–6.4)	6.96 (3.5–11.73)	<0.05
Blood lymphocytes (10 ³ /μl)	0.96 (0.69–1.27)	0.73 (0.59–1.12)	NS
Blood monocytes (10 ³ /μl)	0.42 (0.25–0.6)	0.37 (0.27–0.6)	NS
Blood eosinophils (10 ³ /μl)	0.01 (0–0.05)	0 (0–0.01)	<0.05
Blood basophils (10 ³ /μl)	0.01 (0.01–0.02)	0.02 (0.01–0.03)	NS
Platelets (10 ³ /μl)	195 (157–266)	189 (155–252)	NS
Quick time (%)	83±22	83±13	NS
Quick time (s)	13 (12–13)	13 (12–13)	NS
Fibrinogen (g/l)	5.24±1.61	6.06±2.01	NS
D-dimers (μg/L)	876 (517–1787)	1483 (586–2422)	NS
Erythrocytes sedimentation rate (mm/h)	123 (123–123)	48 (48–48)	NS
Iron (μmol/l)	4.27 (2.95–7.36)	4.61 (3.35–7.06)	NS
Ferritin (μg/l)	827 (499–1677)	1861 (889–4117)	<0.05
Osmolality (mosm/kg)	290±15	286±11	NS
Sodium (mmol/l)	139±5	136±4	<0.05
Chlorides (mmol/l)	102±6	100±5	NS
Potassium (mmol/L)	4.04±0.44	4.16±0.62	NS
Calcium (mmol/l)	2.23±0.18	2.14±0.21	NS
Phosphates (mg/l)	0.99±0.2	1.15±0.34	NS
Bicarbonates (mmol/l)	24 (21–26)	23 (19–26)	NS
Creatinine (mg/dl)	0.93 (0.8–1.31)	1.25 (0.88–1.6)	0.05
Urea (mg/dL)	41 (31–68)	53 (40–84)	<0.05
GFR (MDRD) (ml/min/1.73m ²)	71±33	60±30	NS
Total protein (g/l)	66±8	66±11	NS

Table 1 (continued)

Variables	ICU, No (n=72)	ICU, Yes (n=31)	p value
Albumin (g/l)	37±5	36±4	NS
Uric acid (mg/dl)	61±25	63±25	NS
CRP (mg/l)	58 (26–144)	166 (105–265)	<0.0001
Total bilirubin (mg/dl)	0.62 (0.44–0.82)	0.79 (0.53–1.02)	<0.05
Conjugated bilirubin (mg/dl)	0.25 (0.18–0.34)	0.33 (0.25–0.5)	<0.05
Alkaline phosphatase (U/l)	75 (59–90)	70 (57–95)	NS
GGT (U/l)	52 (30–111)	64 (29–133)	NS
ASAT (U/L)	35 (24–53)	60 (35–80)	<0.001
ALAT (U/L)	27 (17–46)	36 (26–56)	<0.05
LDH (U/l)	310 (244–441)	503 (411–703)	<0.00001
Lipase (U/l)	32 (19–50)	38 (25–53)	NS
Creatine kinase (U/l)	136 (59–266)	229 (101–426)	0.07
YKL-40 (ng/ml)	186 (84–384)	241 (172–827)	<0.05

When the data follow a normal distribution, the results are expressed as mean ± standard deviation, and otherwise, they are expressed as the median (IQR)

M, male; F, female; NS, nonsignificant

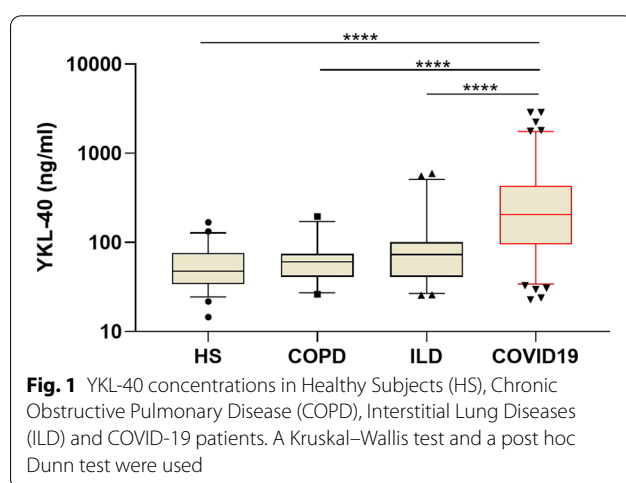


Fig. 1 YKL-40 concentrations in Healthy Subjects (HS), Chronic Obstructive Pulmonary Disease (COPD), Interstitial Lung Diseases (ILD) and COVID-19 patients. A Kruskal-Wallis test and a post hoc Dunn test were used

reached 0.78 ($p < 0.0001$). The positive predictive value was 70%, and the negative predictive value was 83%.

In conclusion, this study showed that firstly the COVID-19 patients had higher levels of YKL-40 compared to a control population (HS, COPD and ILD) and secondly that within the COVID-19 population YKL-40 was an indicator of the seriousness of infection since it is linked to complications such as admission to ICU, ARF or MOF. This marker could also be a predictive marker to anticipate management at the ICU and is useful for the prognosis of the onset of an ILD later. Future studies are also needed to assess the correlation between the levels of YKL-40 and pulmonary sequelae that patients with COVID-19 would develop.

Abbreviations

ICU: Intensive care unit; ILD: Interstitial lung diseases; HS: Healthy subjects; COPD: Chronic obstructive pulmonary disease; MOF: Multiple organ failure; AUC: Area under the ROC curve.

Acknowledgements

The authors would like to thank the COVID-19 clinical investigators of the CHU de Liège: Ancion, A., Berg, J., Bonhomme, O., Bouquegneau, A., Bovy, C., Bruls, S., Darcis, G., Defraigne, J.O., Ghysen, A., Gilbert, A., Heinen, V., Lamberton, B., Louis, R., Malaise, O., Martin, M., Misset, B., Moutschen, M., Nguyen Dang, D., Piazza, J., Szecel, D., Szecel, J., Van Cauwenberge, H., Von Frenckell, C., Vroonen, L.

Authors' contributions

JG, EC and MH contributed to conceptualization. LS, ANF and MH curated the data. MH contributed to formal analysis. LS and EC contributed to methodology. LS contributed to investigation and writing original draft. EC and JG contributed to supervision, validation, visualization and writing—review and editing. All authors read and approved the final manuscript.

Funding

Research grant from Fond Leon Fredericq.

Availability of data and materials

The datasets used and/or analyzed during the current study are available from the corresponding author on reasonable request.

Ethics approval and consent to participate

No specific approval was requested to the ethic committee as a leaflet including the following statement is given to all admitted patients: According to the law of the 19th December 2008, any left-over of biological material collected from patients for their standard medical management and normally destroyed when all diagnostic analyses have been performed, can be used for validation of methods. The law authorizes such use except if the patient expressed an opposition when still alive (presume consent). Written informed consent for participation was not required for this study in accordance with the national legislation and the institutional requirements. However, for HS, COPD and ILD patients, the protocol was approved by the ethics committee of CHU of Liège, and all subjects gave written consent before their enrollment (Belgian Number: B707201422832; ref: 2014/302).

Consent for publication

Not applicable.

Competing interests

All authors declare to have no specific competing interests for this specific publication.

Author details

¹ Department of Clinical Chemistry, University of Liege, CHU de Liège, Domaine Universitaire du Sart-Tilman, B35, 4000 Liège, Belgium. ² Department of Pneumology, CHU de Liège, Liège, Belgium.

Received: 5 November 2020 Accepted: 9 November 2020

Published online: 16 February 2021

References

1. Korthagen NM, van Moorsel CHM, Barlo NP, Ruven HJT, Kruit A, Heron M, et al. Serum and BALF YKL-40 levels are predictors of survival in idiopathic pulmonary fibrosis. *Respir Med*. 2011;105:106–13.
2. Létuvé S, Kozhich A, Arouche N, Grandsaigne M, Reed J, Dombret M-C, et al. YKL-40 is elevated in patients with chronic obstructive pulmonary disease and activates alveolar macrophages. *J Immunol*. 2008;181:5167–73.
3. Nordenbæk C, Johansen JS, Halberg P, Wiik A, Garbarsch C, Ullman S, et al. High serum levels of YKL-40 in patients with systemic sclerosis are associated with pulmonary involvement. *Scand J Rheumatol*. 2005;34:293–7.
4. Inoue Y, Kaner RJ, Guiot J, Maher TM, Tomassetti S, Moiseev S, et al. Diagnostic and prognostic biomarkers for chronic fibrosing interstitial lung diseases with a progressive phenotype. *Chest*. 2020;158:646–59.
5. Guiot J, Moermans C, Henket M, Corhay JL, Louis R. Blood biomarkers in idiopathic pulmonary fibrosis. *Lung*. 2017;195:273–80.
6. Bonhomme O, André B, Gester F, De Seny D, Moermans C, Struman I, et al. Biomarkers in systemic sclerosis-associated interstitial lung disease: review of the literature. *Rheumatol (United Kingdom)*. 2019;58:1534–46.

Publisher's Note

Springer Nature remains neutral with regard to jurisdictional claims in published maps and institutional affiliations.

Ready to submit your research? Choose BMC and benefit from:

- fast, convenient online submission
- thorough peer review by experienced researchers in your field
- rapid publication on acceptance
- support for research data, including large and complex data types
- gold Open Access which fosters wider collaboration and increased citations
- maximum visibility for your research: over 100M website views per year

At BMC, research is always in progress.

Learn more biomedcentral.com/submissions



RESEARCH LETTER

Open Access



YKL-40 as a new promising prognostic marker of severity in COVID infection

Lauranne Schoneveld¹, Aurélie Ladang¹, Monique Henket², Anne-Noëlle Frix², Etienne Cavalier^{1*}& Julien Guiot^{2†} on behalf of the COVID-19 clinical investigators of the CHU de Liège

Keywords: COVID-19, SARS-CoV-2, YKL-40, Chitinase 3-like 1, Interstitial lung disease

The severe acute respiratory syndrome coronavirus 2 (SARS-CoV-2) is responsible for a disease named COVID-19, which may be associated with common symptoms or lead patients to intensive care unit (ICU) or death. The severity of the disease is mainly driven by diffuse interstitial lung diseases (ILD). YKL-40 has a pro-mitogenic action on pulmonary fibroblasts, increases the activity of macrophages and is associated with inflammatory disorders, arteriosclerosis and endothelial dysfunction. In ILD, YKL-40 has been described to be associated with the severity of lung diseases and with the risk of death [1–6]. Yet, in COVID-19 infection, YKL-40 serum levels could therefore be of interest for diagnosis and prognosis since it is at the cross-link between vascular and epithelial lung damage, which are typical characteristics of COVID-19 infection. By closing the gap between those two pathological characteristics, we thought that YKL-40 could be of interest a specific biomarker of severe COVID-19 infection.

We thus retrospectively compared serum levels of YKL-40 in a cohort of 103 patients infected by SARS-CoV-2 hospitalized between March 1 and April 29, 2020, with a group of 58 appariated healthy subjects (HS), 26 patients suffering from chronic obstructive pulmonary disease (COPD) and 53 from non-COVID ILD. Measurement of YKL-40 was taken with the MicroVue™ YKL-40 enzyme immunoassay kit during the 3 first days of admission and

retrospectively analyzed and correlated the results with clinical data [ICU admission, acute renal failure (ARF) or multiple organ failure (MOF)].

Median age of COVID-19 positive patients was 69 yo with a male predominance (67%). A significant proportion of the cohort ($n=103$) experienced ICU admission (30%), ARF (32%) and MOF (28%).

COVID-19 patients who were admitted in ICU had statistically higher CRP, creatinine, LDH and YKL-40 ($p<0.05$) (Table 1). The lymphocyte count was not statistically lower ($p=0.059$) and D-dimers were not higher ($p=0.1297$) compared to the other group.

COVID-19 patients exhibited higher serum levels of YKL-40 than HS, COPD and ILD ($p<0.0001$ for all groups) (Fig. 1). Median serum level of YKL-40 was 206 ng/ml (95–431) in the COVID-19 group, 46 ng/ml (34–67) in the HS subgroup, whereas they were of 60 ng/ml (41–73) in the COPD and 73 ng/ml (42–91) in the ILD groups, respectively.

Patients suffering from more severe diseases had significantly higher YKL-40 values than those who did not experience ICU admission, MOF or ARF ($p<0.05$, $p<0.05$, $p<0.001$, respectively). Patients infected by COVID-19 suffering from prior chronic renal failure and chronic cardiopathy were exhibiting an increased serum level of YKL-40 ($p<0.0001$ and $p<0.001$, respectively). Death was not statistically correlated to levels of YKL-40 within the COVID-19 patient group ($p=0.12$).

The area under the ROC curve (AUC) for the discrimination of patients admitted or not to the ICU in association with the levels of YKL-40, the age and the percentage of lesions visible on the thoracic scanner

*Correspondence: etienne.cavalier@chuliege.be

†Etienne Cavalier and Julien Guiot have contributed equally to this work

¹ Department of Clinical Chemistry, University of Liege, CHU de Liège, Domaine Universitaire du Sart-Tilman, B35, 4000 Liège, Belgium
Full list of author information is available at the end of the article



© The Author(s) 2021. **Open Access** This article is licensed under a Creative Commons Attribution 4.0 International License, which permits use, sharing, adaptation, distribution and reproduction in any medium or format, as long as you give appropriate credit to the original author(s) and the source, provide a link to the Creative Commons licence, and indicate if changes were made. The images or other third party material in this article are included in the article's Creative Commons licence, unless indicated otherwise in a credit line to the material. If material is not included in the article's Creative Commons licence and your intended use is not permitted by statutory regulation or exceeds the permitted use, you will need to obtain permission directly from the copyright holder. To view a copy of this licence, visit <http://creativecommons.org/licenses/by/4.0/>. The Creative Commons Public Domain Dedication waiver (<http://creativecommons.org/publicdomain/zero/1.0/>) applies to the data made available in this article, unless otherwise stated in a credit line to the data.

Table 1 Comparison between COVID-19 patients admitted to intensive care or not

Variables	ICU, No (n=72)	ICU, Yes (n=31)	p value
Age (year)	71 (58–82)	65 (59–69)	<0.05
Gender M/F	44/28	22/9	NS
Height (cm)	169 (162–176)	175 (169–180)	<0.05
Weight (kg)	71 (63–84)	96 (80–105)	<0.0001
BMI (kg/m ²)	25 (22–29)	31 (27–34)	<0.0001
Abnormal lung lesions (%)	20 (10–35)	40 (30–50)	<0.001
SpO ₂ (%)	93 (89–96)	88 (75–90)	<0.0001
Death, No/Yes (%)	92.8/7.2	89.3/10.7	NS
Shock or organ failure, No/Yes (%)	91.3/8.7	26.7/73.3	<0.0001
Cardiopathy, No/Yes (%)	85.5/14.5	75/25	NS
ARF, No/Yes (%)	79.7/20.3	40/60	<0.001
CRF, No/Yes (%)	85.5/14.5	96.7/3.3	NS
Diabetes, No/Yes (%)	85.5/14.5	62.1/37.9	<0.05
Red blood cells (× 10e6/μl)	4.29±0.79	4.48±0.85	NS
Hematocrit (%)	38±7	39±7	NS
Hemoglobin (g/dl)	13±2	14±2	NS
Globular volume (fl)	89±8	89±7	NS
Reticulocytes (%)	0.97 (0.72–1.15)	1 (0.57–1.04)	NS
Reticulocytes (× 10 ³ /μl)	39 (29–50)	39 (24–51)	NS
Leucocytes (× 10e3/μl)	6.15 (4.63–8.03)	7.87 (4.91–13.54)	<0.05
Blood neutrophils (%)	73±12	78±17	<0.05
Blood lymphocytes (%)	15 (10–24)	10 (5–20)	<0.05
Blood monocytes (%)	0.2 (0–0.9)	0 (0–0.1)	<0.01
Blood eosinophils (%)	7.73±4.36	5.63±3.32	NS
Blood basophils (%)	0.2 (0.2–0.4)	0.2 (0.1–0.3)	NS
Blood neutrophils (10 ³ /μl)	4.54 (3.07–6.4)	6.96 (3.5–11.73)	<0.05
Blood lymphocytes (10 ³ /μl)	0.96 (0.69–1.27)	0.73 (0.59–1.12)	NS
Blood monocytes (10 ³ /μl)	0.42 (0.25–0.6)	0.37 (0.27–0.6)	NS
Blood eosinophils (10 ³ /μl)	0.01 (0–0.05)	0 (0–0.01)	<0.05
Blood basophils (10 ³ /μl)	0.01 (0.01–0.02)	0.02 (0.01–0.03)	NS
Platelets (10 ³ /μl)	195 (157–266)	189 (155–252)	NS
Quick time (%)	83±22	83±13	NS
Quick time (s)	13 (12–13)	13 (12–13)	NS
Fibrinogen (g/l)	5.24±1.61	6.06±2.01	NS
D-dimers (μg/L)	876 (517–1787)	1483 (586–2422)	NS
Erythrocytes sedimentation rate (mm/h)	123 (123–123)	48 (48–48)	NS
Iron (μmol/l)	4.27 (2.95–7.36)	4.61 (3.35–7.06)	NS
Ferritin (μg/l)	827 (499–1677)	1861 (889–4117)	<0.05
Osmolality (mosm/kg)	290±15	286±11	NS
Sodium (mmol/l)	139±5	136±4	<0.05
Chlorides (mmol/l)	102±6	100±5	NS
Potassium (mmol/L)	4.04±0.44	4.16±0.62	NS
Calcium (mmol/l)	2.23±0.18	2.14±0.21	NS
Phosphates (mg/l)	0.99±0.2	1.15±0.34	NS
Bicarbonates (mmol/l)	24 (21–26)	23 (19–26)	NS
Creatinine (mg/dl)	0.93 (0.8–1.31)	1.25 (0.88–1.6)	0.05
Urea (mg/dL)	41 (31–68)	53 (40–84)	<0.05
GFR (MDRD) (ml/min/1.73m ²)	71±33	60±30	NS
Total protein (g/l)	66±8	66±11	NS

Table 1 (continued)

Variables	ICU, No (n=72)	ICU, Yes (n=31)	p value
Albumin (g/l)	37±5	36±4	NS
Uric acid (mg/dl)	61±25	63±25	NS
CRP (mg/l)	58 (26–144)	166 (105–265)	<0.0001
Total bilirubin (mg/dl)	0.62 (0.44–0.82)	0.79 (0.53–1.02)	<0.05
Conjugated bilirubin (mg/dl)	0.25 (0.18–0.34)	0.33 (0.25–0.5)	<0.05
Alkaline phosphatase (U/l)	75 (59–90)	70 (57–95)	NS
GGT (U/l)	52 (30–111)	64 (29–133)	NS
ASAT (U/L)	35 (24–53)	60 (35–80)	<0.001
ALAT (U/L)	27 (17–46)	36 (26–56)	<0.05
LDH (U/l)	310 (244–441)	503 (411–703)	<0.00001
Lipase (U/l)	32 (19–50)	38 (25–53)	NS
Creatine kinase (U/l)	136 (59–266)	229 (101–426)	0.07
YKL-40 (ng/ml)	186 (84–384)	241 (172–827)	<0.05

When the data follow a normal distribution, the results are expressed as mean ± standard deviation, and otherwise, they are expressed as the median (IQR)

M, male; F, female; NS, nonsignificant

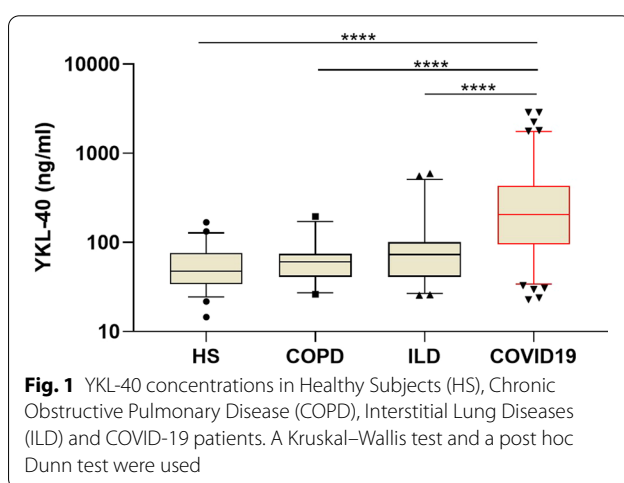


Fig. 1 YKL-40 concentrations in Healthy Subjects (HS), Chronic Obstructive Pulmonary Disease (COPD), Interstitial Lung Diseases (ILD) and COVID-19 patients. A Kruskal-Wallis test and a post hoc Dunn test were used

reached 0.78 ($p < 0.0001$). The positive predictive value was 70%, and the negative predictive value was 83%.

In conclusion, this study showed that firstly the COVID-19 patients had higher levels of YKL-40 compared to a control population (HS, COPD and ILD) and secondly that within the COVID-19 population YKL-40 was an indicator of the seriousness of infection since it is linked to complications such as admission to ICU, ARF or MOF. This marker could also be a predictive marker to anticipate management at the ICU and is useful for the prognosis of the onset of an ILD later. Future studies are also needed to assess the correlation between the levels of YKL-40 and pulmonary sequelae that patients with COVID-19 would develop.

Abbreviations

ICU: Intensive care unit; ILD: Interstitial lung diseases; HS: Healthy subjects; COPD: Chronic obstructive pulmonary disease; MOF: Multiple organ failure; AUC: Area under the ROC curve.

Acknowledgements

The authors would like to thank the COVID-19 clinical investigators of the CHU de Liège: Ancion, A., Berg, J., Bonhomme, O., Bouquegneau, A., Bovy, C., Bruls, S., Darcis, G., Defraigne, J.O., Ghysen, A., Gilbert, A., Heinen, V., Lamberton, B., Louis, R., Malaise, O., Martin, M., Misset, B., Moutschen, M., Nguyen Dang, D., Piazza, J., Szecel, D., Szecel, J., Van Cauwenberge, H., Von Frenckell, C., Vroonen, L.

Authors' contributions

JG, EC and MH contributed to conceptualization. LS, ANF and MH curated the data. MH contributed to formal analysis. LS and EC contributed to methodology. LS contributed to investigation and writing original draft. EC and JG contributed to supervision, validation, visualization and writing—review and editing. All authors read and approved the final manuscript.

Funding

Research grant from Fond Leon Fredericq.

Availability of data and materials

The datasets used and/or analyzed during the current study are available from the corresponding author on reasonable request.

Ethics approval and consent to participate

No specific approval was requested to the ethic committee as a leaflet including the following statement is given to all admitted patients: According to the law of the 19th December 2008, any left-over of biological material collected from patients for their standard medical management and normally destroyed when all diagnostic analyses have been performed, can be used for validation of methods. The law authorizes such use except if the patient expressed an opposition when still alive (presume consent). Written informed consent for participation was not required for this study in accordance with the national legislation and the institutional requirements. However, for HS, COPD and ILD patients, the protocol was approved by the ethics committee of CHU of Liège, and all subjects gave written consent before their enrollment (Belgian Number: B707201422832; ref: 2014/302).

Consent for publication

Not applicable.

Competing interests

All authors declare to have no specific competing interests for this specific publication.

Author details

¹ Department of Clinical Chemistry, University of Liege, CHU de Liège, Domaine Universitaire du Sart-Tilman, B35, 4000 Liège, Belgium. ² Department of Pneumology, CHU de Liège, Liège, Belgium.

Received: 5 November 2020 Accepted: 9 November 2020

Published online: 16 February 2021

References

- Korthagen NM, van Moorsel CHM, Barlo NP, Ruven HJT, Kruit A, Heron M, et al. Serum and BALF YKL-40 levels are predictors of survival in idiopathic pulmonary fibrosis. *Respir Med*. 2011;105:106–13.
- Létuvé S, Kozhich A, Arouche N, Grandsaigne M, Reed J, Dombret M-C, et al. YKL-40 is elevated in patients with chronic obstructive pulmonary disease and activates alveolar macrophages. *J Immunol*. 2008;181:5167–73.
- Nordenbæk C, Johansen JS, Halberg P, Wiik A, Garbarsch C, Ullman S, et al. High serum levels of YKL-40 in patients with systemic sclerosis are associated with pulmonary involvement. *Scand J Rheumatol*. 2005;34:293–7.
- Inoue Y, Kaner RJ, Guiot J, Maher TM, Tomassetti S, Moiseev S, et al. Diagnostic and prognostic biomarkers for chronic fibrosing interstitial lung diseases with a progressive phenotype. *Chest*. 2020;158:646–59.
- Guiot J, Moermans C, Henket M, Corhay JL, Louis R. Blood biomarkers in idiopathic pulmonary fibrosis. *Lung*. 2017;195:273–80.
- Bonhomme O, André B, Gester F, De Seny D, Moermans C, Struman I, et al. Biomarkers in systemic sclerosis-associated interstitial lung disease: review of the literature. *Rheumatol (United Kingdom)*. 2019;58:1534–46.

Publisher's Note

Springer Nature remains neutral with regard to jurisdictional claims in published maps and institutional affiliations.

Ready to submit your research? Choose BMC and benefit from:

- fast, convenient online submission
- thorough peer review by experienced researchers in your field
- rapid publication on acceptance
- support for research data, including large and complex data types
- gold Open Access which fosters wider collaboration and increased citations
- maximum visibility for your research: over 100M website views per year

At BMC, research is always in progress.

Learn more biomedcentral.com/submissions



